

ABSTRACT

Design, Synthesis, and Biological Evaluation of New Anti-cancer Nitrogen-Containing Combretastatins and Novel Cysteine Protease Inhibitors for the Treatment of Chagas

Rogelio Siles

Mentor: Kevin G. Pinney, Ph.D.

In an effort to combat cancer, the development of a relatively new type of anti-cancer drugs known as vascular disrupting agents (VDAs) seems to be a promising clinical approach. VDAs selectively interfere with blood flow in the microvessels that carry nutrients and oxygen to the tumor. Blockage of these vessels will stop tumor growth, produce necrosis, and hence prevent proliferation of cancer cells through the body. The discovery of a group of VDAs known as combretastatins (CA) has sparked an exciting area of anti-cancer drug discovery due to their robust biological activity as evidenced through clinical success, particularly for combretastatin A-4 phosphate (CA-4P) and one nitrogen-based combretastatin CA-4 analogue, AVE8062 which are currently in clinical development. Herein, a small library of seventeen new synthetic oxygen and nitrogen-bearing CA-1 and CA-4 analogues is described. Three of these analogues showed significant inhibition of tubulin assembly (IC_{50} = 2-3 μ M) as well as *in vitro* cytotoxicity against selected human cancer cell lines and *in vivo* blood flow reduction in SCID mice (23-25% at 10 mg/Kg) suggesting that they have potential for

further prodrug modification and development as vascular disrupting agents for the treatment of solid tumor cancers.

A separate research project has concentrated on the development of cysteine protease inhibitors, primarily focused toward the inhibition of cruzain, the major cysteine protease of *Trypanosoma cruzi* which is the agent of the parasitic disease called Chagas' disease. Currently there is no satisfactory treatment for this disease, and the two accepted drugs, nifurtimox and benznidazole, are associated with significant clinical toxicity. A library of fourteen small non-peptidic thiosemicarbazones has been successfully designed, synthesized and tested against cruzain and cathepsin L from which five compounds showed significant cruzain inhibition in the low nanomolar range. Although the most active compound synthesized, which is a bromotetrahydronaphthalene thiosemicarbazone, exhibited an $IC_{50}=12$ nM against cruzain, it also showed activity against cathepsin L ($IC_{50}=134$ nM). This new pharmacophore introduced may prove useful as a lead compound for further optimization. In addition, this research revealed further insights into the complex structure-activity relationship parameters which may lead to the further development of more selective cruzain inhibitors.

Design, Synthesis, and Biological Evaluation of New Anti-Cancer Nitrogen-Containing
Combretastatins and Novel Cysteine Protease Inhibitors for the Treatment of Chagas

by

Rogelio Siles, Licentiate

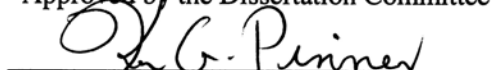
A Dissertation

Approved by the Department of Chemistry and Biochemistry


Marianna A. Busch, Ph.D., Chairperson

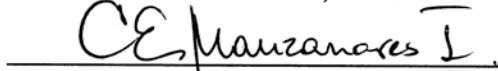
Submitted to the Graduate Faculty of
Baylor University in Partial Fulfillment of the
Requirements for the Degree
of
Doctor of Philosophy

Approved by the Dissertation Committee


Kevin G. Pinney, Ph.D., Chairperson


Robert R. Kane, Ph.D.

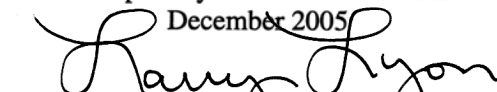

Charles M. Garner, Ph.D.


Carlos E. Manzanares, Ph.D.


William D. Hillis, M.D.

Accepted by the Graduate School

December 2005


J. Larry Lyon, Ph.D., Dean

Copyright © 2005 by Rogelio Siles

All rights reserved

TABLE OF CONTENTS

List of Figures	vii
List of Tables	x
List of Schemes	xi
List of Abbreviations	xiii
Acknowledgments	xvii
Dedication	xix
Chapter One: Introduction	1
Chapter Two: Synthesis and Biological Evaluation of Novel Combretastatin Vascular Disrupting Agents	4
Introduction	4
Background	8
Carcinogenesis and the Cell Cycle	8
Targets for Cancer Chemotherapy	10
Vascular-Targeting Therapies	13
Antiangiogenic Therapy	16
Vascular Disrupting Agents	19
Small Molecule Vascular Disrupting Agents	22
Tubulin Binding Agents	23
Colchicine-Binding Site Agents	31

Chapter Three: Materials and Methods	38
General Section	38
Synthesis of Nitrogen-Based Combretastatin A-4	39
Synthesis of Nitrogen-Based Combretastatin A-1	49
Synthesis of a Combretastatin A-1 Analogue	62
Synthesis of Nitrogen-Based Epoxide Derivatives of Combretastatins A-1 and A-4	66
Synthesis of Cold Precursors of Radio-labeled Combretastatins CA-1 and CA-4	70
Synthesis of OXi8007 and a Nitrogen-Based Indole	75
Biological and Biochemical Evaluation	82
Tubulin polymerization assay	82
MTT assay	84
<i>In vitro</i> cytotoxicity studies	84
Blood flow reduction	85
Chapter Four: Results and Discussion	86
Synthesis of Nitrogen-Based Combretastatin A-4	86
Synthesis of Nitrogen-Based Combretastatin A-1	100
Synthesis of a Combretastatin A-1 Analogue	112
Synthesis of Nitrogen-Based Epoxide Derivatives of Combretastatins A-1 and A-4	114
Synthesis of Cold Precursors of Radio-labeled Combretastatins CA-1 and CA-4	117
Synthesis of OXi8007 and a Nitrogen-Based Indole	122
Biological and Biochemical Results	131

Inhibition of tubulin polymerization, cytotoxicity (MTT) and blood flow reduction	132
<i>In vitro</i> cytotoxicity against P388 and selected human cancer cell lines	134
Chapter Five: Conclusions and Future Directions	140
Chapter Six: Synthesis, Design and Biochemical Evaluation of Cysteine Protease Inhibitors: Novel Compounds for Chagas' Disease Treatment	143
Introduction	143
Background	144
Chemotherapy of Chagas' Disease	148
Chapter Seven: Materials and Methods	157
General Section	157
Synthesis of Propiophenone Thiosemicarbazone Derivatives	158
Synthesis of Benzophenone Thiosemicarbazone Derivatives	165
Synthesis of Tetrahydronaphthalene Derivatives	168
Biochemical Evaluation of Cruzain Inhibitors	189
Cruzain Inhibition	190
Human Liver Cathepsin L	190
Chapter Eight: Results and Discussion	191
Synthesis of Propiophenone Thiosemicarbazone Derivatives	191
Synthesis of Benzophenone Thiosemicarbazone Derivatives	196
Synthesis of Tetrahydronaphthalene Derivatives	199

Biochemical Evaluation of Cruzain Inhibitors	212
Chapter Nine: Conclusions and Future Directions	221
Appendices	228
NMR spectra	229
Appendix A: Vascular Disrupting Agents	240
Appendix B: Cysteine Protease Inhibitors	379
References	483

LIST OF FIGURES

2.1. Major types of cancer that will cause death in USA in 2005	5
2.2. Major types of cancer expected in both men and women in USA in 2005	6
2.3. Causes of death in the US population observed in 1950 and 2002	7
2.4. The cell life cycle	8
2.5. Different steps in the pathway leading to carcinogenesis	9
2.6. Principal characteristics of antiangiogenic and vascular disrupting agents	15
2.7. Five stages of tumor development	16
2.8. Different stages of antiangiogenesis	17
2.9. Some representative antiangiogenic agents with their respective targets	18
2.10. Tumor vasculature	21
2.11. General mechanism of action of VDAs	21
2.12. Structures of the most important small molecule VDAs	22
2.13. Microtubule structure	25
2.14. Microtubule dynamic instability	26
2.15. Ribbon structure of α,β -tubulin dimer refined to 3.5 Å	27
2.16. Hypothetical model showing the three major tubulin active sites	28
2.17. Mechanism of action of a tubulin-binding VDA	29
2.18. The colchicine site in the tubulin-colchicine: RB3-SLD complex	32
2.19. Structures of colchicine and its derivatives	34
2.20. Structures of podophyllotoxin and its derivatives	35
2.21. Structures of some representative carbamates	36

2.22. Structures of some representative naphthyridinones	37
4.1. Aromatic region of the ¹ H-NMR spectrum of <i>E</i> isomer 3a	89
4.2 ¹ H-NMR spectrum of the unknown yellow solid (salt 4a)	91
4.3. Expanded aromatic regions of the ¹ H-NMR spectrum of <i>E</i> isomer 4b	93
4.4. Expanded region of the ¹ H-NMR (CD ₂ Cl ₂) spectrum of compound 13	99
4.5. Minimum-energy structure of compound 13	99
4.6. ¹ H-NMR and DEPT 135 of compound 15a	106
4.7. X-ray crystal structure of 4-methoxy-3,5-dinitrobenzoic acid	107
4.8. Minimum-energy conformation of compound 18 obtained using MOPAC	109
4.9. Minimum-energy conformations of <i>Z</i> epoxide 34 and <i>E</i> epoxide 36	117
4.10. Aromatic region of the ¹ H-NMR spectrum of compound 40d	119
4.11. X-ray crystal structure of compound 45	129
6.1. Countries (in red) that are afflicted with Chagas disease	144
6.2. Life cycle of <i>Trypanosoma cruzi</i>	145
6.3. Different forms that <i>Trypanosoma cruzi</i> adopts during its life cycle	146
6.4. Physical appearance of <i>Triatoma infestans</i> (kissing bug)	147
6.5. Structures of Nifurtimox and Benznidazole	148
6.6. Crystal structure of cruzain complexed with Z-RA-FMK	150
6.7. Proposed catalytic mechanism for cysteine proteases	151
6.8. Active sites of cruzain (S) containing an inhibitor or substrate (P)	152
6.9. Surface representation of cruzain complexed with Z-RA-FMK	153
6.10 Proposed mechanism of action between thiosemicarbazone and cruzain	154
6.11 Structures of tetrahydronaphthalene and benzophenone skeletons	156

8.1. X-ray structure of compound 50	193
8.2. ¹ H-NMR spectrum of compound 51a	194
8.3. X-ray structure of compound 59	197
8.4. X-ray structure of compound 66	202
9.1. Minimum energy conformations of compounds 59 , 62 and 66	223
9.2. One of the best calculated orientations of compound 66 in the active site of cruzain.	225

LIST OF TABLES

2.1. Cell cycle-specific agents used in chemotherapy	12
2.2. Cell cycle-nonspecific agents used in chemotherapy	13
2.3. Major differences between normal and neoplasm vasculature	20
2.4. Small molecule VDAs under development	23
4.1. Inhibition of tubulin polymerization, cytotoxicity and blood flow reduction for compounds 4, 5, 7 and 7a .	134
4.2. Inhibition of tubulin polymerization, cytotoxicity and blood flow reduction of compounds 10, 11, 13 and 14	135
4.3. Inhibition of tubulin polymerization, cytotoxicity and blood flow reduction of compounds 25, 26a, 27a and 27b	136
4.4. Inhibition of tubulin polymerization of compounds 22, 24a, 29, 33-38	137
4.5. <i>In vitro</i> cytotoxicity (GI ₅₀ and ED ₅₀ in μM) against seven human cancer cell lines for compounds 5, 7, 10 and 11	138
4.6. <i>In vitro</i> cytotoxicity (GI ₅₀ and ED ₅₀ in μM) against seven cancer cell lines for compounds 23c, 25, 27a and 33	138
4.7. <i>In vitro</i> cytotoxicity (GI ₅₀ and ED ₅₀ in μM) against seven cancer cell lines for compounds 34, 35, 36, 37 and 38	139
8.1. Inhibition of cruzain and human liver cathepsin L for compounds 49-51 and 56	213
8.2. Inhibition of cruzain and human liver cathepsin L for compounds 59 and 62	214
8.3. Inhibition of cruzain and human liver cathepsin L for compounds 65, 66	215
8.4. Inhibition of cruzain and cathepsin L for compounds 83a, 90, 91, 87 and 88	217
8.5. Inhibition of cruzain and human liver cathepsin L for 73, 74 and 77	218
8.6. <i>In vitro</i> cytotoxicity against seven cancer cell lines for 59, 66, 84, 87 and 88	220

LIST OF SCHEMES

4.1. Synthesis of 3'-amino CA-4 analogue (compound 4)	87
4.2. Generation of hydrogen ions in an aqueous magnesium sulfate solution	92
4.3. Synthesis of AC-7739 and the serinamide CA-4 analogue 7	94
4.4. Synthesis of 2'-amino CA-4 analogue (compound 10)	96
4.5. Synthesis of analogue 13 and hydrochloride salts 11 and 14	98
4.6. Synthesis of phosphonium bromide salt 16 and dinitrobenzaldehyde 21	101
4.7. Proposed mechanism for the formation of benzylic chloride 15a	103
4.8. Synthesis of free diamino 25 and its hydrochloride salt 27	107
4.9. Synthesis of 3,5-diserinamide CA-1 analogue 29	108
4.10. Synthesis of 2,5 and 2,3-dinitro benzaldehydes 20a and 20b	108
4.11. Synthesis of 2,5-dinitrogen-based CA-1 analogues	111
4.12. Synthesis of 2,3-dinitrogen-based CA-1 analogues	113
4.13. Synthesis of CA-1 derivative 33	114
4.14. Epoxidation of some nitrogen containing CA-1 and CA-4 analogues	115
4.15. Methodology suitable for the radiosynthesis of the <i>E</i> isomer of CA-1	121
4.16. Radiosynthesis of the <i>E</i> isomer of CA-1	123
4.17. Scale-up synthesis of OXi8007	124
4.18. Proposed nitrogen containing indole targets	125
4.19. Synthesis of α -bromoketone 43 and nitration of acetamide 44	127
4.20. Synthetic route for nitrogen-based indole derivatives 47a and 47b	128

4.21. Proposed mechanism for the formation of the azirene derivative 47	131
5.1. Proposed structures of future potential vascular disrupting agents	142
8.1. Synthesis of two novel propiophenone thiosemicarbazone derivatives 50 and 51	192
8.2. Synthesis of hydroxythiosemicarbazone 56	195
8.3. Synthesis of benzophenone thiosemicarbazone derivatives 59 and 62	196
8.4. Bromination of α -tetralone under two different conditions	200
8.5. Synthesis of thiosemicarbazones 65 and 66	201
8.6. Bromination of β -tetralone under two different conditions	203
8.7. Synthesis of bromothiosemicarbazone 69	203
8.8. Synthesis of thiosemicarbazone 74	204
8.9. Synthesis of α,β - conjugated ketones 77 and 79	205
8.10. Synthesis of α,β - conjugated ketone 82	207
8.11. Synthesis of thiosemicarbazones 84 and 83a	208
8.12. Bromination and further oxidation of 1,1-dioxo-1-thiochromen-4-one	209
8.13. Synthesis of dioxothiochromane thiosemicarbazones 87 and 88	210
8.14. Synthesis of chromanone thiosemicarbazone 90	211
9.1. Proposed structures of the second generation of more selective tetrahydronaphthalen based cruzain inhibitors	226

LIST OF ABBREVIATIONS

Å	Angstrom (10^{-10} times of an unit)
Ac ₂ O	Acetic anhydride
AcOH	Acetic acid
Ar	Aryl
Bn	Benzyl
Bu	Butyl
n-BuLi	n-Butyl lithium
c	concentrated acid
°C	Degress Celsius
CA-1	Combretastatin A-1
CA-1P	Combretastatin A-1 disodium phosphate prodrug
CA-4	Combretastatin A-4
CA-4P	Combretastatin A-4 disodium phosphate prodrug
CDCl ₃	Deuterated chloroform
COSY	Correlated Spectroscopy
CS Chem 3D	CambridgeSoft Corporation Chem 3D
δ	Chemical shift in ppm
d	doublet (NMR)
DCC	1,3-dicyclohexylcarbodiimide
DEPT	Distortionless enhancement by polarization transfer
DMAP	<i>N,N</i> -dimethylpyridin-4-amine

DMF	<i>N,N</i> -dimethyl formamide
DMSO	Dimethyl sulfoxide
DNA	Deoxyribose nucleic acid
ED ₅₀	Concentration at which 50% of cell growth is inhibited
Eq/ equiv	Equivalents
Et ₃ N	Triethylamine
Et ₂ O	Diethyl ether
EtOAc	Ethyl acetate
EtOH	Ethanol
Fmoc(Ac)	9-Fluorenylmethoxycarbonyl acetate
g	Grams
GB	Gaussian broadening
GC	Gas chromatography
GC-MS	Gas chromatography-mass spectrometry
GDP	Guanosine diphosphate
GI ₅₀	Growth inhibition, the concentration of the compound that inhibits cell growth by 50%
GTP	Guanosine triphosphate
h	Hour(s)
hex	Hexanes
H	Hydrogen atom
HETCOR	Heteronuclear correlation
Hz	Hertz

IC ₅₀	Inhibition constant, the concentration of the compound that inhibits a biological function by 50%
ⁱ Pr	Isopropyl
<i>J</i>	Coupling constant
LB	Line broadening
LDA	Lithium diisopropylamide
μ	Micro
m	milli or multiplet (NMR)
M	Molar (mol/ L)
M ⁺	Molecular ion
Me	Methyl
MeOH	Methanol
MHz	Megahertz
mmol	Milimole (s)
MOPAC	Semiempirical molecular computation application
mp	melting point
MTT	3-(4,5-dimethylthiazol-2-yl)-2,5-diphenyltetrazolium bromide
nM	Nanomolar
NMR	Nuclear magnetic resonance
PBr ₃	Phosphorus tribromide
PCC	Pyridinium chlorochromate
PMA	Phosphomolybdic acid
PPh ₃	Triphenyl phosphine

ppm	Parts per million
q	Quartet
R	Alkyl group
R _f	Retention factor
R _t	Retention time
RT	Room temperature
s	Singlet (NMR)
t	Triplet
T	Temperature
TBAF	Tetrabutylammonium fluoride
TBSCl	<i>tert</i> -butyldimethylsilyl chloride
THF	Tetrahydrofuran
TLC	Thin layer chromatography
TMSCl	Trimethylsilylchloride
<i>p</i> -TSA	<i>para</i> -toluenesulfonic acid
UV	Ultraviolet
VDA	Vascular disrupting agent
VTA	Vascular targeting agent

ACKNOWLEDGMENTS

First of all, I would like to thank my advisor, Dr. Kevin G. Pinney, for the opportunity he gave me to work in his research group. I really appreciate the countless opportunities in which he encourages me to be creative and efficient in order to accomplish the scientific research. Thanks Dr. Pinney for allowing me to start the Chagas' project in your laboratory and allowing me to write a research proposal. Without your support and trust in me, this project would never have been started. I just can tell you once again Dr. Pinney, thanks for being an outstanding mentor.

I am greatly thankful to Dr. Carlos Manzanares, Director of Graduate Studies, for giving me the opportunity to pursue my Ph.D at Baylor University. Thanks to him for the financial aid I received from the Chemistry Department at the beginning of my studies. Thanks for trusting in me.

I would like to thank my committee members, Dr. Bob Kane, Dr. Charles Garner, Dr. Carlos Manzanares and Dr. William Hillis (M.D.) for sparing their valuable time for my defense and for conveying their knowledge to me during the course of my studies.

I take this opportunity to thank Oxigene Inc., Welch Foundation and the Vice-Provost for Research of Baylor University for the generous financial support without which, it would have been impossible to carry out this research work.

I would like to thank the past and current Pinney research group for giving me the opportunity to work in a very pleasant work environment. Thanks Anu, Raj, Hania, Gerardo, John, Graciela, Freeland, Benson, Phyllis, Abi, Ming for your friendship and continuous encouragement. I would like to thank my good friend Malli for his support

when I first joined the group and his valuable friendship. I am particularly thankful to Madhavi Sriram for being present to help me and for sharing with me countless hours of chemistry conversations. Thanks “loquita” for being my good friend. Thanks Freeland for helping me many hours when we were working on our nitrogen-containing CA-1 and CA-4 projects.

I would like to thank Tom, Andy, Dr. Karban, and particularly Dr. Garner for teaching me the theoretical and experimental NMR techniques. Without your help many experiments would not have been possible to carry out for my research.

I am greatly thankful to Dr. Mary Lynn Trawick for working in our Chagas’ project and accepting the task of writing a collaborative research proposal for financial aid. Thanks to my good friend Shen- En Chen for his help in molecular modeling and computer issues. I would also like to thank Dr. Kathleen Kuhler for all her help and suggestions she gave me during the course of my studies.

I am greatly thankful to Nancy Kallus, Barbara Rauls, Adonna Cook and Andrea Johnson for all their help during these years. My special gratitude to Mrs. Beth Walker and other staff members at the office of the International Student and Scholar Services for giving me the proper guidance related to immigration rules. Finally my depp gratitude to Mrs. Sandra Harman for her meticulous revision of my dissertation in order to help me submit a high quality manuscript to the Graduate School at Baylor University.

DEDICATION

To my parents
Oscar and Rosario

They taught me to do anything with love, respect and devotion. Their words are a continuous source of inspiration for my life.

If I hear, I forget
If I see, I remember
If I do, I learn

Chinese Proverb

CHAPTER ONE

Introduction

Chemists play an important role in the search for effective medicines to fight threatening diseases worldwide. In particular, medicinal chemists have the knowledge to identify a drug candidate from an initial lead compound, which incorporates all of the properties that are required to help cure a particular disease or halt its progression. The role of a medicinal chemist in a medicinal chemistry research program is not restricted to the synthesis, purification, and analysis of novel compounds for biological testing, but also, to understand at molecular level how the molecules of the potential drugs interact with a biological, genetic or protein target linked to a particular disease to produce the desired biological activity.¹⁻³

Cancer and parasitic diseases are still the most lethal illnesses known worldwide after heart disease. Although significant research has done to date to treat both diseases, there is still a lack of effective chemotherapeutic treatment to cure them completely. The development of medicinal chemistry programs takes place in pharmaceutical companies as well as in governmental and academic institutions with a common theme of recognizing that health problems concern everyone and require fast and effective solutions from the scientific community.⁴

Herein, two medicinal chemistry projects are presented in order to treat cancer and a parasitic disease called American Trypanosomiasis (Chagas' disease). The first project, which is described from chapters two to five, is related to the lead optimization of a group of anti-cancer compounds called combretastatins. Combretastatins, which

were initially isolated in 1982 from *Combretum caffrum* (a bush willow tree found in Africa) by Professor George Pettit,⁵⁻⁷ are characterized by their remarkable biological activity as inhibitors of tubulin polymerization. They have also shown significant *in vitro* inhibition potency against human cancer cell lines, and demonstrated *in vivo* efficacy as a vascular disrupting agents (VDAs).⁵ Combretastatins can be structurally classified as a *Z* stilbenes that contain one phenyl ring that has three methoxy groups (A-ring) and another benzene ring that has different substituents (B-ring).⁸ In this project, the synthesis of a small library of seventeen new synthetic oxygen and nitrogen-bearing analogues of combretastatins A-1 and A-4 (CA-1 and CA-4) is described. The research work has primarily focused on the substitution of the hydroxyl groups of the B-ring of CA-1 and CA-4 by nitrogen functionalities, such as nitro, amine, and serine.

The second project, that is described from chapters six to nine, focuses on the design and synthesis of fourteen small non-peptidic thiosemicarbazones and unsaturated ketones which were tested against cruzain and cathepsin L in order to treat a devastating parasitic disease known as Chagas which is caused by a parasite called *Trypanosoma cruzi*. Cruzain, which is the major cysteine protease of the *T. cruzi*, is an essential enzyme that is expressed in all life cycle of the parasite and plays an important role in the survival of the microorganism.⁹ Inhibition of cruzain activity will result in death to the parasite and will therefore halt or control the dissemination of the disease in humans.

Because enzymes are essential for different life processes, they are attractive targets for drug therapy. In 2005, Copeland¹⁰ reported that approximately 50% of the drugs in clinical use today are enzyme inhibitors, and worldwide sales of these inhibitors

exceeded 65 billion dollars in 2001,¹⁰ and this market is expected to grow to more than 95 billion dollars by 2006.

CHAPTER TWO

Synthesis and Biological Evaluation Of Novel Combretastatin Vascular Disrupting Agents

Introduction

Despite the fact that cancer is a disease known since ancient times and numerous efforts have been made to prevent, control and eradicate it, in the 21st century, this illness is still one of the most devastating human problems known in the world. Cancer is a group of diseases that are characterized by the abnormal and relatively fast growth of the cells present in some body organs or tissues.¹¹ The uncontrollable cell division, which forms a malignant mass of cells called a neoplasm, is due to mutations that the cell's DNA suffers when a person is exposed to certain cancer-causing agents, called carcinogens, such as ultraviolet light, industrial chemicals, radiation, the tar of cigarettes, viruses and some metabolic products.¹¹⁻¹⁴ Probably, the most important difference that cancer cells have compared to normal cells, is that malignant tumor cells have the ability to spread and infiltrate the tissues around them and may block passage ways, destroy nerves, and erode bone. Cancer cells may spread via blood vessels and lymphatic channels to other parts of the body, where a second neoplasm or metastase will be formed and developed independently.¹¹ Cancer is commonly observed in major organs including the lungs, breast, intestines, skin, stomach, prostate, colon, rectum, ovary, bladder and even in the blood cell-forming tissues of bone marrow.¹¹⁻¹⁴

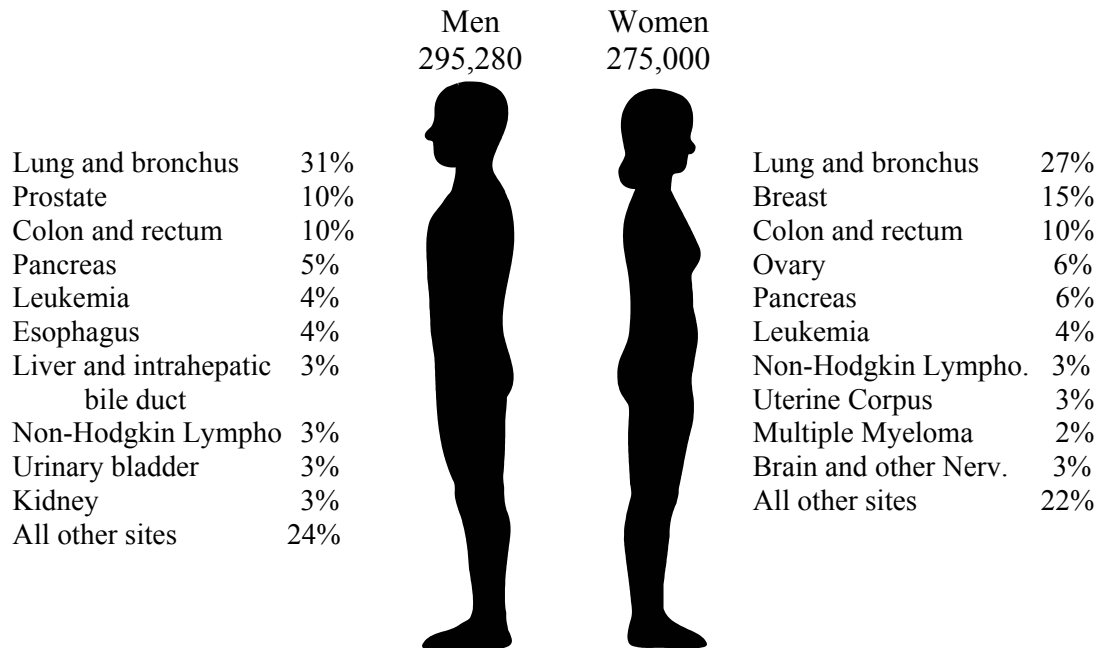


Figure 2.1. Major types of cancer that will cause death in USA in 2005.¹⁵ (Reproduced directly from reference 15).

The American Cancer Society has estimated that in 2005 a total of 1,372,910 new cancer cases and 570,280 deaths are expected in the United States.¹⁵ The major kind of cancer death in 2005 will be from lung and bronchus cancer followed by cancers of the prostate, breast, colon and rectum as Figure 2.1 shows, while Figure 2.2 indicates the most common cancers expected to occur the same year. Although cancer is a disease that often is seen in elderly people, individuals of any age can be stricken by this disease; in fact, in 2002 cancer was the second leading cause of death among children between ages of 1 and 14.¹⁵ Because cancer in the USA is the second cause of death after heart diseases, and because little improvement has been made to reduce the cancer death rates

between 1950 and 2002 (Figure 2.3),¹⁶ the fight against this lethal disease is still one of the biggest challenges for the scientific community.

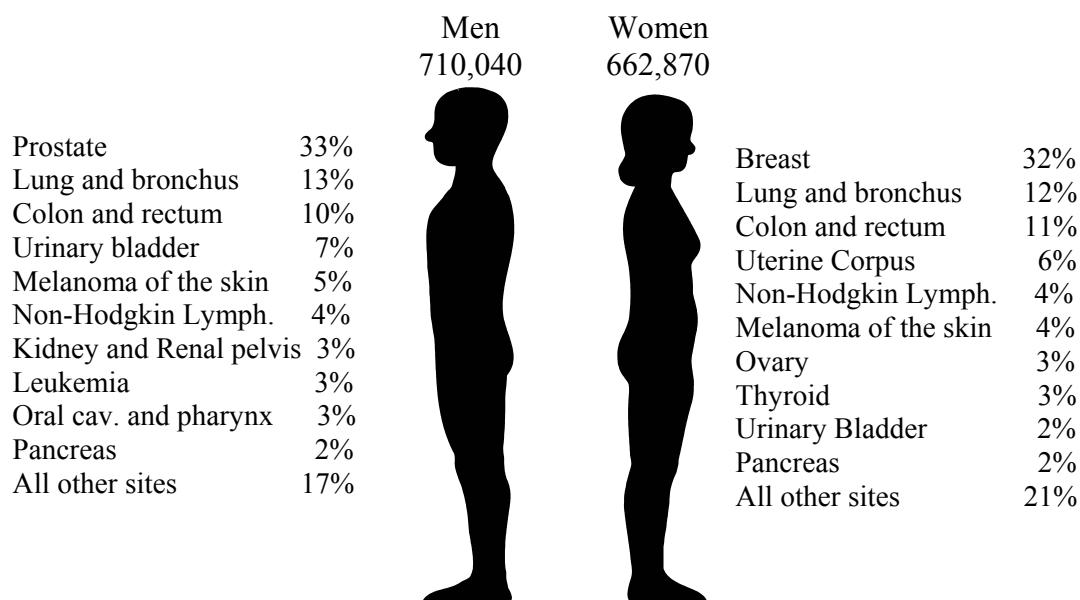


Figure 2.2. Major types of cancer expected to be found in both men and women in USA in 2005.¹⁵ (Reproduced directly from reference 15).

Surgery, radiation, chemotherapy and most recently immunotherapy are the most common methods used to treat cancer. The treatment that is chosen depends on many different factors including the type of cancer, extent of the disease, rate of progression, condition of the patient and response to the therapy; however combination of two or more of these methods has been shown to yield better results.^{11,14} Although chemotherapy is used as a primary treatment or as an adjuvant to the other therapies, it often has unpleasant side effects because of the limited selectivity that these drugs have for cancer cells; unfortunately, healthy cells and tissues are disrupted along with tumor cells. During the past 20 years special attention has been given to the tumor vasculature as a

possible target site to overcome problems associated with selectivity and toxicity. One group of compounds known as Vascular Disrupting Agents (VDAs) has the objective to shut down blood flow selectively in the vessels that carry nutrients and oxygen to the tumor. Blockage of these vessels will stop tumor growth, produce necrosis, and prevent proliferation of cancer cells through the body. Herein, the synthesis of novel VDAs and evaluation of their biological activity against cancer is described.

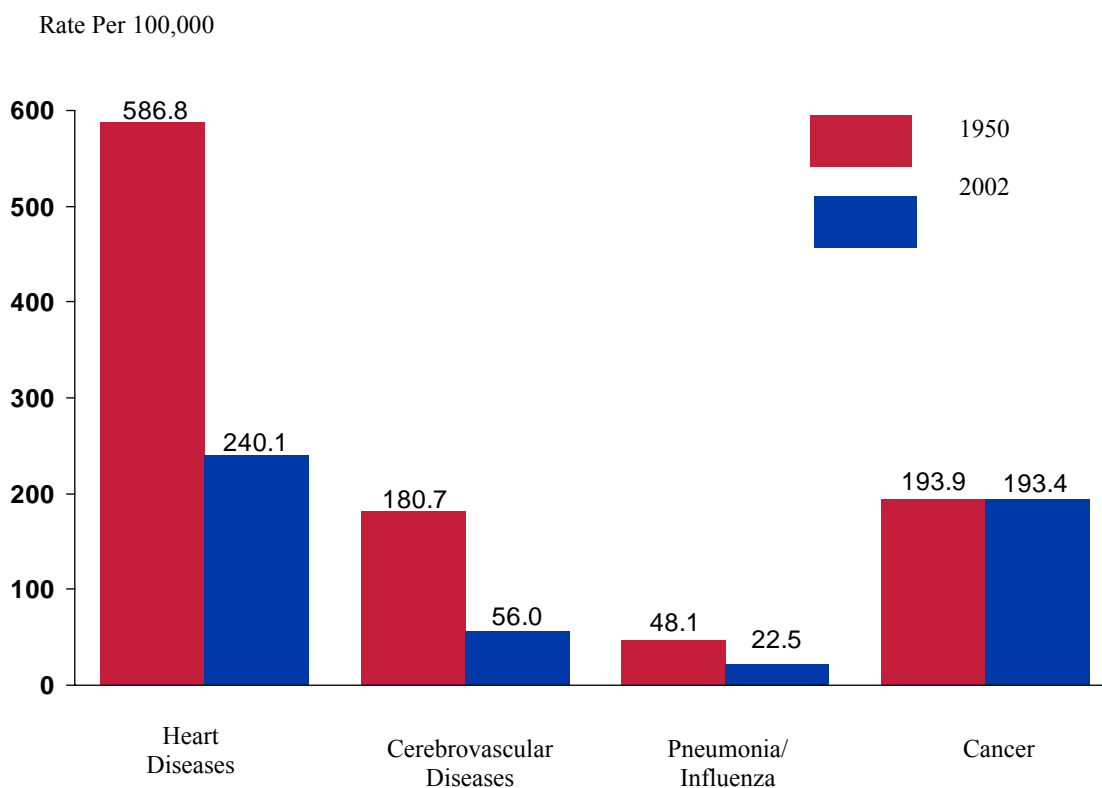


Figure 2.3. Causes of death in the US population observed in 1950 and 2002. The age-adjusted was respect to 2000 US standard population.¹⁶ (Reproduced directly from reference 16).

Background

Carcinogenesis and the Cell Cycle

It is known that cancer is caused by the activation of certain oncogenes which activate different cell-signaling pathways which in turn disrupt the homeostatic mechanism that controls cell differentiation and proliferation. If the body inappropriately regulates the replication of dividing cells, a breakage in the balance between the birth and death of cells will occur and the body's cells will divide abnormally to form tumors.^{17,18}

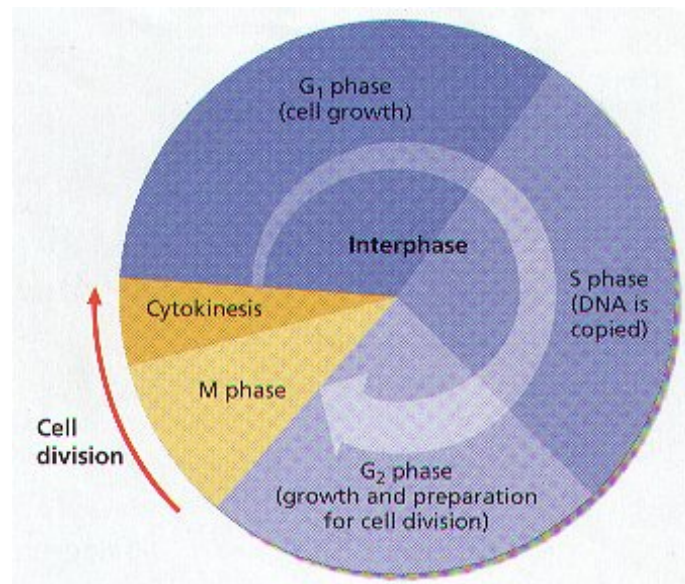


Figure 2.4. The cell life cycle.¹⁹ (Reproduced directly from reference 19).

Like normal cells, cancer cells undergo the different phases of the cell cycle that is depicted in Figure 2.4.¹⁹ Accordingly, the cell has a division phase and a period of growth called the interphase which in turn is divided into three stages called **G₁**, **S**, and **G₂**. **G₁** and **G₂** stand for *Gap 1* and *Gap 2* because they are gaps in the cell cycle that

come between the time of chromosome division and the time of chromosome replication. The **S** stands for synthesis of DNA, and finally the division phase is divided into mitosis (**M**), in which the division of the nucleus occurs, and cytokinesis, in which the division of the cytoplasm occurs.^{12,17} Once the stem cells have divided into daughter cells, these in turn start preferably multiplying to form a malignant tumor which after growing invades other tissues of the body forming metastases that keep this cycle going (Figure 2.5). Therefore, understanding the cell cycle and the steps in the pathway that lead to carcinogenesis is crucial to regulate the stages of growth, division, proliferation, invasion, and rest of malignant tumors.¹²

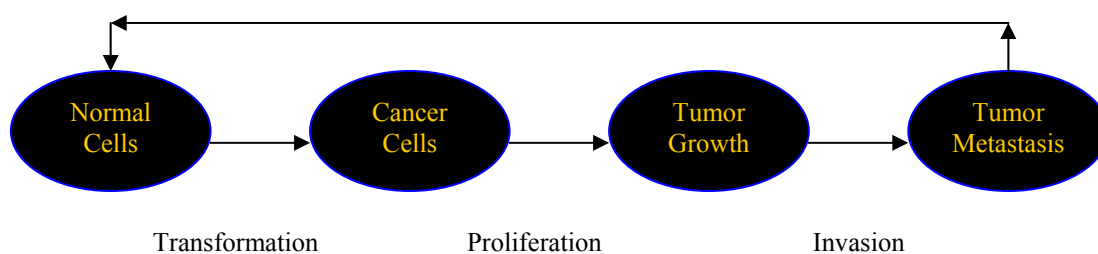


Figure 2.5. Different steps in the pathway leading to carcinogenesis.¹⁸ (Reproduced directly from reference 18).

As Ronald Breslow indicated, there are several approaches that a medicinal chemist uses to combat cancer.¹ In the first approach, bioorganic chemists develop drugs that selectively kill cancer cells without harming normal cells. The second approach focuses on blocking the progress of the disease. This can be carried out, for example, by blocking metastasis, which is the spreading of cancer cells from one place to another in the body, or by blocking the blood supply to the solid tumor so that in the absence of oxygen and nutrients the cells will not survive. The last approach is related to

the synthesis of compounds that induce differentiation and decrease the rate of proliferation of cancerous and precancerous cells. Considerable amounts research has been carried out in all these approaches, and, ultimately time will tell which one is the most effective.

Targets for Cancer Chemotherapy

Compounds that have the property of killing cells are called cytotoxic drugs. When cytotoxic compounds are designed to kill cancer cells, they are referred to as anticancer or antineoplastic agents, and their administration is known as cancer chemotherapy.^{11,20} Unfortunately, these chemicals can also damage healthy cells, especially the ones that are multiplying rapidly, and achieving the desired selectivity over cancer cells is a goal that is far from being completed to date.¹ Although chemotherapy has been used since the 1500s when heavy metals were administered to destroy cancer cells, it was not until the 1940s that the first systematic and successful program of chemotherapy took place when nitrogen mustard and its derivatives were used to treat a patient with lymphoma.^{20,21}

During the first four decades in the history of chemotherapy, a period known as cellular chemotherapy, chemists killed malignant tumors by inhibiting different mechanisms of their cellular division using cytostatic/cytotoxic agents. Later, the rapidly expanding knowledge of molecular biology made possible the identification of specific tumor targets which are responsible for cancer cell replication. These targets may be selectively blocked by molecules designed and synthesized for this purpose, opening the door to a new period called molecular chemotherapy.²¹

Many oncologists define targeted therapy as a drug with a focused mechanism that specifically acts on a well-defined target or biologic pathway that, when inactivated, causes regression or destruction of the malignant process.²² Therefore, before accepting a new compound as an anticancer agent, it is necessary to elucidate its mechanism of action on both cellular and molecular levels.²³ However, first it is important to establish what an ideal target is. Ross and co-workers proposed the following features of the ideal anticancer target:²²

- 1) Crucial to the malignant phenotype
- 2) Not significantly expressed in vital organs and tissues
- 3) A biologically relevant molecular feature
- 4) Reproducibly measurable in readily obtained clinical samples
- 5) Correlated with clinical outcome
- 6) Clinical response in a significant proportion of patients whose tumors express the target when target interrupted, interfered with, or inhibited.
- 7) Minimal responses in patients whose tumors do not express the target.

Although every year new targets for cancer therapy are identified, and several drugs enter clinical trials, the emergence of resistance to targeted cancer therapeutics, the different toxicity profiles, the efficacy and the cost of drug development are still important limitations for chemotherapy to be considered an ideal cancer treatment.²²⁻²⁶

One convenient way to classify antineoplastic agents is based on their mode of action and the phase of the cell cycle in which the drug acts. If the action of the drug is most effective at any particular phase of the cell cycle, the drug is called a cell cycle-specific drug, otherwise the compound is considered to be a nonspecific agent which is

effective through all phases. The cell cycle-specific drugs are known to reduce the growth fraction, that is the number of cells that are in cycle (proliferating cells). On the other hand, cell cycle-non-specific drugs are involved in reduction of the tumor burden, which is the number of cells that make up a tumor. According to the Gompertzian model of tumor growth, tumors in their early stages grow rapidly because they have a high growth fraction. Eventually as the tumor burden increases, its growth reaches a plateau and the growth fraction decreases.¹⁷ Table 2.1 and 2.2 show the most important cell cycle-specific and nonspecific agents which have entered clinical trials. In addition, the stage of the cell cycle in which they interact is also shown.

Table 2.1. Cell cycle-specific agents used in chemotherapy that entered clinical trials.^{17,21} (Directly reproduced from references 17 and 21).

Cell Cycle Stage	Class	Subclass	Representative Compounds
S Phase	antimetabolites	folate analogues	trimetrexate, methotrexate
		purine analogues	fludarabine
		adenosine analogues	cladribine, pentostatine
		pyrimidine analogues	fluoroxidine, gemcitabine
M Phase	mitotic inhibitors	vinca alkaloids	vinblastine, vincristine, vindesine
G ₂ and S Phase		epipodophyllotoxins	Etoposide, teniposide
M Phase		taxanes	Docetaxel, paclitaxel
S Phase	topoisomerase I	camphotecines	Irinotecan, topotecan

Table 2.2. Cell cycle-nonspecific agents used in chemotherapy that entered clinical trials^{17,21} (Directly reproduced from references 17 and 21).

Class	Subclass	Representative Compounds
DNA alkylating agents	Nitrogen mustards	estracyte
	oxazaphosphorines	ifosfamide
	hexitols	mitobronitol, mitolactol
	nitroisoureas	fotemustine, carmustine, lomustine
	triazines	altretamine, temozolomide
	platinum complexes	carboplatin
Antibiotics	glycopeptide	pepleomycin
	anthracyclines	epirubicin, idarubicin, esorubicin
	anthracenedions E	mitoxantrone
	anthapyrazoles E	losoxatrone
Hormonal agents	SnRH analogues	octreotide, lanreotide
	GnRH analogues	leuprolide, buserelin, goserelin, tryptorelin
	aromatase inhibitors	aminoglutethimide, fadrozole, formestane
	antiostrogens	toremifene, raloxifene
	antiandrogens	cyprosterone, flutamide, bicalutamide
	antiprogestins	mifepriston
	others	fluoxymesterone

Vascular-Targeting Therapies

As it was earlier established, current chemotherapy is based on targeting cancer cells. Another interesting strategy to combat cancer centers of producing occlusion of the tumor blood vessels which will produce a prolonged ischemia that in turn will cause cell death and tumor necrosis.²⁷ Although this is a relatively new clinical approach for the

treatment of cancer, the importance of tumor vasculature as a therapeutic target started back in 1923 when Woglom proposed that damage of the capillary system might be the most effective way to inhibit tumor growth. Approximately 60 years later, Denekamp postulated that tumors need to continuously form new blood vessels because of the abrupt and uncontrollable growth of cancer cells.²⁸ These observations were the starting point for the development of a relatively new anti-cancer strategy currently known as vascular-targeted therapies.

In 2005, Siemann and other international scientists met to develop a common terminology and to define and to describe clearly and precisely the variety of agents designed to target the tumor vasculature. Accordingly to their definition, vascular-targeting therapies involve a group of strategies that focus on targeting and disrupting the vascular supply of tumors. In addition, they also mentioned that at any point these therapies should not be called or referred to cytotoxic therapy, a term that is exclusively used for conventional chemotherapeutic agents.²⁷

More than 90% of cancer present in solid tumor form requires a functioning vascular network to provide tumor cells with oxygen and nutrients and also to remove toxic waste products associated with cellular metabolism.²⁸ Therefore, failure in providing adequate blood supply can have detrimental consequences to tumor cell survival, progression and dissemination.²⁹ Even though tumor cells can access the existing blood vessel network from surrounding tissues to grow to a maximum size of one mm³, for further growth and development they must generate their own vasculature (Figure 2.7), a process known as neovascularization or angiogenesis.²⁷⁻³¹

Current vascular-targeted therapy is divided in two broad categories which differ in three important aspects including the physiologic target, the type or extent of disease, and the treatment scheduling.³² The first group is related to compounds that prevent the formation of new blood vessels in tumors, which means that they interfere with the process of angiogenesis and therefore they are called antiangiogenic agents. The second group, which is known as vascular disrupting agents (VDAs), destroys the established tumor vessel network leading to rapid shutdown of the tumor's blood supply.^{27,32} Figure 2.6 shows the most important characteristics and differences between antiangiogenic and vascular disrupting agents.

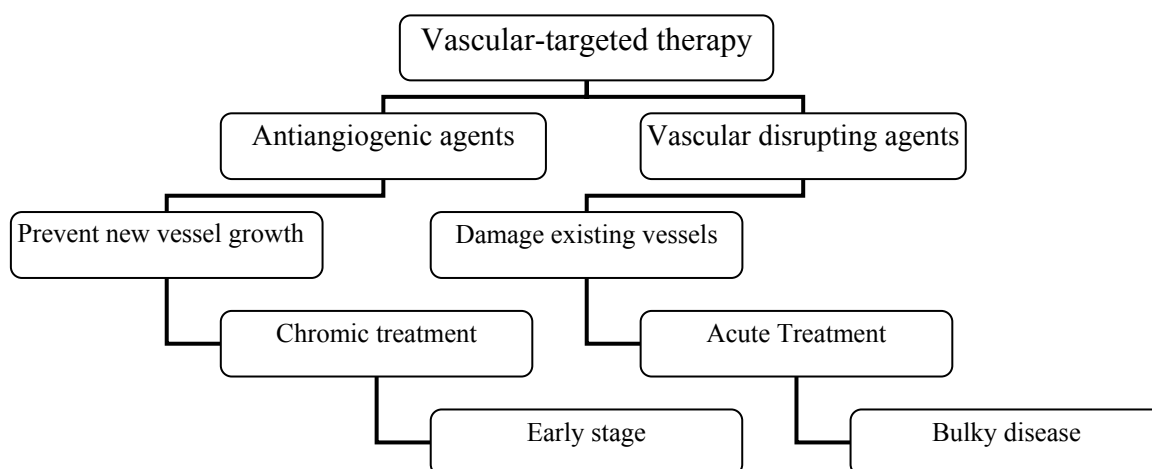


Figure 2.6. Principal characteristics of antiangiogenic and vascular disrupting agents.³²
(Directly reproduced from reference 32).

Before describing each group of vascular therapy, it is important to understand how a tumor is formed. As Figure 2.7 shows, the development of a tumor has five stages. In the first stage called hyperplasia, cells start dividing at a faster rate because of a genetic mutation. During dysplasia, which is the second stage, the structure and

organization of cells become abnormal. In the third stage referred as *in situ* growth, cells continue dividing but in a well-defined area. As the tumor keeps growing, it requires new blood vessels which are formed in the fourth stage called angiogenesis. Finally, in the last stage called invasion, tumor cells break the basement membrane and they are spread to different parts of the body through the circulatory or lymphatic system.¹⁴

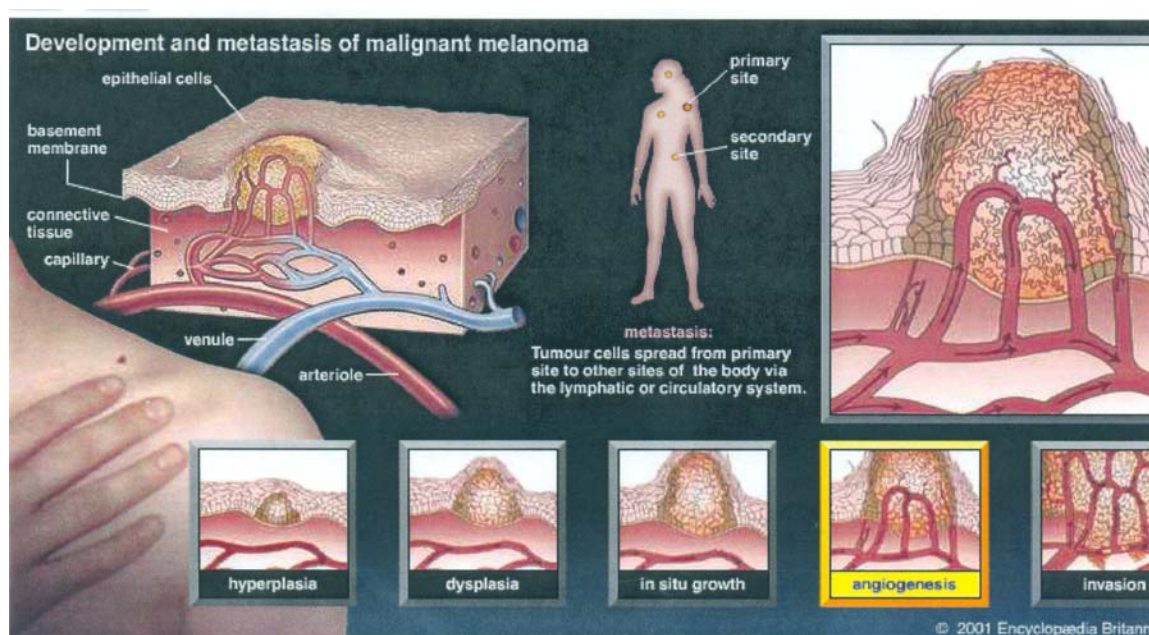


Figure 2.7. Five stages of tumor development.¹⁴ (Directly reproduced from reference 14).

Antiangiogenic Therapy

The principal research work carried out so far in the vascular-targeted therapy is based on the design of antiangiogenic agents. Tumor angiogenesis is a complicated process which involves multiple, sequential, and interdependent steps as shown in Figure 2.8.

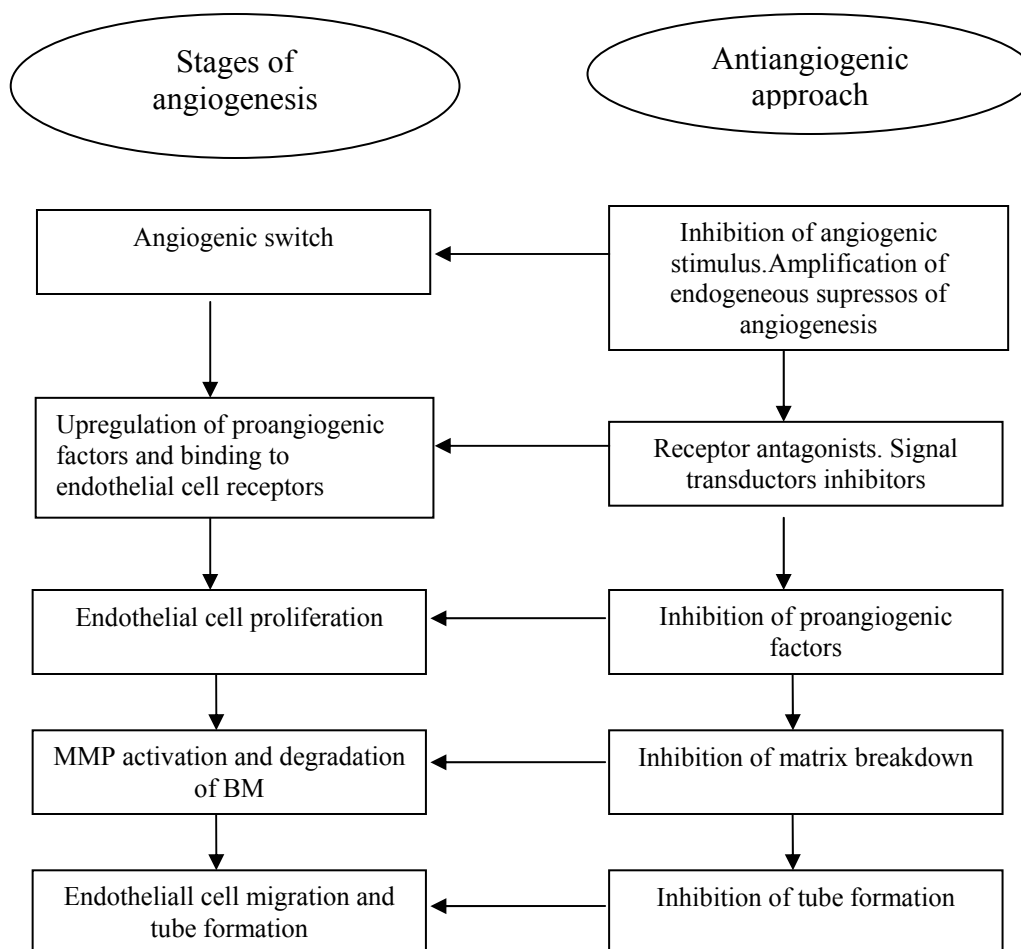


Figure 2.8. Different stages of angiogenesis and the antiangiogenic approach taken on each step. MMP stands for metalloproteinase and BM is the basement membrane.³² (Directly reproduced from reference 32).

Angiogenesis is a process that relies on a delicate balance of biochemical signals and receptors in a variety of cell types. In tumors, vascular endothelial growth factor (VEGF) and basic fibroblast growth factor (bFGF) are considered primary targets to inhibit angiogenesis, the former being the most potent and specific of the many angiogenic factors known. VEGF is not only crucial for endothelial cell proliferation and blood vessel formation, but it also induces significant vascular permeability and plays a key role in endothelial cell survival signaling in newly formed vessels. VEGF is secreted

by tumor cells and the expression can be increased by environmental triggers such as hypoxia, loss of tumor suppression gene function, and oncogene activation.^{32,27-30}

There is evidence that antiangiogenic compounds can also have a direct effect on existing blood vessels, overlapping and possibly having a synergistic effect with the actions of VDAs.²⁹ To date, there are many known compounds that target different stages of the angiogenic process. Figure 2.9 shows some representative antiangiogenic compounds that interact with a specific target.³²

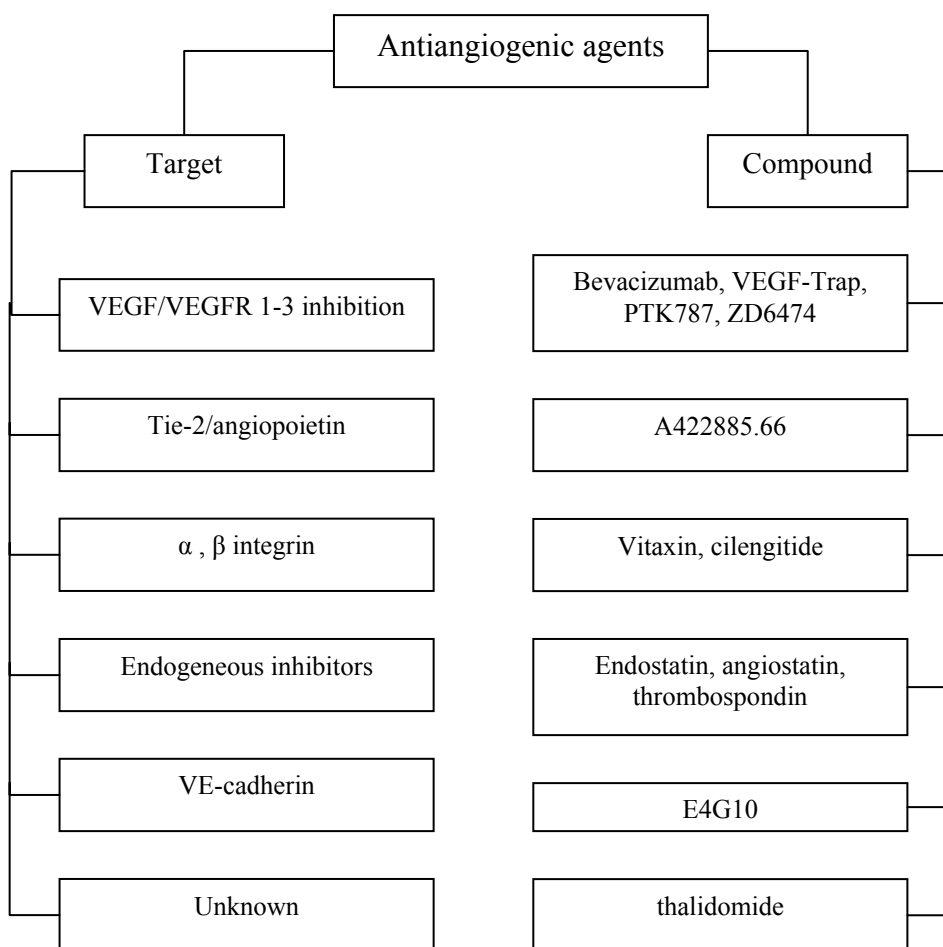


Figure 2.9. Some representative antiangiogenic agents with their respective targets.³²
(Directly reproduced from reference 32).

Vascular Disrupting Agents

One of the reasons that tumor vasculature is considered the “Achilles heel” of solid tumor growth is because of the inherent differences between blood vessels in tumors and those associated with normal tissues.²⁷ In the early 1980s, Denekamp observed that tumor endothelial cells proliferate more rapidly than their counterparts in normal tissues. She proposed that the properties of tumor endothelium may be different from normal tissues, and these differences could be exploited by the use of selective VDAs.²⁹ Table 2.3 shows the most important differences between tumor and normal vasculature; it is clear to notice from the table that tumor blood vessels consist of a chaotic network of immature tortuous, thin-walled vessels with a significant degree of neovasculature and a relatively high proportion of proliferating endothelial cells (Figure 2.10).^{31,33,34}

One potential advantage that VDAs have over other classes of anticancer drugs is evidenced by the observation that blockage of a single vessel, which provides oxygen and nutrients for almost a million tumor cells,³⁴ may cause a massive death of surrounding cancer cells. VDAs do not need to kill the endothelial cells to be effective but rather they simply must change the endothelial cells form or to promote a local coagulation which will stop the blood flow through the vessel.²⁹

In part I of the general mechanism of action of VDAs, depicted in Figure 2.11, the tumor cells (light blue spots) are being continuously fed by the closest blood vessel (red channel) which provides oxygen and nutrients to them. After treatment of the neoplasm with a VDA agent (part II), there is a dysfunction in the endothelial cells which produces partial occlusion of the vessel (green spots). The reduction of the blood flow causes that

tumor cells located further from the vessel to become increasingly hypoxic as represented by the purple spots. As damage in the endothelium progresses (part III), coagulation (dark blue spots) starts taking place and blockage of the vessel finally occurs, which in turn results in widespread tumor cell necrosis (dark spots).²⁷

Table 2.3. Major differences between normal and neoplasm vasculature.²⁹ (Directly reproduced from reference 29).

Increased vessel tortuosity
Vessels thin walled and fragile
Increased interstitial pressure within tumor
Vessel marker immaturity
Increased vessel permeability
Variable flow rates
Huge variability in vascular density
Lack of vascular smooth muscle
Lack of lymphatic drainage
Constant remodeling
Abnormalities of endothelial cell and pericyte shape and function

VDA's can be divided in two groups. The first group called biologics or ligand-directed VDAs includes antibodies or peptides which deliver toxins, procoagulant and proapoptotic effectors to the tumor endothelium. The second category is formed by small-molecule agents which exploit the differences between normal and tumor endothelium to induce vascular shutdown of tumor blood vessels.^{29,27}



Figure 2.10. Tumor vasculature.³⁵ (Directly reproduced from reference 35).

Because the research focuses on the development of small molecule vascular disrupting agents, the rest of the discussion will concentrate on the detailed description of some of these compounds.

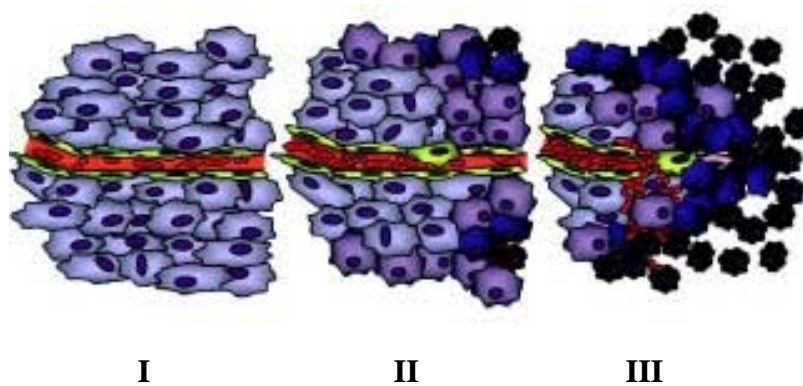


Figure 2.11. General mechanism of action of VDAs.²⁷ (Directly reproduced from reference 27).

Small Molecule Vascular Disrupting Agents

To date, there are two types of agents that cause extensive hemorrhagic necrosis in tumors as a result of vascular collapse.³⁴ The first group includes flavone acetic acid (FAA) and its derivatives while the second group involves tubulin-binding agents.²⁹

Flavonoids are believed to exert their effects on blood vessels via the localized release of TNF α from activated macrophages within the tumor tissue. Evidence for the role of TNF α in the antitumor activity of flavones was provided by the finding that antibodies against TNF α inhibited flavone acetic acid induced vascular collapse. Both FAA and the more potent fused tricyclic compound 5,6-dimethylxanthenone-4 acetic acid (DMXAA) have been shown to stimulate both human and mouse macrophages. Currently DMXAA is considered the leading candidate for continued drug development within the class of flavonoid VDAs (Figure 2.12).²⁷

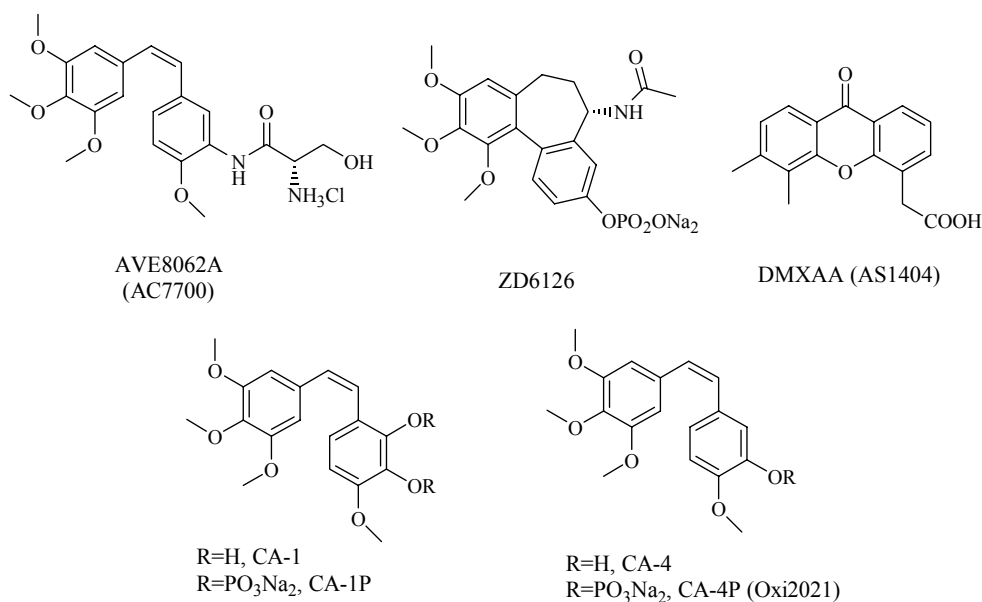


Figure 2.12 Structures of the most important small molecule vascular disrupting agents. AVE8062A, ZD6126, CA-1, CA-1P, CA-4 and CA-4P are the leading tubulin-binding agents; DMXAA is the best flavonoid VDA known to date.^{29,27}

The most important group of small molecule disrupting agents is composed of the tubulin-binding agents, and the attention is going to focus on this class of agents which are described in detail in the next section. Figure 2.12 and Table 2.4 show the structures of six leading compounds that are currently under preclinical and clinical studies.²⁷

Tubulin Binding Agents

In order to understand the mechanism of action of tubulin binding agents against the tumor endothelium, it is first important to evaluate the role that tubulin plays in the life of a cell and how this affects its survival.

The cytoskeleton, which is a group of filaments or fibers present in the cytoplasm of eukaryotic cells, has different functions in the cell such as organization of other constituents in the cell, maintenance of the cell's shape, promotion of locomotion of the cell itself, and the movement of the various organelles within it.¹² There are three types of fibers that make up the cytoskeleton which include the microfilaments which are primarily composed of the protein actin, the intermediate filaments, and finally the microtubules.¹²

Table 2.4. Small molecule VDAs under development.^{27,29}
(Directly reproduced from references 21 and 18).

Agent	Mechanism of action	Stage of development
CA-4P	Tubulin depolymerization	Phase II clinical trials ongoing
ZD6126	Tubulin depolymerization	Phase I clinical trials completed
DMXAA	TNF induction	Phase I clinical trials ongoing
AVE8062	Tubulin depolymerization	Phase I clinical trials ongoing
NPI2358	Tubulin depolymerization	Preclinical
MN029	Tubulin depolymerization	Preclinical
Oxi4503	Tubulin depolymerization	Preclinical

Microtubules are associated with different cellular functions among the most important of which is the formation of the mitotic spindle, involved in the alignment of replicated chromosomes to the equatorial plane to promote further segregation of the chromosomes to the two daughter cells.³⁶ Additional functions include cellular transportation, locomotion of the cell, around its environment, transportation of the organelles inside the cell and construction of the cell shape.³⁷ Microtubules are formed by polymerization of the protein tubulin which exists under physiological conditions as a dimer of two different polypeptide chains known as α and β tubulin subunits attached to each other in a head to tail fashion to form protofilaments.^{38,39} It is known that about 13 of these protofilaments are arranged in parallel making the microtubule wall and forming a polymer with a diameter of 25 nm and an internal bore of around 15 nm as it is shown in Figure 2.13. The ability of microtubules to grow and shrink dynamically is essential for their function, and regulation of this assembly and disassembly can be better understood by looking more closely at the structure of tubulin and its interaction within a microtubule.³⁹

Tubulin as stated above is a dimeric protein of 100 kD that is formed by two 50-kD polypeptide chains called α and β tubulins which share about 40% sequence homology.^{40,41} α -Tubulin is exposed at the less dynamic end (called the minus end), and β tubulin is exposed at the more dynamic end (called the plus end). Within a cell, microtubules are anchored by their minus ends at the microtubule-organizing center while disposing their plus ends towards the cell periphery.^{36,45} Each monomer, which follows a shallow and left handed helix, binds one molecule of the guanidine nucleotide

GTP; the nucleotide bound to α -tubulin, at the so called N-site, is not exchangeable whereas the GTP present at the E-site of β -tubulin is (Figure 2.14).^{39,43,44}

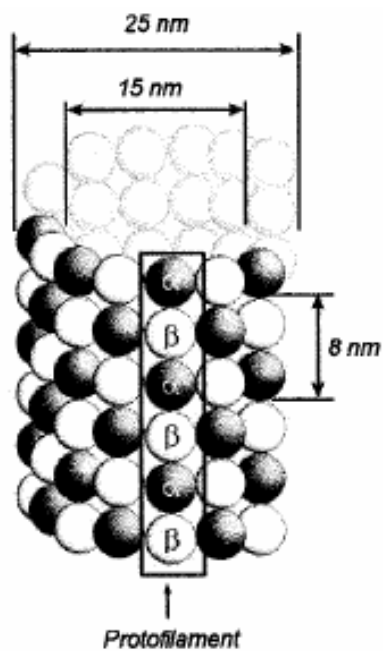


Figure 2.13. Microtubule structure.³⁷ (Directly reproduced from reference 37).

During the association of the α/β heterodimer to the ends of the microtubules, this exchangeable GTP is hydrolyzed to GDP which is unable to exchange once it is formed. However, when the microtubule depolymerizes, the heterodimeric unit is released and the GDP of β -tubulin is now able to exchange to GTP again.³⁶ Therefore, microtubules exhibit two important dynamic properties which are referred as dynamic instability and treadmilling. Dynamic instability (the fluctuations between phases of elongation and shortening) is the process by which microtubule polymers undergo prolonged periods of assembly (rescue) followed by rapid periods of disassembly (catastrophe). Treadmilling is a process by which microtubules incorporate tubulin dimers at their plus ends and

release them from the minus ends. Both properties are important for some cellular functions. For example, during mitosis microtubules continuously polymerize and rapidly depolymerize, forming a pulling device for the duplicated chromosomes. Therefore, disrupting these dynamic properties can cause mitotic arrest, stop cell division and, ultimately induce cell death mainly by the process of apoptosis.^{42,44-46}

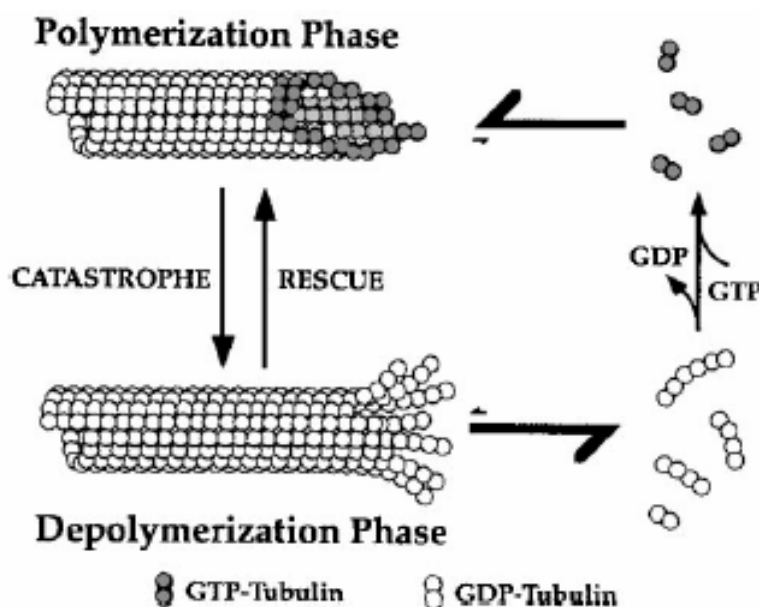


Figure 2.14. Microtubule dynamic instability. The coexistence of polymerizing and depolymerizing microtubules is an important feature of dynamic instability.⁴⁴ (Directly reproduced from reference 44)

In general, tubulin in the dimeric state is reasonably stable, however each monomer is highly unstable in the absence of the other.⁴⁴ Two types of interactions are important in the tubulin polymerization process. The first is the head-to-tail binding which connects two dimeric units along the length of the microtubule and the second is the lateral interaction which joins parallel protofilaments. It is known that longitudinal contacts along protofilaments are much stronger than those between adjacent

profilaments, and therefore the dynamics and regulation of microtubule assembly and disassembly rely on these weak lateral interactions.^{41,46} Figure 2.15 shows a refined structure (3.5 Å resolution) of the α,β -tubulin dimer obtained by electron crystallography with crystalline sheets of tubulin that form in the presence of zinc ions. Notice that this figure shows the non-exchangeable GTP of α -tubulin located at the interface of both subunits by the Mg ion side. In addition, the exchangeable GTP located on β -tubulin after polymerization which has been hydrolyzed to GDP is shown in purple.³⁹



Figure 2.15. Ribbon structure of α,β -tubulin dimer which was refined to 3.5 Å resolution. The structure determination was obtained by electron crystallography with crystalline sheets of tubulin that form in the presence of zinc ions. Non exchangeable GTP (blue) and Mg ion (white inner sphere) are bound in the α -subunit (right polypeptide chain). GDP (magenta) and taxol are bound in the positive end of the β -subunit (left chain). Zinc ion is represented by the outer white sphere close to the α -tubulin.³⁹

Currently, it is known that agents that interact with tubulin can act in one of the three well established sites associated with the β -tubulin subunit: the colchicine, vinblastine or taxoid binding sites.⁴⁶ The vinca domain is located adjacent to the exchangeable GTP binding site in β -tubulin at the plus end. The taxol site is located at the lateral interface between adjacent protofilaments, within the lumen of the assembled microtubule. The colchicine site is found at the intra-dimer interface between β -tubulin and α -tubulin (Figure 2.16 and 1.18).^{26,36,42,46} The existence of another binding site called the laulimalide binding site has been reported. This site is named for the microtubule-stabilizing drug (laulimalide) isolated from the marine sponge *Cacospongia mycofiensis*. The exact location of this binding site on the tubulin/ microtubule protein system is still unknown.³⁶

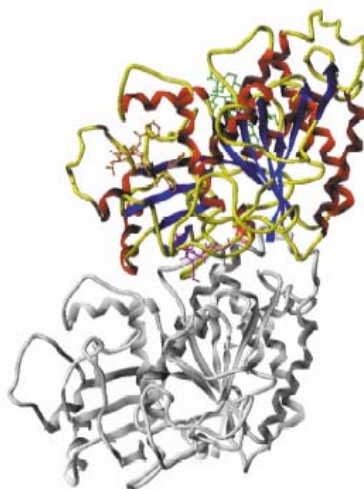


Figure 2.16. Hypothetical model showing the relative positions of the three major types of microtubule-interacting drugs. Vinblastine (green), paclitaxel (orange) and colchicine (magenta) bind β -tubulin (colored top polypeptide chain) at different and specific sites. Vinblastine is at the vinca site which is located at the polar, opposite side of β -tubulin at the plus end interface, adjacent to the exchangeable GTP. Paclitaxel binds the taxol site located at the lateral interface between adjacent protofilaments from the terminal end of the microtubule. Colchicine site is located at the intra-dimer interface between β -tubulin and α -tubulin (grey bottom polypeptide chain).⁴² (Directly reproduced from reference 42)

It is informative to consider how tubulin-binding agents interact with the tumor vasculature to produce necrosis in cancer cells. It is known that mature vasculature of normal endothelium cells have a well-established actin cytoskeleton which plays a significant role in the maintenance of cell shape²⁹ whereas immature tumor cells rely on a tubulin cytoskeleton to maintain their shape.³⁴ This important difference makes it possible to use agents that selectively target tubulin in tumor cells without detrimentally affecting normal cells. Figure 2.17 depicts the basic mechanism of action of a tubulin-binding VDA.³¹

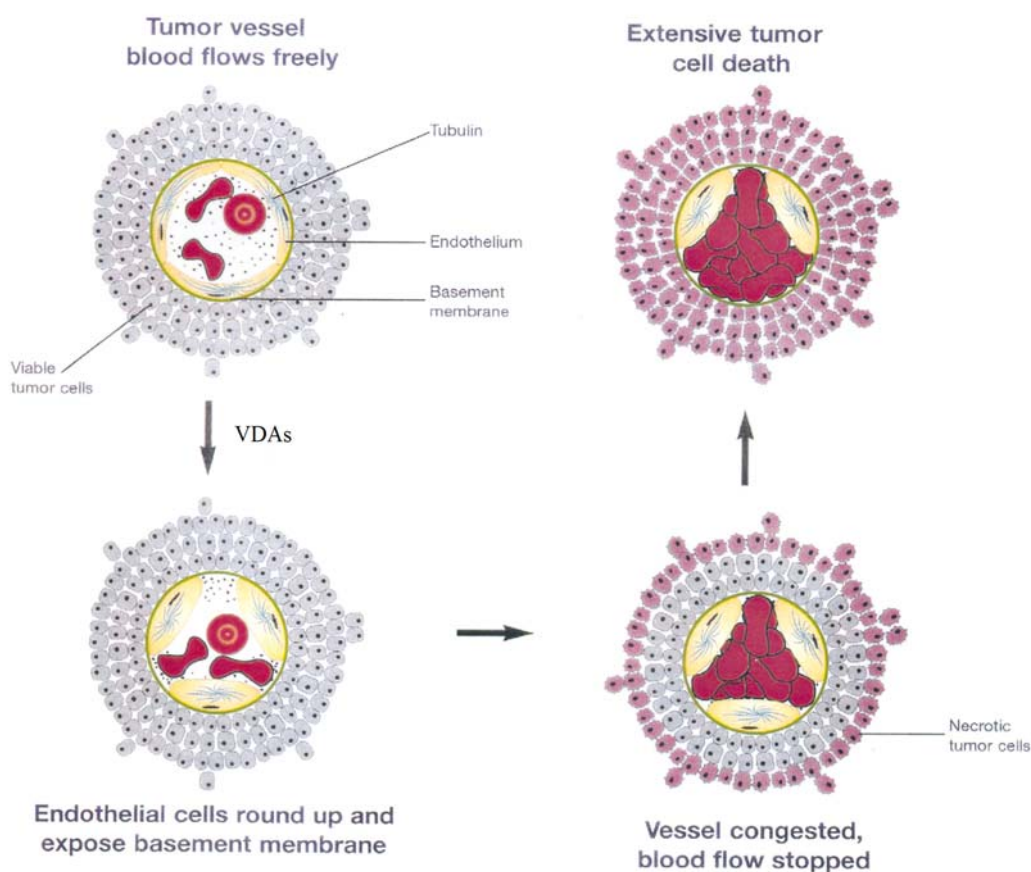


Figure 2.17. Mechanism of action of a tubulin-binding VDA.³¹
(Directly reproduced from reference 31)

Prior to administration of the VDA agent, the blood runs freely through the immature tumor vessel's feeding the surrounding proliferating cells (grey cells). However, after the VDA enters the capillaries, it penetrates the endothelium cells and binds tubulin producing changes in the dynamic instability of the tubulin/ microtubule protein system. The net result is a change in the cell's shape which produces a contraction (rounding up) of the vessel, exposing the basement membrane. As time progresses, interstitial pressure increases, leading to a partial occlusion of the vessel, thereby diminishing blood flow and causing the tumor cells farthest from the vessel to become increasingly hypoxic and inadequately nourished. The complete collapse of the tubulin cytoskeleton, ultimately causes full blood vessel congestion and induces necrosis of the cells furthest from the vessel.^{31,34,29} However, there is evidence that these agents promote necrosis in the cells that are relatively close to the vessel leaving alive the cells at the periphery, called the viable rim cells, which can be fed by the vessels in the surrounding normal tissues.^{33,34} Because of the presence of this residual tumor tissue, which can serve as a foundation of tumor growth, it is often necessary to consider different combination therapies of VDAs with other conventional treatments in order to eradicate completely the tumor cell population.^{27,34} For example, one of the successful treatments involves the sequential treatment of radiation followed by VDAs. It is known that these two treatments interact in a complimentary fashion in such a way that, the VDAs reduce or eliminate the poorly oxygenated cells, which are radioresistant, while radiotherapy destroys the outer cells that are not affected by VDAs. In addition, this treatment regiment has shown better results if VDAs are administrated within a few hours after radiating the tumors.²⁷ A second approach involves the combination of VDAs

with traditional cancer chemotherapy. In this treatment protocol cells surviving vascular targeting treatment can be killed by anticancer drugs following a schedule that requires VDAs to be administered after chemotherapy treatment. This order of treatment is important because VDAs shut down the blood flow making it more difficult for the cytotoxic compounds to actually reach the tumor vasculature.³³ Finally, VDAs exert good antitumor effect when combined with antiangiogenic drugs. The high growth ratio of immature tumor vessels can be targeted with antiangiogenic drugs whereas in the already established more mature vessels, this growth ratio is less and VDAs can have a stronger impact.²⁹ Although VDAs are perhaps not the ideal drugs to completely eradicate tumor cells in single agent therapy schedules, their potential use in the clinic lies in combination therapies with other classical strategies as described above.

Colchicine-Binding Site Agents

Colchicine-binding site agents cause microtubule depolymerization at high concentrations while microtubule dynamics is suppressed at low concentration.³⁶ Inhibition of microtubule depolymerization results when these compounds bind to tubulin at, or near the colchicine site, which was recently further characterized by Ravelli and co-workers.⁴⁶ Figure 2.18 shows the colchicine site a 3.5 Å-resolution structure of tubulin complexed with N-deacetyl-N-(2-mercaptoacetyl)colchicine (DAMA-colchicine) and with the stathmin-like domain (SLD) of RB3. The colchicine molecule is located at the β -subunit, right below the GTP molecule which is located at the α -subunit.

Colchicine and its Derivatives. Colchicine is a highly soluble alkaloid that was first isolated in 1820 from the meadow saffron, *Colchicum autumnale*.

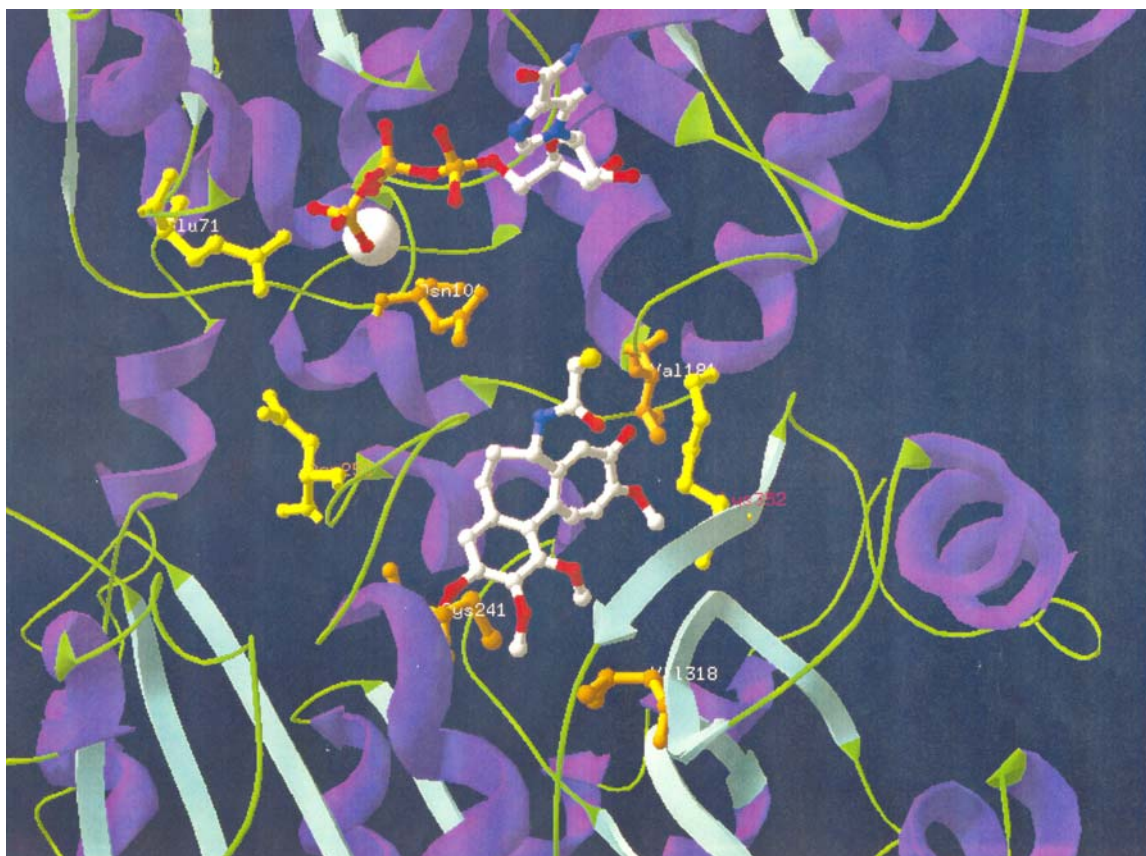


Figure 2.18. The colchicine site in the tubulin-colchicine: RB3-SLD complex. Oxygen atoms are represented by red, carbon by white, nitrogen by blue, sulfur by yellow and phosphorous by mustard. DAMA-Colchicine (top middle structure, Figure 2.19) is bound to β -subunit (bottom polypeptide chain) at the interface with α -subunit (top polypeptide chain). Non-exchangeable GTP (top structure) along with Mg ion (white sphere) is located at the α -subunit close to residues Glu71 (yellow) and Asn101 (mustard). There are five residues close to colchicine molecule: Val181 (pale brown), Asp251 (mustard), Cys241 (mustard), Lys352 (yellow) and Val318 (mustard).⁴⁷

However, it was not until 1960 that the antimotoc activity of colchicine was linked to the binding of tubulin. Colchicine is also used in the treatment of gout, familial Mediterranean fever, and liver cirrhosis and is undergoing clinical trials to treat primary sclerosing cholangitis.^{45,48} It is known that this compound produces a change in the secondary structure of tubulin as a result of binding to a high affinity site on the protein heterodimer. This binding, which is temperature-dependent and irreversible, induces an

alteration in dimer structure that causes an unfolding of the secondary structure of the β -subunits at the carboxyl terminal. This unfolding, in turn, will weaken the lateral bonds at the microtubule end and prohibit the next tubulin dimer from forming the proper lateral bonds within a microtubule. Consequently, microtubule formation will not take place.^{37,48}

Although colchicine is one of the most classical and oldest antimitotic agents, its therapeutic application is affected by its remarkable toxicity and narrow therapeutic window. In the 1970s, the development of new colchicine derivatives, some of which are shown in Figure 2.19, was undertaken in order to overcome this toxicity problem while retaining the desirable activity. Quantitative structure activity relationship (SAR) studies showed that the three methoxy groups located on the A ring (left ring) are important to maintain full tubulin binding affinity and inhibition of tubulin polymerization (ITP). Apparently the seven-membered B-ring and its C7 side chain are believed not to be crucial for tubulin binding while the seven-membered C ring with substituents at C9 and C10 is also important.⁴⁸ Different modifications on all three rings were made to increase the activity, and some of the new compounds exhibited low μM IC_{50} values for inhibition of tubulin assembly as shown in Figure 2.19.⁴⁸

Podophyllotoxin and related Agents. Podophyllotoxin is a lignan that was originally isolated by Podwyssotzki in 1880 from the resin mixture known as podophyllin.⁴⁹ This mixture was obtained from the dried roots and rhizomes of *Podophyllum peltatum*. Although antimitotic activity was first reported more than 50

years ago, one of the medicinal uses of this compound reported in the 19th century was for the treatment of liver and kidney diseases as well as for scrofula and syphilis.

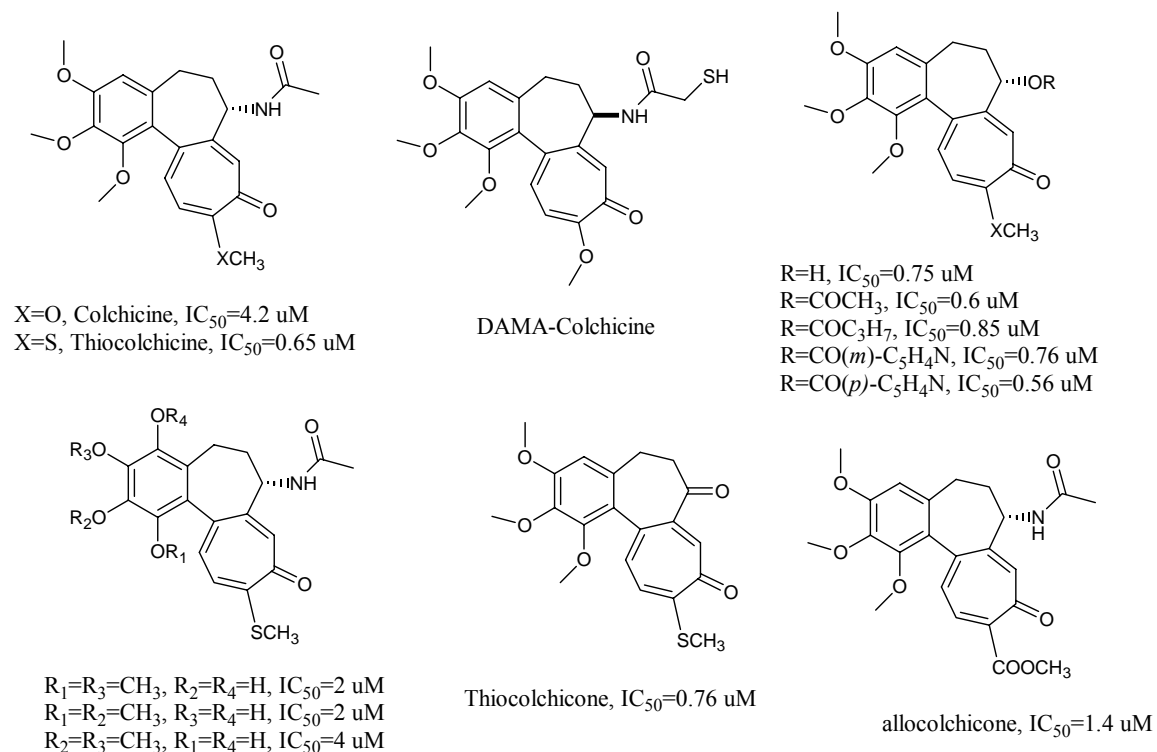


Figure 2.19. Structures of colchicine and its derivatives. The IC_{50} values given are for inhibition of tubulin assembly. Notice that all of these derivatives have lower values than colchicines.⁴⁸ (Directly reproduced from reference 48).

Podophyllotoxin and its analogues, which are competitive inhibitors, bind to tubulin quickly and reversibly close to the colchicine site inducing the inhibition of microtubule assembly.^{37,48} Podophyllotoxin is a molecule composed of five rings among which a tetranaphthalene (tetralin) skeleton forms two of the five rings (rings B and C). A dioxolane ring (A) is attached to left of the tetralin ring while to the right side a 5-membered lactone moiety (D) is present. These four rings form a pseudoplanar system which attaches a perpendicular aromatic ring at the C1 location of ring C (Figure 2.20).

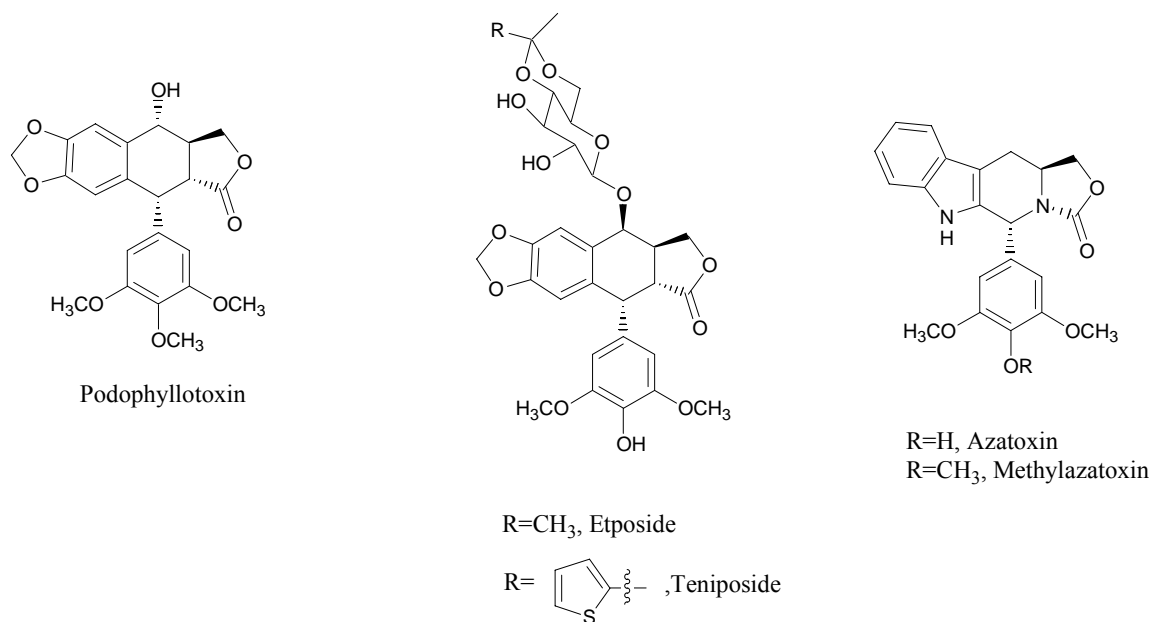


Figure 2.20. Structures of podophyllotoxin and its derivatives.^{48,49}
(Directly reproduced from reference 48 and 49).

Modification of the podophyllotoxin structure led to a variety of derivatives which display biological activity through multiple mechanism of action. For example, etoposide is a potent Topoisomerase II inhibitor but a weak inhibitor of tubulin assembly. Two other synthetic compounds that exhibit the same dual activity are azotoxin and methylazotoxin.⁴⁸

Aromatic Carbamates. These compounds are competitive inhibitors for the colchicine site when binding to tubulin. Most of the carbamates derivatives have at least three rings which are in the same plane; however it has been noted that compounds that are more active have the phenyl and pyrazine rings slightly twisted giving an important structural requirement for activity similar to other tubulin inhibitors as amphetamine,

colchicines and combrestastatin A-4.³⁷ Figure 2.21 shows the structure of some representative carbamates.

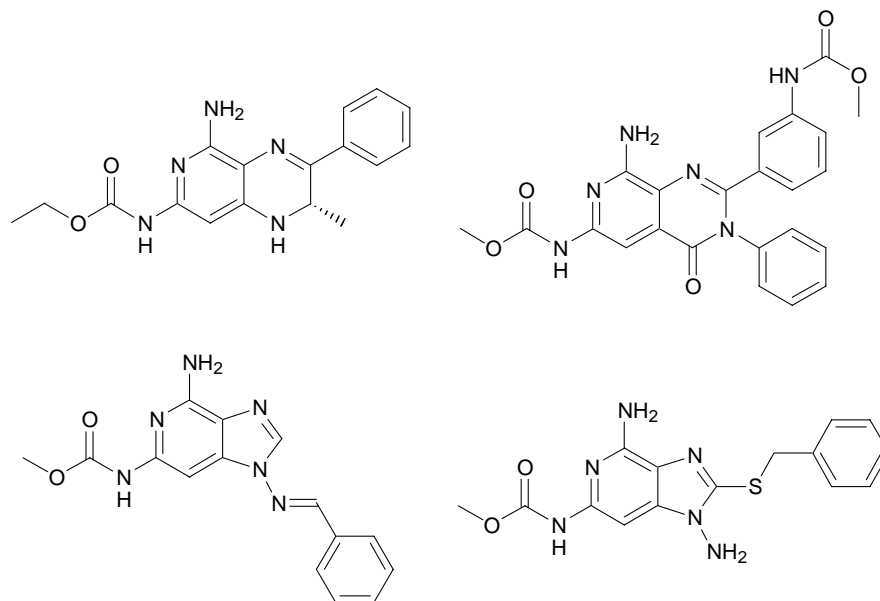


Figure 2.21. Structures of some representative carbamates that are potent antimitotic agents showing activity *in vivo* and *in vitro* against microtubule formation.³⁷ (Directly reproduced from reference 37).

2-Arylnaphthyridinones. Another group of molecules that show anticancer activity by inhibiting tubulin polymerization is composed of the 2-arylnaphthyridinones. These synthetic compounds show high activity when a methoxy group is attached at the 3-position unlike the isomers containing the same group at the 2 or 4 position⁴⁸ as shown in Figure 2.22.

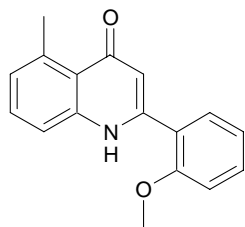
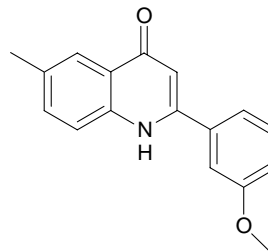
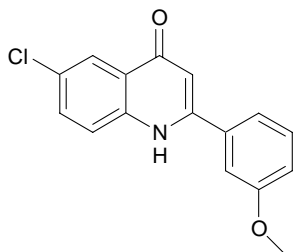
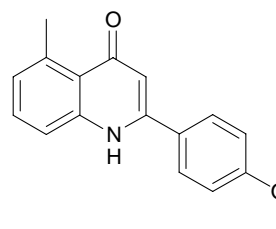
2'-methoxynaphthyridinone, $IC_{50}=20$ μ M3'-methoxynaphthyridinone, $IC_{50}=0.80$ μ M3'-methoxynaphthyridinone, $IC_{50}=0.73$ μ M4'-methoxynaphthyridinone, $IC_{50}=8.8$ μ M

Figure 2.22. Structures of some representative naphthyridinones. The IC_{50} values given are for inhibition of tubulin assembly.⁴⁸ (Directly reproduced from reference 48).

CHAPTER THREE

Materials and Methods

General Section

Chemicals were obtained from commercial companies such as Acros Chemicals, Aldrich Chemical Company, Alfa Aesar, Lancaster Chemicals and Fisher Scientific. Reactions which involved air or moisture sensitive reagents were performed in oven-dried glassware under nitrogen atmosphere using dried syringes, needles and cannulas to transfer solvents and reagents. Reactions were monitored by silica gel thin layer chromatography (TLC) using Merk Kieselgel 60 F₂₅₄ glass backed plates. The plates were visualized by the use of a multiband 254/365 nm UV lamp, iodine or by dipping either in a solution of vanillin (in ethanolic sulphuric acid), PMA (in ethanol), anisaldehyde (in ethanol), ceric sulfate (in sulfuric acid), DNP (in an aqueous ethanolic sulfuric acid) or potassium permanganate (in basic water) followed by heating. Gas chromatography (Hewlett Packard 5890 Series II with a SE-54 column) and /or gas chromatography mass spectrometry (Hewlett Packard GCD system with electron impact ionization) were also used to monitor reactions. Flash chromatography was carried out with silica gel (230-400 mesh) purchased from BODMAN industries. Solvents used for chromatography and workups (CH₂Cl₂, hexanes, THF and acetone) were purified by distillation prior to use. Ethyl acetate, methanol, ethanol, diethyl ether and other solvents were purchased from the above mentioned companies as anhydrous solvents and used without further purification. Evaporation or removal of the solvents was performed in a

rotary evaporator under *vacuum* followed by a further drying of the compounds with a mechanical pump at vacuum pressures of < 0.5 Torr.

Structure elucidation of the products was carried out using spectroscopic techniques such as NMR, IR and MS. ¹H NMR spectra were recorded at 300 or 360 MHz on a Bruker DPX-300 and AMX-360 spectrometers. ¹³C spectra were recorded at 75 or 90 MHz and ³¹P spectra were recorded at 121 MHz. All NMR were recorded in CDCl₃ (0.03% of TMS) unless stated otherwise. Chemical shifts, which are expressed in ppm (δ), are referenced to tetramethylsilane (TMS). The NMR patterns are reported as singlets (s), doublets (d), triplets (t), quartets (q), multiplets (m), etc and the coupling constants (*J*) are reported in Hz. All the spectra are reported in a decoupled mode unless stated otherwise. Special NMR techniques such as low and high temperature NMR and NOESY were carried out on the Bruker AMX-360 spectrometer. Homonuclear decoupling, resolution enhancement, and 2D NMR were performed on both spectrometers. NMR processing data was carried out using WinNMR, Mestrec or Nuts. IR spectra were run either neat (for liquids and solutions) or as nujol mulls (for solids) on a Genesis II FTIR spectrometer. The melting points, which were recorded uncorrected, were determined on a Thomas Hoover capillary melting point apparatus.

*Synthesis of Nitrogen-Based Combretastatin A-4*⁵⁶

4-Methoxy-3-nitrobenzyl bromide (1).⁵⁶

To a well stirred solution of 1-methoxy-4-methyl-2-nitrobenzene (12.6 g, 74.7 mmol) in CCl₄ (150 mL), AIBN (0.132 g, 0.78 mmol) and NBS (13.6 g, 75.4 mmol) were added and, nitrogen gas was passed through the reaction system. After the mixture

was refluxed for 19 h, water was added and, the product was isolated from the aqueous phase with CH₂Cl₂. The resultant organic phase was washed with brine, dried over Na₂SO₄ and the solvent evaporated to yield a solid which was purified by recrystallization (CCl₄). After the solid was dried under vacuum, 11.7 g (47.6 mmol) of the product was obtained in a 64% yield.

¹H NMR (300 MHz, CDCl₃, δ): 7.89 (d, *J*= 2.3, ArH, 1H), 7.58 (dd, *J*= 8.7, 2.3, ArH, 1H), 7.07 (d, *J*= 8.7, ArH, 1H), 4.46 (s, CH₂, 2H), 3.97 (s, OCH₃, 3H).

GC MS *m/z* (% relative intensity, ion): 247 (3, M⁺ + 2), 245 (3, M⁺), 166 (100), 90 (55).

4-Methoxy-3-nitrobenzyl triphenylphosphonium bromide (2).⁵⁶

Bromide **1** (10.3 g, 41.7 mmol) and triphenylphosphine (12.2 g, 45.9 mmol) were dissolved in CH₂Cl₂ (100 mL). The reaction mixture was heated at reflux for 6.5 h at which point water was added and the product extracted by using CH₂Cl₂. The organic phase was washed twice with brine and dried over magnesium sulfate. The resultant solid was washed three times with ethyl ether to afford 20.2 g (50.2 mmol) of the product in a 96% yield.

¹H NMR (300 MHz, CDCl₃, δ): 8.05 (dd, *J*= 8.4, 2.2, ArH, 1H), 7.71 (m, ArH, 15H), 7.43 (d, *J*= 2.6, ArH, 1H), 7.14 (dd, *J*= 8.3, 2.2, ArH, 1H), 5.98 (d, *J*= 14.3, benzylic CH₂, 2H), 3.81 (s, OCH₃, 3H).

(Z)-1-(4-Methoxy-3-nitrophenyl)-2-(3,4,5-trimethoxyphenyl)ethane (3).⁵⁶

Into a round bottom flask containing 3,4,5-trimethoxybenzaldehyde (8.53 g, 43.5 mmol) and 4-methoxy-3-nitrobenzyl-triphenylphosphonium bromide **2** (21.9 g, 43.0

mmol), 150 mL of anhydrous dichloromethane was added, and the mixture was stirred under nitrogen atmosphere. After the reaction mixture was cooled at 0°C, NaH (5.54 g, 231 mmol) was added carefully, and the mixture was stirred for 16 h at room temperature at which point water was added until bubbling stopped. The product was isolated with dichloromethane and the organic phase washed 3 times with brine and dried under sodium sulfate. After evaporation of the solvent, the product was purified by flash chromatography (40% EtOAc/ 20% hex) to afford 6.80 g (19.7 mmol) of the product in a 45% yield.

¹H NMR (300 MHz, CDCl₃, δ): 7.79 (d, *J*= 2.3, ArH, 1H), 7.43 (dd, *J*= 8.8, 2.2, ArH, 1H), 6.93 (d, *J*=8.7, ArH, 1H), 6.58 (d, *J*= 12.1, C=CH, 1H), 6.46 (s, ArH, 2H), 6.44 (d, *J*= 12.3 Hz, C=CH, 1H), 3.91 (s, OCH₃, 3H), 3.84 (s, OCH₃, 3H), 3.71 (s, OCH₃, 6H).

GC MS m/z (% relative intensity, ion): 345 (100, M⁺), 330 (61), 139 (23).

(Z)-1-(3-Amino-4-methoxyphenyl)-2-(3,4,5-trimethoxyphenyl)ethene (**4**).⁵⁶

Cis-stilbene **3** (0.430 g, 1.25 mmol) was dissolved in 45 mL of an acetone-water mixture (2:1 ratio) and, the flask was heated at 50°C. After the solid was completely dissolved, sodium hydrosulfite (4.25 g, 24.4 mmol) was added at once and, the reaction mixture was refluxed for 1.5 h at which point the product was extracted from the aqueous phase with EtOAc (3x10 mL). After the resultant organic phase was washed twice with brine and dried over sodium sulfate, the solvent was evaporated and, the product purified by flash chromatography (30% EtOAc/ 70% hex) to afford 0.300 g (0.952 mmol) of free amine in a 76% yield.

^1H NMR (300 MHz, CDCl_3 , δ): 6.69 (d, $J=1.7$, ArH, 1H), 6.67 (d, $J=7.6$, ArH, 1H), 6.67 (dd, $J=7.6$, 1.7, ArH, 1H), 6.54 (s, ArH, 2H), 6.45 (d, $J=12.2$, C=CH, 1H), 6.36 (d, $J=12.2$, C=CH, 1H), 3.83 (s, OCH₃, 3H), 3.81 (s, OCH₃, 3H), 3.69 (s, OCH₃, 6H).

GC MS m/z (% relative intensity, ion): 315 (100, M^+), 300 (50), 142 (14), 71(16).

(Z)-6-Methoxy-3-[2-(3,4,5-trimethoxyphenyl)vinyl]phenylamine hydrochloride (**5**).^{64,65}

To a well stirred solution of free amine **4** (0.200 g, 0.635 mmol) in dichloromethane (15mL), 0.8 mL of hydrochloride acid (4N-dioxane solution, 3.2 mmol) was added dropwise. The solution was stirred at room temperature for 19 h at which point, the solid that was formed was filtered and purified by recrystallization to obtain 0.117 g (0.333 mmol) of the salt in a 52% yield.

^1H NMR (300 MHz, CDCl_3 , δ): 10.33 (br s, NH_3^+ , 3H), 7.59 (d, $J=1.7$, ArH, 1H), 7.28 (dd, $J=8.7$, 1.6, ArH, 1H), 6.79 (d, $J=8.7$, ArH, 1H), 6.51 (d, $J=12.2$, C=CH, 1H), 6.46 (s, ArH, 2H), 6.44 (d, $J=12.2$, C=CH, 1H), 3.90 (s, OCH₃, 3H), 3.81 (s, OCH₃, 3H), 3.71 (s, OCH₃, 6H).

Dept 90 NMR (75 MHz, CDCl_3): δ 130.8, 130.7, 128.4, 125.7, 111.6, 106.1

Dept 135 NMR (75 MHz, CDCl_3): δ 130.8 (CH), 130.7 (CH), 128.4 (CH), 125.7 (CH), 111.6 (CH), 106.1 (CH), 61.3 (CH₃), 56.7 (CH₃), 56.5 (CH₃).

(Z)-1-(3-Amino-4-methoxyphenyl)-2-(3,4,5-trimethoxyphenyl)ethane-FMOC-L-serinamide (**6**).^{64,65}

To a well stirred solution of free amine **4** (0.582 g, 1.85 mmol) in anhydrous DMF (12 mL), DCC (0.466 g, 2.24 mmol), FMOC(Ac) amino acid (0.831 g, 2.23 mmol), and HOBt.H₂O (0.306 g, 1.96 mmol) were added and the mixture was stirred at room

temperature for 22 h at which point the solid formed was filtered and the filtrate was washed 5 times with water and twice with brine. After the organic phase was dried over sodium sulfate, the solvent was evaporated and the crude reaction mixture was purified by flash chromatography (50% EtOAc/ 50% hex) to afford 0.412 g (0.619 mmol) of the product in a 33% yield.

^1H NMR (300 MHz, CDCl_3 , δ): 8.39 (br s, NH , 1H), 8.30 (d, $J=1.94$, ArH , 1H), 7.77 (d, $J=7.5$, ArH , 2H), 7.60 (d, $J=7.0$, ArH , 2H), 7.41 (t, $J=7.4$, ArH , 2H), 7.31 (td, $J=7.3$, 1.1, ArH , 2H), 7.03 (dd, $J=8.5$, 1.8, ArH , 1H), 6.71 (d, $J=8.6$, ArH , 1H), 6.51 (d, $J=12.1$, $\text{C}=\text{CH}$, 1H), 6.51 (s, ArH , 2H), 6.45 (d, $J=12.2$, $\text{C}=\text{CH}$, 1H), 5.72 (d, $J=6.3$, CH , 1H), 4.63 (br s, CH_2 , 1H), 4.46 (d, $J=6.8$, CH_2 , 2H), 4.31 (dd, $J=11.8$, 5.2, CH_2 , 1H), 4.24 (t, $J=6.8$, CH , 1H), 3.83 (s, OCH_3 , 3H), 3.80 (s, OCH_3 , 3H), 3.68 (s, OCH_3 , 6H), 2.09 (s, CH_3 , 3H).

^{13}C NMR (75 MHz, CDCl_3): δ 170.6, 166.4, 152.8, 147.0, 143.5, 141.2, 137.0, 132.7, 130.1, 129.4, 129.2, 127.8, 127.0, 126.4, 124.9, 120.8, 120.0, 109.5, 105.8, 67.4, 63.9, 60.8, 60.0, 55.8, 54.6, 47.0, 20.7, 14.0.

Dept 45 NMR (75 MHz, CDCl_3): δ 129.9, 129.8, 128.2, 127.5, 125.6, 125.4, 121.3, 120.5, 110.0, 106.3, 67.9, 64.3, 61.3, 56.29, 56.27, 47.5, 21.2, 14.6.

Dept 90 NMR (75 MHz, CDCl_3): δ 129.9, 129.7, 128.3, 127.5, 125.4, 121.3, 120.5, 110.0, 106.3, 56.3, 55.1, 47.5.

Dept 135 NMR (75 MHz, CDCl_3): δ 129.9 ($\underline{\text{CH}}$), 129.7 ($\underline{\text{CH}}$), 128.2 ($\underline{\text{CH}}$), 127.5 ($\underline{\text{CH}}$), 125.5 ($\underline{\text{CH}}$), 125.4 ($\underline{\text{CH}}$), 121.3 ($\underline{\text{CH}}$), 120.5 ($\underline{\text{CH}}$), 110.0 ($\underline{\text{CH}}$), 106.3 ($\underline{\text{CH}}$), 67.9 ($\underline{\text{CH}_2}$), 64.4 ($\underline{\text{CH}_2}$), 61.3 ($\underline{\text{CH}_3}$), 56.31 ($\underline{\text{CH}_3}$), 56.28 ($\underline{\text{CH}_3}$), 47.5 ($\underline{\text{CH}_3}$), 21.2 ($\underline{\text{CH}}$), 14.6 ($\underline{\text{CH}}$).

(Z)-1-(3-Amino-4-methoxyphenyl)-2-(3,4,5-trimethoxyphenyl)ethane-L-serinamide
(7).^{64,65}

Fmoc(Ac)-L-serinamide **6** (0.703 g, 1.06 mmol) was dissolved in 6 mL of a mixture of CH₂Cl₂-MeOH (1:1 ratio) and 1.2 mL of an aqueous solution of 2N- sodium hydroxide (0.0960 g, 2.40 mmol) was added. After the reaction mixture was stirred at room temperature for 6 h, dichloromethane (1 mL) was added and the organic phase was washed once with water, twice with brine and dried under sodium sulfate. After the solvent was evaporated, the resultant oil was purified by flash chromatography (98% CH₂Cl₂-MeOH) to obtain 0.229 g (0.570 mmol) of the product in a 54% yield.

¹H NMR (300 MHz, CDCl₃, δ): δ 9.85 (s, NH, 1H), 8.29 (d, *J*= 1.5, ArH, 1H), 6.95 (dd, *J*= 8.4, 1.6, ArH, 1H), 6.66 (d, *J*= 8.5, ArH, 1H), 6.46 (s, ArH, 2H), 6.45 (d, *J*=12.1, C=CH, 1H), 6.36 (d, *J*=12.2, C=CH, 1H), 3.78 (m, CH₂, 2H), 3.78 (s, OCH₃, 3H), 3.77 (s, OCH₃, 3H), 3.60 (s, OCH₃, 6H), 3.50 (t, *J*=5.0, CH, 1H), 2.50 (br s, OH, NH₂, 3H).

¹³C NMR (75 MHz, CDCl₃): δ 171.4, 152.8, 147.6, 136.8, 132.8, 129.9, 129.7, 129.0, 126.7, 124.7, 120.6, 109.6, 105.8, 64.9, 60.9, 56.6, 55.8, 55.8.

4-Methoxy-2-nitrobenzyl triphenylphosphonium bromide (**8**).^{76,77}

Bromide **17** (12.0 g, 48.8 mmol) and triphenylphosphine (14.2 g, 53.6 mmol) were dissolved in CH₂Cl₂ (150 mL). The reaction mixture was refluxed for 16 h at which point water was added and the product extracted by using CH₂Cl₂. The organic phase was washed twice with brine and dried over magnesium sulfate. The resultant solid was washed three times with ethyl ether to afford 23.4 g (46.0 mmol) of the product in a 95% yield.

^1H NMR (300 MHz, CDCl_3 , δ): δ 7.95 (dd, $J= 8.4, 2.4$, ArH, 1H), 7.75 (m, ArH, 3H), 7.61 (m, ArH, 12H), 7.39 (d, $J= 2.3$, ArH, 1H), 7.09 (dd, $J= 8.6, 2.6$, ArH, 1H), 5.90 (d, $J= 14.3$, benzylic CH_2 , 2H), 3.78 (s, OCH_3 , 3H).

(Z)-2-(2'-Nitro-4'-methoxyphenyl)-1-(3,4,5-trimethoxyphenyl)ethene (**9**).^{76,77}

3,4,5-trimethoxy benzaldehyde (8.27g, 41.7 mmol) and 4-methoxy-2-nitrobenzyltriphenylphosphonium bromide **8** (19.3 g, 37.9 mmol) were dissolved in 150 mL of anhydrous dichloromethane, and the solution was stirred under nitrogen atmosphere. After the reaction mixture was cooled at 0 °C, NaH (5.05 g, 200 mmol) was added and the mixture was stirred for 16 h at room temperature at which point, water (~ 10 mL) was added until bubbling stopped. The product was isolated from the aqueous phase with dichloromethane, and the organic phase was washed with brine and dried over sodium sulfate. After evaporation of the solvent, the product was purified by flash chromatography (15% EtOAc/hex) to afford 5.29 g (15.3 mmol) of the product in a 41% yield. ^1H NMR (300 MHz, CDCl_3 , δ): 7.62 (d, $J= 2.6$, ArH, 1H), 7.27 (d, $J= 8.8$, ArH, 1H), 7.04 (dd, $J= 8.7, 2.7$, ArH, 1H), 6.83 (d, $J= 12.1$, $\text{C}=\text{CH}$, 1H), 6.65 (d, $J= 12.0$, $\text{C}=\text{CH}$, 1H), 6.31 (s, ArH, 2H), 3.89 (s, OCH_3 , 3H), 3.83 (s, OCH_3 , 3H), 3.65 (s, OCH_3 , 6H).

GC MS m/z (% relative intensity, ion): 345 (64, M^+), 196 (93), 181 (100), 149 (25), 122 (32).

(Z)-1-(2-Amino-4-methoxyphenyl)-2-(3,4,5-trimethoxyphenyl)ethene (**10**).^{76,77}

Cis-stilbene **9** (2.57 g, 6.86 mmol) was dissolved in 105 mL of an acetone-water mixture (2:1 ratio) and, the flask was heated at 50°C. After the solid was completely

dissolved, sodium hydrosulfite (7.04 g, 34.4 mmol) was added at once and, the reaction mixture was refluxed for 1.5 h at which point the product was extracted from the aqueous phase with EtOAc (3x10 mL). After the resultant organic phase was washed twice with brine, dried over sodium sulfate and the solvent evaporated, the product was purified by flash chromatography (20% EtOAc/ 80% hex) to afford 0.8173 g (2.59 mmol) of free amine in a 38% yield.

^1H NMR (360 MHz, CDCl_3 , δ): δ 7.03 (d, $J= 8.4$, ArH, 1H), 6.51 (s, ArH, 2H), 6.49 (d, $J= 11.9$, C=CH, 1H), 6.42 (d, $J= 12.0$, C=CH, 1H), 6.30 (dd, $J= 8.4, 2.5$, ArH, 1H), 6.25 (d, $J= 2.4$, ArH, 1H), 3.80 (s, OCH₃, 3H), 3.75 (s, OCH₃, 3H), 3.64 (s, OCH₃, 6H), 1.56 (br s, NH₂, 1H).

^{13}C NMR (75 MHz, CDCl_3): δ 160.1, 152.7, 144.9, 137.2, 132.3, 131.0, 130.6, 125.7, 116.1, 105.8, 104.3, 100.7, 60.9, 55.8, 55.2.

Dept 90 NMR (75 MHz, CDCl_3): δ 131.4, 131.0, 126.1, 106.1, 104.7, 101.1.

Dept 135 NMR (75 MHz, CDCl_3): δ 131.4 (CH), 131.0 (CH), 126.1 (CH), 106.1 (CH), 104.7 (CH), 101.1 (CH), 61.3 (CH₃), 56.2 (CH₃), 55.6 (CH₃).

EIMS: m/z (% rel. intensity) 315 (M^+ , 100), 300 (80), 142 (15).

Anal. Calcd for $\text{C}_{18}\text{H}_{21}\text{O}_4\text{N}$: C, 68.55 H, 6.71 N, 4.44. Found: C, 68.49, H, 6.71, N, 4.25.

(Z)-5-Methoxy-2-[2-(3,4,5-trimethoxyphenyl)vinyl]phenylamine hydrochloride (**11**).^{76,77}

To a well stirred solution of free amine **10** (0.0577 g, 0.183 mmol) in dichloromethane (3 mL), 0.11 mL of hydrochloride acid (4N-dioxane solution, 0.44

mmol) was added dropwise. After the solution was stirred at room temperature for 2.5 h, the solvent was evaporated and the resultant oil formed was triturated at 0 °C with Et₂O forming a solid which after filtration afforded 0.0529 g (0.153 mmol) of the salt in a 83% yield.

¹H NMR (300 MHz, CDCl₃, δ): δ 10.05 (br s, NH₃⁺, 3H), 7.18 (d, *J*=8.6, ArH, 1H), 7.14 (br s ArH, 1H), 6.73 (d, *J*=8.2, ArH, 1H), 6.71 (d, *J*=11.8, C=CH, 1H), 6.56 (d, *J*=11.8, C=CH, 1H), 6.37 (s, ArH, 2H), 3.79 (s, OCH₃, 3H), 3.74 (s, OCH₃, 3H), 3.60 (s, OCH₃, 6H).

(Z)-1-(2-Amino-4-methoxyphenyl)-2-(3,4,5-trimethoxyphenyl)ethane-FMOC-L-serinamide (**12**).^{76,77}

To a well stirred solution of free amine **10** (0.996 g, 3.07 mmol) in anhydrous DMF (10 mL), DCC (0.767 g, 3.68 mmol), FMOC(Ac) amino acid (1.37 g, 3.68 mmol), and HOBt.H₂O (0.508 g, 3.68 mmol) were added and the mixture was stirred at room temperature for 16 h at which point the solid formed was filtered and the filtrate was washed 5 times with water and twice with brine. After the organic phase was dried over sodium sulfate, the solvent was evaporated and the crude reaction mixture was purified by flash chromatography (35% EtOAc/ 65% hex) to afford 1.13 g (1.70 mmol) of the product in a 55% yield.

¹H NMR (300 MHz, CDCl₃, δ): δ 8.11 (br s, NH, 1H), 7.93 (d, *J*=2.2, ArH, 1H), 7.79 (d, *J*=7.4, ArH, 2H), 7.59 (d, *J*=6.5, ArH, 2H), 7.40 (t, *J*=7.5, ArH, 2H), 7.34 (d, *J*=7.0, ArH, 2H), 7.14 (d, *J*=8.6, ArH, 1H), 6.71 (dd, *J*=8.6, 2.5, ArH, 1H), 6.35 (d, *J*=11.7, C=CH, 1H), 6.31 (d, *J*=11.7, C=CH, 1H), 6.23 (s, ArH, 2H), 5.28 (d, *J*=6.6, CH₂, 1H), 4.51 (dd, *J*=12.9, 6.0, CH₂, 1H), 4.40 (br s, CH₂, 2H), 4.20 (d, *J*=5.5, CH, 1H), 4.09

(m, $\underline{\text{CH}}$, 1H), 3.80 (s, OCH_3 , 3H), 3.73 (s, OCH_3 , 3H), 3.48 (s, OCH_3 , 6H), 1.96 (s, $\underline{\text{CH}_3}$, 3H).

^{13}C NMR (75 MHz, CDCl_3): δ 170.8, 166.3, 159.5, 152.9, 143.5, 141.3, 137.8, 135.0, 132.9, 131.1, 129.9, 127.9, 127.8, 127.1, 124.8, 124.7, 123.9, 120.0, 119.9, 111.3, 105.6, 105.5, 63.5, 60.7, 60.4, 55.6, 55.4, 47.1, 20.5, 14.2.

(Z)-1-(3-Amino-4-methoxyphenyl)-2-(3,4,5-trimethoxyphenyl)ethane-L-serinamide
(**13**).^{76,77}

FMOC(Ac)-L-serinamide **12** (0.131 g, 0.196 mmol) was dissolved in 6 mL of a mixture of CH_2Cl_2 -MeOH (1:1 ratio) and 0.22 mL of an aqueous solution of 2N- sodium hydroxide (0.0176 g, 0.44 mmol) was added. After the reaction mixture was stirred at room temperature for 18 h, dichloromethane (1 mL) was added and the organic phase was washed once with water, twice with brine and dried under sodium sulfate. After the solvent was evaporated, the resultant oil was purified by normal-phase preparative TLC (95% CH_2Cl_2 -MeOH) to obtain 0.0529 g (0.132 mmol) of the product in a 67% yield.

^1H NMR (300 MHz, CD_2Cl_2 , δ): δ 9.66 (br s, $\underline{\text{NH}}$, 1H), 7.95 (d, $J=2.6$, ArH , 1H), 7.15 (d, $J=8.5$, ArH , 1H), 6.66 (dd, $J=8.5, 2.6$, ArH , 1H), 6.61 (d, $J=12.0$, $\text{C}=\underline{\text{CH}}$, 1H), 6.49 (d, $J=12.1$, $\text{C}=\underline{\text{CH}}$, 1H), 6.40 (s, ArH , 2H), 3.79 (s, OCH_3 , 3H), 3.70 (s, OCH_3 , 3H), 3.64 (dd, $J=10.7, 5.5$, $\underline{\text{CH}_2}\text{OH}$, 1H), 3.56 (dd, $J=10.6, 5.5$, $\underline{\text{CH}_2}\text{OH}$, 1H), 3.57 (s, OCH_3 , 6H), 3.30 (t, $J=5.4$, $\underline{\text{CH}}\text{NH}_2$, 1H), 2.07 (br s, $\underline{\text{OH}}$, $\underline{\text{NH}_2}$, 3H).

^{13}C NMR (75 MHz, CD_2Cl_2): δ 172.2, 159.8, 153.2, 138.1, 136.3, 132.8, 132.2, 130.4, 124.7, 120.4, 110.5, 106.3, 106.0, 65.2, 60.8, 57.0, 56.1, 55.7.

Dept 45 NMR (75 MHz, CD_2Cl_2): δ 132.5, 130.0, 124.3, 110.1, 105.9, 105.7, 64.9, 60.4, 56.7, 55.7, 55.4.

Dept 90 NMR (75 MHz, CDCl₃): δ 132.9, 130.5, 124.7, 111.3, 106.2, 105.7, 56.8.

Dept 135 NMR (75 MHz, CD₂Cl₂): δ 132.5 (CH), 130.0 (CH), 124.3 (CH), 110.1 (CH), 105.9 (CH), 105.7 (CH), 64.9 (CH₂), 60.4 (CH₃), 56.7 (CH), 55.7 (CH₃), 55.4 (CH₃).

(Z)-2-(2'-Amino-4'-methoxyphenyl)-1-(3,4,5-trimethoxyphenyl)ethene-L-serinamide hydrochloride (**14**).^{76,77}

To a well stirred solution of L-serinamide **13** (0.220g, 0.546 mmol) in methanol (5 mL), 0.57 mL of a dioxane solution of 4N hydrochloride acid (0.0832 g, 2.28 mmol) was added dropwise. After the reaction mixture was stirred at room temperature for 22 h, the solvent was removed and the yellow oil formed was triturated with chloroform at 0 °C forming a solid which was filtered and rinsed with chloroform (3 mL). Purification of the salt by reverse phase preparative TLC (87% CH₂Cl₂- MeOH) afforded 0.0505 g (0.115 mmol) in a 21% yield of the L-serinamide salt.

¹H NMR (300 MHz, methanol-d₆, δ): δ 7.37 (d, J = 2.0, ArH, 1H), 7.10 (d, J = 8.5, ArH, 1H), 6.72 (dd, J = 8.5, 2.3, ArH, 1H), 6.57 (d, J = 11.9, C=CH, 1H), 6.48 (d, J = 12.0, C=CH, 1H), 6.43 (s, ArH, 2H), 4.06 (br s, OH, 1H), 3.78 (m, CH₂, 2H), 3.74 (s, OCH₃, 3H), 3.66 (s, OCH₃, 3H), 3.55 (s, OCH₃, 6H).

Synthesis of Nitrogen-Based Combretastatin A-1

3,4,5-Trimethoxybenzyl bromide (15)

At -5°C and under nitrogen atmosphere, 6.6 mL of a 0 °C CH₂Cl₂ solution of phosphorous tribromide (1.1 mL, 11.6 mmol) was added into a well-stirred solution of 3,4,5-trimethoxybenzyl alcohol (3.22 g, 15.8 mmol) in anhydrous CH₂Cl₂ (15 mL). The

reaction mixture was stirred first at -5°C for 2 hours and the last 4 h at room temperature, at which point, the mixture was slowly added to 100 mL of ice-water and neutralized with NaHCO_3 . The product was extracted twice with CH_2Cl_2 from the aqueous phase and the combined organic phase was washed twice with water and twice with brine. After the organic solution was dried under sodium sulfate, the solvent was evaporated and the pale brown solid formed was purified by recrystallization (hex- Et_2O) to afford 3.15 g (12.1 mmol) of the product in a 77% yield.

^1H NMR (300 MHz, CDCl_3 , δ): δ 6.60 (s, ArH, 2H), 4.45 (s, benzylic CH_2 , 2H), 3.86 (s, OCH_3 , 6H), 3.83 (s, OCH_3 , 3H).

Dept 135 NMR (75 MHz, CDCl_3): δ 106.1 ($\underline{\text{C}}\text{H}$), 60.9 ($\underline{\text{C}}\text{H}_3$), 56.1 ($\underline{\text{C}}\text{H}_3$), 34.3 ($\underline{\text{C}}\text{H}_2$).

EIMS: m/z (% rel. intensity) 262 (4, $\text{M}^+ + 2$), 260 (4, M^+), 181 (100).

3,4,5-Trimethoxybenzyltriphenylphosphonium bromide (16)

Bromide **15** (11.6 g, 44.5 mmol) and triphenylphosphine (11.8 g, 44.5 mmol) were dissolved in CH_2Cl_2 (100 mL) and the reaction mixture was refluxed for 20 h at which point water was added and the product extracted once from the aqueous phase with CH_2Cl_2 . The organic phase was washed twice with water and brine, then dried over sodium sulfate. The crude was triturated at 0°C with ethyl ether to afford 32.4 g (62.0 mmol) of the product in a 77% yield.

^1H NMR (300 MHz, CDCl_3 , δ): δ 7.74 (m, ArH, 9H), 7.60 (m, ArH, 6H), 6.43 (d, $J=2.7$, ArH, 2H), 5.43 (d, $J=14.1$, benzylic CH_2 , 2H), 3.74 (s, OCH_3 , 3H), 3.48 (s, OCH_3 , 6H).

^{31}P NMR (121 MHz, acetone- d_6): δ 23.37.

4-Methoxy-2-nitrobenzyl bromide (17)

To a well stirred solution of 4-methyl-3-nitroanisole (7.45 g, 44.1 mmol) in CCl₄ (70 mL), AIBN (0.740 g, 4.41 mmol) and NBS (8.73 g, 48.6 mmol) were added. After the reaction mixture was refluxed for 16 h under nitrogen atmosphere, water was added and the product extracted from the aqueous phase with CH₂Cl₂. The resultant organic phase was washed with brine, dried under sodium sulfate and the solvent evaporated yielding a solid which was recrystallized (hexanes) to afforded 7.90 g (32.2 mmol) of the bromide in a 73% yield.

¹H NMR (300 MHz, CDCl₃, δ): δ 7.52 (d, *J*= 2.7, ArH, 1H), 7.43 (d, *J*= 8.6, ArH, 1H), 7.11 (dd, *J*= 8.6, 2.7, ArH, 1H), 4.77 (s, benzylic CH₂, 2H), 3.86 (s, OCH₃, 3H).

Dept 135 NMR (75 MHz, CDCl₃): δ 133.6 (CH), 120 (CH), 110 (CH), 56.0 (CH₃), 29.1 (CH₂).

EIMS: *m/z* (% rel. intensity) 247 (4, M⁺ +2), 245 (M⁺, 4), 166 (100), 108 (20).

4-Methoxy-2-nitrobenzylalcohol (18)

Bromide **17** (0.0937 g, 0.38 mmol) was dissolved in 6 mL of a mixture of acetone-water (1:2 ratio) and refluxed for 4 h. At the end of this, water was added into the reaction mixture and the product was extracted with CH₂Cl₂ from the aqueous phase. The organic phase was washed twice with water, twice with brine and dried over sodium sulfate. After recrystallization (hex-EtOAc) of the crude, 0.0635 g (0.347 mmol) of pure product was obtained in a 91% yield.

^1H NMR (CDCl_3 , 300 MHz, δ): δ 7.59 (d, $J=2.6$, ArH, 1H), 7.57 (d, $J=8.4$, ArH, 1H), 7.18 (dd, $J=8.6, 2.7$, ArH, 1H), 4.85 (d, $J=6.4$, benzylic CH_2 , 2H) 3.87 (s, OCH_3 , 3H), 2.56 (t, $J=6.8$, OH, 1H).

^{13}C NMR (75 MHz, CDCl_3): δ 159.4, 148.5, 131.6, 128.7, 120.5, 109.7, 62.4, 55.9.

Dept 135 NMR (75 MHz, CDCl_3): δ 131.6 ($\underline{\text{CH}}$), 120.5 ($\underline{\text{CH}}$), 109.7 ($\underline{\text{CH}}$), 62.4 ($\underline{\text{CH}_2}$), 55.9 ($\underline{\text{CH}}$).

GC MS m/z (% relative intensity, ion): 183 (12, M^+), 165 (M^+-18 , 32), 135 (100), 106 (64), 77 (52).

4-Methoxy-2-nitrobenzaldehyde (19)

30 mL of anhydrous CH_2Cl_2 was poured into a flask containing PCC (3.18 g, 14.7 mmol) and celite (3.2 g). The resultant suspension was stirred at 0 °C under nitrogen atmosphere for 30 minutes after which point, 20 mL of a CH_2Cl_2 solution of **18** (1.80 g, 9.82 mmol) was added. The reaction mixture was stirred for 4.5 h at room temperature. At the end of this period of time, ethyl ether (50 mL) was added and the mixture was filtered through florisil and washed with 20 mL of a mixture of $\text{Et}_2\text{O}-\text{CH}_2\text{Cl}_2$ (1:1 ratio). Purification of the crude by flash chromatography (20% EtOAc/ 80% hex) afforded 1.73 g (9.56 mmol) of pure aldehyde in a 97% yield.

^1H NMR (300 MHz, CDCl_3 , δ): δ 10.27 (d, $J=0.6$, $\underline{\text{CHO}}$, 1H), 7.96 (d, $J=8.7$, ArH, 1H), 7.50 (d, $J=2.5$, ArH, 1H), 7.22 (ddd, $J=8.7, 2.5, 0.5$, ArH, 1H), 3.95 (s, OCH_3 , 3H).

^{13}C NMR (75 MHz, CDCl_3): δ 187.0, 163.7, 131.5, 123.5, 119.1, 109.6, 56.4.

Dept 45 NMR (75 MHz, CDCl_3): δ 187.0, 131.5, 119.1, 109.6, 56.4

GC MS m/z (% relative intensity, ion): 181 (8, M⁺), 151 (100), 134 (24), 106 (36), 63 (36).

4-Methoxy-2,5-dinitrobenzaldehyde (20a)

At 0°C, aldehyde **19** (1.53 g, 8.45 mmol) was dissolved in concentrated sulfuric acid (25 mL). To this well-stirred solution, 7 mL of a 0°C mixture of fuming nitric acid (5.32 g, 84.5 mmol) and concentrated sulfuric acid (5.29 g, 54.0 mmol) were added slowly. After the reaction was stirred for 10 minutes, it was poured slowly into 150 mL of ice-water and allowed the mixture to cool for 2 h at 0°C. The resultant solid formed was filtered, rinsed with ice-water (10 mL) and purified by flash column chromatography (20% EtOAc-hex) to yield 0.8000 g (3.54 mmol) of the aldehyde in a 42% yield.

¹H NMR (300 MHz, CDCl₃, δ): δ 10.30 (s, CHO, 1H), 8.43 (s, ArH, 1H), 7.73 (s, ArH, 1H), 4.14 (s, OCH₃, 3H).

Dept 45 NMR (75 MHz, CDCl₃): δ 184.7, 127.2, 109.7, 57.9.

GC MS m/z (% relative intensity, ion): 226 (4, M⁺), 196 (12), 179 (16), 149 (56), 121 (100), 75 (40), 63 (32).

IR: ν_{max} (CH₂Cl₂): 3054, 2987, 2950, 2908, 2855, 1703, 1622, 1552 cm⁻¹.

4-Methoxy-2,3-dinitrobenzaldehyde (20b)

At 0°C, aldehyde **19** (1.53 g, 8.45 mmol) was dissolved in concentrated sulfuric acid (25 mL). To this well-stirred solution, 7 mL of a 0°C mixture of fuming nitric acid (5.32 g, 84.5 mmol) and concentrated sulfuric acid (5.29 g, 54.0 mmol) were added slowly. After the reaction was stirred for 10 minutes, it was poured slowly into 150 mL of ice-water and the mixture was allowed to cool for 2 h at 0°C. The resultant solid

formed was filtered, rinsed with ice-water (10 mL) and purified by flash column chromatography (20% EtOAc-hex) to yield 0.89 g (3.94 mmol) of the aldehyde in a 47% yield.

$^1\text{H NMR}$ (300 MHz, CDCl_3 , δ): δ 9.95 (d, $J=0.5$, CHO , 1H), 8.15 (d, $J=8.9$, ArH , 1H), 7.38 (dd, $J=8.9, 0.5$, ArH , 1H), 4.08 (s, OCH_3 , 3H).

GC MS m/z (% relative intensity, ion): 132 (40), 120 (48), 103 (84), 75 (100).

IR: ν_{max} (CH_2Cl_2): 3097, 3054, 3005, 2987, 2953, 2900, 2858, 1709, 1612, 1564 cm^{-1} .

4-Methoxy-3,5-dinitrobenzaldehyde (21)

To a round bottom flask containing a mixture of 4-methoxy-3-nitrobenzaldehyde (3.89 g, 21.5 mmol) and 25 mL of concentrated sulfuric acid previously cooled to 0°C in an ice bath, a 0°C mixture of fuming nitric acid (13.6 g, 217 mmol) and concentrated sulfuric acid (15.9 g, 162 mmol) was added slowly. The reaction mixture was stirred for 3.5 h and cautiously added into 100 mL of ice-water at which point, the mixture was cooled for 1 h at 0°C . The resultant solid formed was filtered, rinsed with ice-water (10 mL) and purified by flash column chromatography (10% ethyl acetate/hexanes) to afford 2.31 g (10.2 mmol) of the aldehyde in a 48% yield.

$^1\text{H NMR}$ (300 MHz, CDCl_3 , δ): δ 10.02 (s, ArH , 1H), 8.51 (s, ArH , 2H), 4.13 (s, OCH_3 , 3H).

$^{13}\text{C NMR}$ (75 MHz, CDCl_3): δ 186.5, 131.1, 129.1, 65.1.

Dept 135 NMR (75 MHz, CDCl_3): δ 186.6 ($\underline{\text{C}}\text{H}$), 129.1 ($\underline{\text{C}}\text{H}$), 65.1 ($\underline{\text{C}}\text{H}_3$).

GC MS m/z (% relative intensity, ion): 226 (23, M^+), 196 (100), 119 (30), 75 (45).

IR: ν_{\max} (Nujol): 1531, 1462, 1377 cm^{-1} .

Melting point: 87–89°C.

4-Methoxy-3,5-dinitrobenzoic acid (21a)

After flash chromatography of the crude reaction mixture of compound **21**, 2.06 g (8.51 mmol) of carboxylic acid was separated.

^1H NMR (300 MHz, CDCl_3 , δ): δ 8.87 (s, ArH, 2H), 4.15 (s, OCH_3 , 3H).

^{13}C NMR (75 MHz, CDCl_3): δ 152.1, 144.7, 141.5, 124.2, 65.3.

Dept 45 NMR (75 MHz, CDCl_3): δ 124.2, 65.3.

Dept 135 NMR (75 MHz, CDCl_3): δ 124.2 ($\underline{\text{C}}\text{H}$), 65.3 ($\underline{\text{C}}\text{H}_3$).

GC MS m/z (% relative intensity, ion): 243 (16, M^+), 213 (100), 93 (16), 75 (73), 62 (36).

IR: ν_{\max} (Nujol): 3099, 2987, 2920, 2893, 2821, 1602, 1544, 1344, 1261 cm^{-1} .

(Z)-1-Methoxy-2,6-dinitro -4-[2-(3,4,5-trimethoxyphenyl)ethenyl]benzene (22)

Into a round bottom flask containing NaH (0.824 g, 32.6 mmol), 10 mL of anhydrous dichloromethane was added and the suspension was stirred at 0°C under nitrogen atmosphere for about 10 minutes, at which point, 20 mL of a previously prepared CH_2Cl_2 solution of 3,4,5-trimethoxybenzylphosphonium bromide **16** (2.71 g, 5.19 mmol) was added drop wise. After stirring the mixture for 20 minutes, 10 mL of a CH_2Cl_2 solution of 4-methoxy-dinitrobenzaldehyde **21** (1.29 g, 5.71 mmol) was added to the flask and, the reaction mixture was stirred at room temperature for 2.5 h, at which point, water was added until bubbling stopped. The product was extracted twice with CH_2Cl_2 from the aqueous phase and the resultant organic phase was washed twice with

water, twice with brine and then dried over sodium sulfate. 0.910 g (2.33 mmol) of “Z” stilbene was separated from the crude reaction mixture by flash chromatography (10% EtOAc/ 90% hex) in a 45% yield.

^1H NMR (300 MHz, CDCl_3 , δ): δ 7.91 (s, ArH, 2H), 6.77 (d, $J= 12.1$, $\text{C}=\underline{\text{C}}\text{H}$, 1H), 6.44 (s, ArH, 2H), 6.43 (d, $J = 12.0$, $\text{C}=\underline{\text{C}}\text{H}$, 1H), 4.03 (s, OCH_3 , 3H), 3.86 (s, OCH_3 , 3H), 3.74 (s, OCH_3 , 6H).

^{13}C NMR (75 MHz, CDCl_3): δ 153.6, 145.7, 145.1, 138.7, 134.9, 133.9, 130.4, 128.9, 124.5, 105.8, 64.8, 61.1, 56.2.

Dept 45 NMR (75 MHz, CDCl_3): δ 134.8, 128.9, 124.5, 105.8, 64.8, 61.1, 56.2.

GC MS m/z (% relative intensity, ion): 390 (100, M^+), 375 (36).

(Z)-1-Methoxy-2,3-dinitro -4-[2-(3,4,5-trimethoxyphenyl)ethenyl]benzene (23)

Into a round bottom flask containing NaH (1.32 g, 52.3 mmol), 30 mL of anhydrous dichloromethane was added and the suspension was stirred at 0°C under nitrogen atmosphere for about 10 minutes, at which point, 30 mL of a previously prepared CH_2Cl_2 solution of 3,4,5-trimethoxybenzylphosphonium bromide **16** (5.05 g, 9.68 mmol) was added drop wise. After stirring the mixture for 20 minutes, 20 mL of a CH_2Cl_2 solution of 4-methoxy-dinitrobenzaldehyde **20b** (2.09 g, 8.77 mmol) was added to the flask and, the reaction mixture was stirred at room temperature for 12 h, at which point, water was added until bubbling stopped. The product was extracted twice with CH_2Cl_2 from the aqueous phase and the resultant organic phase was washed twice with water, twice with brine and then dried over sodium sulfate. 1.80 g (4.62 mmol) of “Z” stilbene was separated from the crude reaction mixture by flash chromatography (25% EtOAc/ 75% hex) in a 53% yield.

^1H NMR (300 MHz, CDCl_3 , δ): δ 7.34 (dd, $J=9.0, 0.5$, ArH, 1H), 7.07 (d, $J=8.9$, ArH, 1H), 6.77 (d, $J=11.8$, C=CH, 1H), 6.49 (d, $J=11.8$, C=CH, 1H), 6.29 (s, ArH, 2H), 3.94 (s, OCH₃, 3H), 3.81 (s, OCH₃, 3H), 3.68 (s, OCH₃, 6H).

(Z)-1-Methoxy-2,5-dinitro-4-[2-(3,4,5-trimethoxyphenyl)ethenyl]benzene (**24**)

Into a round bottom flask containing NaH (0.168 g, 6.65 mmol), 5 mL of anhydrous dichloromethane was added and the suspension was stirred at 0°C under nitrogen atmosphere for about 10 minutes, at which point, 5 mL of a previously prepared CH_2Cl_2 solution of 3,4,5-trimethoxybenzylphosphonium bromide **16** (0.288 g, 0.551 mmol) was added drop wise. After stirring the mixture for 20 minutes, 5 mL of a CH_2Cl_2 solution of 4-methoxy-dinitrobenzaldehyde **20a** (0.107 g, 0.474 mmol) was added to the flask and, the reaction mixture was stirred at room temperature for 3 h, at which point, water was added until bubbling stopped. The product was extracted twice with CH_2Cl_2 from the aqueous phase and the resultant organic phase was washed twice with water, twice with brine and then dried over sodium sulfate. 0.0961 g (0.246 mmol) of “Z” stilbene was separated from the crude reaction mixture by flash chromatography (20% EtOAc/ 80% hex) in a 53% yield.

^1H NMR (300 MHz, CDCl_3 , δ): δ 7.73 (s, ArH, 1H), 7.71 (s, ArH, 1H), 6.74 (d, $J=12.2$, C=CH, 1H), 6.68 (d, $J=12.0$, C=CH, 1H), 6.30 (s, ArH, 2H), 4.03 (s, OCH₃, 3H), 3.81 (s, OCH₃, 3H), 3.66 (s, OCH₃, 6H).

GC MS m/z (% relative intensity, ion): 390 (60, M^+), 196 (92), 181 (100).

(Z)-2-Methoxy-5-[2-(3,4,5-trimethoxyphenyl)ethenyl]benzene-1,3-diamine (**25**)

To a 20 mL solution of *cis*-stilbene **22** (0.175, 0.408 mmol) in glacial acetic acid, zinc powder (2.67 g, 40.8 mmol) was added and the resultant suspension was stirred for 35 minutes at room temperature, at which point, the reaction mixture was filtered through celite and the filtrate was washed once with water and once with brine. After the organic phase was dried under Na₂SO₄, and the solvent evaporated at reduced pressure, the product was purified from the crude reaction mixture by flash chromatography (50% EtOAc-hex) to afford 0.0616 g (0.187 mmol) of the diamine in a 46% yield.

¹H NMR (CDCl₃, 360 MHz) δ 6.55 (s, ArH, 2H), 6.40 (d, *J*=12.2, C=CH, 1H), 6.33 (d, *J*=12.2, C=CH, 1H), 6.13 (s, ArH, 2H), 3.82 (3H, s, OCH₃), 3.71 (s, OCH₃, 3H), 3.69 (s, OCH₃, 6H), 3.61 (br s, NH₂, 4H).

¹³C NMR (75 MHz, CDCl₃): δ 152.6, 139.7, 137.0, 134.1, 133.8, 132.6, 130.2, 129.0, 106.7, 106.2, 60.9, 58.3, 55.8.

Dept 45 NMR (75 MHz, CDCl₃): δ 130.3, 129.1, 106.8, 106.2, 60.9, 58.4, 55.9.

GC MS *m/z* (% relative intensity, ion): 330 (60, M⁺), 315 (100).

Anal. Calcd for C₁₈H₂₂O₄N₂: C, 65.44 H, 6.71 N, 8.48. Found: C, 65.27, H, 6.78, N, 8.34.

(Z)-3-Methoxy-4-nitro-6-[2-(3,4,5-trimethoxyphenyl)ethenyl]phenylamine (**26a**)

Z-stilbene **24** (0.580 g, 1.49 mmol) was dissolved in 30 mL of an acetone-water mixture (2:1 ratio) and, the flask was heated at 50°C. After the solid was completely dissolved, sodium hydrosulfite (3.64 g, 17.8 mmol) was added at once and, the reaction mixture was refluxed for 4 h at which point the product was extracted from the aqueous phase with CH₂Cl₂ (3x 5 mL). After the resultant organic phase was washed twice with

brine, dried over sodium sulfate and the solvent evaporated, the product was separated from the crude reaction mixture by flash chromatography (30% EtOAc/ 70% hex) and, then recrystallized (CH₂Cl₂-MeOH) to afford 0.144 g (0.400 mmol) of free amine in a 27% yield.

¹H NMR (300 MHz, CDCl₃, δ): δ 7.97 (s, ArH, 1H), 6.63 (d, *J*=12.0, C=CH, 1H), 6.47 (s, ArH, 2H), 6.32 (d, *J*= 12.0, C=CH, 1H), 6.20 (s, ArH, 1H), 4.38 (br s, NH₂, 2H), 3.91 (s, OCH₃, 3H), 3.81 (s, OCH₃, 3H), 3.65 (s, OCH₃, 6H).

¹³C NMR (75 MHz, CDCl₃): δ 155.6, 153.0, 150.3, 138.1, 133.5, 131.3, 129.7, 129.3, 122.7, 114.5, 105.9, 97.4, 60.9, 56.4, 55.9.

Dept 45 NMR (75 MHz, CDCl₃): δ 133.5, 129.4, 122.7, 105.8, 97.4, 60.9, 56.4, 55.9.

GC MS *m/z* (% relative intensity, ion): 360 (100, M⁺), 345 (14).

(Z)-2-Methoxy-4-nitro-5-[2-(3,4,5-trimethoxyphenyl)ethenyl]phenylamine (**26b**)

Z-stilbene **24** (0.580 g, 1.49 mmol) was dissolved in 30 mL of an acetone-water mixture (2:1 ratio) and, the flask was heated at 50°C. After the solid was completely dissolved, sodium hydrosulfite (3.64 g, 17.8 mmol) was added at once and, the reaction mixture was refluxed for 4 h at which point the product was extracted from the aqueous phase with CH₂Cl₂ (3x 5 mL). After the resultant organic phase was washed twice with brine, dried over sodium sulfate and the solvent evaporated, 0.0235 g (0.0654 mmol) of the product was separated from the crude reaction mixture by flash chromatography (20% EtOAc/ 80% hex) in a 4% yield.

^1H NMR (300 MHz, CDCl_3 , δ): 7.70 (s, ArH, 1H), 6.87 (dd, $J=11.9$, 0.5, C=CH, 1H), 6.53 (d, $J=12.0$, C=CH, 1H), 6.46 (d, $J=0.6$, ArH, 1H), 6.31 (s, ArH, 2H), 4.36 (br s, NH₂, 2H), 3.92 (s, OCH₃, 3H), 3.79 (s, OCH₃, 3H), 3.62 (s, OCH₃, 6H).

^{13}C NMR (75 MHz, CDCl_3): δ 152.8, 145.0, 142.2, 137.5, 137.3, 131.7, 130.1, 129.5, 128.0, 114.7, 106.9, 106.3, 60.9, 56.1, 56.0.

Dept 45 NMR (75 MHz, CDCl_3): δ 129.5, 127.9, 114.6, 106.9, 106.3, 60.9, 56.0, 55.8.

GC MS m/z (% relative intensity, ion): 360 (100, M⁺), 345 (68).

(Z)-3-Methoxy-4-nitro-6-[2-(3,4,5-trimethoxyphenyl)vinyl]benzeneamine hydrochloride (**27a**)

To a well stirred solution of free amine **26** (0.0222 g, 0.0617 mmol) in dichloromethane (3 mL), 0.1 mL of 4N HCl (dioxane solution, 0.40 mmol) was added dropwise. After the solution was stirred at room temperature for 1.5 h, the solvent was evaporated and the resultant oil formed was triturated at 0 °C with Et₂O forming a solid which after filtration afforded 0.0130 g (0.0328 mmol) of the salt in a 53% yield.

^1H NMR (300 MHz, methanol-d₄, δ): 7.78 (s, ArH, 1H), 6.74 (s, ArH, 1H), 6.73 (d, $J=11.9$, C=CH, 1H), 6.55 (s, ArH, 2H), 6.40 (d, $J=11.9$, C=CH, 1H), 3.92 (s, OCH₃, 3H), 3.72 (s, OCH₃, 3H), 3.63 (s, OCH₃, 6H).

(Z)-2-Methoxy-5-[2-(3,4,5-trimethoxyphenyl)vinyl]benzene-1,3-diamine hydrochloride (**27b**)

To a well stirred solution of free amine **25** (0.0558 g, 0.169 mmol) in dichloromethane (3 mL), 0.84 mL of 4N HCl (dioxane solution, 0.84 mmol) was added dropwise. After the solution was stirred at room temperature for 1 h, the solvent was

evaporated and the resultant solid formed was recrystallized with CH₂Cl₂/ EtOH to obtain 0.0176 g (0.0437 mmol) of the product in a 26% yield.

¹H NMR (300 MHz, methanol-d₄, δ): 7.08 (s, ArH, 2H), 6.69 (d, *J*=12.1, C=CH, 1H), 6.54 (d, *J*=12.1, C=CH, 1H), 6.51 (s, ArH, 2H), 3.92 (s, OCH₃, 3H), 3.73 (s, OCH₃, 3H), 3.67 (s, OCH₃, 6H).

Dept 45 NMR (methanol-d₄, 75 MHz): δ 132.2, 126.8, 120.1, 106.0, 61.2, 59.7, 55.1.

(Z)-1-(3,5Diamino-4-methoxyphenyl)-2-(3,4,5-trimethoxyphenyl)ethane-FMOC-L-serinamide (**28**)

To a 5 mL solution (DMF) of free amine **25** (0.441 g, 1.34 mmol), DCC (0.668 g, 3.21 mmol), FMOC (Ac) amino acid (1.20 g, 3.21 mmol), and HOBt.H₂O (0.501 g, 3.21 mmol) were added and, the mixture was stirred for 4h at room temperature, at which point, EtOAc was added and the reaction mixture filtered. After the filtrate was washed 5 times with water and twice with brine, the resultant organic phase was dried over sodium sulfate and the solvent evaporated. The crude reaction mixture was purified by flash chromatography (50% EtOAc/ 50% hex) to afford 0.252 g (0.244 mmol) of the product in a 19% yield.

¹H NMR (300 MHz, CDCl₃, δ): 8.42 (br s, NH, 2H), 7.76 (d, *J*=7.7, ArH, 4H), 7.58 (d, *J*=7.9, ArH, 4H), 7.40 (t, *J*=7.2, ArH, 4H), 7.30 (t, *J*=7.4, ArH, 4H), 6.52 (s, ArH, 2H), 6.50 (s, ArH, 1H), 6.49 (s, ArH, 1H), 6.46 (d, *J*=12.5, C=CH, 1H), 6.41 (d, *J*=12.3, C=CH, 1H), 5.69 (br s, NH, 2H), 4.51 (m, CHNH, CH₂CONH, 8H), 4.33 (dd, *J*=11.9, 5.3, CH₂OCOCH₃, 2H), 4.23 (t, *J*=7.0, CHCH₂O, 2H), 3.82 (s, OCH₃, 3H), 3.68 (s, OCH₃, 3H), 3.64 (s, OCH₃, 6H), 2.09 (s, CH₃, 3H), 2.04 (s, CH₃, 3H).

(Z)-1-(3,5-Diamino-4-methoxyphenyl)-2-(3,4,5-trimethoxyphenyl)ethane-L-serinamide
(**29**)

Into a round bottom flask containing Fmoc-L-serinamide **28** (0.248 g, 0.240 mmol), 6 mL of a mixture of CH₂Cl₂/ MeOH (1:1 ratio) and 0.53 mL (0.0424 g, 1.06 mmol) of an aqueous solution of 2N NaOH were added. After the reaction mixture was stirred at room temperature for 3.5 h, the product was extracted from the aqueous phase with CH₂Cl₂ and the organic phase was washed once with water, twice with brine and dried under sodium sulfate. After the solvent was evaporated, the crude reaction mixture was purified by normal-phase preparative TLC (95% CH₂Cl₂/5% MeOH) to yield 0.0191 g (0.0379 mmol) of the serinamide in a 16% yield.

¹H NMR (360 MHz, CDCl₃, δ): 9.88 (br s NH, 1H), 7.66 (d, *J*= 1.7, ArH, 1H), 6.52 (s, ArH, 2H), 6.47 (d, *J*= 1.9, ArH, 1H), 6.45 (d, *J*= 12.5, C=CH, 1H), 6.39 (d, *J*= 12.3, C=CH, 1H), 3.98 (dd, *J*= 10.7, 5.0, CH₂OH, 1H), 3.81 (s, OCH₃, 3H), 3.77 (m, CH₂OH, CH, 4H), 3.73 (s, OCH₃, 3H), 3.68 (s, OCH₃, 6H), 3.62 (t, *J*=4.5, CH, 1H), 2.40 (br s OH, NH₂, 4H).

¹³C NMR (90 MHz, CDCl₃): δ 171.6, 152.7, 139.0, 137.1, 135.7, 134.2, 132.5, 131.1, 129.9, 129.6, 111.9, 111.2, 106.2, 65.0, 60.9, 59.4, 56.6, 55.9.

Dept 135 NMR (90 MHz, CDCl₃): δ 130.0 (CH), 129.6 (CH), 111.9 (CH), 111.2 (CH), 106.2 (CH), 65.1 (CH₂), 60.9 (CH₃), 59.4 (CH₃), 56.6 (CH), 55.9 (CH₃).

Synthesis of a Combretastatin A-1 Analogue

2, 3-Diisopropyltoluene (30)

To a well-stirred refluxing solution of 3-methylcatechol (5.20 g, 41.1 mmol) in DMF (35 mL), K₂CO₃ (20.3 g, 123 mmol) was added in three portions. After the entire

solid was dissolved (30 minutes), isopropyl bromide (11.7 mL, 123 mmol) was added at once and, the reaction mixture was refluxed for 20 h, at which point, water was added. The product was extracted once from the aqueous phase with CH₂Cl₂ and, the combined organic phase was washed six times with water and twice with brine. After the resultant solution was dried under Na₂SO₄ and filtered through florisil/silica gel, the solvent was evaporated and the product was purified by flash chromatography (2.5% EtOAc/ 97.5% hex) to obtain 5.13 g (24.7 mmol) of protected catechol in a 59% yield.

¹H NMR (300 MHz, CDCl₃, δ): 6.88 (t, *J*= 7.8, ArH, 1H), 6.75 (dd, *J*= 7.9, 2.8, ArH, 2H), 4.52 (sept, *J*= 6.1, CH(CH₃)₂, 1H), 4.49 (sept, *J*= 6.2, CH(CH₃)₂, 1H), 2.25 (s, benzylic CH₃, 3H), 1.34 (d, *J*= 6.1, CH(CH₃)₂, 6H), 1.29 (d, *J*= 6.2 Hz, CH(CH₃)₂, 6H).

Dept 135 NMR (75 MHz, CDCl₃): δ 123.0 (CH), 122.9 (CH), 113.8 (CH), 74.4 (CH), 70.7 (CH), 22.8 (CH₃), 22.3 (CH₃), 16.8 (CH₃).

2, 3-Diisopropyl-4-methylbenzaldehyde (31)

At 0°C, first, TMEDA (4.4 mL, 28.9 mmol) and after BuLi (10.7 mL, 26.8 mmol) were added into a well stirred solution of **30** (4.29 g, 20.6 mmol) in distilled hexanes (50 mL). The reaction mixture was stirred first, at 0°C for 45 minutes and, then for 16 additional hours at room temperature, at which point, DMF (2.72 mL, 35.1 mmol) was added into the reaction mixture cooled at 0°C. After stirring the resultant mixture for 1.5 h at 0°C, 50 mL of 1M HCl solution was added and the reaction mixture stirred for 45 additional minutes. The product was extracted once with ETOAc from the aqueous phase and the combined organic phase was washed twice with water and once with brine. After the organic phase was dried under sodium sulfate and the solvent was evaporated,

the crude reaction mixture was purified by flash chromatography (2.5% EtOAc/ 97.5% hex) to obtain 3.18 g (13.5 mmol) of the aldehyde in a 65% yield.

^1H NMR (300 MHz, CDCl_3 , δ): 10.35 (d, $J= 0.8$, CHO , 1H), 7.47 (d, $J= 8.0$, ArH , 1H), 6.98 (dd, $J= 8.0, 0.6$, ArH , 1H), 4.69 (sept, $J=6.2$, $\text{CH}(\text{CH}_3)_2$, 1H), 4.58 (sept, $J= 6.2$, $\text{CH}(\text{CH}_3)_2$, 1H), 2.29 (s, benzylic CH_3 , 3H), 1.28 (d, $J= 1.8$, $\text{CH}(\text{CH}_3)_2$, 6H), 1.26 (d, $J= 1.8$, $\text{CH}(\text{CH}_3)_2$, 6H).

Dept 135 NMR (75 MHz, CDCl_3): δ 190.6 ($\text{C}=\text{O}$), 126.0 ($\text{C}=\text{O}$), 122.0 ($\text{C}=\text{O}$), 75.5 ($\text{C}=\text{O}$), 74.3 ($\text{C}=\text{O}$), 22.5 (CH_3), 22.3 (CH_3), 17.4 (CH_3).

GC MS m/z (% relative intensity, ion): 236 (5, M^+), 152 (100).

(Z)-1-(2, 3-Diisopropyl -4-methylphenyl)-2-(3, 4, 5-trimethoxyphenyl)ethene (32)

15 mL of anhydrous CH_2Cl_2 was poured into a flask containing NaH (1.06 g, 41.8 mmol) and the resultant suspension was stirred at 0 °C under nitrogen atmosphere for 15 minutes at which point 10 mL of a CH_2Cl_2 solution of phosphonium bromide **16** (4.37 g, 8.36 mmol) was added dropwise. After the reaction mixture was stirred for 10 minutes, 10 mL of a CH_2Cl_2 solution of aldehyde **31** (1.97 g, 8.36 mmol) was added into the flask and the reaction was stirred for 16 h at room temperature at which point water was added until bubbling stopped. After the product was extracted once with CH_2Cl_2 from the aqueous phase, the organic phase was washed twice with water, twice with brine and dried over sodium sulfate. The crude reaction mixture was purified by flash chromatography (5% EtOAc/ 95% hex) to afford 1.53 g (3.83 mmol) of the Z isomer in a 46% yield.

^1H NMR (300 MHz, CDCl_3 , δ): 6.88 (d, $J= 7.9$, ArH , 1H), 6.71 (d, $J= 7.9$, ArH , 1H), 6.64 (d, $J= 12.1$, $\text{C}=\text{CH}$, 1H), 6.48 (s, ArH , 2H), 6.44 (d, $J= 12.2$ Hz, $\text{C}=\text{CH}$, 1H),

4.59 (m, $\text{CH}(\text{CH}_3)_2$, 2H), 3.81 (s, OCH_3 , 3H), 3.63 (s, OCH_3 , 6H), 2.21 (s, benzylic CH_3 , 3H), 1.26 (t, $J=6.3$, $\text{CH}(\text{CH}_3)_2$, 12H).

GC MS m/z (% relative intensity, ion): 400 (73, M^+), 301 (100), 287 (27), 221 (55), 181 (23).

(Z)-1-(2, 3-Dihydroxy-4-methylphenyl)-2-(3, 4, 5-trimethoxyphenyl) ethane (33)

Into a round bottom flask containing 10 mL of a CH_2Cl_2 solution of **32** (0.58 g, 1.46 mmol), TiCl_4 (0.35 mL 3.17 mmol) was added and, the reaction mixture was stirred for 10 minutes at 0°C and under nitrogen atmosphere, at which point ice-water was added until bubbling stopped. The product was extracted once from the aqueous phase with CH_2Cl_2 and the combined organic phase was washed twice with water and once with brine. After the organic solution was dried under sodium sulfate, the solvent was evaporated and the product was purified by flash chromatography (20% EtOAc/ 80% hex) to afford 0.327 g (1.03 mmol) of pure CA-1 analogue in a 71% yield.

^1H NMR (300 MHz, CDCl_3 , δ): 6.70 (d, $J=8.1$, ArH, 1H), 6.67 (d, $J=8.1$, ArH, 1H), 6.62 (d, $J=12.0$, $\text{C}=\text{CH}$, 1H), 6.51 (d, $J=12.0$, $\text{C}=\text{CH}$, 1H), 6.46 (s, ArH, 2H), 5.40 (br s, OH, 1H), 4.96 (br s, OH, 1H), 3.81 (s, OCH_3 , 3H), 3.61 (s, OCH_3 , 6H), 2.23 (s, benzylic CH_3 , 3H).

Dept 45 NMR (75 MHz, CDCl_3): δ 132.1, 124.2, 122.8, 119.9, 105.6, 60.9, 55.8, 15.5

GC MS m/z (% relative intensity, ion): 280 (9, M^+-36), 167 (36), 149 (100).

*Synthesis of Nitrogen-Based Epoxide Derivatives of Combretastatins A-1 and A-4**Z-2-(4-methoxy-3-nitrophenyl)-3-(3,4,5-trimethoxyphenyl)oxirane (34)*

Into a round bottom flask containing 4-phenylpyridine N-oxide (0.50 mg, 0.0028 mmol), stilbene **3** (0.209 g, 0.605 mmol) and R,R-Jacobsen catalyst (3.90 mg, 0.0060 mmol), 3 mL of anhydrous CH₂Cl₂ was added and, the mixture was stirred at 0 °C for 10 minutes before adding 1.45 mL of NaOCl (0.0785 g, 1.06 mmol) and 0.06 mL of a 3M NaOH (0.18 mmol) solution. After the reaction mixture was stirred at 0 °C for 1 h, another 1.45 mL of NaOCl was added and the mixture was stirred for 22 h, at which point the product was extracted from the aqueous phase with CH₂Cl₂, and the resultant organic phase was washed twice with water, once with brine and dried under Na₂SO₄. The crude reaction mixture was purified by flash chromatography (25% EtOAc/ 75% hex) to obtain 0.0226 g (0.0626 mmol) of the epoxide in an 11% yield.

¹H NMR (300 MHz, CDCl₃, δ): 7.79 (d, *J*=2.2, ArH, 1H), 7.31 (ddd, *J*=8.7, 2.2, 0.3, ArH, 1H), 6.90 (d, *J*=8.7, ArH, 1H), 6.39 (s, ArH, 2H), 4.31 (d, *J*=4.1, CH, 1H), 4.28 (d, *J*=4.1, CH, 1H), 3.88 (s, OCH₃, 3H), 3.75 (s, OCH₃, 3H), 3.74 (s, OCH₃, 6H).

¹³C NMR (75 MHz, CDCl₃): δ 153.0, 152.4, 138.9, 137.5, 132.3, 129.0, 126.9, 124.4, 113.1, 103.6, 60.8, 60.0, 58.5, 56.5, 56.0.

Dept 45 NMR (75 MHz, CDCl₃): δ 132.4, 124.4, 113.1, 103.7, 60.8, 60.0, 58.5, 56.6, 56.1.

E-2-(4-methoxy-2,5-dinitrophenyl)-3-(3,4,5-trimethoxyphenyl)oxirane (35)

Into a round bottom flask containing 4-phenylpyridine N-oxide (1.50 mg, 0.0085 mmol), a mixture of cis/trans (1:1 ratio) stilbene **24** (0.683 g, 1.75 mmol) and R,R-

Jacobsen catalyst (11.4 mg, 0.0176 mmol), 10 mL of anhydrous CH₂Cl₂ was added and, the mixture was stirred at 0 °C for 10 minutes before adding 4.22 mL of NaOCl (0.228 g, 3.07 mmol) and 0.18 mL of a 3M NaOH (0.54 mmol) solution. After the reaction mixture was stirred at 0 °C for 1 h, another 4.22 mL of NaOCl was added and the mixture was stirred for 48 h, at which point the product was extracted from the aqueous phase with CH₂Cl₂, and the resultant organic phase was washed twice with water, once with brine and dried under Na₂SO₄. The crude reaction mixture was purified by flash chromatography (20% EtOAc/ 80% hex) to obtain 0.0845 g (0.208 mmol) of the epoxide in a 41% yield.

¹H NMR (300 MHz, CDCl₃, δ): 8.05 (s, ArH, 1H), 7.86 (s, ArH, 1H), 6.60 (s, ArH, 2H), 4.39 (d, *J* = 1.9, CH, 1H), 4.06 (s, OCH₃, 3H), 3.87 (s, OCH₃, 6H), 3.85 (s, OCH₃, 3H), 3.76 (d, *J* = 1.9, CH, 1H).

¹³C NMR (75 MHz, CDCl₃): δ 153.6, 152.0, 149.2, 142.8, 138.4, 131.0, 126.5, 124.3, 110.1, 102.6, 62.5, 60.9, 58.7, 57.4, 56.1.

E-2-(4-Methoxy-3-nitrophenyl)-3-(3,4,5-trimethoxyphenyl)oxirane (**36**)

Into a round bottom flask containing 4-phenylpyridine N-oxide (0.6 mg, 0.0034 mmol), *E* isomer of stilbene **3** (0.216 g, 0.627 mmol) and R,R-Jacobsen catalyst (4.1 mg, 0.0063 mmol), 3 mL of anhydrous CH₂Cl₂ was added and, the mixture was stirred at 0 °C for 10 minutes before adding 1.5 mL of NaOCl (0.0812 g, 1.09 mmol) and 0.06 mL of a 3M NaOH (0.18 mmol) solution. After the reaction mixture was stirred at 0 °C for 1 h, another 1.5 mL of NaOCl was added and the mixture was stirred for 39 h, at which point the product was extracted from the aqueous phase with CH₂Cl₂, and the resultant organic phase was washed twice with water, once with brine and dried under Na₂SO₄.

The crude reaction mixture was purified by flash chromatography (30% EtOAc/ 70% hex) to obtain 0.0380 g (0.105 mmol) of the epoxide in a 17% yield.

^1H NMR (300 MHz, CDCl_3 , δ): 7.81 (d, $J=2.2$, ArH, 1H), 7.51 (dd, $J=8.6, 2.1$, ArH, 1H), 7.10 (d, $J=8.7$, ArH, 1H), 6.55 (s, ArH, 2H), 3.97 (s, OCH_3 , 3H), 3.86 (s, OCH_3 , 6H), 3.84 (s, OCH_3 , 3H), 3.82 (d, $J=1.4$, CH, 1H), 3.79 (d, $J=1.7$, CH, 1H).

^{13}C NMR (75 MHz, CDCl_3): δ 153.6, 152.9, 139.7, 138.2, 131.9, 131.1, 129.5, 122.8, 113.8, 102.2, 62.9, 61.3, 60.9, 56.7, 56.1

E-2-(4-Methoxy-2-nitro-phenyl)-3-(3,4,5-trimethoxy-phenyl)oxirane (**37**)

Into a round bottom flask containing 4-phenylpyridine N-oxide (0.4 mg, 0.0023 mmol), *E* isomer of stilbene **9** (0.170 g, 0.492 mmol) and R,R-Jacobsen catalyst (3.2 mg, 0.0049 mmol), 3 mL of anhydrous CH_2Cl_2 was added and, the mixture was stirred at 0 °C for 10 minutes before adding 1.2 mL of NaOCl (0.065 g, 0.873 mmol) and 0.05 mL of a 3M NaOH (0.15 mmol) solution. After the reaction mixture was stirred at 0 °C for 1 h, another 1.2 mL of NaOCl was added and the mixture was stirred for 20 h, at which point the product was extracted from the aqueous phase with CH_2Cl_2 , and the resultant organic phase was washed twice with water, once with brine and dried under Na_2SO_4 . The crude reaction mixture was purified by flash chromatography (20% EtOAc/ 80% hex) to obtain 0.0869 g (0.241 mmol) of the epoxide in a 49% yield.

^1H NMR (300 MHz, CDCl_3 , δ): 7.6 (d, $J=2.6$, ArH, 1H), 7.59 (d, $J=8.7$, ArH, 1H), 7.21 (dd, $J=8.7, 2.7$, ArH, 1H), 6.74 (s, ArH, 2H), 4.34 (d, $J=2.0$, CH, 1H), 4.04 (d, $J=2.0$, C=CH, 1H), 3.91 (s, OCH_3 , 3H), 3.88 (s, OCH_3 , 3H), 3.87 (s, OCH_3 , 3H), 3.86 (s, OCH_3 , 3H).

^{13}C NMR (75 MHz, CDCl_3): δ 159.6, 152.6, 150.0, 148.4, 143.2, 129.6, 128.1, 125.2, 120.7, 119.5, 109.4, 104.0, 61.2, 61.1, 59.6, 59.5, 56.2, 55.9.

Dept 45 NMR (75 MHz, CDCl_3): δ 128.2, 120.8, 109.5, 104.1, 61.2, 61.2, 59.61, 59.58, 56.2, 56.0.

Z-2-(4-Methoxy-3,5-dinitrophenyl)-3-(3,4,5-trimethoxyphenyloxirane (38)

Into a round bottom flask containing 4-phenylpyridine N-oxide (0.0191 g, 0.108 mmol), stilbene **22** (0.116 g, 0.271 mmol) and R,R-Jacobsen catalyst (3.5 mg, 0.0054 mmol), 2 mL of anhydrous CH_2Cl_2 was added and, the mixture was stirred at 0 °C for 10 minutes before adding 0.63 mL of NaOCl (0.065 g, 0.873 mmol) and 0.05 mL of a 3M NaOH (0.15 mmol) solution. The reaction mixture was stirred for 21.5 h, at which point the product was extracted from the aqueous phase with CH_2Cl_2 , and the resultant organic phase was washed twice with water, once with brine and dried under Na_2SO_4 . The crude reaction mixture was purified by flash chromatography (20% EtOAc/ 80% hex) to obtain 0.0410 g (0.101 mmol) of the epoxide in a 37% yield.

^1H NMR (300 MHz, CDCl_3 , δ): 7.94 (d, $J= 0.4$, ArH, 2H), 6.42 (d, $J= 0.5$, ArH, 2H), 4.42 (dd, $J= 4.1, 0.5$, CH, 1H), 4.34 (dd, $J= 4.1, 0.6$, CH, 1H), 3.99 (s, OCH₃, 3H), 3.79 (s, OCH₃, 6H), 3.77 (s, OCH₃, 3H).

^{13}C NMR (75 MHz, CDCl_3): δ 153.3, 147.0, 144.7, 137.9, 131.7, 127.7, 127.3, 103.4, 64.8, 60.8, 60.4, 57.8, 56.1.

Dept 45 NMR (75 MHz, CDCl_3): δ 127.3, 103.4, 64.8, 60.9, 60.4, 57.8, 56.1.

*Synthesis of Cold Precursors of Radio Labeled Combretastatins CA-1 and CA-4*¹⁰⁵

1-Bromomethyl-2,3-diisopropoxy-4-methoxybenzene (39a)

At -5°C and under nitrogen atmosphere, 10 mL of a 0 °C CH₂Cl₂ solution of phosphorous tribromide (0.94 mL, 9.94 mmol) was added into a well-stirred solution of 2,3-diisopropoxy-4-methoxyphenylmethanol (3.37 g, 13.3 mmol) in anhydrous CH₂Cl₂ (30 mL). The reaction mixture was stirred first at -5°C for 2 hours and the last 2.5 h at room temperature, at which point, the mixture was slowly added to 50 mL of ice-water and neutralized with NaHCO₃. The product was extracted twice with CH₂Cl₂ from the aqueous phase and the combined organic phase was washed twice with water and twice with brine. After the organic solution was dried under sodium sulfate, the solvent was evaporated to afford 3.79 g (12.0 mmol) of the product in a 90% yield.

¹H NMR (300 MHz, CDCl₃, δ): 7.10 (d, *J*=8.6, ArH, 1H), 6.64 (d, *J*=8.6, ArH, 1H), 4.87 (sept., *J*=6.2, CH(CH₃)₂, 1H), 4.58 (s, CH₂, 2H), 4.40 (sept., *J*=6.2, CH(CH₃)₂, 1H) 3.83 (s, OCH₃, 3H) 1.29 (d, *J*=5.1, CH(CH₃)₂, 6H), 1.27 (d, *J*=5.2, CH(CH₃)₂, 6H).

(2,3-Diisopropoxy-4-methoxyphenyl)triphenylphosphonium bromide (39b)

Bromide **39a** (10.3 g, 32.6 mmol) and triphenylphosphine (8.64 g, 32.6 mmol) were dissolved in CH₂Cl₂ (100 mL) and the reaction mixture was refluxed for 10 h at which point water was added and the product extracted once from the aqueous phase with CH₂Cl₂. The organic phase was washed twice with water and brine, then dried over sodium sulfate. The crude was triturated at 0 °C with ethyl ether to afford 17.3 g (29.9 mmol) of the product in a 92% yield.

^1H NMR (300 MHz, CDCl_3 , δ): 7.68 (m, ArH, 15H), 7.04 (dd, $J= 8.6, 2.9$, ArH, 1H), 6.48 (d, $J= 8.6$, ArH, 1H), 5.14 (d, $J= 13.8$, CH₂, 1H), 4.69 (sept., $J= 6.2$, CH(CH₃)₂, 1H), 3.94 (sept., $J= 6.2$, CH(CH₃)₂, 1H), 3.74 (s, OCH₃, 3H), 1.09 (d, $J= 2.7$, CH(CH₃)₂, 6H), 1.07 (d, $J= 2.7$, CH(CH₃)₂, 6H).

4-[(Z)-2-(3,5-Dimethoxyphenyl-4-t-butyltrimethylsilyloxy)vinyl]-2,3-diisopropoxy-1-methoxybenzene (40a)

30 mL of anhydrous CH_2Cl_2 was poured into a flask containing NaH (3.77 g, 149 mmol) and the resultant suspension was stirred at 0 °C under nitrogen atmosphere for 15 minutes at which point 50 mL of a CH_2Cl_2 solution of phosphonium bromide **39b** (17.3 g, 29.8 mmol) was added carefully. After the reaction mixture was stirred for 10 minutes, 20 mL of a CH_2Cl_2 solution of 3,5-dimethoxy-4-t-butyltrimethylsilyloxybenzaldehyde (8.36 g, 29.9 mmol) was added into the flask and the reaction was stirred for 3 h at room temperature at which point water was added until bubbling stopped. After the product was extracted once with CH_2Cl_2 from the aqueous phase, the organic phase was washed twice with water, twice with brine and dried over sodium sulfate. The crude reaction mixture was purified by flash chromatography (2% EtOAc/ 98% hex) to afford 1.75 g (3.39 mmol) of the *Z* isomer in a 12% yield.

Z- isomer: ^1H NMR (300 MHz, CDCl_3 , δ): 6.90 (d, $J= 8.6$, ArH, 1H), 6.56 (d, $J= 12.1$, C=CH, 1H), 6.44 (s, ArH, 2H), 6.43 (d, $J= 8.6$, ArH, 1H), 6.42 (d, $J= 12.1$ Hz, C=CH, 1H), 4.68 (sept., $J= 6.1$, CH(CH₃)₂, 1H), 4.41 (sept., $J= 5.9$, CH(CH₃)₂, 1H), 3.77 (s, OCH₃, 3H), 3.57 (s, OCH₃, 6H), 1.28 (d, $J= 6.2$, CH(CH₃)₂, 12H), 0.98 (s, CH(CH₃)₂, 9H), 0.10 (s, Si(CH₃)₂, 6H).

^{13}C NMR (75 MHz, CDCl_3): δ 153.6, 151.1, 150.4, 140.3, 133.3, 129.9, 129.2, 125.6, 125.4, 124.9, 106.4, 106.1, 75.1, 74.8, 55.8, 55.4, 25.8, 22.6, 22.5, 18.7, -4.7.

Dept 90 NMR (75 MHz, CDCl_3): δ 129.6, 126.0, 125.3, 106.7, 106.4, 75.5, 75.2.

Dept 135 NMR (75 MHz, CDCl_3): δ 129.6 ($\underline{\text{C}}\text{H}$), 126.0 ($\underline{\text{C}}\text{H}$), 125.3 ($\underline{\text{C}}\text{H}$), 106.7 ($\underline{\text{C}}\text{H}$), 106.5 ($\underline{\text{C}}\text{H}$), 75.5 ($\underline{\text{C}}\text{H}$), 75.2 ($\underline{\text{C}}\text{H}$), 56.2 ($\underline{\text{C}}\text{H}_3$), 55.8 ($\underline{\text{C}}\text{H}_3$), 26.2 ($\underline{\text{C}}\text{H}_3$), 23.0 ($\underline{\text{C}}\text{H}_3$), 22.9 ($\underline{\text{C}}\text{H}_3$), -4.7 ($\underline{\text{C}}\text{H}_3$).

E- isomer (**40b**): 6.99 g was obtained in a 48% yield. ^1H NMR (300 MHz, CDCl_3 , δ): 7.29 (d, J = 8.7, ArH, 1H), 7.26 (d, J = 16.3, C=CH, 1H), 6.87 (d, J = 16.4 Hz, C=CH, 1H), 6.70 (s, ArH, 2H), 6.67 (d, J = 8.5, ArH, 1H), 4.59 (sept., J = 6.2, CH(CH₃)₂, 1H), 4.44 (sept., J = 6.2, CH(CH₃)₂, 1H), 3.84 (s, OCH₃, 3H), 3.82 (s, OCH₃, 6H), 1.29 (d, J = 6.2, CH(CH₃)₂, 12H), 1.00 (s, CH(CH₃)₂, 9H), 0.13 (s, Si(CH₃)₂, 6H).

4-[(E)-2-(3,4,5-Trimethoxyphenyl)vinyl]-2,3-diisopropoxy-1-methoxybenzene (40c)

Into a round bottom flask containing *E*-isomer **40b** (0.343 g, 0.663 mmol), 3 mL of anhydrous CH_3CN was added, and the solution was stirred at 0 °C before adding 0.17 mL of CH_3I (0.0384 g, 2.70 mmol). After the reaction mixture was stirred at 0 °C, 0.73 mL of a 1M TBAF solution (THF, 0.191 g, 0.73 mmol) was added, and the contents were stirred for 20 minutes at 0 °C, at which point, H_2O was added to the reaction mixture. The product was extracted once from the aqueous phase with EtOAc, and the resultant organic phase was washed once with H_2O , once with brine and dried under Na_2SO_4 . After the organic phase was filtered through silica gel and evaporated under vacuum, 0.248 g (0.596 mmol) of the product was obtain in a 90% yield.

^1H NMR (300 MHz, CDCl_3 , δ): 7.30 (d, J = 8.7, ArH, 1H), 7.28 (d, J = 16.9, C=CH, 1H), 6.86 (d, J = 16.4, C=CH, 1H), 6.69 (s, ArH, 2H), 6.64 (d, J = 8.8, ArH, 1H),

4.56 (sept., $J= 6.2$, $\text{CH}(\text{CH}_3)_2$, 1H), 4.41 (sept., $J= 6.2$, $\text{CH}(\text{CH}_3)_2$, 1H), 3.86 (s, OCH_3 , 6H), 3.81 (s, OCH_3 , 3H), 3.80 (s, OCH_3 , 3H), 1.26 (d, $J= 7.1$, $\text{CH}(\text{CH}_3)_2$, 12H).

^{13}C NMR (75 MHz, CDCl_3): δ 153.8, 153.2, 149.9, 140.2, 137.3, 133.8, 126.7, 125.2, 123.5, 119.9, 107.2, 103.1, 75.4, 74.9, 60.7, 55.8, 55.7, 22.4, 22.3.

GC MS m/z (% relative intensity, ion): 416 (66, M^+), 374 (11), 333 (39), 317 (100), 303 (16), 222 (23), 166 (23).

4-[(Z)-2-(3,5-Dimethoxyphenyl-4-t-butyltrimethylsilyloxy)vinyl]-2-isopropoxy-1-methoxybenzene (40d)

2.24 g of a mixture of cis/trans (6.7:1 ratio) was purified by column chromatography (2% EtOAc/ 98% hex) to afford 2.09 g (4.56 mmol) of pure Z isomer in a 93% recovery yield.

^1H NMR (300 MHz, CDCl_3 , δ): 6.87 (d, $J= 1.9$, ArH, 1H), 6.83 (dd, $J= 8.2$, 2.0, ArH, 1H), 6.75 (d, $J= 8.2$, ArH, 1H), 6.47 (s, ArH, 2H), 6.45 (d, $J= 12.0$, $\text{C}=\text{CH}$, 1H), 6.40 (d, $J= 12.0$, $\text{C}=\text{CH}$, 1H), 4.28 (sept., $J= 6.0$, $\text{CH}(\text{CH}_3)_2$, 1H), 3.82 (s, OCH_3 , 3H), 3.62 (s, OCH_3 , 6H), 1.25 (d, $J= 6.1$, $\text{CH}(\text{CH}_3)_2$, 6H), 0.99 (s, $\text{CH}(\text{CH}_3)_2$, 9H), 0.11 (s, $\text{Si}(\text{CH}_3)_2$, 6H).

^{13}C NMR (75 MHz, CDCl_3): δ 151.3, 149.4, 146.8, 133.5, 130.2, 129.8, 129.1, 128.9, 122.1, 116.0, 111.5, 106.0, 71.2, 56.0, 55.6, 25.8, 22.0, 18.7, -4.65.

4-[(Z)-2-(3,4,5-Trimethoxyphenyl)vinyl]-2-isopropoxy-1-methoxybenzene (40e)

Into a round bottom flask containing Z-isomer **40d** (0.200 g, 0.437 mmol), 5 mL of anhydrous CH_3CN was added, and the solution was stirred at 0 °C for before adding 0.11 mL of CH_3I (0.248 g, 1.75 mmol). After the reaction mixture was stirred at 0 °C for

15 minutes, 0.48 mL of a 1M TBAF solution (THF, 0.126 g, 0.48 mmol) was added, and the contents were stirred for 15 minutes at 0 °C, at which point, H₂O was added to the reaction mixture. The product was extracted once from the aqueous phase with EtOAc, and the resultant organic phase was washed once with H₂O, once with brine and dried under Na₂SO₄. After the solvent was evaporated under vacuum, the crude reaction mixture was purified by flash chromatography (25% EtOAc/ 75% hex) to obtain 0.148 g (0.413 mmol) of the product in a 94% yield.

¹H NMR (300 MHz, CDCl₃, δ): 6.84 (dd, *J*= 2.0, 8.2, ArH, 1H), 6.79 (d, *J*= 1.9, ArH, 1H), 6.76 (d, *J*= 8.3, ArH, 1H), 6.50 (d, *J*= 12.1, C=CH, 1H), 6.49 (s, ArH, 2H), 6.43 (d, *J*= 12.1, C=CH, 1H), 4.24 (sept., *J*= 6.1, CH(CH₃)₂, 1H), 3.82 (s, OCH₃, 3H), 3.81 (s, OCH₃, 3H), 3.69 (s, OCH₃, 6H), 1.22 (d, *J*= 6.1, CH(CH₃)₂, 6H).

¹³C NMR (75 MHz, CDCl₃): δ 153.0, 149.5, 146.8, 137.0, 133.2, 129.9, 129.8, 128.7, 122.2, 115.9, 111.5, 105.8, 71.1, 60.9, 56.0, 55.9, 22.0.

2-Methoxy-5-[(Z)-2-(3,4,5-trimethoxyphenyl)vinyl]phenol (40f)

Into a round bottom flask keeping nitrogen gas and containing 4 mL of a CH₂Cl₂ solution of **40e** (0.127 g, 0.354 mmol), 0.05 mL of TiCl₄ (0.0864 g, 0.456 mmol) was added and, the reaction mixture was stirred for 19 minutes at 0°C, at which point, ice-water was added until bubbling stopped. The product was extracted once from the aqueous phase with CH₂Cl₂ and the combined organic phase was washed twice with water and once with brine. After the organic solution was dried under sodium sulfate, the solvent was evaporated and the product was purified by recrystallization (hex-EtOAc) to afford 0.104 g (0.329 mmol) of CA-1 in a 93% yield.

^1H NMR (300 MHz, CDCl_3 , δ): 6.91 (d, $J= 1.9$, ArH, 1H), 6.79 (dd, $J= 8.3, 1.9$, ArH, 1H), 6.72 (d, $J= 8.3$, ArH, 1H), 6.52 (s, ArH, 2H), 6.46 (d, $J= 12.2$, C=CH, 1H), 6.40 (d, $J= 12.2$, C=CH, 1H), 5.52 (s, OH, 1H), 3.85 (s, OCH₃, 3H), 3.83 (s, OCH₃, 3H), 3.69 (s, OCH₃, 6H).

^{13}C NMR (75 MHz, CDCl_3): δ 152.8, 145.7, 145.2, 137.1, 132.7, 130.6, 129.5, 129.0, 121.1, 115.0, 110.3, 106.0, 60.9, 55.94, 55.91.

*Synthesis of OXi8007 and a Nitrogen-Based Indole*¹¹³⁻¹¹⁵

*1-(4-Methoxy-3-*t*-butyldimethylsilyloxyphenyl)ethanone (41a)*

The product was purified by column chromatography (20% EtOAc/ 80% hex) to obtain the protected acetophenone in high purity.

^1H NMR (300 MHz, CDCl_3 , δ): 7.57 (dd, $J= 8.5, 2.2$, ArH, 1H), 7.45 (d, $J= 2.2$, ArH, 1H), 6.86 (d, $J= 8.5$, ArH, 1H), 3.86 (s, OCH₃, 3H), 2.52 (s, COCH₃, 3H), 0.90 (s, CH(CH₃)₂, 9H), 0.16 (s, Si(CH₃)₂, 6H).

^{13}C NMR (75 MHz, CDCl_3): δ 196.8, 155.3, 144.8, 130.6, 123.5, 120.5, 110.8, 55.5, 26.3, 25.7, 18.5, -4.6.

*1-Methoxy-2-*t*-butyldimethylsilyloxy-4-(1-trimethylsilyloxyvinyl)benzene (41b)*

Into a round bottom flask keeping N_2 gas, and containing 8.1 mL of diisopropylamine (5.77 g, 57.1 mmol), 50 mL of Et₂O was added. After the solution was cooled at 0°C, BuLi (22.9 mL, 26.8 mmol) was added, and the mixture was stirred for 15 minutes before adding 40 mL of a Et₂O solution of ketone **41a** (10.7, 38.3mmol). After the reaction mixture was stirred for 20 minutes, 7.4 mL of TMSCl (6.23 g, 57.3 mmol)

was added, and the reaction mixture was stirred for 13 h at room temperature, at which point, 70 mL of a 10% NaHCO₃ solution was added. The product was extracted twice with hexanes from the aqueous phase, and the combined organic phase was dried under K₂CO₃. After the solvent was evaporated, 15.0 g (42.6 mmol) of the crude reaction mixture was obtained.

¹H NMR (300 MHz, CDCl₃, δ): 7.15 (dd, *J*= 8.5, 2.2, ArH, 1H), 7.08 (d, *J*= 2.2, ArH, 1H), 6.78 (d, *J*= 8.5, ArH, 1H), 4.75 (d, *J*= 1.6, C=CH, 1H), 4.31 (d, *J*= 1.5, C=CH, 1H), 3.80 (s, OCH₃, 3H), 0.99 (s, CH(CH₃)₂, 9H), 0.24 (s, Si(CH₃)₃, 9H) 0.15 (s, Si(CH₃)₂, 6H).

*2-Bromo-1-(4-methoxy-3-*t*-butyldimethylsilyloxyphenyl)ethanone (41c)*

Into a round bottom flask containing TMS ether **41b** (15.0 g, 42.6 mmol), 70 mL of anhydrous CH₂Cl₂ and 0.6 g of K₂CO₃ were poured and N₂ gas was passed through the system. After the solution was cooled at 0 °C, 2 mL of Br₂ (6.22 g, 38.9 mmol) was added drop-wise, and the reaction mixture was stirred for 30 minutes, at which point, a saturated solution of Na₂S₂O₃ (40 mL) was added. The product was extracted three times from the aqueous phase with CH₂Cl₂, and the resultant organic phase was dried under Na₂SO₄ followed by evaporation of the solvent. The crude reaction mixture was purified by flash chromatography (2.5% EtOAc/ 97.5% hex) to obtain 3.90 g (10.9 mmol) of the product in a 28% yield.

¹H NMR (300 MHz, CDCl₃, δ): 7.61 (dd, *J*= 8.5, 2.2, ArH, 1H), 7.48 (d, *J*= 2.2, ArH, 1H), 6.88 (d, *J*= 8.5, ArH, 1H), 4.37 (s, CH₂, 2H), 3.88 (s, OCH₃, 3H), 0.99 (s, CH(CH₃)₂, 9H), 0.24 (s, Si(CH₃)₃, 9H) 0.16 (s, Si(CH₃)₂, 6H).

^{13}C NMR (75 MHz, CDCl_3): δ 189.9, 156.1, 145.1, 127.1, 124.3, 121.1, 111.0, 55.6, 30.7, 25.7, 18.5, -4.6.

Dept 135 NMR (75 MHz, CDCl_3): δ 124.3 ($\underline{\text{C}}\text{H}$) , 121.1 ($\underline{\text{C}}\text{H}$), 111.0 ($\underline{\text{C}}\text{H}$), 55.6 ($\underline{\text{C}}\text{H}_3$), 30.7 ($\underline{\text{C}}\text{H}_2$), 25.7 ($\underline{\text{C}}\text{H}_3$), -4.6 ($\underline{\text{C}}\text{H}_3$).

*6-Methoxy-2-(4-methoxy-3-*t*-butyldimethylsilyloxyphenyl)-1H-indole (41d)*

Into a 3-neck round bottom flask containing a refluxing mixture of 3.6 mL of *m*-anisidine (3.87 g, 31.4 mmol) and 13 mL of *N,N*-dimethylaniline, 22 mL of a EtOAc solution of bromide **41c** was added, and the mixture was refluxed at 140 °C for 13 h. After the reaction mixture was cooled at room temperature, water was added (25 mL), and the product was extracted three times from the aqueous phase with EtOAc, the resultant organic phase washed with water and brine and dried under Na_2SO_4 . The crude reaction mixture was purified by flash chromatography (20% EtOAc/ 80% hex) to obtain 2.83 g (7.38 mmol) of the product in a 49% yield.

^1H NMR (300 MHz, CDCl_3 , δ): 8.09 (br s, $\underline{\text{N}}\text{H}$, 1H), 7.45 (d, J = 8.6, $\underline{\text{A}}\text{rH}$, 1H), 7.16 (dd, J = 8.3, 2.2, $\underline{\text{A}}\text{rH}$, 1H), 7.11 (d, J = 2.2, $\underline{\text{A}}\text{rH}$, 1H), 6.89 (d, J = 8.4, $\underline{\text{A}}\text{rH}$, 1H), 6.88 (d, J = 2.2, $\underline{\text{A}}\text{rH}$, 1H), 6.77 (dd, J = 8.6, 2.3, $\underline{\text{A}}\text{rH}$, 1H), 6.60 (dd, J = 2.1, 0.8, $\text{C}=\underline{\text{C}}\text{H}$, 1H), 3.85 (s, $\text{O}\underline{\text{C}}\text{H}_3$, 3H), 3.83 (s, $\text{O}\underline{\text{C}}\text{H}_3$, 3H), 1.02 (s, $\text{CH}(\underline{\text{C}}\text{H}_3)_2$, 9H), 0.18 (s, $\text{Si}(\underline{\text{C}}\text{H}_3)_2$, 6H).

*3,4,5-Trimethoxy-*N*-(3-methoxyphenyl)benzamide (42)*

Into a 2-neck round bottom flask containing 45 mL of an *o*-dichlorobenzene solution of indole **41d** (3.00 g, 7.83 mmol), benzoyl chloride (4.60 g, 19.5 mmol) was added, and the mixture was heated at 160 °C for 12 h. After the reaction mixture was

cooled at room temperature, water was added (25 mL), and the product was extracted twice from the aqueous phase with CH₂Cl₂. The resultant organic phase was washed with water, brine and dried under Na₂SO₄ followed by isolation of the product from the crude reaction mixture by flash chromatography (20% EtOAc/ 80% hex). The resultant yellow solid obtained was dissolved with CH₂Cl₂ (15 mL), washed with a saturated NaHCO₃ solution (2x 10 mL), and dried under Na₂SO₄. After evaporation of the solvent, 1.00 g (3.15 mmol) of the product was obtained in a 40% yield.

¹H NMR (300 MHz, CDCl₃, δ): 9.21 (br s, NH, 1H), 7.38 (t, *J*= 2.0, ArH, 1H), 7.24 (ddd, *J*= 8.0, 1.9, 1.0, ArH, 1H), 7.15 (t, *J*= 8.1, ArH, 1H), 7.09 (s, ArH, 2H), 6.64 (ddd, *J*= 8.1, 2.5, 1.0, ArH, 1H), 3.82 (s, OCH₃, 3H), 3.69 (s, OCH₃, 6H), 3.68 (s, OCH₃, 3H).

¹³C NMR (75 MHz, CDCl₃): δ 165.9, 159.6, 152.5, 140.4, 139.1, 129.8, 129.1, 112.7, 109.8, 106.1, 104.3, 60.4, 55.5, 54.7.

Dept 135 NMR (75 MHz, CDCl₃): δ 129.5 (CH), 113.0 (CH), 110.2 (CH), 106.5 (CH), 104.6 (CH), 60.7 (CH₃), 55.9 (CH₃), 55.0 (CH₃).

2-Bromo-1-(4-methoxy-3-nitrophenyl)ethanone (43)

Into a round bottom flask containing 15 mL of a CHCl₃ solution of 1-(4-methoxy-3-nitrophenyl)ethanone (2.04 g, 10.5 mmol), 15 mL of a CHCl₃ solution of Br₂ (1.68 g, 10.5 mmol) was added for 15 minutes. After the reaction mixture was stirred for 2 h, water (20 mL) was added and the organic phase was washed twice with water, once with brine and dried under Na₂SO₄. After the solvent was evaporated, the solid obtained was purified by recrystallization with EtOH to afford 1.79 g (6.53 mmol) of the product in a 64% yield.

^1H NMR (300 MHz, CDCl_3 , δ): 8.47 (d, $J= 2.3$, ArH, 1H), 8.20 (dd, $J= 8.9, 2.3$, ArH, 1H), 7.19 (d, $J= 8.9$, ArH, 1H), 4.38 (s, CH_2 , 2H), 4.05 (s, OCH_3 , 3H).

GC MS m/z (% relative intensity, ion): 275 (3, $\text{M}^+ + 2$), 273 (3, M^+), 180 (100), 105 (16), 90 (9), 76 (9).

N-(3-Methoxyphenyl)acetamide (**44**)

Into a round bottom flask containing 3-methoxyaniline (1.06 g, 8.55 mmol), 1.6 mL of triethylamine (1.14 g, 11.3 mmol), and DMAP (0.106 g, 0.85 mmol), 25 mL of CH_2Cl_2 was added and the contents were stirred under nitrogen gas for 15 minutes before adding 1.1 mL of acetic anhydride (1.18 g, 11.5 mmol). After the reaction was stirred for 16.5 h, water (20 mL) was added and the organic phase was washed once with brine followed by drying under Na_2SO_4 . After the solvent was evaporated, the solid formed was recrystallized with Et_2O - EtOAc to afford 1.20 g (7.27 mmol) of the product in an 84% yield.

^1H NMR (300 MHz, CDCl_3 , δ): 7.42 (br s, NH, 1H), 7.28 (t, $J= 2.2$, ArH, 1H), 7.20 (t, $J= 8.1$, ArH, 1H), 6.97 (dd, $J= 8.0, 1.1$, ArH, 1H), 6.66 (ddd, $J= 8.3, 2.4, 0.7$, ArH, 1H), 3.79 (s, OCH_3 , 3H), 2.18 (s, COCH_3 , 3H).

GC MS m/z (% relative intensity, ion): 165 (68, M^+), 123 (100), 94 (38).

N-(5-Methoxy-2-nitrophenyl)acetamide (**45**)

Acetic anhydride (55 mL) was poured into a flask containing acetamide **44** (5.76 g, 34.9 mmol), and the solution was stirred at 0 °C before adding 22.2 mL of a 0 °C mixture of AcOH (19.2 g, 320 mmol) and HNO_3 (c) (3.93 g, 62.4 mmol) during a 10-

minute period. After the reaction mixture was stirred for 15 minutes, it was poured into ice-water (200 mL) and cooled at 0 °C for an hour, at which point, the green solid formed was filtered, and the product was extracted twice from the filtrate with CH₂Cl₂. The resultant organic phase was washed with brine, dried under Na₂SO₄, and the solvent evaporated to afford a red solid. Both solids were mixed together and purified by flash chromatography (15% EtOAc/ 85% hex) to obtain 3.06 g (14.6 mmol) of the product in a 42% yield.

¹H NMR (300 MHz, CDCl₃, δ): 10.75 (br s, NH, 1H), 8.43 (d, *J*= 2.8, ArH, 1H), 8.20 (d, *J*= 9.5, ArH, 1H), 6.65 (dd, *J*= 9.5, 2.8, ArH, 1H), 3.90 (s, OCH₃, 3H), 2.29 (s, COCH₃, 3H).

¹³C NMR (75 MHz, CDCl₃): δ 169.4, 165.8, 137.8, 129.4, 128.1, 110.8, 104.2, 56.1, 25.9.

GC MS *m/z* (% relative intensity, ion): 210 (30, M⁺), 168 (78), 164 (100), 138 (45), 122 (25).

Mp 126.5 °C (126.0- 127.0 °C)

5-Methoxy-2-nitroaniline (46)

Into a round bottom flask containing acetamide **45** (0.187 g, 0.892 mmol), 5 mL of boiling water was added and the mixture was refluxed for 30 minutes before adding 0.51 mL of concentrated HCl (0.223 g, 6.12 mmol). After the reaction mixture was refluxed for 15 h, a saturated solution of K₂CO₃ was added until the solution became neutral. The heterogeneous mixture was cooled at 0 °C for an hour and the solid formed was filtered and dried under vacuum to afford 0.146 g (0.869 mmol) of the product in a 97% yield.

^1H NMR (300 MHz, CDCl_3 , δ): 8.06 (d, $J=9.5$, ArH, 1H), 6.28 (dd, $J=9.5, 2.6$, ArH, 1H), 6.20 (br s, NH, 2H), 6.14 (d, $J=2.6$, ArH, 1H), 3.82 (s, OCH₃, 3H).

^1H NMR (300 MHz, acetone- d_6 , δ): 7.99 (d, $J=9.6$, ArH, 1H), 7.10 (br s, NH, 2H), 6.50 (d, $J=2.7$, ArH, 1H), 6.28 (dd, $J=9.5, 2.7$, ArH, 1H), 3.83 (s, OCH₃, 3H).

^{13}C NMR (300 MHz, acetone- d_6): δ 166.2, 149.3, 128.6, 107.0, 100.1, 56.1

Dept 45 NMR (300 MHz, acetone- d_6): δ 128.6, 107.0, 100.0, 56.1

GC MS m/z (% relative intensity, ion): 168 (100, M^+), 138 (27), 122 (23), 107 (14), 95 (18), 79 (16), 52 (16).

1-(5-Methoxy-2-nitrophenyl)-2-(4-methoxyphenyl)-1H-azirene (47).

Into a 3-neck round bottom flask containing a 100 °C mixture of aniline **46** (1.34 g, 7.99 mmol) and 25 mL of *N,N*-dimethylaniline, 5 mL of a CH_2Cl_2 solution of 2-bromo-1-(4-methoxyphenyl)ethanone (1.00 g, 4.23 mmol) was added, and the mixture was refluxed at 190 °C for 24 h under nitrogen atmosphere. After the reaction mixture was cooled at room temperature, CH_2Cl_2 (15 mL) and a 10% HCl solution (15 mL) were added, and the resultant organic phase was washed with water, brine and dried under Na_2SO_4 . The product was isolated from the crude reaction mixture by flash chromatography (10% EtOAc/ 90% hex) to obtain a solid which was further recrystallized with hex/ EtOAc to obtain 0.230 g (0.772 mmol) of the product in an 18% yield.

^1H NMR (360 MHz, CDCl_3 , δ): 9.12 (br s, NH, 1H), 8.13 (d, $J=8.9$, ArH, 2H), 7.95 (d, $J=9.1$, ArH, 1H), 7.39 (d, $J=2.7$, ArH, 1H), 7.34 (dd, $J=9.1, 2.8$, ArH, 1H), 7.06 (d, $J=8.9$, ArH, 2H), 3.98 (s, OCH₃, 3H), 3.89 (s, OCH₃, 3H).

^{13}C NMR (75 MHz, CDCl_3): δ 161.4, 161.0, 151.6, 144.0, 140.5, 137.4, 130.0, 129.5, 128.9, 122.3, 114.6, 106.8, 55.8, 55.4.

Dept 45 NMR (75 MHz, CDCl_3): δ 140.5, 130.0, 128.9, 122.3, 114.6, 106.8, 55.8, 55.4.

Dept 90 NMR (75 MHz, CDCl_3): δ 140.5, 130.0, 128.9, 122.3, 114.6, 106.8.

Dept 135 NMR (75 MHz, CDCl_3): δ 140.5 ($\underline{\text{C}}\text{H}$), 130.0 ($\underline{\text{C}}\text{H}$), 128.9 ($\underline{\text{C}}\text{H}$), 122.3 ($\underline{\text{C}}\text{H}$), 114.6 ($\underline{\text{C}}\text{H}$), 106.8 ($\underline{\text{C}}\text{H}$), 55.8 ($\underline{\text{C}}\text{H}_3$), 55.4 ($\underline{\text{C}}\text{H}_3$).

Biological and Biochemical Evaluation

The biological and biochemical activity of the compounds synthesized in the present research work were evaluated through a collaborative effort with Dr. Mary Lynn Trawick (Baylor University, Waco, Texas) and Dr. Ernest Hamel (National Cancer Institute, Frederick, Maryland) who performed the inhibition of tubulin assembly assays. The cancer cell growth inhibitory activity assays with selected human cancer cell lines which were carried out in the laboratory of Dr. George Pettit (Arizona State University). The evaluation of the *in vitro* cytotoxicity using MTT and the *in vivo* blood flow reduction studies were carried out in the laboratory of Dr. Klaus Edvardsen (University of Lund, Sweden).

Tubulin Polymerization Assay

Tubulin was purified from calf brain according to the method of Hamel and Lin.⁵⁰ This method is based on six selective polymerization / cold depolymerization cycles. Tubulin purity was determined by SDS-PAGE and by its ability to polymerize. The purified tubulin was flash frozen and stored in liquid nitrogen. The tubulin concentration

was determined by a two-component⁵¹ analysis using the absorption measured at 278 and 255 nm and the following extinction coefficients: for tubulin, $1.2 \text{ L g}^{-1} \text{ cm}^{-1}$ at 278 nm (Harrison et al.)⁵² and $0.65 \text{ L g}^{-1} \text{ cm}^{-1}$ at 255 nm; for GTP, 12.17×10^3 and $7.66 \times 10^3 \text{ M}^{-1} \text{ cm}^{-1}$ at 255 and 278 nm, respectively. Tubulin polymerization was induced in the presence of organic acid (sodium glutamate) and GTP by a temperature jump to $30 \text{ }^\circ\text{C}$ according to the method of Verdier-Pinard et al.^{53,54} Polymerization was followed turbidimetrically at 350 nm on an Agilent 8453 spectrophotometer equipped with kinetics program software, a jacketed cell holder, and two circulating water baths. To ice chilled tubulin at 1.0 mg / mL in 1.0 M glutamate, pH 6.6 ($10 \mu\text{M}$), pure DMSO (4% v/v final concentration) was added for the control or $2.5 - 1000 \mu\text{M}$ of the analog to be analyzed in DMSO, giving a final concentration of $0.1 - 40.0 \mu\text{M}$ compound in a total volume of $200 \mu\text{l}$ of reaction mixture. The mixture was incubated at 30°C for 15 min and cooled at 0°C for 15 min. An aliquot of 10mM GTP (final concentration of 0.4mM), was added to the reaction mixture on ice, mixed, and immediately transferred into a pre-cooled $250 \mu\text{l}$ quartz microcuvette. The baseline was established at 350 nm at 0°C and after 100 seconds, polymerization was initiated by a temperature jump to 30°C . After 1500 seconds, the cell was cooled to 0°C to induce depolymerization. Turbidity (Absorbance) readings were recorded every 10 s. IC_{50} values of the various analogs were determined from the data using nonlinear regression analysis with the Prism software (GraphPad) 3.02 version.

MTT Assay

The MTT cell proliferation assay was used to quantify the cell viability, measuring cell survival and proliferation spectrophotometrically.⁵⁵ This colorimetric assay measures the reduction of 3-(4,5-dimethylthiazol-2-yl)-2,5-diphenyl tetrazolium bromide (MTT), reflecting the changes in cell proliferation. The mechanism of this assay involves the cleavage of the tetrazolium ring by active mitochondria in living cells, producing a dark blue formazan product which can be quantified in a rapid colorimetric fashion. The reduction of MTT can only occur with living cells containing active mitochondria. Comparison of the cells treated with the drug to an untreated control group provides the relative cytotoxicity, reflecting the loss of cell viability as MTT reduction decreases. Heart endothelioma cells (MHEC5-T) from mice were exposed to serial dilutions of the reported compounds, and cell viability was determined after incubation at 37 °C at one hour and at 5 days by the MTT method, yielding the drug concentration which reduced cell viability by 50% of the control (IC₅₀).

In Vitro Cytotoxicity Studies

Some of the synthesized compounds were tested for inhibition of human cancer cell growth by using National Cancer Institute's standard sulforhodamine B (SRB) assay. SRB is a protein-binding dye that binds to the basic amino acids of cellular components, and is used to stain the cells. The cell lines in a suitable medium are preincubated for 24 hours in 96-well microliter plates followed by treatment with serial dilutions of the compounds. After 48 hours, the plates are fixed with trichloroacetic acid and stained with SRB. The solubilized stain is then measured spectrophotometrically, and the GI₅₀ is calculated from optical density data with Immunosoft software.(ref malli)

Blood Flow Reduction

In vivo experiments were performed in the MHEC5-T tumor model established by the injection of cultured MHEC5-T cells into the right flank of SCID mice.¹³⁵ When the established tumor reached the size of 300 mm³ (a mass without the development of necrosis), mice were injected i.p. with doses of the various compounds at 100 mg/kg or 10 mg/kg. At 24 hours after injection, the animals were injected in the tail vein with 0.25 mL of diluted FluoSphere beads (1:6 in physiological saline). The mice were sacrificed 3 minutes thereafter, and cryosections at a thickness of 8 μm were removed from the tumor, heart, liver, spleen, and kidney. These cryosections were directly examined under a fluorescent microscope, providing a blue fluorescence from the injected microbeads. The results were quantified from three sections of three tumors in each group and in each section, recording more than 70% of the area using a microscopic digital camera at 100 x magnification. The computer program Stage Pro (Media Cybernetics, MD) was used to control the picture recording, and image analysis was performed using Image Plus software (Media Cybernetics, MD).

CHAPTER FOUR

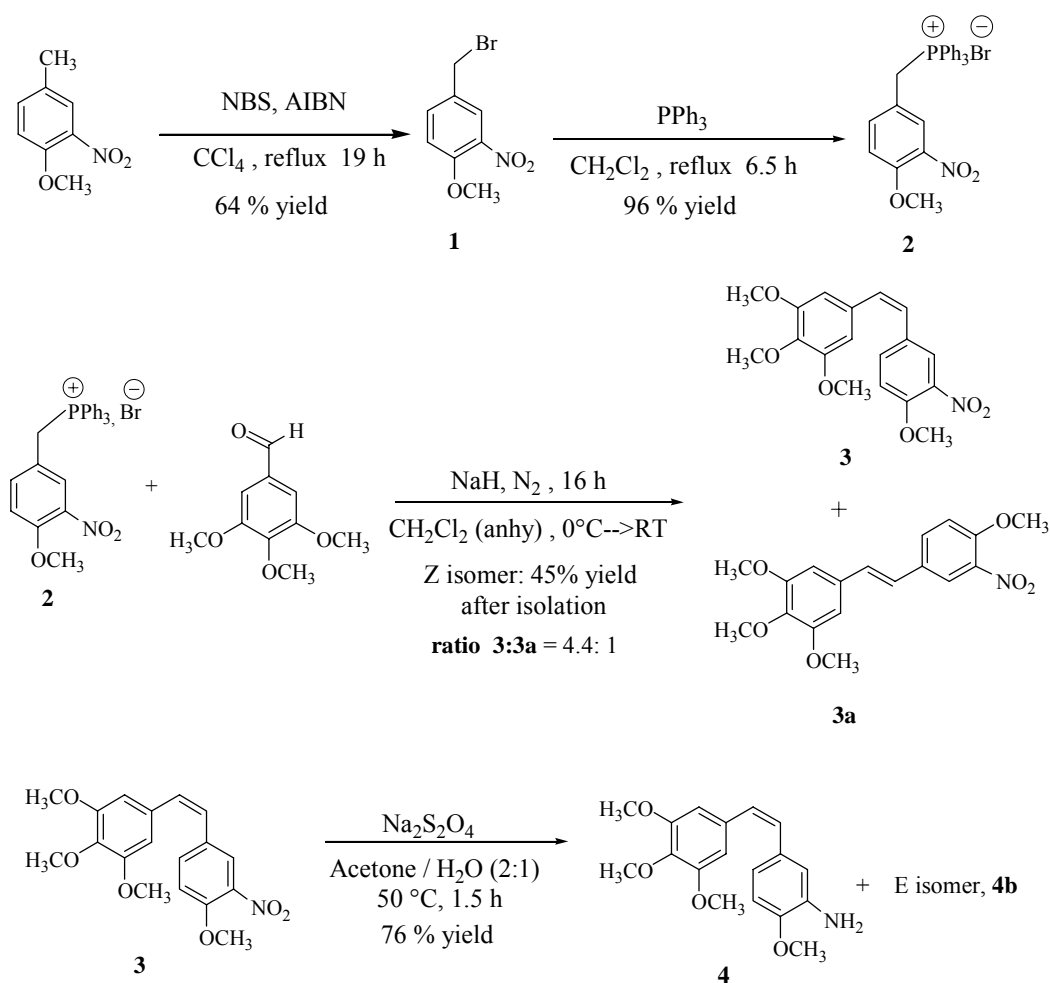
Results and Discussion

In this chapter, the synthesis of different CA-1 and CA-4 combretastatin derivatives and indole-based analogues will be presented. The discussion will first focus on the synthesis of nitrogen-containing derivatives, on which the substitution of the phenol group(s) of CA-1 and CA-4 were replaced by nitro, amino or serinamide moieties. The second part will concentrate on the synthesis of nitro-based epoxide derivatives, on which the double bond of both combretastatins was transformed into the epoxy functionality. Synthetic strategies useful for the radiolabeling of both combretastatins will be discussed in part three of this chapter and, finally, the synthesis of an indole-containing compound will be presented at the end of the chapter. Along with explanations for the synthetic methodologies used for these compounds, important observations of reaction conditions, spectroscopic data, and unexpected product formation will be explained in detail.

Synthesis of Nitrogen-Based Combretastatin A-4

Scheme 4.1 shows the synthesis of the 3'-amino CA-4 analogue **4** which was synthesized following the procedure previously reported by Pinney and co-workers.⁵⁶ Initial bromination of 1-methoxy-4-methyl-2-nitrobenzene with NBS in the presence of AIBN formed monobromide **1** in a 64% yield. It was noted that if the reaction is carried out for more than 19 hours, the yield of the product starts decreasing because of the formation of the dibromo derivative which is the major by-product found under these

reaction conditions. Monitoring of the reaction by GC-MS showed that the reaction mixture at 6.5 h contained 50% of starting material, 46% of the product, and nearly 2% of the dibromo derivative. At 17 h, there was 11% of the starting material, 75% of the product and almost 14% of dibromo analog. At 19 h, the reaction mixture contained 4% of starting material, 81% of the product, and 15% of dibromo analog. Therefore, reaction times longer than 19 h are not needed because the longer reaction times facilitate formation of the undesirable dibromo analog.



Scheme 4.1. Synthesis of 3'-amino CA-4 analogue (compound **4**).⁵⁶

Characterization of the product and the by-product was carried out by analysis of their $^1\text{H-NMR}$ and low-resolution MS. For example, the monobromide derivative showed in its MS two peaks in a ratio 1:1 corresponding to the M^+ (243) and $\text{M}^+ + 2$ (245) demonstrating the presence of just one bromine.^{57,58} The presence of two bromines in the by-product was shown by the typical triplet (ratio 1:2:1) corresponding to M^+ (323) and $\text{M}^+ + 2$ (325) and $\text{M}^+ + 4$ (327).^{57,58} Triphenylphosphonium bromide **2** was obtained in a 96% yield after refluxing bromide **1** with triphenylphosphine for 6.5 h. Its NMR spectrum showed a doublet at 5.98 ppm exhibiting a $J = 14.3$ Hz, a typical value for a two-bond H-P coupling.⁵⁸ The *Z* stilbene **3** was formed by a Wittig reaction of bromide **2** with 3,4,5-trimethoxybenzaldehyde using NaH as the base. The structure assignment of the product was based on the magnitude of the coupling constant measured for the vinylic protons which was $J = 12.1$ Hz, a typical $^3J_{\text{HH}}$ value for *Z* alkenes.^{57,58} Different experiments carried out showed that the reaction is complete after 15 h and longer reaction times are not required. The crude reaction mixture analyzed by GC-MS showed an average *Z-E* ratio of 4.4:1 after work up and the separation of these isomers by flash chromatography allowed characterization of the more polar *E* isomer **3a** by measuring its vinylic coupling constant which gave a value of 16.6 Hz, a typical $^3J_{\text{HH}}$ value for *E* alkenes.^{57,58} Interestingly, as Figure 4.1 shows, the *E* isomer $^1\text{H-NMR}$ has exactly the same patterns in the same sequence as observed for the *Z* isomer; however all the peaks are shifted more downfield presumably because of the anisotropic deshielding produced by the benzene rings.^{57,58} Reduction of the nitro group of stilbene **3** yielded free amine **4** in a 76% yield after refluxing the stilbene with sodium hydrosulfite.^{59,60} Interestingly, when the organic phase (EtOAc) was dried over magnesium sulfate, a pale yellow solid

precipitated. This solid was filtered and purified by recrystallization with EtOAc and different NMR spectrum was obtained (Figure 4.2) to elucidate its structure.

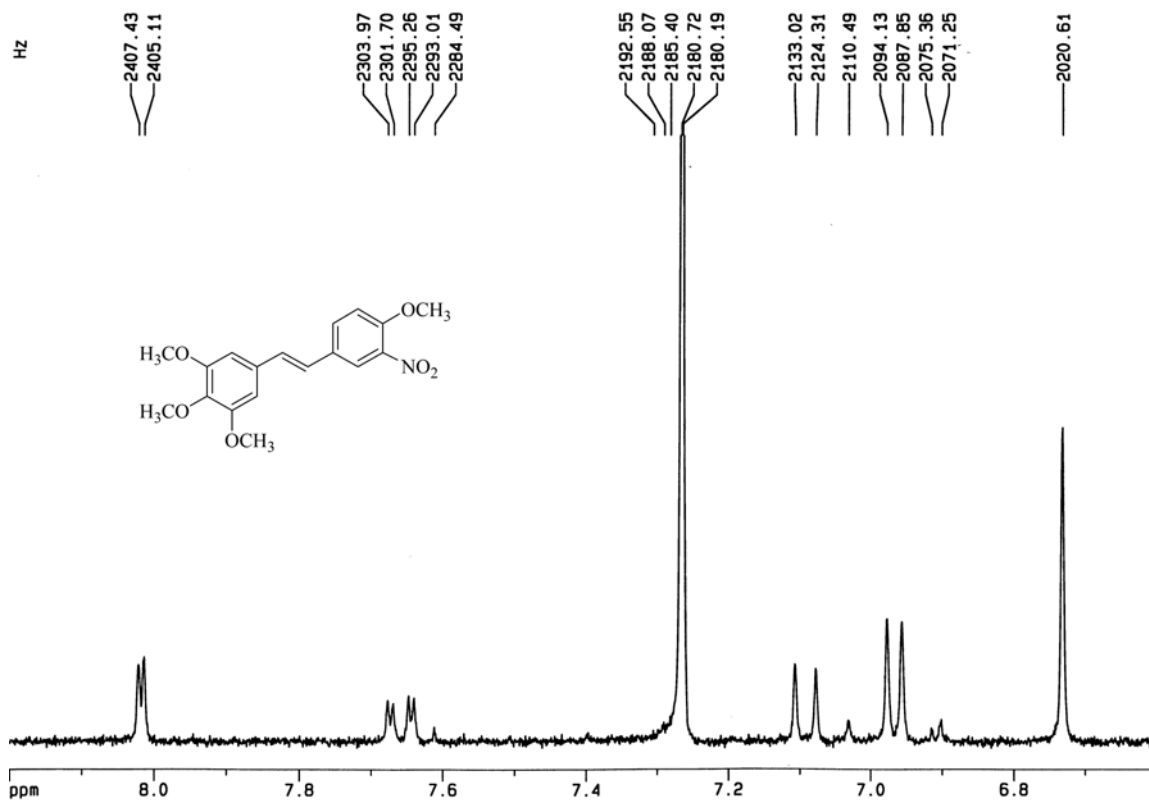


Figure 4.1. Aromatic region of the ^1H -NMR spectrum of *E* isomer **3a**

We were surprised to find that its ^1H and ^{13}C -NMR did not match with the free amine **4** previously reported in the literature.⁵⁶ We postulated that the possible structure belonged to the arylaminium salt **4a** shown in Scheme 4.2 since the only sort of acidic chemical used was the dehydrating agent magnesium sulfate. Comparable to some small highly charged metal ions, Mg^{+2} in water becomes hexahydrated, which in turn suffers a hydrolysis generating hydrogen ions⁶¹ as depicted in part “a” of Scheme 4.2. The positively charged magnesium ion, which is directly attached to the water oxygen,

induces, by an electronic effect, a weakness of the O-H bond making this proton considerably acidic to protonate water.⁶¹ After the hydronium ions are formed, protonation of the free amine takes place to form the salt **4a**. In Figure 4.2, it is clearly seen how an increment in the concentration of the sample shifts downfield the peak for the hydrogens attached to the nitrogen suggesting an increment in the strength of the hydrogen bond associated with this compound.

In order to test the hypothesis we decided to treat this solid with a base with the hope of regenerating the free amine **4**. Approximately 98 mg of the solid was treated with 0.8 mL of a 10% solution of NaOH followed by extraction of the product with Et₂O. The ethereal phase was dried, this time with sodium sulfate, evaporated, and another ¹H-NMR was taken which showed a direct match with the expected NMR. Therefore, this demonstrated the hypothesis and illustrated the care we must employ when drying acid-sensitive groups like amines.⁶²

One important observation in the ¹H-NMR of the aminium salt **4a** is that the aromatic protons, which are more downfield than their respective protons in the free amine, have unusually broad peaks making it difficult to easily recognize the patterns for each type of hydrogen. In addition, the two vinyl hydrogens are accidentally equivalent giving a second-order pattern. At first glance, it seems that the two doublets appear as a singlet but careful analysis of the spectrum shown in Figure 4.2 reveals the presence of two tiny peaks located on each side of the peak at 6.33 ppm.

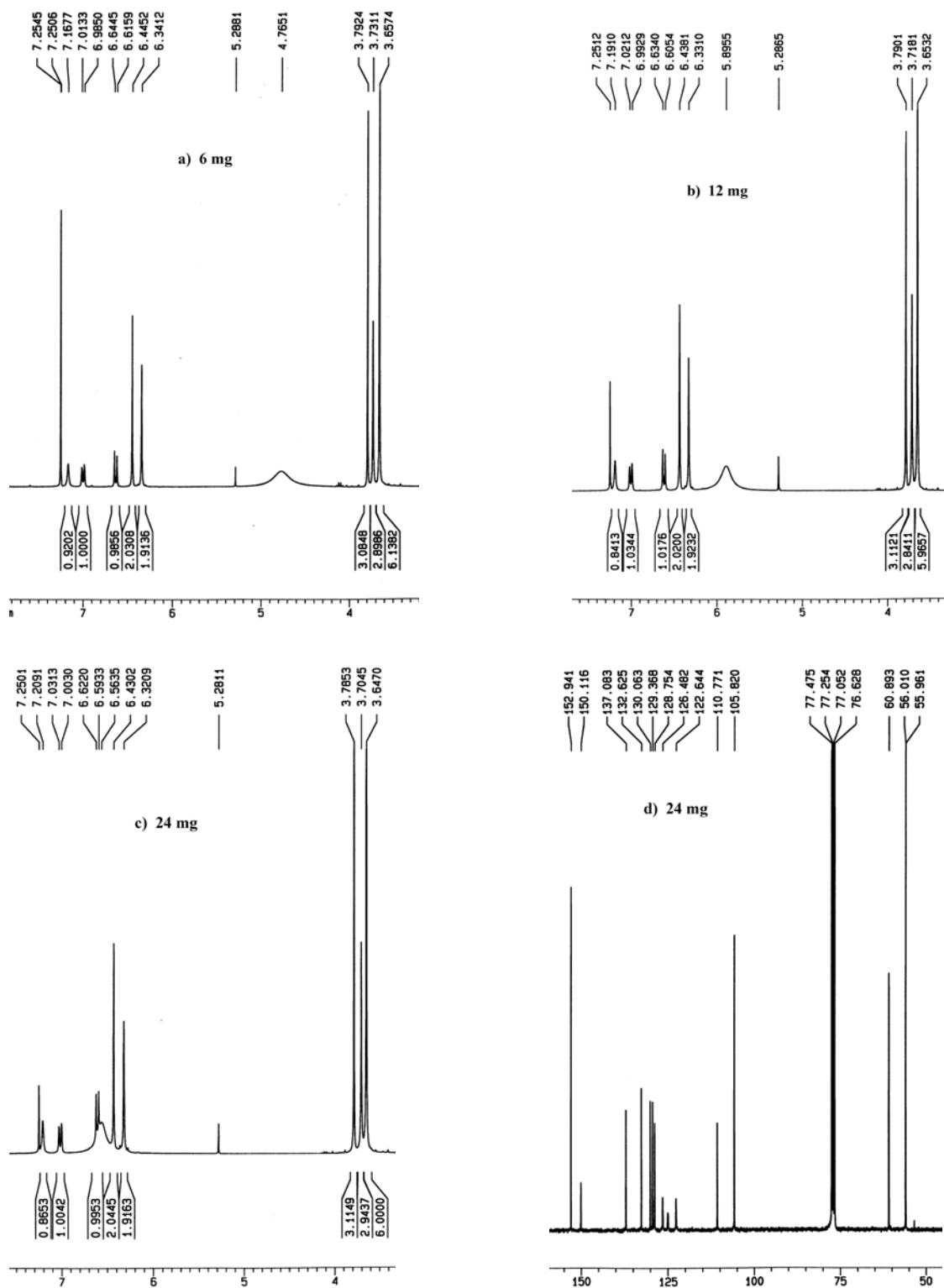
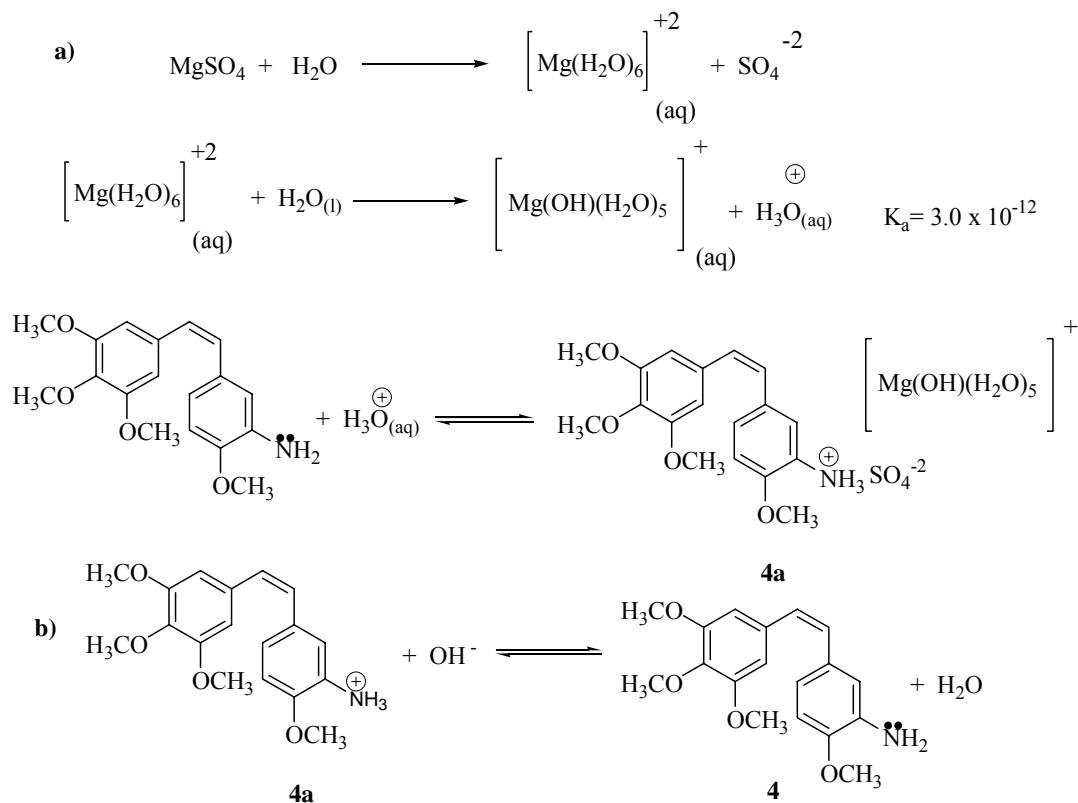


Figure 4.2. ¹H-NMR spectrum of the unknown yellow solid (salt **4a**) taken at different concentrations in CDCl₃. a) 6 mg b) 12 mg and c) 24 mg d) ¹³C-NMR taken from 24 mg of sample. All the samples were prepared using the same volume of CDCl₃.



Scheme 4.2. Generation of hydrogen ions in an aqueous magnesium sulfate solution.⁶¹
 a) protonation of free amine **4**. b) Neutralization of the ammonium salt with NaOH to regenerate free amine **4**.

The *E* isomer **4b** was separated from the crude reaction mixture to confirm the structure of compound **4**. Figure 4.3 shows the expanded aromatic region of the ¹H-NMR spectrum of the *E* isomer before and after applying resolution enhancement. It is clearly seen that resolution enhancement of these peaks aided in determining the different coupling patterns for each proton in the structure of this isomer. Careful analysis of this set of peaks, shown in the bottom spectrum of Figure 4.3, allowed for the identification of two doublets of about $J = 16.1$ Hz (2078.4 Hz - 2062.4 Hz and 2058.7 Hz - 2042.4 Hz) indicating that the structure belongs to the *E* isomer.^{57,58} Note also, that free amine **4b** has all its aromatic hydrogens located more downfield than the respective *Z* isomer **4** probably because these protons are in the deshielding cone of the two benzene rings.

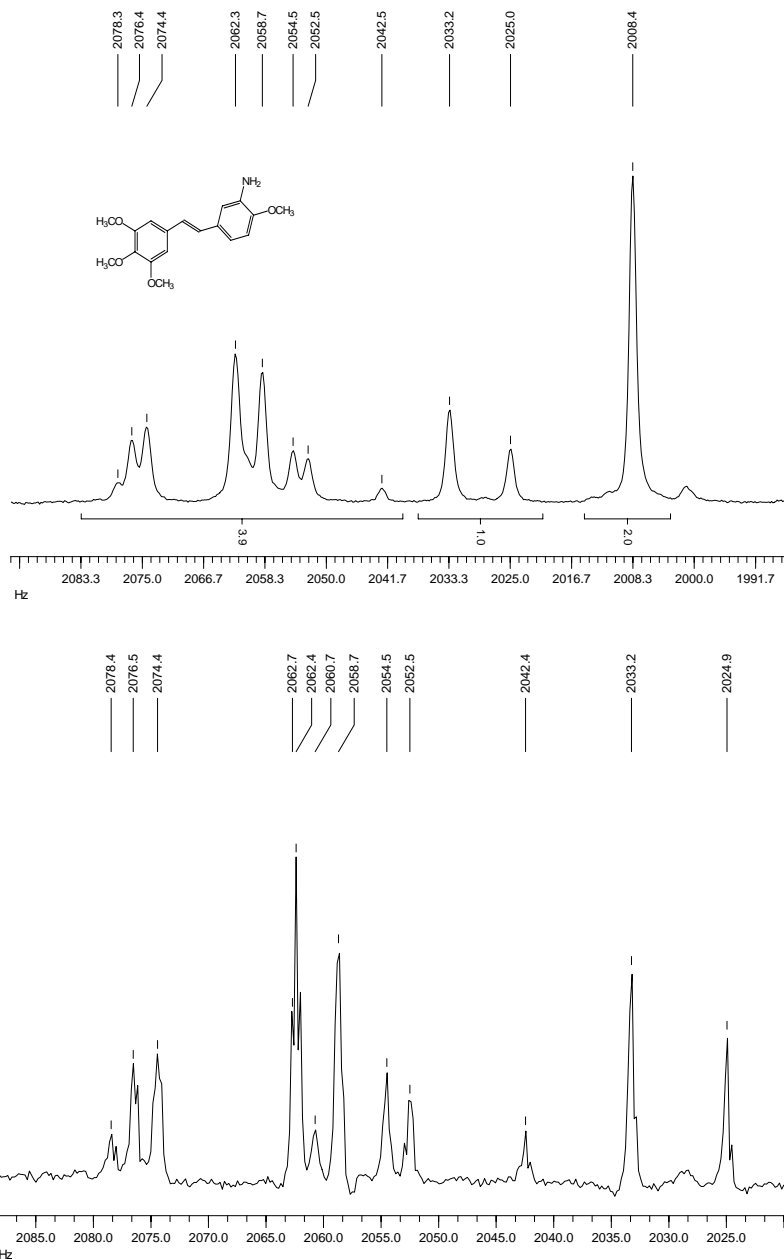
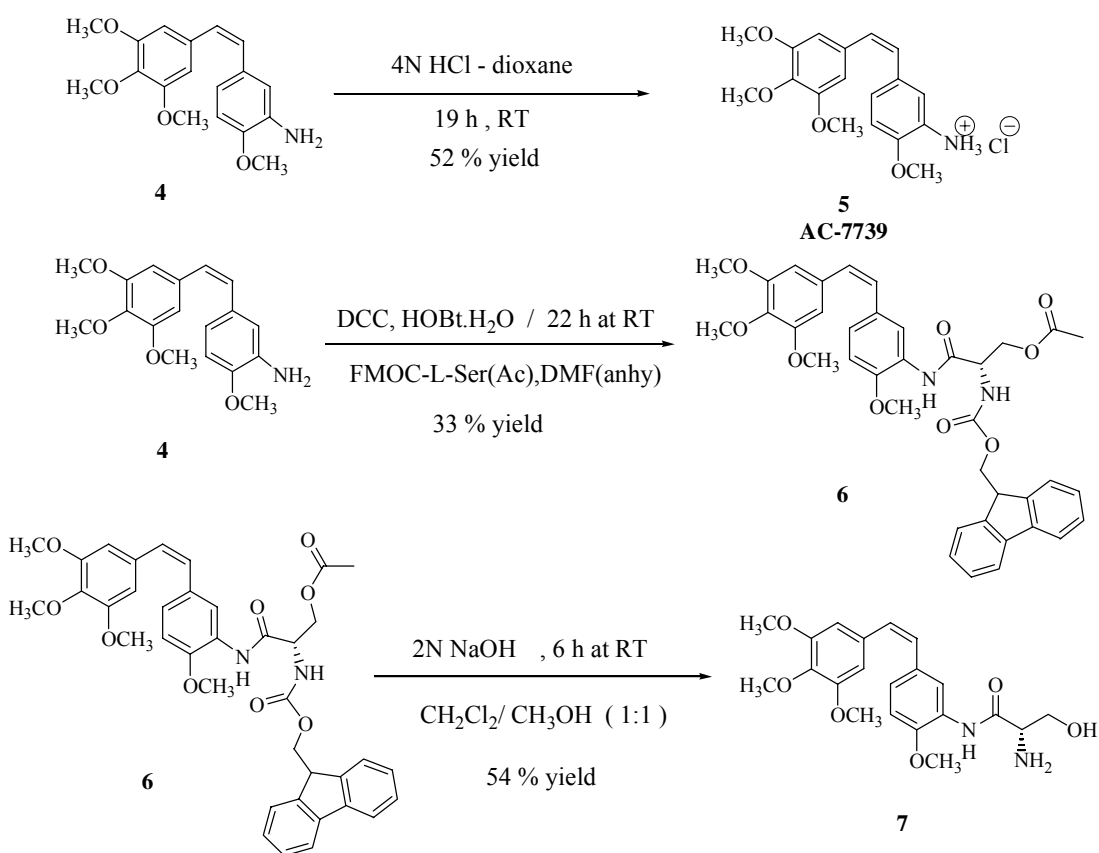


Figure 4.3. Expanded aromatic regions of the 300 MHz ^1H -NMR spectrum of *E* isomer **4b**. The top spectrum corresponds to the spectrum before applying resolution enhancement while the bottom spectrum was obtained after enhancement of its resolution.

Following a procedure developed by Ohsumi and co-workers,^{63,64} acidification of the free amine **4** was performed with a 4N HCl solution in dioxane to form the respective hydrochloride salt **5** in a 52% yield. This compound, which is known today as AC-7739,

was presented publically for the first time by the Ajinomoto pharmaceutical company group and later by Pinney and co-workers independently.⁵⁶ Because of its outstanding properties as a VDA, The Ajinomoto researchers directed their efforts towards the synthesis of different amino acid-based combrestastatin A-4 analogues. One of them, AC-7700 (AVE8062), which is the hydrochloride salt of the serinamide **7**, which has been introduced in clinical development by Aventis Inc.⁶⁵⁻⁷⁵



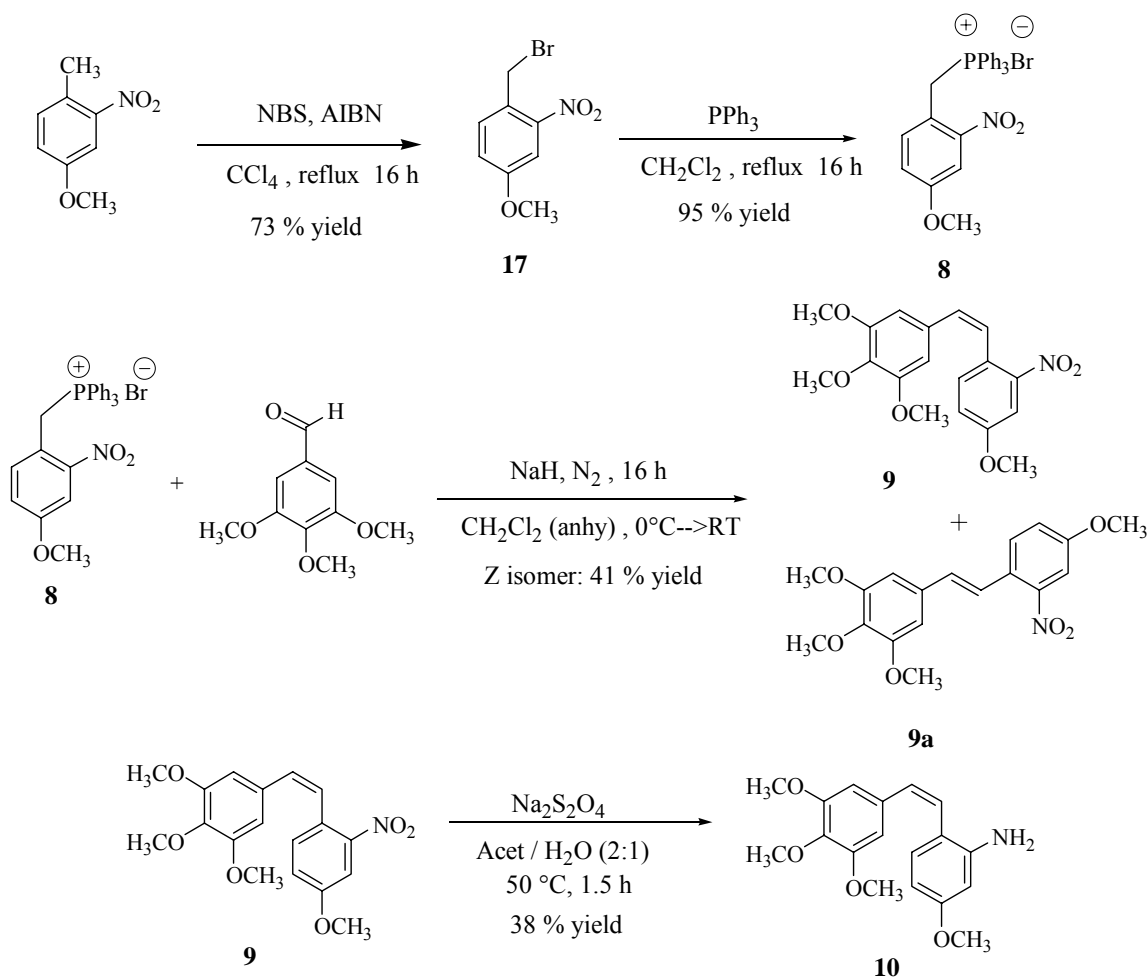
Scheme 4.3. Synthesis of AC-7739 and the serinamide CA-4 analogue **7**.^{63,64}

The synthesis of serinamide **7** involved initial reaction of amine **4** with Fmoc-L-Ser(Ac), DCC and HOBT to form, in a 33% yield, the protected Fmoc serinamide **6** which in turn, after reacting with an aqueous 2N-NaOH solution, formed the aminoacid

analogue **7** in a 54% yield.^{63,64} One important observation in the ¹H-NMR spectrum of compound **7** is that the methine hydrogen attached to the chiral α -carbon that contains the amine group appears as a broad triplet. However these peaks most likely correspond to an overlap of a doublet of doublets of $J= 5.0$ Hz because the methylene hydrogens are not magnetically equivalent as a consequence of the adjacent chiral center. In fact, although it is not easy to see, all of the peaks for these two hydrogens (overlapping two methoxy groups) appear as a doublet of doublet.

Encouraged by the potential anticancer activity of AC7739 and AC7700, we decided to synthesize the 2'-nitrogen analogue^{76,77,89} to compare its activity against the 3'-isomer giving further insights into the structural requirements for the interaction of these agents with tubulin.

The synthesis of free amine **10**, which is shown in Scheme 4.4, starts with the benzylic bromination of 4-methoxy-1-methyl-2-nitrobenzene using the same procedure already described for the 3'-isomer.⁵⁶ Monitoring of the reaction mixture was performed by GC-MS and indicated that carrying out the reaction for more than 17 h was not recommended due to the conversion of the monobromide into its dibromo derivative. For instance, after 17 h the average composition of the crude mixture was 7% of starting material, 88% of bromide **17**, and 5% of the dibromo derivative. However, when the reaction was allowed to proceed for 20, 22 and 35 h the crude mixture contained (in each case) 6% of starting material, 80% of monobromide, and 14% of dibromide. As noted from these data, no further conversion of the starting material occurs however further reaction of the desired product takes place decreasing its yield.



Scheme 4.4. Synthesis of 2'-amino CA-4 analogue (compound 10).⁷⁶

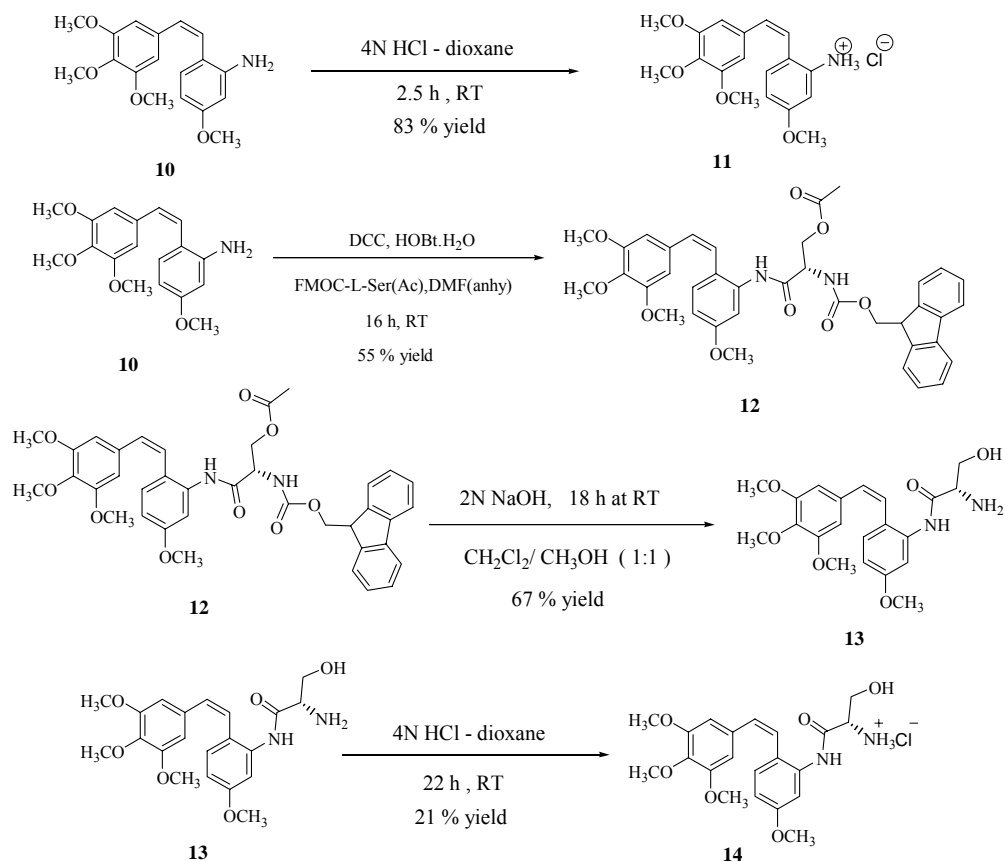
The low-resolution MS of bromide **17** showed the presence of two peaks in a ratio of 1:1 (M^+ and $M^+ + 2$) indicating that the molecule has just one bromine atom. By the other hand, the existence of two bromine atoms was deduced by the presence of a triplet in a ratio of 1:2:1 corresponding to the peaks $M^+ = 323$, $M^+ + 2 = 325$ and $M^+ + 4 = 327$.

After bromide **17** was treated with triphenylphosphine for 16 h, triphenylphosphonium bromide **8** was formed in a 95% yield. Its $^1\text{H-NMR}$ spectrum, like isomer **2**, showed the expected $J = 14.3$ Hz, indicating the coupling between hydrogen and phosphorous.^{57,58} A Wittig reaction of phosphonium salt **8** and 3,4,5-

trimethoxybenzaldehyde produced *Z* stilbene **9** and its *E* isomer **9a** in a 1:1 ratio. Careful flash chromatography of the crude reaction mixture made it possible to separate these isomers to obtain the *Z* stilbene in a 41% yield. Both structures were again assigned based on the values of the coupling constants of the vinylic protons, almost 12 Hz for the *Z* isomer and 16 Hz for the *E*.^{57,58} Reduction of the nitro group of stilbene **9** was performed using sodium hydrosulfite^{59,60} giving the free amine **10** in a 38% yield. Formation of the hydrochloride salt **11** in an 83% yield was achieved by treating the free amine **10** with a 4N HCl solution in dioxane using CH₂Cl₂ as a solvent as shown in Scheme 4.5.

The synthesis of the 2'-serinamide CA-4 analogue **13** and its hydrochloride salt **14** was achieved by incorporating first the protected serinamide moiety into the free amine **10** by reacting with Fmoc-L-Ser(Ac), DCC and HOBT in DMF followed by basic hydrolysis of this intermediate **12** with a 2N NaOH aqueous solution^{63,64} to afford serinamide **13** in a 67% yield. Finally, acidification of serinamide **13** produced its hydrochloride salt in a 21% yield after stirring at room temperature with a 4N HCl solution using CH₂Cl₂ as a solvent.

Interestingly, the ¹H-NMR (CD₂Cl₂) spectrum of compound **13** as compared to its 3'-isomer **7** showed a good separation of the peaks that belong to the methylene which contains the hydroxyl group. Because these hydrogens, H_a and H_b, are attached to a carbon adjacent to a chiral center, we expect them to be magnetically non-equivalent and appear as a double of doublets. In fact, this is exactly what Figure 4.4 shows and this observation allows calculating two different values for the two possible coupling constants.



Scheme 4.5. Synthesis of 2'-serinamide CA-4 analogue **13** and hydrochloride salts **11** and **14**.⁷⁶

One constant has $J = 10.7$ Hz (1101.8-1091.1 Hz) and the other has $J = 5.5$ Hz (1101.8-1096.3 Hz). The former is the value associated with a coupling between geminal hydrogens (H_a and H_b) separated one from the other with an approximate angle of 110° according to Karplus's graph,^{57,58,78} while the second coupling constant can be associated with a vicinal coupling between H_c and both H_a and H_b . Based on Karplus's equation, a range of angles between 45° and 135° can satisfy this requirement.^{57,58,78}

A stable conformation for the structure of compound **13** was obtained by using a semiempirical method called MOPAC⁷⁹ in order to measure distances, angles, and to see how the different hydrogens of analysis are orientated in three dimensional space.

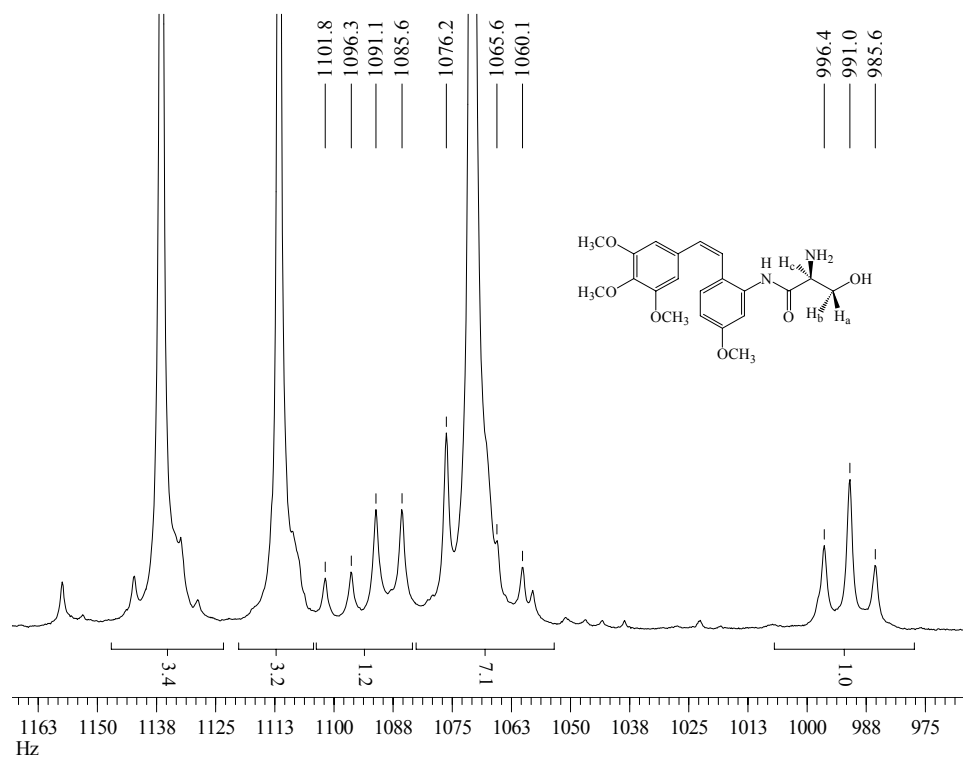


Figure 4.4. Expanded region of the $^1\text{H-NMR}$ (CD_2Cl_2) spectrum of compound **13** showing the methine hydrogen H_c and the two magnetically nonequivalent methylene hydrogens H_a and H_b . Note that both, H_a and H_b , appear as a doublet of doublet at about 1098 and 1070 Hz ; the methine hydrogen H_c , attached to the α -carbon, appears more upfield as a triplet at 991 Hz.

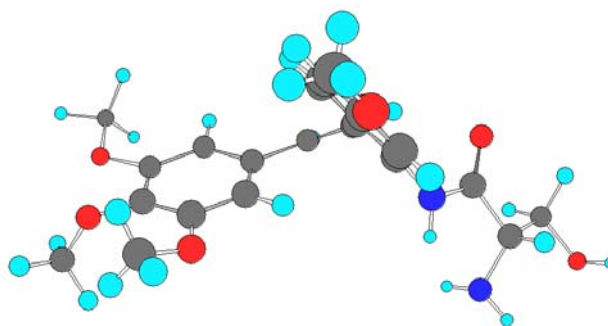


Figure 4.5. Minimum-energy structure of compound **13** generated using the MOPAC method incorporated in CS Chem3D.⁷⁹ The angles between H_c and both H_b and H_a are approximately 58 and 179 degrees. Also there is hydrogen bond (2.52 Å) between one of the amine hydrogens and the oxygen of the hydroxyl group forming a 5-membered ring. It also possible to see another hydrogen bond (2.56 Å) between the amine nitrogen and the amide hydrogen forming another 5-membered ring.

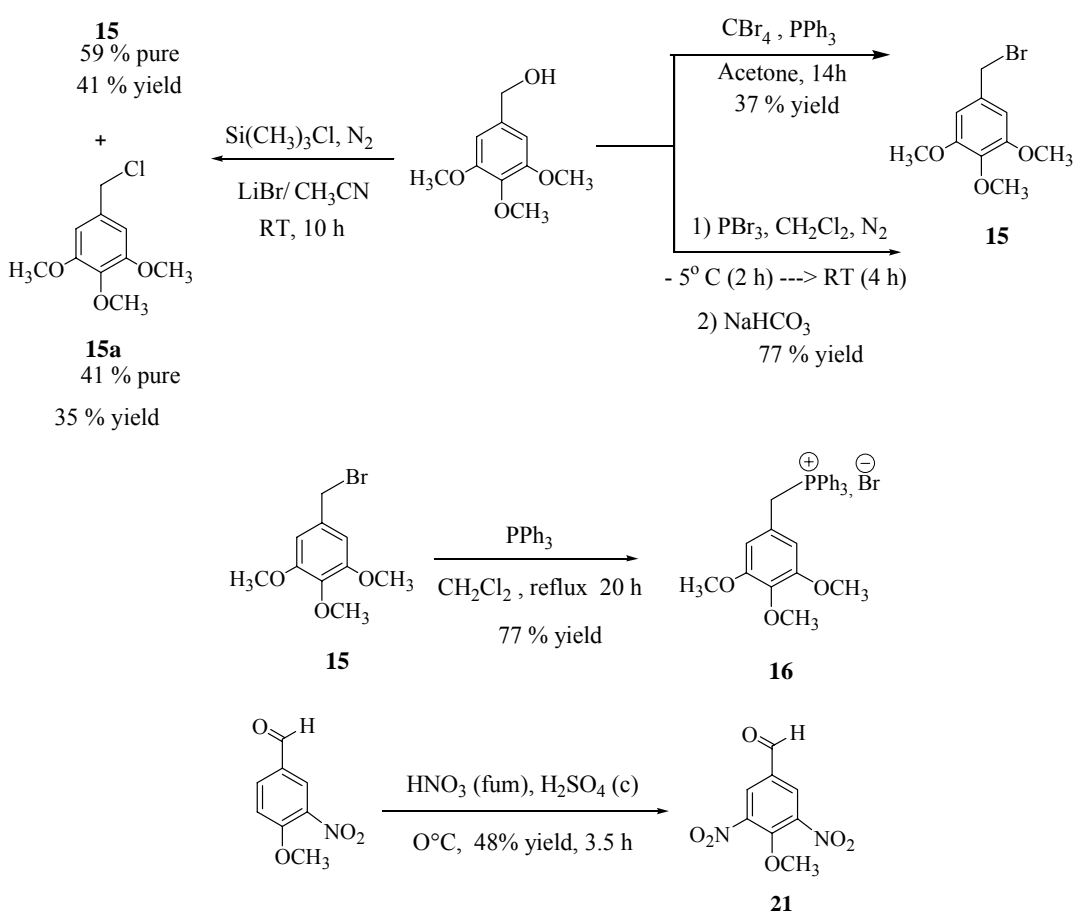
Figure 4.5 shows a conformation from which it was possible to measure the dihedral angles between H_c and both H_a and H_b which are 58° and 179° respectively. In Figure 4.4, it is possible to see that the methine hydrogen H_c appears as a triplet with $J=5.5$ Hz suggesting that the dihedral angle with these two hydrogens is the same. Although the conformation shown in Figure 4.4 demonstrates one angle (179°) that is outside of the predicted range, it is possible that the C-C bond is rotating and on average gives the same dihedral angle for both hydrogens. It is also important to mention that in this particular conformation two hydrogen bonds are observed. The first one involves the bond between the amine hydrogen and the oxygen of the hydroxyl group with a distance of 2.52 \AA ; the second involves the bond between amine nitrogen and the amide hydrogen with a distance of (2.56 \AA). In other conformations it may be possible to see a hydrogen bond between the oxygen carbonyl and either the hydrogens of the amine or hydroxyl group.

Synthesis of Nitrogen-Based Combretastatin A-1

The following discussion details the synthesis of dinitrogen-based analogues of CA-1. Functional groups such as nitro, amino, serinamide and their respective hydrochloride salts were incorporated at positions 2 and 3, 2 and 5, and 3 and 5 of the B-ring of combretastatin CA-1 with the hope of identifying more potent anti-cancer agents. The purpose on this project was to explore how the nature and location of these substituents can ultimately affect inhibition of tubulin assembly and the activity of the resultant compounds.

The key step in the synthetic strategy to prepare dinitrogen-based derivatives was to use a Wittig reaction to form the *Z* isomer. In order to reach this goal, the

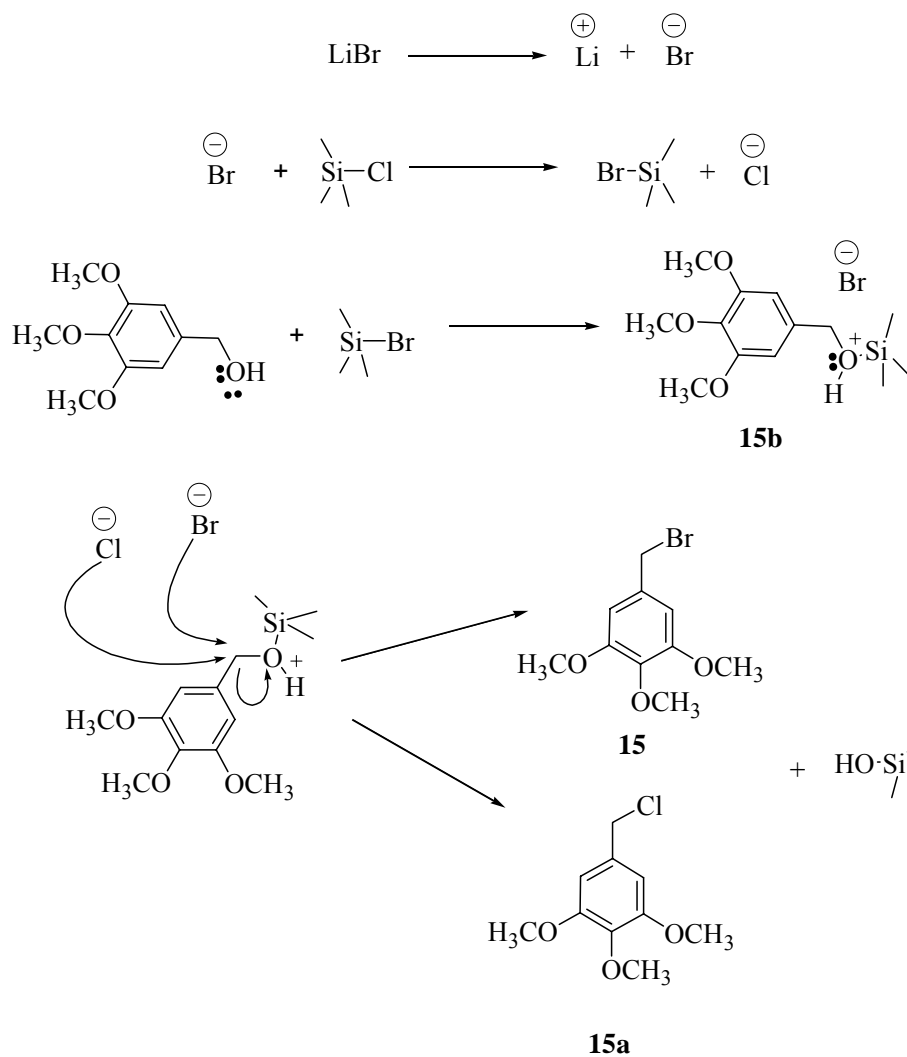
phosphonium bromide fragment⁸⁷ and the aldehyde counterpart which can be assembled using NaH as the base in a Wittig reaction were independently prepared. The aldehyde was designed to contain the nitro groups, which after Wittig reaction can be reduced to the respective amino groups.^{59,60,80-86} The resulting amine analogs subsequently undergo the analogous reactions used to form the serinamide and hydrochloride salt derivatives^{63,64} previously described. In Scheme 4.6, the synthesis of 3,4,5-trimethoxybenzyltriphenylphosphonium bromide⁸⁷ **16** and 4-methoxy-3,5-dinitrobenzaldehyde⁸⁸ **21** is shown.



Scheme 4.6. Synthesis of phosphonium bromide salt⁸⁷ **16** and dinitrobenzaldehyde⁸⁸ **21**.

Benzylic bromide **15** was obtained using three different methods⁹⁰⁻⁹³ which are described below. In the first method, commercially available 3,4,5-trimethoxybenzyl alcohol was reacted with CBr_4 and PPh_3 to form the requisite bromide⁹³ in just 37% yield after stirring for 14 h at room temperature. Because of this low yield and the long reaction time the decision was made to evaluate two other methods to improve both the yield and the reaction time. The second approach^{90,92} involved treating the alcohol with PBr_3 to form highly pure bromide in a 77% yield and just 4 h. The presence of the bromine atom was confirmed by its MS which showed the two expected peaks at 262 ($\text{M}^+ + 2$) and 260 (M^+). Alternatively, a third method was employed in which the alcohol was reacted with TMSCl and LiBr in acetonitrile at room temperature for 10 h.⁹¹ After the reaction was complete, the solid which formed was recrystallized and characterized by $^1\text{H-NMR}$, DEPT 135, and MS. Interestingly, the solid obtained was actually a mixture of two compounds, one of them with a molecular weight of 260, which belongs to the expected product, and the other with a molecular weight of 216. Its MS also showed another peak with m/z of 218 which had approximately one third of the intensity of the molecular ion 216. The DEPT 135 spectrum showed two methylene carbons, one that corresponds to the product and the other (a less intense peak) which is attributed to the impurity. In addition, the same spectrum showed two methine carbons, one for the product and the other for the unknown. The $^1\text{H-NMR}$ showed all the peaks of the bromide derivative along with extra small peak close, to the signal for the product methylene, which belongs to the impurity. It was possible to observe other small peaks that were overlapping the aromatic and methoxy peaks of the product as shown in Figure 4.6. Based on all of these spectroscopic findings the structure of the impurity was

assigned to the chlorine derivative **15a**. The proposed mechanism for the formation of this product is depicted in Scheme 4.7. The first step of this mechanism most likely starts with the dissociation of LiBr in acetonitrile generating lithium cations and bromine anions. In the second step, bromide ions attack TMSCl to displace the chlorine atom as a chloride ion through a substitution mechanism.⁹⁴ In the third step, the trimethyl silyl bromide formed is attacked by the benzylic alcohol through a substitution mechanism releasing a bromide ion and forming protonated silyl ether **15b**.



Scheme 4.7. Proposed mechanism for the formation of benzylic chloride **15a**.⁹⁴

The hydroxyl group of the alcohol has been now converted into a better leaving group which is surrounded by both bromide and chloride ions. It is well known that bromide is a better nucleophile than chloride and the reaction will take place faster with the former than the latter when the reaction goes by an S_N2 mechanism.⁹⁴ Accordingly, the fourth step most likely consists of nucleophilic attack of bromide or chloride to the back side of the protonated silyl ether forming the respective benzylic bromide **15** and the chloride **15a** in a ratio of 1.4: 1 respectively as the GC-MS showed.

In summary, we found that the most suitable method for preparing bromide **15** from the alcohol involved treating the benzylic alcohol with PBr_3 . After bromide **15** reacted with PPh_3 for 20 h, the triphenylphosphonium bromide was formed in a 77% yield.

The dinitrobenzaldehyde **21** was obtained in a 48% yield by nitration of the benzene ring with HNO_3 (fum) and H_2SO_4 (c) after stirring the mixture at 0 °C for 3.5 h.⁸⁸ The crude reaction mixture was actually a mixture of two compounds which were separated afterwards by column chromatography and fully characterized. The first less polar compound isolated showed a molecular weight of 243 and after analyzing carefully its 1H NMR, ^{13}C NMR, DEPT 135, and DEPT 45, it was deduced that this compound was the 4-methoxy-3,5-dinitro benzoic acid. An X-ray structure of this compound confirmed the structural analysis as seen in Figure 4.7 which illustrates the carboxylic acid that crystallizes as a dimer.

The second, more polar compound, showed a molecular mass of 226 which corresponds to the mass of the expected dinitrobenzaldehyde. From its spectrum it was deduced that this compound was the expected 4-methoxy-3,5-dinitrobenzaldehyde **21** in

agreement with the theoretical prediction that the methoxy will direct to its only open ortho position. The ratio of these compounds depends on the reaction time. The reaction was monitored by GC-MS and it was found that in an average at 3.5 h the crude reaction mixture contained 55% of **21** and 45% of the carboxylic acid **21a**. Longer reaction times decreased the amount of aldehyde and increased the amount of carboxylic acid formed.

A Wittig reaction performed with phosphonium salt **16** and aldehyde **21** formed the *Z* stilbene **22** in a 45% yield as Scheme 4.8 shows. The crude reaction mixture, after 2 h, contained (as shown by GC-MS) both the *Z* and *E* isomers in a ratio of 1.9: 1. Both isomers were separated by column chromatography and characterized by NMR; their ¹H-NMR showed a *J*= 12 Hz for the *Z* isomer and *J*= 16.2 Hz for the *E* isomer. Reduction of stilbene **22** was carried out using two different methods. In the first method sodium hydrosulfite was used to form the 3,5-diamine **25** in a 20% yield after refluxing for 4.5 h.^{59,60} However, when Zn in acetic acid was used,⁸⁶ the reduction took place in a 46% yield after stirring at room temperature for 35 minutes. Therefore the second method is more convenient to reduce both nitro groups in better yields and in a shorter period of time.

Hydrochloride salt **27** was formed in a 26% yield after reacting free diamine **25** with a 4N-dioxane solution of HCl.

The synthesis of diserinamide **29**, which is shown in Scheme 4.9, starts with the Fmoc-Ser(Ac) protection of the free diamine to afford compound **28** in a 19% yield. The final serinamide **29** was obtained in a 19% yield after deprotecting the Fmoc-protected stilbene **28** with a 2N solution of NaOH.⁷⁷

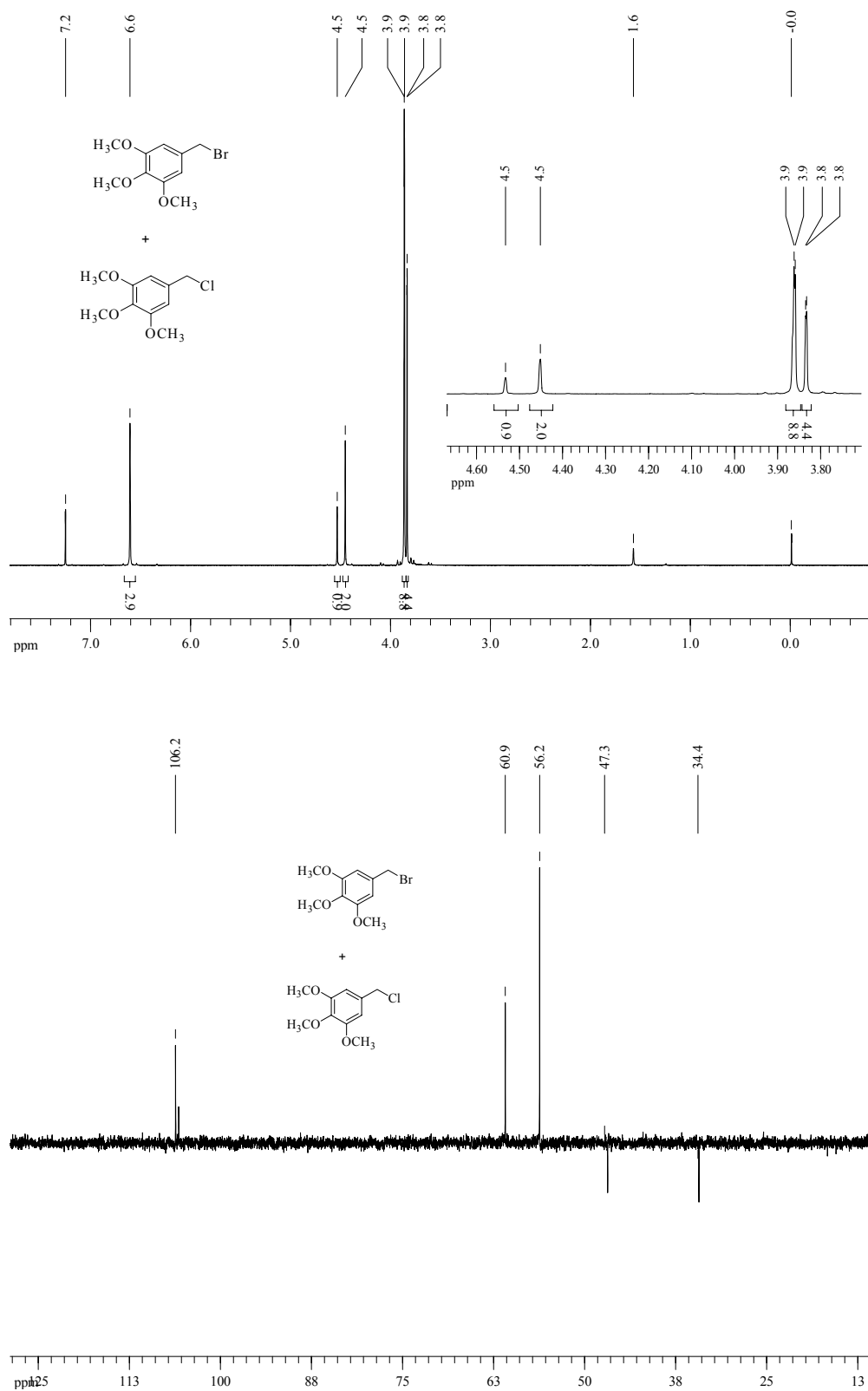


Figure 4.6. $^1\text{H-NMR}$ and DEPT 135 of compound **15a**

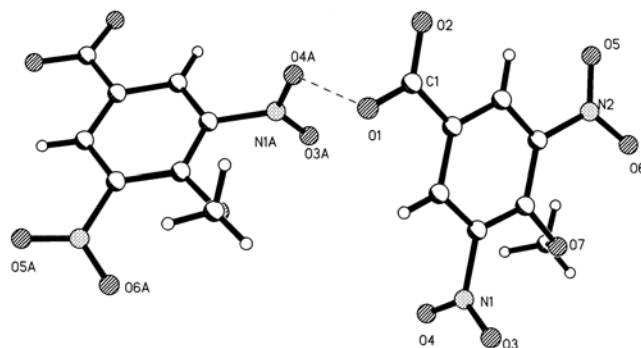
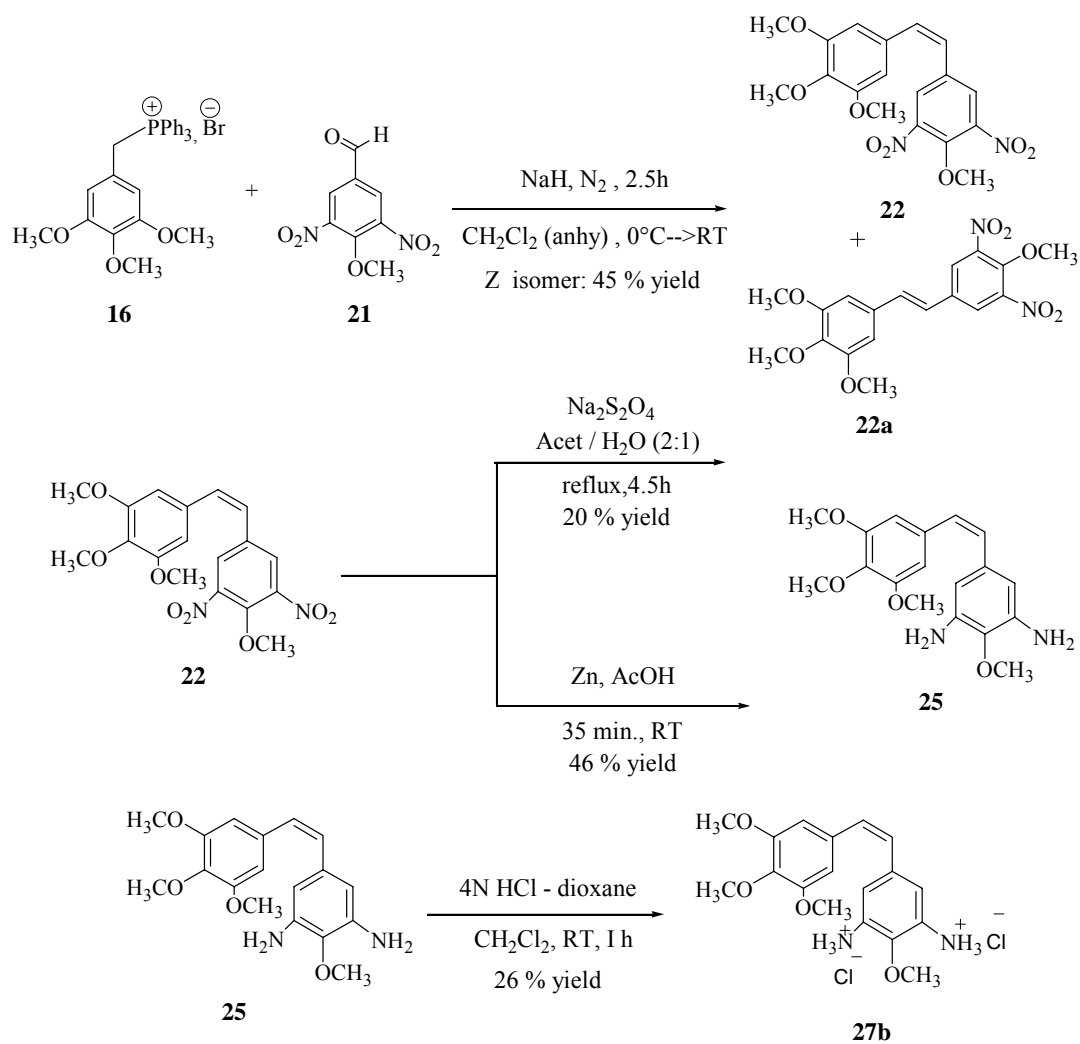
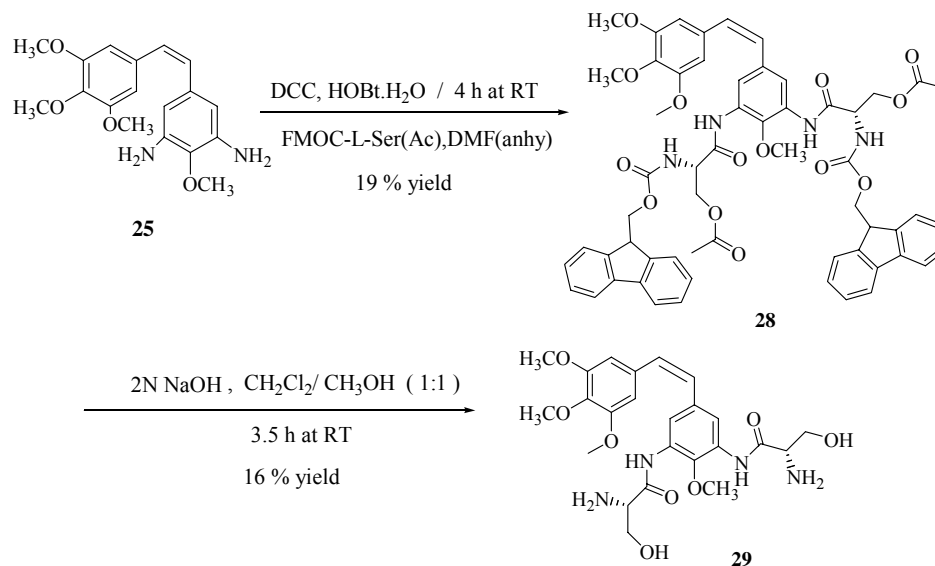


Figure 4.7. X-ray crystal structure of 4-methoxy-3,5-dinitrobenzoic acid.⁹⁵

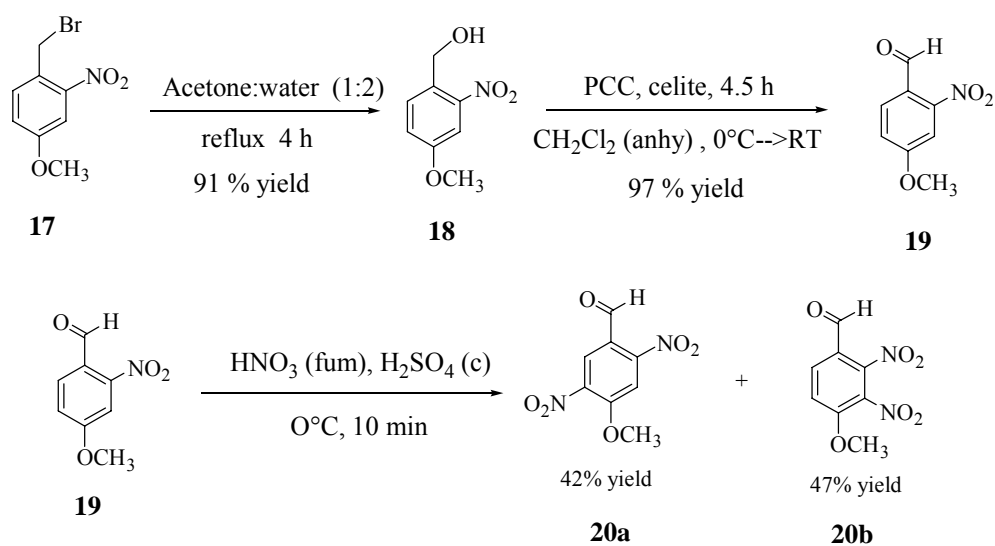


Scheme 4.8. Synthesis of free diamino analog **25** and its corresponding hydrochloride salt **27**.

The synthesis of the 2,5 and the 2,3 dinitrogen-based derivatives are discussed next. The Wittig reaction is the key step in the formation of the *Z* stilbenes, hence the synthesis will utilize the dinitro requisite benzaldehydes, which later will be reacted with the phosphonium bromide salt **16** to form the desired *Z* stilbenes.



Scheme 4.9. Synthesis of 3,5-diserinamide CA-1 analogue **29**.⁷⁷



Scheme 4.10. Synthesis of 2,5 and 2,3-dinitro benzaldehydes **20a** and **20b**.

Hydrolysis of bromide **17** produced the benzylic alcohol **18** in a 91% yield after refluxing for 4 h.⁹⁶ It was interesting to notice that the ¹H-NMR of this alcohol showed a coupling of the hydrogen of the hydroxyl group with the two benzylic hydrogen atoms. A minimum-energy conformation of this alcohol was obtained using MOPAC⁷⁹ as shown in Figure 4.8. Based on this structure, it is postulated that a hydrogen bond occurs between the hydrogen of the hydroxyl group and one of the oxygen atoms of the nitro group forming a seven-membered ring. The distance measured for this hydrogen bond is 2.83 Å, which is within the range of distances that hydrogen bonds are known to occur.⁹⁷ This intramolecular hydrogen-bond presumably limits hydrogen exchange with other alcohol molecules and hence the hydroxyl group is locked in such position that has a specific dihedral angle with the benzylic hydrogen atoms. The dihedral angle measured from the model is 49°, which is a value that is in the range of angles that explains the coupling constant measured (6.8 Hz) based on Karplus's graph.^{57,58}

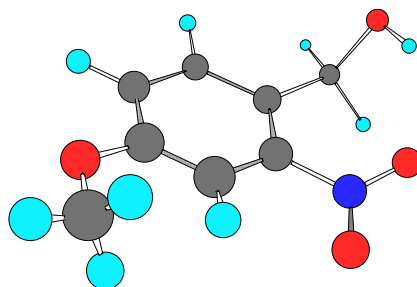


Figure 4.8. Minimum-energy conformation of compound **18** obtained using MOPAC.⁷⁹ A hydrogen bond is observed between the hydrogen of the hydroxyl group and one of the oxygens of the nitro group. The distance measured for this hydrogen bond was 2.83 Å.

Oxidation of the benzylic alcohol **18** with PCC⁹⁸⁻¹⁰¹ afforded benzaldehyde **19** in a 97% yield after stirring for 4.5 h at room temperature. The nitrobenzaldehyde **19** was

further nitrated with H₂SO₄ (c) and HNO₃ (fum)¹⁰² forming a mixture of two dinitrobenzaldehydes **20a** and **20b**. The reaction was monitored by GC-MS and the observation was made that if the reaction was stirred for more than 1 h, both aldehydes started to oxidize to their respective carboxylic acids. For example, after carrying out many experiments it was noted that on average the composition of the crude reaction mixture, after 10 min and 1 h, approximately 45% of **20a** and 55% of **20b**. However, when the reaction was stirred for 4h, the crude mixture contained 60% of **20a**, 11% of **20b** and 29% of the carboxylic acids. After column separation, both aldehydes were separated from each other but unfortunately only a very little amount of their carboxylic acids was present in the final product compositions even after pursuing recrystallization. The less polar compound **20a** came out first followed by **20b**. Both structures were confirmed by their ¹H-NMRs.

A Wittig reaction was performed with dinitrobenzaldehyde **20a** and phosphonium salt **16** to form the *Z* dinitrostilbene **24** in a 53% yield as Scheme 4.11 shows. After 3h, the crude reaction mixture showed that the *Z* and *E* isomer were formed in a ratio of 9.6:1 respectively as determined by ¹H-NMR. Because the R_f values for both isomers were close, the column separation was difficult, but it was possible to separate both of them in high purity. The *Z* isomer, as usual, showed a vinyl coupling constant of 12 Hz and the *E* isomer **24a** exhibited a coupling constant of *J*= 16 Hz. It was noted once again that all the aromatic peaks of the *E* isomer were more downfield than the *Z* isomer, particularly the methine hydrogen atoms present on the B-ring, which is the ring containing the two nitro groups.

The GC-MS of the crude reaction mixture showed that these isomers were present in a ratio of 2.5: 1 after the reaction was carried out for 4 h. After carefully analyzing their MS and NMR spectra it was deduced that these compounds contained just one reduced nitro group; in one case an amino group attached at 2' position and in the second case an amino group at 5' position. After column separation, the less polar compound was obtained in a 4% yield and the more polar compound in a 27% yield. The assignment of the structures for each isomer was based on a comparison of their ^1H and ^{13}C -NMR with the theoretical values predicted with ChemDraw 3D Predictor.¹⁰³ Hence, the spectral data of compound **26b** matched with the less polar compound and the more polar matched with **26a**. However, structural assignments just based on this comparison are not conclusive. The reduction of both nitro groups was achieved by treating the dinitrostilbene **24** with Zn in AcOH⁸⁶ to form diamino combretastatin **26c** in a 61% yield.¹⁰⁴

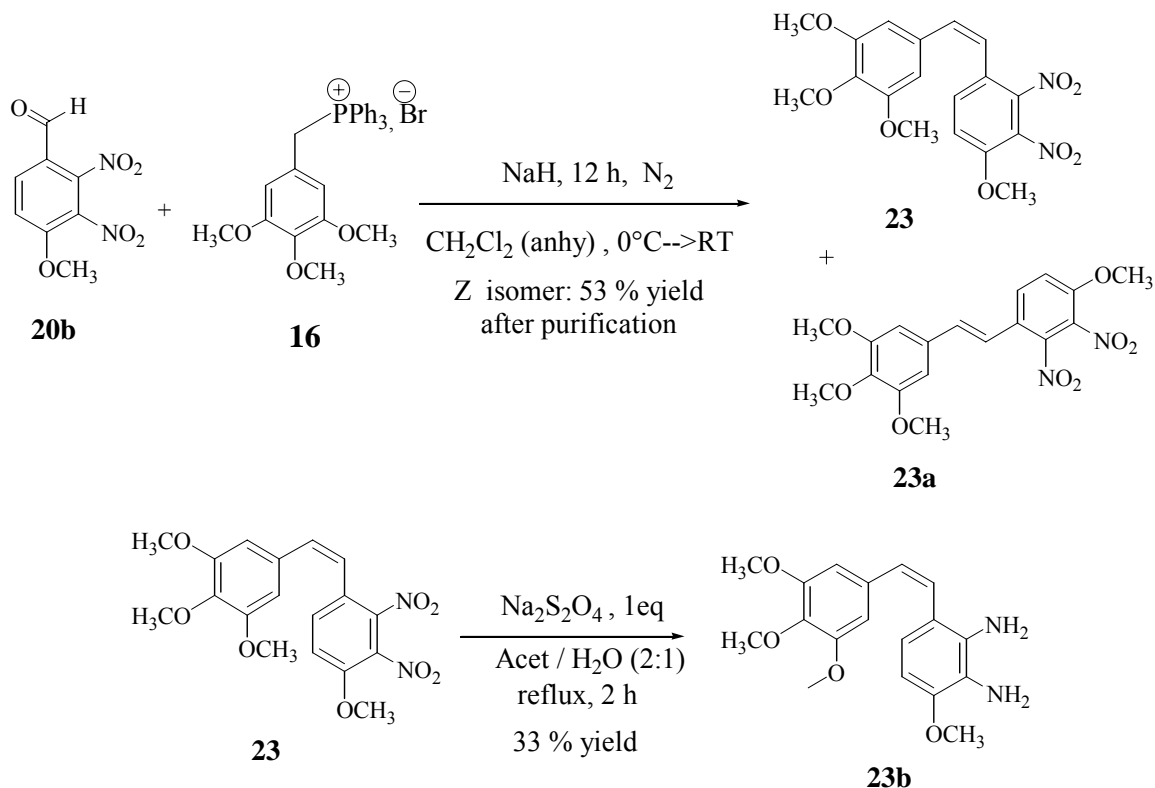
The hydrochloride salt **27a**, as shown in Scheme 4.11, was formed in a 53% yield by treating the stilbene **26a** with a 4N solution of HCl in dioxane.^{64,65}

In Scheme 4.12, the synthesis of the 2,3-dinitro-based derivatives is depicted. After the Wittig reaction was performed for 12 h with benzaldehyde **20b** and phosphonium salt **16**, the *Z* isomer **23** was formed in 53% yield. Separation of both isomers was carried out by column chromatography; the less polar *Z* isomer was afterwards treated with sodium hydrosulfite to form free diamine **23b** in a 33% yield.

Synthesis of a Combretastatin A-1 Analogue

In this project, the goal was to incorporate a substitution of the B-ring methoxy group of CA-1 for a methyl group. We were curious to see the effect of this substitution

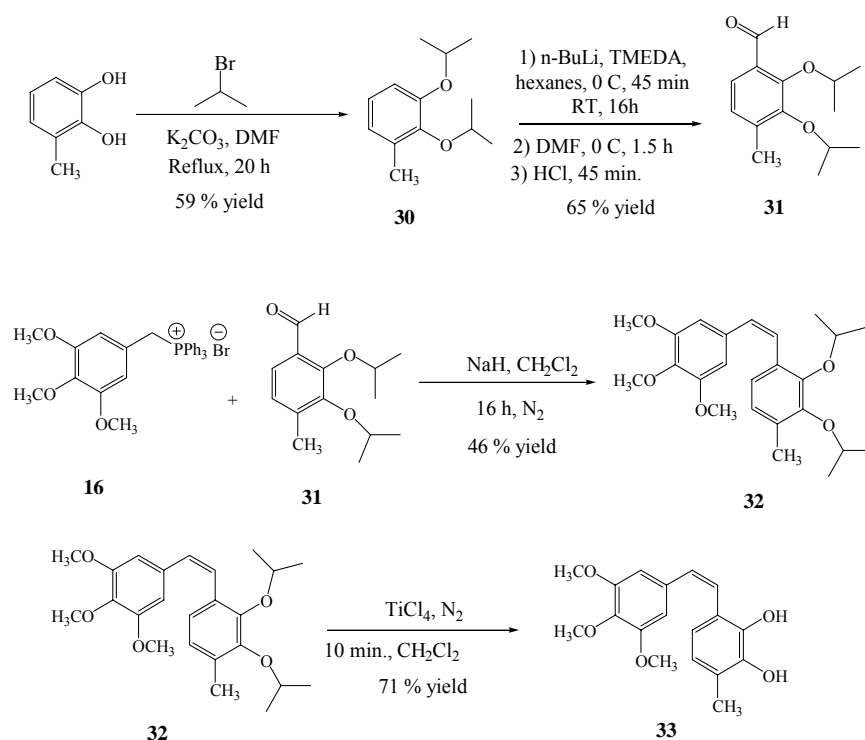
towards inhibition of tubulin assembly and *in vivo* blood flow shutdown activity in SCID mice. The synthesis of CA-1 analogue **33**, which is depicted in Scheme 4.13, starts with the isopropyl protection of the two hydroxyl groups¹⁰⁵ of 3-methylbenzene-1,2-diol with isopropyl bromide and potassium carbonate to form the protected diol **30** in a 59% yield.



Scheme 4.12. Synthesis of 2,3-dinitrogen-based CA-1 analogues

One of the key steps in the synthetic strategy was the formation of benzaldehyde **31**. An analogous procedure, which was reported in 1996 by Kaufman¹⁰⁶, was used to incorporate the formyl group at the ortho position with respect to one of the isopropyl groups on the benzene ring. In the first part of the reaction, the isopropyl protected alcohol reacted with BuLi in TMEDA at 0 °C for 16 h to form the respective aryl lithium intermediate which subsequently was reacted with DMF. Following, acidic hydrolysis

the product was formed in a 65% yield. A Wittig reaction, which was carried out by reacting phosphonium bromide **16** with aldehyde **31**, constituted the second key step in the synthetic plan. After the contents were stirred for 16 h, the *Z* and *E* isomers were formed in a ratio of 4.8: 1 respectively. Column chromatography facilitated the separation of both isomers and obtaining the less polar *Z* stilbene **32** was obtained in a 46% yield. Finally, deprotection of the isopropyl groups was carried out by reacting stilbene **32** with TiCl_4 ¹⁰⁵ to form the CA-1 analogue **33** in a 71% yield.

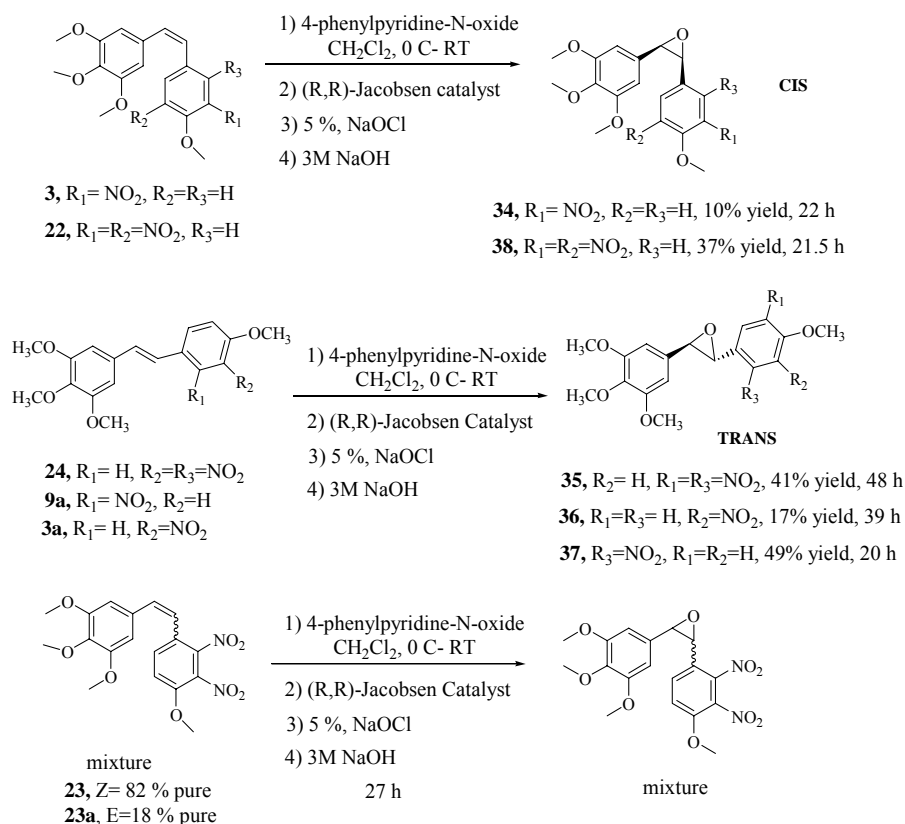


Scheme 4.13. Synthesis of CA-1 derivative **33**.

Synthesis of Nitrogen-Based Epoxide Derivatives of Combretastatins A-1 and A-4

In this project, different nitrogen containing epoxides of CA-1 and CA-4 were synthesized. Epoxides of *Z* and *E* isomers containing one or two nitro groups attached at

the 2, 3 and 5 positions of the B-ring were prepared as shown in Scheme 4.14. Epoxidation of the appropriate stilbenes was carried out by using a procedure reported previously by Pettit and co-workers¹⁰⁷ in which the alkene reacts with NaOCl catalyzed by (R,R)-Jacobsen reagent in the presence of 4-phenylpyridine-N-oxide. In the top part of the Scheme 4.14, the synthesis of two *Z* epoxides **34** and **38** derived from *Z* stilbenes **3** and **22** is illustrated. Products were obtained in percentage yields of 10 and 41% respectively.



Scheme 4.14. Epoxidation of some nitrogen containing CA-1 and CA-4 analogues.

After epoxidation of stilbene **3**, the crude reaction mixture contained, as evidenced by TLC, two compounds besides the starting material. The desired *Z* epoxide, which was the more polar compound, was obtained in just 10% yield and its structure

was confirmed by DEPT 45, ^{13}C and ^1H -NMR spectroscopy. The first spectrum (DEPT45) showed nine peaks as expected, the ^{13}C -NMR showed a total of 15 peaks and finally, in the ^1H -NMR it was possible to see the methine hydrogens of the epoxide which appeared as doublets with a coupling constant of $J= 4.1$ Hz. The structure of the less polar compound, which was separated as the major product, was identified as (4-methoxy-3-nitrophenyl)-(3,4,5-trimethoxyphenyl)methanone. The formation of this product presumably is the result of an initial aryl shift of the epoxide to form the corresponding diarylacetaldehyde which in turn undergoes an oxidative cleavage to form the ketone.¹⁰⁷ In 1998, George Pettit and coworkers attempted to form the epoxide of CA-4 using the same procedure but instead they found as final products the corresponding 1,1-diphenylacetaldehyde and the benzophenone derivative.¹⁰⁷ They deduced that a rearrangement under basic conditions was taking place to form the deoxybenzoin and diphenylacetaldehyde via migration of a phenyl group.¹⁰⁷ They also reported that the presence of the epoxide was observed by NMR but never could be separated after column chromatography. Under the conditions¹⁰⁸⁻¹⁰⁹ and with the nitrogen-containing stilbenes we could form the respective epoxides which were isolated by column chromatography in relatively low yields. Epoxidation of stilbene **22** formed the respective *Z* oxirane **38** in a 37% yield. Again it was noted that the methine hydrogen atoms of the epoxide had a coupling constant of $J= 4.1$ Hz which is the same as was observed for oxirane **34**.

In Scheme 4.14, the synthesis of epoxides from three *E* stilbenes is also shown. The yields that were obtained using these *E* isomers starting materials were much better compared to the *Z* isomer-based epoxides although the reaction times used were longer.

It was noted that the $^1\text{H-NMR}$ of these epoxides showed a coupling constant for the epoxide hydrogen atoms of approximately $J= 1.7$ Hz, a value that is smaller than the corresponding value for the *Z* oxiranes.⁵⁷ In Figure 4.9 the minimum-energy conformations of epoxides **34** (left model) and **36** (right model) are shown. As noted, the dihedral angle of the epoxide hydrogen atoms of the *Z* isomer is smaller (a value closer to 0°) than for the *E* oxirane (close to 120°). Based on Karplus's graph,^{57,58,78} it is observed that as the angle approaches 0° , the value of the coupling constant increase. Furthermore if the angle approaches 90° , the values of the coupling constants goes to zero. These models can explain, in part, why the values for the coupling constants of the *Z* isomers ($J= 4.1$ Hz) are higher than the corresponding values for the *E* isomers ($J= 1.7$ Hz).

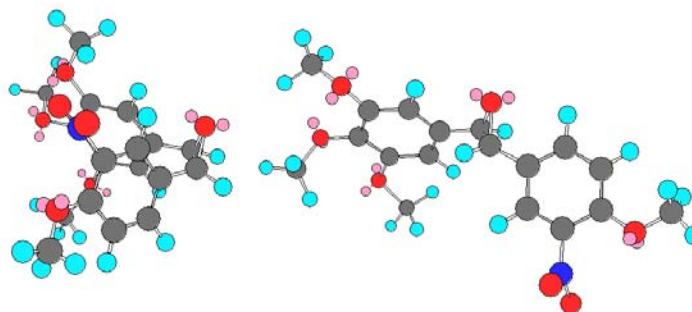


Figure 4.9. Minimum-energy conformations of *Z* epoxide **34** (left) and *E* epoxide **36** (right). The dihedral angle between the epoxide hydrogen atoms of the *cis* isomer is smaller than the *E* epoxide as the models show.

Synthesis of Cold Precursors of Radiolabeled Combretastatins CA-1 and CA-4

As part of a team effort, in 2001, the synthesis of a cold precursor appropriate to label combretastatin CA-4 with the radioisotope ^{14}C was initiated.¹⁰⁵ The main objective of this project was to devise a synthetic methodology suitable to incorporate the

radioisotope into the A-ring of CA-4 in order to ultimately provide a pathway which others can follow to actually incorporate the radioisotope. Radiolabeled CA-4 may prove valuable in advanced preclinical studies. Therefore, once the radiolabeled CA-4 enters the body, it will allow a better understanding of the mechanisms associated with the biological pathways that this class of compounds have while interacting with the tumor vasculature. The overall synthesis¹⁰⁵ of cold precursors of CA-4 is depicted in Scheme 4.15. The steps that have solid arrows are the ones in which I was directly involved and detailed description will be given for each of them. The first synthesis involved was the formation of the phosphonium bromide salt **40i** in a 99% yield which in turn reacted with 4-*t*-butyldimethylsilyloxy-3,5-dimethoxybenzaldehyde using NaH as the base to form the *Z* stilbene **40d**. In the ¹H-NMR spectrum, it was difficult to observe one of the vinylic hydrogen peaks. Therefore as Figure 4.10 shows, resolution enhancement of this spectrum was obtained with values of LB= - 0.5 and GB= 0.55 to separate these peaks that were located in the region of 6.38 and 6.48 ppm.

A strategy ultimately useful for the radiolabeling of stilbene **40d** was thought to involve replacement of the TBS group¹¹⁰ by a ¹⁴C-labeled methyl group. Initially, deprotection of the TBS group took place releasing a phenoxide group which in turn reacted with radiolabeled iodomethane through an S_N2 reaction to form the isopropyl stilbene **40e** in a 94% yield. The final step consisted of the deprotection of the isopropyl group¹⁰⁵ with TiCl₄ to form CA-4 in a 93% yield. Under these conditions, no significant isomerization occurred after the reaction was stirred for 19 minutes (the crude contained 92% of *Z* and 8% of *E* isomer).

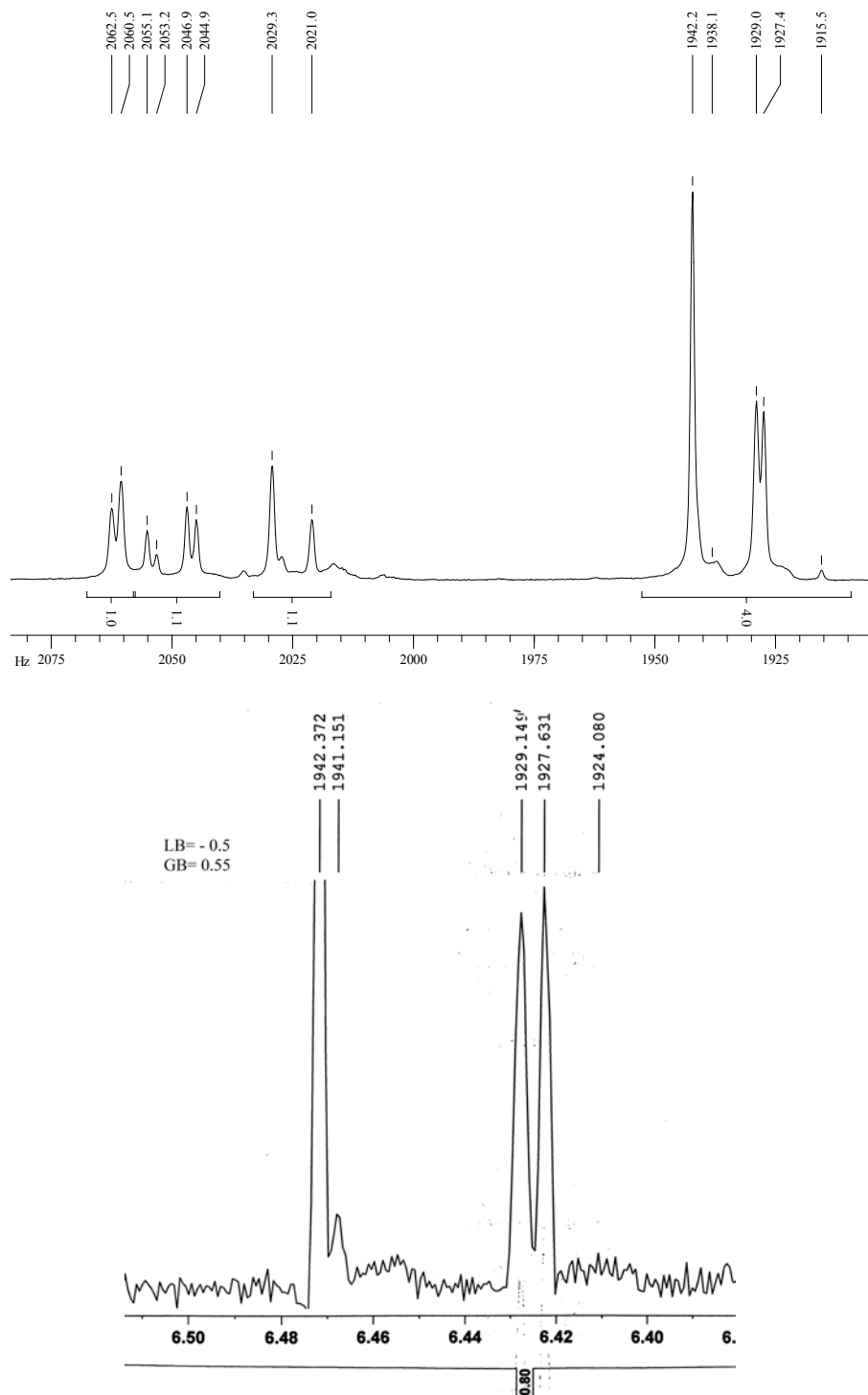


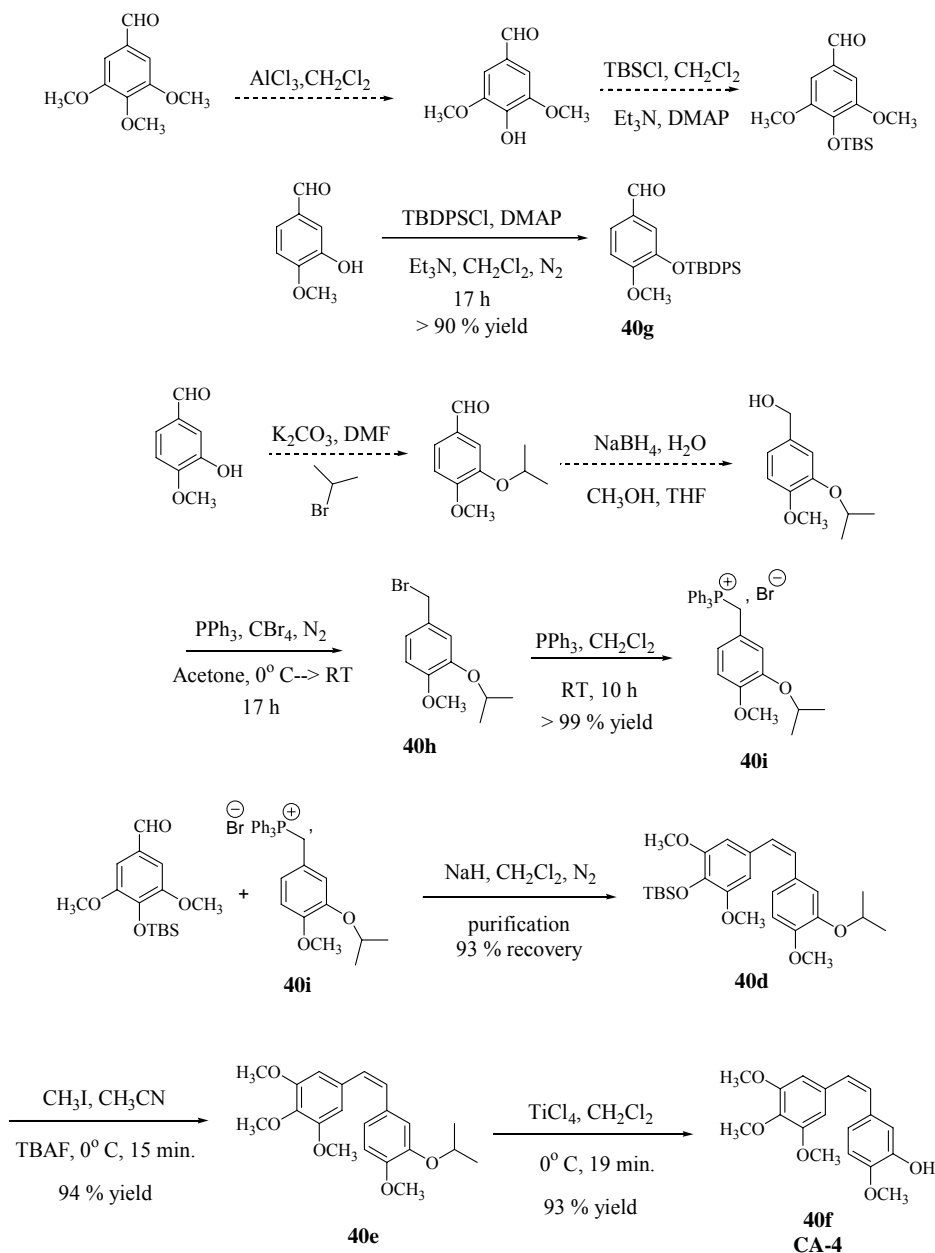
Figure 4.10. a) Expansion of the aromatic region of the $^1\text{H-NMR}$ spectrum of compound **40d** b) resolution enhancement of the $^1\text{H-NMR}$ spectrum using a LB= - 0.5 and GB= 0.55. Notice that a small peak located at 1941.2 Hz was separated from the large peak located at 1942.4 Hz. The coupling constant measured after resolution was 12.0 Hz (1941.151- 1929.149 Hz).

In 2004, Pinney and coworkers¹¹¹ observed that the use of a brand new bottle of TiCl_4 from Aldrich Chemical Co. formed the *Z* isomer in a high ratio compare to the *E* isomer of CA-1. So, we decided to use the same procedure in order to optimize the yield for the formation of stilbene **40f**.

In 2002, the project was continued by synthesizing the cold precursors ultimately necessary for the radiosynthesis of CA-1.¹⁰⁵ The general strategy was the same approach that was used as for the CA-4 radiosynthesis project (Scheme 4.16). After purification of the (2,3-diisopropoxy-4-methoxyphenyl)-methanol, bromination⁹⁰ was carried out with PBr_3 for 2.5 h at room temperature to obtain the bromide **39a** in a 90% yield. Phosphonium bromide salt **39b** was used in the Wittig reaction along with the TBS protected benzaldehyde to form a mixture of *Z* and *E* diisopropyl stilbenes **40a** and **40b** in a ratio of 1: 4 respectively. It is thought that the steric hindrance of the isopropyl groups facilitates formation of the *E* isomer in a much higher amount. After column separation, the *Z* isomer **40a**, which was obtained in a 12% yield, showed (in its $^1\text{H-NMR}$) the vinyl coupling constant of $J= 12.1$ Hz while the trans isomer **40b** exhibited $J= 16.4$ Hz.

The next step was carried out for both isomers in order to have a comparison of the coupling constants for the vinylic hydrogen atoms in the resultant products. The reaction with the *E* isomer **40b** will be described. In the next step, initial deprotection of the TBS group with TBAF^{110} occurs forming the phenoxide which in turn will attack the iodomethane molecule. If a ^{14}C -labeled iodomethane is used instead, this is a convenient way to label CA-1 by incorporating a radiolabeled methyl group.¹⁰⁵ The reaction of the *E* isomer was carried out in 20 minutes to form the diisopropyl stilbene **40c** in a 90% yield.

The $^1\text{H-NMR}$ of stilbene **40c** showed a $J= 16.4$ Hz for the coupling between the vinylic protons while the coupling constant for the *Z* isomer, which was synthesized by Shirali,¹⁰⁵ showed a value of $J= 12.1$ Hz in agreement with Karplus's graph.^{57,58,78}



Scheme 4.15. Synthesis of cold precursors suitable for the radiosynthesis of CA-4.¹⁰⁵

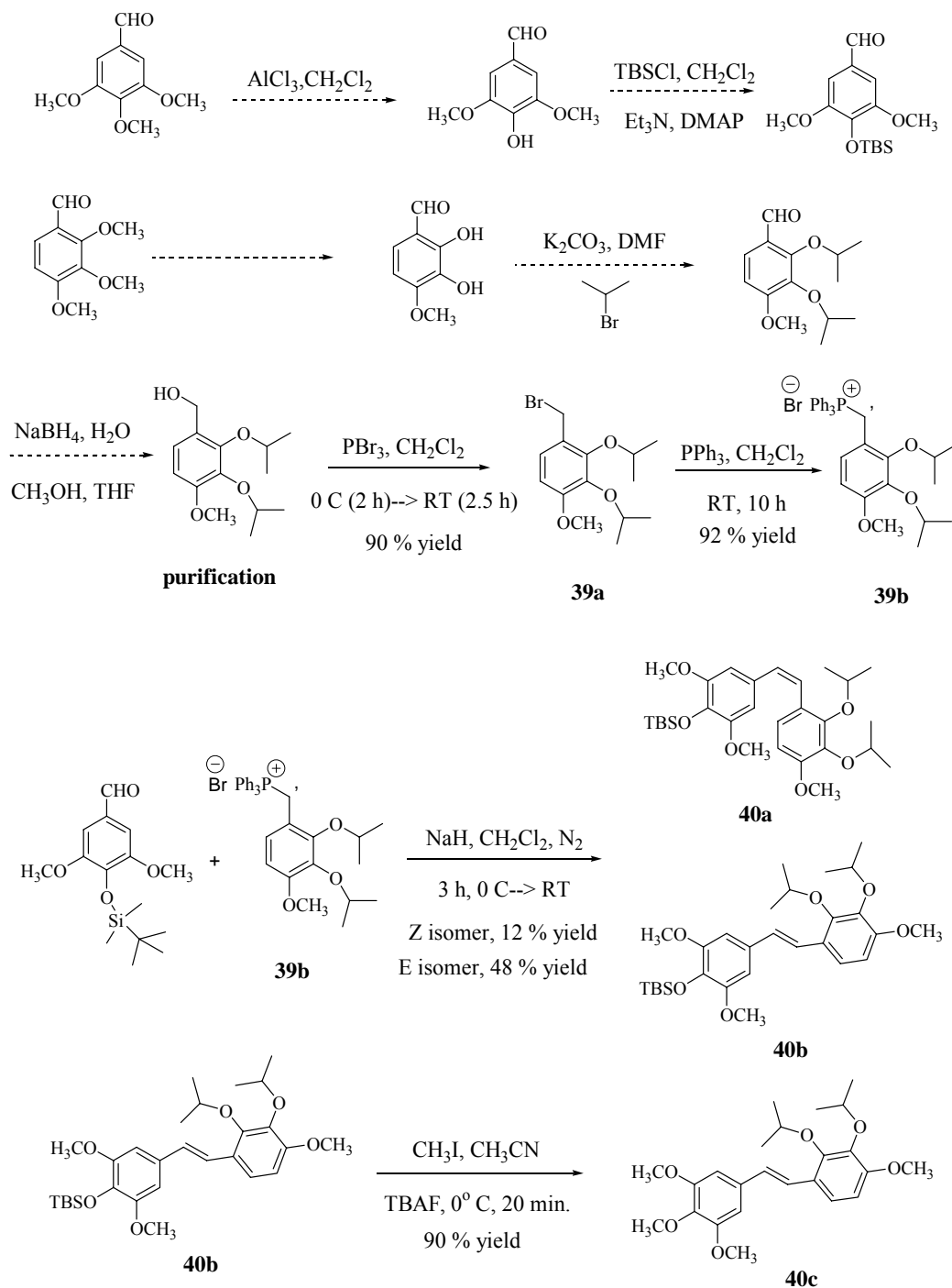
Synthesis of OXi8007 and a Nitrogen-Based Indole

In 2000, Pinney and coworkers¹¹² reported the synthesis of benzo[*b*]thiophenes as potent anti-tubulin inhibitors and potential vascular disrupting agents. Inspired for the good biological activity that these compounds exhibited, Pinney some years later designed the synthesis of different indole-based inhibitors, in particular the phosphate prodrug **OXi8007** which displayed remarkable cytotoxicity against some human cancer cell lines and good inhibition of tubulin assembly.¹¹³⁻¹¹⁵ Because of these excellent results, in 2003 and 2004, two scale-up syntheses of **OXi8007** were performed by the Pinney research group members to provide more compound for further pre-clinical biological evaluations. I was personally involved in the second scale-up project working on the steps of phase II as Scheme 4.17 shows.

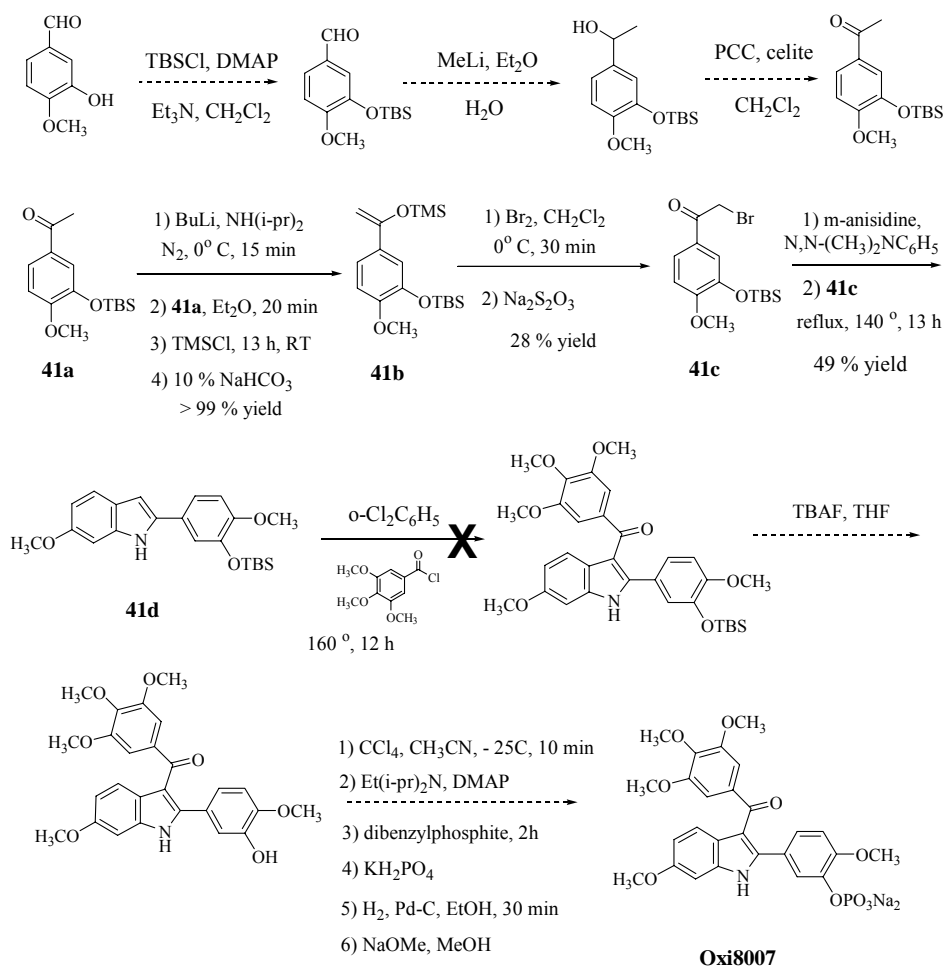
The overall synthetic strategy was divided into three phases. The first phase involved the first three reactions up to the formation of the TBS protected acetophenone **41a**. The second phase involved the next four steps up to the acylation of the TBS protected indole **41d**. Finally, the last phase consisted of the deprotection of the TBS group followed by the formation of the disodium phosphate salt to form the final product **OXi8007**.

Herein, the reactions are described which were performed in the second phase of the overall synthesis project. Synthesis of the TMS enol-ether **41b** was carried out first by removing one of the α -hydrogen atoms of the acetophenone **41a** with LDA formed *in situ*,¹⁰⁴ once the enolate was formed, a nucleophilic substitution took place on TMSCl to form the TMS enol-ether **41b** in almost 99% yield. Bromination of the enol-ether was performed by addition of bromine at 0°C to form the α -bromoketone **41c** in a 28% yield. Indole cyclization was carried out by a Bischler indole type synthesis¹¹⁶⁻¹¹⁹ of

bromoketone **41c** and excess of *m*-methoxyaniline at 140 °C for 13 h to form the TBS protected indole **41d**.



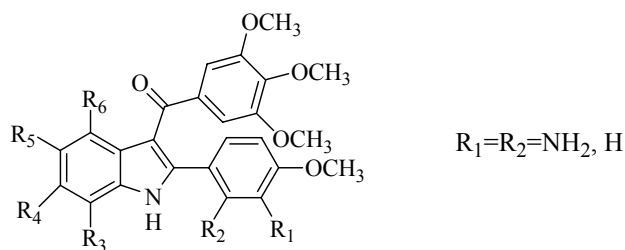
Scheme 4.16. Methodology suitable for the radiosynthesis of the *E* isomer of CA-1.¹⁰⁵



Scheme 4.17. Scale-up synthesis of OXi8007.¹¹³⁻¹¹⁵

Encouraged by the outstanding biological properties of **OXi8007** another project was initiated based on nitrogen containing indoles. The basic idea was to incorporate nitrogen-based functionalities such as nitro, amino, and serinamide into the indole ring at different positions. In addition, this project had the aim to synthesize dinitrogen containing indoles incorporating the other nitrogen-based moiety into the benzene ring as Scheme 4.18 shows. The intended synthetic strategy was similar to that used for the **OXi8007**.¹¹³⁻¹¹⁵ First, it was necessary to synthesize independently the nitroaniline and the α -bromoacetophenone, which, after undergoing a Bishler type indole synthesis,¹¹⁶⁻¹¹⁹

would form the respective indole which in turn could be acylated to form the nitro derivative. It was hoped that the final product could be obtained by reducing the nitro group (s) by a suitable reducing agent^{59,60,80-86} like Zn/AcOH or sodium hydrosulfite. Once amino indole was prepared, a serinamide moiety could be incorporated following the same procedure used for the CA-1 and CA-4 analogues.⁷⁶



47a. R₆=OCH₃, R₁=R₃=NH₂, R₂=R₄=R₅=H

47b. R₆=OCH₃, R₃=NH₂, R₁=R₂=R₄=R₅=H

47c. R₆=OCH₃, R₃=NH₂, R₆=R₅=H

47d. R₆=OCH₃, R₅=NH₂, R₆=R₃=H

47e. R₄=OCH₃, R₆=NH₂, R₅=R₃=H

47f. R₅=OCH₃, R₃=NH₂, R₄=R₆=H

47g. R₅=OCH₃, R₄=NH₂, R₃=R₆=H

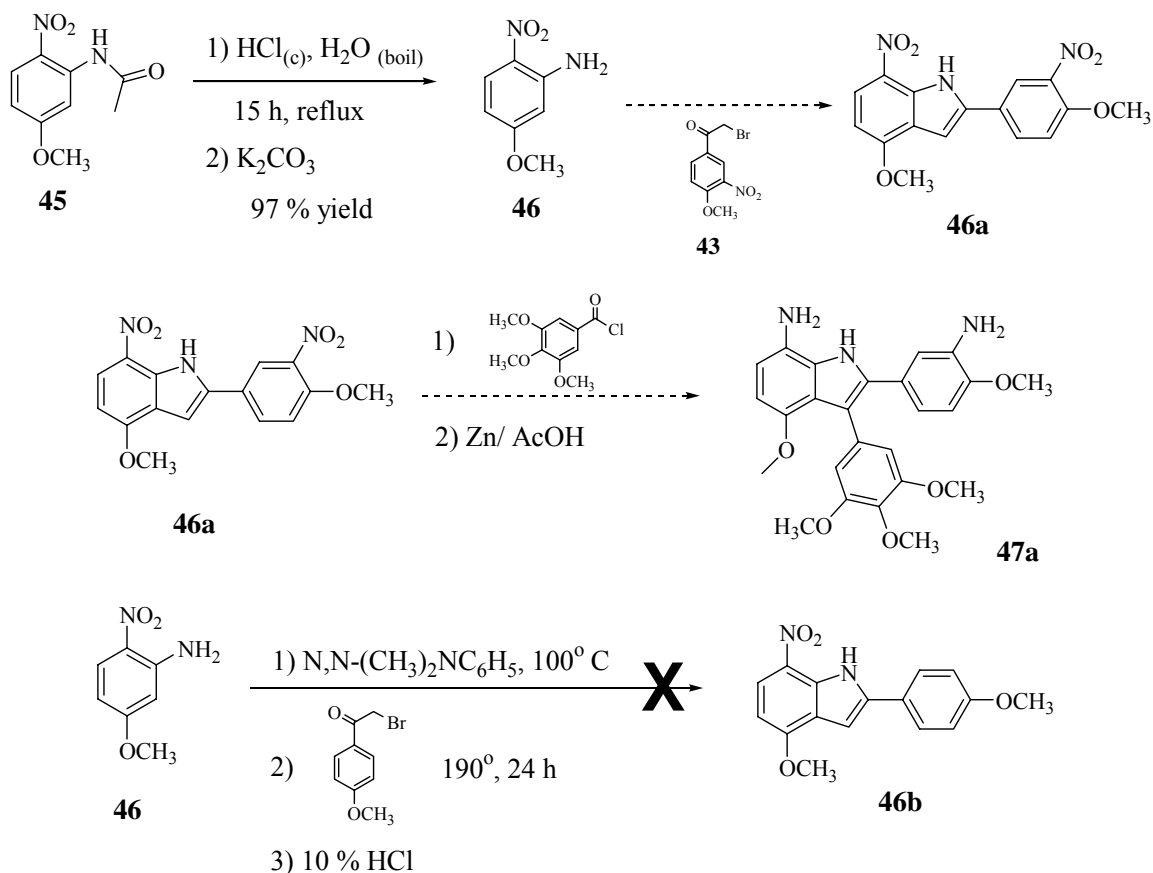
47h. R₅=OCH₃, R₆=NH₂, R₃=R₄=H

Scheme 4.18. Proposed nitrogen containing indole targets. As noted, the first objective was to put the nitrogen functionality into the indole ring at different positions and later to incorporate the second nitrogen-based group into the benzene ring. The nitrogen-based groups to be incorporated were nitro, amino and serinamide as well as the hydrochloride salts of the last two functionalities.

It was our intention to start this project by synthesizing indoles **47a** and **47b** as illustrated in Scheme 4.20. The synthesis of the α -bromoacetophenone **43** was straightforward. Commercially available 4-methoxy-3-nitroacetophenone was reacted with bromine¹²⁰ during 2h at room temperature to form the bromoketone **43** in a 64% yield. The crude reaction mixture was analyzed by GC-MS and it was observed that the product was present in 74% yield along with 13% of the starting material and 9% of the dibromo derivative. The MS of the product showed values of m/z for M^+ at 273 and for $M^+ + 2$ at 275. The presence of the dibromoderivative was confirmed by its MS ($M^+ =$

351, $M^+ + 2 = 353$ and $M^+ + 4 = 355$) and the $^1\text{H-NMR}$ of the crude reaction mixture. The synthesis of nitro aniline **46** started with protection of the amino group of *m*-anisidine with the acetyl group after treating the aniline with Et_3N , DMAP and Ac_2O ¹²¹ to form the amide **44** in an 84% yield. Nitration of amide **44** was performed using three different methods as shown in Scheme 4.19. In the first method,¹⁰² the nitration was carried out with fuming HNO_3 and concentrated H_2SO_4 for 10 minutes at 0 °C. After workup, it was found that two major compounds were formed in a ratio of 1: 2.5 (as illustrated by NMR); both compounds were separated by column chromatography and their structures were elucidated by NMR spectroscopy. Comparison of the ^1H and $^{13}\text{C-NMR}$ chemical shifts with the ones calculated by the Chewdraw NMR predictor,¹⁰³ allowed us to assign the structure of the less polar compound to dinitroacetamide **45a** and the more polar compound to acetamide **45b**. These results are in agreement with the theoretical prediction of the nitration of acetamide **44** which indicates that the nitration will most likely take place at *ortho* and *para* positions with respect to the methoxy group. Because the reactant mixture contained a strong nitrating agent, a subsequent nitration occurred forming preferentially dinitroacetamide **45a** due to the decreased steric hindrance of the second nitro group observed in this compound as compared to the other isomer **45b** in which the nitro group is located between the acetamido and the methoxy groups.

In the second nitrating method, after concentrated nitric acid and acetic acid¹²⁶ were used, the crude reaction mixture contained three major compounds. $^1\text{H-NMR}$ showed that acetamide **45** was primarily formed with a very small amount of another compound which is presumably isomer **45c**.



Scheme 4.20. Synthetic route for nitrogen-based indole derivatives **47a** and **47b**.

A third method used simply treated acetamide **44** with a mixture of concentrated nitric acid, glacial acetic acid, and acetic anhydride¹²²⁻¹²⁵ at 0°C for 15 minutes to form a mixture of two isomers of molecular mass of 210 (determined by GC-MS) in a ratio of 4.9: 1 (determined by NMR and GC) which corresponds to the mass of the expected product **45**. The crude $^1\text{H-NMR}$ showed that both isomers contained the same aromatic patterns (*meta* doublet, *ortho* doublet and *ortho-meta* doublet of doublets). Theoretically, as stated early, three mono-nitro derivatives can be formed but just two of them matched the patterns found in the crude. The probable structures of the two compounds are acetamides **45** and **45c** but it was not completely clear which of these compounds was the

major and which one the minor isomer.^{122,128} After both isomers were separated by flash chromatography, an X-ray crystal structure of the major isomer, which was obtained in 42% yield, was taken and showed that this compound was acetamide **45** as shown in Figure 4.11.

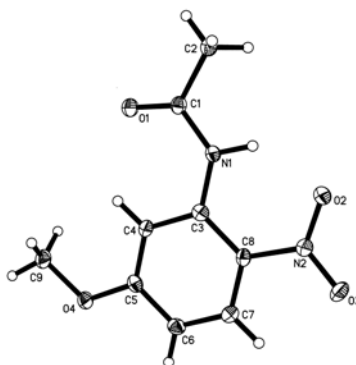
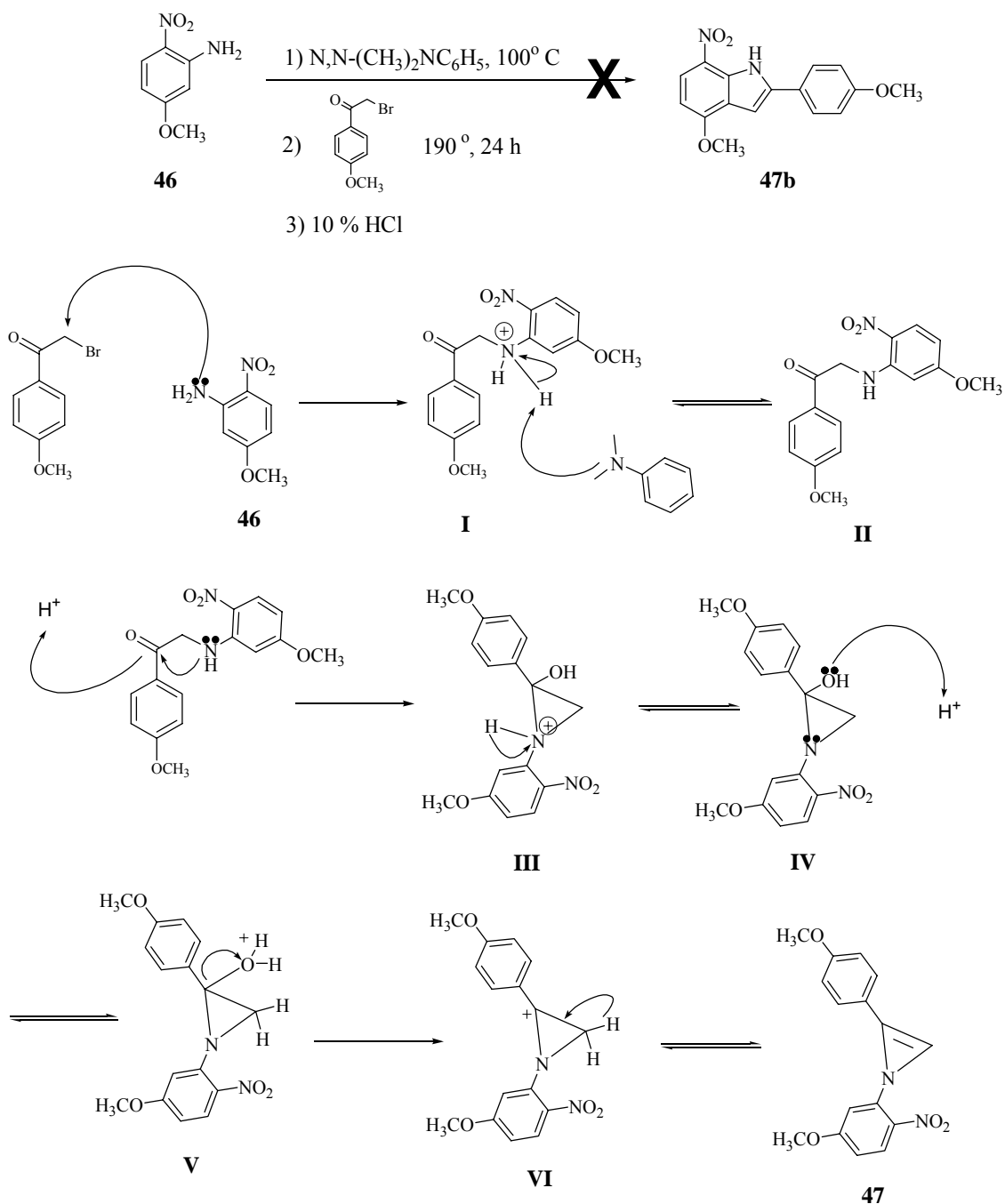


Figure 4.11. X-ray crystal structure of compound **45**.⁹⁵

Deprotection of the acetyl group of acetamide **45** was performed with concentrated hydrochloride acid and boiling water. After the mixture was refluxed for 15 h, the ortho nitroaniline **46** was obtained in a 97% yield as Scheme 4.20 shows. Before synthesizing indole **46a**, we first wanted to prepare indole **46b** and use this reaction as a model for the other targets that are shown in Schem 2.18. Commercially available 2-bromo-1-(4-methoxyphenyl)ethanone was refluxed at 190 °C for 24 h with nitroaniline **46** using *N,N*-dimethylaniline as a solvent.¹⁰⁴ The crude reaction mixture contained 5 compounds among them the most polar was the major product which was successfully separated by flash chromatography and later its structure was fully characterized. Although the ¹H-NMR accounted for a total of 14 hydrogen atoms, the aromatic region did not match with the expected patterns to be found in the compound. The ¹³C-NMR showed 14 different types of carbon atoms but DEPT 45, 90 and 135 surprisingly

indicated the presence of six types of aromatic protons instead of the expected five. The decision was made to take a COSY ^1H - ^1H and a COSY ^1H - ^{13}C NMR to analyze more carefully the coupling among the protons to correlate these atoms with the respective carbon atoms present in the molecule. It was interesting to notice that HETCOR showed a correlation between the proton located at the most downfield chemical shift (9.12 ppm) with the respective more unshielded carbon atom (140.5 ppm) indicating that this hydrogen atom was not attached to the nitrogen atom as initially thought. In addition, COSY ^1H - ^1H showed no coupling of this proton with any other hydrogen present in the molecule explaining in this way why this hydrogen appeared as a singlet. Additional support and information about the different couplings of the hydrogen atoms in the molecule was obtained with different homonuclear decoupling experiments. It is proposed that the structure that best satisfies the spectroscopic data found is compound **47**. The reaction mechanism for its formation is depicted in Scheme 4.21.

The first step of the mechanism starts with nucleophilic attack of the aniline **46** to the bromoketone to form the protonated amine **I** and a bromide ion. In the second step, an acid-base reaction happens between *N,N*-dimethylaniline and the intermediate **I** to form the α -aminoacetophenone **II**. In the third step, an intramolecular nucleophilic addition takes place in which the lone pair of electrons of the nitrogen attack the electrophilic carbon of the carbonyl. Protonation of the carbonyl oxygen makes the carbon more susceptible toward an electrophilic attack. The fourth step involves a deprotonation of intermediate **III** to form the azirene type intermediate **IV** which in turn undergoes a protonation of the hydroxyl group to form **V**. In the last step the elimination of water and hydrogen ion drives to formation of the final azirene product **47**.



Scheme 4.21. Proposed mechanism for the formation of the azirene derivative **47**.⁹⁴

Biological and Biochemical Results

Biological evaluation of these new modified CA-4 and CA-1 analogs involved both *in vitro* and *in vivo* tests. Initially, some compounds were screened for their ability

to inhibit tubulin assembly in a cell free assay using purified tubulin. Secondly, some compounds were evaluated in terms of *in vitro* cytotoxicity (MTT assay) and for their ability to selectively impair blood flow (*in vivo*) to tumors in SCID mice. The combination of enhanced activity towards tubulin and *in vivo* blood flow capability has proven to be indicative of pre-clinical efficacy and predictive of potential clinical success. Additionally, *in vitro* cytotoxicity for some of the compounds against mouse P388 leukemia and selected human cancer cell lines will be shown. Evaluation of these assays is a key component in our overall drug design and development program related to the synthesis of novel anticancer drugs.

*Inhibition of tubulin polymerization, cytotoxicity (MTT) and blood flow reduction*⁷⁶

Three compounds, CA-4, CA-1, and AC7739, and their water-soluble prodrug derivatives, CA-4P, OXi4503, and AVE8062 (AC-7700) serve as benchmark reference compounds in order to evaluate new VDA candidates in a pre-clinical sense. CA-4, CA-1, and AC7739 all inhibit tubulin assembly with IC₅₀ values in the range of 1-2 μM while CA-4P and OXi4503 demonstrate the ability to shutdown tumor blood flow on the order of 80-100% at a dose of 100 mg/kg as Table 1 shows. Additionally, it is interesting to note that the replacement of the amino group in compound **4** by its hydrochloride salt decreased the inhibition of tubulin assembly value from 2.6 to 1.3 μM. However, when the hydrochloride salt of the serinamide **7** was formed, the inhibition increased from 9.6 to 11.3 μM. In Table 1, it is also noted that free amine **4** exhibited less cytotoxicity and more percentage of blood flow shutdown than its respective serinamide **7**.

Table 4.2 shows the effects on the biological activity of changing the amino group of compound **4** from the 3' position to the 2' position. The results indicate that there was

a considerable improvement in the inhibition of tubulin assembly (from 2.6 to 1.4 μM) when the amino group was at 2' position of the B-ring instead of the 3' position. However, it was noted that the hydrochloride salt **11** was not as active as its free amine **10** as was also observed in the case of the 3' isomer in which the salt significantly improved notoriously the biological activity. Both serinamide **13** and its hydrochloride salt **14** did not show any good antitubulin activity ($\text{IC}_{50} > 40 \mu\text{M}$) but they contained significant activity in terms of blood flow reduction (24 and 22.8% respectively at a dose of 10 mg/Kg). It was also noted that the free amine **10** is less cytotoxic than the respective serinamide **13** and compound **4** exhibited more blood flow shutdown than free amine **10** (36% and 25% respectively at a dose of 10 mg/ Kg).

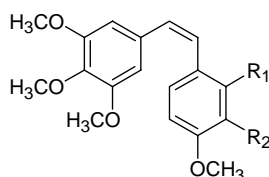
In Tables 2.3 and 2.4, the biological data for nitrogen-containing derivatives is shown. Among all of these derivatives, the 2,3-diamine **23b** and its hydrochloride salt **23c** exhibited good inhibition of tubulin assembly values (2.9 and 1.8 μM respectively) followed by next in terms of inhibition of tubulin assembly compound **26a**.

In addition, compound **23b** showed lower cytotoxicity and a higher percentage of blood flow reduction than compounds **25**, **26a**, **27a** and **27b** which showed relatively high cytotoxicity and either none or low blood flow reduction. Interestingly, in the 3,5-dinitrogen-based derivatives, compound **22**, which incorporates two nitro groups, showed a better inhibition of tubulin assembly value than the respective diamine **25** (7.4 and $> 40 \mu\text{M}$ respectively).

As Table 4.4 shows, none of the five epoxides showed good inhibition of tubulin assembly values ($> 40 \mu\text{M}$). One of the compounds that showed comparable inhibition of tubulin assembly values with CA-1 was its analogue **33**. Apparently, the substitution

of the B-ring methoxy group for a methyl group did not significantly affect the activity because it produced an increment of just 0.2 μM .

Table 4.1. Inhibition of tubulin polymerization, cytotoxicity, and blood flow reduction for compounds **4**, **5**, **7** and **7a**.⁷⁶



Compound ^a	R ₁	R ₂	Tubulin inhibition IC ₅₀ [μM]	MTT (IC ₅₀ <i>in vitro</i> cytotoxicity) [μM]		<i>In vivo</i> blood Flow shutdown [%]	
				1h	5days	10mg/kg	100mg/kg
CA-4	H	OH	1.2 (1.2) ^c	na ^b		na	
CA-1	OH	OH	1.9 (2) ^d	na		na	
CA-4P	H	OPO ₃ Na ₂	na	0.8	0.0020	10	88
CA-1P	OPO ₃ Na ₂	OPO ₃ Na ₂	na	3.2	0.0046	70	99
AC-7739 (5)	H	NH ₃ Cl	1.3 (1) ^e	na		na	
AC-7700 (7a)	H	NH-SerHCl	11.3	na		na	
4	H	NH ₂	2.6 (1.2) ^c	0.8	0.0080	36	100
7	H	NH-Ser	9.6	5.0	0.0140	0	100

^a CA-4, CA-1, CA-4P, CA-1P, AC-7739, AC-7700, 4 and 7 have all been previously synthesized and reported in literature. They are included here for the purpose of comparison (see references 56, 67,87,129-132).

^b na: not analyzed

^c Ref 56

^d Ref. 130

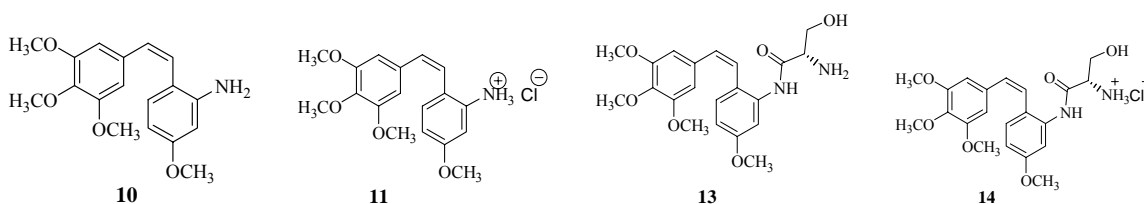
^e Ref 133

In vitro cytotoxicity against P388 and some human cancer cell lines⁷⁶

In Tables 2.5, 2.6 and 2.7, the *in vitro* cytotoxicity against six human cancer cell lines of ten synthesized compounds is shown. The values are reported as ED₅₀ expressed in μM . Each compound was tested against P388 mouse leukemia, pancreas (BXPC-3),

breast adn (MCF-7), CNS Gliobl (SF268), lung-NSC (NCI-H460), colon (KM20L2) and prostate (DU-145) cell lines.

Table 4.2. Inhibition of tubulin polymerization, cytotoxicity, and blood flow reduction of compounds **10**, **11**, **13** and **14**.⁷⁶



Compound	Tubulin inhibition IC ₅₀ [μM]	MTT (IC ₅₀ <i>in vitro</i> cytotoxicity) [μM]		<i>In vivo</i> blood Flow shutdown [%]	
		1h	5days	10mg/kg	100mg/kg
10	1.4	2.0	0.0080	25	50
11	3.1	na ^a		1.5	
13	> 40	10.0	0.08	24	43
14	> 40	na		22.8	

^a na: not analyzed

After analyzing carefully all the data of all the inhibitors and references, they can be arranged in the following order of decreasing activity against each cancer cell line:

P388: 5 > **11** > 7 > **10** > **38** > **35** > 25 > 33 > 27a > 36 > 34 > 37

BXPC-3: 5 > 7 > 23c > **11** > **10** > 27a > 25 > 35 > 33 > 34 > 36 > 38 > 37

MCF-7: 5 > **10** > 7 > **11** > 23c > 33 > 25, 27a > 35 > 34 > 37 > 36 > 38

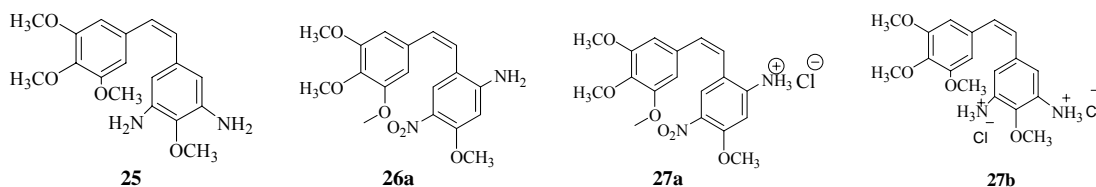
SF268: 5 > **10** > 7 > **11** > 23c > 27a > 25 > 33 > 35 > 34 > 37 > 38 > 36

NCI: 5 > 7 > 23c > **11** > **10** > 33 > 25 > 35 > 27a > 34 > 36 > 37 > 38

KM20: 5 > 7 > **10** > **11** > 23c > 27a > 25 > 35 > 33 > 34 > 36 > 38 > 37

DU145: 5 > 7 > **11** > **10** > 23c > 25 > 33 > 27a > 35 > 36 > 34 > 38 > 37

Table 4.3. Inhibition of tubulin polymerization, cytotoxicity, and blood flow reduction of compounds **25**, **26a**, **27a** and **27b**.



Compound	Tubulin inhibition IC ₅₀ [μM]	MTT (IC ₅₀ <i>in vitro</i> cytotoxicity) [μM]		<i>In vivo</i> blood Flow shutdown [%]	
		1h	5days	10mg/kg	100mg/kg
25	> 40	> 44.8	> 1.4	3.1	4.6
26a	17.4	37.7	> 1.4	0	0
27a	> 40	na ^a		0	13.7
27b	na ^a	> 44.8	> 1.4	0	6
23b *	2.9	2.4	0.0043	40	
23c *	1.8	na ^a			na ^a

- **23b** and **23c** have all been previously synthesized and reported in literature. They are included here for the purpose of comparison. See Table 4.6 (see reference 104) ..

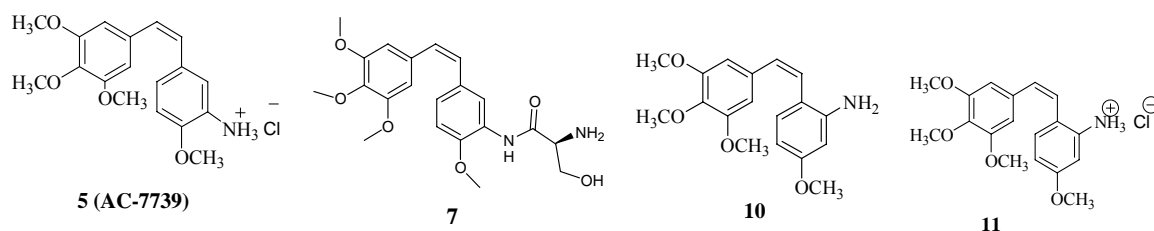
The first important observation is that two of the novel compounds, stilbenes **10** and **11**, are among the top five most active compounds against all the cancer cell lines. As noted, their activity depends on the type of cancer cell line with which they are interacting. For example, the hydrochloride salt **11** is more active than its free amine **10** in mouse leukemia (P388), pancreas (BXPC-3), lung (NCI-H460) and prostate (DU-145) but less active in breast (MCF-7), central nervous system (SF268) and colon (KM20L2). Another important observation is that substitution at the 3'-position definitively is crucial for good anticancer activity. As the results indicate, for all cancer cell lines, **AC-7739 (5)** is always more active than its regioisomer **11**. In the CA-1 series, two of the compounds,

stilbenes **27a** and **25** showed good activity, with the former being more active than the latter.

Table 4.4. Inhibition of tubulin polymerization of compounds **22**, **24a**, **29**, **33-38**.

Compound	Tubulin inhibition IC ₅₀ [μM]	
22	7.4	
24a	> 40	
29	> 40	
33	2.1	
34	> 40	
35	> 40	
36	> 40	
37	> 40	
38	> 40	

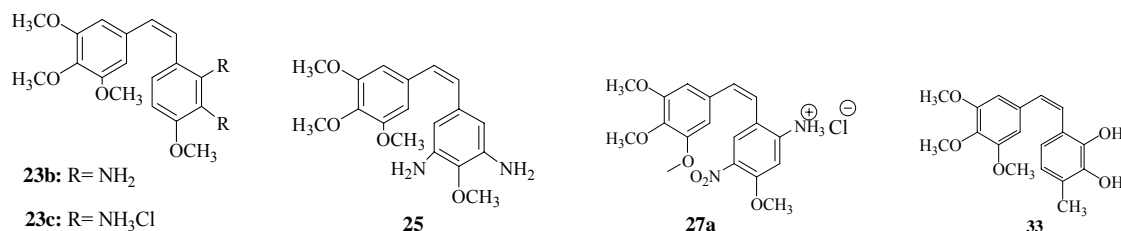
Table 4.5. *In vitro* cytotoxicity (GI₅₀ and ED₅₀ in μM) against six cancer cell lines and P388 mouse leukemia for compounds **5**, **7**, **10** and **11**.⁷⁶



Compound	P388 (ED ₅₀)	BXPC-3	MCF-7	SF268	NCI-H460	KM20L2	DU-145
OXi8006 ^a		0.097	0.054	0.12	0.10	0.050	<3.7
5 ^a	0.0060	<0.0028	<0.0028	<0.0028	<0.0028	<0.0028	<0.0028
7 ^a	0.045	0.011	0.0097	0.0089	0.0077	0.0064	0.0079
10	0.11	0.018	0.0083	0.0092	0.011	0.0098	0.010
11	0.037	0.016	0.01	0.01	0.01	0.01	0.0088

^a **OXi8006**, **5** and **7** have all been previously synthesized and reported in literature. They are included here for the purpose of comparison (see references 64,65,104)

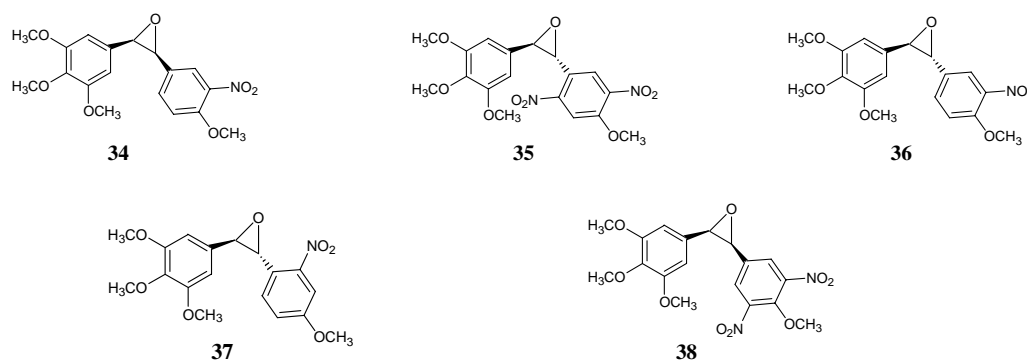
Table 4.6. *In vitro* cytotoxicity (GI₅₀ and ED₅₀ in μM) against six cancer cell lines and P388 mouse leukemia for compounds **23c**, **25**, **27a** and **33**.



Compound	P388 (ED ₅₀)	BXPC-3	MCF-7	SF268	NCI-H460	KM20L2	DU-145
OXi8006 ^a		0.097	0.054	0.12	0.10	0.050	<3.7
CA-1	3.0						
CA-4	0.010						
23c ^a		0.014	0.011	0.011	0.009	0.019	0.012
25	5.2	1.5	1.5	1.5	2.4	1.1	2.1
27a	6.6	1.2	1.5	1.2	4.3	0.98	3.5
33	5.4	5.1	0.25	3.2	2.0	6.3	2.9

^a **OXi8006** and **23c** have all been previously synthesized and reported in literature. They are included here for the purpose of comparison (see reference 104)

Table 4.7. *In vitro* cytotoxicity (GI₅₀ and ED₅₀ in μM) against six cancer cell lines and P388 mouse leukemia for compounds **34**, **35**, **36**, **37** and **38**



Compound	P388 (ED ₅₀)	BXPC-3	MCF-7	SF268	NCI-H460	KM20L2	DU-145
OXi8006^a		0.097	0.054	0.12	0.10	0.050	<3.7
34	>27.7	9.1	10	8.0	8.6	10	8.6
35	3.9*	3.4	2.3	4.2	2.9	3.4	3.7
36	19*	11	21	28	12	23	6.6
37	> 28*	> 28	17	21	22	> 28	> 28
38	0.89*	> 25	> 25	> 25	> 25	> 25	11

Values were determined in suspension.

However, it is clearly noted that the dihydrochloride salt **23c** is much more active than any of the other dinitrogen-containing derivatives. In the epoxide series, the *trans* epoxide **35** is the best inhibitor against of all the cancer cell lines evaluated followed by compound **34**. Furthermore, in this series, the *Z* epoxide **34** is more active than its respective *E* isomer **36** which is consistent with the previous knowledge that *Z* stilbenes are more active than their corresponding *E* isomers.¹³⁴ In addition, it is noted that when the nitro group is attached at 3'-position, as in compound **36**, the activity is superior as compared to compound **37** in which the nitro group is located at the 2'-position. Finally, it is observed that the CA-1 analogue **33** is reasonably active against most of the cell lines but not as good as the nitrogen-based stilbenes **10** and **11**.

CHAPTER FIVE

Conclusions and Future Directions

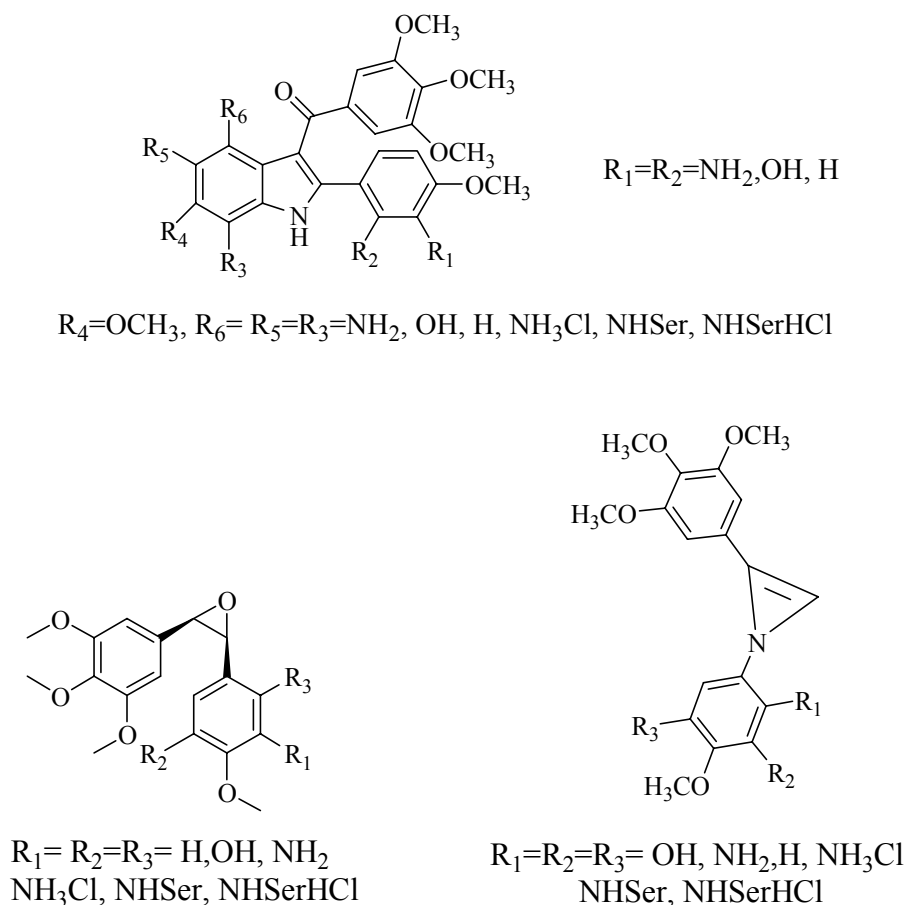
The development of a small library of new, synthetic, oxygen and nitrogen-bearing combrestastatin CA-1 and CA-4 analogues was successfully achieved. Out of seventeen synthesized compounds, four derivatives, **10**, **11**, **13** and **33** have emerged as potential candidates for further pre-clinical trials. Particularly, stilbenes **10** and **11** are the best candidates with respect to their potent inhibition of tubulin assembly and their significant cytotoxicity against seven cancer cell lines comparable to **AC-7739 (5)** and compound **7 (AC-7700)**. Although compound **13** did not show acceptable inhibition of tubulin assembly, it exhibited a significant *in vivo* blood flow shutdown capability along with compounds **10** and **14**. Among all of the compounds, three analogues, **10**, **33** and **11** demonstrated most potent inhibition of tubulin assembly. This novel nitrogen-modified CA-1 and CA-4 compound library enhances the overall structure-activity relationship profile that is known for the combretastatins and related analogues. Even though a complete set of biochemical and biological data for all the compounds does not yet exist, it is still possible to address the most significant structural requirements that combretastatins need to have for anticancer activity:

- 1) Incorporation of an amino or serinamide group and the respective hydrochloride salts at either the 2' or 3' position of the B-ring of combretastatins is essential for inhibition of tubulin assembly and *in vivo* blood flow shutdown.

- 2) Monosubstituted combrestastatins containing a nitrogen-based functionality at the 3' position exhibited better biological activity than the corresponding analogs functionalized at the 2' position.
- 3) In the disubstituted combretastatin series, significant activity was observed when the substituents were preferentially attached at the 2' and 3' positions and in less extension at 2' and 5' or at 3' and 5' positions.
- 4) In general, the monosubstituted nitrogen-based derivatives show better activity than the respective disubstituted analogues against tubulin assembly, MTT cytotoxicity, blood flow reduction, and cytotoxicity against human cancer cell lines.
- 5) Replacement of the B-ring methoxy of CA-1 by a methyl group slightly reduced inhibition of tubulin assembly and cytotoxicity against mouse leukemia P388.
- 6) In the epoxide series, the *Z* epoxide CA-4 nitro analogue showed better activity than the respective *E* epoxide derivatives against the human cancer cell lines.
- 7) All of the nitro-epoxides were not active against tubulin assembly
- 8) Nitrogen-containing combretastatin analogues showed comparable values of activity with respect to their parents, CA-1 and CA-4.

Incorporation of the nitrogen-based functionalities such as amino or serinamide and their respective hydrochloride salts to the combretastatin skeleton introduced a new scaffold that improved significantly the tumor vascular targeting properties of the molecules. Currently, **AC-7700** is under clinical development (sponsored by Aventis

Inc.)⁶⁵⁻⁷⁵ and therefore, future efforts need to be carried out towards the incorporation of these nitrogen functionalities into other pharmacophores with the aim of obtaining more effective vascular disrupting agents. Recently, a research effort developed by Monk¹³⁵ showed that the incorporation of an amino and a hydroxy group in the B-ring of combretastatin significantly improved the activity of inhibition of tubulin assembly and the blood flow reduction. Hence, we propose the following pharmacophores to which the nitrogen functionalities in combination with hydroxyl groups and their pro-drugs can be attached.



Scheme 5.1. Proposed structures of future potential vascular disrupting agents.

CHAPTER SIX

Synthesis, Design and Biochemical Evaluation Of Cysteine Protease Inhibitors: Novel Compounds for Chagas' disease Treatment

Introduction

It is estimated that 18-20 million people including 500,000 in the United States are infected with Chagas' disease (American trypanosomiasis) and that 20,000 to 50,000 deaths occur each year from this devastating parasitic illness.^{136,137} This disease is found in twenty-one countries from the southern part of the United States to the southern part of Argentina and it is the leading cause of heart disease in Latin America.¹³⁸ Chagas' disease is a parasitic illness caused by infection with the flagellate protozoan *Trypanosoma cruzi*, which is transmitted to humans by hematophagous reduviid vectors (blood-sucking insects called kissing bugs) or by blood transfusion.¹³⁹⁻¹⁴² The complex life cycle of *T. cruzi* is characterized by proliferative stages in both human and other mammalian hosts (intracellular amastigotes) and vectors (epimastigotes) and by infectious phases in both types of hosts (trypomastigotes) that are non-replicative.^{142,143} The initial phase of the disease, called acute, has an associated mortality of less than 10% and is often undiagnosed and even asymptomatic. It is followed by a chronic infection that in 30-40% of the individuals progresses to irreversible heart and/or gastrointestinal damage, which lead to sudden death.¹⁴⁴⁻¹⁴⁶

Background

American trypanosomiasis or Chagas' disease was first described in 1909 by the Brazilian physician Carlos Justiniano Ribeiro Chagas who also discovered its etiological agent, the vector, the host and the mode of transmission. This lethal protozoan disease, which causes the death of six people in one hour, and infects 38 people per minute in the world, is one of the leading causes of sudden death after coronary artery disease.¹³⁷ People infected with *Trypanosoma cruzi* (*T. cruzi*) are afflicted with many ailments, the most common being swelling or denervation of nervous tissue in the heart, colon and esophagus. Some infected people live many years without any visible symptoms, while others painfully endure constipation, fatigue, choking, and heart attacks.¹⁴⁷ Among all the parasitic illnesses, Chagas' disease is third after malaria and schistosomiasis and no vaccine or effective treatment is known to date.



Figure 6.1. Countries (in red) that are afflicted with Chagas disease.¹⁴⁷ (Reproduced directly from reference 147).

In Figure 6.1, the countries in the world that are afflicted with Chagas disease are shown. As noticed in Figure 6.1, although this disease is endemic to Latin America, its social and economical impact is already found in USA where it is believed that 500,000 people are infected.¹³⁷

As stated above, Chagas' disease is caused by *Trypanosoma cruzi*, a microorganism that belongs to the subkingdom protozoa. These flagellar organisms live one stage of their lives in the blood and/or tissues of vertebrate hosts and during other stages they live in the digestive tracts of invertebrate vectors (temporary hosts) as Figure 6.2 shows.

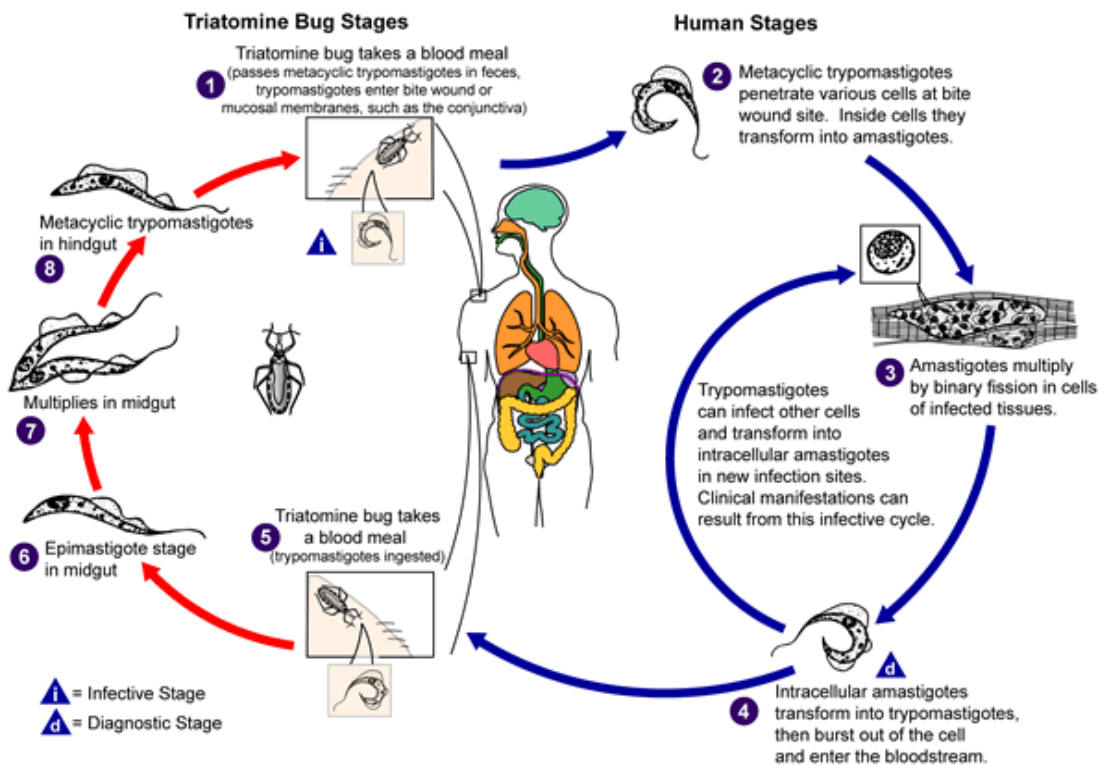


Figure 6.2. Life cycle of *Trypanosoma cruzi*.¹⁴⁸
(Reproduced directly from reference 148).

The parasite, which develops its infectious stage in the insect's digestive tract, is passed to humans through the feces of an infected kissing bug which bites the person's skin. The parasite enters the bite wound or through abrasions on the skin caused by the victim scratching the sore bite. The three different forms that *Trypanosoma cruzi* has during its life cycle as it travels from insects to humans are shown in Figure 6.3.

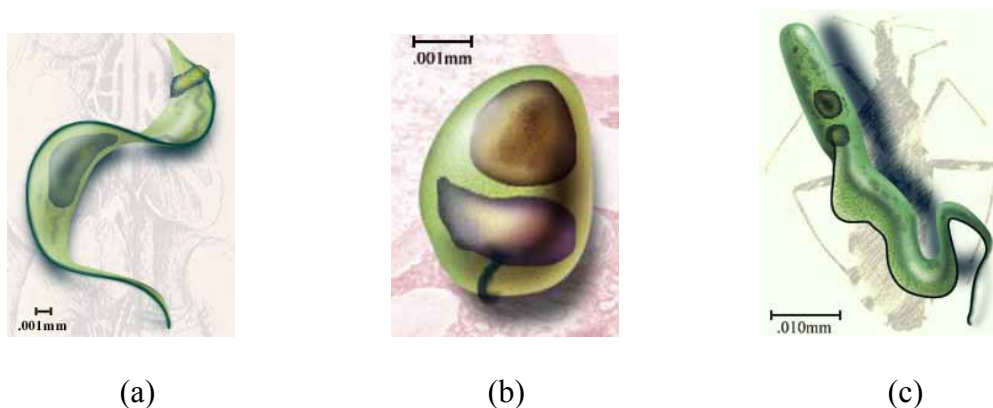


Figure 6.3. Different forms that *Trypanosoma cruzi* adopts during its life cycle. a) trypomastigote b) amastigote c) epimastigote.¹⁴⁷ (Reproduced directly from reference 147).

Metacyclic trypomastigotes are effective forms of *T. cruzi* that pass from the insect's hindgut in the fecal matter and burrow into the skin. These parasites, which are 20 microns long and 3 microns wide, have a free flagellum attached to an undulating membrane on the body. The flagella whip them along in the person's blood and attaches to the insect's intestinal wall. After trypomastigotes pass through the skin, they briefly travel in the blood stream and then colonize in muscle and neuron tissue, areas less vulnerable to attack, where they encyst and form amastigotes, microorganisms of 1.5-5 microns long. This new form of *T. cruzi*, is an intracellular oval-shaped microorganism that multiplies within the cell and then differentiates to trypomastigotes which are

released later into the blood stream to invade other tissue cells. When the kissing bug bites an infected person, they ingest stumpy trypomastigotes and as soon as these reach the insect's midgut, they are transformed into epimastigotes which are more adaptable to survive the insect's intestines. Epimastigotes are 10 to 20 microns long at first, but grow another 10 microns as they travel to the insect's hindgut where they transform into metacyclic trypomastigotes.¹⁴⁷

The vectors of Chagas' disease are insects of the order Hemiptera, family Reduviidae and subfamily Triatominae.¹⁴⁹ Of the 118 species of triatomines, a relatively small number are epidemiologically significant as vectors of *Trypanosoma cruzi*. These are species that colonize poorer quality rural houses, where colonies of thousands of individuals can be found.¹⁴⁹ One of the most common species of insects that are responsible for transmitting the disease is the *Triatoma infestans* which is a nocturnal predator that feeds from mammals' blood while they are asleep (Figure 6.4). This bug, which prefers a warm and humid climate, is commonly found in areas at elevations from 1100 to 11200 feet (330 to 3450 m) above sea level, although they have been found in areas as high as 13300 feet (4100 m).¹⁴⁷



Figure 6.4. Appearance of *Triatoma infestans* (kissing bug) before and after the blood meal (left and right respectively).¹⁵⁰ (Reproduced directly from reference 150).

Chemotherapy of Chagas' Disease

Currently there is no satisfactory treatment for Chagas' disease. The only two clinically accepted drugs, nifurtimox and benznidazole, shown in Figure 6.5, are associated with significant clinical toxicity and a poor therapeutic index for long-term use. In the parasites, the nitro groups of both nifurtimox and benznidazole are reduced to radical anions that in turn produce reactive oxygen species resulting in widespread DNA and protein damage in the parasite, in the case of nifurtimox, or covalent modification of essential biomolecules with benznidazole.¹⁵⁵ While these compounds work well in the acute phase, they have little effect on the chronic phase of the disease. Application of the antifungal and antiprotozoan agent itraconazole or allopurinol (used to treat gout), which blocks purine salvage, have not proved very effective. Several triazoles currently under evaluation as general antifungal/ antiprotozoans may prove to be more useful.^{9,151-153}



Figure 6.5. Structures of Nifurtimox(4-[(5-nitrofurfurylidene)amino]-3-methylthiomorpholin-1,1-dioxide),and Benznidazole (N-benzyl-2-(2-nitroimidazole) acetamide).^{154,156}

The urgent need for an effective therapy against Chagas' disease has stimulated the search for a suitable drug target in the parasite. There are several possibilities for intervention including inhibition of sterol biosynthesis. *T. cruzi* requires specific sterols and is affected by ergosterol biosynthesis inhibitors. Commercially available inhibitors

of cytochrome P-450 dependent C14 α sterol demethylase such as itraconazole or ketoconazole, however, do not eliminate the disease from chronically infected individuals. Trypanosomatid parasites contain acidocalcisomes, specialized organelles involved in calcium and polyphosphate storage. Inhibitors of enzymes which involve inorganic and organic pyrophosphate metabolism is a potential anti-trypanosomal chemotherapy target. Since trypanosomal parasites do not biosynthesize purines *de novo*, depletion of purine biosynthesis in the host is another potential strategy. The biochemical pathway for the synthesis of trypanothione is unique to protozoa and therefore presents an additional site for intervention.^{9,151-153}

The most promising target is the protein cruzain or cruzipain gp 57/51, a cysteine protease that is essential for replication and metabolism throughout the life cycle of the *T. cruzi* parasite. Several compounds that block the action of cruzain have been used to cure this infection in mouse models.^{142,157}

The high-resolution crystal structure of Cruzain (Figure 6.6) shows that this papain-like enzyme has 215 amino acid residues folded in two domains.¹⁵⁸ One domain is mainly α -helical (L domain) and the other consists of extensive antiparallel β -sheet interactions (R domain). The L domain includes residues 12 to 112 and 208 to 212 with helical regions 25 to 40, 50 to 56 and 68 to 78. The R domain is made up of residues 1 to 11 and 113 to 207 with residues 117 to 127 and 139 to 142 as helices.¹⁵⁸

The active site of cruzain contains residues Cys25, His159 and Asn175 as a catalytic triad.^{158,159} The thiol group of Cys25 has enhanced nucleophilicity due to the close proximity of the imadazole side-chain of His159 forming a thiolate-imidazolium pair stabilized by Asn175. It is believed that the indole ring of Trp177 helps position the

protease's catalytic triad asparagine in an orientation with the triad's histidine via a JI-NH interaction as Figure 6.7 shows.¹⁶⁰

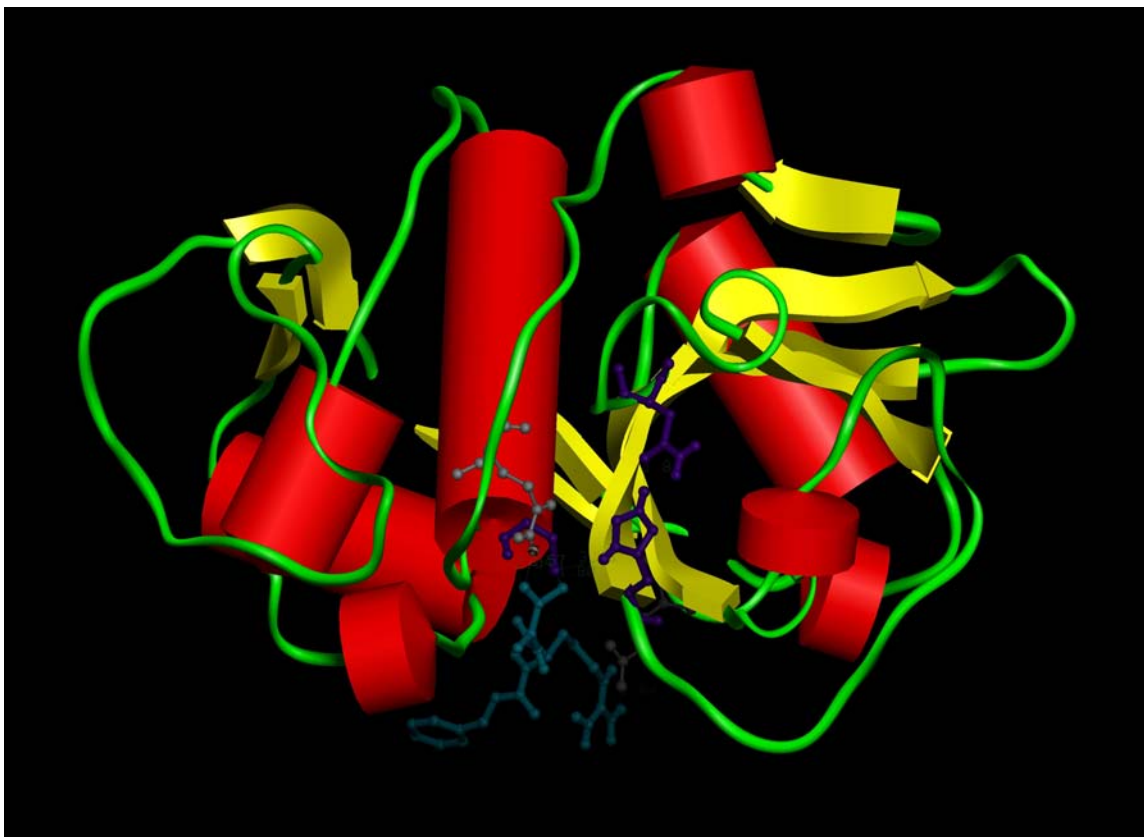


Figure 6.6. Crystal structure of cruzain complexed with Z-RA-FMK (benzyloxycarbonyl argininyalanyl fluoromethyl ketone) colored in aqua marina. The L-domain, which is located at the left side, is mainly α -helices and the right domain is mainly antiparallel β -sheets. The catalytic triad, Cys25, His159 and Asn175 is colored in purple and Gln19 is colored grey.¹⁵⁹ This picture was generated by using Accelrys Insight II software.

During hydrolysis of the substrate, carried out by the enzyme, the oxyanion hole is stabilized by hydrogen bond donors, mainly the Gln 19 residue.^{158,159,161} M. Sajid and co-workers reported that the main interactions of papain-like cysteine proteases with their substrates occur at sub-sites S'_1 , S_1 and S_2 as shown in Figure 6.9.¹⁶¹ Cruzain, which contains the key residue Glu205, has a primary substrate specificity at S_2 having a

preference for hydrophobic amino acids like Leu > Tyr > Phe > Val and positively charged groups. Although S₁ and S₃ specificities are broader than S₂, residues like Arg and Leu and Arg and Lys are preferred respectively while S₄ has no preference for any specific residue but does not bind well to aromatic or bulky hydrophobic side-chains (see Figure 6.8).^{143,159,161,162}

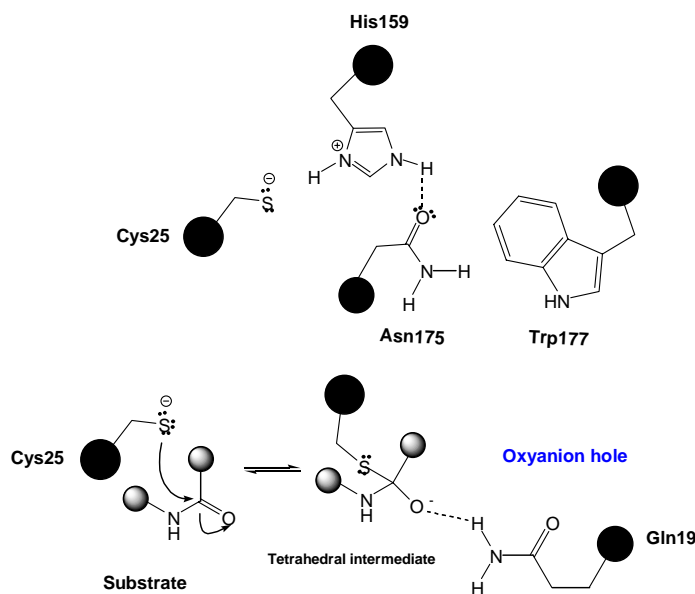


Figure 6.7. Proposed catalytic mechanism for cysteine proteases.^{160,161,163,164}

The development of cruzain inhibitors should take into consideration the potential interactions between inhibitor and host cysteine proteases such as the cathepsins B and L to avoid toxic effects. As pointed out by McKerrow, some of the protease inhibitors already known such as vinyl sulfones, can effectively inhibit human lysosomal proteases such as cathepsins B, L and S.¹⁶⁵ Serveau and co-workers studied the substrate specificity of cruzain by using cystatin derivatives, and they found that when a prolyl residue was introduced into the substrate at P'₂, the activity of cruzain increased much more than that of cathepsins B and L. These studies suggest the importance in

considering the P' sites of the inhibitor in order to discriminate between cruzain and mammalian cathepsins.¹⁶⁶

Another potential host enzyme that can cause toxic effects if it is inhibited is a threonine protease called the Proteasome. A three-dimensional structure of the proteasome subunit showed that its active site has well-defined hydrophobic subsites S₁ and S₃ (Phenylalanine, homophenylalanine and leucine or valine) but not a S₂ pocket which is a well-defined subsite in the parasite cysteine proteases.¹⁶⁵⁻¹⁶⁷

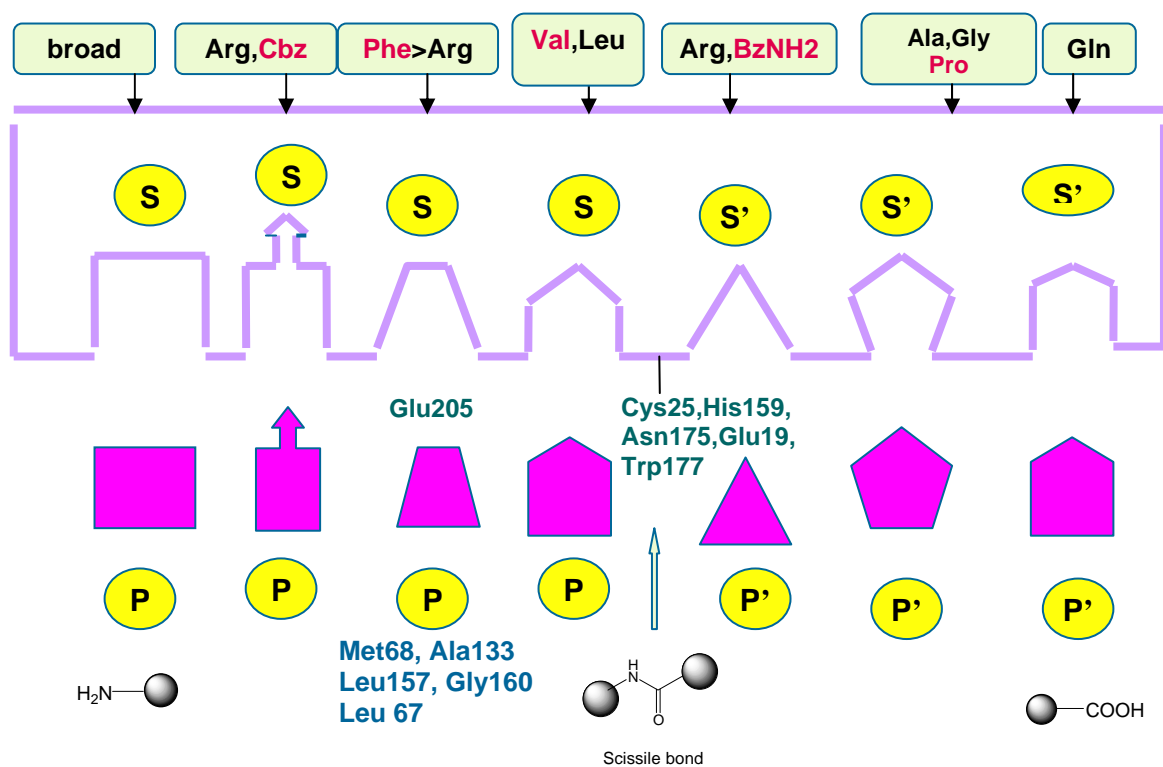


Figure 6.8. Active site of cruzain (S) with inhibitor or substrate (P). S₂ pocket is the major site of specificity in the interaction between the enzyme and the substrate. The substrate needs to have either a hydrophobic or a positively charged group to interact with Glu205 in the S₂ pocket. S₁ and S₃ are less important sub-sites for interaction. S' subsites are promising in order to increase the substrate discrimination for cruzain compared to mammalian cathepsins B, L and K.¹⁶⁵⁻¹⁶⁷

Many peptides derivatives have been synthesized that demonstrate excellent inhibition of cruzain but do not affect the parasite in tissues or, in the case of fluoromethyl ketone analogs, may be metabolized to toxic compounds (fluoroacetate). For this reason, one important goal focuses on the development of different type of bioisoster. While a vinyl sulfone derivative of a dipeptide is currently in clinical trials (K777), its lack of selectivity against different cysteine proteases is of concern.¹⁶⁸

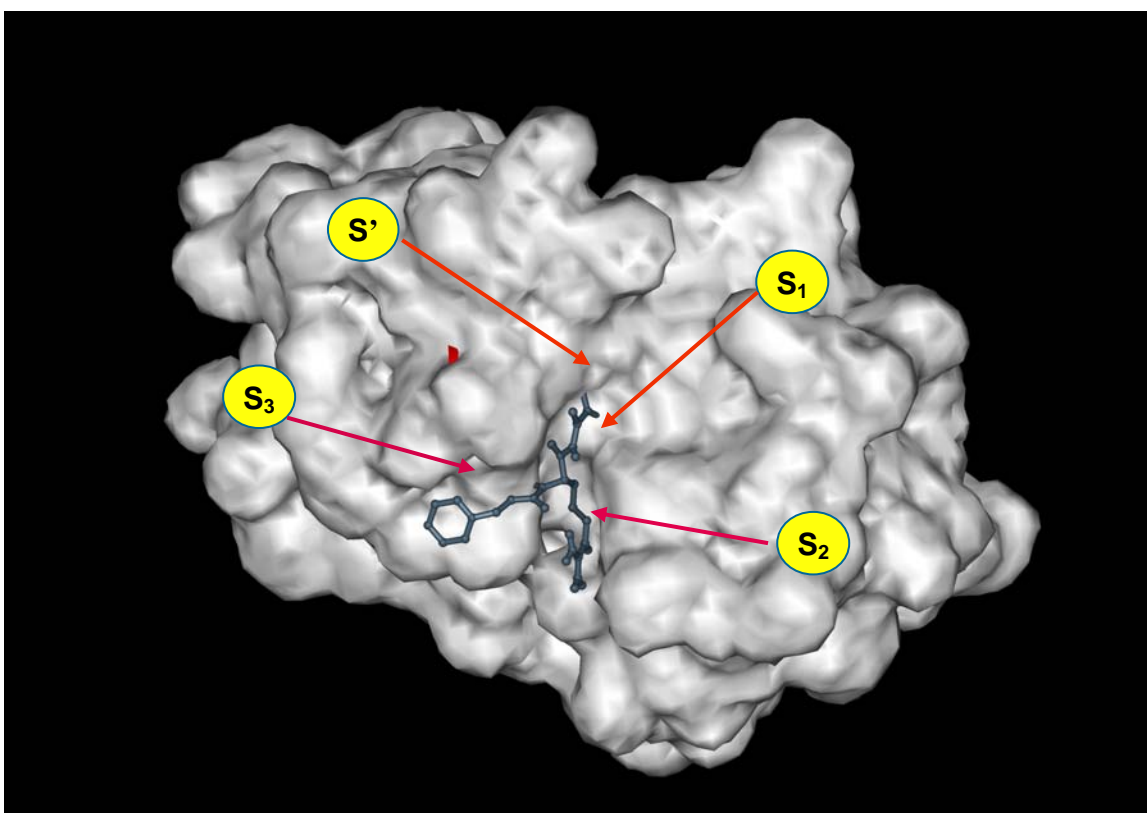


Figure 6.9. Surface representation of cruzain complexed with Z-RA-FMK (benzyloxycarbonyl argininy alanyl fluoromethyl ketone) showing the most important pockets of the active site. Note that the S₂ pocket is a deep subsite that can accommodate preferentially hydrophobic residues. This picture was generated bu using Accelrys Insight II software.¹⁶⁹

In 2002, Xiaohui Du and coworkers¹⁶⁹ from the University of California, San Francisco, were the first research team to introduce the thiosemicarbazone scaffold into drugs designed to treat Chagas' disease by targeting cruzain.²⁷ Among the more than 100 non-peptidic small molecules they synthesized, some of them were potent cruzain inhibitors and did not show significant toxicity. In particular, the 3'-bromopropiophenone thiosemicarbazone derivative was among the best cruzain inhibitor that exhibited no toxicity for mammalian cells at concentrations that were trypanocidal.¹⁶⁹ The proposed mechanism of action of these compounds with cruzain consists of a reversible 1,2-polar addition to the C=S bond. As Figure 6.10 shows, the acidic hydrogen of the imidazole ring of His159 attaches to the partial negatively charged sulfur atom and the resulting thiolate group (R-S⁻) formed from Cys25 binds to the electrophilic carbon of the double bond.²⁷

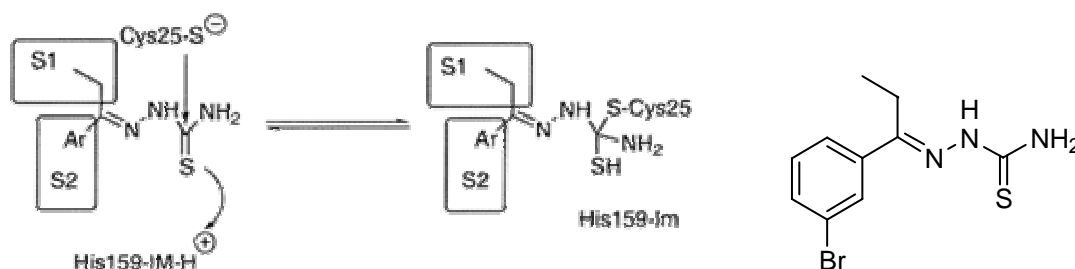


Figure 6.10 Left picture shows the proposed mechanism of Du and coworkers of reversible covalent interaction between thiosemicarbazones and cruzain based on experimental and modeling results. The right picture shows the structure of 3'-bromopropiophenone thiosemicarbazone, the best compound developed by this research team which showed significant cruzain activity and low toxicity against mammalian cells.²⁷ (Reproduced directly from reference 27).¹⁶⁹

In 2003, Idan Chiyanzu and coworkers used the same thiosemicarbazone scaffold to incorporate into the basic skeleton of a natural product called isatin and evaluated their

activity against cruzain and other two enzymes, Falcipain-2 and Rhodesain. The first enzyme is the major cysteine of *Plasmodium falciparum*, which is the causative agent of Malaria and the second is the cysteine protease of *Trypanosoma brucei rhodesiense*, a parasite that causes African sleeping sickness. Their results showed one more time that the presence of this scaffold improved the anti cruzain activity.¹⁷⁰ Additional support for the importance of this functional group used in the design of cysteine proteases was shown most recently by Fujii and coworkers who synthesized a small library of ten two-benzene ring containing thiosemicarbazones that showed antiparasitic activity against rhodesain and cruzain.¹⁷¹ Therefore, we thought that the incorporation of this scaffold into other pharmacophores might generate another generation of improved cysteine protease inhibitors.

We proposed, as convenient pharmacophores, the tetrahydronaphthalene and benzophenone skeletons as shown in Figure 6.11. In addition, the discover of other bioisosteres that retain or improve upon the activity of thiosemicarbazone derivatives is a further area of research focus. These alternative functional groups that we propose include an α,β -conjugated carbonyl group¹⁷² and epoxide functionalities which are also shown in Figure 6.11.

In summary, the main goal of this project is to generate a convenient pharmacophore that inhibits cruzain with the same or better efficacy than 3'-bromopropiophenone thiosemicarbazone does. Secondly, we will incorporate other functional groups different from the thiosemicarbazone moiety and evaluate the biological activities of these new analogs.

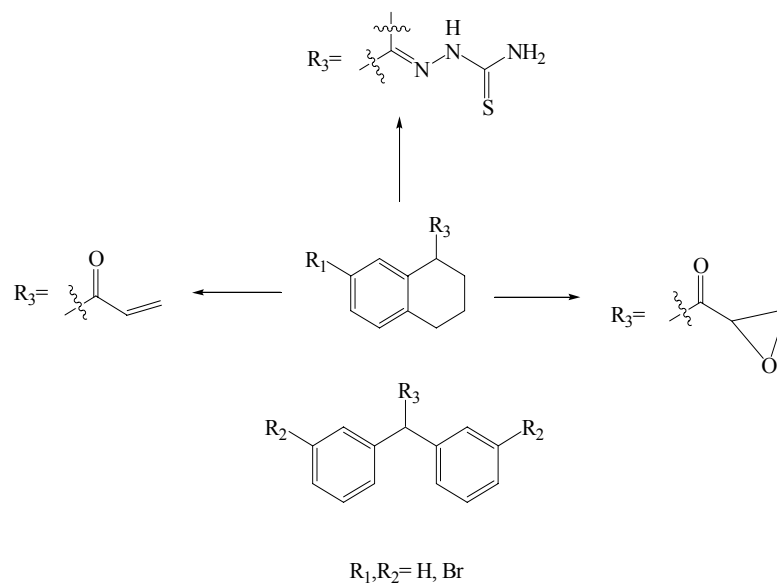


Figure 6.11. Structures of tetrahydronaphthalene (middle structure) and benzophenone (bottom) skeletons used as pharmacophores containing thiosemicarbazone (top), conjugated carbonyl (left) and epoxide (right) functionalities to inhibit cruzain and related cysteine proteases.

Although the primarily target is cruzain, it is conceivable that this first generation of compounds might be active against other cysteine proteases as well including the mammalian cathepsins L and B and other parasitic related proteases. Therefore, in a second generation of compounds (which is out the scope of this current project), selectivity will be incorporated.

CHAPTER SEVEN

Materials and Methods

General Section

Chemicals were obtained from commercial companies such as Acros Chemicals, Aldrich Chemical Company, Alfa Aesar, Lancaster Chemicals, and Fisher Scientific. Reactions which involved air or moisture sensitive reagents were performed in oven-dried glassware under nitrogen atmosphere using dried syringes, needles and cannulas to transfer solvents and reagents. Reactions were monitored by silica gel thin layer chromatography (TLC) using Merk Kieselgel 60 F₂₅₄ glass backed plates. The plates were visualized by the use of a multiband 254/365 nm UV lamp, iodine or by dipping either in a solution of vanillin (in ethanolic sulphuric acid), PMA (in ethanol), anisaldehyde (in ethanol), ceric sulfate (in sulfuric acid), DNP (in an aqueous ethanolic sulfuric acid) or potassium permanganate (in basic water) followed by heating. Gas chromatography (Hewlett Packard 5890 Series II with a SE-54 column) and /or gas chromatography mass spectrometry (Hewlett Packard GCD system with electron impact ionization) were also used to monitor reactions. Flash chromatography was carried out with silica gel (230-400 mesh) purchased from BODMAN industries. Solvents used for chromatography and workups (CH₂Cl₂, hexanes, THF and acetone) were purified by distillation prior to use. Ethyl acetate, methanol, ethanol, diethyl ether and other solvents were purchased from the above mentioned companies as anhydrous solvents and used without further purification. Evaporation or removal of the solvents were performed with

a rotary evaporator in *vacuo* followed by a further drying of the compound with a mechanical pump at vacuum pressures of < 0.5 Torr.

Structure elucidation of the products was carried out using spectroscopic techniques such as NMR, IR and MS. ^1H NMR spectra were recorded at 300 or 360 MHz on a Bruker DPX-300 and AMX-360 spectrometers. ^{13}C spectra were recorded at 75 or 90 MHz and ^{31}P spectra were recorded at 121 MHz. All NMRs were recorded in CDCl_3 (0.03% of TMS) unless stated otherwise. Chemical shifts, which are expressed in ppm (δ), are referenced to tetramethylsilane (TMS). The NMR patterns are reported as singlets (s), doublets (d), triplets (t), quartets (q), multiplets (m), etc and the coupling constants (J) are reported in Hz. All the spectra are reported in a decoupled mode unless stated otherwise. Special NMR techniques such as low and high temperature NMR and NOESY were carried out on the Bruker AMX-360 spectrometer. Homonuclear decoupling, resolution enhancement, 2D NMR was performed on both spectrometers. NMR processing data was carried out using WinNMR, Mestrec or Nuts. IR spectra were run either neat (for liquids and solutions) or as nujol mulls (for solids) on a Genesis II FTIR spectrometer. The melting points, which were recorded uncorrected, were determined on a Thomas Hoover capillary melting point apparatus.

Synthesis of Propiophenone Derivatives

3-Bromopropiophenone thiosemicarbazone (49).¹⁶⁹ Into a round bottom flask containing 3-bromopropiophenone (0.508 g, 2.34 mmol), 20 mL of anhydrous methanol were added and the solution was refluxed for 15 minutes. To the warm ketone solution, thiosemicarbazide (0.184 g, 2.04 mmol) and 1% solution of HOAc (0.2 mL) were added.

The reaction mixture was refluxed under nitrogen atmosphere for 17 h, at which point, the solvent was evaporated and, the crude reaction mixture was purified by flash chromatography (30% EtOAc/ 70% hex) to obtain 0.2498 g (0.873 mmol) of the product in a 37% yield.

^1H NMR (300 MHz, methyl sulfoxide- d_6 , δ): 10.39 (s, NH , 1H), 8.35 (br s, NH_2 , 1H), 8.17 (t, $J = 1.7$, ArH , 1H), 8.12 (br s, NH_2 , 1H), 7.87 (ddd, $J = 7.9, 1.6, 0.8$, ArH , 1H), 7.57 (ddd, $J = 7.9, 1.9, 0.8$, ArH , 1H), 7.34 (t, $J = 7.9$, ArH , 1H), 2.86 (q, $J = 7.4$, CH_2 , 2H), 0.99 (t, $J = 7.5$, CH_3 , 3H).

^{13}C NMR (75 MHz, methyl sulfoxide- d_6): δ 179.0, 150.3, 138.8, 131.9, 130.5, 129.0, 125.8, 122.2, 19.1, 10.8.

Dept 135 NMR (75 MHz, methyl sulfoxide- d_6): δ 132.3 ($\underline{\text{C}}\text{H}$), 130.9 ($\underline{\text{C}}\text{H}$), 129.5 ($\underline{\text{C}}\text{H}$), 126.3 ($\underline{\text{C}}\text{H}$), 19.6 ($\underline{\text{C}}\text{H}_2$), 11.3 ($\underline{\text{C}}\text{H}_3$).

3-Nitropropiophenone thiosemicarbazone (50). Into a round bottom flask containing 3-nitropropiophenone (1.02 g, 5.53 mmol), 30 mL of anhydrous methanol were added and the solution was refluxed for about 15 minutes. To the warm ketone solution, thiosemicarbazide (0.485 g, 5.33 mmol) and 1% solution of HOAc (0.4 mL) were added. The reaction mixture was refluxed under nitrogen atmosphere for 30 h, at which point, the solvent was evaporated and, the crude reaction mixture was purified by flash chromatography (50% EtOAc/ 50% hex) to obtain 0.8119 g (3.22 mmol) of the product in a 58% yield.

^1H NMR (300 MHz, acetone- d_6 , δ): 9.62 (br s, NH , 1H), 8.66 (t, $J = 1.9$, ArH , 1H), 8.38 (ddd, $J = 7.9, 1.8, 1.0$, ArH , 1H), 8.25 (ddd, $J = 8.2, 2.3, 1.0$, ArH , 1H), 8.07

(br s, NH_2 , 1H), 7.72 (t, $J = 8.1$, ArH, 1H), 7.66 (br s, NH_2 , 1H), 3.09 (q, $J = 7.7$, CH_2 , 2H), 1.23 (t, $J = 7.7$, CH_3 , 3H).

3-Aminopropiophenone thiosemicarbazone (51). Into a round bottom flask containing 3-nitropropiophenone (0.102 g, 0.406 mmol), Zn (0.884 g, 13.5 mmol) and CaCl_2 (0.0398 g, 0.271 mmol), 7.5 mL of EtOH- H_2O (4:1 ratio) were added and the solution was refluxed for about 1.5 h. At the end of this time, the reaction mixture was filtered through celite and silica gel, rinsed twice with EtOH (2 x 5 mL) and the solvent evaporated. The product was purified by flash chromatography (40% EtOAc/ 60% hex) to obtain 0.0420 g (0.189 mmol) of the amine in a 47% yield.

E- isomer: ^1H NMR (300 MHz, acetone- d_6 , δ): 9.39 (br s, NH , 1H), 7.79 (br s, NH_2 , 1H), 7.54 (br s, NH_2 , 1H), 7.24 (m, ArH, 1H), 7.09 (m, ArH, 2H), 6.72 (m, ArH, 1H), 4.70 (br s, NH , 2H), 2.89 (q, $J = 7.6$, CH_2 , 2H), 1.16 (t, $J = 7.4$, CH_3 , 3H).

Dept 135 NMR (75 MHz, acetone- d_6): δ 129.0 ($\underline{\text{C}}\text{H}$), 115.5 ($\underline{\text{C}}\text{H}$), 115.2 ($\underline{\text{C}}\text{H}$), 112.3 ($\underline{\text{C}}\text{H}$), 19.6 ($\underline{\text{C}}\text{H}_2$), 10.5 ($\underline{\text{C}}\text{H}_3$).

*3-(*t*-Butyldimethylsilyloxy)benzaldehyde (52)*. Into a round bottom flask containing 3-hydroxybenzaldehyde (0.658 g, 5.23 mmol) and DMAP (0.0646 g, 0.52 mmol), first 10 mL of anhydrous CH_2Cl_2 and then 0.89 mL of NEt_3 (0.634 g, 6.27 mmol) were added. After the reaction mixture was stirred under nitrogen at 0 °C for 10 minutes, 5 mL of a CH_2Cl_2 solution of TBSCl (0.976 g, 6.28 mmol) were added. The reaction mixture was stirred for 2.5 h at room temperature and, then it was filtered through silica gel-florisil, rinsed with CH_2Cl_2 and the organic phase dried under Na_2SO_4 . After

evaporating the solvent, 1.1308 g (4.79 mmol) of pure product was obtained in a 92% yield.

^1H NMR (300 MHz, CDCl_3): δ 9.94 (s, CHO , 1H), 7.46 (td, $J = 7.5, 1.3$, ArH, 1H), 7.39 (t, $J = 7.7$, ArH, 1H), 7.31 (dd, $J = 2.5, 1.5, 1.0$, ArH, 1H), 7.09 (ddd, $J = 7.9, 2.5, 1.2$, ArH, 1H), 0.98 (s, $\text{C}(\text{CH}_3)_3$, 9H), 0.21 (s, $\text{Si}(\text{CH}_3)_2$, 6H).

3-(t-Butyldimethylsilyloxyphenyl)-1-propanol (53). 9 mL of anhydrous Et_2O were poured into a dry flask containing Mg (0.442 g, 18.0 mmol) and few crystals of I_2 . While the reaction mixture was being stirred at room temperature under nitrogen, 10 drops of ethyl bromide (1.86 g, 17.1 mmol) were added. After the reaction mixture became cloudy (approximately 10 minutes after bromide addition), the rest of the ethyl bromide (1.3 mL) was added during a 50-minute period and the reaction mixture was refluxed at 45 °C for 2 h. When almost all the Mg was consumed, the reaction flask was put in ice bath and 5 mL of an ethereal solution of aldehyde **52** (1.85 g, 7.82 mmol) were added during 15 minutes. The reaction mixture was stirred for 4 h at room temperature, at which point, first H_2O was added and, then 3 mL of HCl (6M). The product was extracted twice from the aqueous phase with Et_2O and the resultant organic phase was washed once with H_2O and once with brine. After drying the organic phase under Na_2SO_4 , the solvent was evaporated and 1.9952 g (7.50 mmol) of pure product was obtained in a 91% yield.

^1H NMR (300 MHz, CDCl_3 , δ): 7.18 (t, $J = 7.8$, ArH, 1H), 6.91 (ddd, $J = 7.5, 2.6, 0.6$, ArH, 1H), 6.82 (dd, $J = 2.3, 1.8$, ArH, 1H), 6.74 (ddd, $J = 8.0, 2.5, 1.0$, ArH, 1H), 4.53 (t, $J = 6.6$, CHOH , 1H), 1.83 (br s, OH, 1H), 1.75 (m, CH_2 , 2H), 0.97 (s, $\text{C}(\text{CH}_3)_3$, 9H), 0.90 (dd, $J = 8.6, 6.3$, CH_3 , 3H), 0.18 (s, $\text{Si}(\text{CH}_3)_2$, 6H).

*1-(3-*t*-Butyldimethylsilyloxyphenyl)propan-1-one (54)*. 30 mL of anhydrous CH₂Cl₂ were poured into a flask containing PCC (2.63 g, 12.0 mmol) and celite (2.6 g). The suspension was stirred at 0°C under nitrogen for 10 minutes, at which point, 12 mL of a CH₂Cl₂ solution of alcohol **53** (2.00 g, 7.50 mmol) were added. After the reaction was stirred at room temperature for 4 h, 20 mL of Et₂O were added and the reaction mixture was filtered through fluorisil - silica gel and rinsed with extra Et₂O (10 mL). The organic phase was dried under Na₂SO₄ and the solvent was evaporated to afford 1.842 g (6.98 mmol) of pure product in an 86% yield.

¹H NMR (300 MHz, CDCl₃, δ): 7.54 (ddd, *J* = 7.7, 1.6, 1.0, ArH, 1H), 7.41 (dd, *J* = 2.5, 1.6, ArH, 1H), 7.30 (t, *J* = 7.9, ArH, 1H), 7.01 (ddd, *J* = 8.0, 2.5, 1.0, ArH, 1H), 2.96 (q, *J* = 7.2, CH₂, 2H), 1.20 (t, *J* = 7.2, CH₃, 3H), 0.98 (s, C(CH₃)₃, 9H), 0.20 (s, Si(CH₃)₂, 6H).

¹³C NMR (75 MHz, CDCl₃): δ 200.6, 156.0, 138.4, 129.5, 124.7, 121.1, 119.3, 31.9, 25.7, 18.2, 8.3, -4.4

Dept 135 NMR (75 MHz, CDCl₃): δ 129.5 (CH), 124.7 (CH), 121.11 (CH), 119.3 (CH), 31.9 (CH₂), 25.7 (CH₃), 8.3 (CH₃), -4.4 (CH₃).

*1-(3-*t*-Butyldimethylsilyloxyphenyl)propan-1-one thiosemicarbazone (55)*. Into a round bottom flask containing the TBS protected ketone **54** (0.645 g, 2.44 mmol), 20 mL of anhydrous methanol were added and the solution was refluxed for about 15 minutes. To the warm ketone solution, thiosemicarbazide (0.214 g, 2.85 mmol) and 1% solution of HOAc (0.5 mL) were added. The reaction mixture was refluxed under nitrogen atmosphere for 23 h, at which point, the solvent was evaporated and, the crude reaction

mixture was purified by flash chromatography (20% EtOAc/ 80% hex) to obtain 0.6741 g (2.07 mmol) of a mixture of *E/Z* thiosemicarbazones (1.2: 1 ratio) in an 85% yield.

E- isomer: ^1H NMR (300 MHz, CDCl_3 , δ): 8.80 (br s, NH , 1H), 7.35 (t, $J = 7.9$, ArH , 1H), 7.34 (br s, NH_2 , 1H), 7.15 (dd, $J = 1.6, 0.6$, ArH , 1H), 6.91 (ddd, $J = 8.3, 2.4, 0.9$, ArH , 1H), 6.90 (dt, $J = 7.2, 2.2$, ArH , 1H), 6.42 (br s, NH_2 , 1H), 2.70 (q, $J = 7.8$, CH_2 , 2H), 1.21 (t, $J = 7.7$, CH_3 , 3H), 1.00 (s, $\text{C}(\text{CH}_3)_3$, 9H), 0.22 (s, $\text{Si}(\text{CH}_3)_2$, 6H).

^{13}C NMR (75 MHz, CDCl_3): δ 179.4, 156.0, 152.7, 137.6, 129.6, 121.6, 119.4, 118.1, 25.7, 20.4, 18.2, 10.6, -4.3.

Dept 135 NMR (75 MHz, CDCl_3): δ 129.6 ($\underline{\text{C}}\text{H}$), 121.7 ($\underline{\text{C}}\text{H}$), 119.5 ($\underline{\text{C}}\text{H}$), 118.1 ($\underline{\text{C}}\text{H}$), 25.7 ($\underline{\text{C}}\text{H}$), 20.4 ($\underline{\text{C}}\text{H}_2$), 10.7 ($\underline{\text{C}}\text{H}_3$), -4.3 ($\underline{\text{C}}\text{H}_3$).

Z- isomer: ^1H NMR (300 MHz, CDCl_3 , δ): 8.62 (br s, NH , 1H), 7.29 (br s, NH_2 , 1H), 7.26 (t, $J = 7.7$, ArH , 1H), 6.79 (ddd, $J = 7.5, 1.4, 1.1$, ArH , 1H), 6.66 (dd, $J = 2.2, 1.9$, ArH , 1H), 6.29 (br s, NH_2 , 1H), 2.56 (q, $J = 7.4$, CH_2 , 2H), 1.11 (t, $J = 7.4$, CH_3 , 3H), 1.00 (s, $\text{C}(\text{CH}_3)_3$, 9H), 0.24 (s, $\text{Si}(\text{CH}_3)_2$, 6H).

^{13}C NMR (75 MHz, CDCl_3): δ 178.9, 156.8, 155.4, 134.2, 131.0, 121.6, 119.4, 118.4, 31.5, 25.6, 18.2, 10.6, -4.3.

Dept 135 NMR (75 MHz, CDCl_3): δ 131.0 ($\underline{\text{C}}\text{H}$), 121.7 ($\underline{\text{C}}\text{H}$), 119.4 ($\underline{\text{C}}\text{H}$), 118.4 ($\underline{\text{C}}\text{H}$), 31.5 ($\underline{\text{C}}\text{H}_2$), 25.7 ($\underline{\text{C}}\text{H}_3$), 10.7 ($\underline{\text{C}}\text{H}_3$), -4.3 ($\underline{\text{C}}\text{H}_3$).

1-(3-Hydroxyphenyl)-1-propanone thiosemicarbazone (56). At 0 °C and under nitrogen, the TBS protected thiosemicarbazone **55** (0.344g, 1.06 mmol) was dissolved with 10 mL of anhydrous CH_2Cl_2 . To the well stirred solution, 1.6 mL of a solution (1M in THF) of TBAF (0.418 g, 1.6 mmol) was added and the reaction mixture was stirred at room temperature for 1.5 h. At the end of this period of time, H_2O was added to the

reaction mixture, the product was extracted once from the aqueous phase with CH_2Cl_2 and the resultant organic phase was washed once with H_2O , once with brine and dried under Na_2SO_4 . The product was purified from the crude of reaction by flash chromatography (30% EtOAc/ 70% hex) to afford 0.2338 g (1.05 mmol) of thiosemicarbazone in a 99% yield.

E- isomer: ^1H NMR (360 MHz, CDCl_3 , δ): 9.38 (br s, NH , 1H), 7.72 (br s, NH_2 , 1H), 7.47 (br s, NH_2 , 1H), 7.34 (m, ArH , 1H), 7.26 (m, ArH , 2H), 6.96 (m, ArH , 1H), 2.80 (q, $J = 7.6$, CH_2 , 2H), 1.20 (t, $J = 7.5$, CH_3 , 3H).

Dept 135 NMR (90 MHz, CDCl_3): δ 134.7 ($\underline{\text{C}}\text{H}$), 123.3 ($\underline{\text{C}}\text{H}$), 122.1 ($\underline{\text{C}}\text{H}$), 118.6 ($\underline{\text{C}}\text{H}$), 25.4 ($\underline{\text{C}}\text{H}_2$), 15.9 ($\underline{\text{C}}\text{H}_3$).

1-Phenyl-1-(3-bromophenyl)methanol (57) 6 mL of anhydrous Et_2O were poured into a dry flask containing Mg (0.448 g, 18.2 mmol) and few crystals of I_2 . While the reaction mixture was stirred at room temperature under nitrogen, 14 drops of bromobenzene (2.74 g, 17.5 mmol) were added. After the reaction mixture became cloudy (approximately 5 minutes after bromide addition), the rest of the bromobenzene (1.86 mL) was added during a 30-minute period and, the reaction mixture was refluxed at 40 °C for 2.5 h. When almost all the Mg was consumed, the reaction flask was put in ice bath and 3 mL of an ethereal solution of *m*-bromobenzaldehyde (1.50 g, 7.93 mmol) were added during 10 minutes. The reaction mixture was stirred for 2 h at room temperature, at which point, first H_2O was added and, then 6.6 mL of HCl (6M). The product was extracted twice from the aqueous phase with Et_2O and the resultant organic phase was washed once with H_2O and once with brine. After drying the organic phase under Na_2SO_4 , the solvent was evaporated and the product was purified by flash

chromatography (10% EtOAc/ 90% hex). 1.8611 g (7.08 mmol) of pure alcohol was obtained in a 89% yield.

^1H NMR (300 MHz, CDCl_3 , δ): 7.56 (t, $J = 1.8$, ArH, 1H), 7.34 (m, ArH, 7H), 7.19 (t, $J = 7.8$, ArH, 1H), 5.79 (s, CHOH, 1H), 2.23 (br s, OH, 1H).

Dept 135 NMR (75 MHz, CDCl_3): δ 130.6 ($\underline{\text{C}}\text{H}$), 130.1 ($\underline{\text{C}}\text{H}$), 129.5 ($\underline{\text{C}}\text{H}$), 128.7 ($\underline{\text{C}}\text{H}$), 128.0 ($\underline{\text{C}}\text{H}$), 126.6 ($\underline{\text{C}}\text{H}$), 125.1 ($\underline{\text{C}}\text{H}$), 75.7 ($\underline{\text{C}}\text{HOH}$).

EIMS: m/z (% rel. intensity) 264 ($\text{M}^+ + 2$, 16), 262 (M^+ , 16), 185 (23), 183 (28), 105 (100), 77 (40).

Synthesis of Benzophenone Thiosemicarbazones Derivatives

Phenyl(3-bromophenyl) ketone (58) 30 mL of anhydrous CH_2Cl_2 were poured into a flask containing PCC (2.34 g, 10.6 mmol) and celite (2.3 g). The suspension was stirred at 0°C under nitrogen for 10 minutes, at which point, 10 mL of a CH_2Cl_2 solution of alcohol **57** (1.86 g, 7.08 mmol) were added. After the reaction was stirred at room temperature for 4 h, 15 mL of Et_2O were added and the reaction mixture was filtered through Fluorisil - silica gel bed and rinsed with extra Et_2O (10 mL). The organic phase was dried under Na_2SO_4 and the solvent was evaporated to afford 1.7852 g (6.84 mmol) of pure product in a 97% yield.

^1H NMR (300 MHz, CDCl_3 , δ): 7.93 (t, $J = 1.8$, ArH, 1H), 7.78 (m, ArH, 2H), 7.71 (dd, $J = 8.1, 1.6$, ArH, 2H), 7.61 (tt, $J = 7.4, 1.3$, ArH, 1H), 7.49 (tt, $J = 6.8, 1.5$, ArH, 2H), 7.36 (t, $J = 7.8$, ArH, 1H).

Dept 45 NMR (75 MHz, CDCl_3): δ 135.3 ($\underline{\text{C}}\text{H}$), 132.9 ($\underline{\text{C}}\text{H}$), 132.8 ($\underline{\text{C}}\text{H}$), 130.1 ($\underline{\text{C}}\text{H}$), 129.9 ($\underline{\text{C}}\text{H}$), 128.6 ($\underline{\text{C}}\text{H}$), 128.5 ($\underline{\text{C}}\text{H}$).

EIMS: m/z (% rel. intensity) 262 ($M^+ + 2$, 25), 260 (M^+ , 25), 185 (16), 183 (16), 105(100), 77 (33).

Phenyl(3-bromophenyl) ketone thiosemicarbazone (59) Into a round bottom flask containing ketone **58** (1.79 g, 6.84 mmol), 30 mL of anhydrous methanol were added and the solution was refluxed for about 15 minutes. To the warm ketone solution, thiosemicarbazide (0.600 g, 6.59 mmol) and 1% solution of HOAc (0.8 mL) were added. The reaction mixture was refluxed under nitrogen atmosphere for 26 h, at which point, the solvent was evaporated and, the crude reaction mixture was purified by flash chromatography (30% EtOAc/ 70% hex) to obtain 0.7739 g (2.32 mmol) of the product in a 34% yield.

E- isomer: ^1H NMR (300 MHz, methyl sulfoxide- d_6 , δ): 8.69 (br s, NH , 1H), 8.57 (br s, NH_2 , 1H), 8.42 (br s, NH_2 , 1H), 8.07 (s, ArH , 1H), 7.59 (m, ArH , 4H), 7.36 (m, ArH , 4H).

1,1-Bis(3-bromophenyl)methanol (60) 7 mL of anhydrous Et_2O were poured into a dry flask containing Mg (0.530 g, 21.6 mmol) and few crystals of I_2 . While the reaction mixture was being stirred at room temperature under nitrogen, 6 drops of *m*-dibromobenzene (4.92 g, 20.9 mmol) were added. After the reaction mixture became cloudy (approximately 30 minutes after bromide addition), the rest of the dibromobenzene (2.6 mL) was added during a 30-minute period and, the reaction mixture was refluxed at 30 °C for 1.5 h. When almost all the Mg was consumed, the reaction flask was put in ice bath and, 5 mL of an ethereal solution of *m*-bromobenzaldehyde (1.77 g, 9.38 mmol) were added during 10 minutes. The reaction mixture was stirred for

3.5 h at room temperature, at which point, first H₂O (4 mL) was added and, then 5 mL of HCl (6M). The product was extracted twice from the aqueous phase with Et₂O and the resultant organic phase was washed once with H₂O and once with brine. After drying the organic phase under Na₂SO₄, the solvent was evaporated and the product was purified by flash chromatography (10% EtOAc/ 90% hex). 1.99 g (5.82 mmol) of pure alcohol was obtained in a 62% yield.

¹H NMR (360 MHz, CDCl₃, δ): 7.53 (t, *J* = 1.8, ArH, 2H), 7.41 (ddd, *J* = 7.7, 2.0, 1.4, ArH, 2H), 7.27 (dtd, *J* = 7.5, 1.6, 0.4, ArH, 2H), 7.21 (t, *J* = 7.7, ArH, 2H), 5.75 (s, CHOH, 1H), 2.31 (br s, OH, 1H).

Dept 135 NMR (90 MHz, CDCl₃): δ 131.0 (CH), 130.3 (CH), 129.6 (CH), 125.2 (CH), 75.0 (CHOH).

EIMS: *m/z* (% rel. intensity) 344 (M⁺ + 4, 8), 342 (M⁺ + 2, 17), 340 (M⁺, 8), 185 (100), 183(89), 157 (25), 77 (50).

Bis(3-bromophenyl) ketone (61) 30 mL of anhydrous CH₂Cl₂ were poured into a flask containing PCC (1.92 g, 8.73 mmol) and celite (1.9 g). The suspension was stirred at 0°C under nitrogen for 10 minutes, at which point, 10 mL of a CH₂Cl₂ solution of alcohol **60** (1.99 g, 5.82 mmol) were added. After the reaction was stirred at room temperature for 5.5 h, 15 mL of Et₂O were added and the reaction mixture was filtered through fluorisil - silica gel and rinsed with extra Et₂O (10 mL). The organic phase was dried under Na₂SO₄ and the solvent was evaporated to afford 1.673 g (4.92 mmol) of pure product in a 85% yield.

^1H NMR (300 MHz, CDCl_3 , δ): 7.92 (t, $J = 1.8$, ArH, 2H), 7.73 (ddd, $J = 8.0, 2.0, 1.1$, ArH, 2H), 7.68 (ddd, $J = 7.7, 1.6, 1.2$, ArH, 2H), 7.37 (t, $J = 7.8$, ArH, 2H).

^{13}C NMR (75 MHz, CDCl_3): δ 193.7, 138.8, 135.7, 132.7, 130.0, 128.5, 122.8.

Bis(3-bromophenyl) ketone thiosemicarbazone (62) Into a round bottom flask containing ketone **61** (1.044 g, 3.07 mmol), 35 mL of anhydrous methanol were added and the solution was refluxed for about 15 minutes. To the warm ketone solution, thiosemicarbazide (0.294 g, 3.23 mmol) and 1% solution of HOAc (1.5 mL) were added. The reaction mixture was refluxed under nitrogen atmosphere for 46 h, at which point, the solvent was evaporated and, the crude reaction mixture was purified by flash chromatography (20% EtOAc/ 80% hex) to obtain 0.231 g (0.559 mmol) of the product in an 18% yield.

^1H NMR (360 MHz, CDCl_3 , δ): 8.59 (br s, NH, 1H), 7.72 (s, ArH, 2H), 7.41 (m, ArH, 6H), 6.92 (br s, NH₂, 1H).

Synthesis of Tetrahydronaphthalene Derivatives

5-Bromo-1-tetralone (63).¹⁷³ Into a round bottom flask kept at 0 °C, AlCl_3 (19.6 g, 146.8 mmol) was added and the reaction system was put under nitrogen. 8 mL of tetralone (8.62 g, 58.9 mmol) were added during a 10-minute period, at which point, the reaction mixture was heated in an oil bath at 90 °C for about 45 minutes before adding 3.6 mL of Br_2 (11.2 g, 70.1 mmol). The reaction mixture was stirred at 90 °C for an hour before 30 mL of ice-water and 20 mL of NaHCO_3 were added. The product was extracted twice from the aqueous phase with Et_2O and, the resultant organic phase was

washed once with NaHCO₃, once with brine and dried under Na₂SO₄. The crude reaction mixture was purified by flash chromatography (2.5% EtOAc/ 97.5% hex) which afforded 5.87 g (26.1 mmol) of the product in a 44% yield.

¹H NMR (300 MHz, CDCl₃, δ): 8.01 (dd, *J* = 7.8, 1.3, ArH, 1H), 7.73 (dd, *J* = 7.9, 1.3, ArH, 1H), 7.18 (tt, *J* = 7.9, 0.6, ArH, 1H), 3.01 (t, *J* = 6.2, CH₂, 2H), 2.64 (dd, *J* = 6.7, 5.6, CH₂, 2H), 2.15 (td, *J* = 13.0, 6.5, CH₂, 2H).

¹³C NMR (75 MHz, CDCl₃): δ 197.5, 143.4, 137.3, 134.9, 127.7, 126.5, 124.8, 38.2, 30.0, 22.3.

Dept 135 NMR (75 MHz, CDCl₃): δ 137.3 (CH), 127.7 (CH), 126.5 (CH), 38.2 (CH₂), 30.0 (CH₂), 22.3 (CH₂).

EIMS: *m/z* (% rel. intensity) 226 (M⁺ + 2, 93), 224 (M⁺, 93), 211 (25), 209 (25), 198(100), 196 (100), 170 (50), 168 (50), 145 (25), 115 (45), 89 (60), 63 (28).

7-Bromo-1-tetralone (**64**).¹⁷³ Into a round bottom flask kept at 0 °C, AlCl₃ (19.6 g, 146.8 mmol) was added and the reaction system was put under nitrogen. 8 mL of tetralone (8.62 g, 58.9 mmol) were added during a 10-minute period, at which point, the reaction mixture was heated in an oil bath at 90 °C for about 45 minutes before adding 3.6 mL of Br₂ (11.2 g, 70.1 mmol). The reaction mixture was stirred at 90 °C for an hour before 30 mL of ice-water and 20 mL of NaHCO₃ were added. The product was extracted twice from the aqueous phase with Et₂O and, the resultant organic phase was washed once with NaHCO₃, once with brine and dried under Na₂SO₄. The crude reaction mixture was purified by flash chromatography (2.5% EtOAc/ 97.5% hex) which afforded 5.36 g (23.8 mmol) of the product in a 40% yield.

^1H NMR (300 MHz, CDCl_3 , δ): 8.14 (d, $J = 2.2$, ArH, 1H), 7.56 (dd, $J = 8.1, 2.2$, ArH, 1H), 7.13 (d, $J = 8.2$, ArH, 1H), 2.90 (t, $J = 6.1$, CH_2 , 2H), 2.64 (dd, $J = 5.7, 5.5$, CH_2 , 2H), 2.12 (td, $J = 12.7, 6.4$, CH_2 , 2H).

Dept 135 NMR (75 MHz, CDCl_3): δ 136.1 ($\underline{\text{C}}\text{H}$), 130.7 ($\underline{\text{C}}\text{H}$), 130.0 ($\underline{\text{C}}\text{H}$), 38.8 ($\underline{\text{C}}\text{H}_2$), 29.2 ($\underline{\text{C}}\text{H}_2$), 23.1 ($\underline{\text{C}}\text{H}_2$).

EIMS: m/z (% rel. intensity) 226 ($\text{M}^+ + 2$, 100), 224 (M^+ , 100), 211 (25), 209 (25), 198(75), 196 (75), 170 (60), 168 (60), 145 (25), 115 (45), 89 (58), 63 (28).

5-Bromo-1-tetralone thiosemicarbazone (65) Into a round bottom flask containing ketone **63** (0.343 g, 1.52 mmol), 16 mL of anhydrous methanol were added and the solution was refluxed for about 15 minutes. To the warm ketone solution, thiosemicarbazide (0.182 g, 2.00 mmol) and about 80 mg of TsOH were added. The reaction mixture was refluxed under nitrogen atmosphere for 7.5 h, at which point, the white solid formed was filtered and, rinsed with cold MeOH. After drying the solid under reduced pressure, 0.3577 g (1.20 mmol) of the product was obtained in a 79% yield.

^1H NMR (300 MHz, acetone- d_6 , δ): 9.25 (s, NH, 1H), 8.22 (dd, $J = 8.0, 1.2$, ArH, 1H), 7.87 (br s, NH_2 , 1H), 7.55 (dd, $J = 7.9, 1.2$, ArH, 1H), 7.47 (br s, NH_2 , 1H), 7.10 (tt, $J = 7.9, 0.6$, ArH, 1H), 2.88 (t, $J = 6.2$, CH_2 , 2H), 2.79 (t, $J = 6.5$, CH_2 , 2H), 1.99 (tt, $J = 6.6, 1.1$, CH_2 , 2H).

Dept 135 NMR (75 MHz, acetone- d_6): δ 133.1 ($\underline{\text{C}}\text{H}$), 127.4 ($\underline{\text{C}}\text{H}$), 124.4 ($\underline{\text{C}}\text{H}$), 29.5 ($\underline{\text{C}}\text{H}_2$), 24.7 ($\underline{\text{C}}\text{H}_2$), 21.0 ($\underline{\text{C}}\text{H}_2$).

7-Bromo-1-tetralone thiosemicarbazone (66) Into a round bottom flask containing ketone **64** (0.347 g, 1.54 mmol), 10 mL of anhydrous methanol were added and the solution was refluxed for about 10 minutes. To the warm ketone solution, thiosemicarbazide (0.246 g, 2.70 mmol) and 0.7 mL of 1% solution of HOAc were added. The reaction mixture was refluxed under nitrogen atmosphere for 18 h, at which point, the solvent was evaporated. The crude reaction mixture was purified by flash chromatography (30% EtOAc/ 70% hex) which afforded 0.314 g (1.05 mmol) of the product in a 68% yield.

^1H NMR (300 MHz, acetone- d_6 , δ): 9.31 (br s, NH , 1H), 8.38 (d, $J = 2.1$, ArH, 1H), 8.15 (br s, NH_2 , 1H), 7.57 (br s, NH_2 , 1H), 7.43 (dd, $J = 8.2, 2.2$, ArH, 1H), 7.16 (d, $J = 8.2$, ArH, 1H), 2.82 (t, $J = 6.6$, CH_2 , 2H), 2.79 (t, $J = 6.5$, CH_2 , 2H), 1.96 (m, CH_2 , 2H).

Dept 135 NMR (75 MHz, acetone- d_6): δ 131.8 (CH), 130.6 (CH), 127.3 (CH), 28.6 (CH_2), 25.0 (CH_2), 21.2 (CH_2).

7-Bromo-2-tetralone (67) Into a round bottom flask kept at 0 °C, AlCl_3 (3.93 g, 29.5 mmol) and, 5 mL of CH_2Cl_2 were added. The reaction system was put under nitrogen and stirred for about 7 minutes before adding 20 mL of a CH_2Cl_2 solution of β -tetralone (2.16 g, 14.7 mmol). After the reaction mixture was stirred for almost 10 minutes, 10 mL of Br_2 (2.58 g, 16.2 mmol) were added and, the reaction mixture was stirred at room temperature for an hour. At the end of this period of time, the reaction mixture was poured into 50 mL of ice-water and, the product was extracted 3 times from the aqueous phase with EtOAc. The resultant organic phase was washed once with brine and dried under Na_2SO_4 . After the crude reaction mixture was purified by flash

chromatography (5% EtOAc/ 95% hex), 2.364 g (10.5 mmol) of monobromide was obtained in a 71% yield.

^1H NMR (300 MHz, CDCl_3 , δ): 7.33 (dd, $J = 8.1, 2.0$, ArH, 1H), 7.27 (d, $J = 2.0$, ArH, 1H), 7.10 (d, $J = 8.0$, ArH, 1H), 3.55 (s, CH_2 , 2H), 3.02 (t, $J = 6.6$, CH_2 , 2H), 2.53 (t, $J = 6.7, 6.4$, CH_2 , 2H).

^{13}C NMR (75 MHz, CDCl_3): δ 209.2, 135.6, 135.5, 130.9, 129.8, 129.2, 120.4, 44.5, 37.8, 27.8.

Dept 135 NMR (75 MHz, CDCl_3): δ 131.0 ($\underline{\text{C}}\text{H}$), 129.9 ($\underline{\text{C}}\text{H}$), 129.3 ($\underline{\text{C}}\text{H}$), 44.6 ($\underline{\text{C}}\text{H}_2$), 37.9 ($\underline{\text{C}}\text{H}_2$), 27.9 ($\underline{\text{C}}\text{H}_2$).

5,7-Dibromo-2-tetralone and 6,8-dibromo-2-tetralone (68) Into a round bottom flask kept at 0 °C, AlCl_3 (2.26 g, 16.9 mmol) was added and the reaction system was put under nitrogen. 1 mL of β -tetralone (1.08 g, 7.37 mmol) were added during a 10-minute period, at which point, the reaction mixture was heated in an oil bath at 90 °C for about 30 minutes before adding 0.45 mL of Br_2 (1.41 g, 8.82 mmol). The reaction mixture was stirred at 85 °C for an hour before 15 mL of ice-water and 8 mL of NaHCO_3 were added. The product was extracted twice from the aqueous phase with Et_2O and, the resultant organic phase was washed once with NaHCO_3 , once with brine and dried under Na_2SO_4 . The crude reaction mixture was purified by flash chromatography (10% EtOAc/ 90% hex) which afforded 2 major compounds. 0.110 g (0.362 mmol) of 6,8-dibromo-2-tetralone (less polar compound) was obtained in a 6% yield.

^1H NMR (300 MHz, CDCl_3 , δ): 7.34 (s, ArH, 2H), 3.66 (s, CH_2 , 2H), 3.24 (t, $J = 6.8$, CH_2 , 2H), 2.60 (t, $J = 6.9$, CH_2 , 2H).

^{13}C NMR (75 MHz, CDCl_3): δ 207.8, 137.9, 135.1, 131.93, 131.90, 123.2, 122.9, 44.6, 37.9, 29.4.

Dept 135 NMR (75 MHz, CDCl_3): δ 131.99 ($\underline{\text{CH}}$), 131.95 ($\underline{\text{CH}}$), 44.7 ($\underline{\text{CH}_2}$), 38.0 ($\underline{\text{CH}_2}$), 29.5 ($\underline{\text{CH}_2}$).

The more polar compound was recrystallized (MeOH – hex) to yield 0.2602 g (0.856 mmol) of 5,7-dibromo-2-tetralone in a 10% yield.

^1H NMR (300 MHz, CDCl_3 , δ): 7.64 (d, $J = 1.8$, ArH, 1H), 7.34 (d, $J = 1.8$, ArH, 1H), 3.58 (s, $\underline{\text{CH}_2}$, 2H), 3.06 (t, $J = 6.5$, $\underline{\text{CH}_2}$, 2H), 2.57 (t, $J = 6.7$, $\underline{\text{CH}_2}$, 2H).

^{13}C NMR (75 MHz, CDCl_3): δ 207.9, 140.1, 133.3, 133.2, 130.4, 124.7, 120.6, 44.1, 38.1, 29.0.

Dept 135 NMR (75 MHz, CDCl_3): δ 133.2 ($\underline{\text{CH}}$), 130.1 ($\underline{\text{CH}}$), 44.1 ($\underline{\text{CH}_2}$), 38.1 ($\underline{\text{CH}_2}$), 29.0 ($\underline{\text{CH}_2}$).

7-Bromo-2-tetralone thiosemicarbazone (69) Into a round bottom flask containing ketone **67** (0.358 g, 1.59 mmol), 10 mL of anhydrous methanol were added and the solution was refluxed for about 15 minutes. To the warm ketone solution, thiosemicarbazide (0.269 g, 2.96 mmol) and about 50 mg of TsOH were added. The reaction mixture was refluxed under nitrogen atmosphere for 16.5 h, at which point, the solid formed was filtered and recrystallized with MeOH. After drying the solid under reduced pressure, 0.333 g (1.12 mmol) of the product was obtained in a 70% yield.

^1H NMR (300 MHz, acetone- d_6 , δ): 9.25 (s, $\underline{\text{NH}}$, 1H), 8.22 (dd, $J = 8.0, 1.2$, ArH, 1H),

1-Tetralone p-toluensulfonhydrazone (71) Into a round bottom flask containing 1-tetralone (4.40 g, 30.1 mmol), 30 mL of anhydrous methanol were added and the solution was refluxed for about 15 minutes. To the warm ketone solution, p-toluensulfonhydrazide (8.49 g, 44.2 mmol) and about 57 mg of TsOH were added. The reaction mixture was refluxed under nitrogen atmosphere for 4.5 h, at which point, the solid formed was filtered and recrystallized with MeOH. After drying the solid under reduced pressure, 8.064 g (25.7 mmol) of the product was obtained in an 87% yield.

^1H NMR (300 MHz, CDCl_3 , δ): 7.95 (dd, $J = 7.6, 1.5$, ArH, 1H), 7.94 (d, $J = 8.4$, ArH, 2H), 7.85 (br s, NH, 1H), 7.32 (dd, $J = 8.6, 0.5$, ArH, 2H), 7.21 (m, ArH, 2H), 7.08 (dd, $J = 7.0, 1.8$, ArH, 1H), 2.70 (t, $J = 6.0$, CH_2 , 2H), 2.47 (t, $J = 6.6$, CH_2 , 2H), 2.41 (s, CH_3 , 3H), 1.88 (p, $J = 6.4$, CH_2 , 2H).

Dept 135 NMR (75 MHz, CDCl_3): δ 129.61 ($\underline{\text{C}}\text{H}$), 129.57 ($\underline{\text{C}}\text{H}$), 128.3 ($\underline{\text{C}}\text{H}$), 128.2 ($\underline{\text{C}}\text{H}$), 126.5 ($\underline{\text{C}}\text{H}$), 125.0 ($\underline{\text{C}}\text{H}$), 29.3 ($\underline{\text{C}}\text{H}_2$), 25.5 ($\underline{\text{C}}\text{H}_2$), 21.6 ($\underline{\text{C}}\text{H}_3$), 21.4 ($\underline{\text{C}}\text{H}_2$).

1-[1-(3,4-Dihydronaphthalenyl)]-1-ethanol (72a) Into a dry round bottom flask containing 1-tetralone p-toluenensulfonhydrazone **71** (0.957 g, 3.05 mmol), 20 mL of TMEDA were added and, nitrogen was circulated through the reaction system. After the solution was cooled at $-50\text{ }^\circ\text{C}$, 4.9 mL of BuLi (2.5 M/hex, 12.3 mmol) were added and, the reaction mixture was stirred first at $-50\text{ }^\circ\text{C}$ for 30 minutes and then at room temperature for another 30 minutes. After bubbling stopped, the flask was cooled at $0\text{ }^\circ\text{C}$ and, 1 mL of acetaldehyde (0.786 g, 17.9 mmol) was added. The reaction was stirred at $0\text{ }^\circ\text{C}$ for 2 h, at which point, 10 mL of ice water were added. The product was extracted once from the aqueous phase with EtOAc and, the combined organic phase was washed 3 times with H_2O and with brine. The organic phase was dried under Na_2SO_4 and, the

solvent was removed under vacuum. After the product was purified by flash chromatography (20% EtOAc/ 80% hex), 0.155 g (0.891 mmol) was obtained in a 29% yield.

^1H NMR (300 MHz, CDCl_3 , δ): 7.38 (d, $J= 7.3$, ArH, 1H), 7.18 (m, ArH, 3H), 6.17 (td, $J= 4.6, 1.0$, C=CH, 1H), 4.89 (q, $J= 6.3$, CHOH, 1H), 2.72 (t, $J = 8.0$, CH₂, 2H), 2.27 (m, CH₂, 2H), 1.76 (br s, OH, 1H), 1.45 (d, $J = 6.4$, CH₃, 3H).

^{13}C NMR (75 MHz, CDCl_3): δ 140.4, 136.9, 133.3, 127.8, 126.9, 126.4, 123.8, 122.9, 67.4, 28.3, 22.8, 22.6.

Dept 135 NMR (75 MHz, CDCl_3): δ 127.8 (CH), 126.9 (CH), 126.4 (CH), 123.8 (CH), 122.9 (CH), 67.4 (CH), 28.2 (CH₂), 22.8 (CH₃), 22.6 (CH₂).

[1-(3,4-Dihydronaphthalenyl)]methyl ketone (73) Into a round bottom flask containing 15 mL of a 15% w/w solution of Dess-Martin reagent (3.07 g, 7.24 mmol), 10 mL of a CH_2Cl_2 solution of alcohol **72** (0.470 g, 2.70 mmol) were added and, the reaction mixture was stirred under nitrogen for 2 h at room temperature. The crude reaction mixture was poured into 75 mL of a mixture of $\text{NaHCO}_3 - \text{Na}_2\text{S}_2\text{O}_3$ (2:1 ratio) and stirred for 10 minutes. The product was extracted twice from the aqueous phase with Et_2O and, the resultant organic phase was washed once with H_2O , once with brine and dried under Na_2SO_4 . The ethereal solution was filtered through silica gel and concentrated under vacuum to afford 0.460 g (2.67 mmol) of the product in a 99% yield.

^1H NMR (300 MHz, CDCl_3 , δ): 7.69 (dd, $J= 8.7, 2.2$, ArH, 1H), 7.19 (m, ArH, 3H), 7.01 (t, $J= 4.9$, C=CH, 1H), 2.74 (t, $J = 7.4$, CH₂, 2H), 2.46 (s, CH₃, 3H), 2.42 (m, CH₂, 2H).

^{13}C NMR (75 MHz, CDCl_3): δ 199.4, 139.2, 136.4, 130.9, 130.8, 127.7, 127.6, 126.6, 126.5, 27.8, 27.5, 23.7.

Dept 135 NMR (75 MHz, CDCl_3): δ 139.2 ($\underline{\text{C}}\text{H}$), 127.7 ($\underline{\text{C}}\text{H}$), 127.6 ($\underline{\text{C}}\text{H}$), 126.6 ($\underline{\text{C}}\text{H}$), 126.5 ($\underline{\text{C}}\text{H}$), 27.9 ($\underline{\text{C}}\text{H}_3$), 27.5 ($\underline{\text{C}}\text{H}_2$), 23.8 ($\underline{\text{C}}\text{H}_2$).

5,7-Dibromo-2-tetralone thiosemicarbazone (74) Into a round bottom flask containing ketone **73** (0.0783 g, 0.455 mmol), 10 mL of anhydrous methanol were added and the solution was refluxed for about 15 minutes before adding thiosemicarbazide (0.0683 g, 0.856 mmol) and 13 mg of TsOH. The reaction mixture was refluxed under nitrogen atmosphere for 15 h. The crude reaction mixture was purified by column chromatography (40% EtOAc/ 60% hex) which afforded 0.028 g (0.114 mmol) of the product (65% *trans* isomer and 35% *cis*) in a 25% yield.

Trans isomer: ^1H NMR (300 MHz, CDCl_3 , δ): 8.62 (br s, $\underline{\text{N}}\text{H}$, 1H), 7.26 (br s, $\underline{\text{N}}\text{H}_2$, 1H), 7.17 (m, $\text{Ar}\underline{\text{H}}$, 3H), 6.76 (d, $J=7.1$, $\text{Ar}\underline{\text{H}}$, 1H), 6.27 (br s, $\underline{\text{N}}\text{H}_2$, 1H), 6.02 (t, $J=4.5$, $\text{C}=\underline{\text{C}}\text{H}$, 1H), 2.85 (t, $J=8.1$, $\underline{\text{C}}\text{H}_2$, 2H), 2.34 (m, $\underline{\text{C}}\text{H}_2$, 2H), 2.15 (s, $\underline{\text{C}}\text{H}_3$, 3H).

Dept 135 NMR (75 MHz, CDCl_3): δ 129.6 ($\underline{\text{C}}\text{H}$), 128.7 ($\underline{\text{C}}\text{H}$), 128.5 ($\underline{\text{C}}\text{H}$), 127.2 ($\underline{\text{C}}\text{H}$), 123.6 ($\underline{\text{C}}\text{H}$), 27.2 ($\underline{\text{C}}\text{H}_2$), 24.2 ($\underline{\text{C}}\text{H}_3$), 22.7 ($\underline{\text{C}}\text{H}_2$).

Cis isomer: ^1H NMR (300 MHz, CDCl_3 , δ): 8.67 (br s, $\underline{\text{N}}\text{H}$, 1H), 7.26 (br s, $\underline{\text{N}}\text{H}_2$, 1H), 7.17 (m, $\text{Ar}\underline{\text{H}}$, 4H), 6.31 (t, $J=4.8$, $\text{C}=\underline{\text{C}}\text{H}$, 1H), 6.27 (br s, $\underline{\text{N}}\text{H}_2$, 1H), 2.76 (t, $J=7.6$, $\underline{\text{C}}\text{H}_2$, 2H), 2.46 (m, $\underline{\text{C}}\text{H}_2$, 2H), 2.13 (s, $\underline{\text{C}}\text{H}_3$, 3H).

Dept 135 NMR (75 MHz, CDCl_3): δ 130.9 ($\underline{\text{C}}\text{H}$), 127.9 ($\underline{\text{C}}\text{H}$), 127.6 ($\underline{\text{C}}\text{H}$), 126.4 ($\underline{\text{C}}\text{H}$), 125.3 ($\underline{\text{C}}\text{H}$), 27.9 ($\underline{\text{C}}\text{H}_2$), 23.3 ($\underline{\text{C}}\text{H}_2$), 15.6 ($\underline{\text{C}}\text{H}_3$).

7-Bromo-1-tetralone p-toluensulfonhydrazone (75) Into a round bottom flask containing tetralone **64** (2.20 g, 9.78 mmol), 40 mL of anhydrous methanol were added and the solution was refluxed for about 15 minutes. To the warm ketone solution, p-toluenesulfonhydrazide (2.82 g, 14.7 mmol) and about 20 mg of TsOH were added. The reaction mixture was refluxed under nitrogen atmosphere for 7 h, at which point, the solid formed was filtered and recrystallized with MeOH. After drying the solid under reduced pressure, 3.44 g (8.75 mmol) of the product was obtained in a 90% yield.

^1H NMR (360 MHz, methanol- d_6 , δ): 8.00 (d, $J= 2.1$, ArH, 1H), 7.86 (d, $J= 8.3$, ArH, 2H), 7.67 (br s, NH, 1H), 7.35 (d, $J= 8.2$, ArH, 2H), 7.31 (dd, $J= 8.2, 2.1$ ArH, 1H), 6.98 (d, $J= 8.2$, ArH, 1H), 2.66 (t, $J= 5.8$, CH $_2$, 2H), 2.49 (t, $J= 6.6$, CH $_2$, 2H), 2.40 (s, CH $_3$, 3H), 1.83 (p, $J= 6.1$, CH $_2$, 2H).

^{13}C NMR (75 MHz, methanol- d_6): δ 152.7, 145.0, 139.6, 136.9, 134.8, 132.8, 131.0, 130.3, 128.8, 128.4, 120.8, 29.6, 26.4, 22.2, 21.7.

Dept 135 NMR (75 MHz, methanol- d_6): δ 132.8 (CH), 131.0 (CH), 130.3 (CH), 128.8 (CH), 128.4 (CH), 29.6 (CH $_2$), 26.4 (CH $_2$), 22.2 (CH $_2$), 21.7 (CH $_3$).

1-(7-Bromo-3,4-dihydronaphthalen-1-yl)-2-propen-1-ol (76) Into a dry round bottom flask containing hydrazone **75** (3.44 g, 8.76 mmol), 30 mL of TMEDA were added and, nitrogen was circulated through the reaction system. After the solution was cooled at $-50\text{ }^\circ\text{C}$, 14 mL of BuLi (2.5 M/hex, 35 mmol) were added and, the reaction mixture was stirred first at $-50\text{ }^\circ\text{C}$ for 40 minutes and then at room temperature for another 40 minutes. After bubbling stopped, the flask was cooled at $0\text{ }^\circ\text{C}$ and, 2.4 mL of acrolein (1.96 g, 34.9 mmol) were added. The reaction was stirred at $0\text{ }^\circ\text{C}$ for 3 h, at which point, 30 mL of ice water were added. The product was extracted once from the

aqueous phase with EtOAc and, the combined organic phase was washed 3 times with H₂O and with brine. The organic phase was dried under Na₂SO₄ and, the solvent was removed under vacuum. After the product was purified by flash chromatography (10% EtOAc/ 90% hex), 0.246 g (0.928 mmol) was obtained in an 11% yield.

¹H NMR (300 MHz, CDCl₃, δ): 7.60 (d, *J* = 2.0, ArH, 1H), 7.26 (dd, *J* = 8.0, 2.0, ArH, 1H), 7.00 (d, *J* = 8.0, ArH, 1H), 6.22 (td, *J* = 4.6, 0.7, C=CH, 1H), 6.05 (ddd, *J* = 17.3, 10.5, 5.4, CH=CH₂, 1H), 5.40 (dt, *J* = 17.3, 1.5, C=CH₂, 1H), 5.25 (dt, *J* = 10.4, 1.4, C=CH₂, 1H), 5.10 (dd, *J* = 5.3, 1.0, CHOH, 1H), 2.67 (t, *J* = 8.0, CH₂, 2H), 2.30 (m, CH₂, 2H), 1.92 (br s, OH, 1H).

Dept 135 NMR (75 MHz, CDCl₃): δ 138.9 (CH), 129.6 (CH), 129.2 (CH), 128.2 (CH), 126.7 (CH), 116.1 (CH₂), 72.6 (CHOH), 27.5 (CH₂), 22.8 (CH₂).

1-(7-Bromo-3,4-dihydronaphthalen-1-yl)propenone (77) Into a round bottom flask containing 2.4 mL of a 15% w/w solution of Dess-Martin reagent (0.471 g, 1.11 mmol), 10 mL of a CH₂Cl₂ solution of alcohol **76** (0.123 g, 0.463 mmol) were added and, the reaction mixture was stirred under nitrogen for 1 h at room temperature. The crude reaction mixture was poured into 50 mL of a mixture of NaHCO₃–Na₂S₂O₃ (1:1 ratio) and stirred for 10 minutes. The product was extracted twice from the aqueous phase with Et₂O and, the resultant organic phase was washed once with H₂O, once with brine and dried under Na₂SO₄. After the crude reaction mixture was purified by flash chromatography (5% EtOAc/ 95% hex), 0.0683 g (0.260 mmol) of the product was obtained in a 67% yield.

¹H NMR (300 MHz, CDCl₃, δ): 7.68 (d, *J* = 2.0, ArH, 1H), 7.30 (dd, *J* = 8.0, 2.1, ArH, 1H), 7.03 (d, *J* = 8.0, ArH, 1H), 6.85 (t, *J* = 4.8, C=CH, 1H), 6.77 (dd, *J* = 17.2, 10.5,

$\text{CH}=\text{CH}_2$, 1H), 6.32 (dd, $J= 17.2, 1.5$, $\text{C}=\text{CH}_2$, 1H), 5.90 (dd, $J= 10.5, 1.5$, $\text{C}=\text{CH}_2$, 1H), 2.73 (t, $J= 7.9$, CH_2 , 2H), 2.45 (td, $J= 8.0, 4.9$, CH_2 , 2H).

^{13}C NMR (75 MHz, CDCl_3): δ 192.6, 139.0, 137.7, 135.0, 134.7, 132.9, 130.6, 130.2, 129.1, 128.9, 120.2, 26.9, 23.3.

Dept 135 NMR (75 MHz, CDCl_3): δ 138.9 ($\underline{\text{C}}\text{H}$), 134.7 ($\underline{\text{C}}\text{H}$), 130.6 ($\underline{\text{C}}\text{H}$), 130.2 ($\underline{\text{C}}\text{H}_2$), 129.2 ($\underline{\text{C}}\text{H}$), 128.9 ($\underline{\text{C}}\text{H}$), 26.9 ($\underline{\text{C}}\text{H}_2$), 23.3 ($\underline{\text{C}}\text{H}_2$).

Dept 90 NMR (75 MHz, CDCl_3): δ 138.9 ($\underline{\text{C}}\text{H}$), 134.6 ($\underline{\text{C}}\text{H}$), 130.6 ($\underline{\text{C}}\text{H}$), 129.1 ($\underline{\text{C}}\text{H}$), 128.8 ($\underline{\text{C}}\text{H}$).

1-(3,4-Dihydronaphthalen-1-yl)prop-2-en-1-ol (78) Into a dry round bottom flask containing hydrazone **71** (1.995 g, 6.35 mmol), 20 mL of TMEDA were added and, nitrogen was circulated through the reaction system. After the solution was cooled at -50 °C, 10.2 mL of BuLi (2.5 M/hex, 25.5 mmol) were added and, the reaction mixture was stirred first at -50 °C for 40 minutes and then at room temperature for 35 minutes. After bubbling stopped, the flask was cooled at 0 °C and, 2.0 mL of acrolein (1.63 g, 29.1 mmol) were added. The reaction was stirred at 0 °C for 5 h, at which point, 30 mL of ice water were added. The product was extracted once from the aqueous phase with EtOAc and, the combined organic phase was washed 3 times with H_2O and with brine. The organic phase was dried under Na_2SO_4 and, the solvent was removed under vacuum. After the product was purified by flash chromatography (10% EtOAc/ 90% hex), 0.1165 g (0.626 mmol) was obtained in a 10% yield.

^1H NMR (300 MHz, CDCl_3 , δ): 7.46 (d, $J= 6.7$, ArH , 1H), 7.18 (m, ArH , 3H), 6.19 (td, $J= 4.6, 0.9$, $\text{C}=\text{CH}$, 1H), 6.12 (ddd, $J= 17.2, 10.4, 5.3$, $\text{CH}=\text{CH}_2$, 1H), 5.42 (dt, $J= 17.2, 1.5$, $\text{C}=\text{CH}_2$, 1H), 5.24 (dt, $J= 10.4, 1.5$, $\text{C}=\text{CH}_2$, 1H), 5.18 (d, $J= 3.9$, CHOH ,

1H), 2.75 (t, $J = 8.0$, $\underline{\text{CH}}_2$, 2H), 2.31 (dddd, $J = 6.3, 4.7, 3.2, 0.9$, $\underline{\text{CH}}_2$, 2H), 1.95 (br s, $\underline{\text{OH}}$, 1H).

^{13}C NMR (75 MHz, CDCl_3): δ 139.3, 137.8, 136.7, 133.0, 127.7, 126.9, 126.6, 126.3, 123.4, 115.6, 72.6, 28.1, 22.9.

Dept 135 NMR (75 MHz, CDCl_3): δ 139.4 ($\underline{\text{CH}}$), 127.8 ($\underline{\text{CH}}$), 127.0 ($\underline{\text{CH}}$), 126.7 ($\underline{\text{CH}}$), 126.3 ($\underline{\text{CH}}$), 123.5 ($\underline{\text{CH}}$), 115.7 ($\underline{\text{CH}}_2$), 72.7 ($\underline{\text{CHOH}}$), 28.1 ($\underline{\text{CH}}_2$), 23.0 ($\underline{\text{CH}}_2$).

1-(3,4-Dihydronaphthalen-1-yl)propenone (**79**) Into a round bottom flask containing 2.6 mL of a 15% w/w solution of Dess-Martin reagent (0.532 g, 1.26 mmol), 9 mL of a CH_2Cl_2 solution of alcohol **78** (0.117 g, 0.626 mmol) were added and, the reaction mixture was stirred under nitrogen for 2 h at room temperature. The crude reaction mixture was poured into 75 mL of a mixture of NaHCO_3 – $\text{Na}_2\text{S}_2\text{O}_3$ (2:1 ratio) and stirred for 10 minutes. The product was extracted twice from the aqueous phase with Et_2O and, the resultant organic phase was washed once with H_2O , once with brine and dried under Na_2SO_4 . After the crude reaction mixture was purified by flash chromatography (10% EtOAc / 90% hex), 0.0825 g (0.448 mmol) of the product was obtained in a 72% yield.

^1H NMR (300 MHz, CDCl_3 , δ): 7.46 (d, $J = 8.7$, ArH , 1H), 7.18 (m, ArH , 3H), 6.77 (dd, $J = 17.3, 10.5$, $\underline{\text{CH}}=\text{CH}_2$, 1H), 6.77 (t, $J = 4.8$, $\text{C}=\underline{\text{CH}}$, 1H), 6.32 (dd, $J = 17.3, 1.6$, $\text{C}=\underline{\text{CH}}_2$, 1H), 5.87 (dd, $J = 10.5, 1.6$, $\text{C}=\underline{\text{CH}}_2$, 1H), 2.79 (t, $J = 7.9$, $\underline{\text{CH}}_2$, 2H), 2.45 (ddd, $J = 8.7, 7.2, 4.9$, $\underline{\text{CH}}_2$, 2H).

^{13}C NMR (75 MHz, CDCl_3): δ 193.4, 138.8, 137.4, 136.1, 135.1, 131.1, 129.7, 127.8, 127.6, 126.5, 125.9, 27.4, 23.4.

Dept 135 NMR (75 MHz, CDCl_3): δ 137.4 ($\underline{\text{C}}\text{H}$), 135.2 ($\underline{\text{C}}\text{H}$), 129.8 ($\underline{\text{C}}\text{H}_2$), 127.8 ($\underline{\text{C}}\text{H}$), 127.7 ($\underline{\text{C}}\text{H}$), 126.6 ($\underline{\text{C}}\text{H}$), 125.9 ($\underline{\text{C}}\text{H}$), 27.5 ($\underline{\text{C}}\text{H}_2$), 23.4 ($\underline{\text{C}}\text{H}_2$).

5-Bromo-1-tetralone p-toluenesulfonylhydrazone (80) Into a round bottom flask containing tetralone **63** (2.28 g, 10.1 mmol), 40 mL of anhydrous methanol were added and the solution was refluxed for about 15 minutes. To the warm ketone solution, p-toluenesulfonylhydrazide (2.92 g, 15.2 mmol) and 20 mg of TsOH were added. The reaction mixture was refluxed under nitrogen atmosphere for 7 h, at which point, the solid formed was filtered and recrystallized with MeOH. After drying the solid under reduced pressure, 3.494 g (8.89 mmol) of the product was obtained in an 88% yield.

^1H NMR (360 MHz, methanol- d_6 , δ): 7.90 (dd, $J = 8.0, 1.2$, ArH , 1H), 7.85 (d, $J = 8.4$, ArH , 2H), 7.54 (s, NH , 1H), 7.47 (dd, $J = 7.9, 1.2$, ArH , 1H), 7.30 (dd, $J = 8.6, 0.6$, ArH , 2H), 7.02 (t, $J = 7.9$, ArH , 1H), 2.78 (t, $J = 6.2$, $\underline{\text{C}}\text{H}_2$, 2H), 2.48 (t, $J = 6.6$, $\underline{\text{C}}\text{H}_2$, 2H), 2.38 (s, $\underline{\text{C}}\text{H}_3$, 3H), 1.85 (p, $J = 6.5$, $\underline{\text{C}}\text{H}_2$, 2H).

^{13}C NMR (75 MHz, methanol- d_6): δ 153.2, 144.6, 139.4, 136.5, 134.9, 133.9, 130.1, 128.6, 127.9, 125.0, 124.9, 30.0, 25.8, 21.7.

Dept 135 NMR (75 MHz, methanol- d_6): δ 133.9 ($\underline{\text{C}}\text{H}$), 130.07 ($\underline{\text{C}}\text{H}$), 128.6 ($\underline{\text{C}}\text{H}$), 127.9 ($\underline{\text{C}}\text{H}$), 124.9 ($\underline{\text{C}}\text{H}$), 29.9 ($\underline{\text{C}}\text{H}_2$), 25.8 ($\underline{\text{C}}\text{H}_2$), 21.73 ($\underline{\text{C}}\text{H}_3$), 21.69 ($\underline{\text{C}}\text{H}_2$).

1-(5-Bromo-3,4-dihydronaphthalen-1-yl)-2-propen-1-ol (81) Into a dry round bottom flask containing hydrazone **80** (3.49 g, 8.89 mmol), 30 mL of TMEDA were added and, nitrogen was circulated through the reaction system. After the solution was cooled at $-50\text{ }^\circ\text{C}$, 14.2 mL of BuLi (2.5 M/hex, 35 mmol) were added and, the reaction mixture was stirred first at $-50\text{ }^\circ\text{C}$ for 40 minutes and then at room temperature for

another 40 minutes. After bubbling stopped, the flask was cooled at 0 °C and, 2.4 mL of acrolein (1.96 g, 34.9 mmol) were added. The reaction was stirred at 0 °C for 4 h, at which point, 30 mL of ice water were added. The product was extracted once from the aqueous phase with EtOAc and, the combined organic phase was washed 3 times with H₂O and with brine. The organic phase was dried under Na₂SO₄ and, the solvent was removed under vacuum. After the product was purified by flash chromatography (10% EtOAc/ 90% hex), 0.319 g (1.20 mmol) was obtained in a 14% yield.

¹H NMR (300 MHz, CDCl₃, δ): 7.42 (dd, *J*= 8.8, 1.0, ArH, 1H), 7.39 (dd, *J*= 9.3, 1.2, ArH, 1H), 7.03 (t, *J*= 7.9, ArH, 1H), 6.21 (td, *J*= 4.7, 0.8, C=CH, 1H), 6.04 (ddd, *J*= 17.2, 10.4, 5.3, CH=CH₂, 1H), 5.39 (dt, *J*= 17.3, 1.5, C=CH₂, 1H), 5.23 (dt, *J*= 10.4, 1.4, C=CH₂, 1H), 5.13 (dd, *J*= 5.3, 1.0, CHOH, 1H), 2.88 (t, *J*= 8.1, CH₂, 2H), 2.32 (m, CH₂, 2H), 1.94 (br s, OH, 1H).

¹³C NMR (90 MHz, CDCl₃): δ 139.0, 137.4, 136.0, 135.2, 131.2, 127.7, 127.3, 124.0, 122.8, 115.9, 77.6, 27.3, 22.5.

Dept 135 NMR (90 MHz, CDCl₃): δ 139.1 (CH), 131.3 (CH), 127.8 (CH), 127.4 (CH), 122.9 (CH), 116.0 (CH₂), 72.7 (CHOH), 27.6 (CH₂), 22.6 (CH₂).

1-(5-Bromo-3,4-dihydronaphthalen-1-yl)propenone (82) Into a round bottom flask containing 5 mL of a 15% w/w solution of Dess-Martin reagent (1.02 g, 2.41 mmol), 10 mL of a CH₂Cl₂ solution of alcohol **81** (0.319 g, 1.21 mmol) were added and, the reaction mixture was stirred under nitrogen for 1.5 h at room temperature. The crude reaction mixture was poured into 50 mL of a mixture of NaHCO₃–Na₂S₂O₃ (1:1 ratio) and stirred for 10 minutes. The product was extracted twice from the aqueous phase with Et₂O and, the resultant organic phase was washed once with H₂O, once with brine and

dried under Na_2SO_4 . After the crude reaction mixture was purified by flash chromatography (10% EtOAc/ 90% hex), 0.146 g (0.555 mmol) of the product was obtained in a 46% yield.

^1H NMR (300 MHz, CDCl_3 , δ): 7.43 (dd, J = 8.0, 1.1, ArH, 1H), 7.39 (d, J = 7.7, ArH, 1H), 7.05 (t, J = 7.9, ArH, 1H), 6.78 (t, J = 4.8, C=CH, 1H), 6.73 (dd, J = 17.3, 10.5, CH=CH₂, 1H), 6.30 (dd, J = 17.3, 1.5, C=CH₂, 1H), 5.88 (dd, J = 10.5, 1.5, C=CH₂, 1H), 2.93 (t, J = 8.0, CH₂, 2H), 2.46 (td, J = 8.0, 4.8, CH₂, 2H).

^{13}C NMR (75 MHz, CDCl_3): δ 192.9, 138.4, 137.8, 135.5, 135.0, 133.1, 132.0, 130.2, 127.5, 125.2, 123.7, 26.7, 23.0.

Dept 135 NMR (75 MHz, CDCl_3): δ 137.9 (CH), 135.1 (CH), 132.1 (CH), 130.2 (CH₂), 127.6 (CH), 125.3 (CH), 26.8 (CH₂), 23.1 (CH₂).

1,1-Dioxo-1-thiochroman-4-one (**83**) Into a round bottom flask containing thiochroman-4-one (0.804 g, 4.75 mmol), 6 mL of glacial HOAc and, 2.3 mL of a 35% w/w solution of H_2O_2 (0.914 g, 26.9 mmol) were added and, the solution was heated at 100 °C for 1 h. After the reaction mixture was cooled at room temperature, 10 mL of H_2O were added and the product was extracted twice with CH_2Cl_2 from the aqueous layer. The resultant organic phase was washed once with brine and dried under Na_2SO_4 . After the solvent was removed, a solid was formed which was purified by recrystallization with EtOH. After drying the solid under reduced pressure, 0.649 g (3.31 mmol) of the product was obtained in a 70% yield.

^1H NMR (300 MHz, acetone- d_6 , δ): 8.07 (ddd, J = 7.7, 1.3, 0.6, ArH, 1H), 7.99 (ddd, J = 7.8, 2.2, 0.7, ArH, 1H), 7.95 (td, J = 7.8, 1.5, ArH, 1H), 7.86 (ddd, J = 7.7, 6.7, 2.1, ArH, 1H), 3.94 (t, J = 6.3, CH₂, 2H), 3.37 (t, J = 6.3, CH₂, 2H).

^{13}C NMR (75 MHz, acetone- d_6): δ 191.3, 142.9, 135.6, 134.1, 131.6, 129.1, 124.0, 49.6, 37.5.

Dept 45 NMR (75 MHz, acetone- d_6): δ 134.8 ($\underline{\text{C}}\text{H}$), 133.2 ($\underline{\text{C}}\text{H}$), 128.2 ($\underline{\text{C}}\text{H}$), 123.1 ($\underline{\text{C}}\text{H}$), 48.8 ($\underline{\text{C}}\text{H}_2$), 36.7 ($\underline{\text{C}}\text{H}_2$).

5,7-Dibromo-2-tetralone thiosemicarbazone (84) Into a round bottom flask containing ketone **83** (0.379 g, 1.93 mmol), 15 mL of anhydrous methanol were added and the solution was refluxed for about 15 minutes before adding thiosemicarbazide (0.160 g, 1.76 mmol) and 4 mg of TsOH. After the reaction mixture was refluxed under nitrogen atmosphere for 5 h, a solid was formed which was filtered and further rinsed with MeOH. After the solid was dried under vacuum, 0.361 g (1.34 mmol) of the product was obtained in a 70% yield.

^1H NMR (300 MHz, methyl sulfoxide- d_6 , δ): 10.62 (s, $\underline{\text{N}}\text{H}$, 1H), 8.56 (dd, $J= 8.2$, 2.1, $\text{Ar}\underline{\text{H}}$, 1H), 8.55 (br s, $\underline{\text{N}}\text{H}_2$, 1H), 8.25 (br s, $\underline{\text{N}}\text{H}_2$, 1H), 7.84 (m, $\text{Ar}\underline{\text{H}}$, 1H), 7.65 (m, $\text{Ar}\underline{\text{H}}$, 2H), 3.69 (t, $J= 6.3$, $\underline{\text{C}}\text{H}_2$, 2H), 3.30 (t, $J= 6.3$, $\underline{\text{C}}\text{H}_2$, 2H).

^{13}C NMR (75 MHz, Methyl Sulfoxide- d_6): δ 179.4, 139.8, 137.6, 132.7, 132.6, 129.9, 127.1, 122.4, 45.7, 24.4.

6-Bromothiochroman-4-one and 6,8-Dibromothiochroman-4-one (85a) Into a round bottom flask kept at room temperature, AlCl_3 (1.81 g, 13.5 mmol) and, 1 mL of CH_2Cl_2 were added. The reaction system was put under nitrogen and stirred for about 7 minutes before adding 1 mL of a CH_2Cl_2 solution of thiochroman-4-one (1.11 g, 6.77 mmol). After the reaction mixture was stirred for almost 10 minutes, 2 mL of a CH_2Cl_2 solution of Br_2 (1.19 g, 7.44 mmol) were added and, the reaction mixture was stirred at

room temperature for 16 h. At the end of this period of time, the reaction mixture was poured into 50 mL of ice-water and, the product was extracted 3 times from the aqueous phase with EtOAc. The resultant organic phase was washed once with brine and dried under Na₂SO₄. After the crude reaction mixture was purified by flash chromatography (15% EtOAc/ 85% hex), 0.648 g of a mixture of 6-monobromide (34% pure, 13% yield) and 6,8-dibromo (66% pure, 20% yield) was obtained.

6,8-Dibromo-thiocroman-4-one: ¹H NMR (300 MHz, CDCl₃, δ): 8.18 (dd, *J* = 2.2, 0.7, ArH, 1H), 7.77 (dd, *J* = 2.2, 0.7, ArH, 1H), 3.22 (m, CH₂, 2H), 2.94 (m, CH₂, 2H).

¹³C NMR (75 MHz, CDCl₃): δ 192.0, 142.5, 139.1, 136.0, 131.0, 122.2, 118.2, 37.8, 26.0.

6-Bromo-thiocroman-4-one: ¹H NMR (300 MHz, CDCl₃, δ): 8.19 (dd, *J* = 2.2, 0.4, ArH, 1H), 7.44 (ddd, *J* = 8.5, 2.3, 0.6, ArH, 1H), 7.13 (dd, *J* = 8.5, 0.3, ArH, 1H), 3.22 (m, CH₂, 2H), 2.93 (m, CH₂, 2H).

¹³C NMR (75 MHz, CDCl₃): δ 192.7, 141.1, 133.3, 132.1, 131.8, 129.2, 118.7, 39.1, 26.5.

8-Bromothiochroman-4-one (85b) Into a round bottom flask kept at 0 °C, AlCl₃ (2.01 g, 15.1 mmol) and, 9 mL of CH₂Cl₂ were added. The reaction system was put under nitrogen and stirred for about 7 minutes before adding 2 mL of a CH₂Cl₂ solution of thiochroman-4-one (1.24 g, 7.54 mmol). After the reaction mixture was stirred for almost 10 minutes, 4 mL of a CH₂Cl₂ solution of Br₂ (1.28 g, 7.98 mmol) were added during a 30-minute period and, the reaction mixture was stirred at 0 °C for 4 h. At the end of this period of time, the reaction mixture was poured into 50 mL of ice-water and,

the product was extracted 3 times from the aqueous phase with EtOAc. The resultant organic phase was washed once with brine and dried under Na₂SO₄. After the crude reaction mixture was purified by flash chromatography (20% EtOAc/ 80% hex), 1.34 g of a mixture of 6-bromide (63% pure, 46% yield), 8-bromide (20% pure, 15% yield), and 6,8-dibromo (17% pure, 10% yield) was obtained.

8-Bromo-thiocroman-4-one: ¹H NMR (300 MHz, CDCl₃, δ): 8.07 (ddd, *J* = 7.9, 1.4, 0.7, ArH, 1H), 7.63 (ddd, *J* = 7.7, 1.4, 0.7, ArH, 1H), 7.03 (td, *J* = 7.9, 0.7, ArH, 1H), 3.22 (m, CH₂, 2H), 2.93 (m, CH₂, 2H).

6,8-Dibromo-1,1-dioxo-1-thiochroman-4-one (86a) Into a round bottom flask containing 0.548 g of **85a** (0.361 g, 1.12 mmol of dibromo and 0.186 g, 0.766 mmol of monobromide), 6 mL of glacial HOAc and, 1 mL of a 35% w/w solution of H₂O₂ (0.400 g, 11.7 mmol) were added and, the solution was heated at 100 °C for 2 h. After the reaction mixture was cooled at room temperature, a solid was formed which was filtered and purified by recrystallized with EtOH-MeOH. After drying the solid under reduced pressure, 0.265 g (0.749 mmol) of the product was obtained in a 67% yield.

¹H NMR (300 MHz, CD₂Cl₂, δ): 8.22 (d, *J* = 2.1, ArH, 1H), 8.16 (d, *J* = 2.1, ArH, 1H), 3.75 (m, CH₂, 2H), 3.37 (m, CH₂, 2H).

¹³C NMR (75 MHz, CD₂Cl₂): δ 188.8, 143.4, 139.5, 133.6, 131.6, 127.8, 119.4, 50.8, 36.6.

6-Bromo-1,1-dioxo-1-thiochroman-4-one (86b) Into a round bottom flask containing 1.31 g of **85b** (0.824 g, 3.39 mmol of 6-bromo, 0.262 g, 1.08 mmol of 8-bromo and 0.222 g, 0.69 mmol of 6,8-dibromo-thiocroman-4-one), 15 mL of glacial

HOAc and, 2.5 mL of a 35% w/w solution of H₂O₂ (0.993 g, 29.2 mmol) were added and, the solution was heated at 100 °C for 2 h. After the reaction mixture was cooled at room temperature, 10 mL of H₂O were added and the product was extracted twice with CH₂Cl₂ from the aqueous layer. The resultant organic phase was washed once with brine and dried under Na₂SO₄. After the solvent was removed, a solid was formed which was purified by recrystallized with EtOH-CH₂Cl₂. After drying the solid under reduced pressure, 0.653 g (1.76 mmol) of the product (74% pure) was obtained in a 52% yield.

¹H NMR (300 MHz, CD₂Cl₂, δ): 8.21 (d, *J*= 2.0, ArH, 1H), 7.95 (dd, *J*= 8.3, 2.0, ArH, 1H), 7.84 (d, *J*= 8.3, ArH, 1H), 3.71 (m, CH₂, 2H), 3.38 (m, CH₂, 2H).

¹³C NMR (75 MHz, CD₂Cl₂): δ 189.5, 143.4, 140.6, 138.1, 131.9, 128.6, 125.6, 49.6, 37.1.

6,8-Dibromo-1,1-dioxo-1-thiochroman-4-one thiosemicarbazone (87) Into a round bottom flask containing thiochroman-4-one **86** (0.218 g, 0.617 mmol), 15 mL of anhydrous methanol were added and the solution was refluxed for about 15 minutes before adding thiosemicarbazide (0.0512 g, 0.563 mmol) and 1.2 mg of TsOH. After the reaction mixture was refluxed under nitrogen atmosphere for 4 h, a solid was formed which was filtered and, then purified by recrystallization with CH₂Cl₂-EtOH. After the solid was dried under vacuum, 0.115 g (0.269 mmol) of the product was obtained in a 44% yield.

¹H NMR (300 MHz, Methyl Sulfoxide-d₆, δ): 10.69 (s, NH, 1H), 8.82 (d, *J*= 1.9, ArH, 1H), 8.59 (br s, NH₂, 1H), 8.53 (br s, NH₂, 1H), 8.11 (d, *J*= 1.9, ArH, 1H), 3.76 (t, *J*= 5.6, CH₂, 2H), 3.26 (t, *J*= 5.6, CH₂, 2H).

^{13}C NMR (75 MHz, Methyl Sulfoxide- d_6): δ 179.4, 139.3, 137.6, 136.5, 135.7, 128.9, 126.4, 117.8, 47.4, 23.0.

6-Bromo-1,1-dioxo-1-thiochroman-4-one thiosemicarbazone (88) Into a round bottom flask containing 0.198 g of thiochroman-4-one **86b** (0.147 g, 0.534 mmol), 10 mL of anhydrous methanol were added and the solution was refluxed for about 15 minutes before adding thiosemicarbazide (0.0598 g, 0.657 mmol) and 1.4 mg of TsOH. After the reaction mixture was refluxed under nitrogen atmosphere for 10 h, a solid was formed which was filtered and, then purified by column chromatography (30% EtOAc/ 70% hex). 0.0618 g (0.178 mmol) of the product was obtained in a 33% yield.

^1H NMR (300 MHz, Methyl Sulfoxide- d_6 , δ): 10.59 (s, NH , 1H), 8.77 (d, $J= 1.8$, ArH , 1H), 8.58 (br s, NH_2 , 1H), 8.52 (br s, NH_2 , 1H), 7.80 (dd, $J= 8.4, 1.9$, ArH , 1H), 7.74 (d, $J= 8.4$, ArH , 1H), 3.69 (t, $J= 6.3$, CH_2 , 2H), 3.27 (t, $J= 6.5$, CH_2 , 2H).

^{13}C NMR (75 MHz, Methyl Sulfoxide- d_6): δ 179.4, 138.8, 136.6, 134.5, 132.7, 129.1, 127.1, 124.6, 45.5, 24.5.

7-Bromo-4-chromanone (89) Into a round bottom flask kept at 0 °C, AlCl_3 (0.533 g, 3.99 mmol) and, 5 mL of CH_2Cl_2 was added. The reaction system was put under nitrogen and stirred for about 7 minutes before adding 10 mL of a CH_2Cl_2 solution of 4-chromanone (0.296 g, 1.99 mmol). After the reaction mixture was stirred for 10 minutes, 10 mL of Br_2 (0.352 g, 2.20 mmol) was added and, the reaction mixture was stirred at room temperature for an hour. At the end of this period of time, the reaction mixture was poured into 30 mL of ice-water and, the product was extracted 3 times from the aqueous phase with EtOAc. The resultant organic phase was washed once with brine and dried

under Na₂SO₄. After the solvent was evaporated, the solid formed was filtered and dried to obtain 0.361 g (1.51 mmol) of the product (93% pure) in a 74% yield.

¹H NMR (300 MHz, CDCl₃, δ): 7.90 (dd, *J* = 2.6, 0.3 ArH, 1H), 7.47 (dd, *J* = 8.8, 2.5, ArH, 1H), 6.82 (dd, *J* = 8.8, 0.2, ArH, 1H), 4.48 (t, *J* = 6.5, CH₂, 2H), 2.75 (t, *J* = 6.5, CH₂, 2H).

7-Bromo-4-chromanone thiosemicarbazone (90) Into a round bottom flask containing 0.198 g of chroman-4-one **89** (0.336 g, 1.48 mmol), 20 mL of anhydrous methanol were added and the solution was refluxed for about 15 minutes before adding thiosemicarbazide (0.274 g, 3.01 mmol) and 38 mg of TsOH. After the reaction mixture was refluxed under nitrogen atmosphere for 12 h, the solid formed was filtered and, then purified by column chromatography (20% EtOAc/ 80% hex) to obtain 0.363 g (1.21 mmol) of the product in an 82% yield.

¹H NMR (300 MHz, CDCl₃, δ): 8.73 (s, NH, 1H), 8.01 (d, *J* = 2.5, ArH, 1H), 7.38 (dd, *J* = 8.8, 2.5, ArH, 1H), 7.35 (br s, NH₂, 1H), 6.83 (1H, d, *J* = 8.7, ArH), 6.42 (br s, NH₂, 1H), 4.31 (t, *J* = 6.2, CH₂, 2H), 2.76 (t, *J* = 6.2, CH₂, 2H).

Biochemical Evaluation

The biochemical evaluation of the compounds synthesized in the current research work was performed through a collaborative effort with Dr. Mary Lynn Trawick (Baylor University) who performed the *in vitro* cruzain inhibition for most of the compounds and the *in vitro* human liver cathepsin L inhibition for selected inhibitors. Cruzain was obtained as a generous gift from Dr. James McKerrow and Ms. Elizabeth Hansell (University of California San Francisco)

*Cruzain Inhibition*¹⁶⁹

Cruzain (0.15 nM final concentration) was incubated with potential inhibitors at 20 different concentrations (from 0.05 nM to 50 μ M) at 25 °C for 5 minutes before 20 μ L of substrate benzyloxycarbonyl-L-phenylalanyl-L-arginyl-7-amido-4-methylcoumarin (abbreviated as Z-FR-AMC, 10 μ M in final assay condition) was added to the enzyme-inhibitor mixture to make a total volume of 300 μ L. The assay conditions were 100 mM sodium acetate, 5 mM DTT, pH 5.5. Excitation wavelength and emission wavelength were 355 nm and 460 nm, respectively. Velocity of enzyme reaction was measured as the rate of release of 7-amino-4-methylcoumarin (AMC) per unit time. IC₅₀ values were determined by plotting velocity versus logarithm of inhibitor concentrations and fit to a sigmoid dose-response equation with GraphPad Prism 3.02.

$$y = \text{bottom} + (\text{top} - \text{bottom}) / (1 + 10^{((\log \text{EC}_{50} - x) * \text{HillSlope})})$$

Human Liver Cathepsin L Inhibition

Cathepsin L (0.25 nM final concentration) was incubated with potential inhibitors at 20 different concentrations (from 5.0 pM to 50 μ M) at 25 °C for 5 minutes before 100 μ L substrate (benzyloxycarbonyl-L-phenylalanyl-L-arginyl-7-amido-4-methylcoumarin, abbreviated as Z-FR-AMC, 50 μ M in final assay condition) was added to the enzyme-inhibitor mixture; total volume was 200 μ L. The assay conditions were 100 mM sodium acetate, 2 mM DTT, 1 mM EDTA, pH 5.5. Excitation wavelength and emission wavelength were 355 nm and 460 nm, respectively. Velocity of enzyme reaction was measured as the rate of release of 7-amino-4-methylcoumarin (AMC) per unit time. IC₅₀ values were determined by plotting velocity versus logarithm of inhibitor concentrations and fit to a sigmoid dose-response equation with GraphPad Prism 3.02.

CHAPTER EIGHT

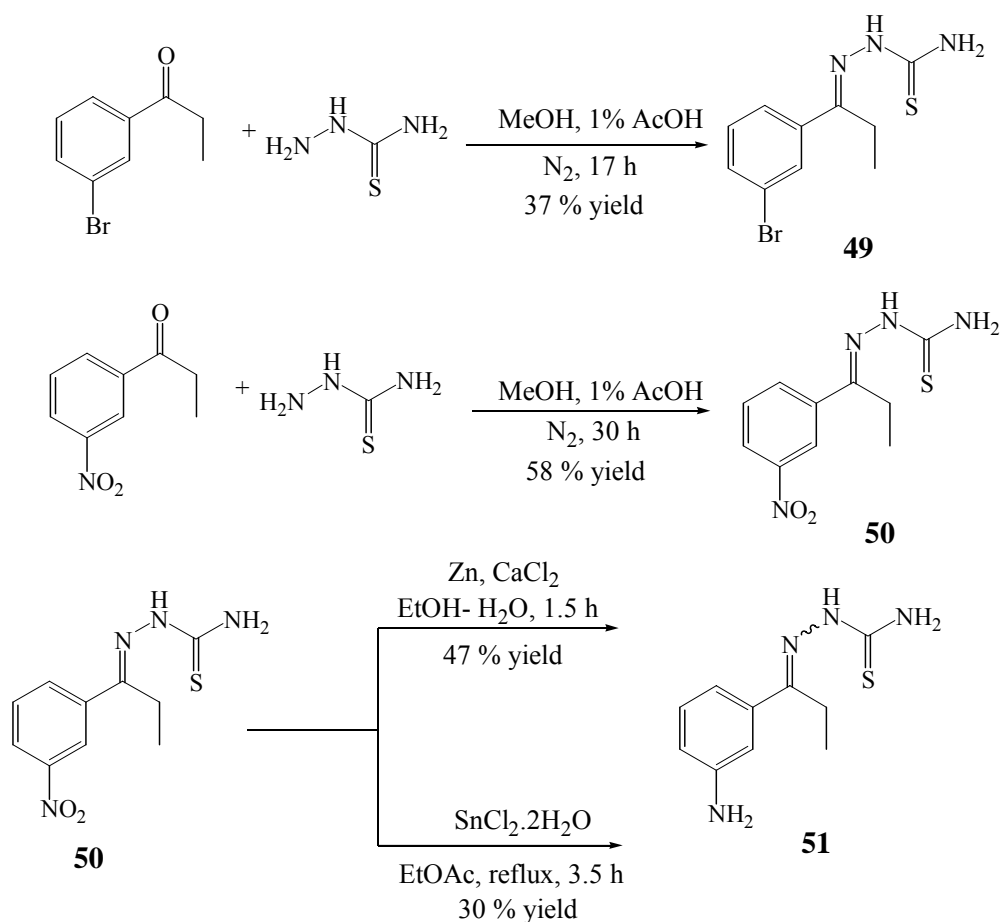
Results and Discussion

In this chapter, the synthesis of a variety of new cruzain inhibitors will be discussed and the most important observations associated with the reactions will be presented. All of the inhibitors are classified in the following groups: propiophenone thiosemicarbazone derivatives, benzophenone thiosemicarbazone derivatives and tetrahydronaphthalene analogues. Finally, the biochemical results will be presented along with the discussion of the structure-activity relationship of these compounds against cruzain.

Synthesis of Propiophenone Thiosemicarbazone Derivatives

In 2002, Cohen and McKerrow reported the synthesis and structure-activity relationship studies of small nonpeptide thiosemicarbazone molecules which are active *in vitro* and *in vivo* against cruzain.¹⁶⁹ They found that the best inhibitor, which exhibited a low nanomolar value of IC₅₀ for cruzain inhibition and trypanocidal activity, was compound **49** shown in Scheme 8.1. In order to understand the impressive biological activity exhibited for these novel derivatives, they docked compound **49** in the crystal structure of cruzain showing that this small molecule interacts with the catalytic triad of cruzain by forming reversibly and covalently a tetrahedral intermediate between the thiosemicarbazone group and Cys25 of the enzyme.¹⁶⁹ In addition, the study showed that the phenyl ring containing a bromine atom at position three is important in order to effectively bind the enzyme at the most important subsite S2.

Encouraged by these results, the designed synthesis of other novel propiophenone thiosemicarbazone derivatives containing other substituents rather than bromine was undertaken in order to better understand the type of interaction taking place inside the S2 pocket and therefore ultimately obtain more potent inhibitors against cruzain. The decision was made to incorporate on the aromatic ring an electron-withdrawing group like nitro and two hydrogen bond donor-acceptor groups such as amino and hydroxyl and to compare their biochemical effect against cruzain.



Scheme 8.1. Synthesis of two novel propiophenone thiosemicarbazone derivatives **50** and **51**.

The synthesis of derivative **50** was carried out following the procedure reported by Du and co-workers¹⁶⁹ treating the commercially available 3-nitro propiophenone with thiosemicarbazide to form the respective nitrothiosemicarbazone in a 58% yield. Because of the possibility of forming the *E* or *Z* isomers at the C=N bond, an X-ray crystal structure⁹⁵ was obtained to determine the geometry of this double bond. Figure 8.1 shows that the structure of compound **50** belongs to the *E* isomer as expected since its most likely the more stable isomer.

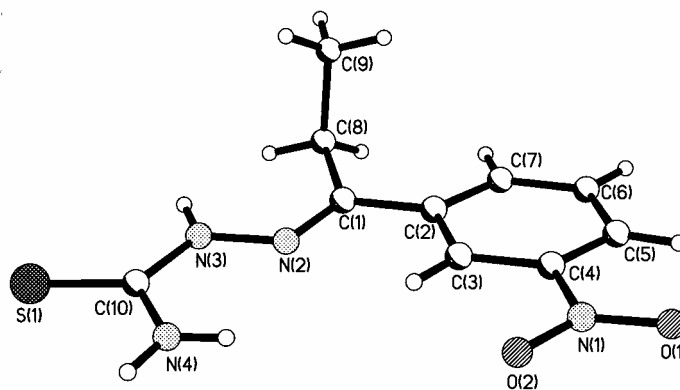


Figure 8.1. X-ray structure of compound **50**.⁹⁵

The reduction of nitrothiosemicarbazone **50** was performed using two methods. In the first method,⁸⁵ compound **50** was treated with Zn and CaCl₂ to form the amine derivative **51** in a 47% yield. However, when the reduction was carried out with SnCl₂·2H₂O^{80,81} the same product was obtained in a 30% yield, however this reaction also formed 1-(3-aminophenyl)-propan-1-one as a by-product. It seems that this reducing agent, besides reducing the nitro group, also reduces the thiosemicarbazone group breaking the C=N bond and forming the aminoketone **51a**. The low resolution mass spectrum of this by-product showed a peak of 149 corresponding to the molecular weight

of the ketone. It was also noticed that the base peak had an m/z value of 120 corresponding to the loss of an ethyl group ($M^+ - 29$) and another important peak of 92 ($M^+ - 57$) corresponding to the loss of a propanoyl ion.^{57,58,78} The ^{13}C -NMR showed nine different peaks, and the Dept 135 spectrum showed four aromatic methines, one methylene, and one methyl group as expected. The presence of the amino group was confirmed by the ^1H -NMR that is shown in Figure 8.2.

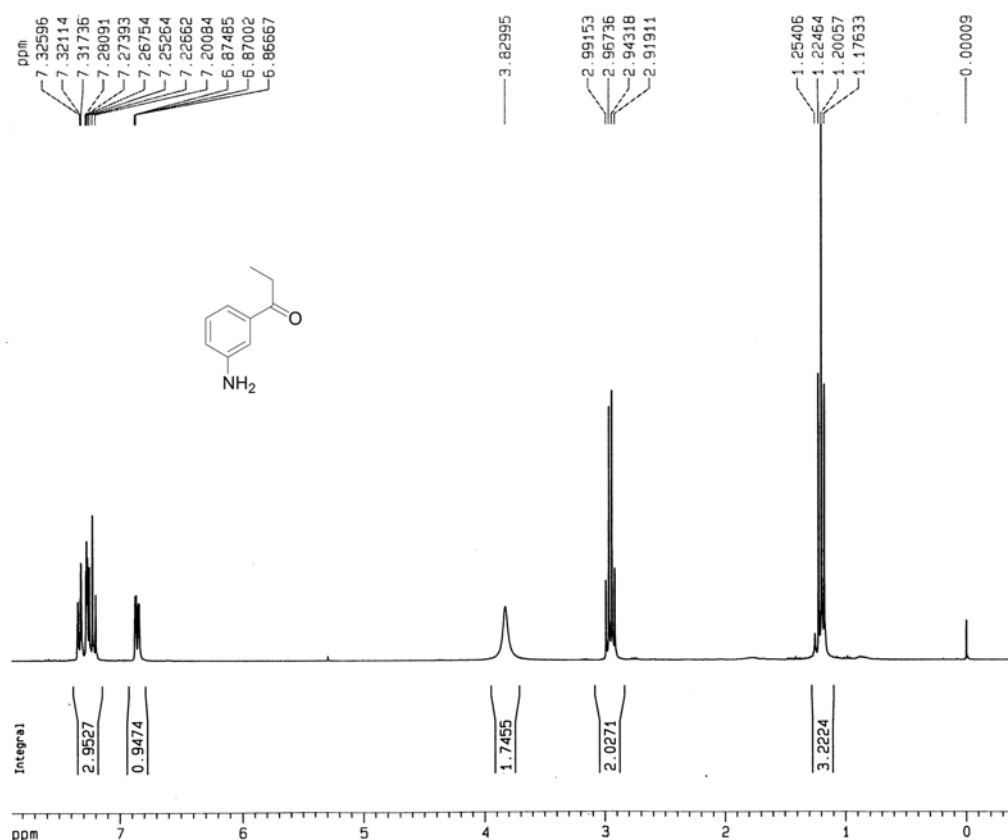
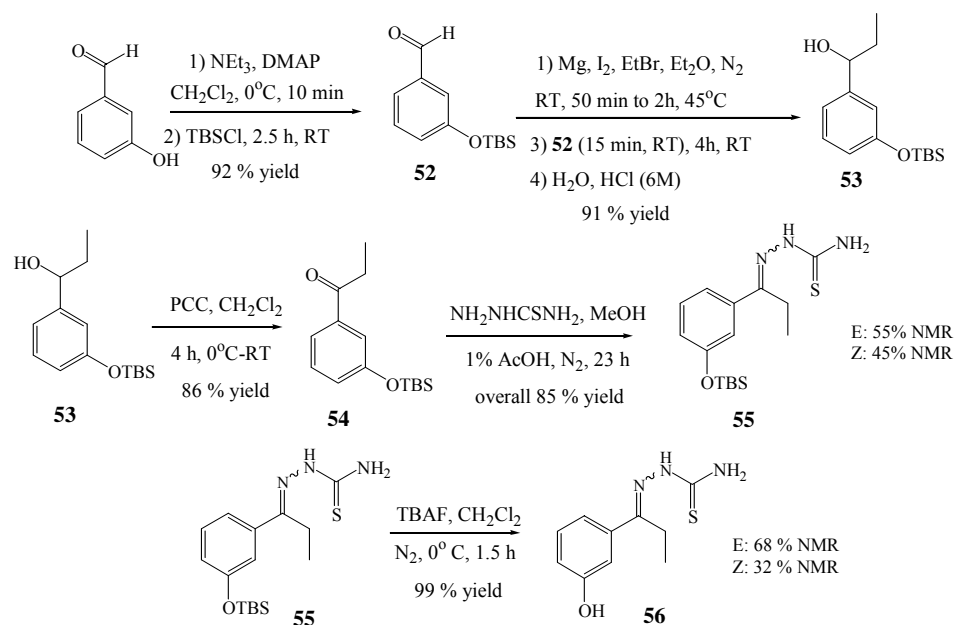


Figure 8.2 ^1H -NMR (300 MHz) spectrum of compound **51a** obtained as a by-product after reacting compound **50** with $\text{SnCl}_2 \cdot 2\text{H}_2\text{O}$.

The acetone- d_6 ^1H -NMR of the only product obtained from the reaction of Zn/CaCl_2 with compound **50** showed, at room temperature, a mixture of the *E* and *Z* isomers

presumably in a ratio of 5.1: 1 respectively. The ^{13}C -NMR and Dept 135 spectra showed twice the number of carbons in different ratios suggesting the presence of both isomers.

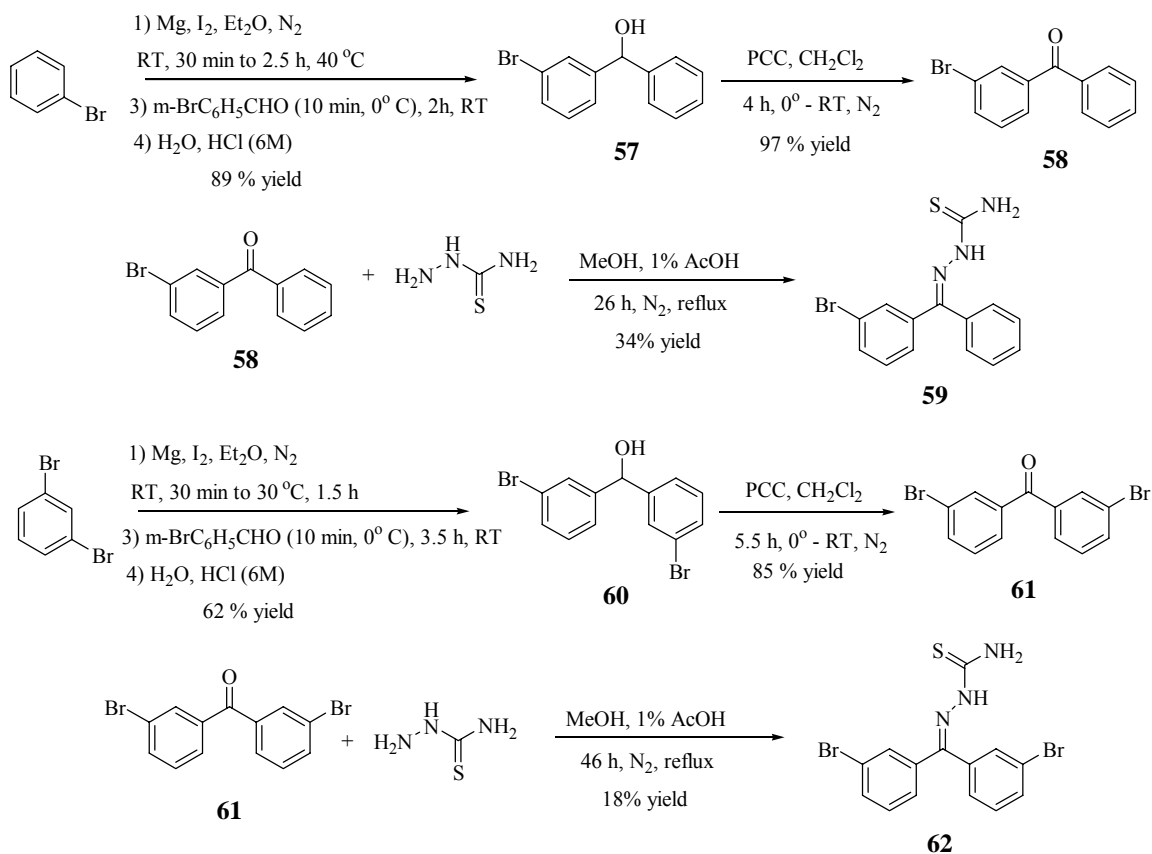
The synthesis of the hydroxythiosemicarbazone **56** is depicted in Scheme 8.2. TBS protection¹¹⁰ of the phenol group was carried out with TBSCl in the presence of NEt_3 and DMAP to form the protected aldehyde **52** in a 92% yield. Grignard reaction¹⁷⁴ of this aldehyde was performed with ethyl magnesium bromide, which was formed *in situ*, to afford the secondary alcohol **53** in a 91% yield which in turn was oxidized with PCC⁹⁸⁻¹⁰¹ to obtain ketone **54** in an 86% yield. Again a mixture of *Z* and *E* isomers (1: 1.2 NMR ratio respectively) was formed in an overall yield of 85% after treating ketone **54** with thiosemicarbazide. Deprotection of the TBS group of thiosemicarbazone **55** was performed using TBAF¹¹⁰ which afforded the hydroxythiosemicarbazone **56** in a 99% yield. Once again the CDCl_3 ^1H -NMR of the purified fraction, which was taken at room temperature, showed a mixture of both isomers in a ratio *E*: *Z* = 2.1: 1.



Scheme 8.2. Synthesis of hydroxythiosemicarbazone **56**.

Synthesis of Benzophenone Thiosemicarbazone Derivatives

The objective of this second project was to substitute the ethyl moiety of compound **49** by a benzene ring either containing or not containing a bromine atom substitution. In Scheme 8.3, the synthesis of thiosemicarbazones **59** and **62** is shown. The secondary alcohol **57** was formed in an 89% yield after performing a Grignard¹⁷⁴ reaction of phenyl magnesium bromide and *m*-bromobenzaldehyde. Its low resolution MS showed the molecular ion peak of 262 and the $M^+ + 2$ peak of the same intensity as M^+ characteristic of molecules containing one bromine atom.^{57,58,78}



Scheme 8.3. Synthesis of benzophenone thiosemicarbazone derivatives **59** and **62**.

PCC oxidation⁹⁸⁻¹⁰¹ of alcohol **57** afforded the respective benzophenone **58** in a 97% yield which after reacting with thiosemicarbazide formed bromobenzophenone thiosemicarbazone **59** in a 34% yield. The structure of ketone **58** was confirmed by its ¹H-NMR and the MS which showed one more time the M⁺ and M⁺ + 2 peaks confirming the presence of one bromine atom in the molecule.^{57,58,78} An X-ray structure of compound **59** showed that the structure belongs to the *E* isomer.⁹⁵ However, when the ¹H-NMR spectrum of this compound was taken in different solvents, a mixture of both isomers was observed.¹⁷⁵⁻¹⁷⁹

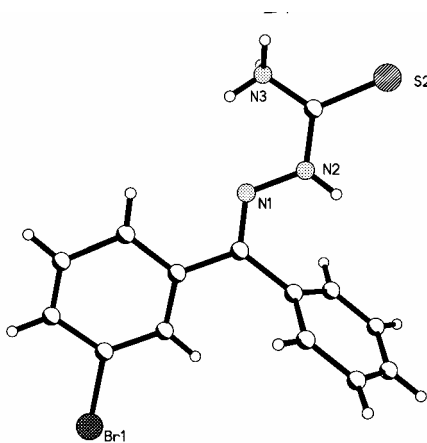


Figure 8.3. X-ray structure of compound **59**.⁹⁵

The first solvent used in the ¹H-NMR was CDCl₃, however in this solvent the peaks of the aromatic region overlapped making it difficult to assign all the peaks for both isomers. The spectrum shows that the compound is a mixture of both isomers in a ratio *E*: *Z* = 2.4: 1. Therefore, acetone-d₆ was used as the second solvent to induce a change in the chemical shifts of the peaks (SIS, solvent-induced shift)⁷⁸ in an effort to identify the respective peaks for both isomers. There was a slight improvement in the separation of some aromatic peaks but it was still complicated enough to cause

difficulties in differentiating some peaks from the others. One important observation noted in the acetone- d_6 $^1\text{H-NMR}$ spectrum was that the hydrogen atoms attached to the different nitrogen atoms appeared more downfield than in CDCl_3 . Based on these results, we decided to perform a low-temperature study of the acetone- d_6 $^1\text{H-NMR}$ of compound **59** in order to separate, as much as possible, the peaks associated with both isomers. Ten $^1\text{H-NMR}$ spectrum were taken starting from 20 °C and decreasing the temperature in intervals of 10 ° until -70 °C. The results showed that there was not significant improvement in the aromatic region. In fact most of the peaks were overlapped as the temperature decreased.⁵⁸ However, at low temperatures it was possible to observe six broad peaks of different intensities moving downfield as the temperature was decreasing. Most likely these peaks correspond to the hydrogen atoms of the thiosemicarbazone functionality the *E* and *Z* isomers which were found in a ratio of 3:1 respectively. The results so far obtained demonstrate that apparently compound **59**, in both solvents, exists as a mixture of *Z* and *E* isomers but the question still remained whether compound **59** is an actual mixture of both isomers after the reaction that could not be separated or if this compound, which presumably is the *E* isomer based on the X-ray structure, in solution starts exhibiting interconversion into its *Z* isomer. To answer this question a $^1\text{H-NMR}$ spectrum was taken in methyl sulfoxide- d_6 and performed high temperature studies.⁵⁸ If an interconversion is taking place as the temperature increases, a simple average $^1\text{H-NMR}$ spectrum is expected to be seen for both isomers because it will be easy and fast for one isomer to reach the activation energy to be converted into the other isomer.⁵⁸ Conversely, if compound **59** is a mixture of both isomers in a specific ratio, regardless of the increase of temperature this ratio will be basically the same all the time. Five

DMSO- d_6 $^1\text{H-NMR}$ spectra were taken starting from 23 °C and increasing the temperature in intervals of about 20 ° until 107 °C. Interestingly, at room temperature the hydrogen atoms of the thiosemicarbazone group for both isomers were more downfield than in CDCl_3 or acetone. However, when the temperature was increased, all these peaks started moving upfield and were overlapped at higher temperatures. All of the spectra showed a ratio of $E:Z=2:1$, and basically the peaks of the aromatic region were not considerably affected. This suggests that compound **59** is most likely a mixture of both isomers.

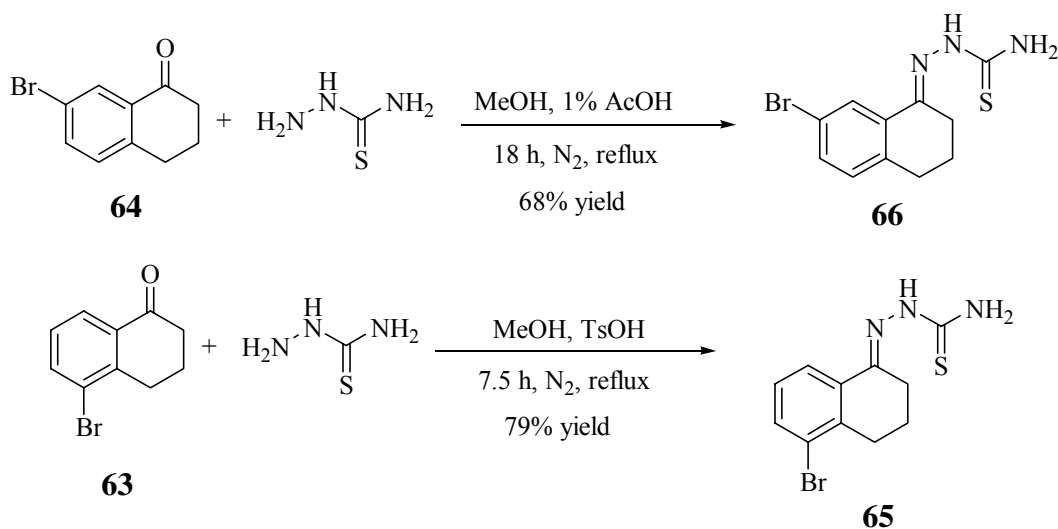
The synthesis of thiosemicarbazone **62** started with a Grignard reaction of *m*-dibromobenzene and *m*-bromobenzaldehyde to form the secondary alcohol **60** in a 62% yield. Oxidation of this alcohol with PCC^{98-101} afforded the respective ketone **61** in an 85% yield which, after reacting with thiosemicarbazide, afforded thiosemicarbazone **62**. The structure of alcohol **60** was confirmed by its $^1\text{H-NMR}$, DEPT 135, and MS which showed three expected peaks (M^+ , $M^+ + 2$ and $M^+ + 4$) in a ratio 1: 2: 1 as an evidence for the presence of two bromine atoms.^{57,58,78} The $^1\text{H-NMR}$, in CDCl_3 , of thiosemicarbazone **62** showed again a mixture of both isomers in a ratio $E:Z=2.7:1$.

Synthesis of Tetrahydronaphthalene Derivatives

After analyzing carefully the cruzain structure and because it is well known that proteases have a better interaction with inhibitors or substrates that have planar structure to fit their active site,³ we decided to incorporate this structural requirement in the novel inhibitors by forming a new ring next to the aromatic moiety. One of the simplest skeletons that seemed to fill this requirement was the tetrahydronaphthalene skeleton.

After column purification, bromotetralone **64** was obtained in high purity in a 40% yield. However, tetralone **63** after purification by column chromatography was just 93% pure having as a contaminant dibromide **64a**. Therefore it was purified by recrystallization with hexanes to obtain a purer product in a 44% yield. The structure of **64a** was elucidated by its $^1\text{H-NMR}$ and MS which showed the presence of two bromine atoms.^{57,58,78}

When bromination of α -tetralone was carried out using CH_2Cl_2 as the solvent at room temperature,¹⁸⁰ a longer reaction time was required, however only tetralones **63** and **64** were obtained in a ratio of 1: 1.5 respectively. The spectroscopic data did not show the presence of dibromide **64a** and, under these conditions, it was apparent that compound **64** was the major product. After column separation both isomers were obtained in high purity, however the yields for these tetralone derivatives were low (38% for **64** and 26% for **63**).



Scheme 8.5. Synthesis of thiosemicarbazones **65** and **66**.

Tetralones **63** and **64** were reacted with thiosemicarbazide to form thiosemicarbazones **65** and **66** in a 79% and 68% yield respectively (Scheme 8.5). The X-ray structure⁹⁵ of tetralone **66** (Figure 8.4) confirms that the structure of this compound is the *E* isomer as in earlier cases. The ¹H-NMR of this compound suggests that it exists as a single pure isomer and not as mixture of both isomers. Although an X-ray crystal structure of tetralone **65** is not available, its ¹H-NMR spectrum indicates that this compound is pure and exists as the *E* isomer too.

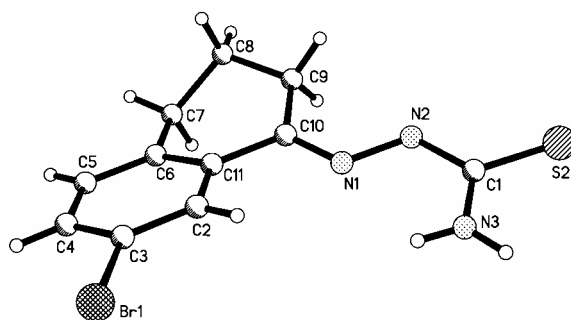
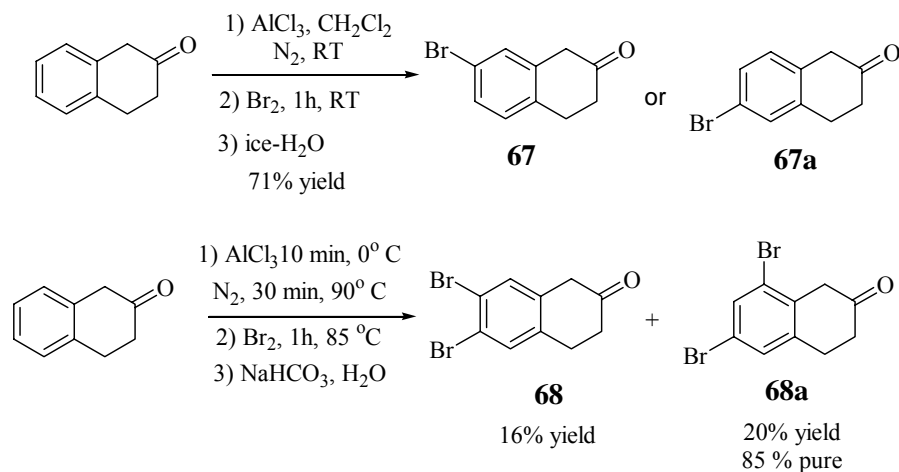


Figure 8.4. X-ray structure of compound **66**.⁹⁵

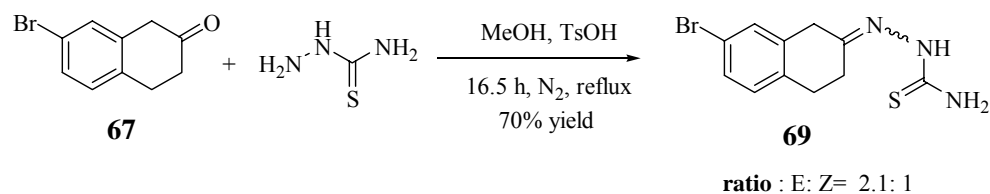
Bromination of β -tetralone was carried out using two different conditions. In the first approach, the tetralone was heated with AlCl_3 at 90 °C before and after adding Br_2 ¹⁷³ which formed primarily dibromotetralones **68** and **68a**. After column separation, the less polar compound **68** was obtained as a pure component in a 16% yield; however, the more polar dibromo compound **68a** was obtained as a pure component in a 85% purity, even after recrystallization (Scheme 8.6).



Scheme 8.6. Bromination of β -tetralone under two different conditions.

Unfortunately, X-ray crystallographic structures are not available for compounds **68** and **68a**, and the assignment of their structures was based entirely on their ^1H -NMR and ^{13}C -NMR spectra. The experimental chemical shifts for ^1H and ^{13}C NMR have been carefully compared with the ones obtained using ChemNMR predictor software.¹⁰³

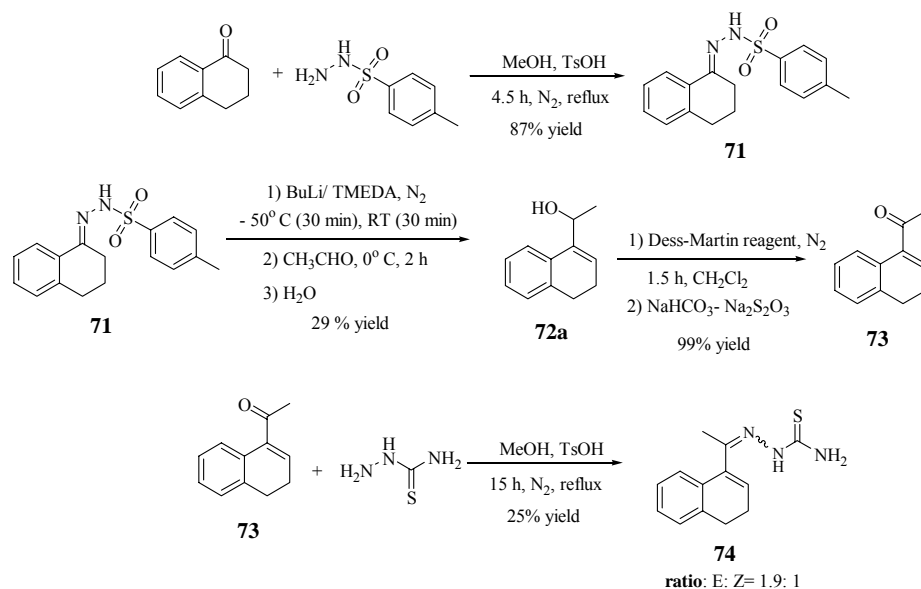
When the bromination was carried out at room temperature using CH_2Cl_2 as the solvent,¹⁸⁰ a monobromide tetralone was formed in a 71% yield. After carefully analyzing the ^1H -NMR and ^{13}C -NMR spectra and comparing with the values obtained from the ChemDraw NMR predictor,¹⁰³ compound **67** was the product that most likely was formed instead of **67a**.



Scheme 8.7. Synthesis of bromothiosemicarbazone **69**.

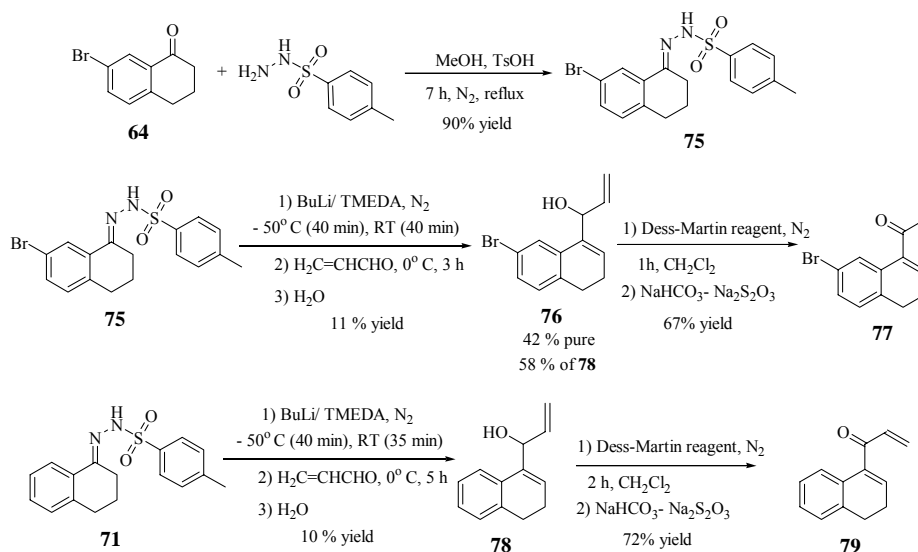
After tetralone **67** was reacted with thiosemicarbazide, the respective thiosemicarbazone **69** was formed in a 70% yield. The $^1\text{H-NMR}$ of compound **69** showed that this solid was a mixture of presumably *E* and *Z* isomers in a ratio of 2.1: 1, respectively. Additional support for the structural assignment was found in the DEPT 135 of this compound which showed twice the number of methines and methylenes as anticipated for a single isomer.

The next group of compounds synthesized contained an exo-cyclic conjugated carbonyl group instead of the thiosemicarbazone scaffold. The introduction of these other functional groups would inhibit the activity of cruzain by reacting with the thiolate of Cys25 of the enzyme. The incorporation of an α,β -conjugated carbonyl group into the tetranaphthalene skeleton would allow the inhibitor to react with the nucleophilic thiolate of Cys25 through an 1,4-Michael addition¹⁷² and, hence the catalytic activity of the enzyme will be suppressed.



Scheme 8.8. Synthesis of thiosemicarbazone **74**.

The synthesis of thiosemicarbazone **74** is depicted in Scheme 8.8. The incorporation of the ethanoyl moiety starts with the formation of *p*-toluensulfonylhydrazone **71** which is formed in an 87% yield after reacting α -tetralone with *p*-toluensulfonylhydrazine.¹⁸¹ Hydrazone **71** reacted initially with BuLi to form 3,4-dihydronaphthalenen-1-yl lithium *in situ*¹⁸²⁻¹⁸⁴ which in turn attacked the electrophilic carbon of acetaldehyde. Subsequent hydrolysis produced the secondary alcohol **72a** in a 29% yield. Unfortunately, the major by-product of this reaction was 1,2-dihydronaphthalene **72b** which was formed after the lithium derivative reacted with moisture instead of acetaldehyde. Its structure was confirmed by its ¹H-NMR which showed the two vinylic protons and its DEPT 135 which showed two methylenes and six methines. Dess-Martin oxidation¹⁸⁵⁻¹⁸⁶ of alcohol **72a** formed the conjugated ketone **73** in a 99% yield, which after reacting with thiosemicarbazide formed thiosemicarbazone **74** in a 25% yield. Compound **74** is actually a mixture of two isomers with a ratio of 1.9:1.



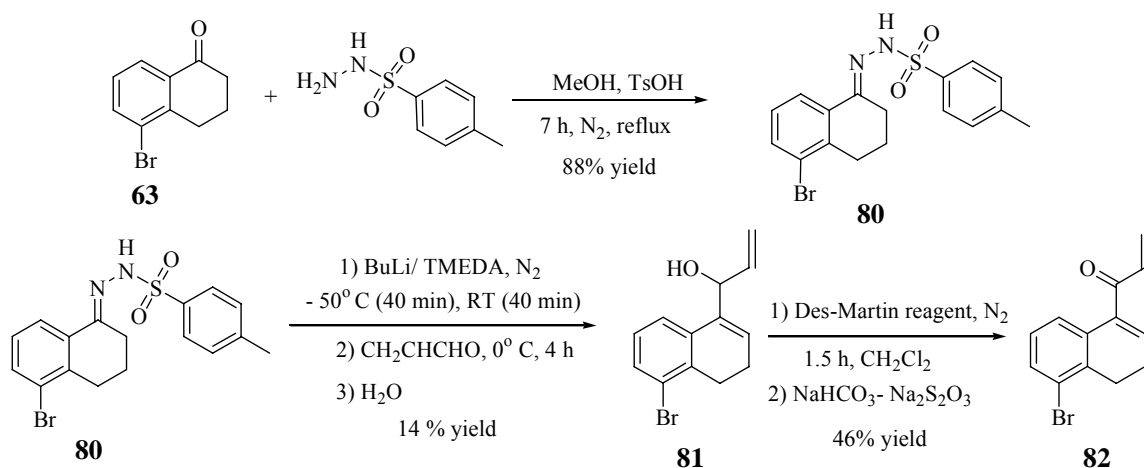
Scheme 8.9. Synthesis of α,β -conjugated ketones **77** and **79**.

In Scheme 8.9, the synthesis of the first exo-cyclic α,β - conjugated ketones is shown. Because the presence of a bromine atom seems important for activity against cruzain,¹⁶⁹ again this atom was attached to the 7 position of the benzene ring. Hydrazone **75**, which was formed in a 90% yield after tetralone **64** reacted with *p*-toluensulfonhydrazone, produced the allylic alcohol **76** by a Shapiro-type reaction¹⁸²⁻¹⁸⁴ after reacting with BuLi and acrolein. Interestingly, after column chromatography compound **76** was just 42% pure having 58% of alcohol **78** as the by-product as its ¹H-NMR confirms. Attempted separation of this impurity was unsuccessful by flash chromatography (two additional columns). Unfortunately the R_f values for both compounds are too close to allow separation by this technique. The formation of this alcohol can be explained by the fact that halogen-metal exchange takes place after the nucleophilic addition of the bromolithium intermediate to acrolein. This mixture of alcohols **76** and **78** was oxidized with Dess-Martin reagent¹⁸⁵⁻¹⁸⁶ to form ketones **77** and **79** which were successfully separated by column chromatography to yield the former in a 67% and the latter in a 48% yield.

Synthesis of ketone **79** started with the Shapiro-type reaction¹⁸²⁻¹⁸⁴ of hydrazone **71** to form the allylic alcohol **78** in a 10% yield. One more time it has been observed that the major by-product was 1,2-dihydronaphthalene **72b**. Finally oxidation of this alcohol with Dess-Martin reagent¹⁸⁵⁻¹⁸⁶ afforded the α,β - conjugated ketone **79** in a 72% yield.

The synthesis of the isomeric α,β - conjugated ketone **82** containing the bromine atom at position 5 was performed in order to compare how these positions affect the biochemical activity. The synthesis of this ketone, which is depicted in Scheme 8.10, starts with the reaction of tetralone **63** and *p*-toluensulfonhydrazide¹⁸¹ to form, in an 88%

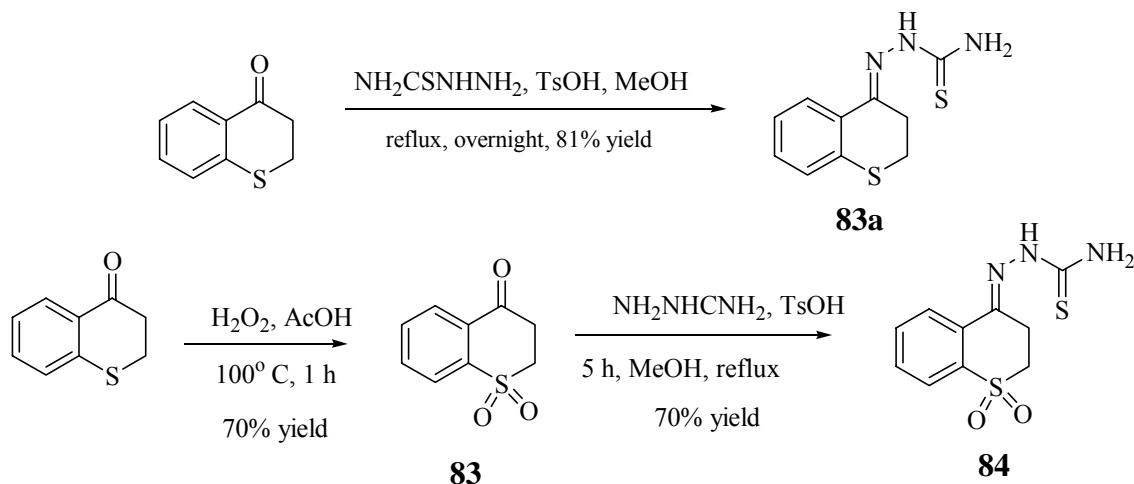
yield, the respective hydrazone **80**. After the hydrazone was reacted with BuLi and acrolein,¹⁸²⁻¹⁸⁴ the allylic alcohol **81** was formed in a 14% yield. Once again alcohol **78** was observed in the reaction mixture but it was formed in less amount compare to the reaction of the isomer **76** already discussed. Finally, Dess-Martin oxidation¹⁸⁵⁻¹⁸⁶ of alcohol **81** formed the α,β - conjugated ketone **82** in a 46% yield.



Scheme 8.10. Synthesis of α,β - conjugated ketone **82**

The last group of molecules that are going to be discussed is the series that contains tetrahydronaphthalene derivatives that have a heteroatom such as O and S replacing one benzylic carbon of the cyclohexane ring. It was of interest to know how the presence of these elements could affect cruzain inhibition. Scheme 8.11 shows the synthesis of the first thiosemicarbazone inhibitor containing sulfur and a sulfone group attached at the benzylic position of α -tetralone. A one-step reaction of 2,3-dihydro-4H-thiochromen-4-one with thiosemicarbazide formed in a 81% yield the respective thiosemicarbazone **83a**. Oxidation of 2,3-dihydro-4H-thiochromen-4-one with H_2O_2 ¹⁸⁷

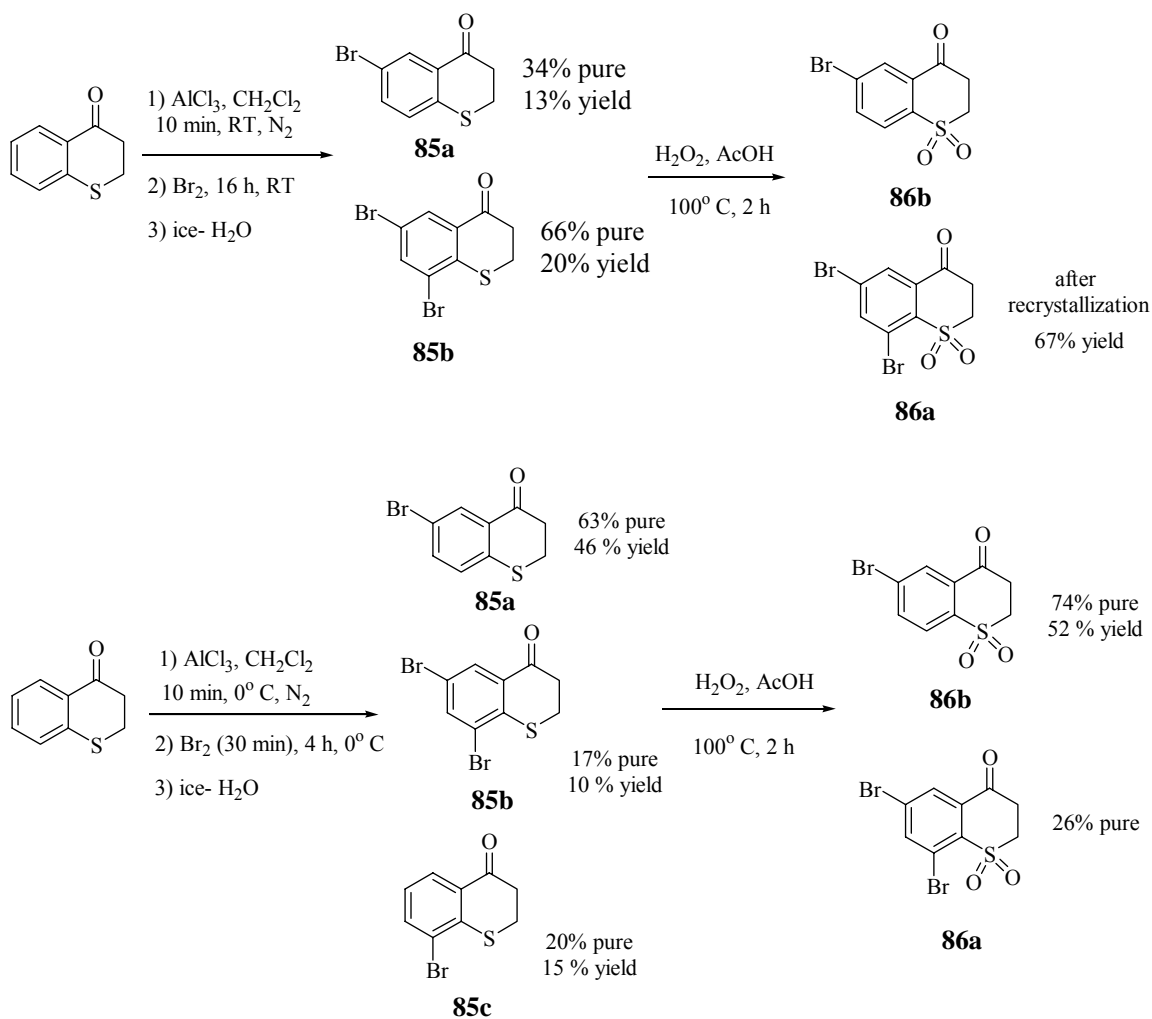
produced sulfone **83** in a 70% yield which afterwards reacted with thiosemicarbazide to afford thiosemicarbazone **84** in a 70% yield.



Scheme 8.11. Synthesis of thiochromen-4-one thiosemicarbazone **84** and thiosemicarbazone **83a**.

Bromination of 2,3-dihydro-4H-thiochromen-4-one was carried out under two sets of reaction conditions as shown in Figure 8.12. In the first case, thiochromen-4-one reacted with Br_2 and AlCl_3 for 16 h at room temperature¹⁸⁰ to form a mixture of two bromide derivatives. Based on their ^1H and ^{13}C -NMR spectra and the comparison made with the values predicted by Chemdraw predictor¹⁰³ we think that the first compound obtained in a 34% purity is **85a** and the second product is **85b** which was obtained in a 66% purity. The experimental assignment of these structures agrees with the theoretical prediction towards the electrophilic aromatic substitution of thiochromen-4-one. As we can see from the structure, the sulfur atom directly attached to the ring activates it toward the substitution and directs to *ortho* and *para* positions. The deactivating carbonyl group, which is *ortho* to the sulfur atom, is a *meta* director that will not have any effect in the

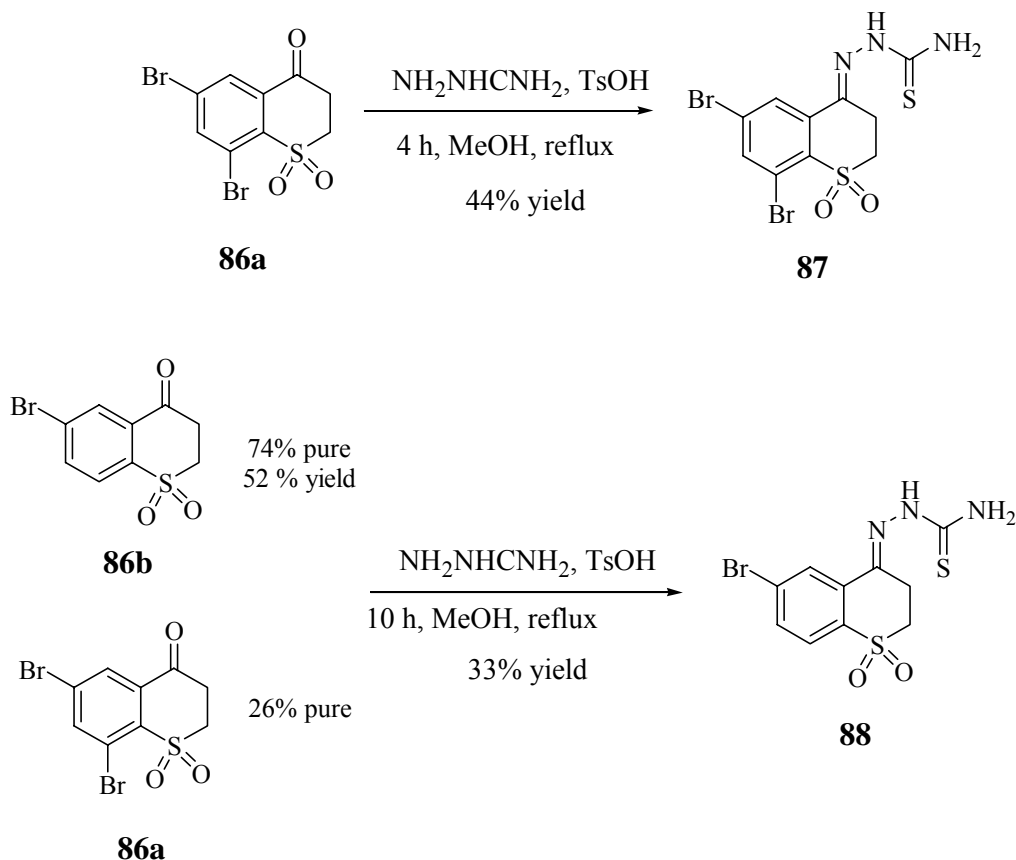
aromatic substitution in the presence of the activating sulfur group. Therefore the products that will result are the ones attached at positions 6 or 8, the former most likely being the major. In the event that disubstitution takes place, both positions are expected to be substituted.



Scheme 8.12. Bromination and further oxidation of 1,1-dioxo-1-thiochromen-4-one.

Unfortunately compounds **85a** and **85b** could not be separated by column chromatography because of their close R_f values; so, the next reaction was performed with this mixture which produced, after oxidation with H_2O_2 ,¹⁸⁷ sulfones **86a** and **86b**.

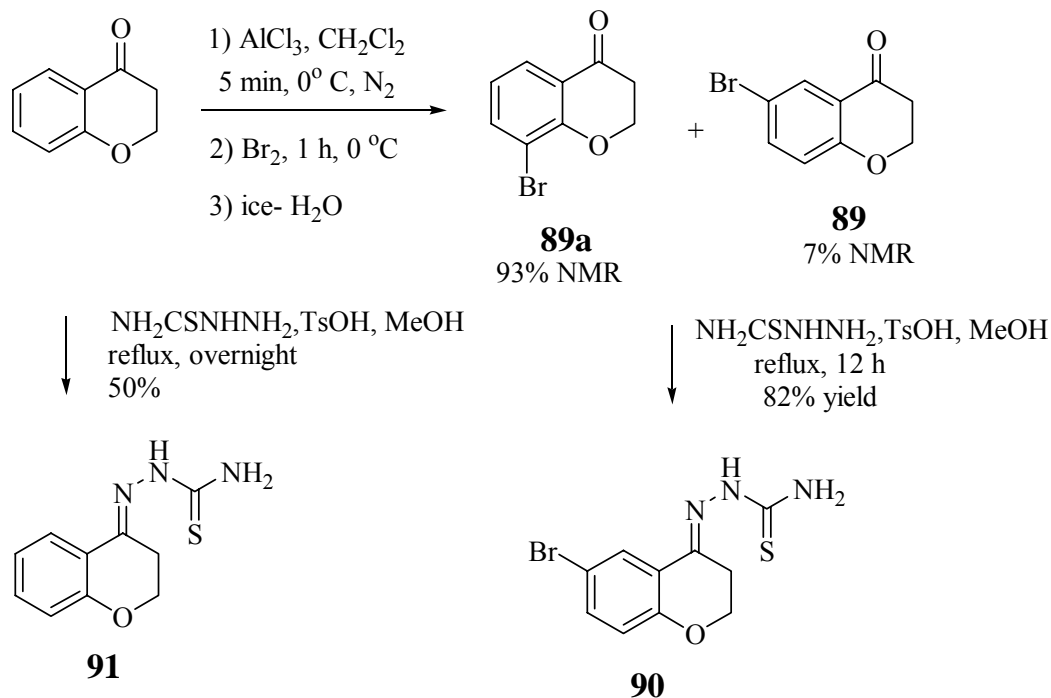
This time both compounds were separated by recrystallization obtaining the dibromo sulfone **86a** in a 67% yield.



Scheme 8.13. Synthesis of dioxothiochromane thiosemicarbazones **87** and **88**.

In the second bromination reaction, the thiochromen-4-one reacted with Br_2 and AlCl_3 for 4 h at $0\text{ }^\circ\text{C}$.¹⁸⁰ Interestingly, after column separation the ^1H -NMR showed that there was a mixture of the three thiochromen-4-one **85a** (63% pure), **85b** (17% pure), and **85c** (20% pure). The mixture could not be separated and was carried on to the oxidation with H_2O_2 which afforded a crude reaction mixture that contained the three respective sulfones. After the crude solid was recrystallized, a mixture of compounds **86a** and **86b** were obtained in ratio of 1: 2.8 respectively. Attempts to obtain a more pure

compound were unsuccessful and this mixture was carried on to the next reaction with thiosemicarbazide to form the final thiosemicarbazone **88** in a 33% yield as shown in Scheme 8.13. The synthesis of thiosemicarbazone **88**, which was obtained in a 44% yield, is also depicted in the same scheme.



Scheme 8.14. Synthesis of chromanone thiosemicarbazone **90**.

Finally, Scheme 8.14 presents the synthesis of compounds that have an oxygen atom attached at the benzylic position. Direct reaction of thiosemicarbazide with 2,3-dihydro-4H-chromen-4-one formed thiosemicarbazide **91** in a 50% yield. Reaction of chromen-4-one with Br_2 and AlCl_3 , which was carried out at 0°C for 1 h,¹⁸⁰ formed a mixture of two isomers. Even after column chromatography and recrystallization the product consisted of a mixture of chromen-4-ones **89** and **89a** in a ratio of 13.3: 1 respectively. As predicted by theory, the aromatic substitution took place at positions 6

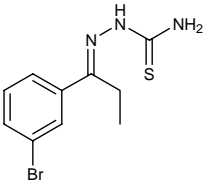
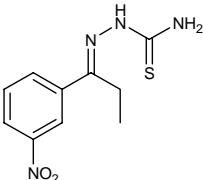
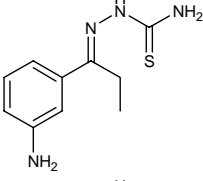
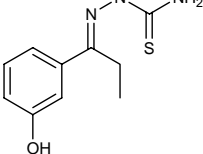
and 8 in agreement with the patterns found in the ^1H -NMR spectrum. Finally, a reaction of this mixture with thiosemicarbazide was carried out to form the final product **90** in a 65% yield in two steps.

Biochemical Evaluation of Cruzain Inhibitors

In tables 8.1 through 8.5, the IC_{50} values (in nM) of many of the new inhibitors are reported against cruzain and for some selected compounds against, human liver cathepsin L. Compound **49**, which was already reported in the literature¹⁶⁹ as a potent cruzain inhibitor, is considered as the benchmark reference to measure the biochemical activity of these potential cysteine protease inhibitors against both enzymes.

In Table 8.1, the biochemical results of the propiophenone thiosemicarbazone derivatives are shown. As noticed, the substitution of bromine atom by a nitro, amino or hydroxyl group resulted in a remarkable reduction of cruzain inhibition. Among all three of these compounds, the thiosemicarbazone **56** was 215 times less active than **66** while propiophenones **50** and **51** decreased the activity 4 and 18 times, respectively. Du and coworkers reported^{169,188} in their SAR studies that the presence in the benzene ring of a bromine atom, chlorine atom, or a trifluoromethyl group was important for cruzain inhibition, incorporation of the bromine atom leading to the best results. The results obtained in the present research work give additional information about the nature of the substituents needed to be present on the aromatic ring. It has noticed that groups capable of forming hydrogen-bond such as NH_2 an OH are not good for cruzain inhibition but conversely the former showed good activity against cathepsin L (0.25 nM).

Table 8.1. Inhibition of cruzain and human liver cathepsin L for compounds **49-51** and **56**.¹⁸⁹

Compound ^a	Structure	Cruzain Inhibition IC ₅₀ [nM]	Human cathepsin L Inhibition IC ₅₀ [nM]
49		200 (100) ^b , (60) ^d , (310) ^e	68.3
50		850	na ^c
51		3640	0.25
56		43000	na ^c

a: Compound **49** has been previously synthesized and reported in the literature. It is included here for the purpose of comparison (see reference 169)

b: Ref. 169

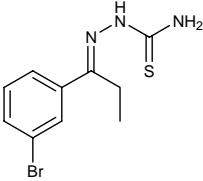
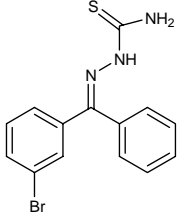
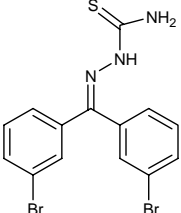
c: na= not analyzed

d: Ref. 188

e: Ref. 171

In Table 8.2, the biochemical results of the two benzophenone derivatives are shown. In the case of the benzophenone derivatives **59** and **62**, a significant improvement in cruzain inhibition was noticed compared to reference compound **49**. In the first case substitution of the ethyl group of compound **49** by a benzene ring increased the enzyme inhibition about 2.7 times.

Table 8.2. Inhibition of cruzain and human liver cathepsin L for compounds **59** and **62**.¹⁸⁹

Compound ^a	Structure	Cruzain Inhibition IC ₅₀ [nM]	Human cathepsin L Inhibition IC ₅₀ [nM]
49		200 (100) ^b , (60) ^d , (310) ^e	68.3
59		73.4	81.6
62		47.0	na ^c

a: Compound **49** has been previously synthesized and reported in the literature. It is included here for the purpose of comparison (see reference 169)

b: Ref. 169

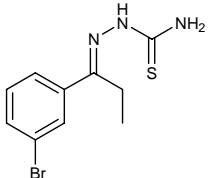
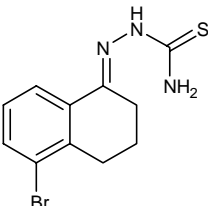
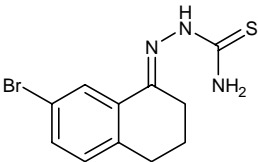
c: na= not analyzed

d: Ref. 188

e: Ref. 171

However, when the substitution of the ethyl group was made by a bromobenzene ring, (compound **62**) the cruzain inhibition was much more effective, showed with an IC₅₀ value of 47 nM. Compound **59** is less active against cathepsin L than thiosemicarbazones **49** and **51**. Cruzain inhibition was significantly improved in the tetrahydronaphthalene derivative **66** as Table 8.3 shows.

Table 8.3. Inhibition of cruzain and human liver cathepsin L for compounds **65**, **66**.¹⁸⁹

Compound ^a	Structure	Cruzain Inhibition IC ₅₀ [nM]	Human cathepsin L Inhibition IC ₅₀ [nM]
49		200 (100) ^b , (60) ^d , (310) ^e	68.3
65		1200	0.30
66		12.2	134

a: Compound **49** has been previously synthesized and reported in the literature. It is included here for the purpose of comparison (see reference 169)

b: Ref. 169

d: Ref. 188

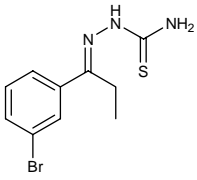
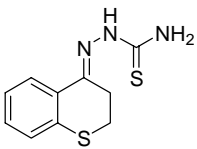
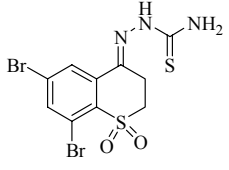
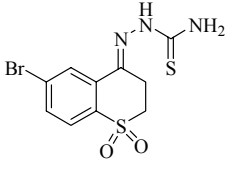
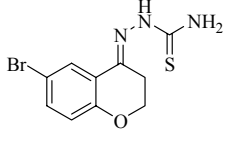
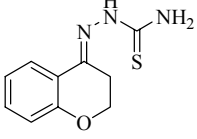
e: Ref. 171

The activity of this compound was almost 16 times better than compound **49** (the chosen reference analog) and almost 100 times more active than its isomer **65**. As note, the formation of a six-member ring next to the benzene ring significantly improved the activity even more than compounds **59** and **62**. In addition, the results suggest that the position of a bromine atom in the benzene ring is crucial for activity, with the 7-position being much more important than the 5-position. Interestingly, once again it was noticed that among similar structures the more active the compound is against cruzain,

the less active it is against cathepsin L. For example, compound **66** is more active than **65** against cruzain (12.2 and 1200 nM respectively) but less active against cathepsin L (134 and 0.30 nM respectively).

In Table 8.4, the biochemical results of tetrahydronaphthalenes containing a heteroatom are shown. Compounds **88** and **90** were more active than the chosen reference compound **49** but less active than compound **66**. Clearly, it is seen that the substitution of the carbon atom in **66** by a sulfur atom or an oxygen atom caused reduction in the enzyme activity. Additionally, when a bromine atom is not present on the benzene ring, the activity decreased almost 155 times as compounds **90** and **91** showed (110 and >17000 nM respectively). Another important observation that was noted in Table 8.4 is that comparing the activities of compounds **83a** and **91**, it seems that a sulfur atom causes more detrimental reduction (in fact no activity at all was observed) in the cruzain activity than an oxygen atom does. When a sulfone group is attached, as in compound **88**, the activity basically is the same as in compound **90**, however the introduction of another bromine atom, as in compound **87**, reduces the activity almost 600%. This suggests that more than one bromine atom is not effective for cruzain inhibition and the position of this atom is important as well. Finally, it was also observed that compound **90** is significantly active against cathepsin L almost in the same magnitude as compound **51**. Among all three dihydronaphthalenes, compound **77** was the most active against cruzain followed by the exoacetyl dihydronaphthalene **73**. It is interesting to observe that the exo unsaturated carbonyl group is a potential scaffold for the inhibition of cysteine proteases as reported earlier by Palmer and coworkers¹⁷² and it can be successfully incorporated in the design of cruzain inhibitors.

Table 8.4. Inhibition of cruzain and human liver cathepsin L for compounds **83a**, **90**, **91**, **87** and **88**.¹⁸⁹

Compound ^a	Structure	Cruzain Inhibition IC ₅₀ [nM]	Human cathepsin L Inhibition IC ₅₀ [nM]
49		200 (100) ^b , (60) ^d , (310) ^e	68.3
83a		no effect	na ^c
87		820	na ^c
88		118	na ^c
90		110	0.35
91		> 17000	na ^c

a: Compound **49** has been previously synthesized and reported in the literature. It is included here for the purpose of comparison (see reference 169)

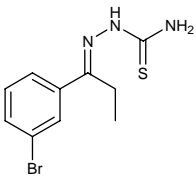
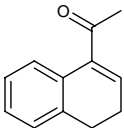
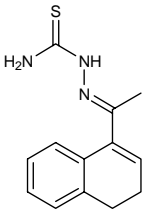
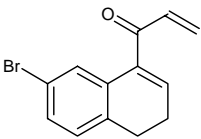
b: Ref. 169

c: na= not analyzed

d: Ref. 188

e: Ref. 171

Table 8.5. Inhibition of cruzain and human liver cathepsin L for compounds **73**, **74** and **77**.¹⁶⁹

Compound ^a	Structure	Cruzain Inhibition IC ₅₀ [nM]	Human cathepsin L Inhibition IC ₅₀ [nM]
49		200 (100) ^b , (60) ^d , (310) ^e	68.3
73		1360	0.16
74		> 20000	na ^c
77		802	na ^c

a: Compound **49** has been previously synthesized and reported in the literature. It is included here for the purpose of comparison (see reference 27)

b: Ref. 169

c: na= not analyzed

d: Ref. 188

e: Ref. 171

After carefully analyzing the biochemical results of the tested inhibitors, they were arranged in the following order of decreasing activity against cruzain and human liver cathepsin L:

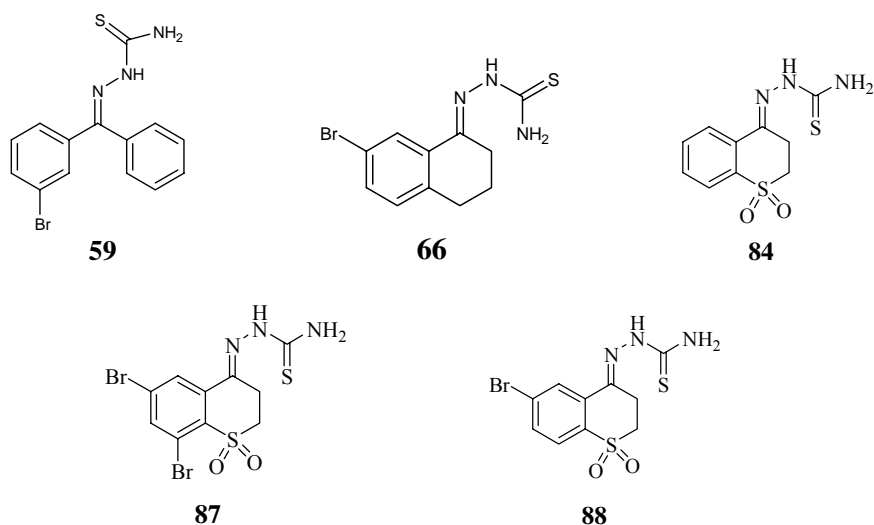
Cruzain: 66 > 62 > 59 > 90 > 88 > **49** > 77 > 87 > 50 > 65 > 73 > 51 > 74 > 56 > 83a

Cathepsin L: 73 > 51 > 65 > 90 > **49** > 59 > 66 >

One important observation in this arrangement is that most of the compounds that are less active against cruzain (farthest to the right in the cruzain list) are more active against cathepsin L (farthest to the left side in the cathepsin L list). One important structural requirement for cruzain inhibition is that the molecules need to have hydrophobic moieties, particularly aliphatic and/or aromatic rings containing at least one bromine atom. By the other hand it seems that for cathepsin L activity, the presence of negatively charged oxygen-based functional groups such as nitro or sulfone is required. In addition, it was noticed that functional groups containing either nitrogen or oxygen with lone pairs of electrons (NH₂, OH, ether, thioether) significantly improve cathepsin activity.

Interestingly, when compounds **59**, **66**, **84**, **87** and **88** were tested against the seven cancer cell lines used to evaluate vascular disrupting agents, the first two exhibited significant activity against all cell lines and in particular against breast and colon (Table 8.6).

Table 8.6. *In vitro* cytotoxicity (ED₅₀ and GI₅₀ in μM) against seven cancer cell lines of compounds **59**, **66**, **84**, **87** and **88**.



Compound	P388 (ED ₅₀)	BXPC-3	MCF-7	SF268	NCI- H460	KM20L2	DU-145
OXi8006^a		0.097	0.054	0.12	0.10	0.050	<3.7
59	1.4	11.4	10.1	11.4	10.2	9.9	13.8
66	5.7	> 33	8.0	21.5	>33	25.8	> 33
84	> 37.1	> 37.1	> 37.1	> 37.1	> 37.1	> 37.1	> 37.1
87	> 23.4	> 23.4	> 23.4	> 23.4	> 23.4	> 23.4	> 23.4
88	> 28.7	> 28.7	> 28.7	> 28.7	> 28.7	> 28.7	> 28.7

OXi8006 has been previously synthesized and reported in literature. It is included here for the purpose of comparison (see reference 104).

CHAPTER NINE

Conclusions and Future Directions

A unique library of small non-peptidic molecules was synthesized with the aim of primarily targeting the trypanosomal peptidase cruzain, the major cysteine protease of *Trypanosoma cruzi*, which is the causative agent of the lethal parasitic disease called American trypanosomiasis or Chagas' disease. The lead discovery project started with the synthesis of low-molecular weight compounds containing primarily the thiosemicarbazone scaffold previously reported in the literature as an important functional group that effectively targets cruzain and other parasite-derived cysteine proteases.^{169-171,188} Out of fourteen synthesized new compounds, five of them inhibited cruzain more effectively than 3'-bromopropiophenone thiosemicarbazone **49** a compound reported by Cohen and coworkers¹⁶⁹ in 2002 as one of the most potent cruzain inhibitors and trypanocidal agents known. The structures of the three best cruzain inhibitors included a bromotetrahydronaphthalene thiosemicarbazone derivative **66**, which showed an IC₅₀ value of 12.2 nM, followed by two benzophenone thiosemicarbazones **59** and **62** with IC₅₀ values of 73.4 and 47.0 nM respectively. The structure-activity relationship study of this new library of compounds allowed to conclude the following structural requirements for the design of cruzain inhibitors:

- 1) The presence of a benzene ring containing a bromine atom attached at the *meta* position is important for activity.

- 2) The substitution of the ethyl group of reference compound **49** by another benzene (bromo substituted or not) or a cyclohexene ring increases the enzymatic inhibition activity.
- 3) Benzene substituents such as NH₂, OH, and NO₂ are not good for activity because they decreased cruzain inhibition
- 4) The isosteric replacement of the benzylic methylene group in the tetrahydronaphthalene derivative **66** by an oxygen or a sulfur atom and a sulfone group resulted in a reduction in cruzain inhibition.
- 5) Although the unsaturated carbonyl system is a less effective bioisoster than thiosemicarbazone, their low micromolar (μM) values still allow utilizing this functional group as a potential warhead for the development of cysteine proteases inhibitors.

The outstanding activity against cruzain that thiosemicarbazones **66**, **62** and **59** exhibited compared to reference compound **49** can be explained based on the general understanding that proteases universally recognize beta strand-conformation inhibitors or substrates in their active sites. Tyndall and coworkers¹⁹⁰ proposed that cyclization of a protease inhibitor might force the molecule to adopt a β -strand type conformation which mimics the ideal protease-binding shape required for better interaction with the enzyme. Effective enzyme affinity is achieved by designing molecules that have the required functionalities arranged in the space with the right orientation towards the active site of the receptor. Therefore, locking the inhibitor structure in the right conformation to interact with the active site of the enzyme can be carried out by incorporating conformational restriction in the molecule. This structural restriction can be obtained by

introducing a methyl group which sterically restricts free bond rotation, by using intramolecular hydrogen bonds, by introducing double bonds that fix the relative positions of the substituents attached to the unsaturated atoms, due to the non-rotatable double bond, or by cyclization, which fixes the relative positions of the substituents either exocyclic or within the ring.¹⁹¹ Small and flexible molecules like compound **49** can exist in many conformations and selective fixation of their bond functionalities into the active site of a particular enzyme will be somewhat harder to achieve. Tyndall also showed in his research work that twelve of the known cruzain inhibitors bound the enzyme by adopting a β -strand like conformation as Figure 9.1 shows.¹⁹⁰ The minimum energy conformations⁷⁹ of the three best inhibitors might superimpose to the twelve inhibitors structures shown by Tyndall.

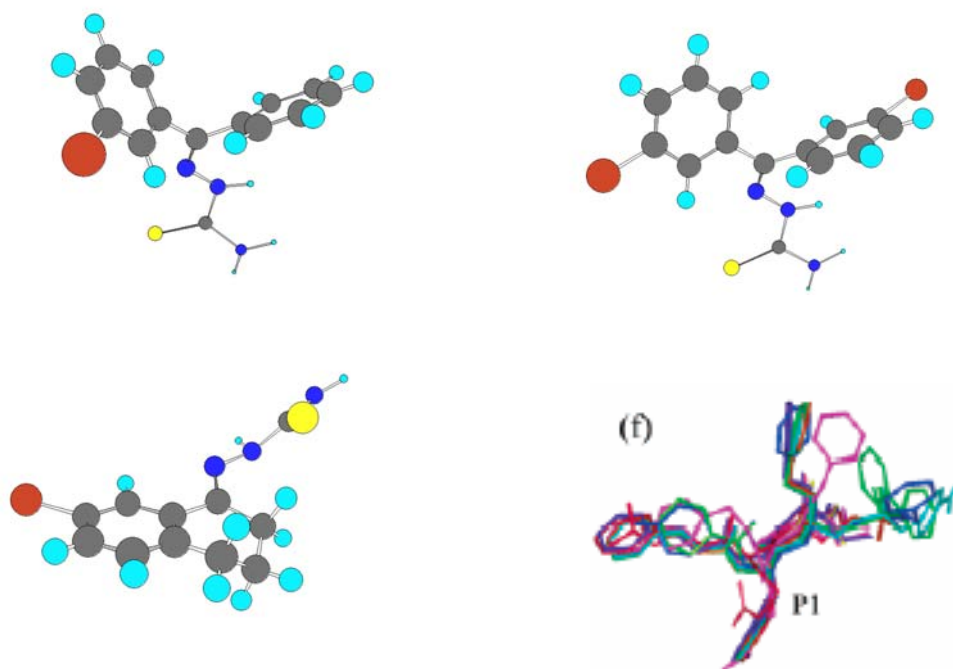


Figure 9.1. Minimum energy conformations⁷⁹ of compounds **59** (top left), **62** (top right) and **66** (bottom left) generated by MOPAC. The bottom right picture shows the structures of twelve known superimposed cruzain inhibitors with their main chains running horizontally N to C terminal from left to right.¹⁹⁰

Therefore, it is believed that improvement of the inhibitor-enzyme affinity can be successfully achieved by designing cyclic molecules instead of acyclic analogues.

Although the best five inhibitors that were synthesized have low IC_{50} values in the nanomolar range against cruzain, all of them showed activity against human liver cathepsin L, in some cases, this activity was even more pronounced than activity for cruzain itself. The main objective of this project was successfully accomplished after a suitable pharmacophore was generated that might serve as a good starting point for drug development. In the current work, the tetrahydronaphthalene thiosemicarbazone **66** has been established as a lead compound. It is important to incorporate structural moieties within compound **66** that lead to selective binding of cruzain's active site rather than binding to the human cathepsin enzyme. In Figure 9.2, one of the best calculated orientations of thiosemicarbazone **66** is shown. This conformation was generated by DOCK 4.0.1 software with which the structure of the inhibitor was docked into the cruzain active site. It is important to mention that this is not necessarily the best conformation and, with this calculation, no conclusive results can be obtained. However, it gives at least valuable information about the way that this inhibitor interacts with cruzain. It is well known that in papain-like cysteine proteases, the S_2 pocket is the primary subsite for substrate specificity.^{159,160,162} In the series of inhibitors synthesized apparently the bromobenzene moiety fits perfectly in both cruzain and cathepsin L subsites. In the picture, the bromobenzene moiety is buried into the deep S_2 pocket with the bromine atom facing down as was predicted. This explains how important the bromine atom is for activity.

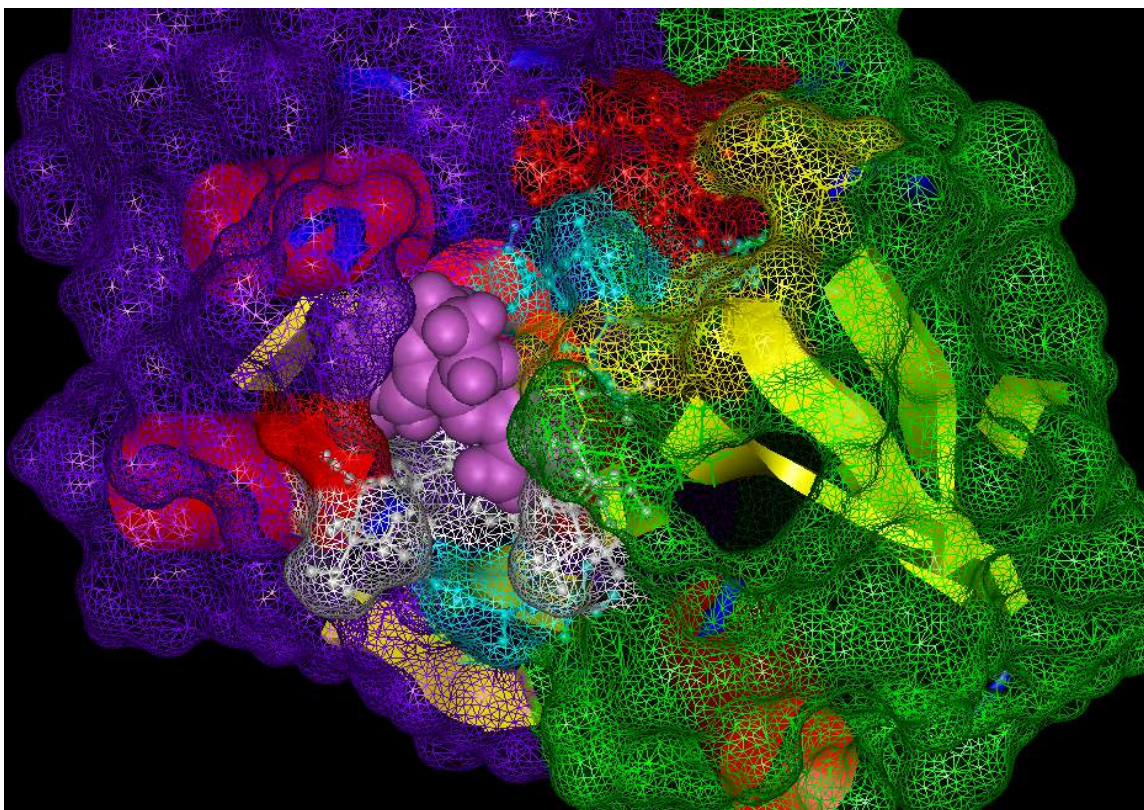
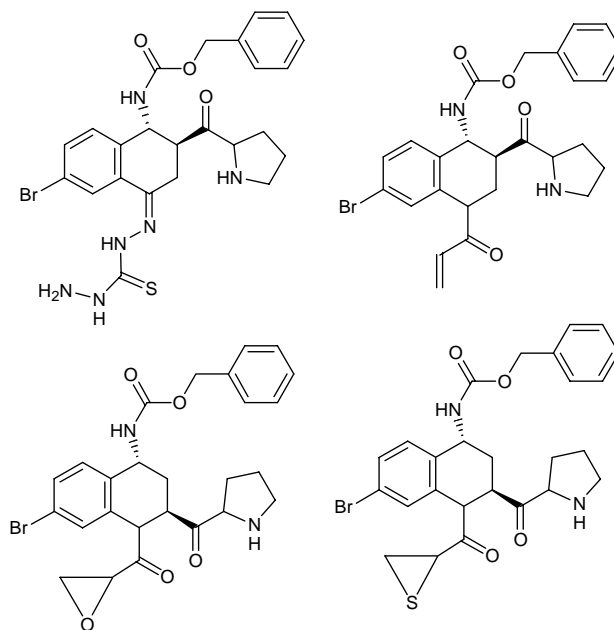


Figure 9.2. One of the best calculated orientations of compound **66** in the active site of cruzain. The L-domain is colored in blue and the R-domain is in green. The inhibitor is represented in space-filling model colored in purple with the bromine atom buried into the deep S_2 pocket. Glu205 is located at the bottom of the S_2 pocket and is colored in aquamarina. The catalytic triad, Cys25, His159 and Asn175 (colored in aquamarina) is located right above of the inhibitor. Trp177 and Gln19 are located above of the catalytic triad and colored in red. In white are represented the other important aminoacid residues Leu157, Gly160, Leu67, Met68 and Ala133 present in the S_2 pocket.

In 1996, Serveu and coworkers investigated the substrate specificity of cruzain and they concluded that the incorporation of a prolyl residue at the P'_2 position of the substrate increased significantly the selectivity for cruzain against rat cathepsin L.¹⁶⁶ Hence, a proline-type residue should be attached to the tetrahydronaphthalene skeleton of compounds **66**, **59** and **62** in order to discriminate cathepsin L from cruzain. Additionally, most of the potent cruzain inhibitors have a benzyloxycarbonyl group (Cbz) present at P_3 position and the presence of this structural moiety into the second

generation of the cruzain inhibitors is proposed. In Scheme 9.1, the proposed structures of the second generation of cruzain inhibitors are shown.



Scheme 9.1. Proposed structures of the second generation of more selective tetrahydronaphthalene based cruzain inhibitors.

As seen in the structures of the proposed targets, new isosteres, which potentially might react with the catalytic triad of cruzain, have been attached to the tetrahydronaphthalene skeleton. The proposed functional groups are oxirane and thiirane rings along with the exo-cyclic unsaturated carbonyl group.

Biological assays (*in vitro* and *in vivo*) are proposed to be performed for the next generation of inhibitors in order to evaluate the trypanocidal activity of the compounds not just against cruzain but also against other important parasitic cysteine proteases such as rhodesain (major cysteine of *T. brucei rhodesiense*) and falcipain-2 (cysteine protease of *Plasmodium falciparum*).^{170,171}

The *in vitro* cytotoxicity assays against different cancer cell lines for compounds **59**, **66**, **84**, **87** and **88** gave further insight into the use of these compounds as anti-cancer agents. Among all five tested compounds, thiosemicarbazones **59** and **66** exhibited low ED₅₀ values in the low micromolar range, being particularly effective against breast and colon. The screening of new cysteine protease inhibitors against the same cancer cell lines might generate a new class of potential anti-cancer agents.

APPENDICES

NMR Spectra

Appendix A: Vascular Disrupting Agents

¹ H-NMR (300 MHz, CDCl ₃) of Compound 1	240
¹ H-NMR (300 MHz, CDCl ₃) of Compound 2	241
¹ H-NMR (300 MHz, CDCl ₃) of Compound 3	242
¹ H-NMR (300 MHz, CDCl ₃) of Compound 4	243
¹ H-NMR (300 MHz, CDCl ₃) of Compound 5	244
Dept 135-NMR (75 MHz, CD ₂ Cl ₂) of Compound 5	245
¹ H-NMR (300 MHz, CDCl ₃) of Compound 6	246
¹³ C-NMR (75 MHz, CDCl ₃) of Compound 6	247
Dept 45-NMR (75 MHz, CDCl ₃) of Compound 6	248
Dept 90-NMR (75 MHz, CDCl ₃) of Compound 6	249
Dept 135-NMR (75 MHz, CDCl ₃) of Compound 6	250
COSY ¹ H- ¹ H NMR (300 MHz, CDCl ₃) of Compound 6	251
COSY ¹ H- ¹ H NMR (300 MHz, CDCl ₃) of Compound 6	252
¹ H-NMR (300 MHz, CDCl ₃) of Compound 7	253
¹³ C-NMR (75 MHz, CDCl ₃) of Compound 7	254
¹ H-NMR (300 MHz, CDCl ₃) of Compound 8	255
¹ H-NMR (300 MHz, CDCl ₃) of Compound 9	256
¹ H-NMR (360 MHz, CDCl ₃) of Compound 10	257
¹³ C-NMR (75 MHz, CDCl ₃) of Compound 10	258
Dept 135-NMR (75 MHz, CDCl ₃) of Compound 10	259
COSY- ¹ H- ¹ H NMR (300 MHz, CDCl ₃) of Compound 10	260

	230
¹ H-NMR (360 MHz, CDCl ₃) of Compound 11	261
¹ H-NMR (300 MHz, CDCl ₃) of Compound 12	262
¹³ C-NMR (75 MHz, CDCl ₃) of Compound 12	263
COSY- ¹ H- ¹ H NMR (300 MHz, CDCl ₃) of Compound 12	264
¹ H-NMR (300 MHz, CD ₂ Cl ₂) of Compound 13	265
¹³ C-NMR (75 MHz, CD ₂ Cl ₂) of Compound 13	266
Dept 45-NMR (75 MHz, CD ₂ Cl ₂) of Compound 13	267
Dept 135-NMR (90 MHz, CD ₂ Cl ₂) of Compound 13	268
¹ H-NMR (300 MHz, methanol-d ₄) of Compound 14	269
¹ H-NMR (300 MHz, CDCl ₃) of Compound 15	270
¹ H-NMR (300 MHz, CDCl ₃) of Compound 16	271
³¹ P-NMR (121 MHz, acetone-d ₆) of Compound 16	272
¹ H-NMR (300 MHz, CDCl ₃) of Compound 17	273
Dept 135-NMR (75 MHz, CDCl ₃) of Compound 17	274
¹ H-NMR (300 MHz, CDCl ₃) of Compound 18	275
¹³ C-NMR (75 MHz, CDCl ₃) of Compound 18	276
Dept 135-NMR (75 MHz, CDCl ₃) of Compound 18	277
¹ H-NMR (300 MHz, CDCl ₃) of Compound 19	278
¹³ C-NMR (75 MHz, CDCl ₃) of Compound 19	279
Dept 45-NMR (75 MHz, CDCl ₃) of Compound 19	280
¹ H-NMR (300 MHz, CDCl ₃) of Compound 20a	281
Dept 45-NMR (75 MHz, CDCl ₃) of Compound 20a	282
¹ H-NMR (300 MHz, CDCl ₃) of Compound 20b	283

	231
¹ H-NMR (300 MHz, CDCl ₃) of Compound 21	284
¹³ C-NMR (75 MHz, CDCl ₃) of Compound 21	285
Dept 135-NMR (75 MHz, CDCl ₃) of Compound 21	286
Infrared Spectrum (nujol, cm ⁻¹) of Compound 21	287
¹ H-NMR (300 MHz, CDCl ₃) of Compound 21a	288
¹³ C-NMR (75 MHz, CDCl ₃) of Compound 21a	289
Dept 45-NMR (75 MHz, CDCl ₃) of Compound 21a	290
Dept 135-NMR (75 MHz, CDCl ₃) of Compound 21a	291
COSY- ¹ H- ¹³ C NMR (75 MHz, CDCl ₃) of Compound 21a	292
Infrared Spectrum (Nujol, cm ⁻¹) of Compound 21a	293
¹ H-NMR (300 MHz, CDCl ₃) of Compound 22	294
¹³ C-NMR (75 MHz, CDCl ₃) of Compound 22	295
COSY- ¹ H- ¹ H NMR (75 MHz, CDCl ₃) of Compound 22	296
¹ H-NMR (300 MHz, CDCl ₃) of Compound 23	297
¹ H-NMR (300 MHz, CDCl ₃) of Compound 24	298
¹ H-NMR (300 MHz, CDCl ₃) of Compound 25	299
¹³ C-NMR (75 MHz, CDCl ₃) of Compound 25	300
Dept 45-NMR (75 MHz, CDCl ₃) of Compound 25	301
¹ H-NMR (300 MHz, CDCl ₃) of Compound 26a	302
¹³ C-NMR (75 MHz, CDCl ₃) of Compound 26a	303
Dept 45-NMR (75 MHz, CDCl ₃) of Compound 26a	304
COSY- ¹ H- ¹ H NMR (300 MHz, CDCl ₃) of Compound 26a	305
COSY ¹ H- ¹³ C NMR (75 MHz, CDCl ₃) of Compound 26a	306

	232
¹ H-NMR (300 MHz, CDCl ₃) of Compound 26b	307
¹³ C-NMR (75 MHz, CDCl ₃) of Compound 26b	308
Dept 45-NMR (75 MHz, CDCl ₃) of Compound 26b	309
COSY ¹ H- ¹ H NMR (300 MHz, CDCl ₃) of Compound 26b	310
COSY ¹ H- ¹³ C NMR (75 MHz, CDCl ₃) of Compound 26b	311
¹ H-NMR (300 MHz, MeOH-d ₄) of Compound 27a	312
¹ H-NMR (300 MHz, MeOH-d ₄) of Compound 27b	313
Dept 45-NMR (75 MHz, MeOH-d ₄) of Compound 27b	314
¹ H-NMR (300 MHz, CDCl ₃) of Compound 28	315
¹ H-NMR (360 MHz, CDCl ₃) of Compound 29	316
¹³ C-NMR (90 MHz, CDCl ₃) of Compound 29	317
Dept 135-NMR (90 MHz, CDCl ₃) of Compound 29	318
¹ H-NMR (300 MHz, CDCl ₃) of Compound 30	319
Dept 135-NMR (75 MHz, CDCl ₃) of Compound 30	320
¹ H-NMR (300 MHz, CDCl ₃) of Compound 31	321
Dept 135-NMR (75 MHz, CDCl ₃) of Compound 31	322
¹ H-NMR (300 MHz, CDCl ₃) of Compound 32	323
¹ H-NMR (300 MHz, CDCl ₃) of Compound 33	324
Dept 45-NMR (75 MHz, CDCl ₃) of Compound 33	325
¹ H-NMR (300 MHz, CDCl ₃) of Compound 34	326
¹³ C-NMR (75 MHz, CDCl ₃) of Compound 34	327
Dept 45-NMR (75 MHz, CDCl ₃) of Compound 34	328
¹ H-NMR (300 MHz, CDCl ₃) of Compound 35	329

¹³ C-NMR (75 MHz, CDCl ₃) of Compound 35	330
¹ H-NMR (300 MHz, CDCl ₃) of Compound 36	331
¹³ C-NMR (75 MHz, CDCl ₃) of Compound 36	332
¹ H-NMR (300 MHz, CDCl ₃) of Compound 37	333
¹³ C-NMR (75 MHz, CDCl ₃) of Compound 37	334
Dept 45-NMR (75 MHz, CDCl ₃) of Compound 37	335
¹ H-NMR (300 MHz, CDCl ₃) of Compound 38	336
¹³ C-NMR (75 MHz, CDCl ₃) of Compound 38	337
Dept 45-NMR (75 MHz, CDCl ₃) of Compound 38	338
¹ H-NMR (300 MHz, CDCl ₃) of Compound 39a	339
¹ H-NMR (300 MHz, CDCl ₃) of Compound 39b	340
¹ H-NMR (300 MHz, CDCl ₃) of Compound 40a	341
¹³ C-NMR (75 MHz, CDCl ₃) of Compound 40a	342
Dept 90-NMR (75 MHz, CDCl ₃) of Compound 40d	343
Dept 135-NMR (75 MHz, CDCl ₃) of Compound 40a	344
¹ H-NMR (300 MHz, CDCl ₃) of Compound 40a	345
¹ H-NMR (300 MHz, CDCl ₃) of Compound 40c	346
¹³ C-NMR (75 MHz, CDCl ₃) of Compound 40c	347
¹ H-NMR (300 MHz, CDCl ₃) of Compound 40d	348
¹³ C-NMR (75 MHz, CDCl ₃) of Compound 40d	349
¹ H-NMR (300 MHz, CDCl ₃) of Compound 40e	350
¹³ C-NMR (75 MHz, CDCl ₃) of Compound 40e	351
¹ H-NMR (300 MHz, CDCl ₃) of Compound 40f	352

¹³ C-NMR (75 MHz, CDCl ₃) of Compound 40f	353
¹ H-NMR (300 MHz, CDCl ₃) of Compound 41a	354
¹³ C-NMR (75 MHz, CDCl ₃) of Compound 41a	355
¹ H-NMR (300 MHz, CDCl ₃) of Compound 41b	356
¹ H-NMR (300 MHz, CDCl ₃) of Compound 41c	357
¹³ C-NMR (75 MHz, CDCl ₃) of Compound 41c	358
Dept 135-NMR (75 MHz, CDCl ₃) of Compound 41c	359
¹ H-NMR (300 MHz, CDCl ₃) of Compound 41d	360
¹ H-NMR (300 MHz, CDCl ₃) of Compound 42	361
¹³ C-NMR (75 MHz, CDCl ₃) of Compound 42	362
Dept 135-NMR (75 MHz, CDCl ₃) of Compound 42	363
¹ H-NMR (300 MHz, CDCl ₃) of Compound 43	364
¹ H-NMR (360 MHz, CDCl ₃) of Compound 44	365
¹ H-NMR (300 MHz, CDCl ₃) of Compound 45	366
¹³ C-NMR (75 MHz, CDCl ₃) of Compound 45	367
¹ H-NMR (300 MHz, CDCl ₃) of Compound 46	368
¹ H-NMR (300 MHz, acetone-d ₆) of Compound 46	369
¹³ C-NMR (75 MHz, acetone-d ₆) of Compound 46	370
Dept 45-NMR (75 MHz, acetone-d ₆) of Compound 46	371
¹ H-NMR (360 MHz, CDCl ₃) of Compound 47	372
¹³ C-NMR (75 MHz, CDCl ₃) of Compound 47	373
Dept 45 -NMR (75 MHz, CDCl ₃) of Compound 47	374
Dept 90 -NMR (75 MHz, CDCl ₃) of Compound 47	375

Dept 135 -NMR (75 MHz, CDCl ₃) of Compound 47	376
COSY ¹ H- ¹ H NMR (300 MHz, CDCl ₃) of Compound 47	377
COSY ¹ H- ¹³ C NMR (75 MHz, CDCl ₃) of Compound 47	378

Appendix B: Cysteine Protease Inhibitors

¹ H-NMR (300 MHz, methyl Sulfoxide-d ₆) of Compound 49	379
¹³ C-NMR (75 MHz, methyl Sulfoxide-d ₆) of Compound 49	380
Dept 135-NMR (75 MHz, methyl Sulfoxide-d ₆) of Compound 49	381
¹ H-NMR (300 MHz, acetone-d ₆) of Compound 50	382
¹ H-NMR (300 MHz, acetone-d ₆) of Compound 51	383
Dept 135-NMR (75 MHz, acetone-d ₆) of Compound 51	384
¹ H-NMR (300 MHz, CDCl ₃) of Compound 52	385
¹ H-NMR (300 MHz, CDCl ₃) of Compound 53	386
¹ H-NMR (300 MHz, CDCl ₃) of Compound 54	387
¹³ C-NMR (75 MHz, CDCl ₃) of Compound 54	388
Dept 135-NMR (75 MHz, CDCl ₃) of Compound 54	389
¹ H-NMR (300 MHz, CDCl ₃) of Compound 55	390
¹³ C-NMR (75 MHz, CDCl ₃) of Compound 55	391
Dept 135-NMR (75 MHz, CDCl ₃) of Compound 55	392
¹ H-NMR (300 MHz, CDCl ₃) of Compound 56	393
Dept 135-NMR (75 MHz, CDCl ₃) of Compound 56	394
¹ H-NMR (300 MHz, CDCl ₃) of Compound 57	395
Dept 135-NMR (75 MHz, CDCl ₃) of Compound 57	396

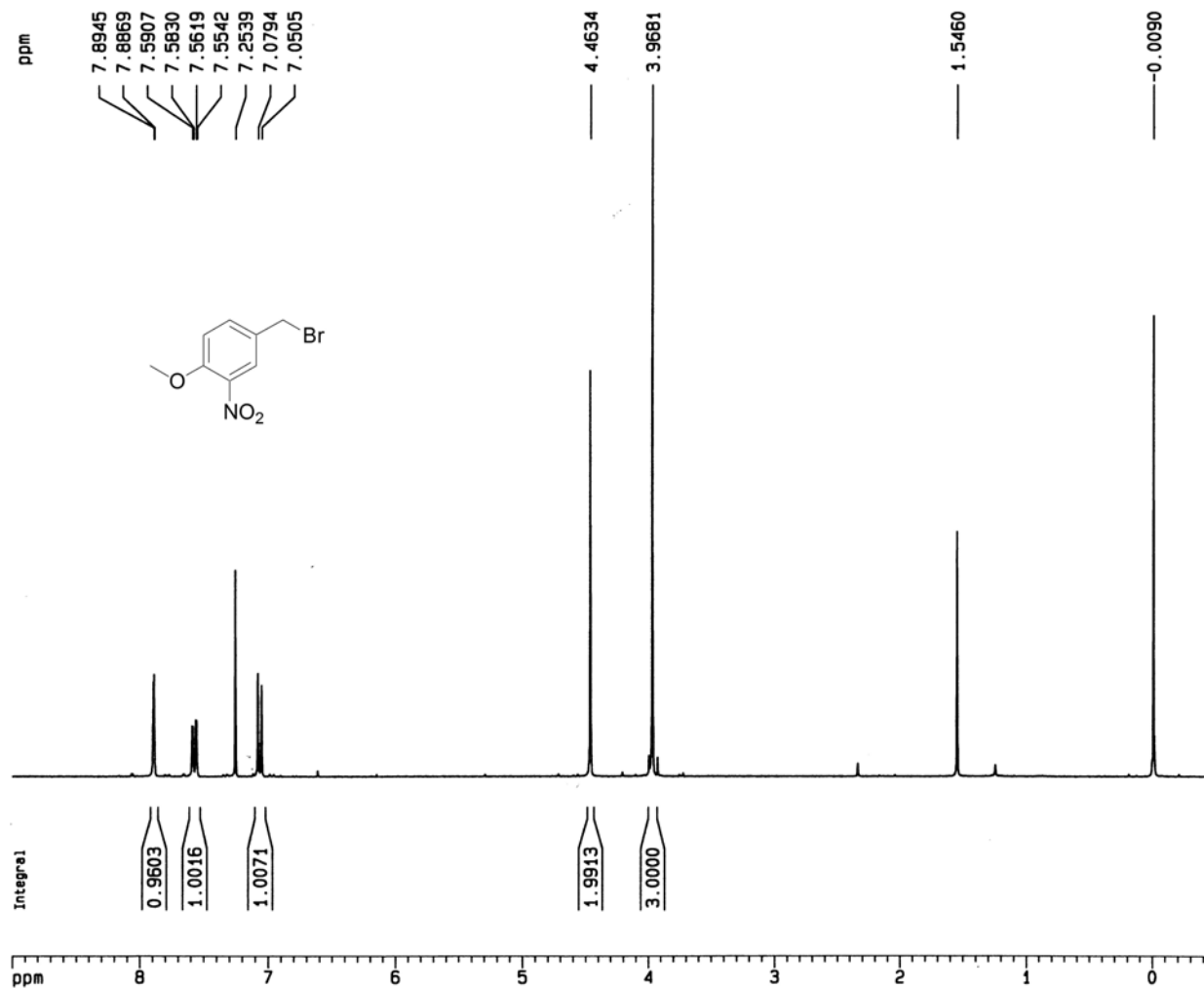
¹ H-NMR (300 MHz, CDCl ₃) of Compound 58	397
Dept 45-NMR (75 MHz, CDCl ₃) of Compound 58	398
¹ H-NMR (300 MHz, CDCl ₃) of Compound 59	399
¹ H-NMR (360 MHz, acetone-d ₆) at 17°C of Compound 59	400
¹ H-NMR (360 MHz, acetone-d ₆) at 10°C of Compound 59	401
¹ H-NMR (360 MHz, acetone-d ₆) at 0°C of Compound 59	402
¹ H-NMR (360 MHz, acetone-d ₆) at -10°C of Compound 59	403
¹ H-NMR (360 MHz, acetone-d ₆) at -20°C of Compound 59	404
¹ H-NMR (360 MHz, acetone-d ₆) at -30°C of Compound 59	405
¹ H-NMR (360 MHz, acetone-d ₆) at -40°C of Compound 59	406
¹ H-NMR (360 MHz, acetone-d ₆) at -50°C of Compound 59	407
¹ H-NMR (360 MHz, acetone-d ₆) at -60°C of Compound 59	408
¹ H-NMR (360 MHz, acetone-d ₆) at -70°C of Compound 59	409
Dept 45-NMR (75 MHz, acetone-d ₆) of Compound 59	410
¹ H-NMR (360 MHz, CDCl ₃) of Compound 60	411
Dept 135-NMR (90 MHz, CDCl ₃) of Compound 60	412
¹ H-NMR (300 MHz, CDCl ₃) of Compound 61	413
¹³ C-NMR (75 MHz, CDCl ₃) of Compound 61	414
¹ H-NMR (360 MHz, CDCl ₃) of Compound 62	415
¹ H-NMR (300 MHz, CDCl ₃) of Compound 63	416
Dept 135-NMR (75 MHz, CDCl ₃) of Compound 63	417
¹ H-NMR (300 MHz, CDCl ₃) of Compound 64	418
Dept 135-NMR (75 MHz, CDCl ₃) of Compound 64	419

¹ H-NMR (300 MHz, acetone-d ₆) of Compound 65	420
¹ H -NMR (75 MHz, Acetone-d ₆) of Compound 66	421
¹ H-NMR (300 MHz, CDCl ₃) of Compound 67	422
¹³ C-NMR (75 MHz, CDCl ₃) of Compound 67	423
Dept 135-NMR (75 MHz, CDCl ₃) of Compound 67	424
¹ H-NMR (300 MHz, CDCl ₃) of Compound 68	425
¹³ C-NMR (75 MHz, CDCl ₃) of Compound 68	426
¹ H-NMR (300 MHz, CDCl ₃) of Compound 68a	427
¹³ C-NMR (75 MHz, CDCl ₃) of Compound 68a	428
Dept 135-NMR (75 MHz, CDCl ₃) of Compound 68a	429
¹ H-NMR (300 MHz, CDCl ₃) of Compound 69	430
Dept 135-NMR (75 MHz, CDCl ₃) of Compound 69	431
¹ H-NMR (300 MHz, CDCl ₃) of Compound 71	432
Dept 135-NMR (75 MHz, CDCl ₃) of Compound 71	433
¹ H-NMR (300 MHz, CDCl ₃) of Compound 72a	434
¹³ C-NMR (75 MHz, CDCl ₃) of Compound 72a	435
Dept 135-NMR (75 MHz, CDCl ₃) of Compound 72a	436
¹ H-NMR (300 MHz, CDCl ₃) of Compound 72b	437
¹³ C-NMR (75 MHz, CDCl ₃) of Compound 72b	438
Dept 135-NMR (75 MHz, CDCl ₃) of Compound 72b	439
¹ H-NMR (300 MHz, CDCl ₃) of Compound 73	440
¹³ C-NMR (75 MHz, CDCl ₃) of Compound 73	441
Dept 135-NMR (75 MHz, CDCl ₃) of Compound 73	442

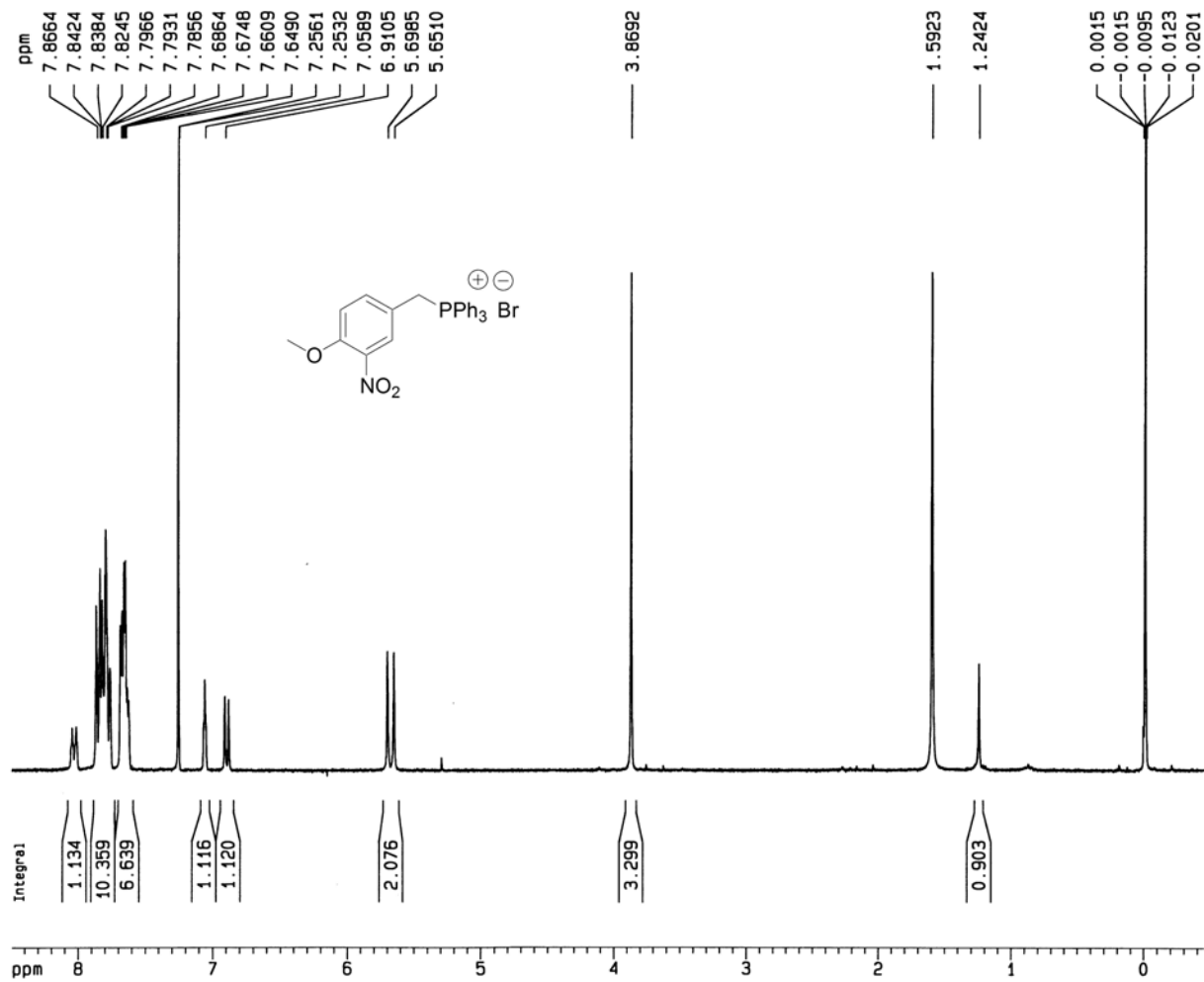
¹ H-NMR (300 MHz, CDCl ₃) of Compound 74	443
Dept 135-NMR (75 MHz, CDCl ₃) of Compound 74	444
¹ H-NMR (360 MHz, methanol-d ₄) of Compound 75	445
¹³ C-NMR (75 MHz, methanol-d ₄) of Compound 75	446
¹ H-NMR (300 MHz, CDCl ₃) of Compound 76	447
¹ H-NMR (300 MHz, CDCl ₃) of Compound 77	448
¹³ C-NMR (75 MHz, CDCl ₃) of Compound 77	449
Dept 90-NMR (75 MHz, CDCl ₃) of Compound 77	450
¹ H-NMR (300 MHz, CDCl ₃) of Compound 78	451
¹³ C-NMR (75 MHz, CDCl ₃) of Compound 78	452
Dept 135-NMR (75 MHz, CDCl ₃) of Compound 78	453
¹ H-NMR (300 MHz, CDCl ₃) of Compound 79	454
¹³ C-NMR (75 MHz, CDCl ₃) of Compound 79	455
¹ H-NMR (300 MHz, methanol-d ₄) of Compound 80	456
¹³ C-NMR (75 MHz, methanol-d ₄) of Compound 80	457
Dept 135-NMR (75 MHz, methanol-d ₄) of Compound 80	458
¹ H-NMR (300 MHz, CDCl ₃) of Compound 81	459
¹³ C-NMR (90 MHz, CDCl ₃) of Compound 81	460
Dept 135-NMR (90 MHz, CDCl ₃) of Compound 81	461
¹ H-NMR (300 MHz, CDCl ₃) of Compound 82	462
¹³ C-NMR (75 MHz, CDCl ₃) of Compound 82	463
Dept 135-NMR (75 MHz, CDCl ₃) of Compound 82	464
¹ H-NMR (300 MHz, acetone-d ₆) of Compound 83	465

¹³ C-NMR (75 MHz, acetone-d ₆) of Compound 83	466
Dept 45-NMR (75 MHz, acetone-d ₆) of Compound 83	467
¹ H-NMR (300 MHz, methyl sulfoxide-d ₆) of Compound 84	468
¹³ C-NMR (75 MHz, methyl sulfoxide-d ₆) of Compound 84	469
¹ H-NMR (300 MHz, CDCl ₃) of Compound 85a	470
¹³ C-NMR (75 MHz, CDCl ₃) of Compound 85a	471
¹ H-NMR (300 MHz, CDCl ₃) of Compound 85b	472
¹ H-NMR (300 MHz, CD ₂ Cl ₂) of Compound 86a	473
¹³ C-NMR (75 MHz, CD ₂ Cl ₂) of Compound 86a	474
¹ H-NMR (300 MHz, CD ₂ Cl ₂) of Compound 86b	475
¹³ C-NMR (75 MHz, CD ₂ Cl ₂) of Compound 86b	476
¹ H-NMR (300 MHz, methyl Sulfoxide-d ₆) of Compound 87	477
¹³ C-NMR (75 MHz, methyl Sulfoxide-d ₆) of Compound 87	478
¹ H-NMR (300 MHz, methyl Sulfoxide-d ₆) of Compound 88	479
¹³ C-NMR (75 MHz, methyl Sulfoxide-d ₆) of Compound 88	480
¹ H-NMR (300 MHz, CDCl ₃) of Compound 89	481
¹ H-NMR (300 MHz, CDCl ₃) of Compound 90	482

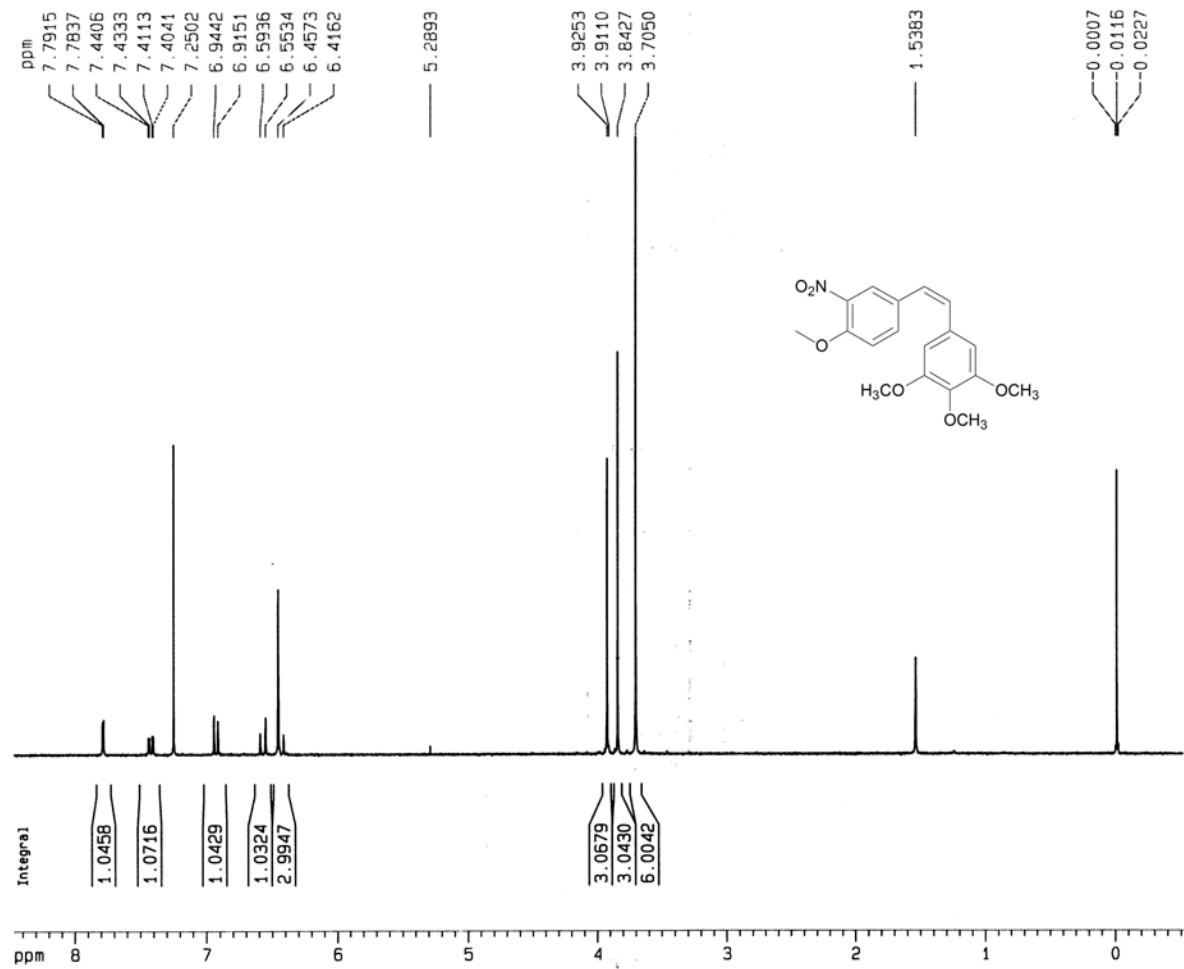
$^1\text{H-NMR}$ (300 MHz, CDCl_3) of Compound 1



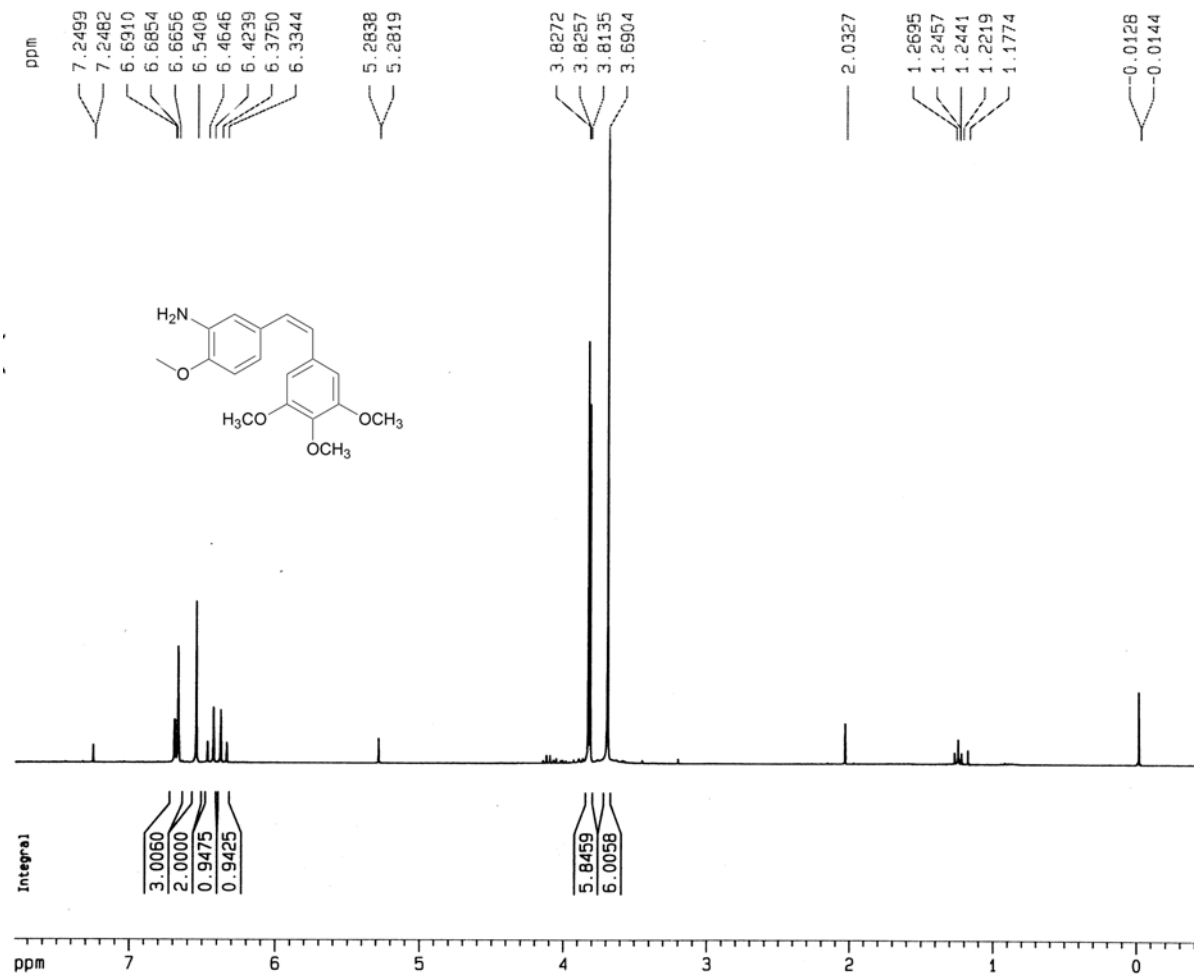
$^1\text{H-NMR}$ (300 MHz, CDCl_3) of Compound 2



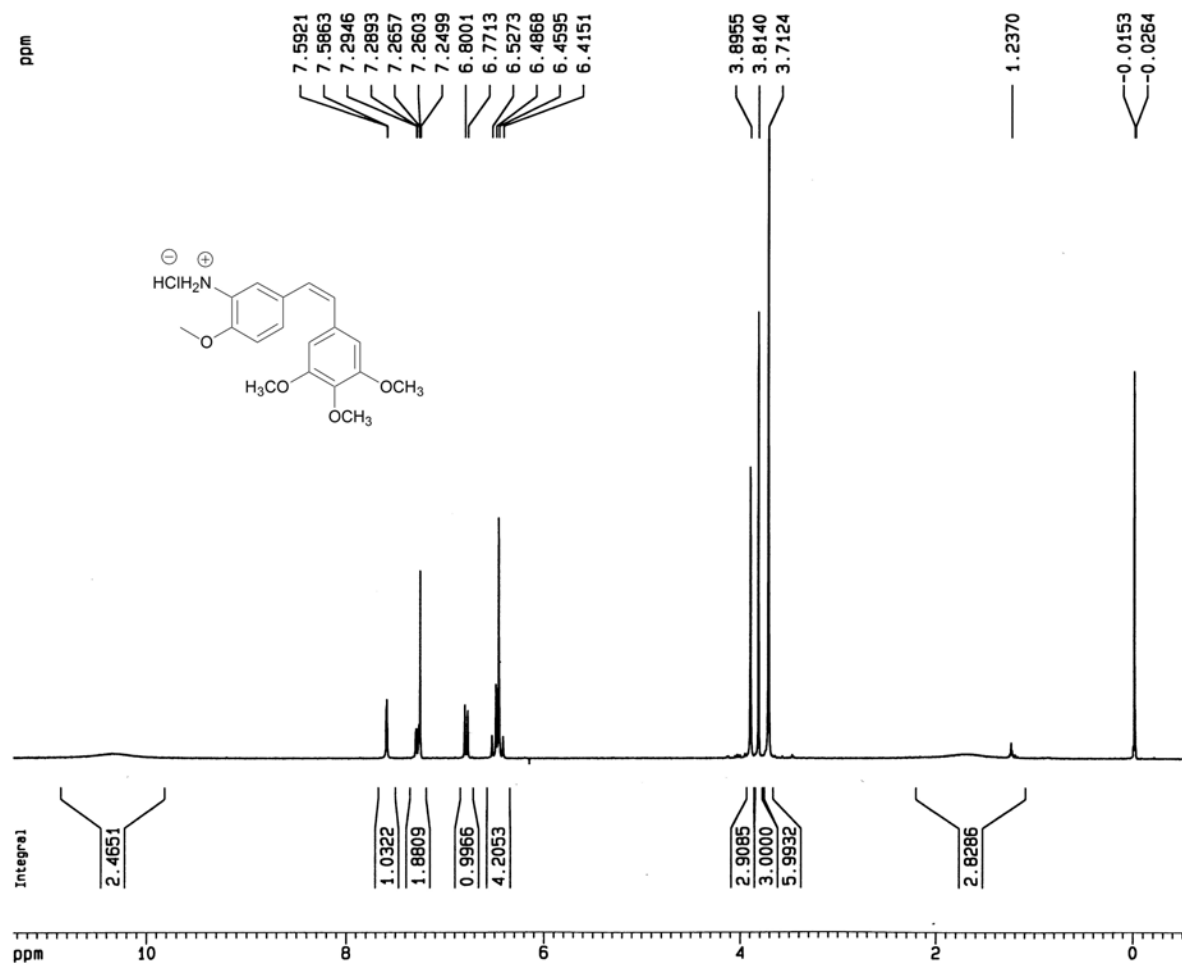
¹H-NMR (300 MHz, CDCl₃) of Compound 3



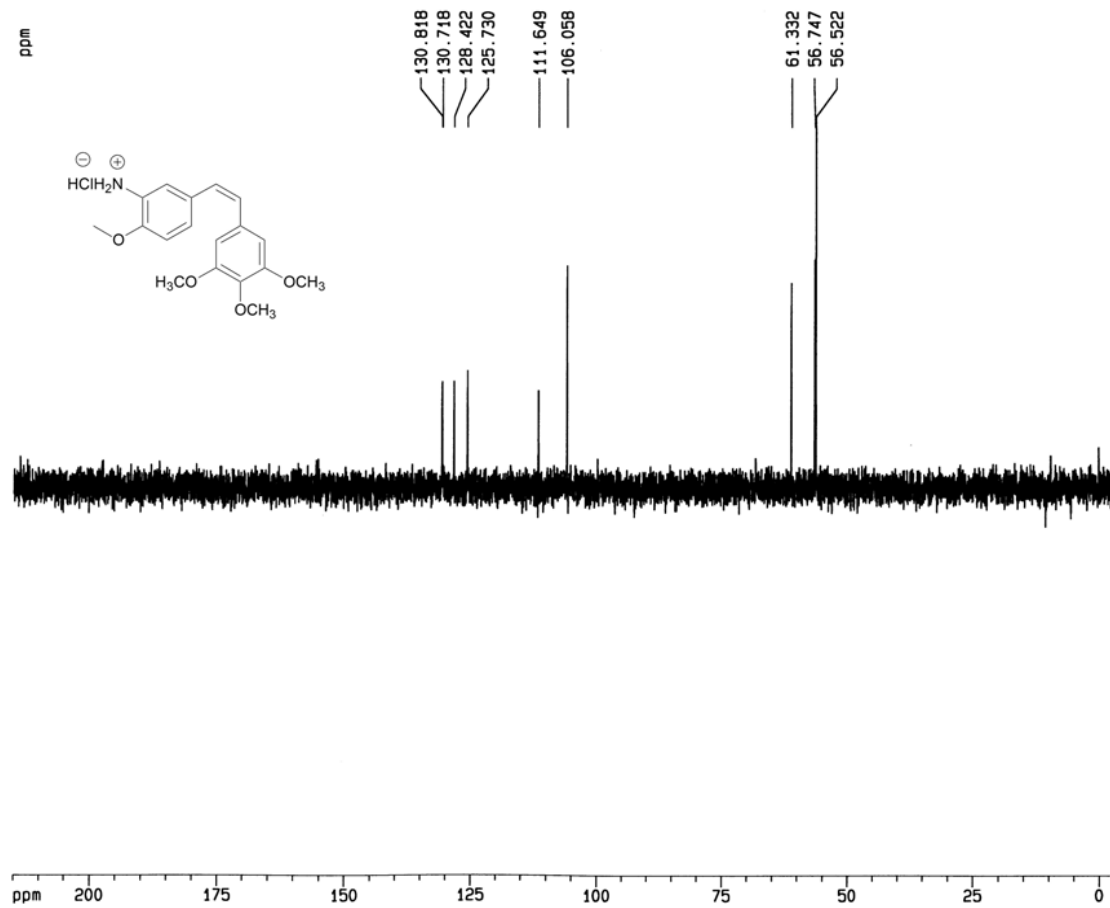
¹H-NMR (300 MHz, CDCl₃) of Compound 4



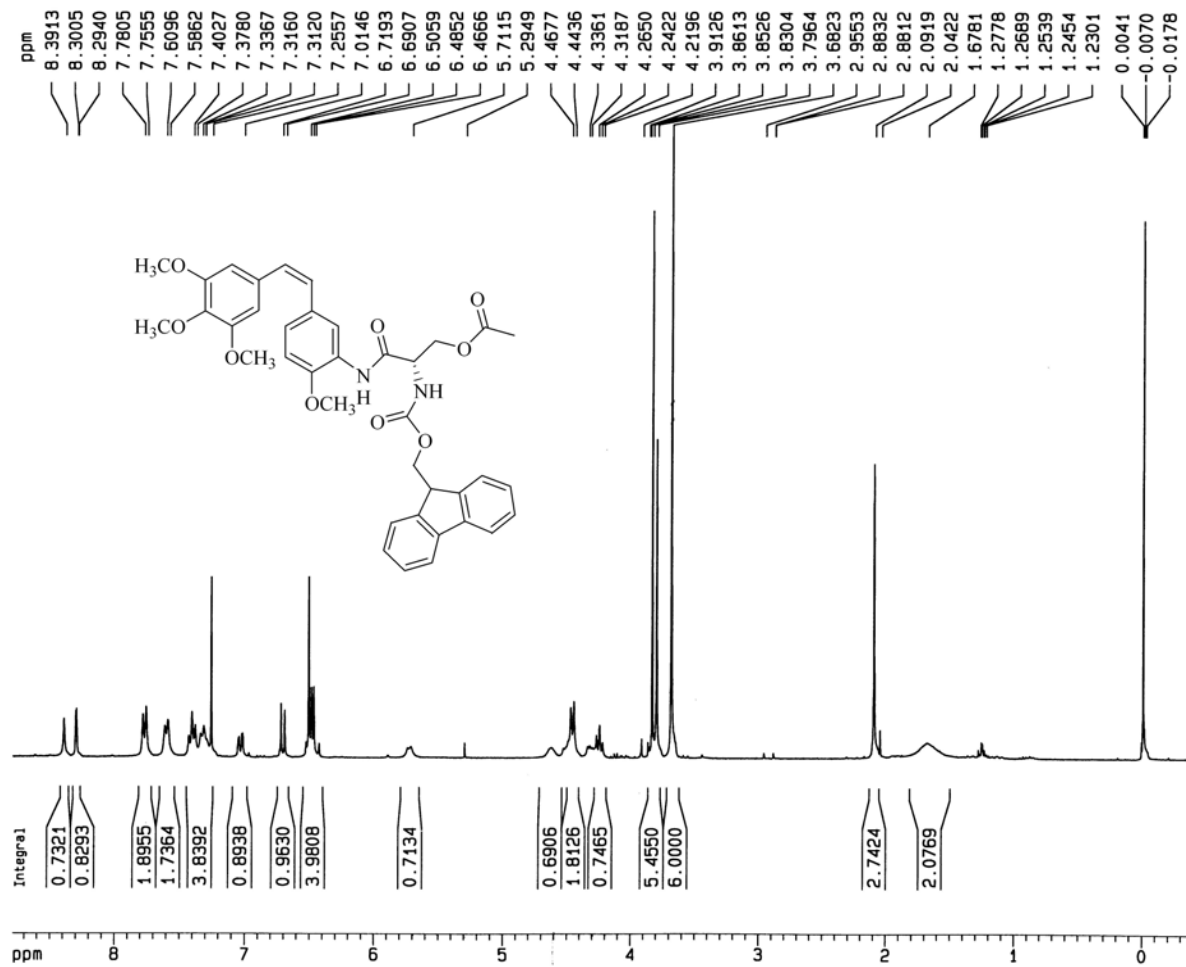
¹H-NMR (300 MHz, CDCl₃) of Compound 5



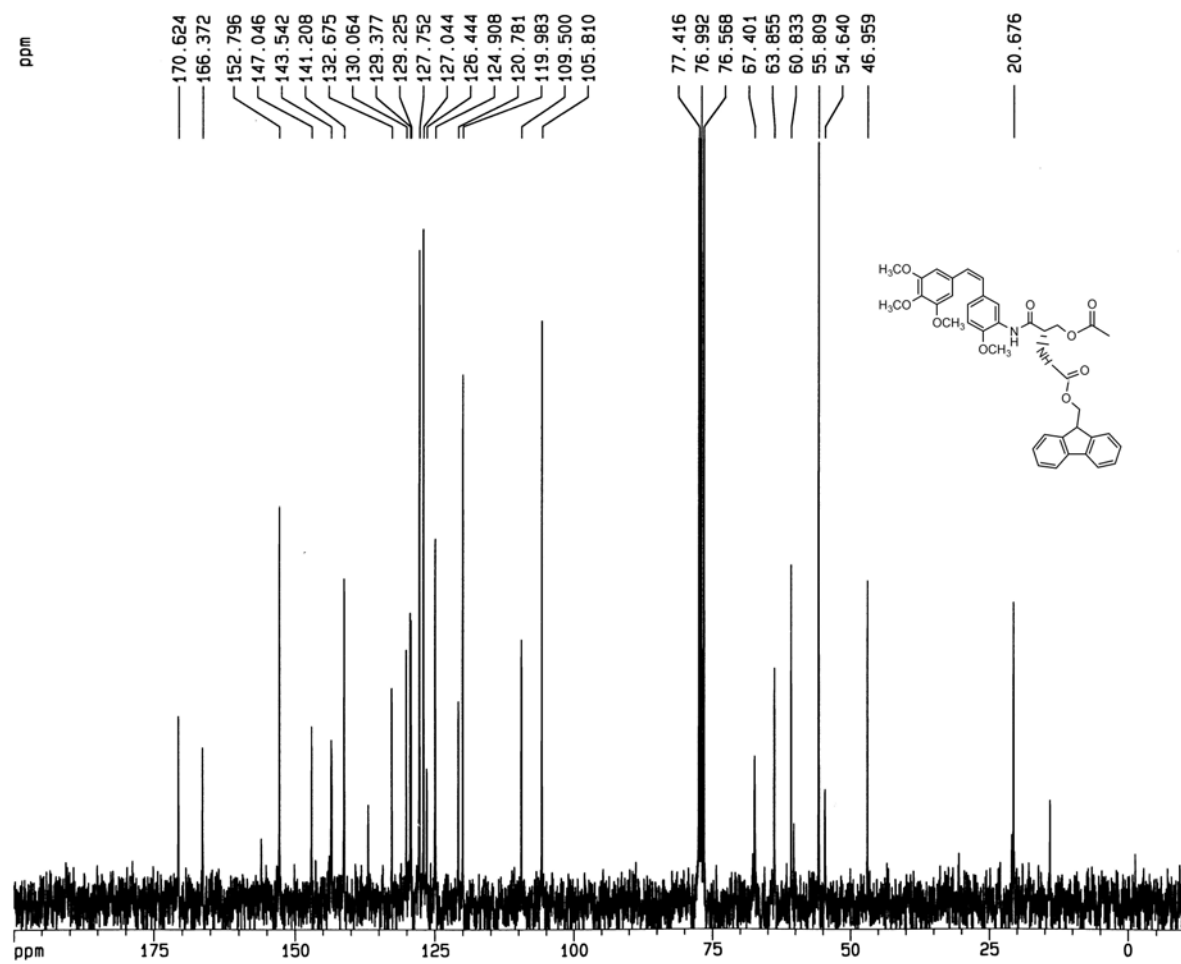
Dept 135-NMR (75 MHz, CD₂Cl₂) of Compound 5



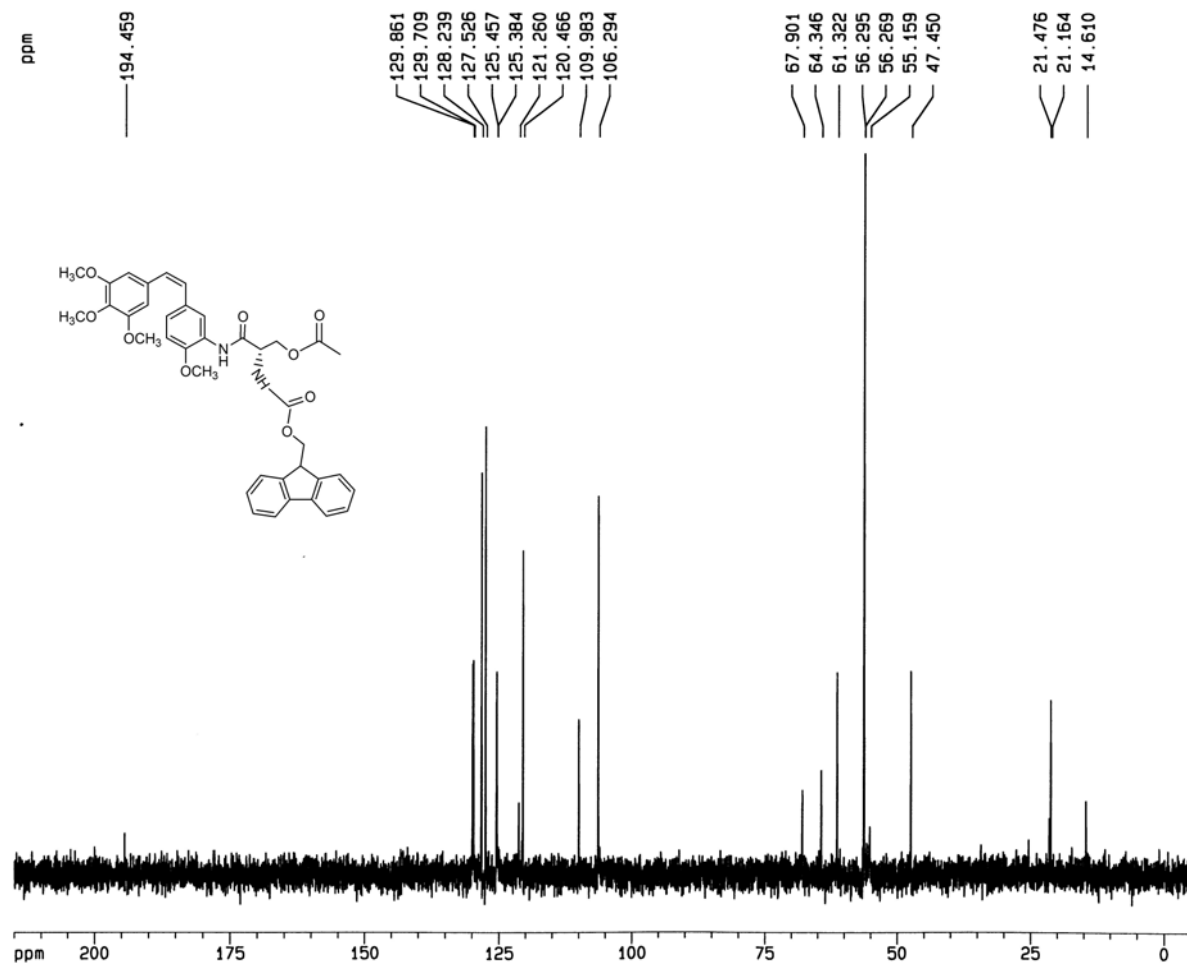
¹H-NMR (300 MHz, CDCl₃) of Compound 6



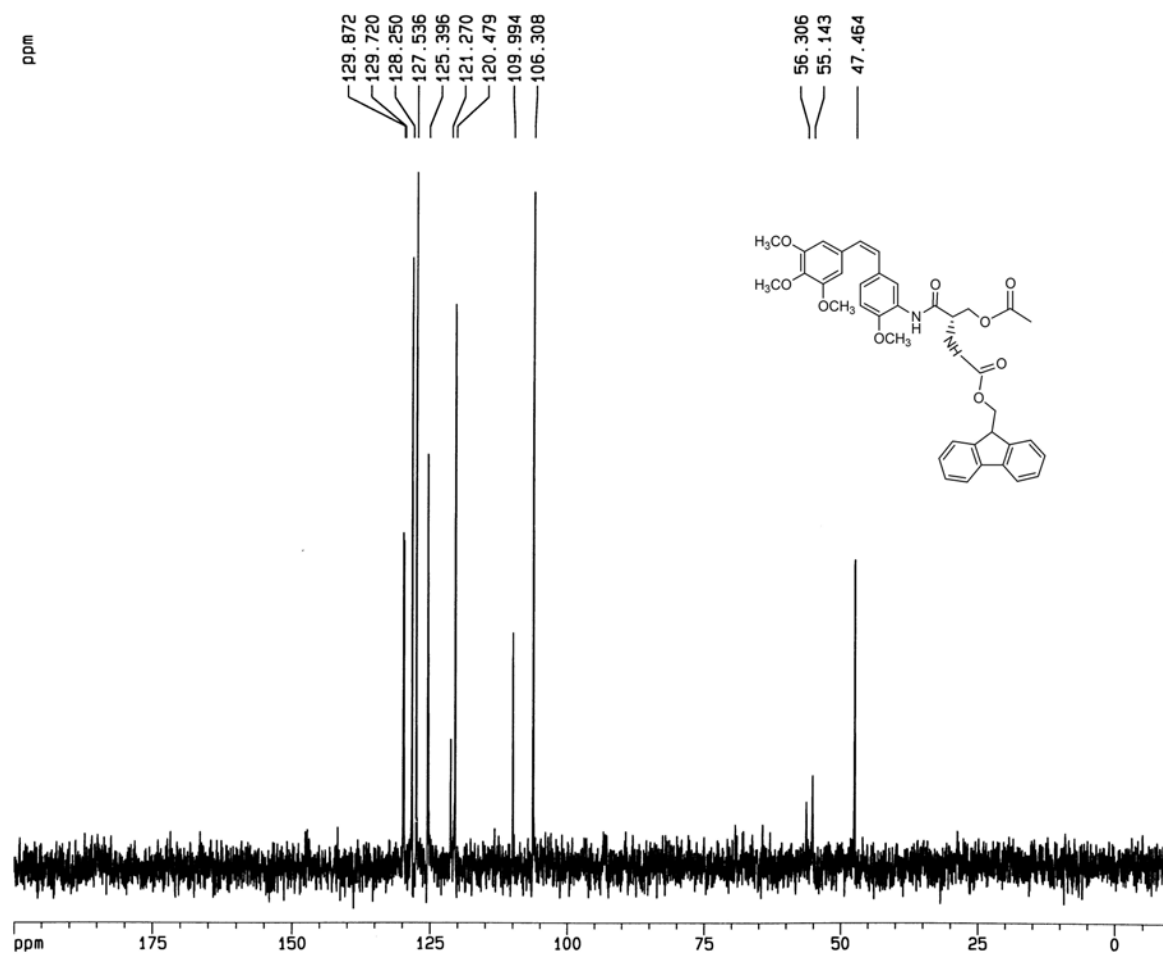
¹³C-NMR (75 MHz, CDCl₃) of Compound 6



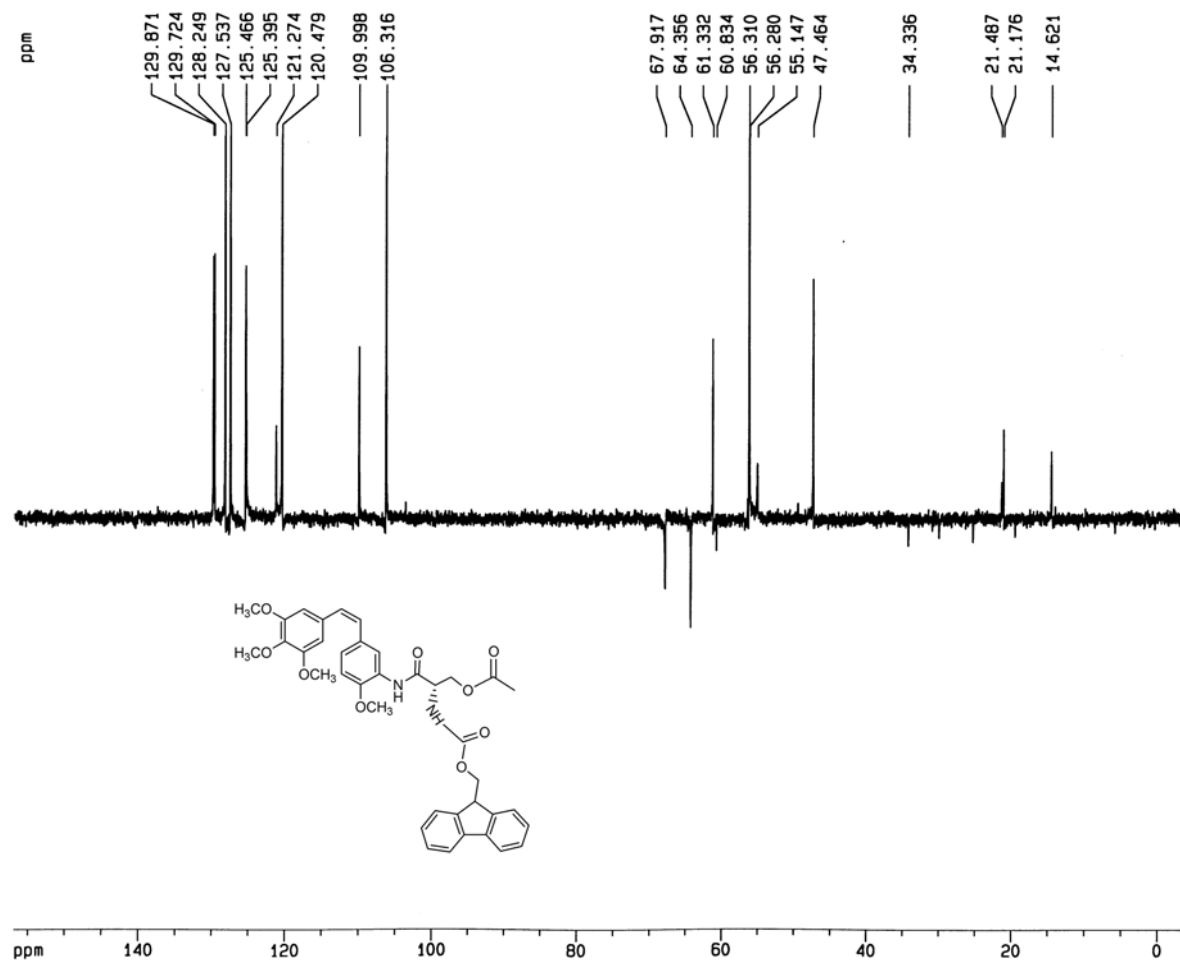
Dept 45-NMR (75 MHz, CDCl₃) of Compound 6



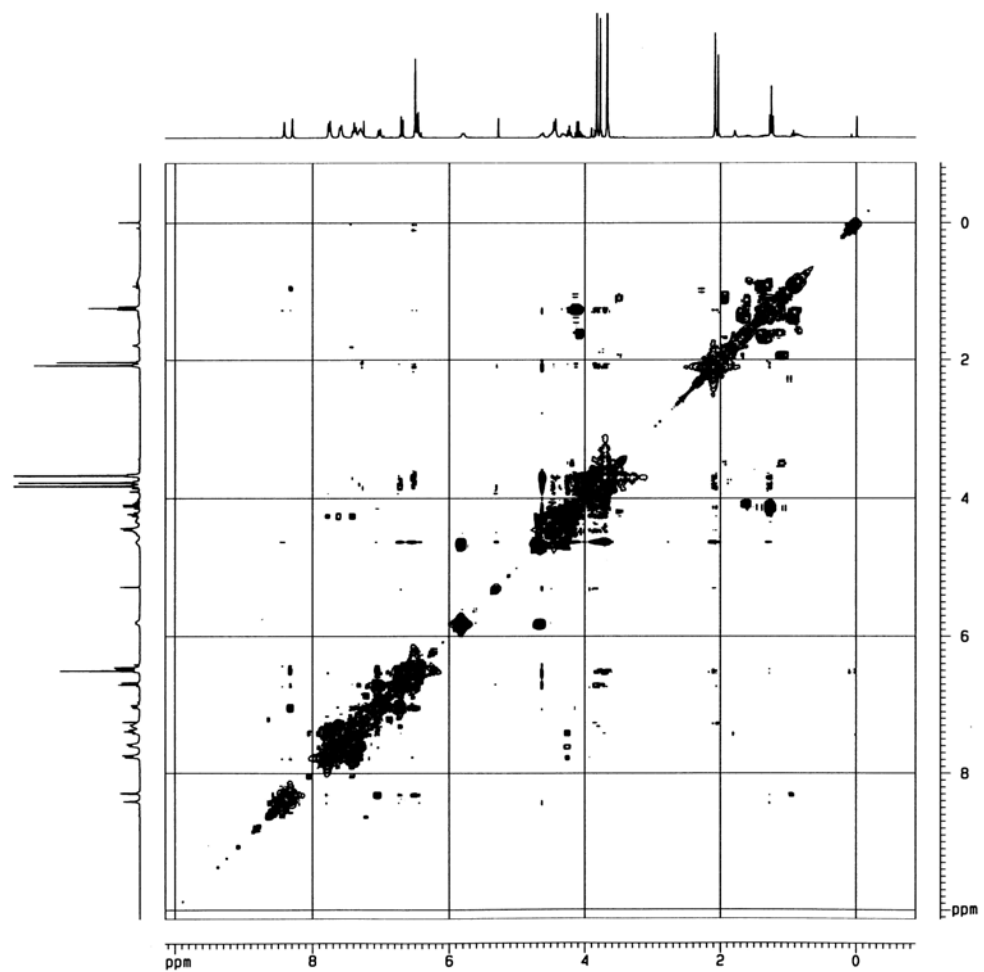
Dept 90-NMR (75 MHz, CDCl₃) of Compound 6



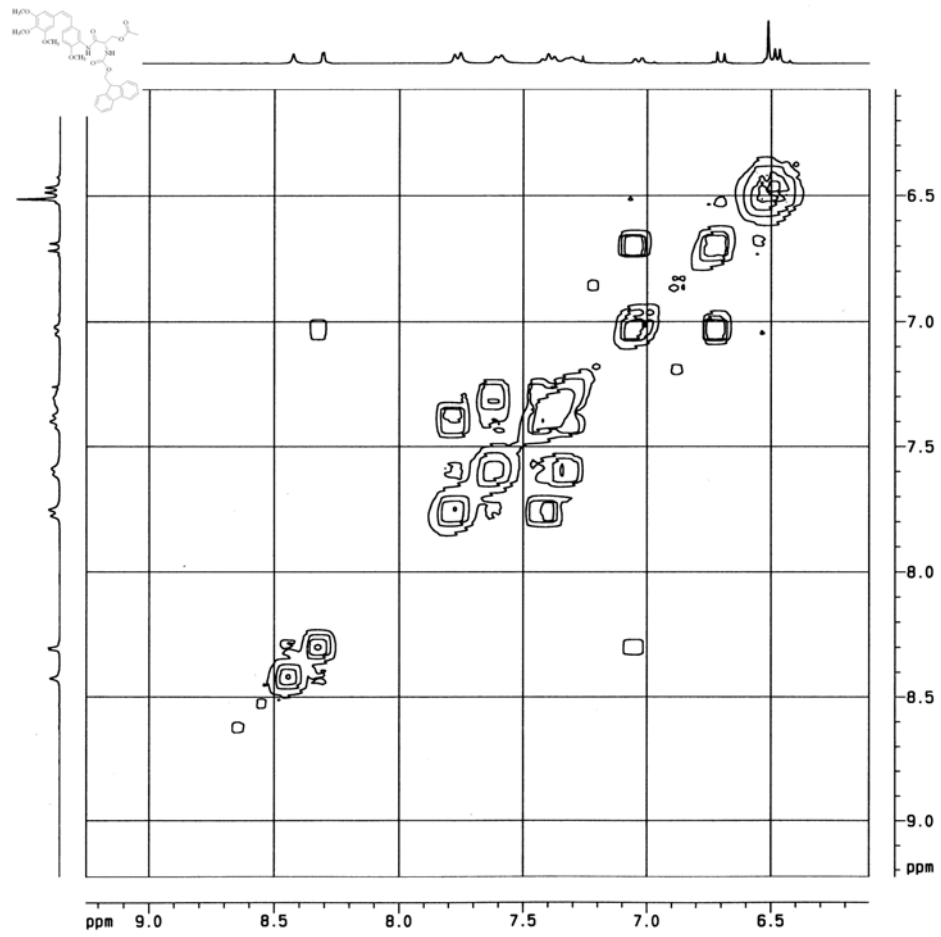
Dept 135-NMR (75 MHz, CDCl₃) of Compound 6



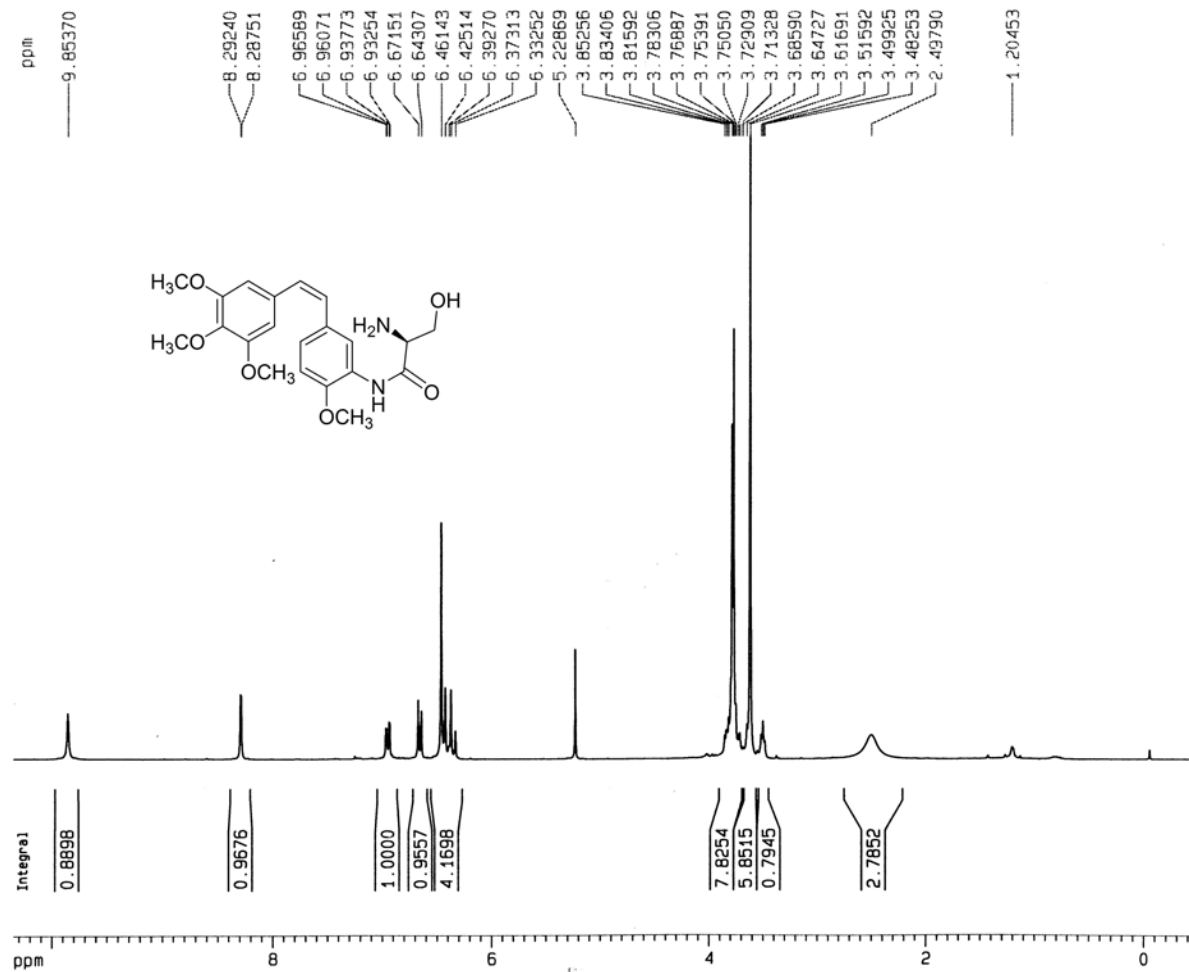
COSY ^1H - ^1H NMR (300 MHz, CDCl_3) of Compound 6



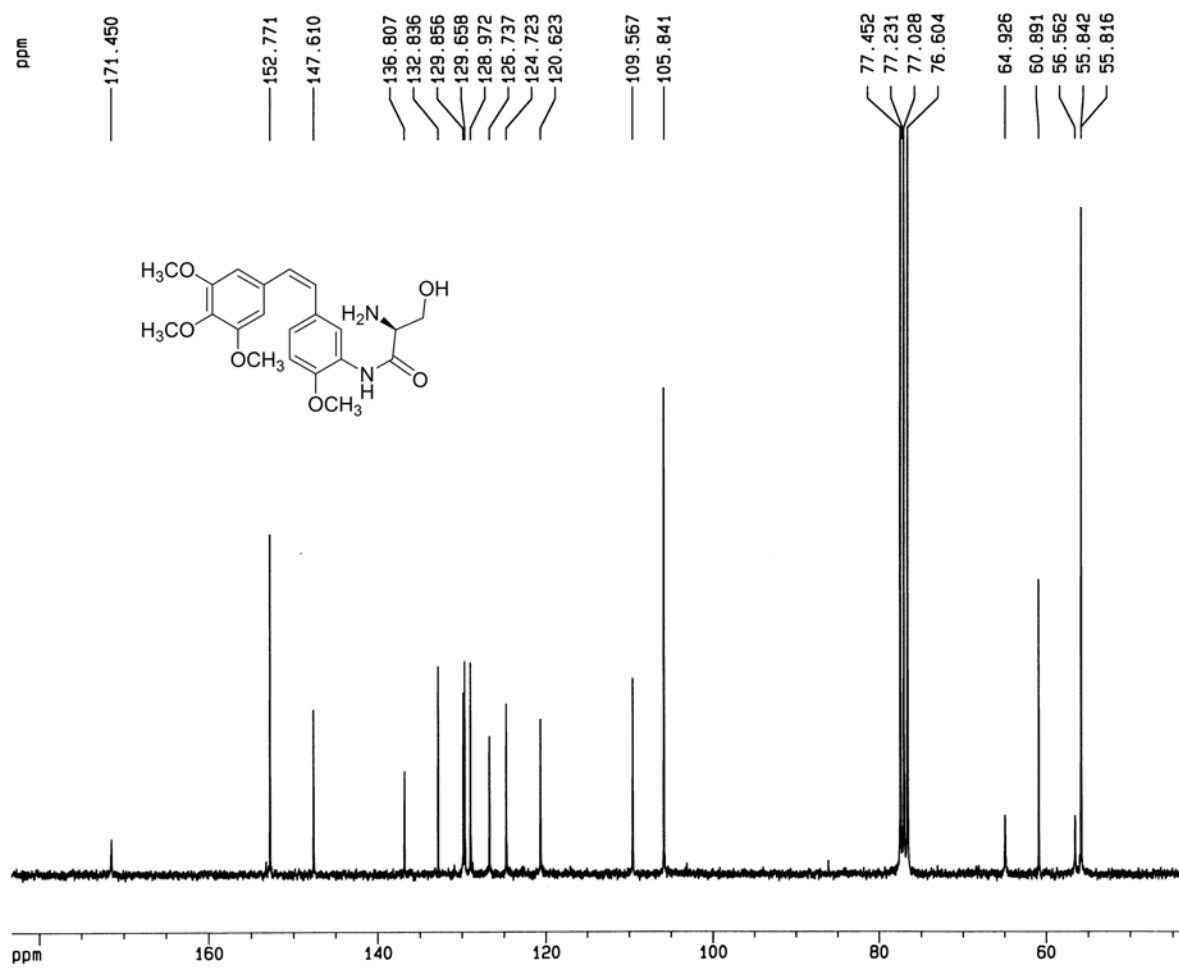
COSY ^1H - ^1H NMR (300 MHz, CDCl_3) of Compound 6



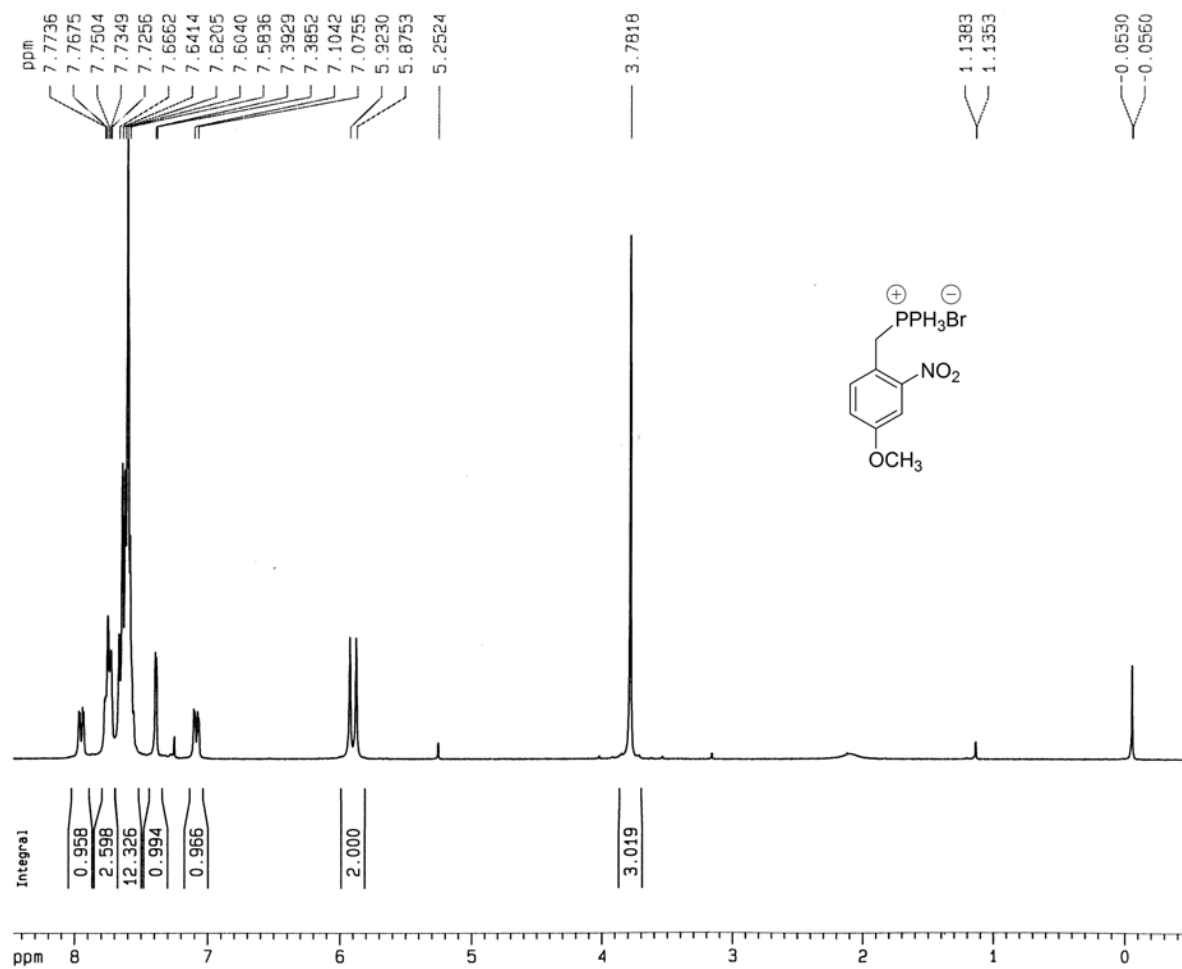
¹H-NMR (300 MHz, CDCl₃) of Compound 7



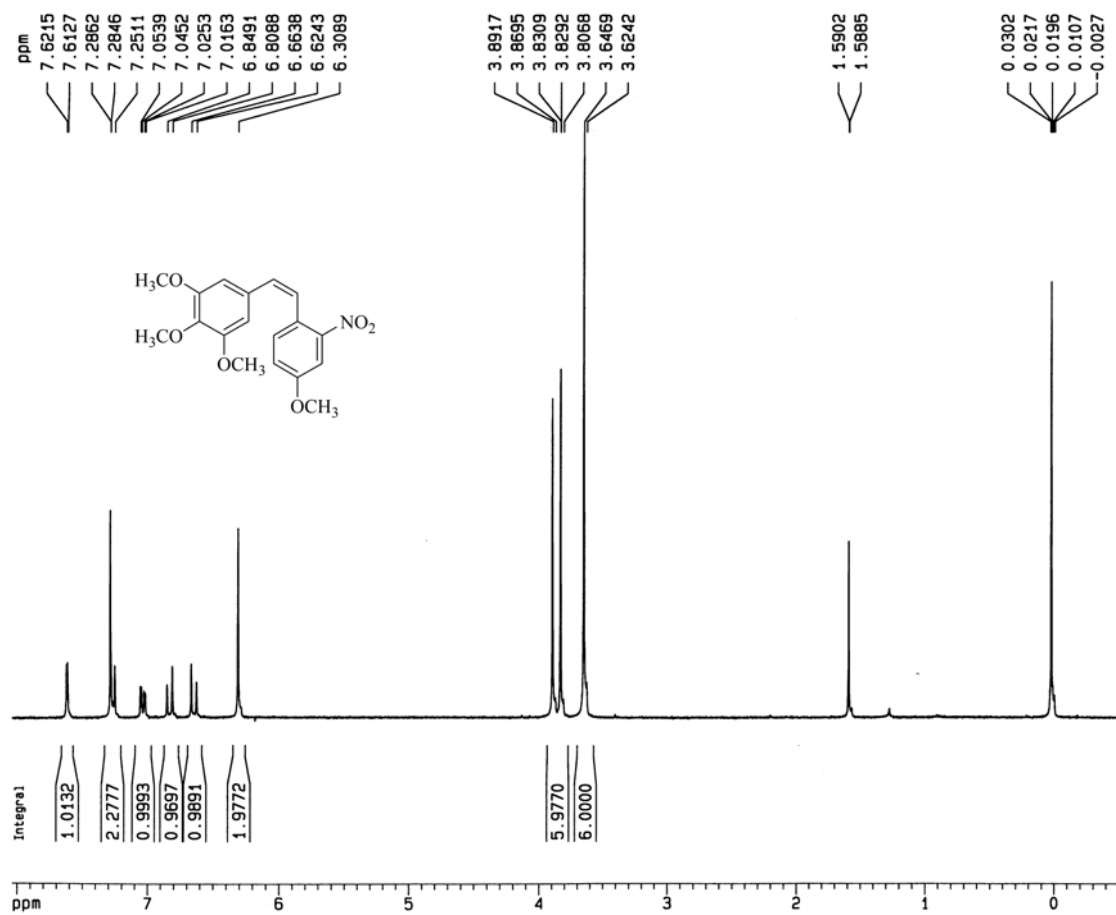
¹³C-NMR (75 MHz, CDCl₃) of Compound 7



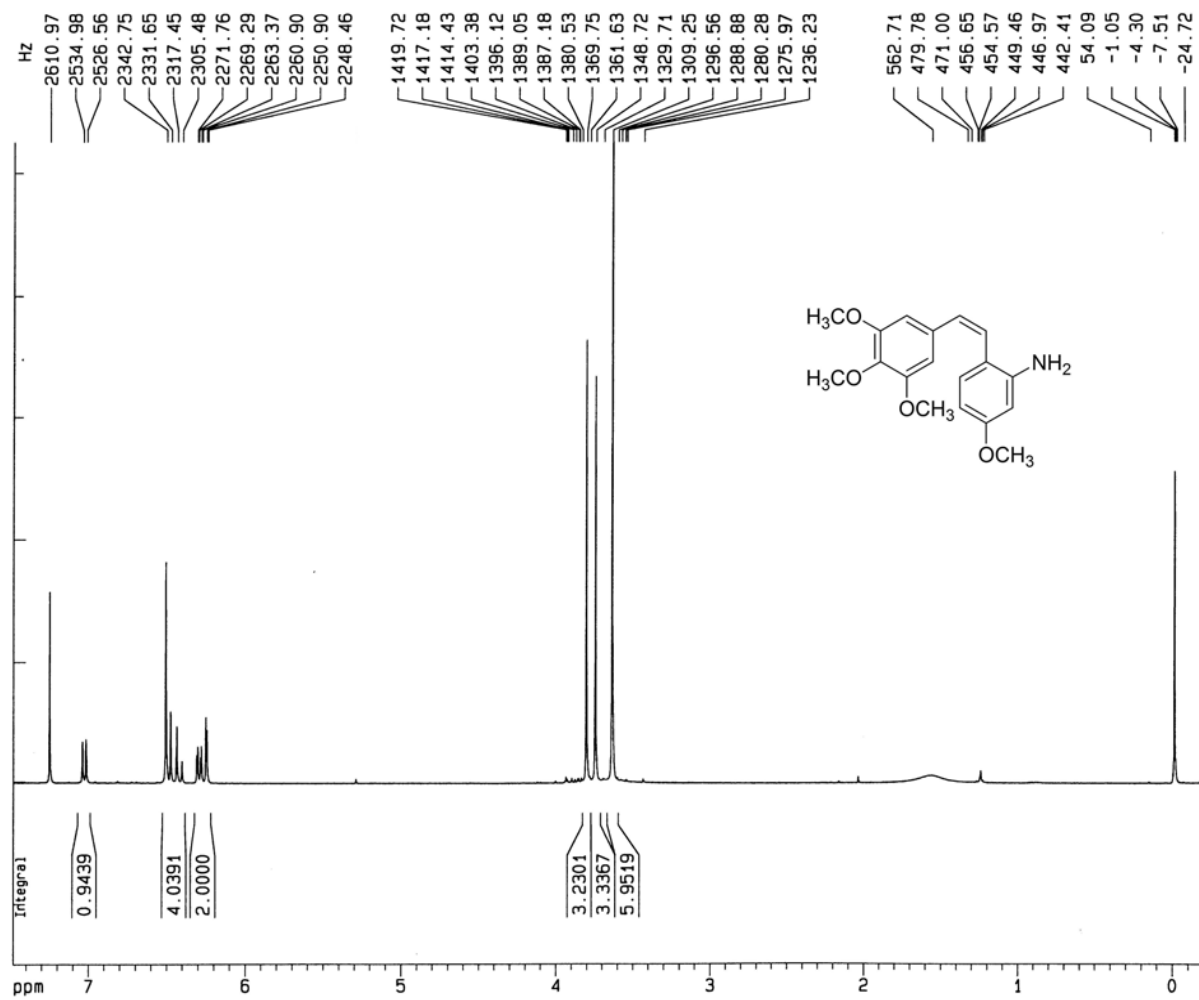
¹H-NMR (300 MHz, CDCl₃) of Compound 8



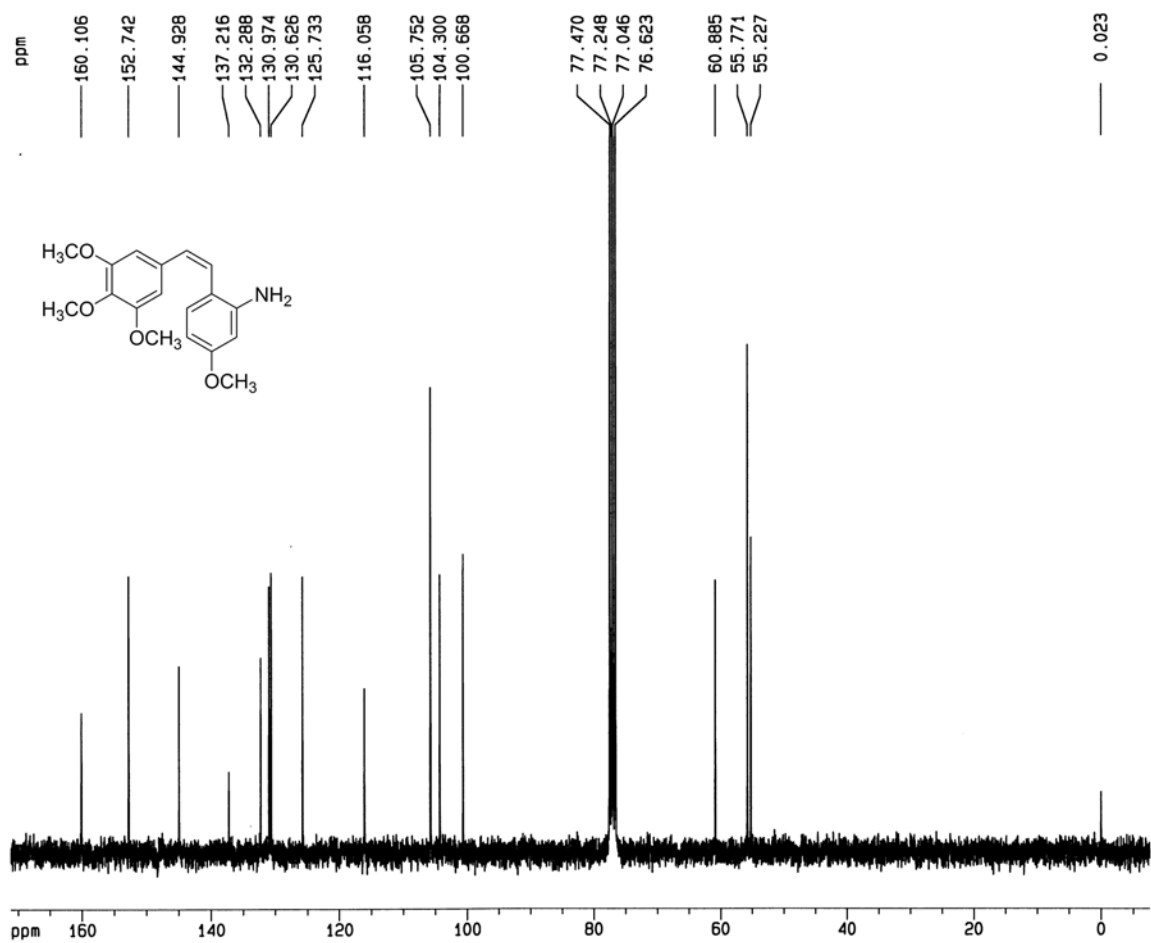
¹H-NMR (300 MHz, CDCl₃) of Compound 9



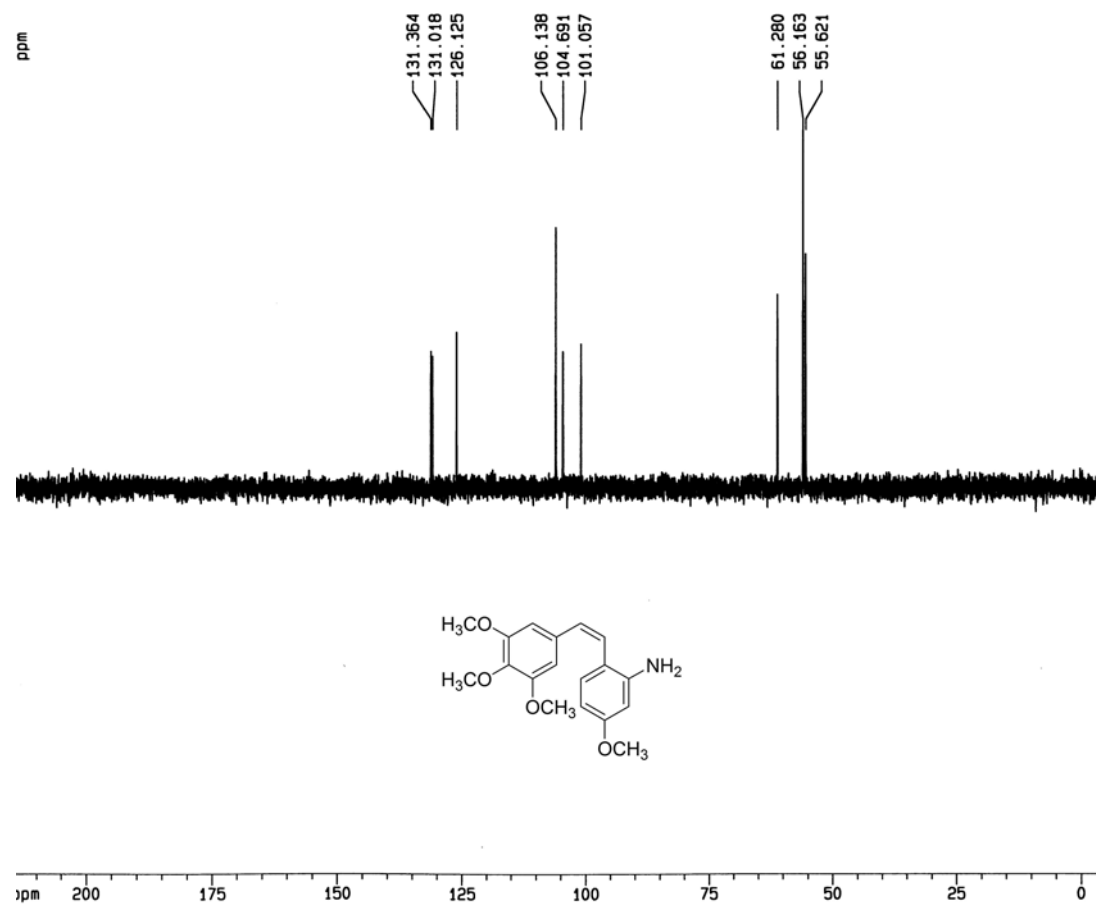
¹H-NMR (360 MHz, CDCl₃) of Compound 10



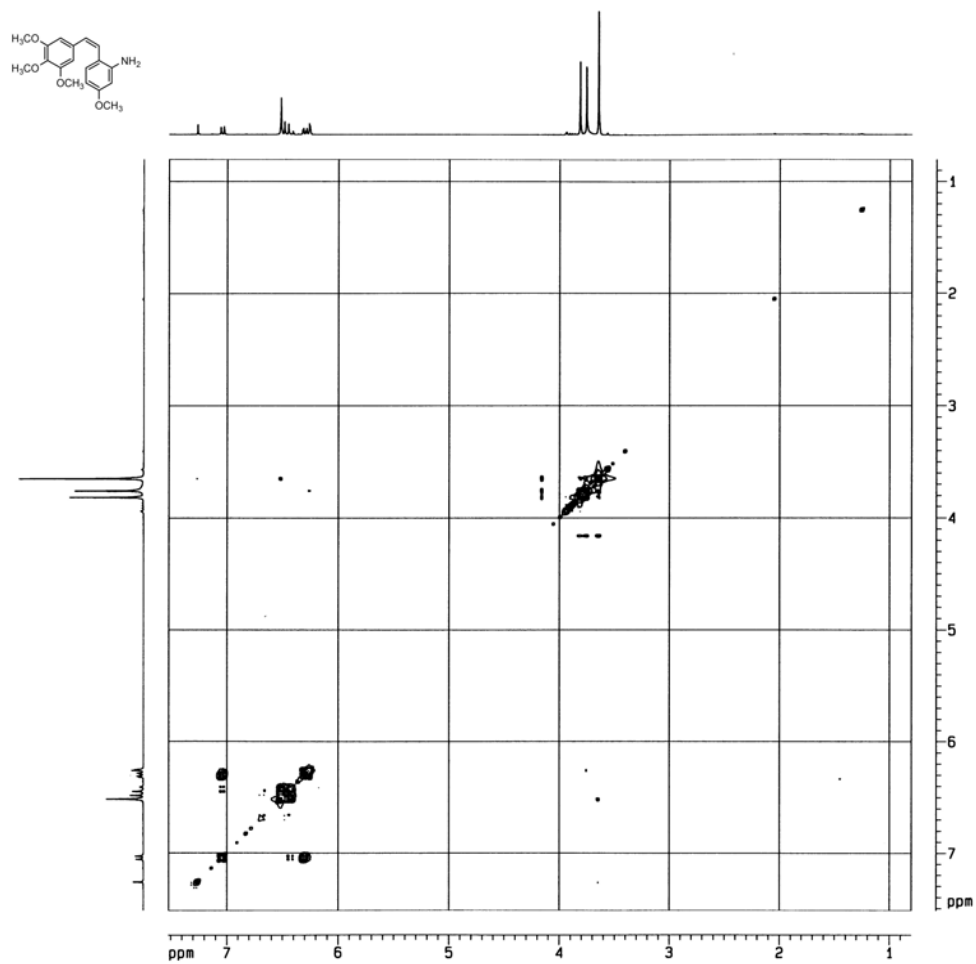
¹³C-NMR (75 MHz, CDCl₃) of Compound **10**



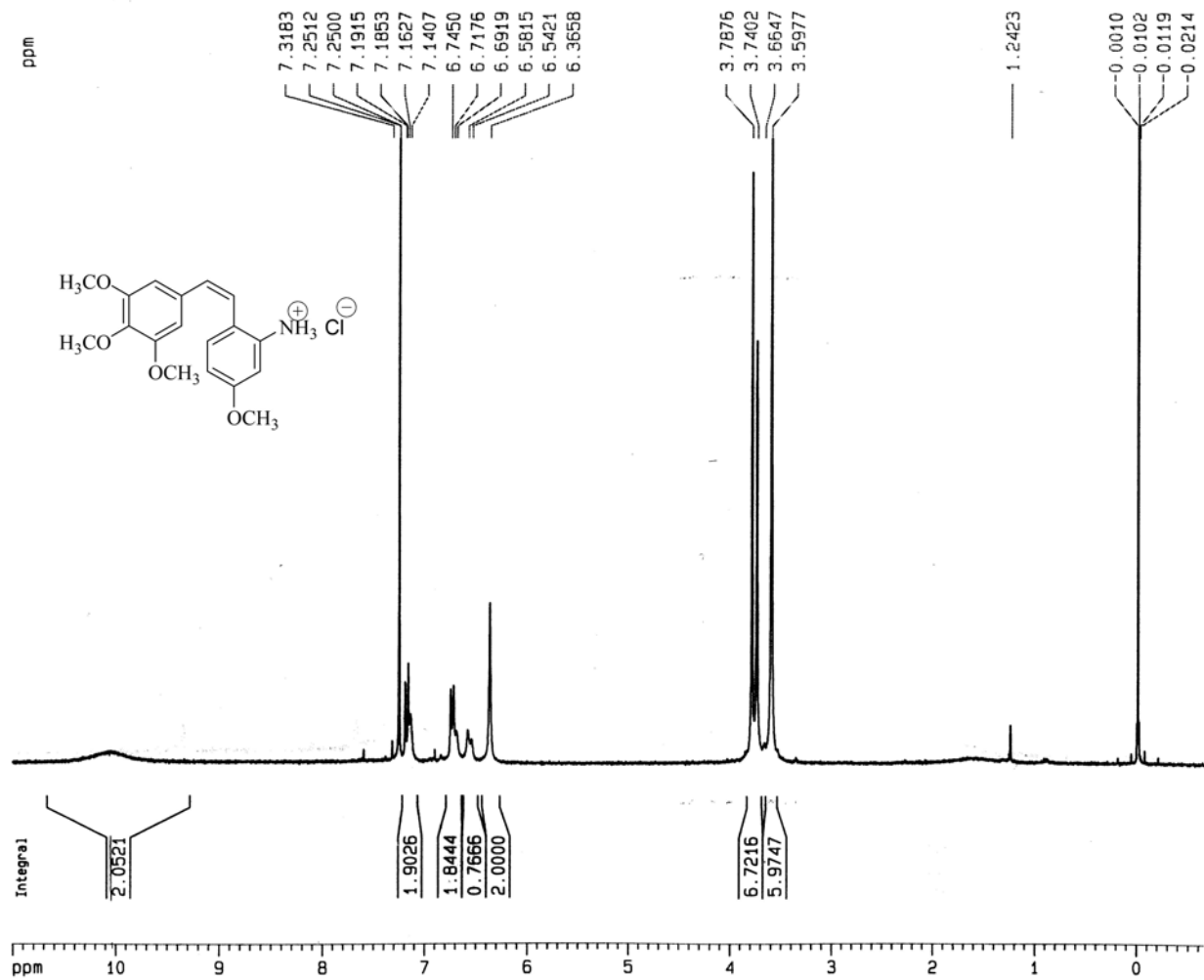
Dept 135-NMR (75 MHz, CDCl₃) of Compound 10



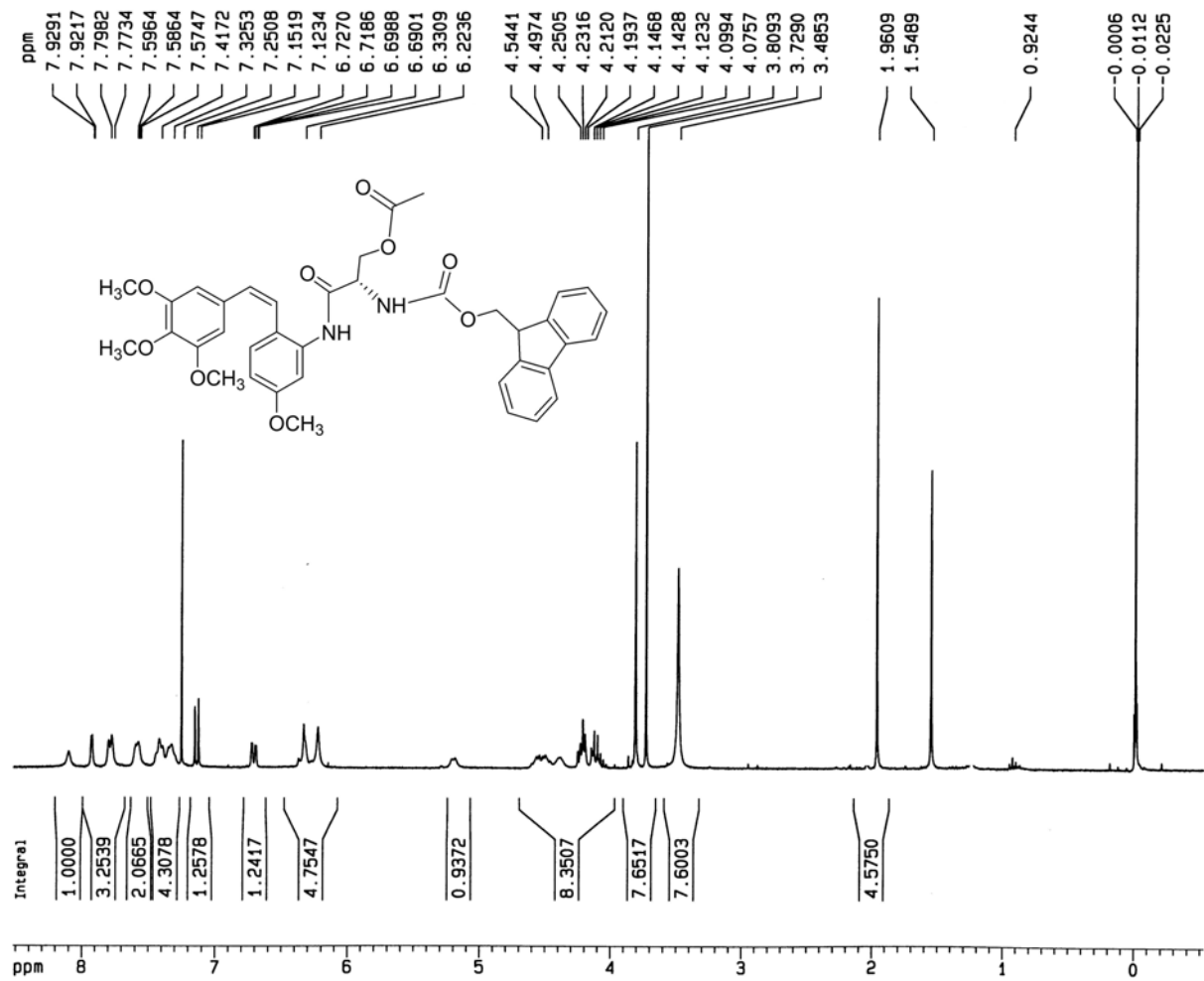
COSY-¹H-¹H NMR (300 MHz, CDCl₃) of Compound **10**



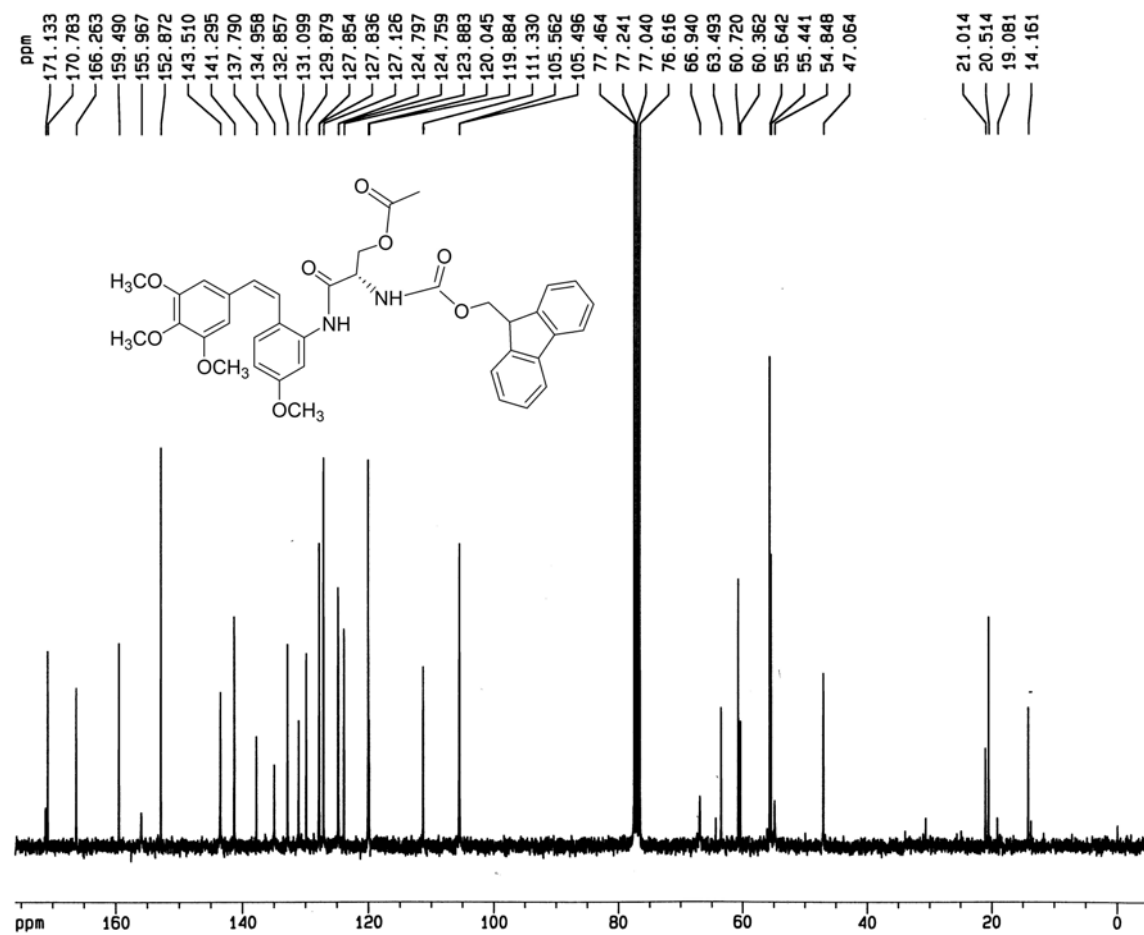
¹H-NMR (360 MHz, CDCl₃) of Compound 11



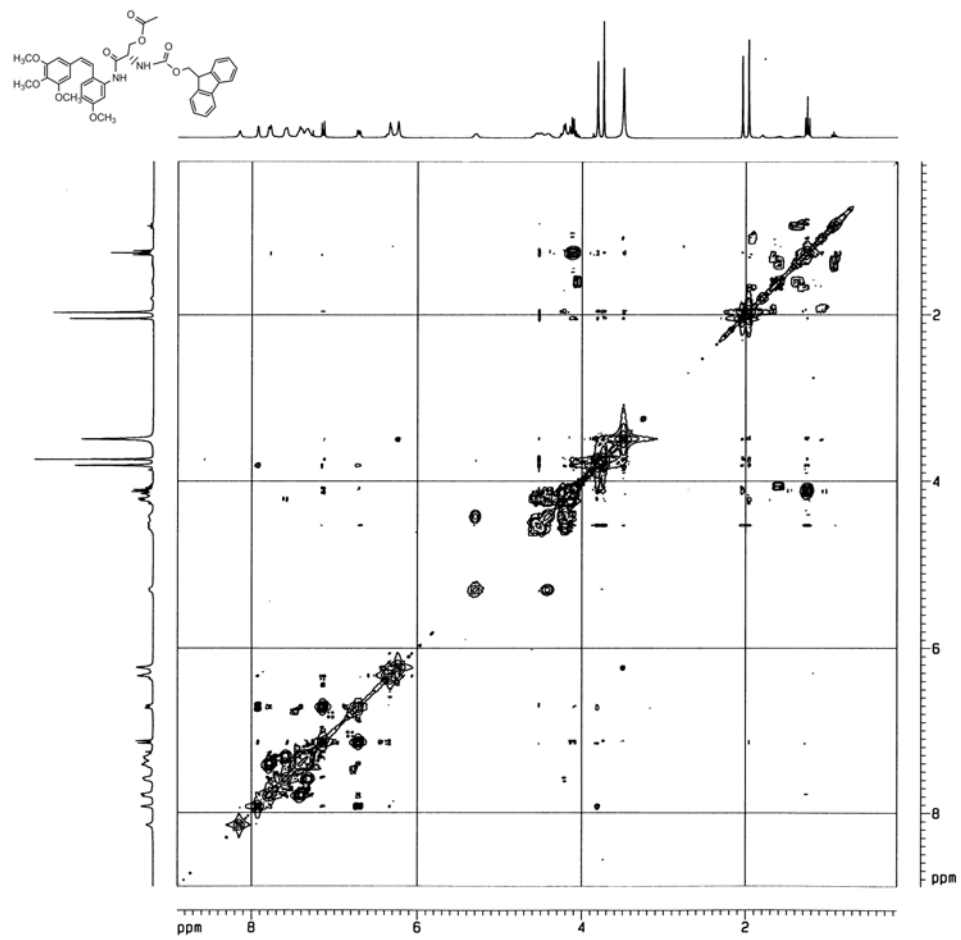
¹H-NMR (300 MHz, CDCl₃) of Compound 12



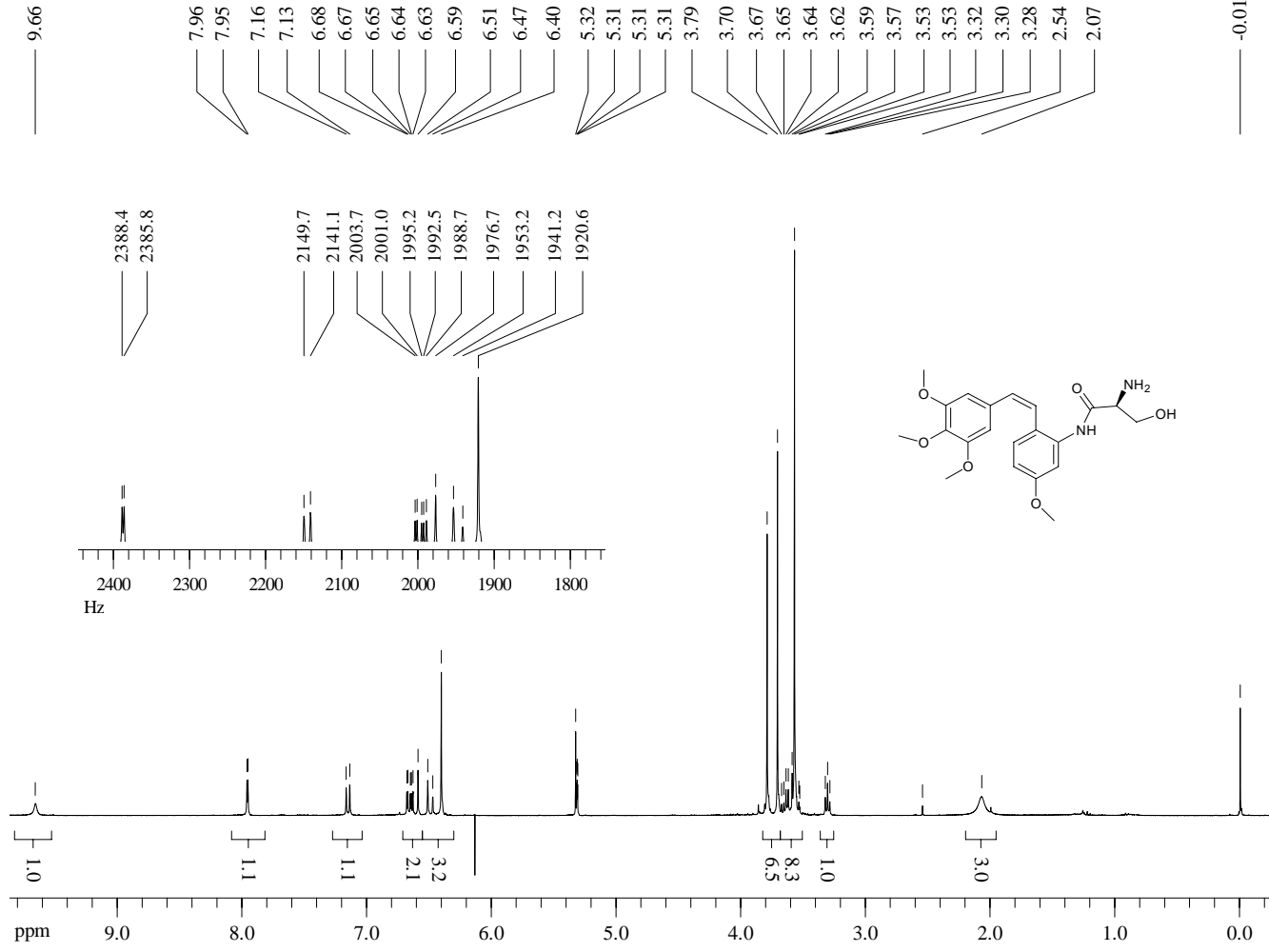
$^{13}\text{C-NMR}$ (75 MHz, CDCl_3) of Compound **12**



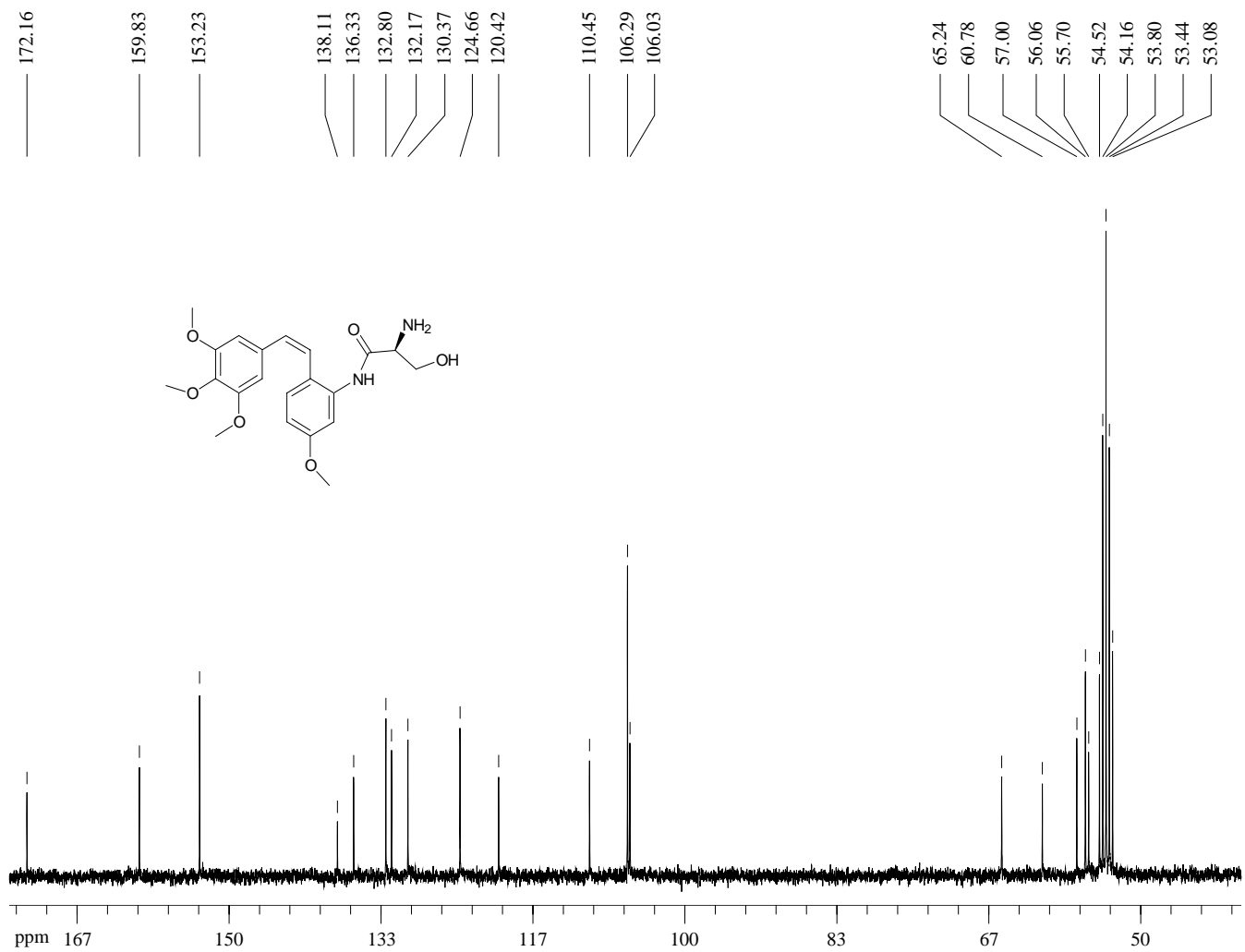
COSY-¹H-¹H NMR (300 MHz, CDCl₃) of Compound 12



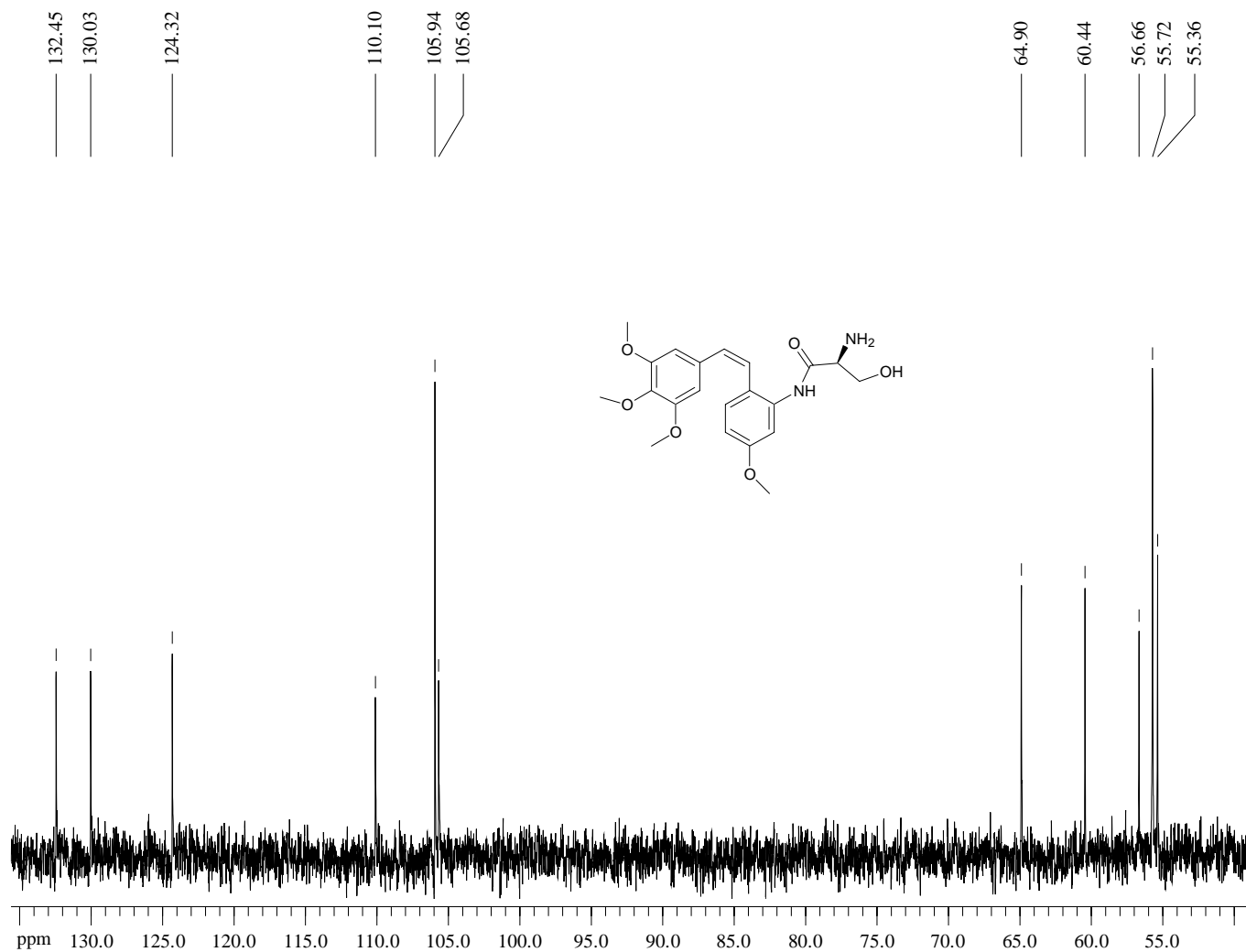
¹H-NMR (300 MHz, CD₂Cl₂) of Compound 13



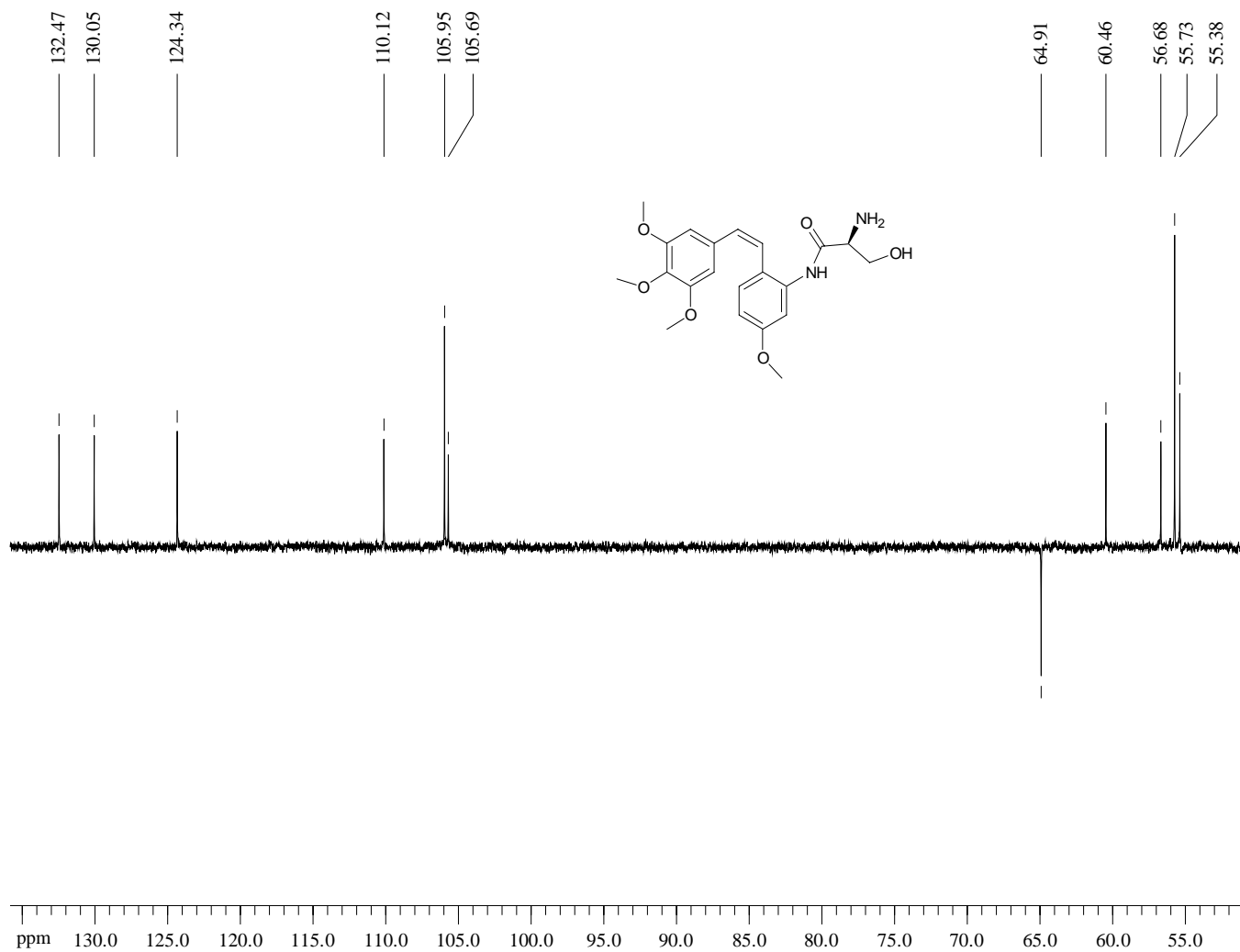
¹³C-NMR (75 MHz, CD₂Cl₂) of Compound **13**



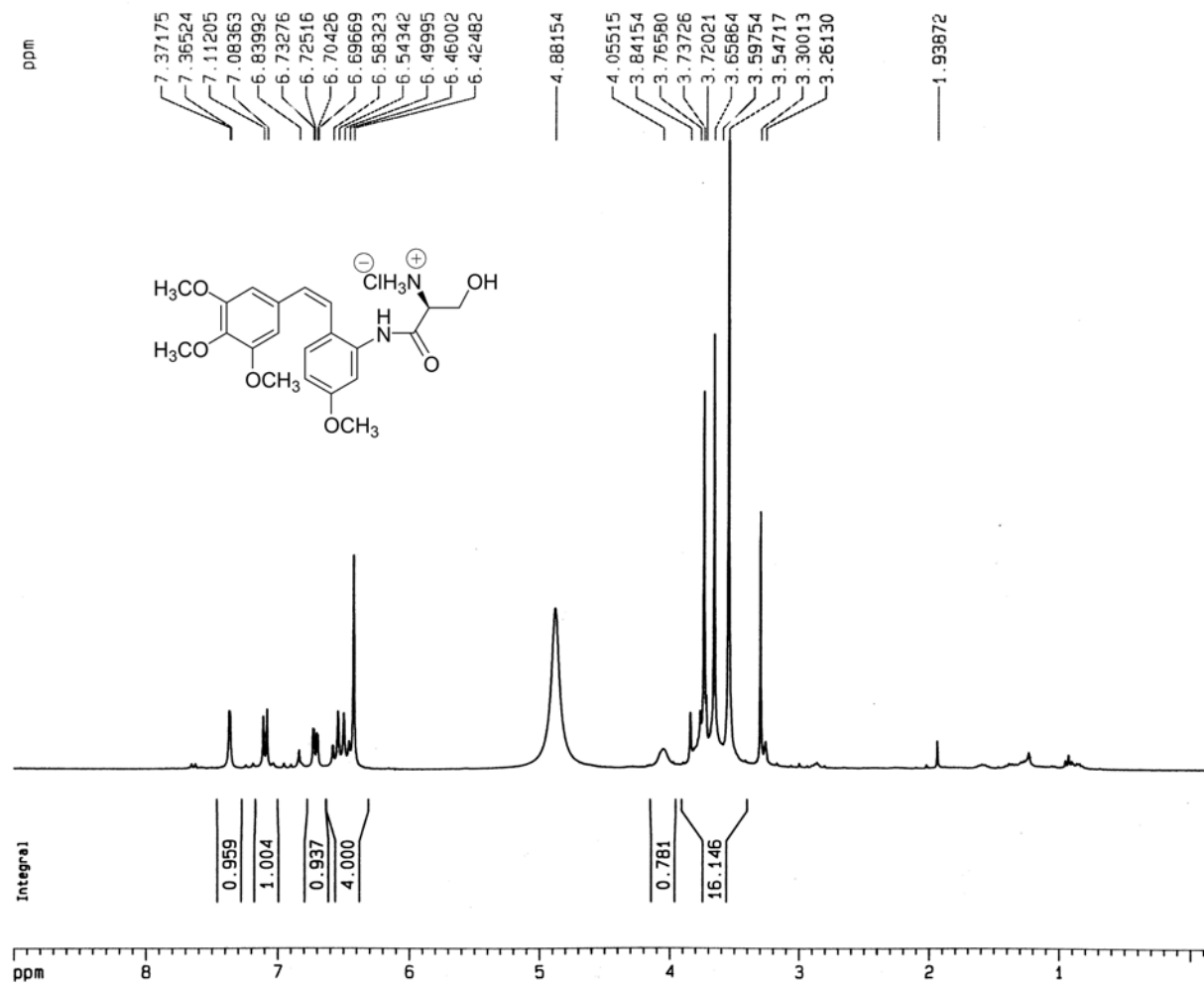
Dept 45-NMR (75 MHz, CD₂ Cl₂) of Compound **13**



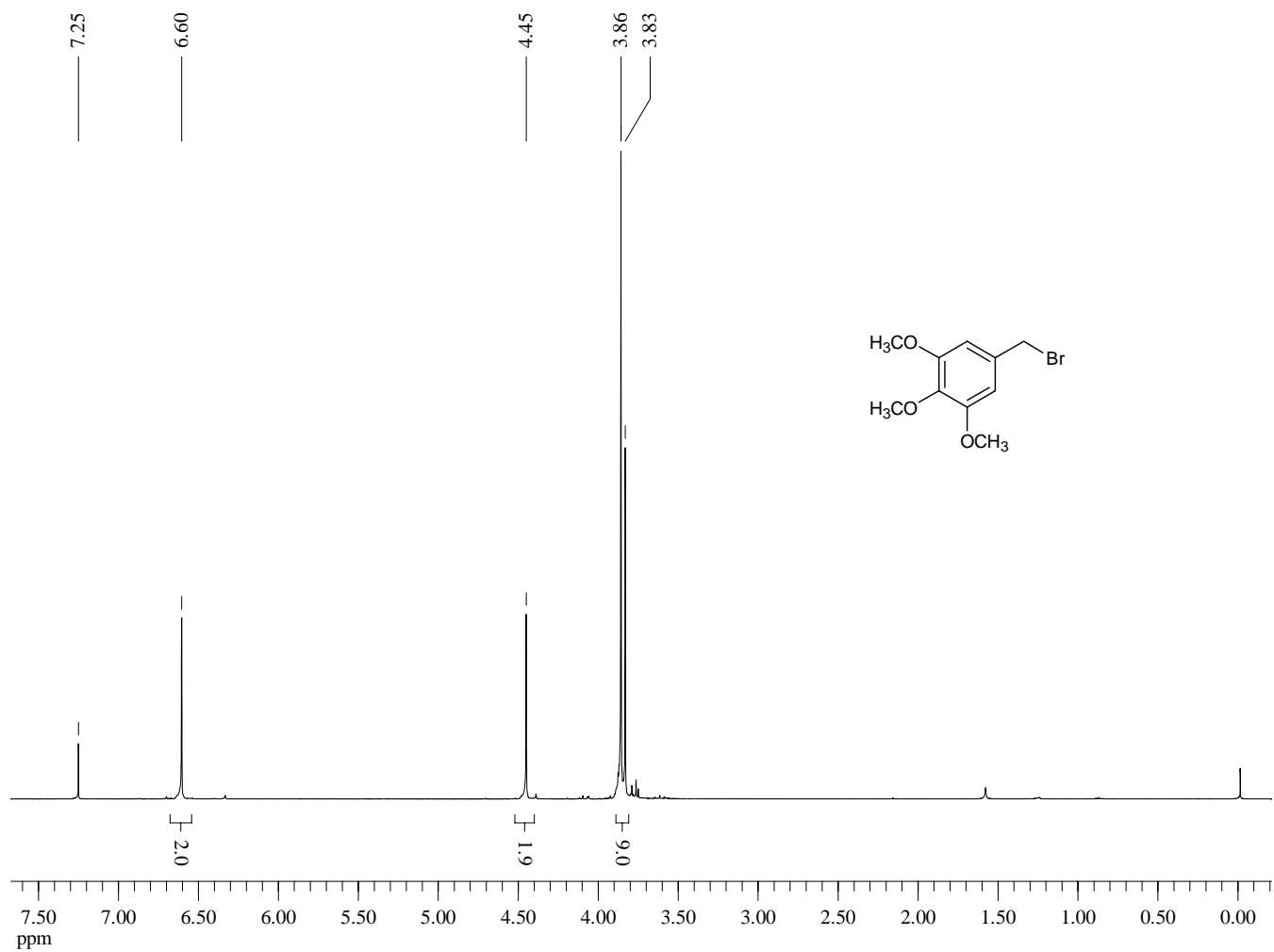
Dept 135-NMR (90 MHz, CD₂ Cl₂) of Compound **13**



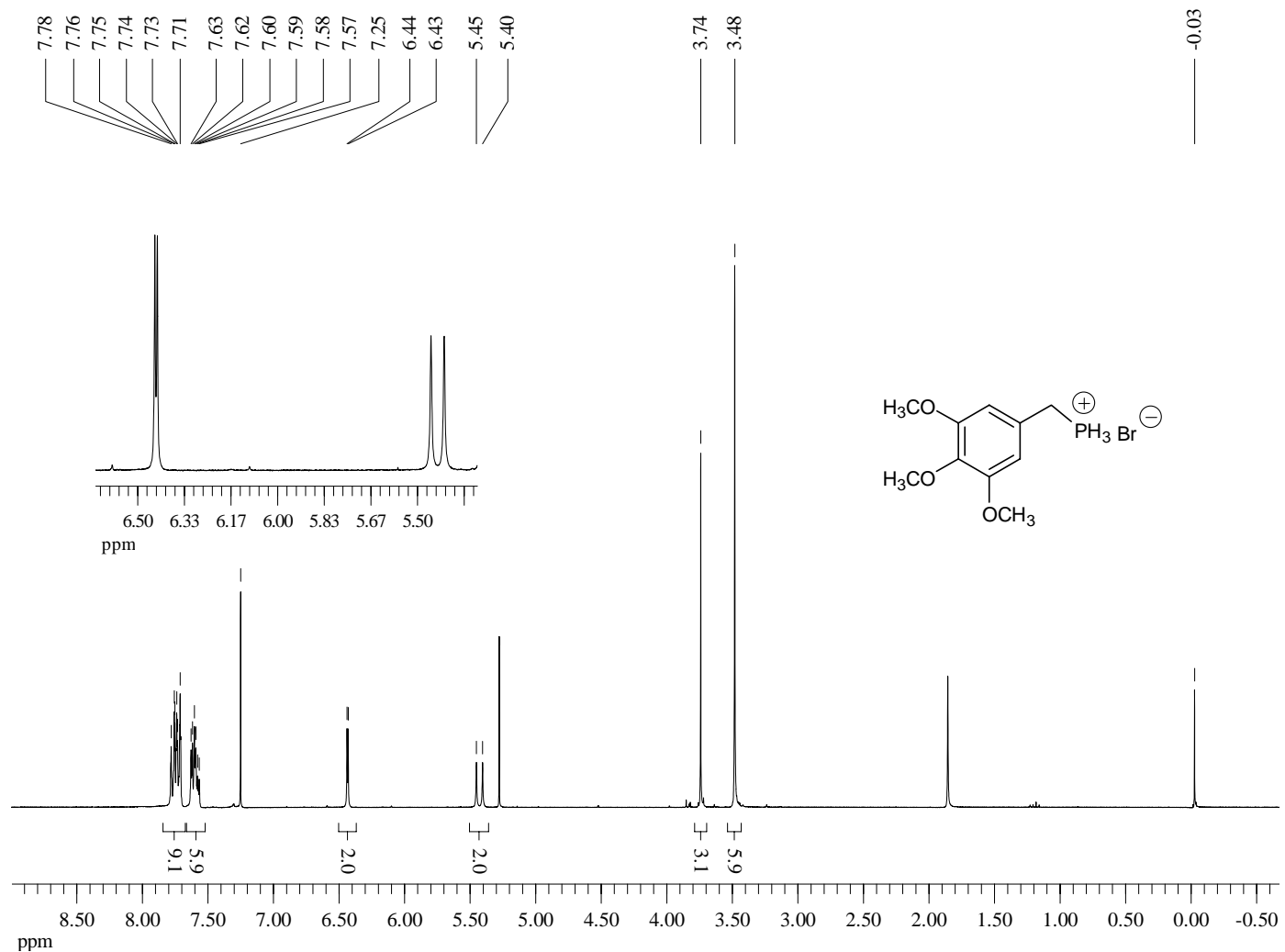
¹H-NMR (300 MHz, Methanol-d₄) of Compound 14



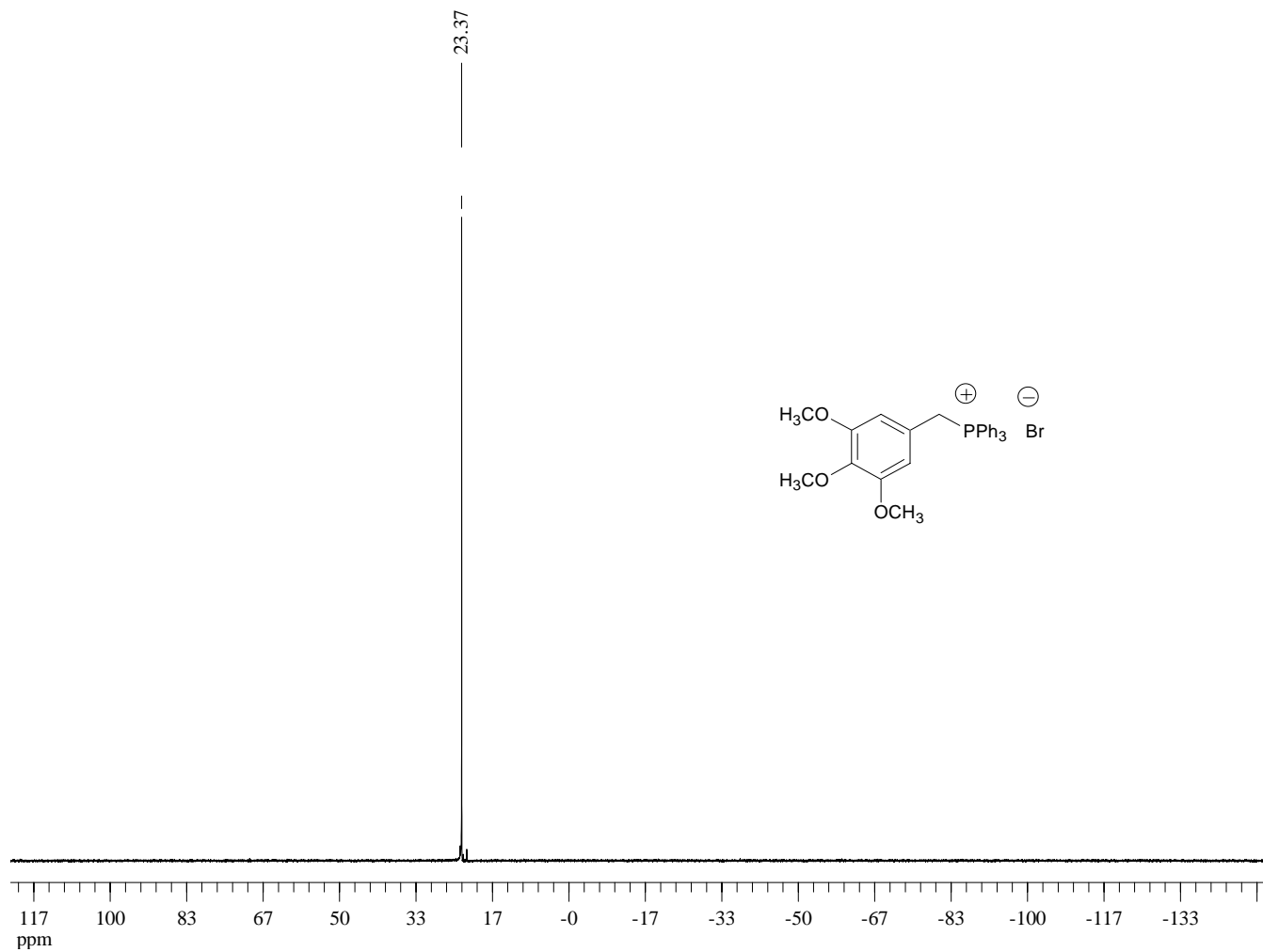
¹H-NMR (300 MHz, CDCl₃) of Compound **15**



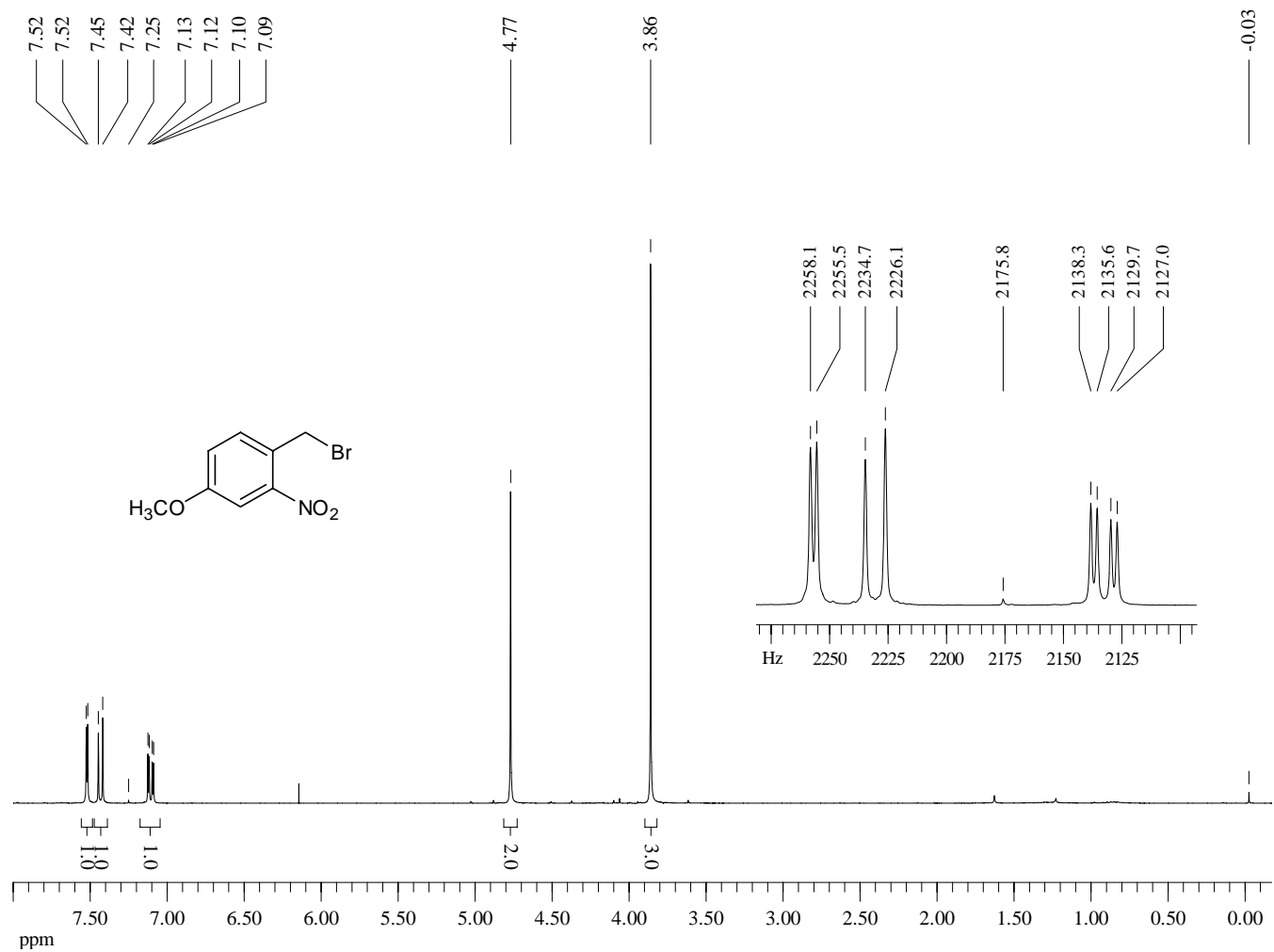
¹H-NMR (300 MHz, CDCl₃) of Compound 16



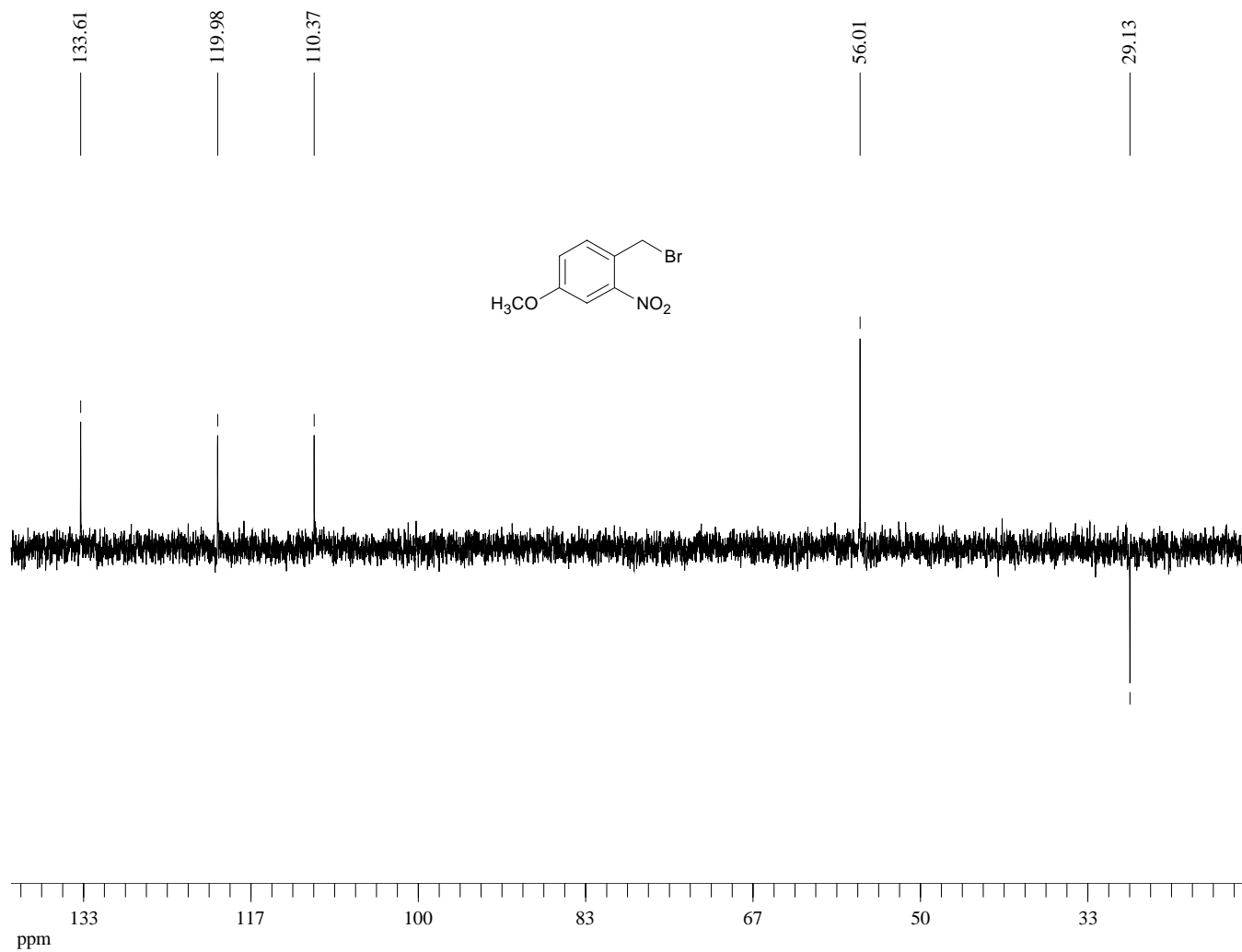
^{31}P -NMR (121 MHz, Acetone- d_6) of Compound **16**



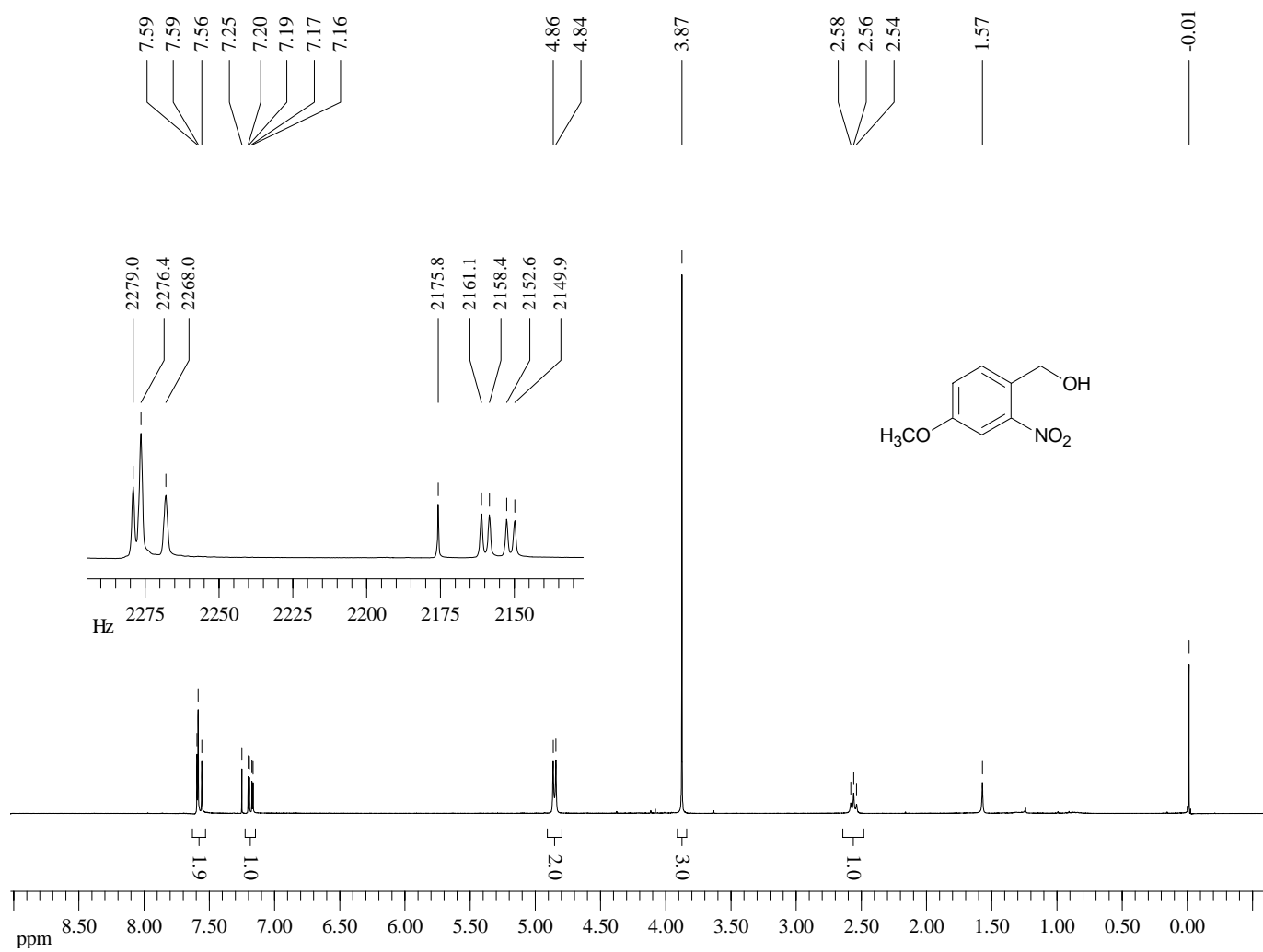
¹H-NMR (300 MHz, CDCl₃) of Compound **17**



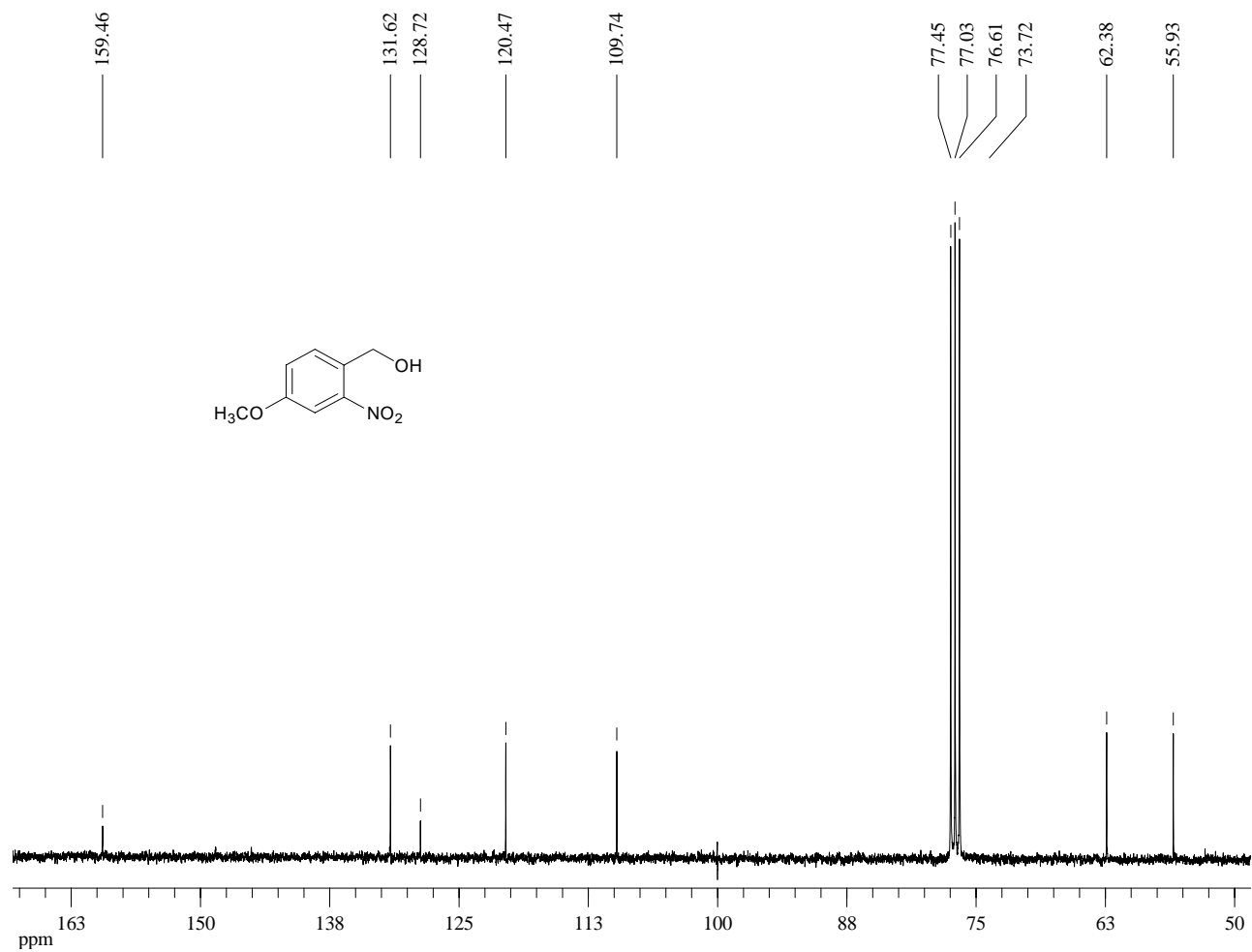
Dept 135-NMR (75 MHz, CDCl₃) of Compound 17



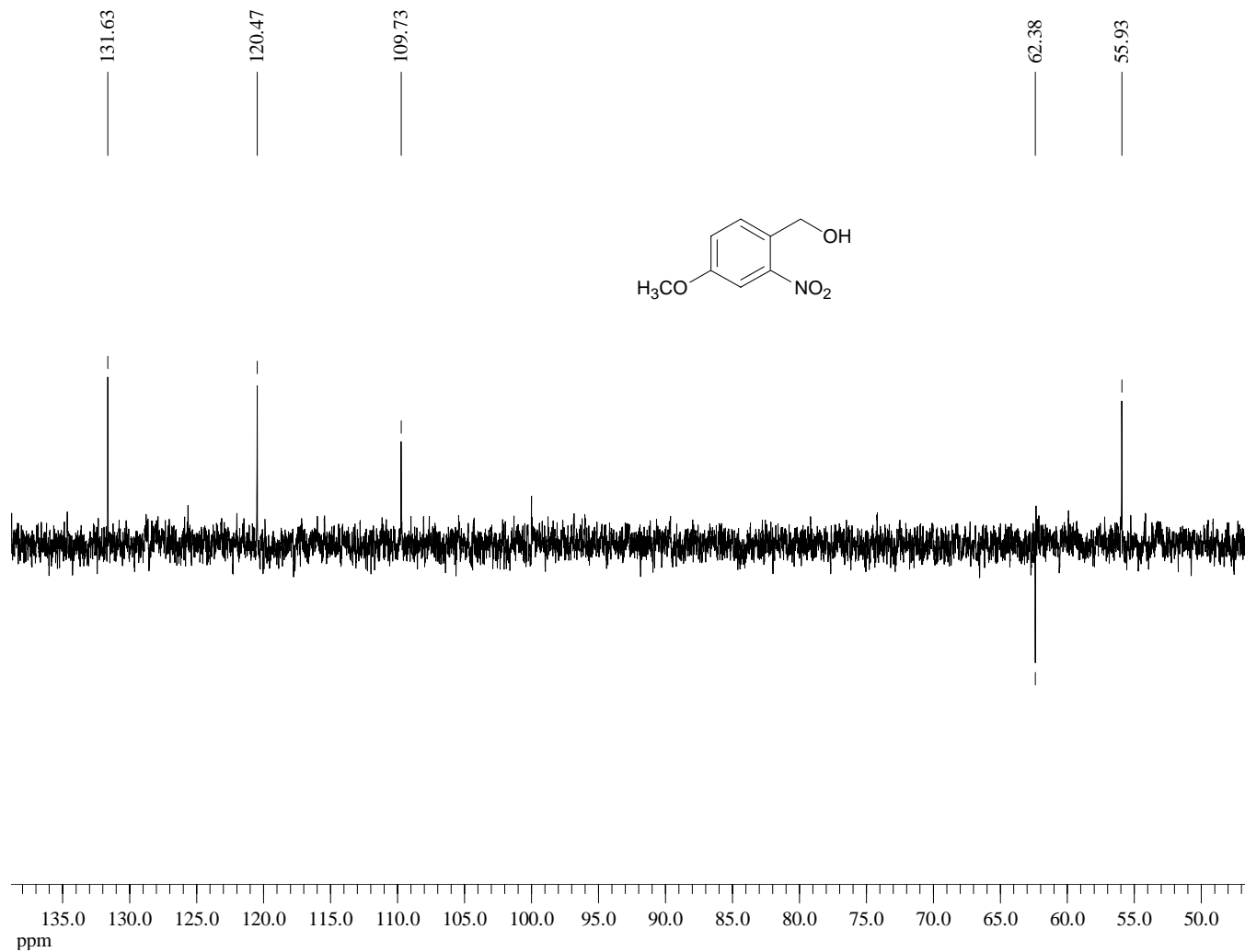
¹H-NMR (300 MHz, CDCl₃) of Compound **18**



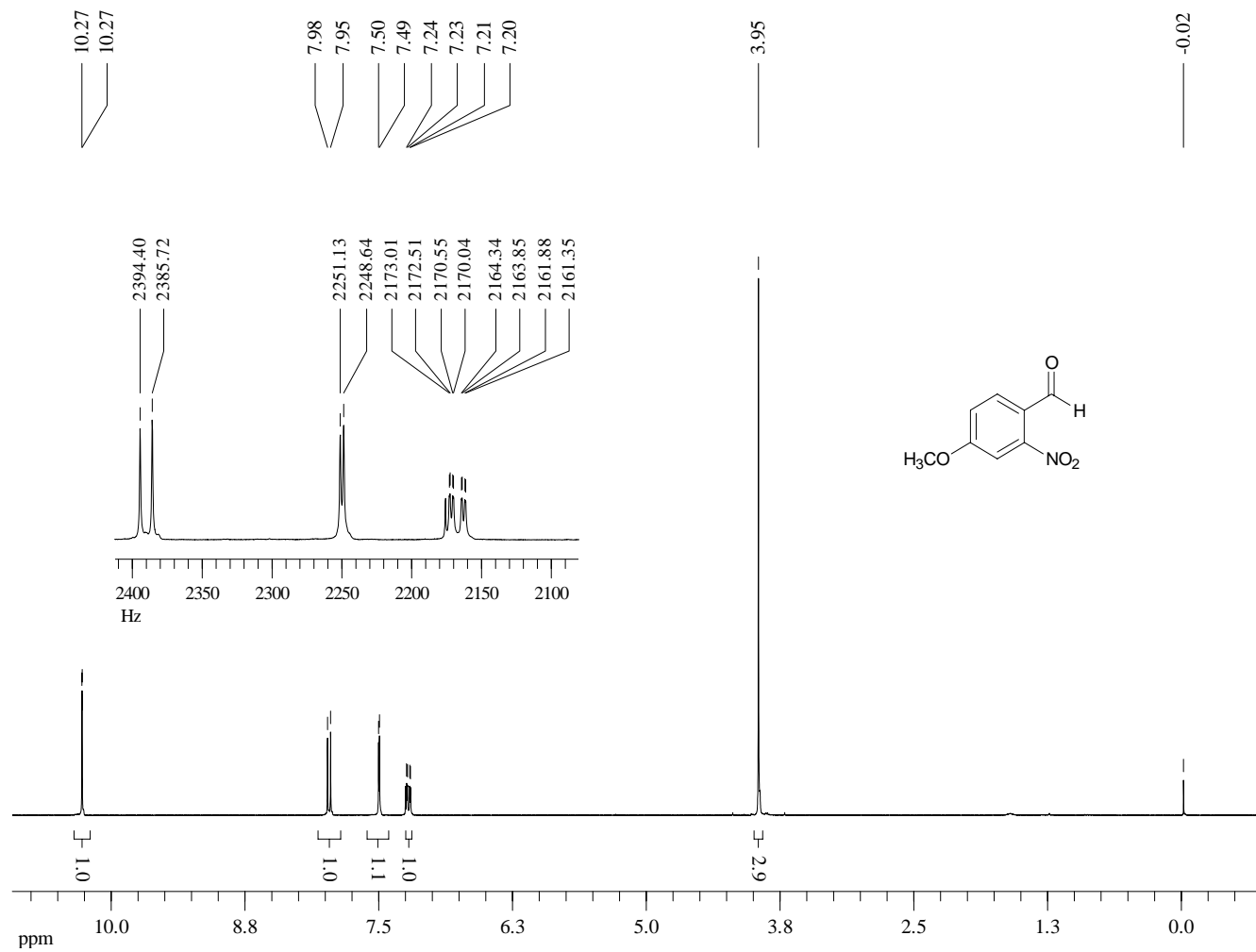
^{13}C -NMR (75 MHz, CDCl_3) of Compound **18**



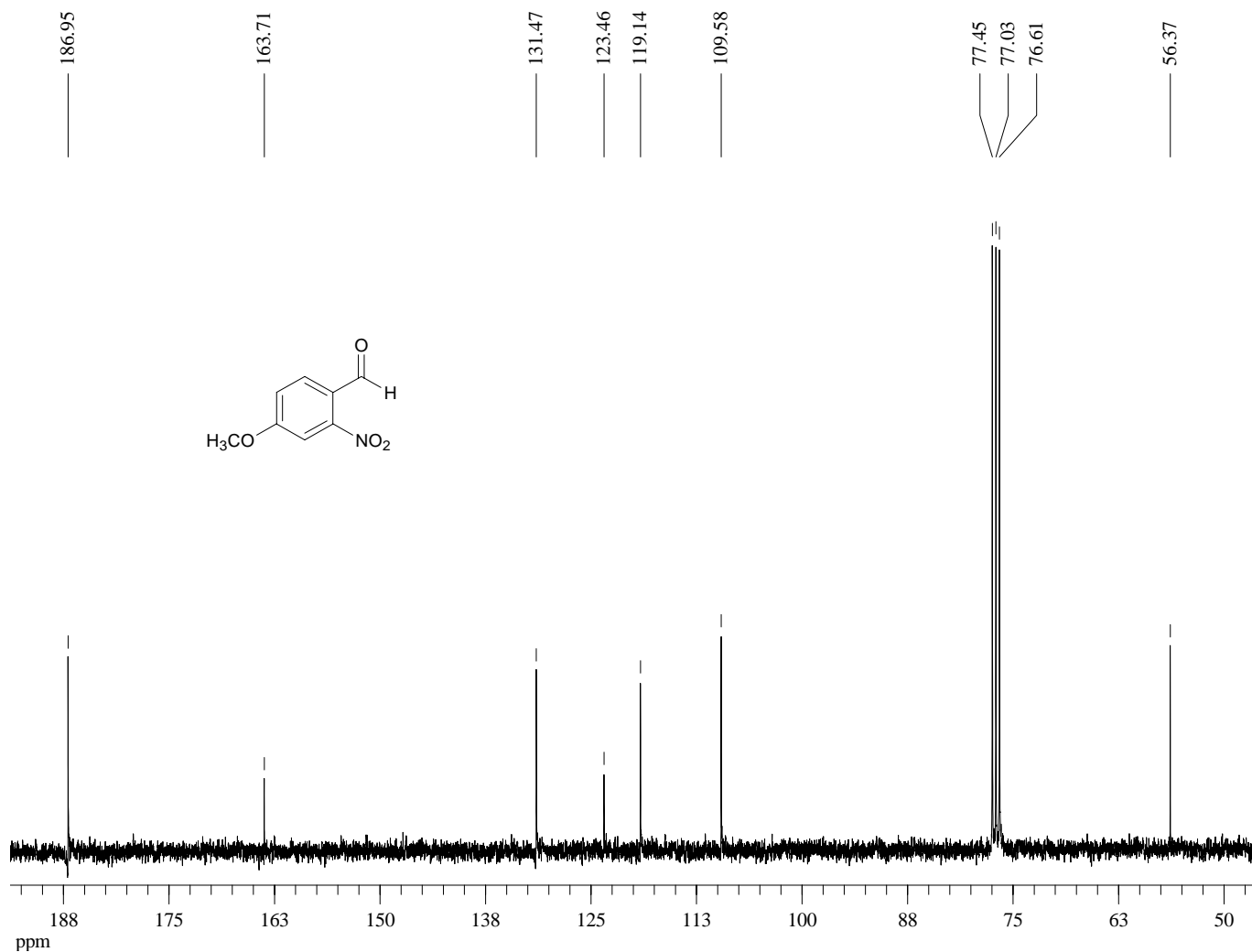
Dept 135-NMR (75 MHz, CDCl₃) of Compound 18



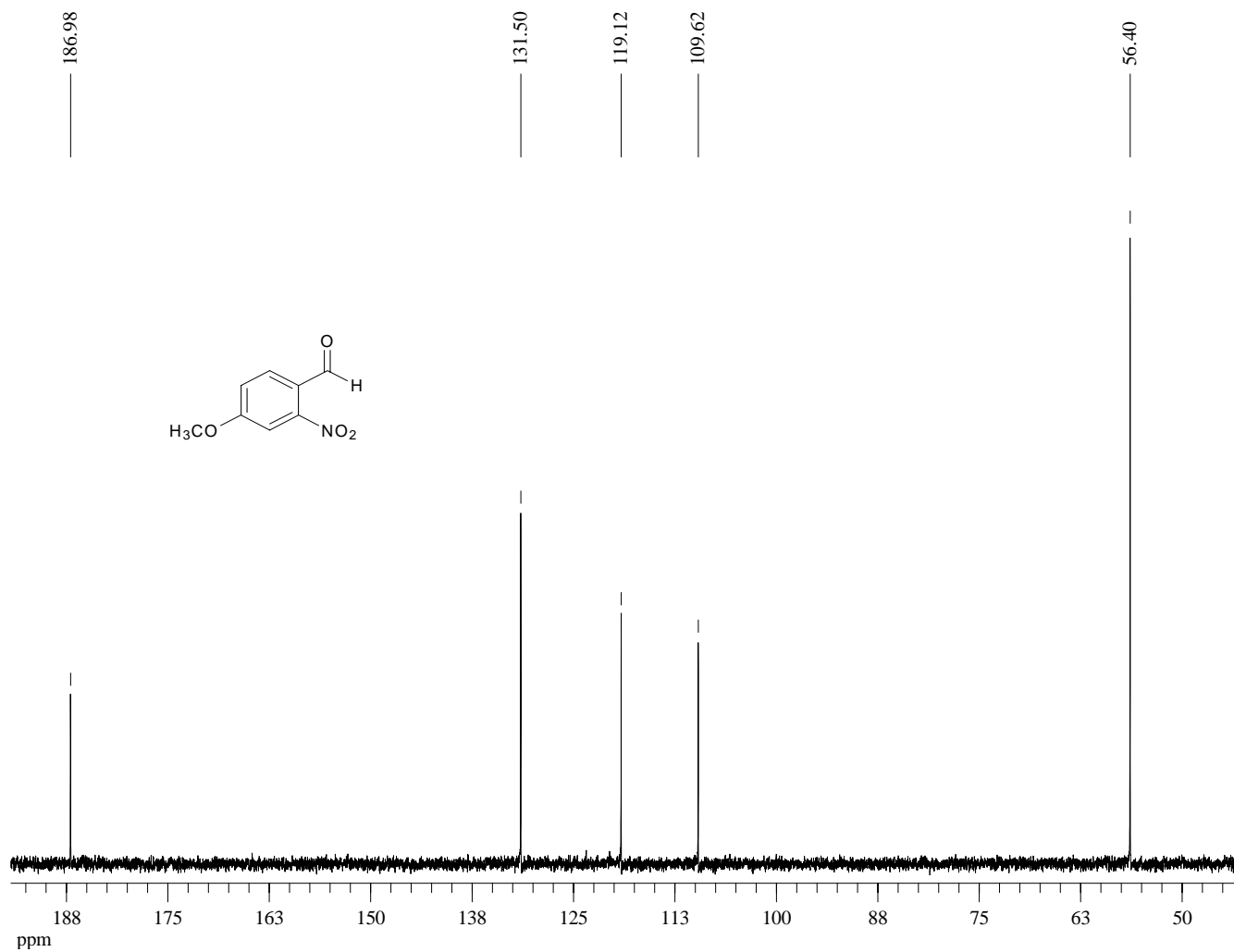
¹H-NMR (300 MHz, CDCl₃) of Compound **19**



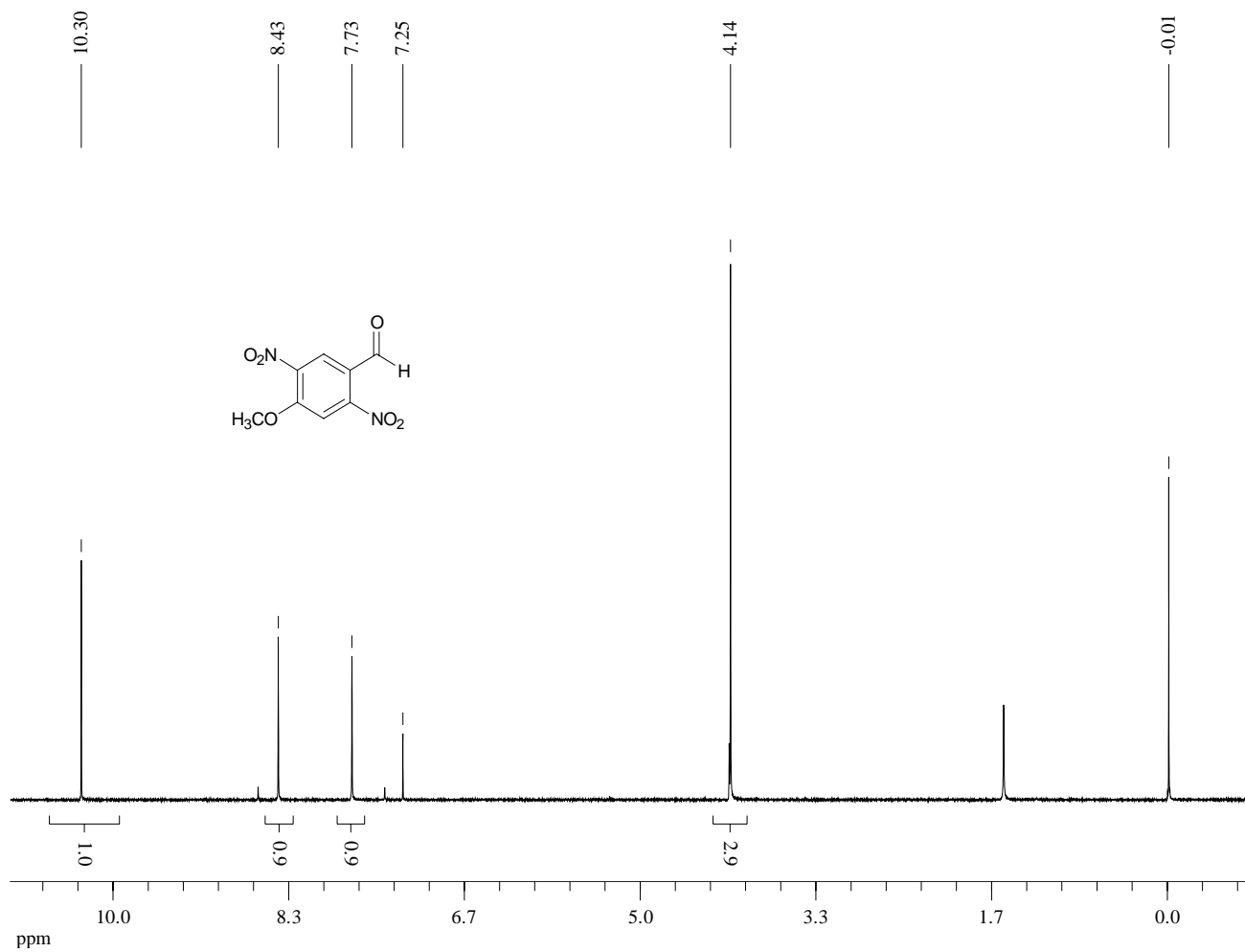
¹³C-NMR (75 MHz, CDCl₃) of Compound **19**



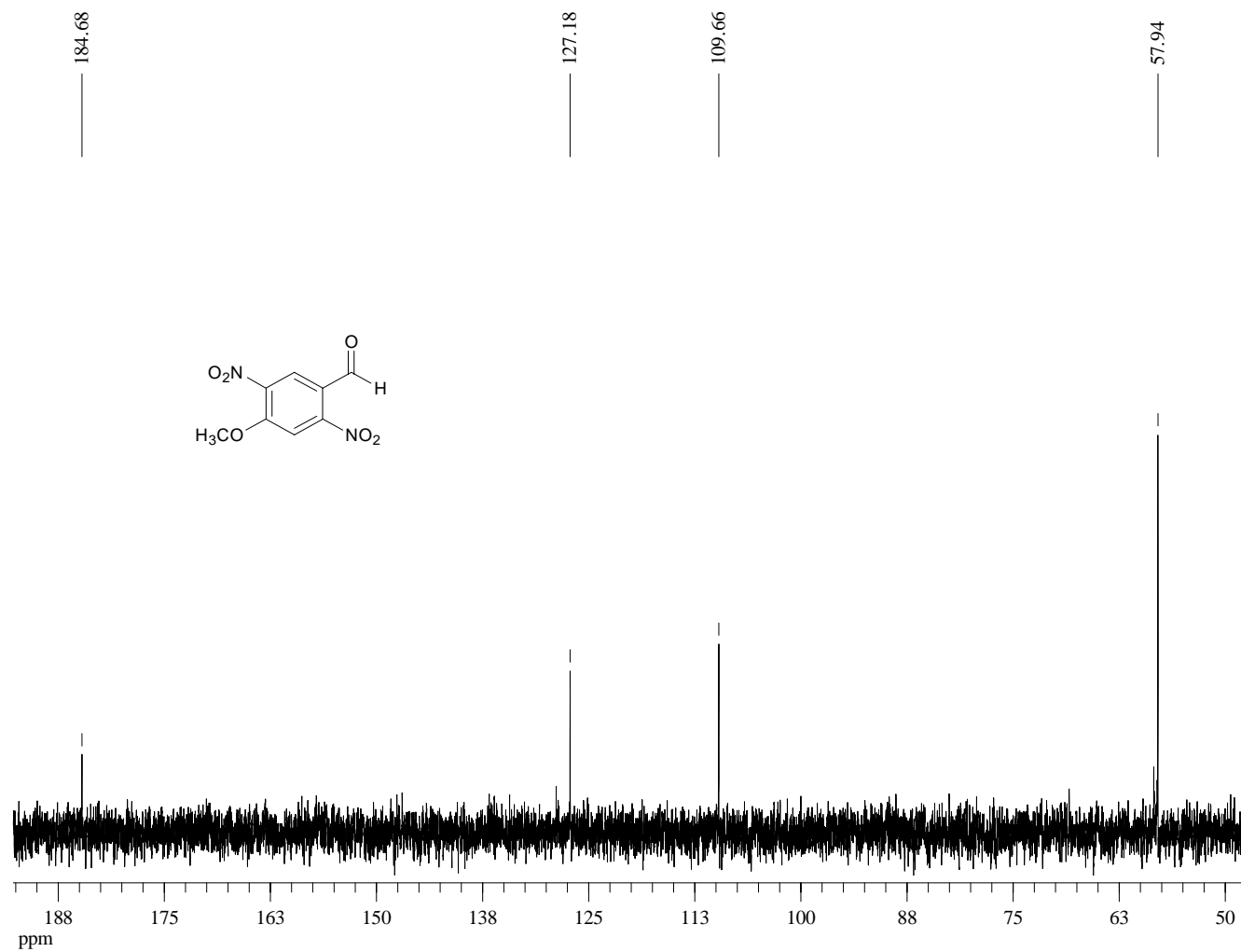
Dept 45-NMR (75 MHz, CDCl₃) of Compound **19**



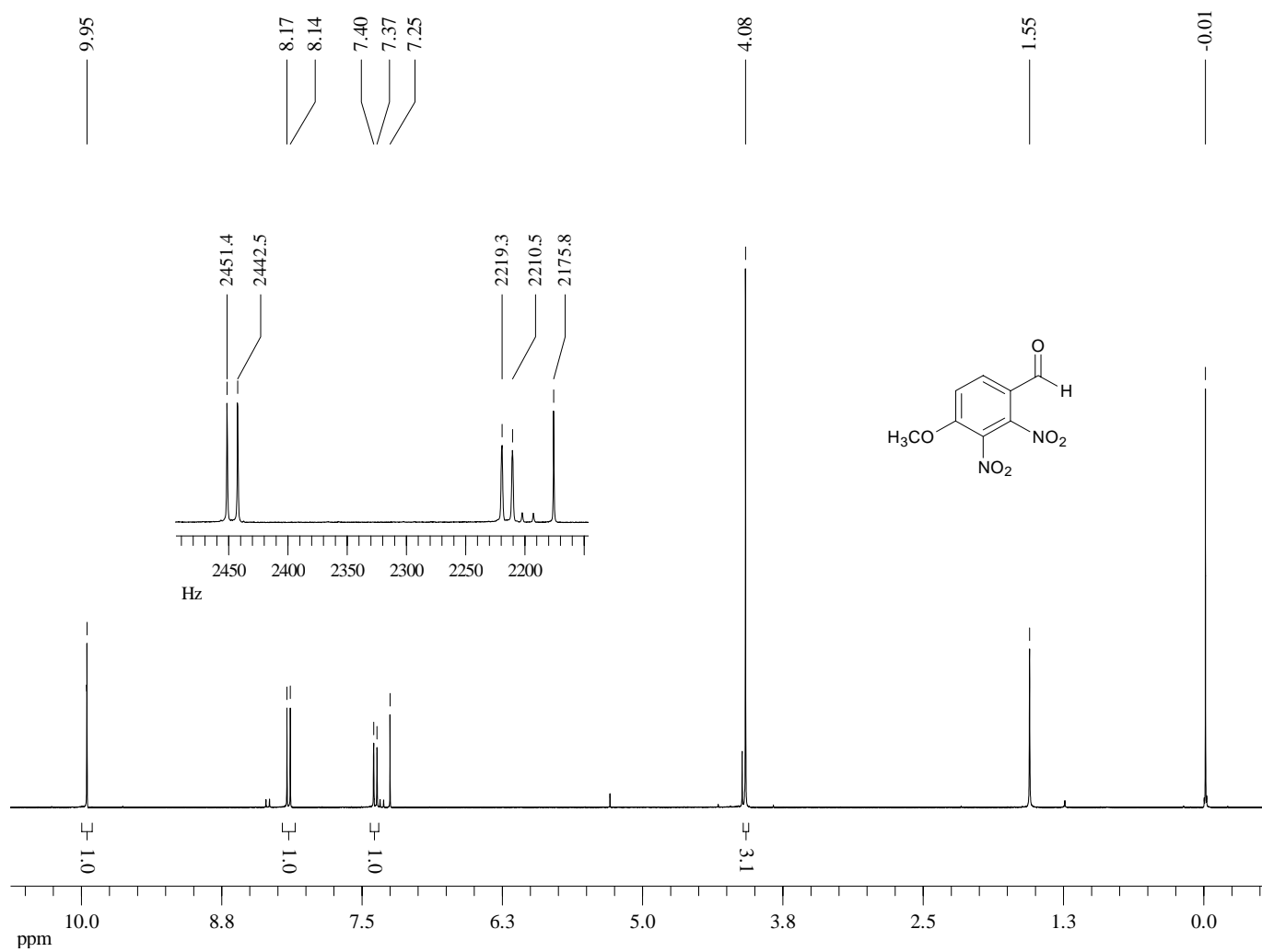
¹H-NMR (300 MHz, CDCl₃) of Compound **20a**



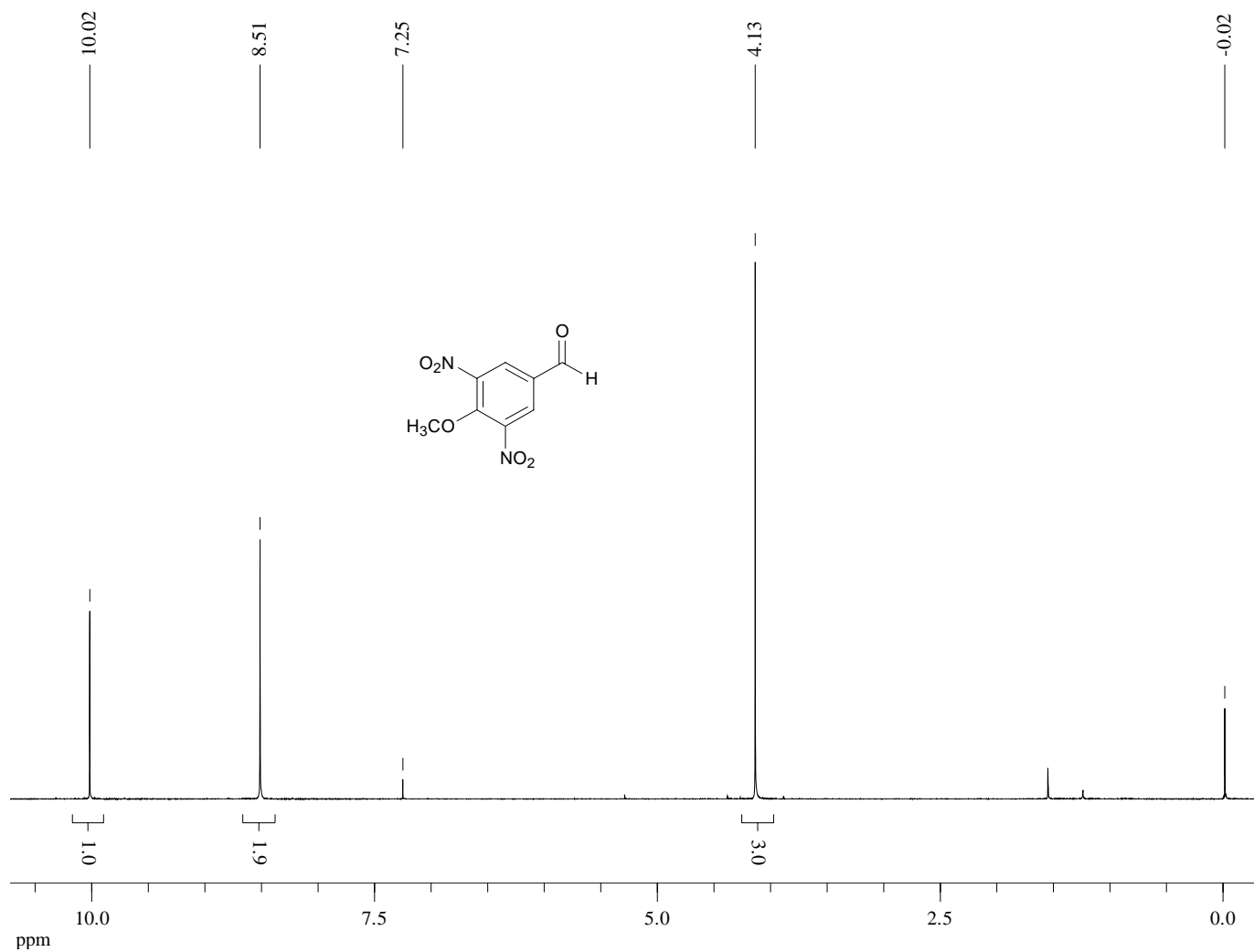
Dept 45-NMR (75 MHz, CDCl₃) of Compound **20a**



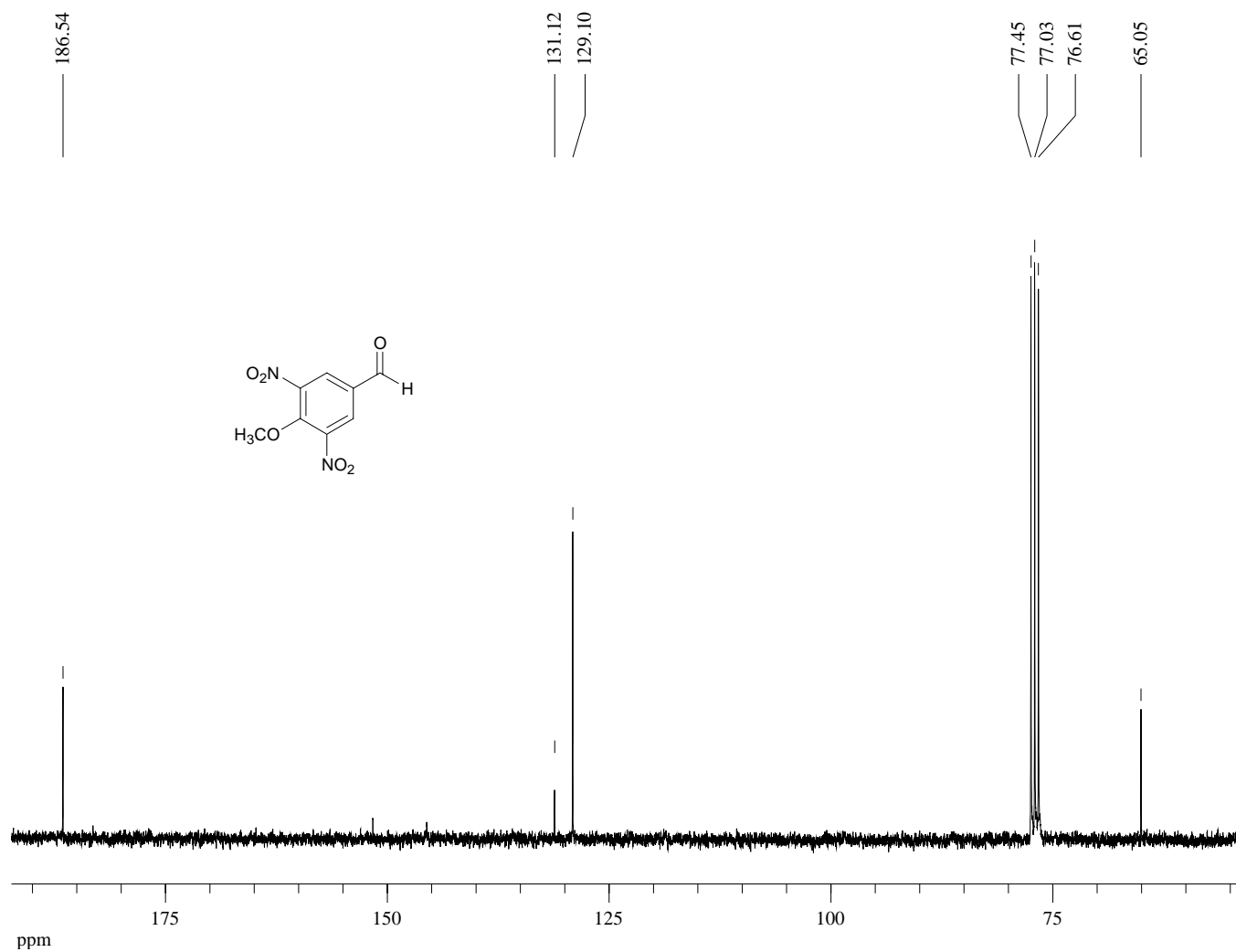
¹H-NMR (300 MHz, CDCl₃) of Compound **20b**



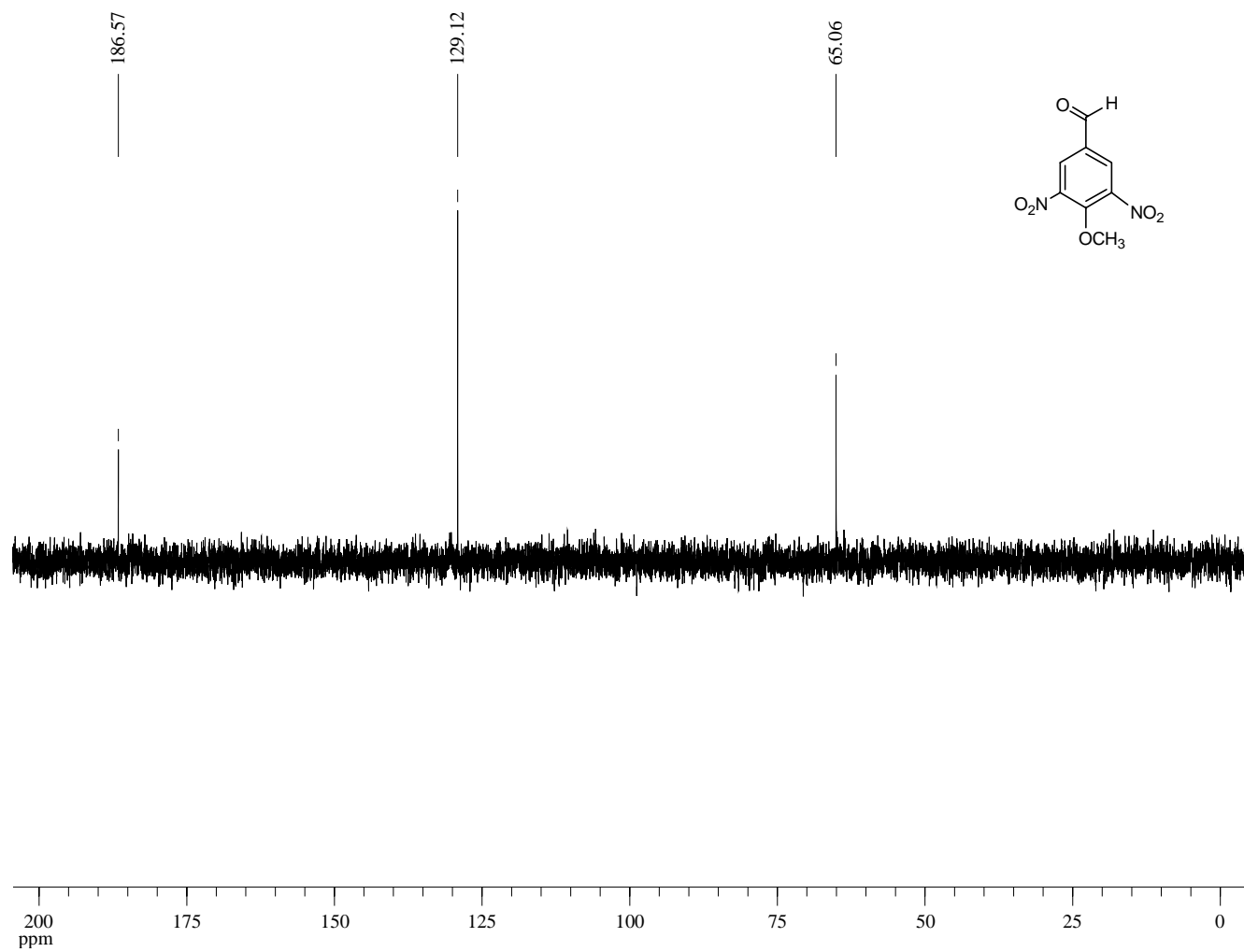
¹H-NMR (300 MHz, CDCl₃) of Compound **21**



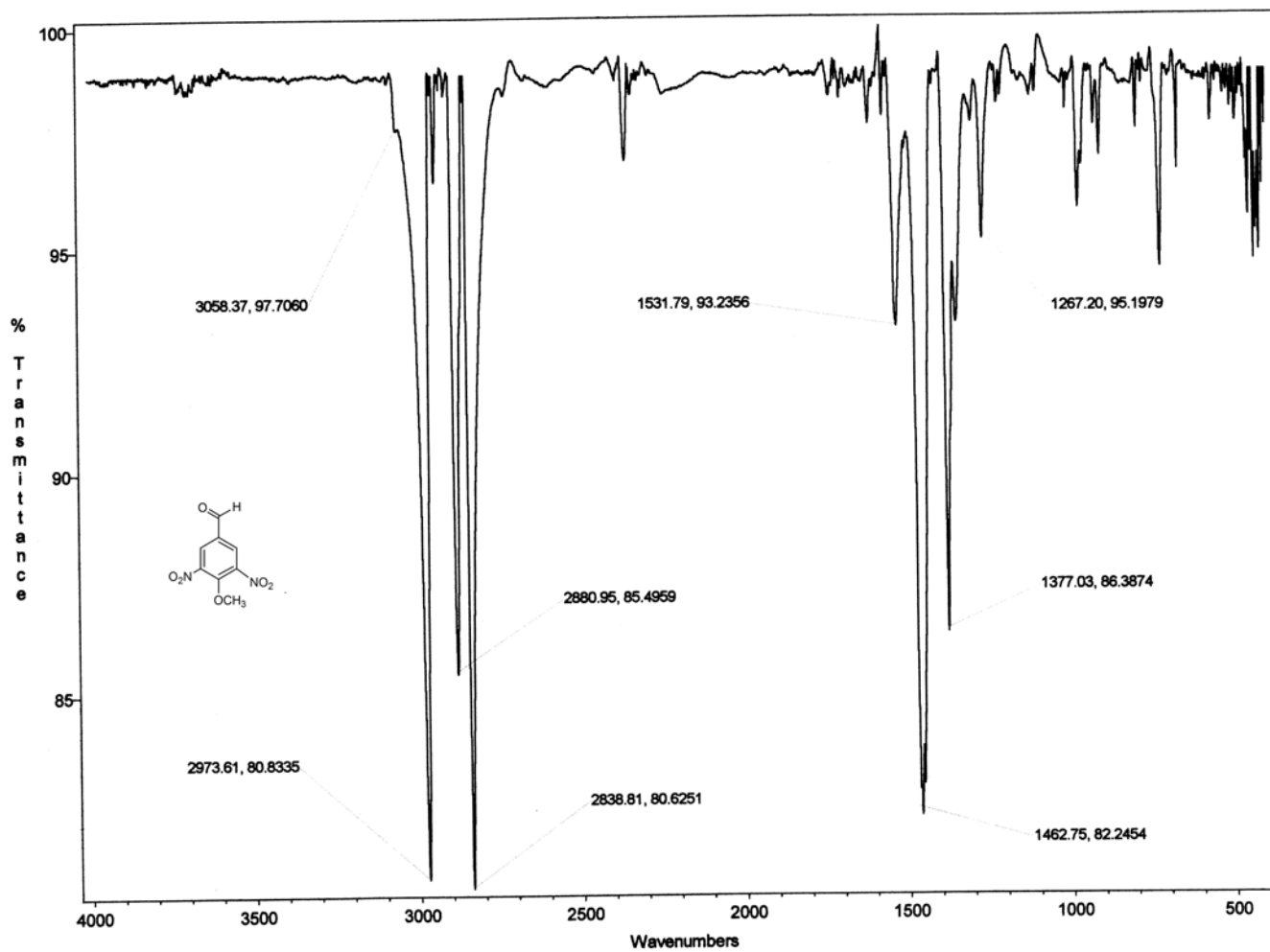
^{13}C -NMR (75 MHz, CDCl_3) of Compound **21**



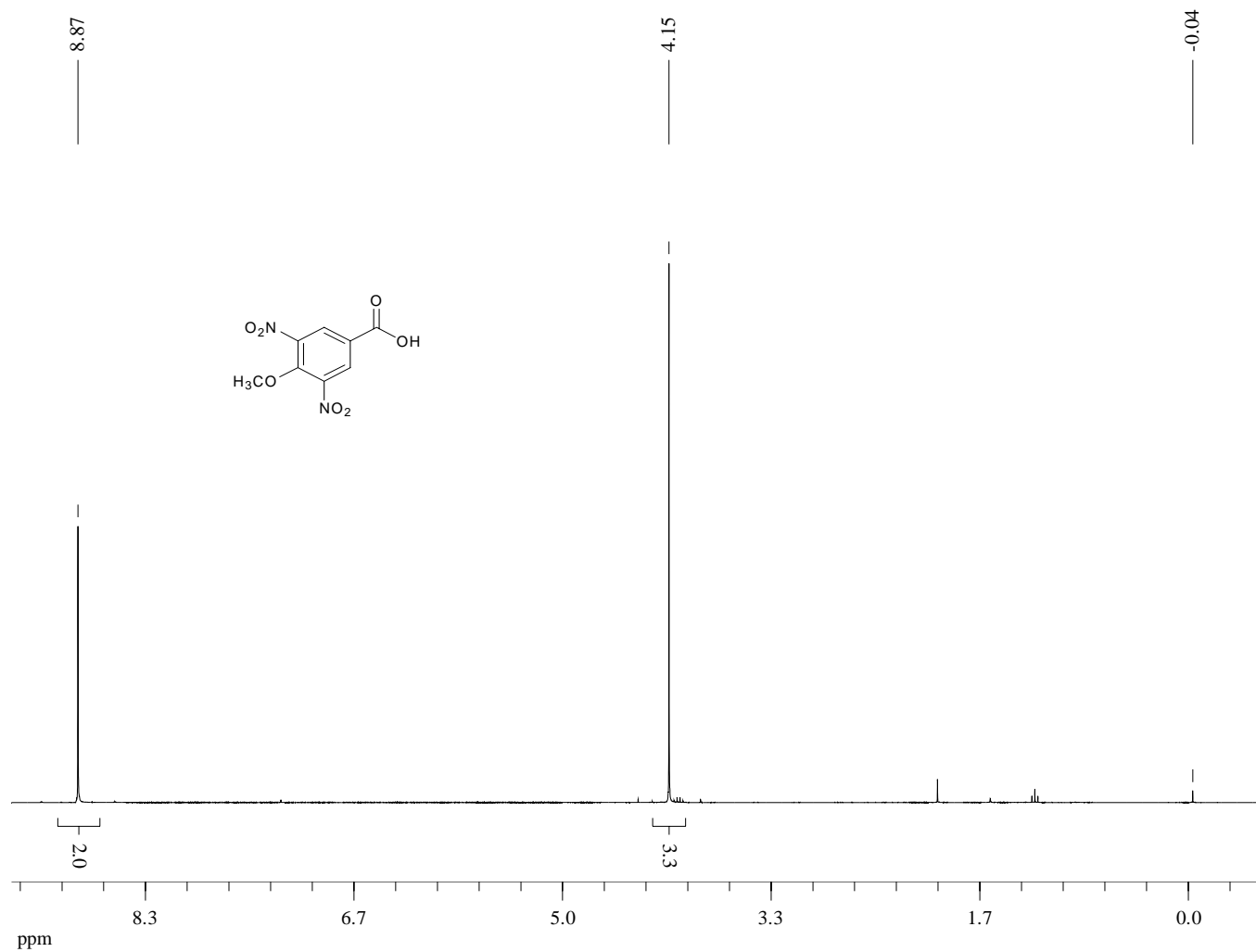
Dept 135-NMR (75 MHz, CDCl₃) of Compound 21



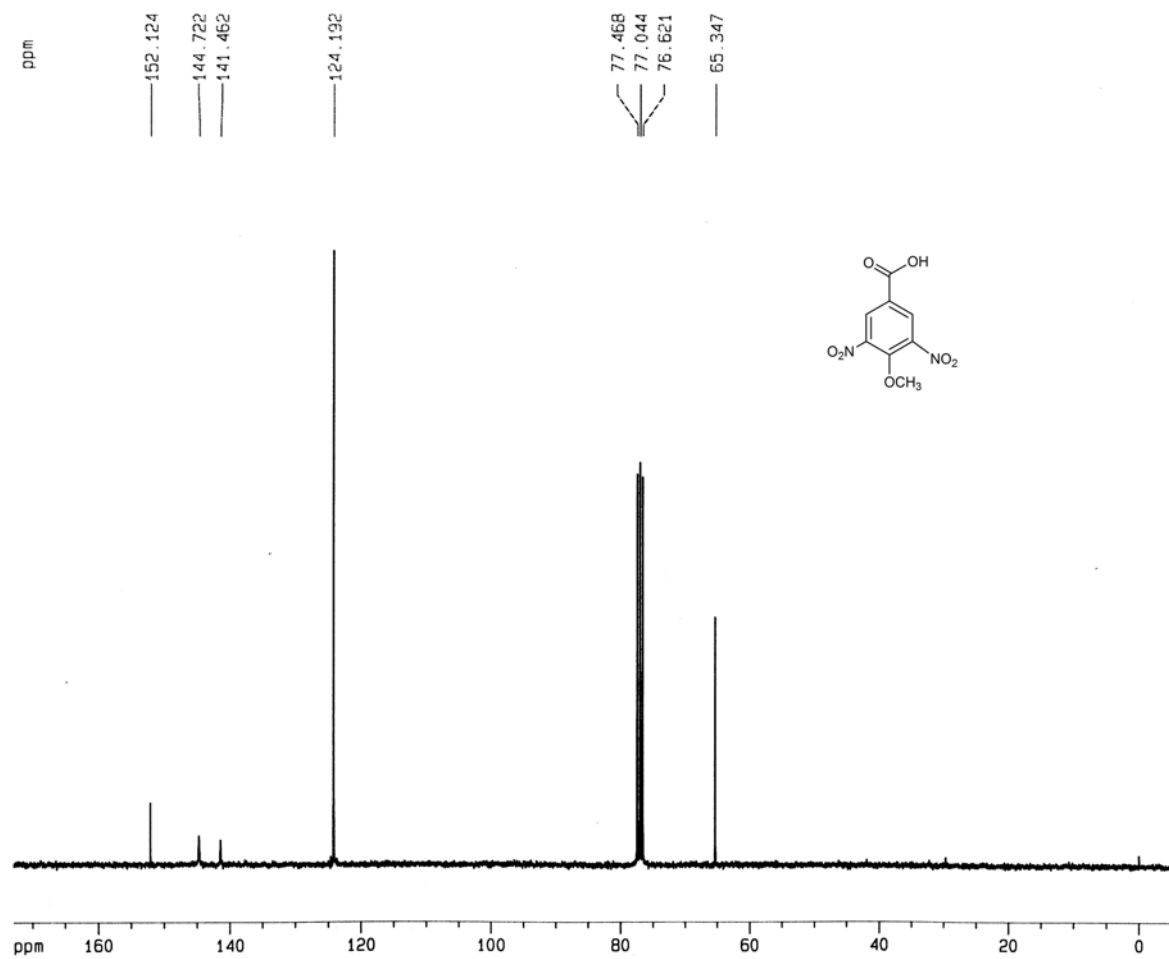
Infrared Spectrum (nujol, cm^{-1}) of Compound **21**



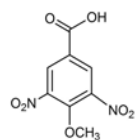
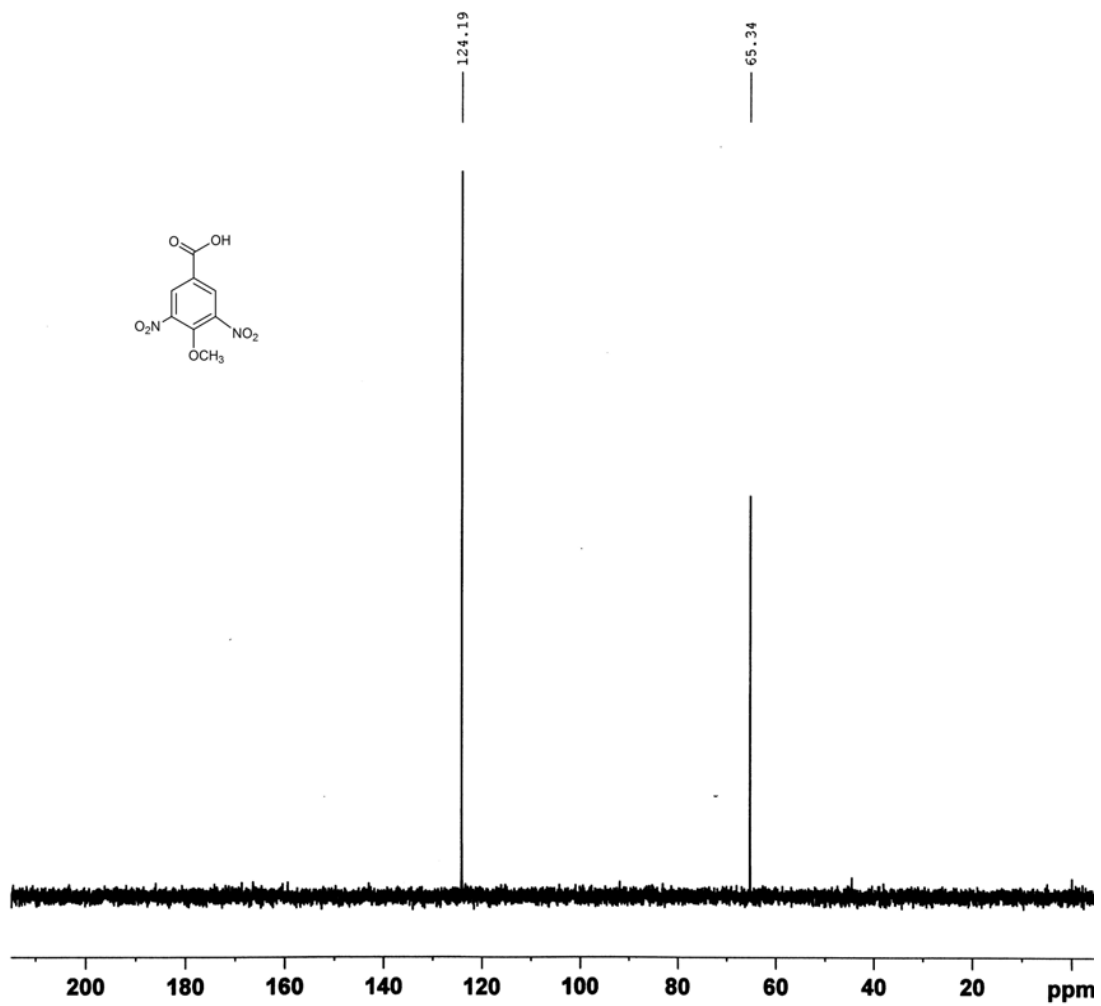
¹H-NMR (300 MHz, CDCl₃) of Compound **21a**



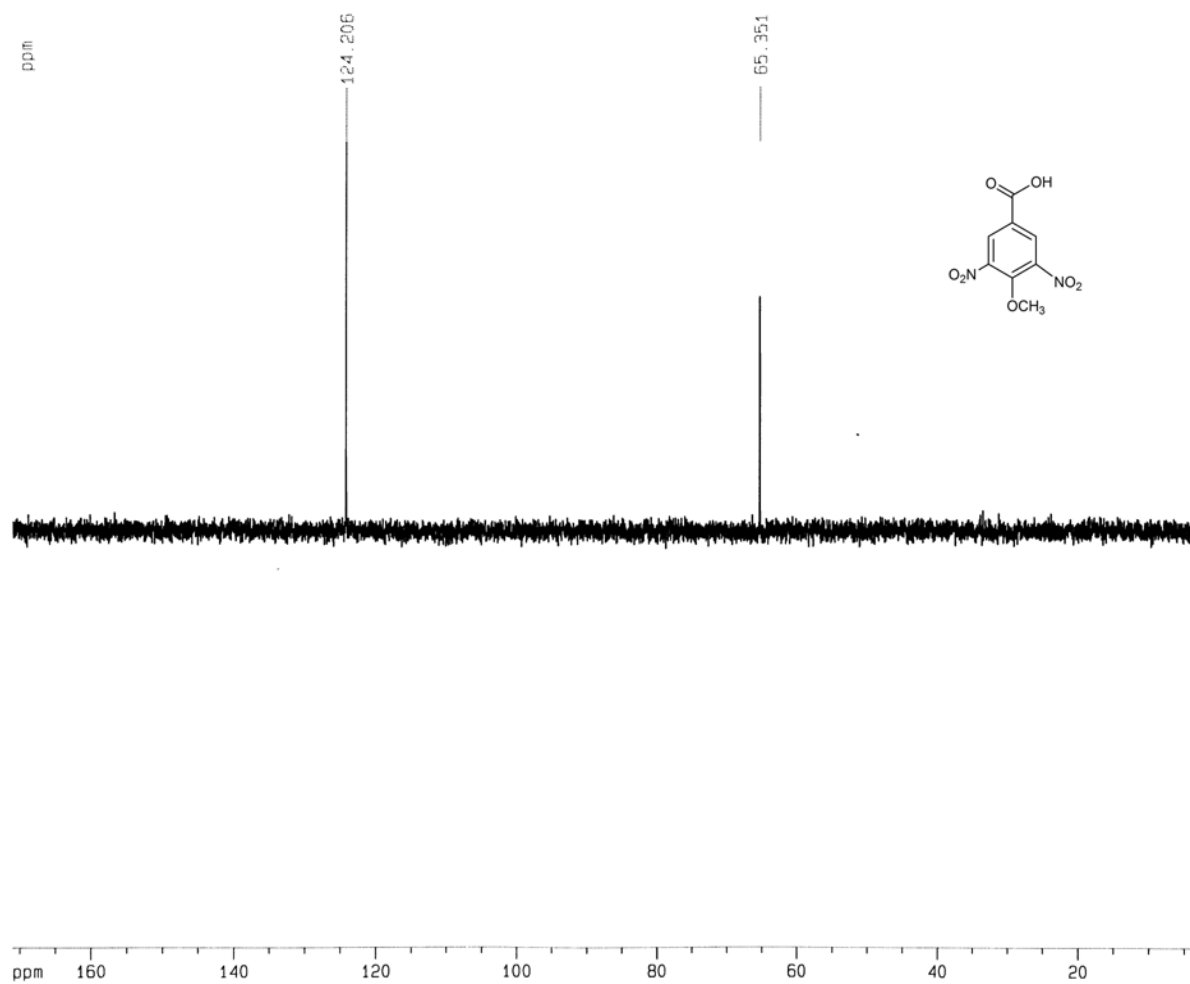
^{13}C -NMR (75 MHz, CDCl_3) of Compound **21a**



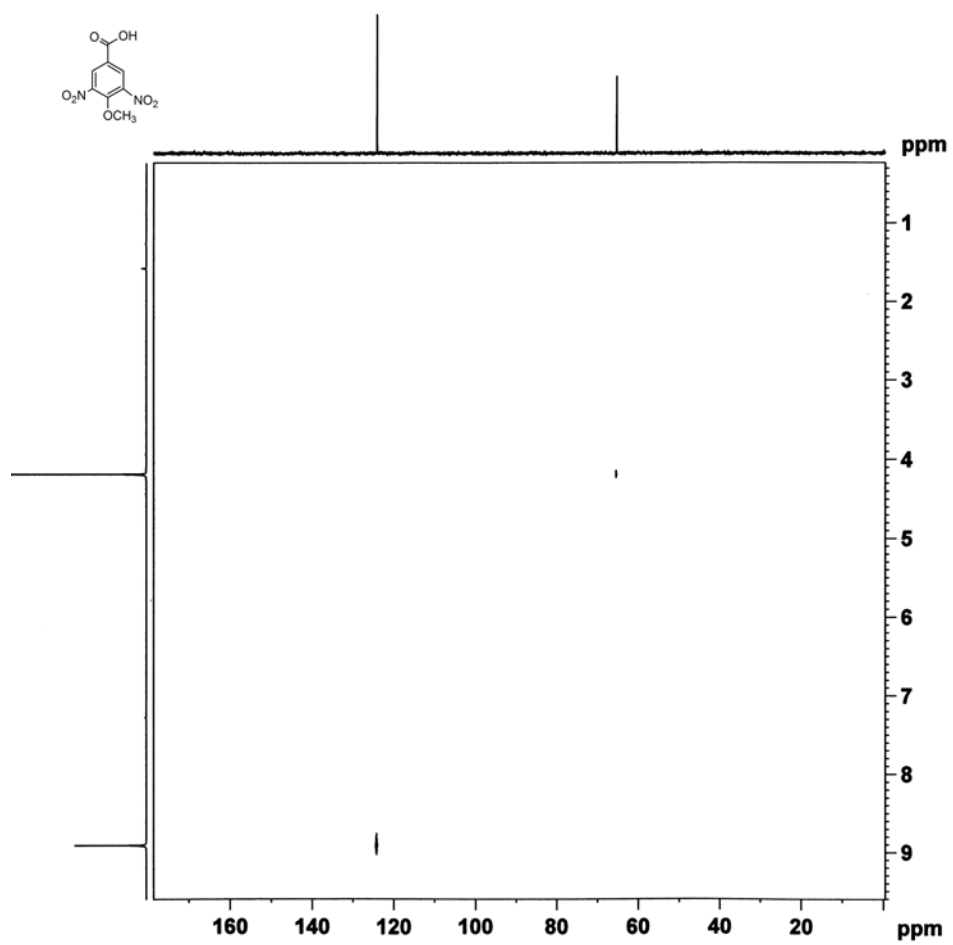
Dept 45-NMR (75 MHz, CDCl₃) of Compound **21a**



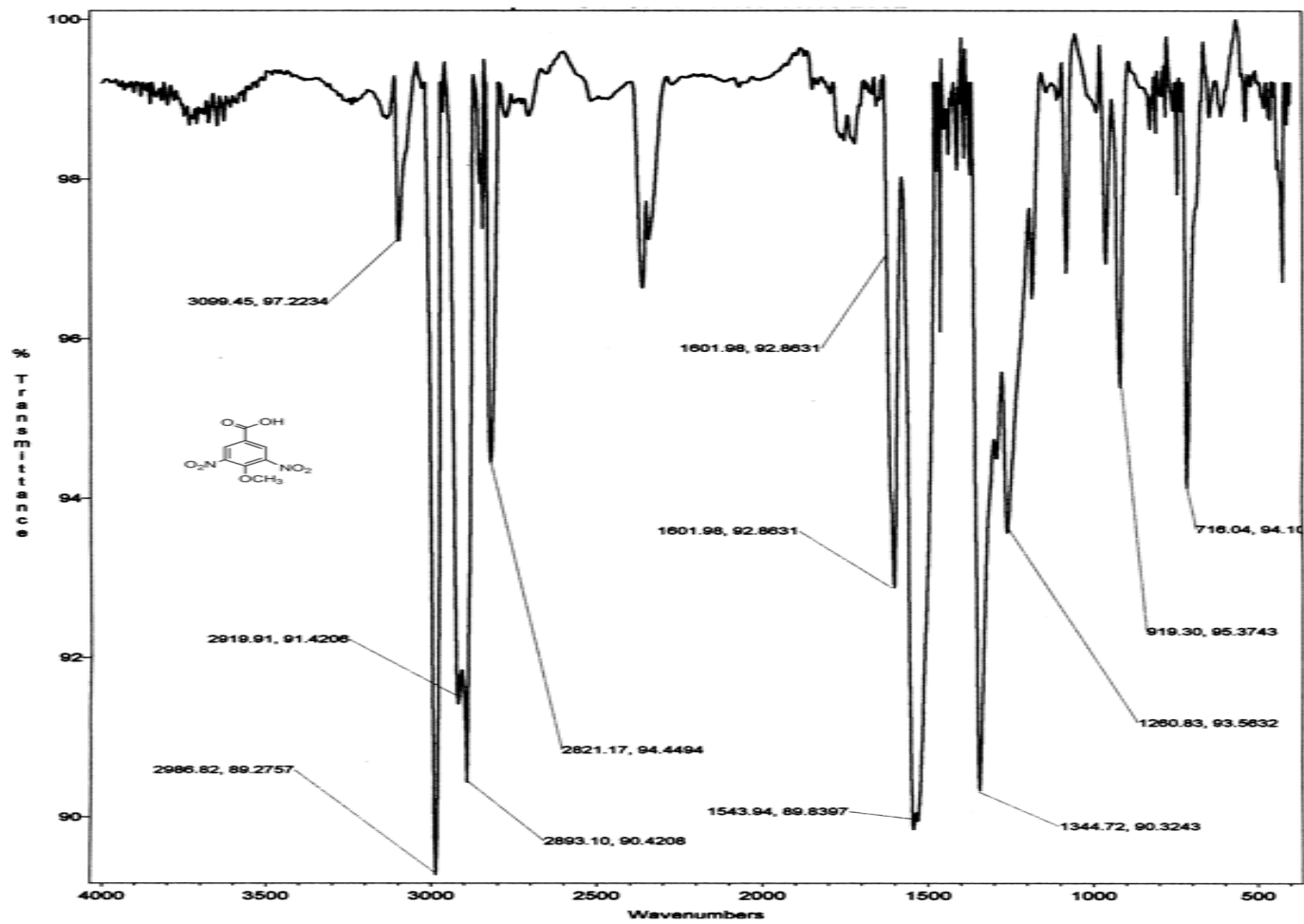
Dept 135-NMR (75 MHz, CDCl₃) of Compound **21a**



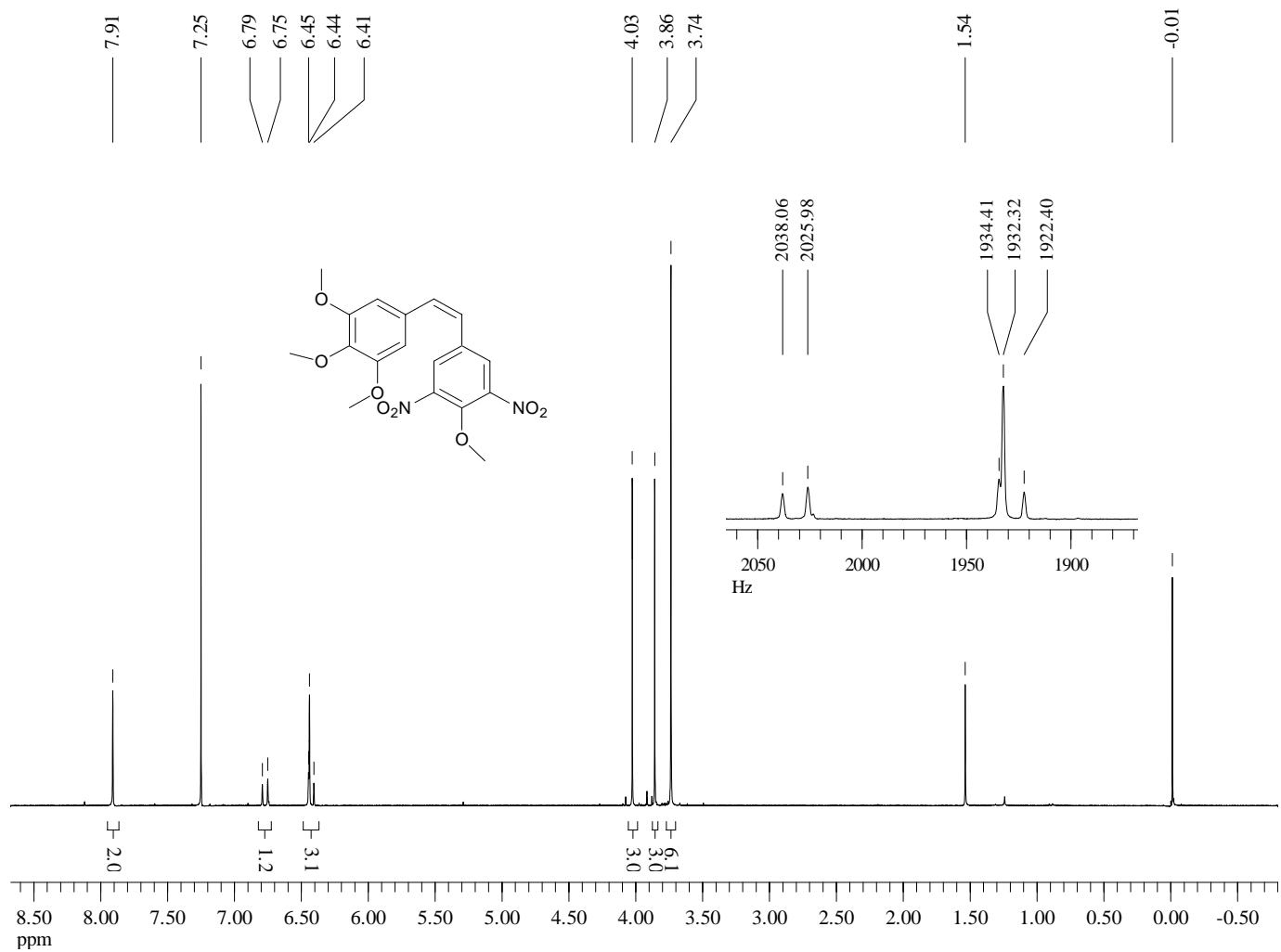
COSY- ^1H - ^{13}C NMR (75 MHz, CDCl_3) of Compound **21a**



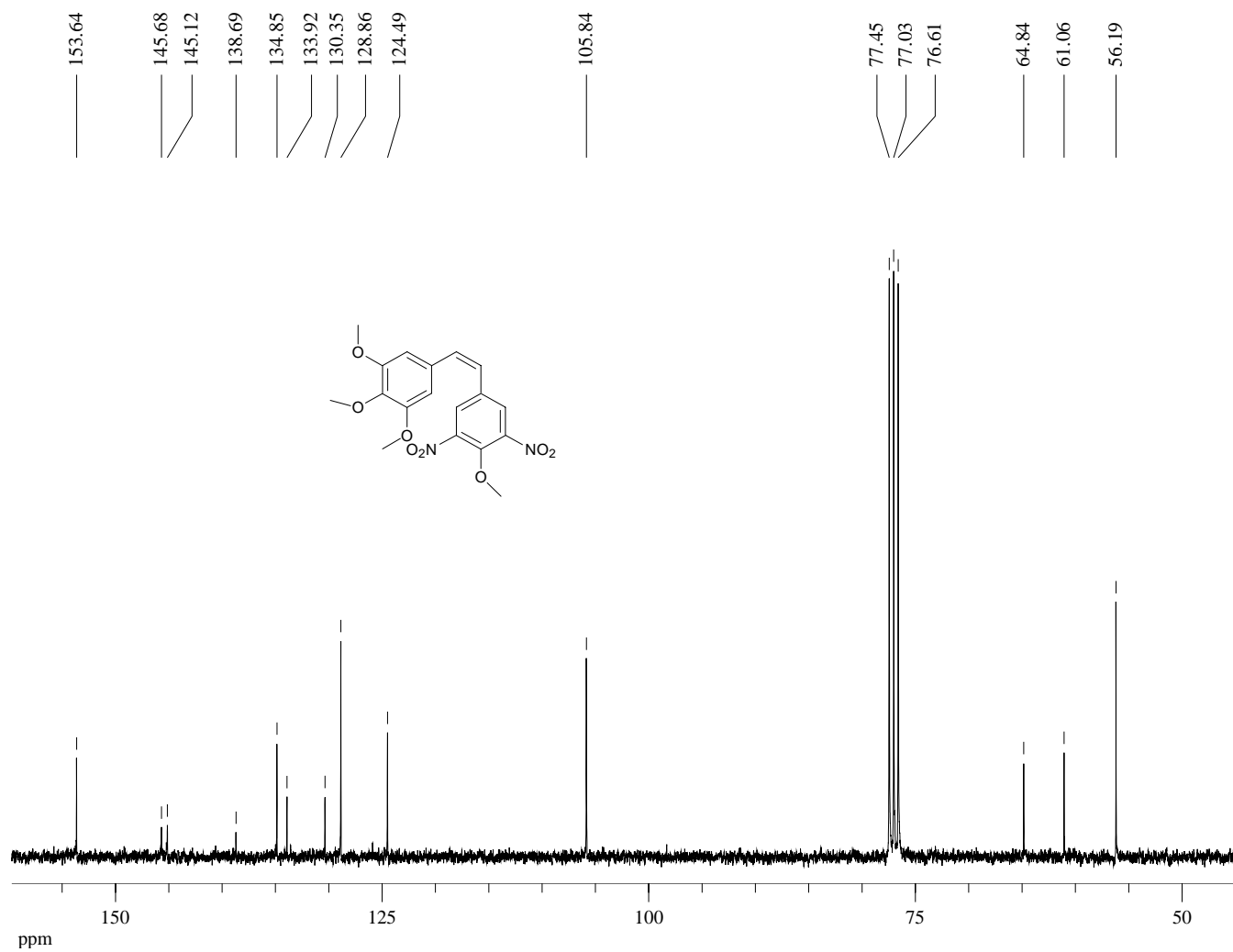
Infrared Spectrum (Nujol, cm^{-1}) of Compound 21a



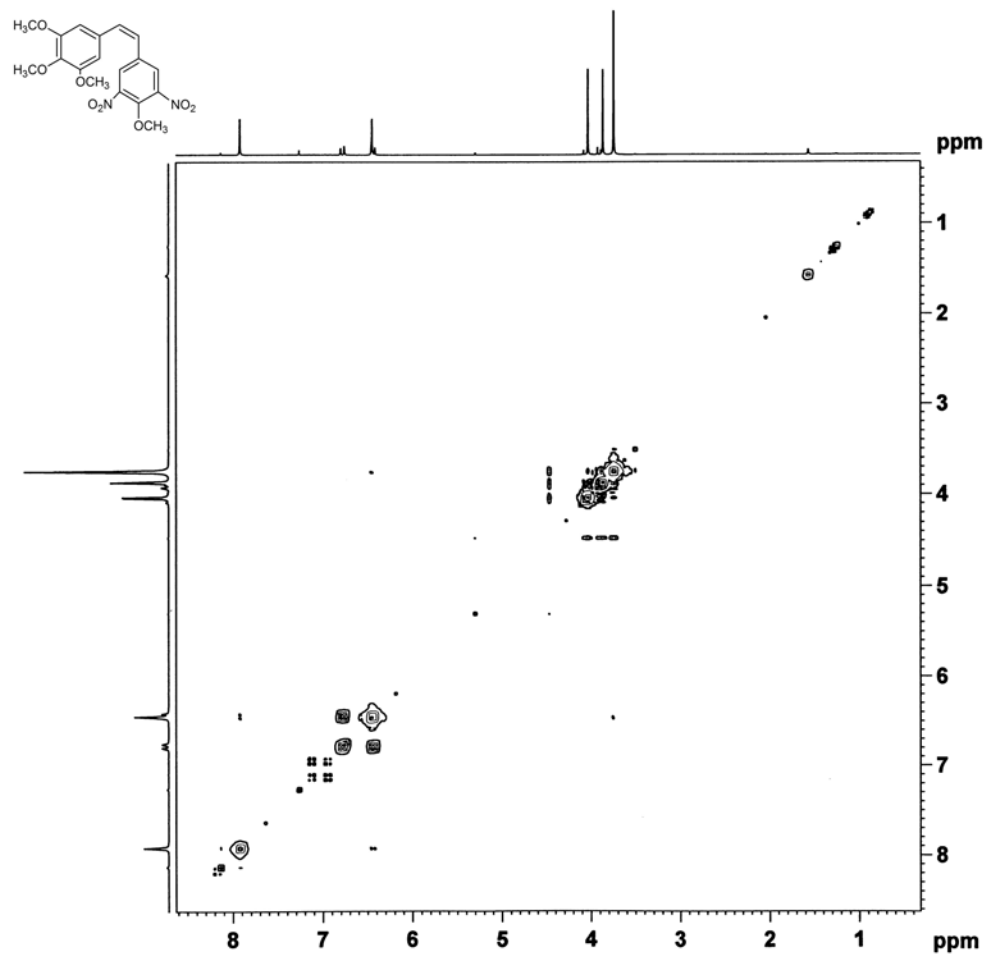
¹H-NMR (300 MHz, CDCl₃) of Compound **22**



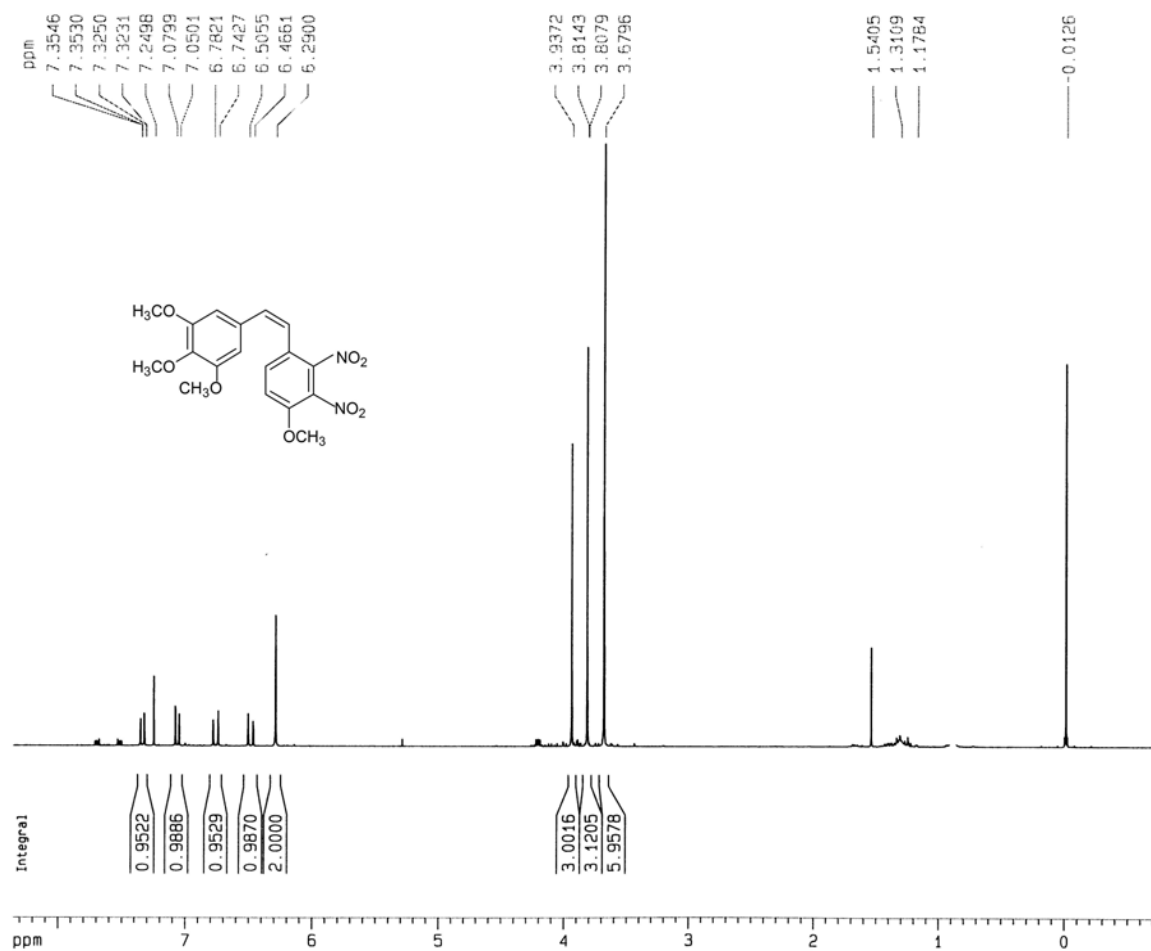
¹³C-NMR (75 MHz, CDCl₃) of Compound **22**



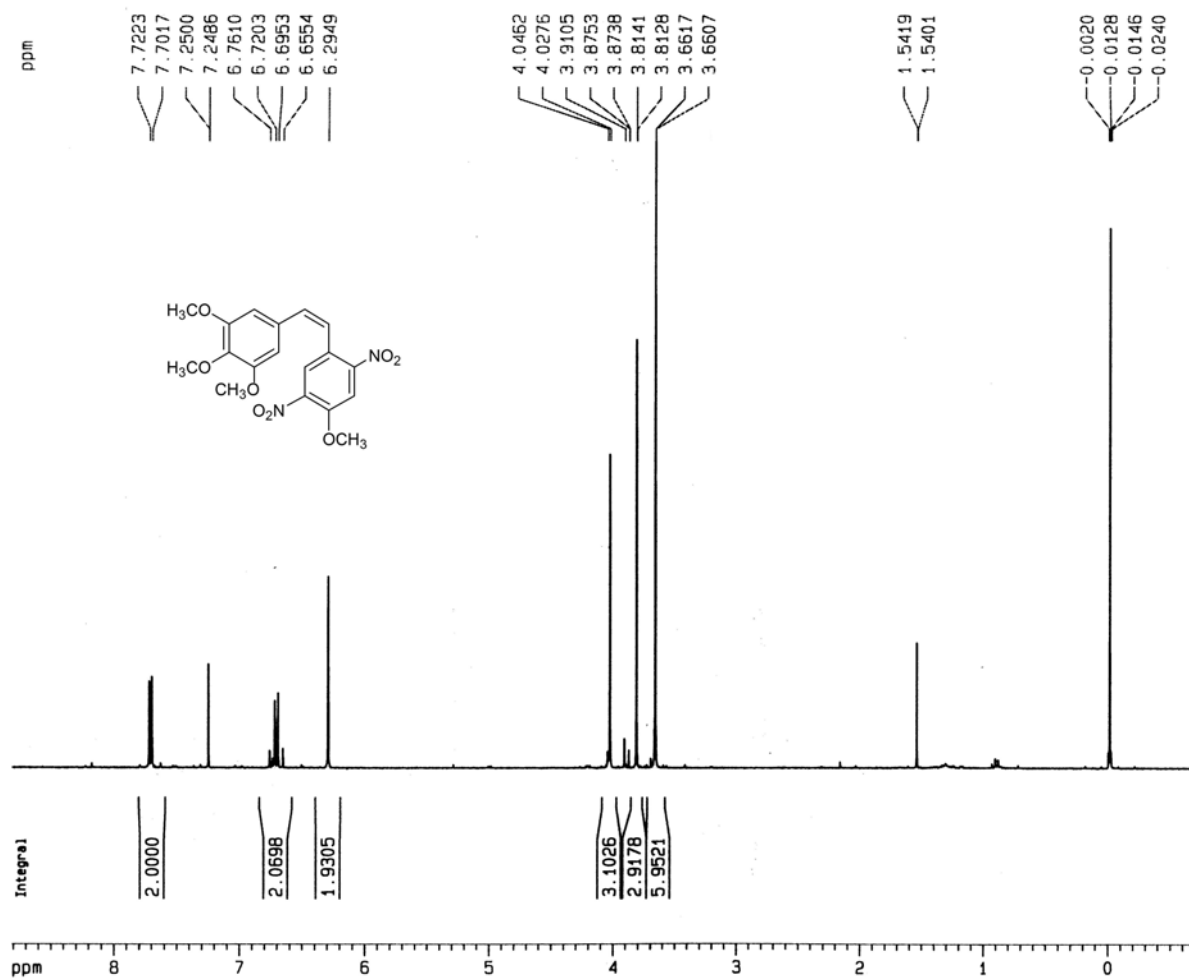
COSY-¹H-¹H NMR (75 MHz, CDCl₃) of Compound 22



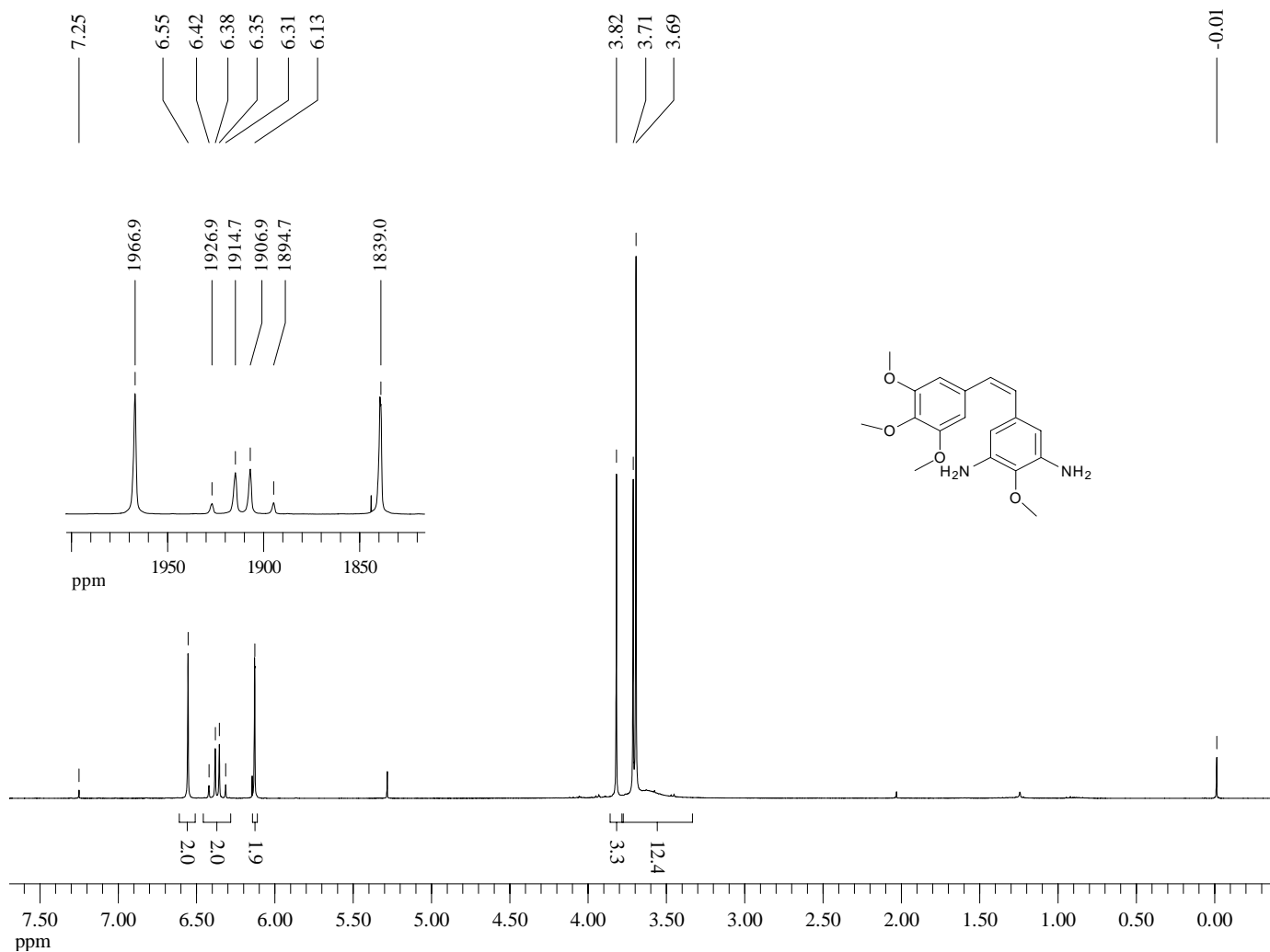
¹H-NMR (300 MHz, CDCl₃) of Compound **23**



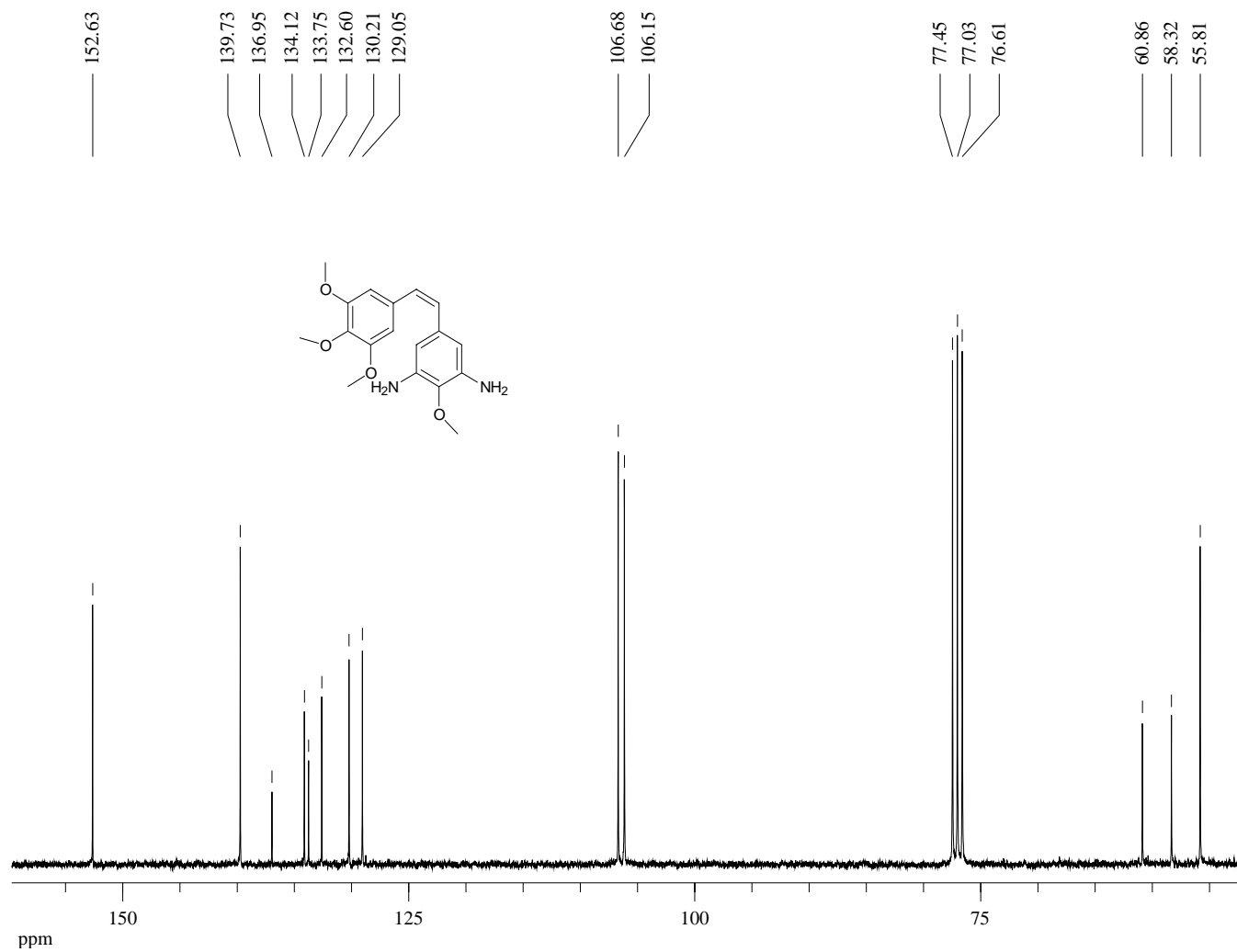
¹H-NMR (300 MHz, CDCl₃) of Compound 24



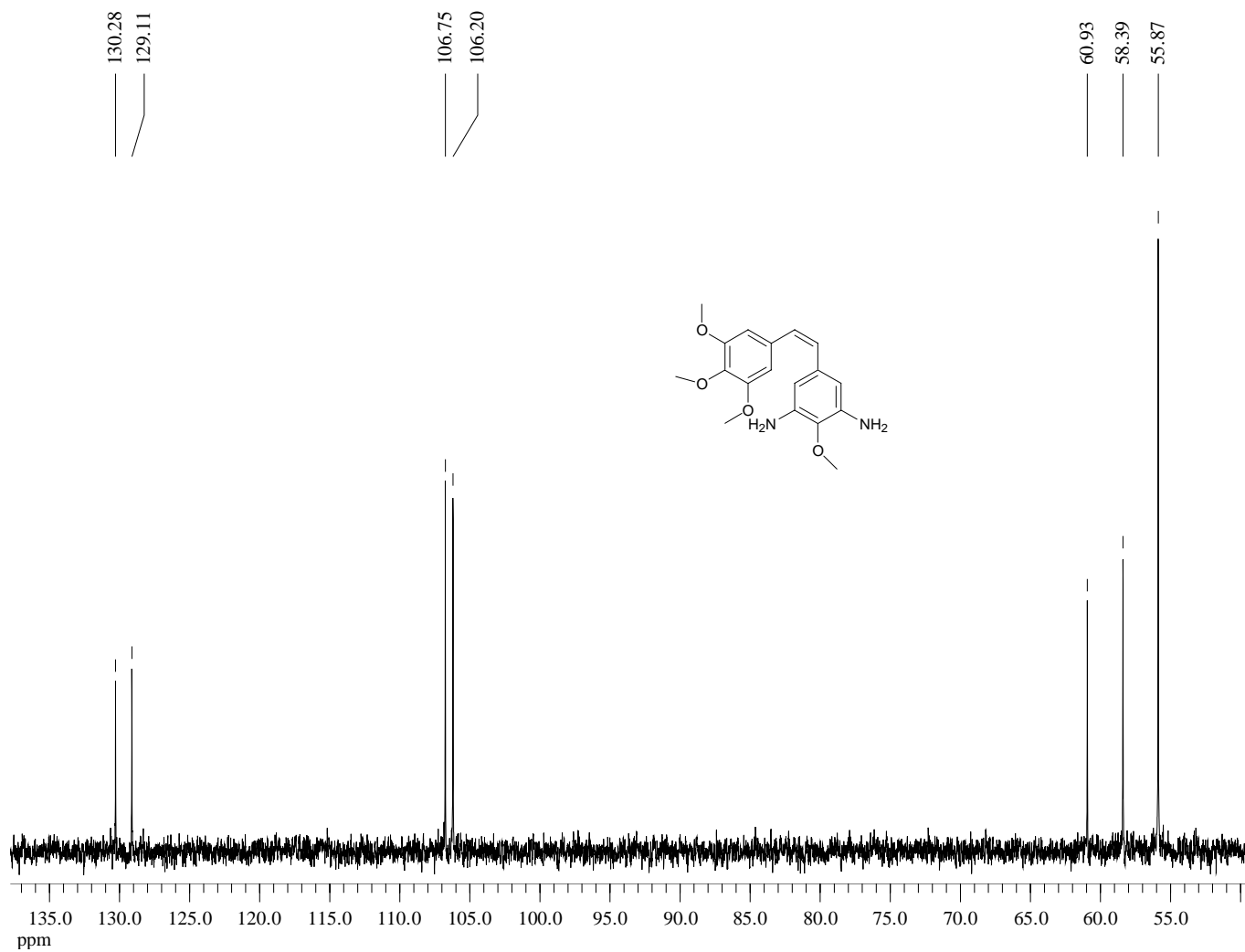
¹H-NMR (300 MHz, CDCl₃) of Compound **25**



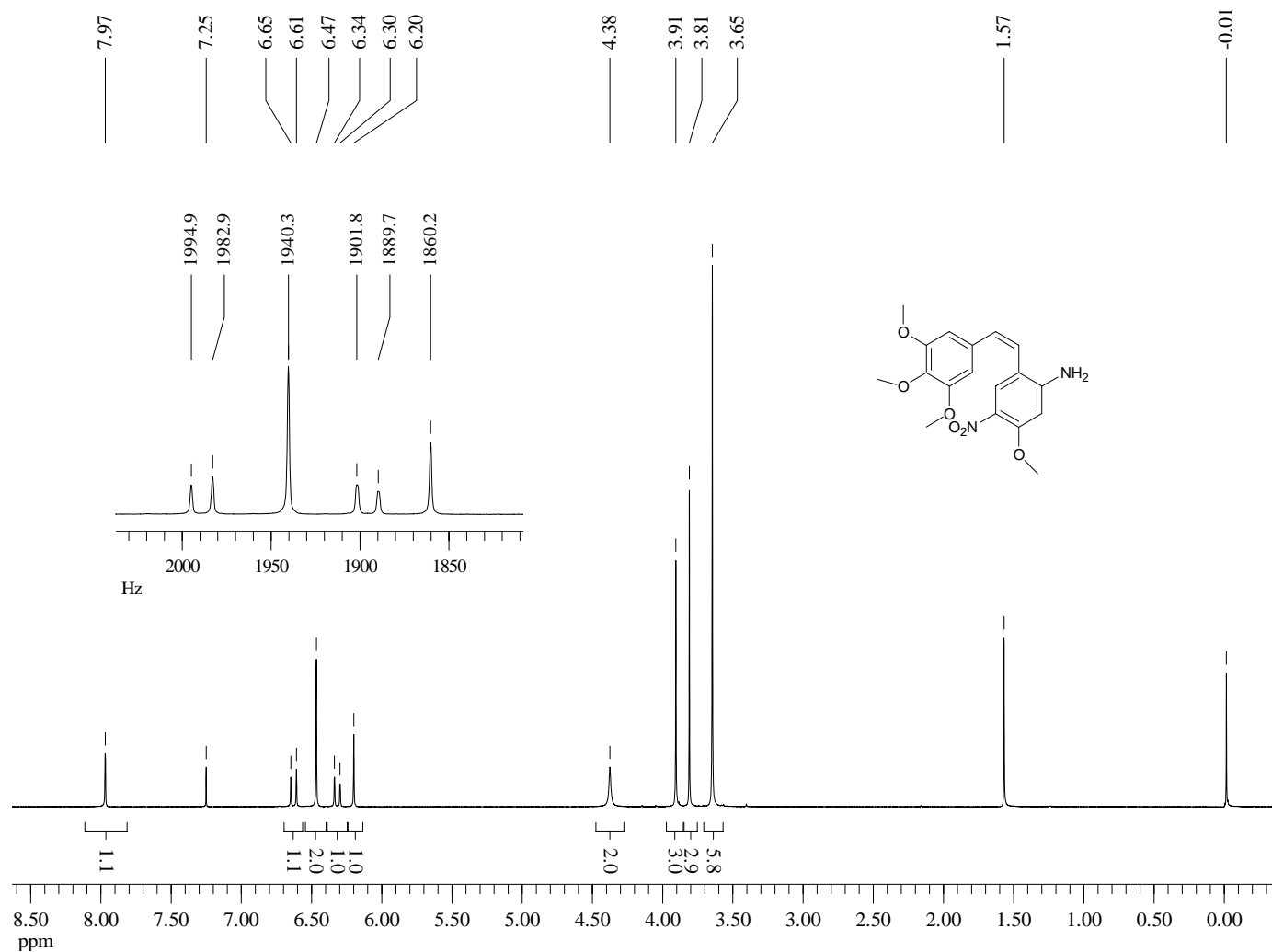
¹³C-NMR (75 MHz, CDCl₃) of Compound **25**



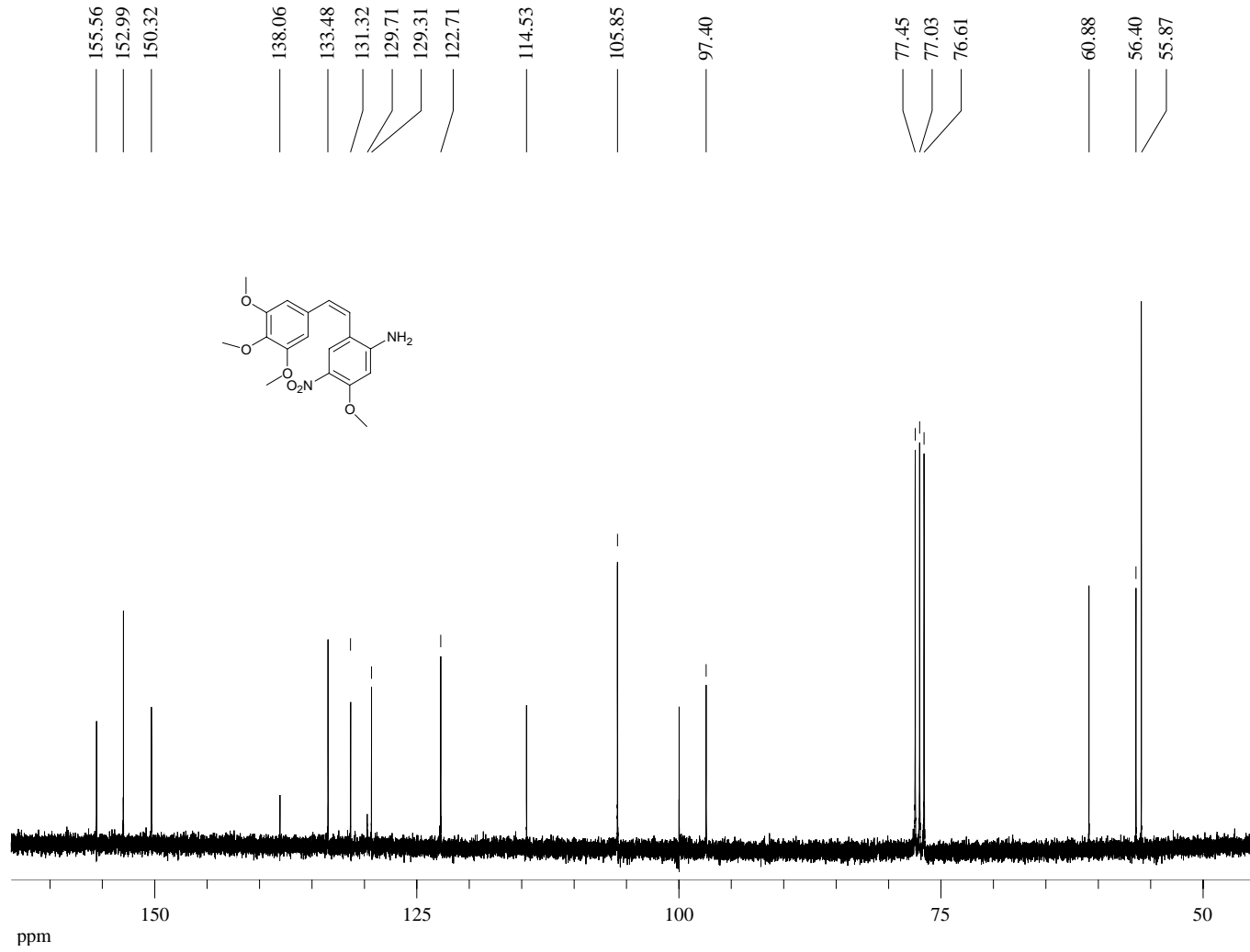
Dept 45-NMR (75 MHz, CDCl₃) of Compound **25**



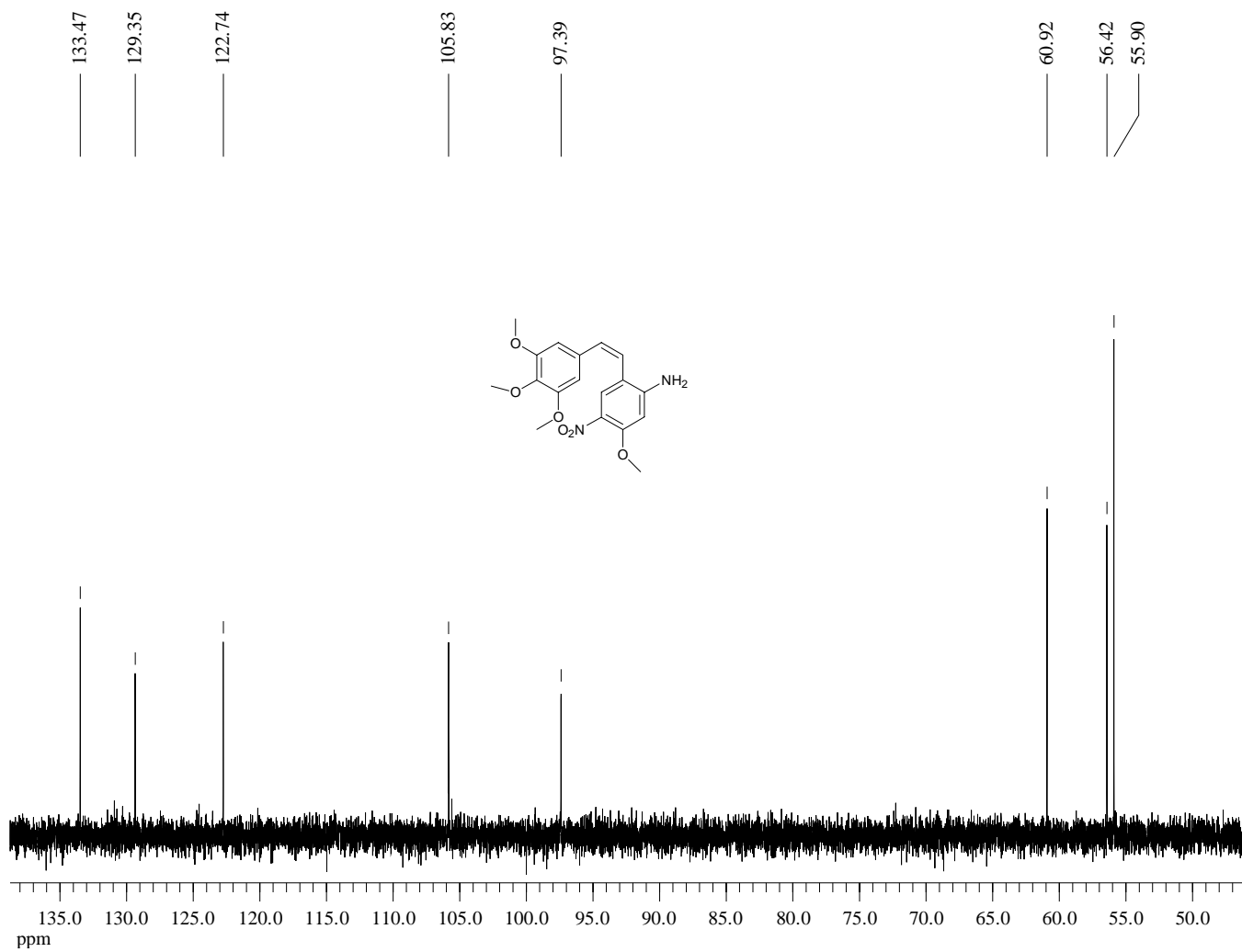
¹H-NMR (300 MHz, CDCl₃) of Compound **26a**



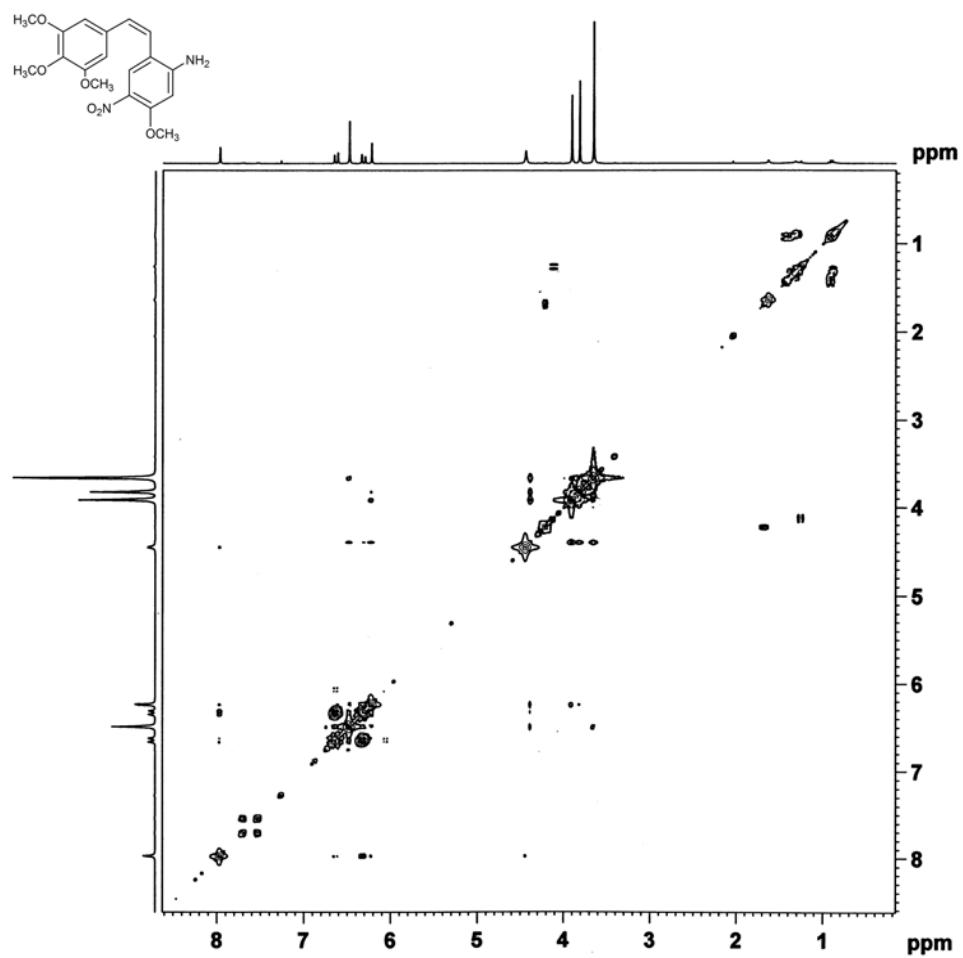
¹³C-NMR (75 MHz, CDCl₃) of Compound **26a**



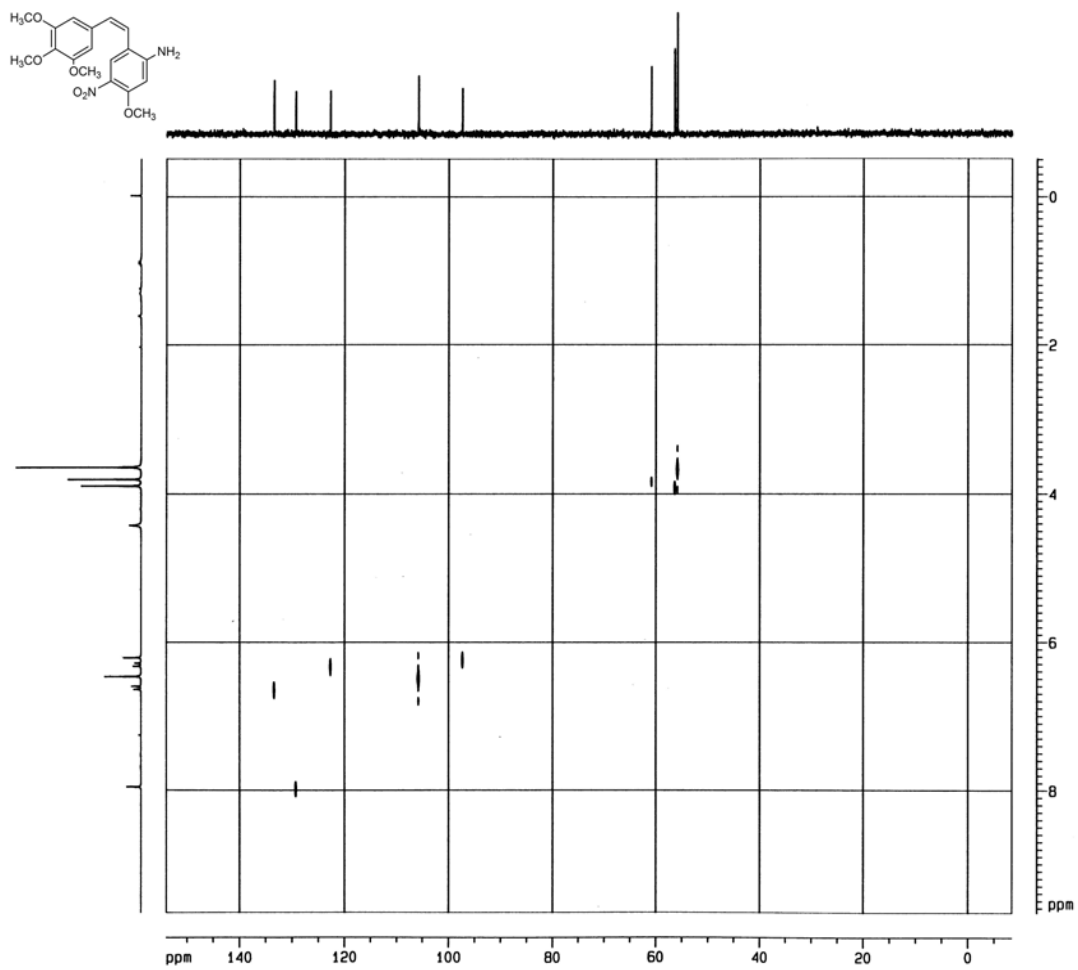
Dept 45-NMR (75 MHz, CDCl₃) of Compound **26a**



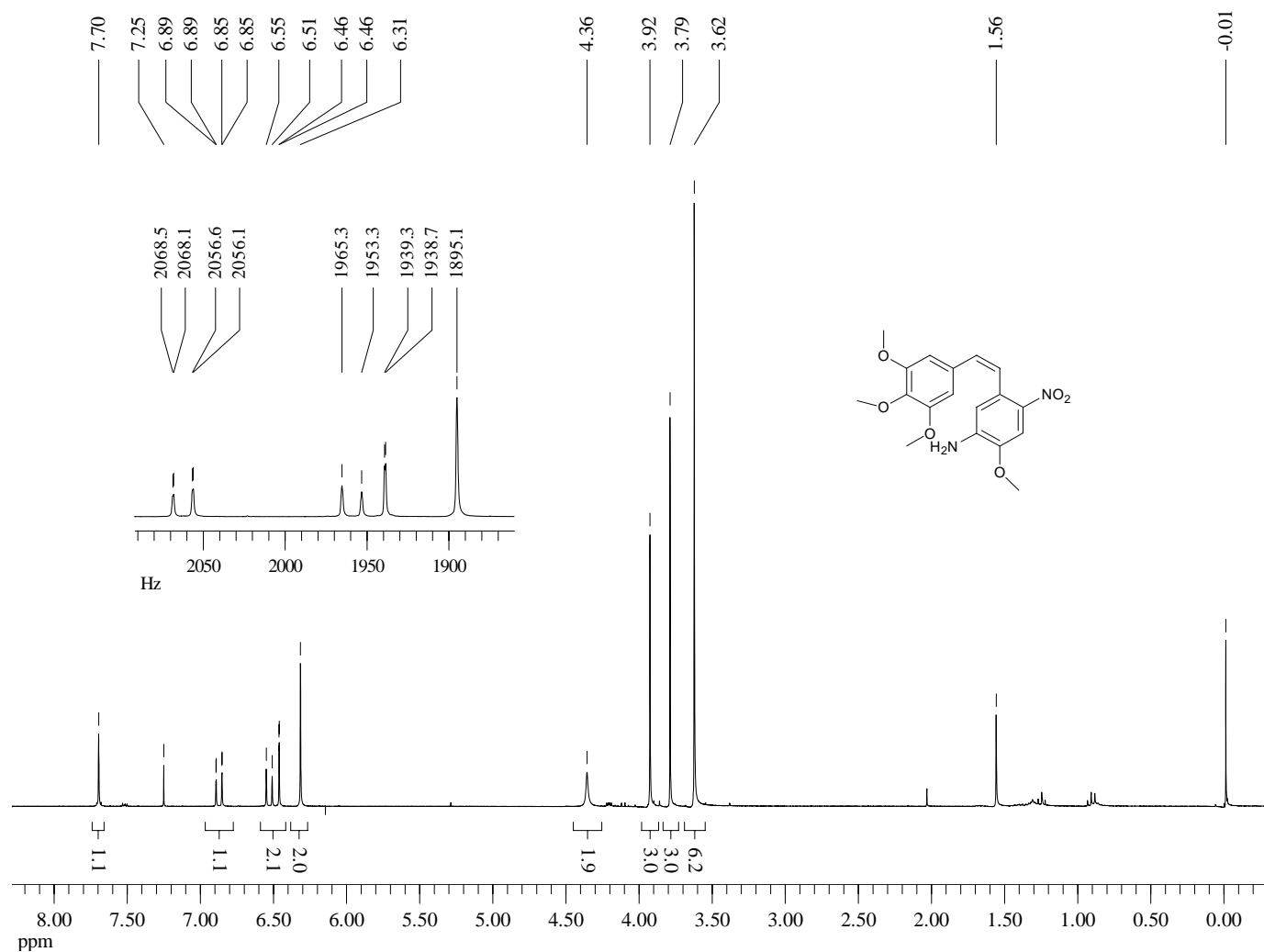
COSY-¹H-¹H NMR (300 MHz, CDCl₃) of Compound 26a



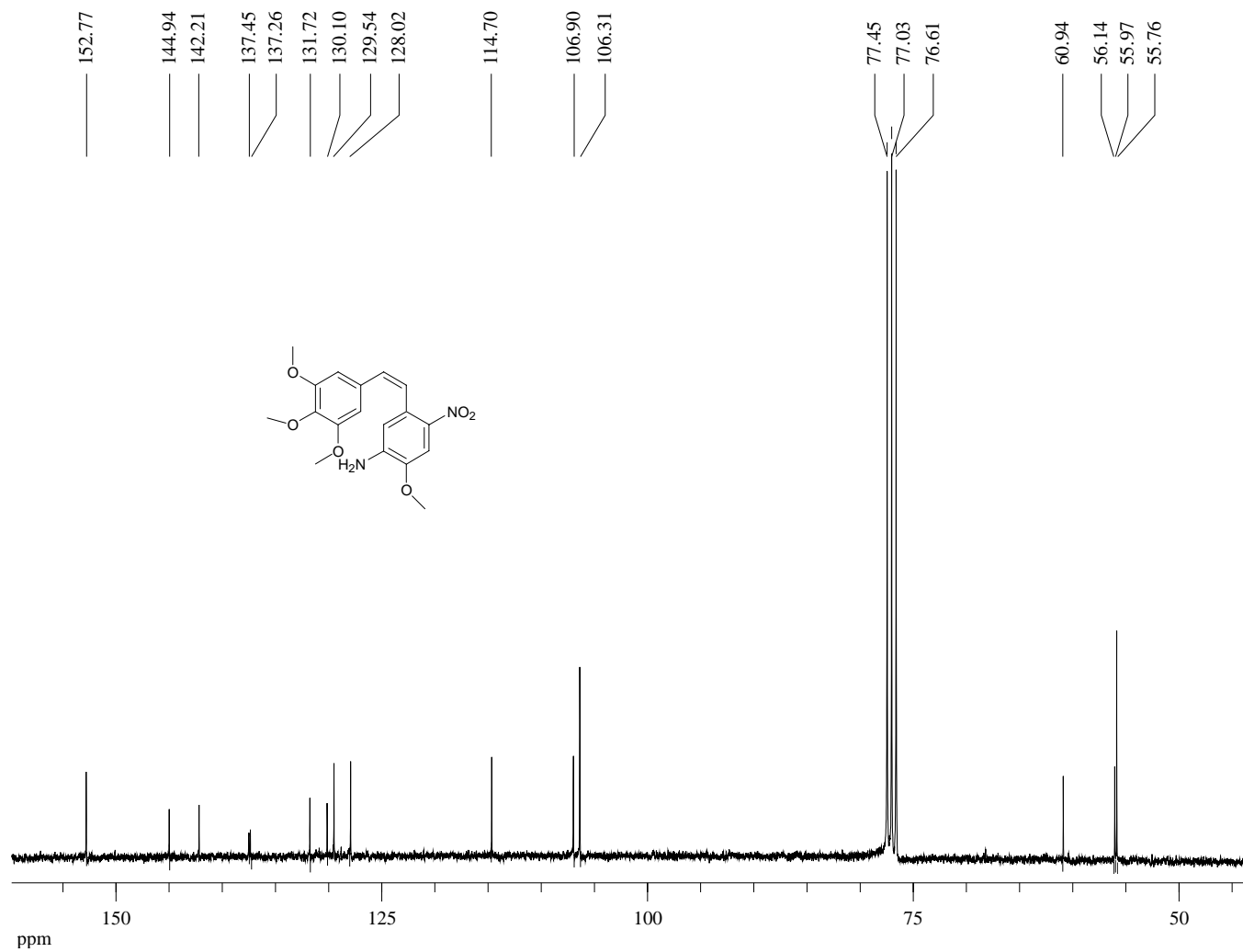
COSY ^1H - ^{13}C NMR (75 MHz, CDCl_3) of Compound **26a**



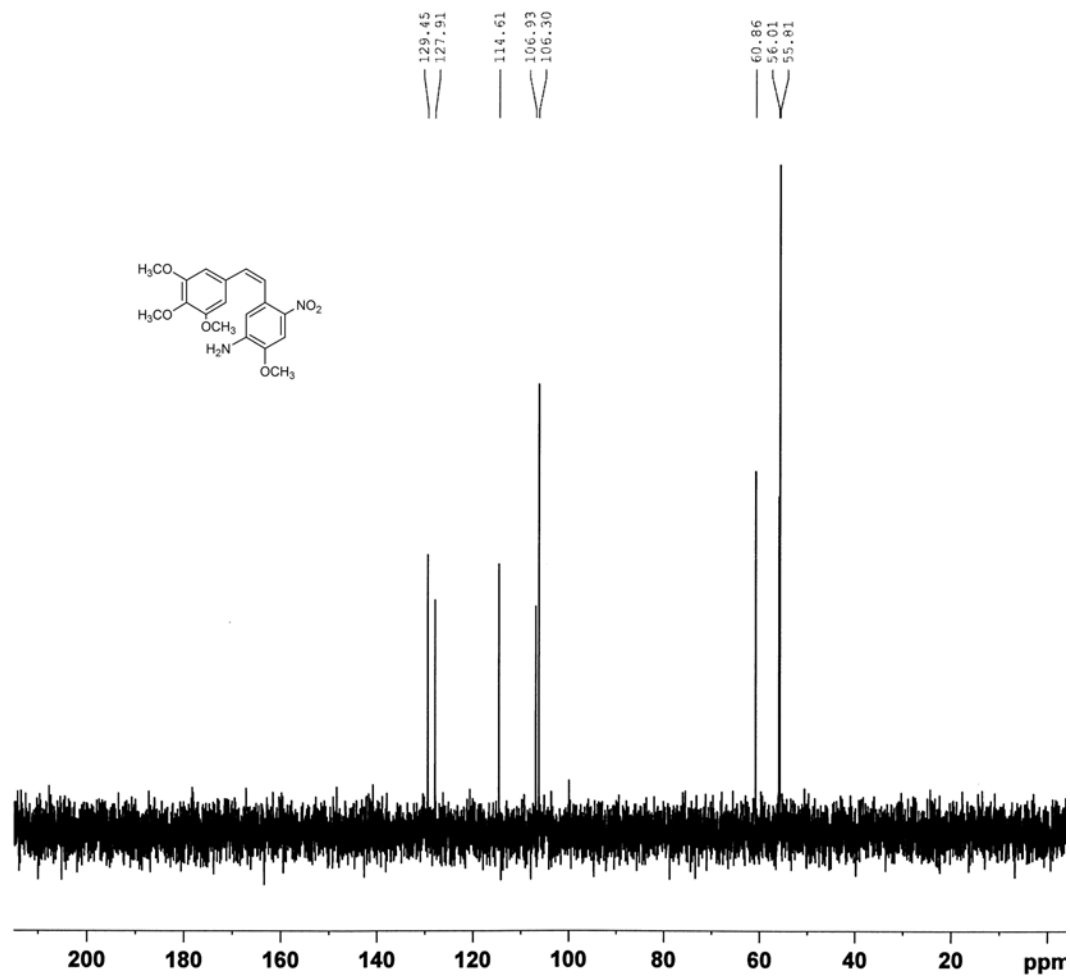
¹H-NMR (300 MHz, CDCl₃) of Compound **26b**



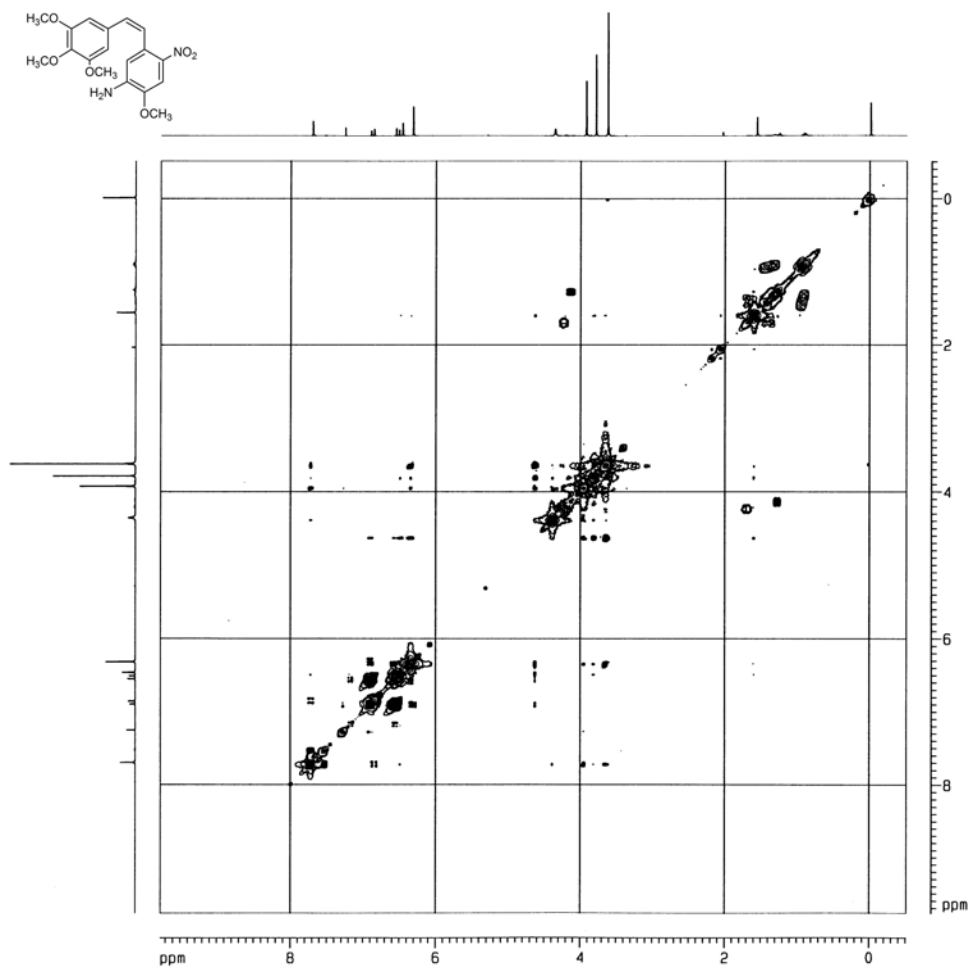
¹³C-NMR (75 MHz, CDCl₃) of Compound **26b**



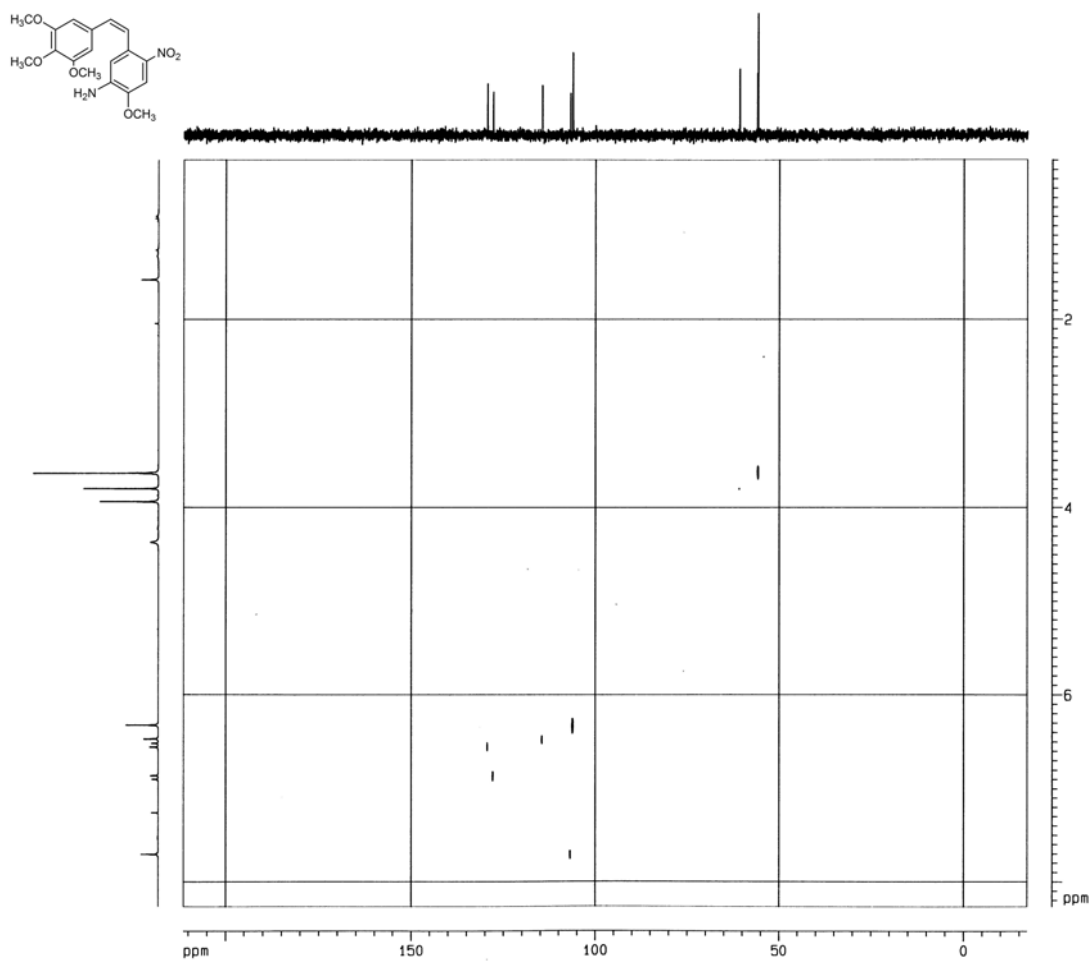
Dept 45-NMR (75 MHz, CDCl₃) of Compound **26b**



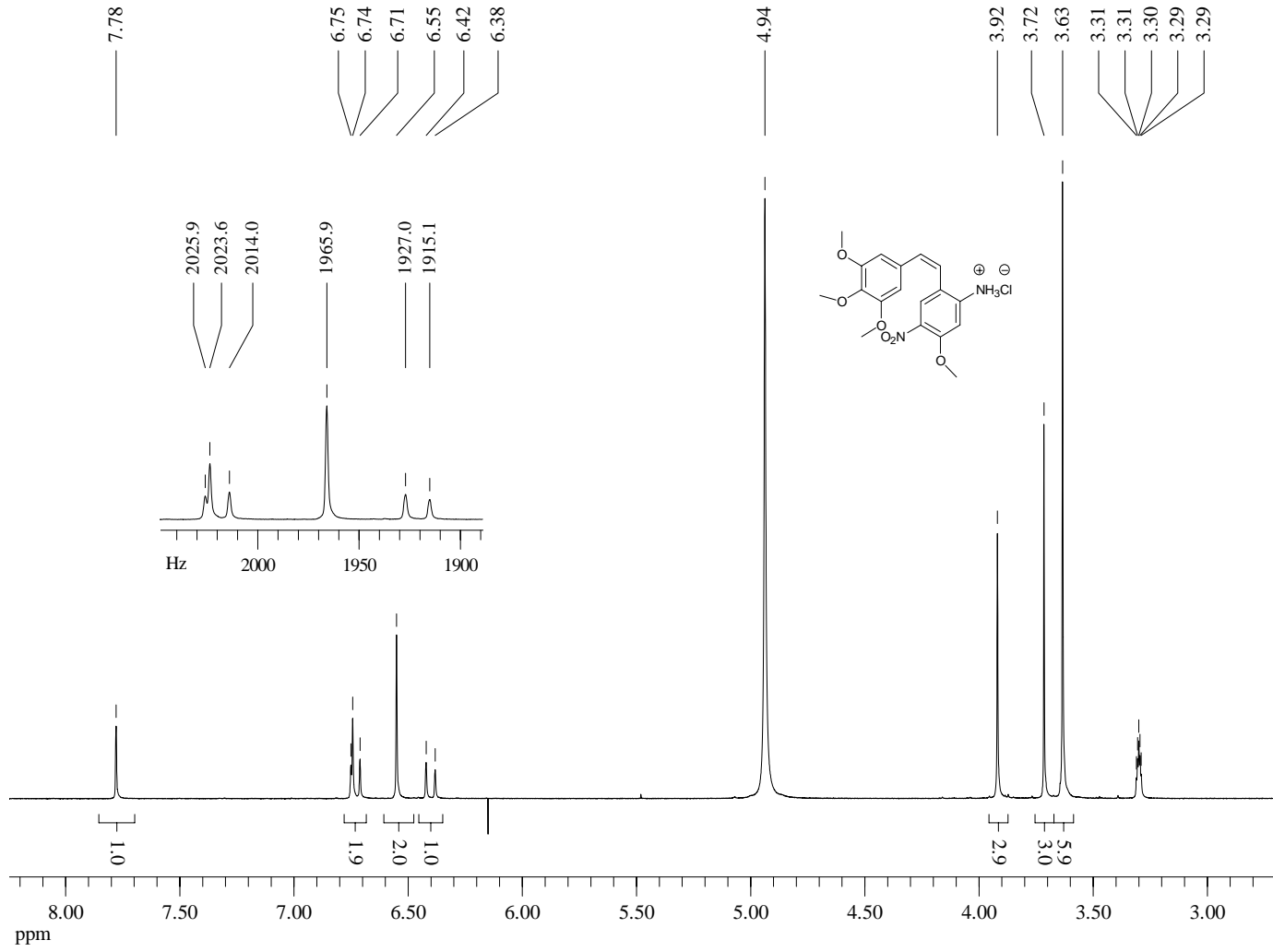
COSY ^1H - ^1H NMR (300 MHz, CDCl_3) of Compound **26b**



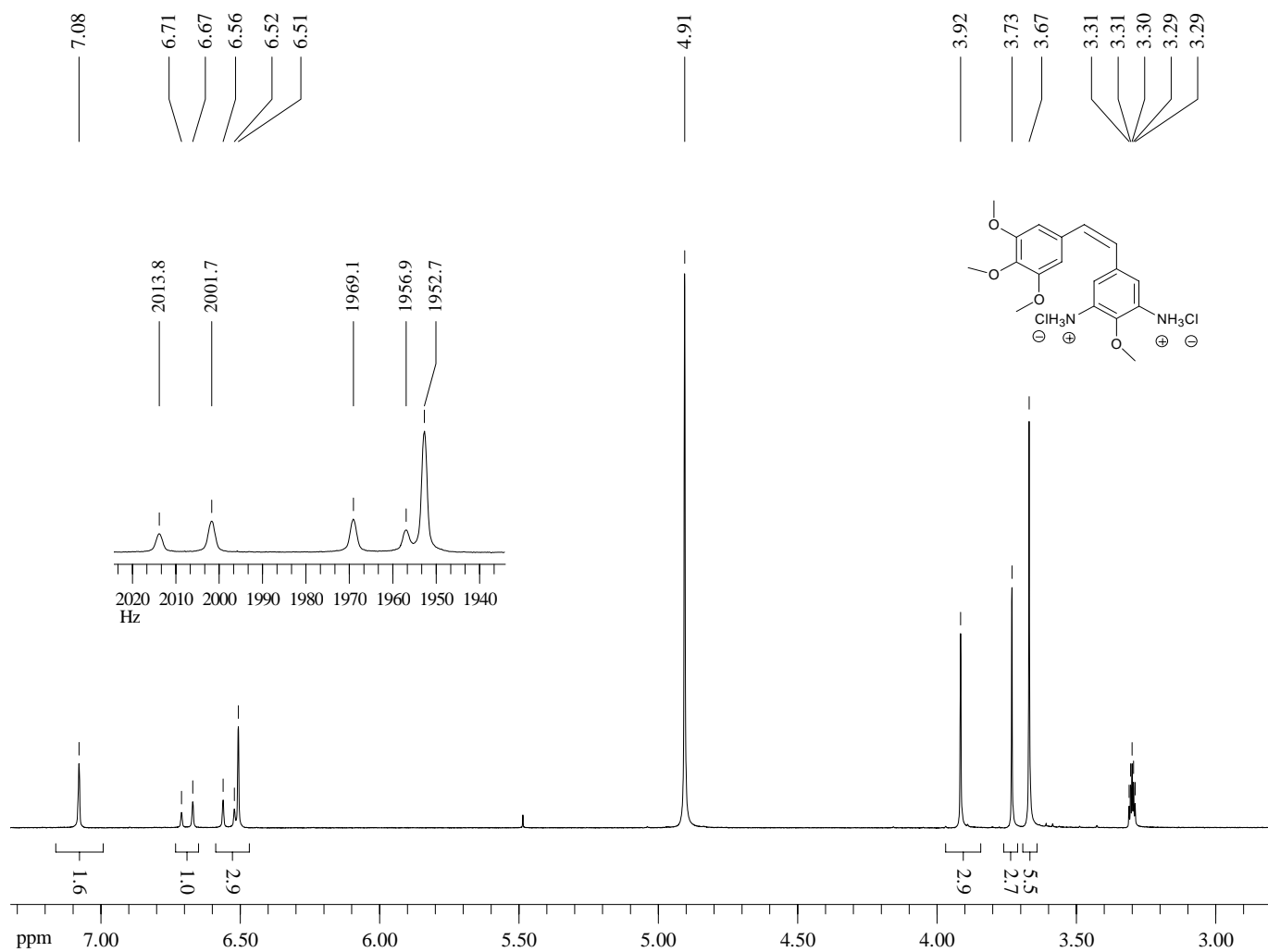
COSY ^1H - ^{13}C NMR (75 MHz, CDCl_3) of Compound **26b**



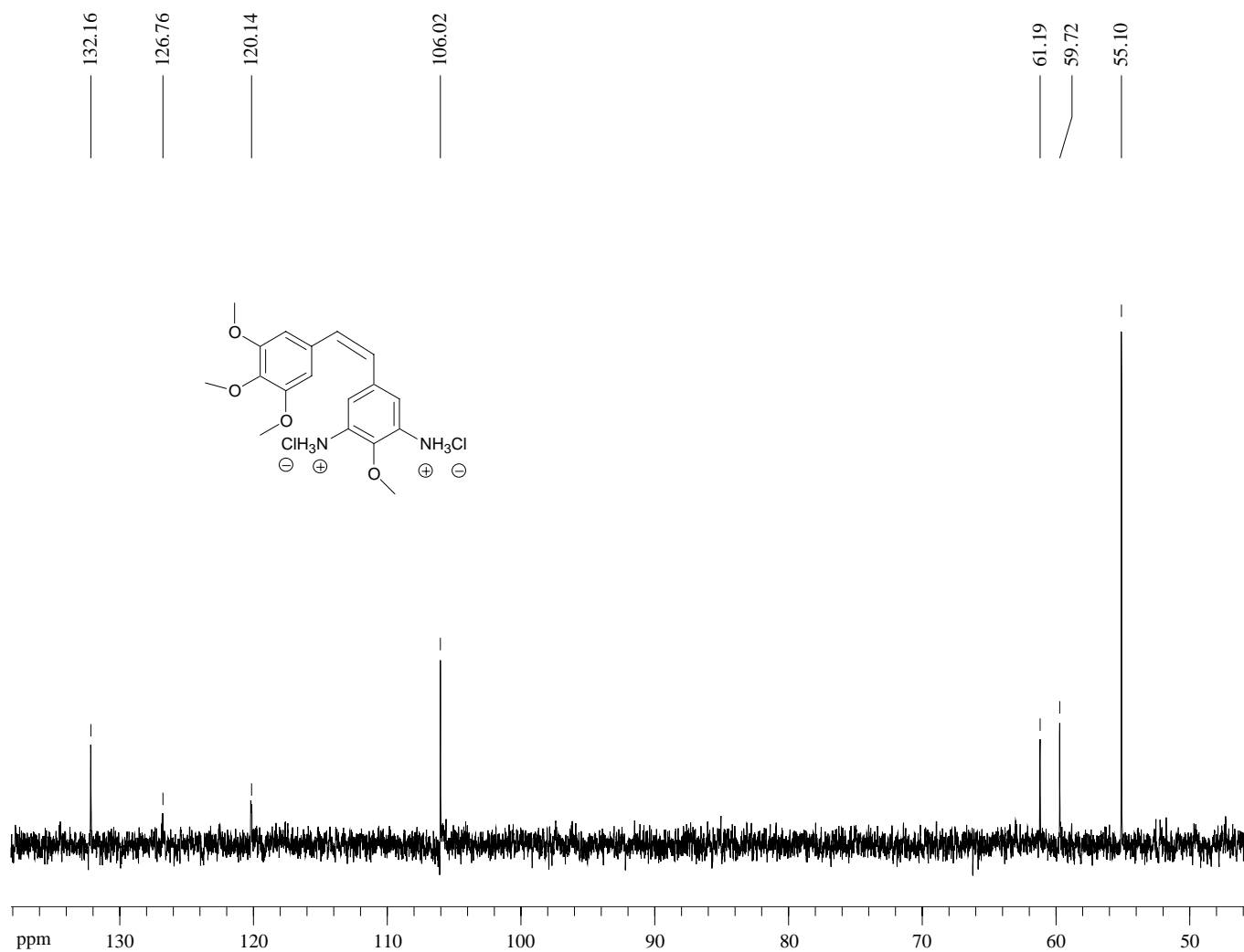
¹H-NMR (300 MHz, MeOH-d₄) of Compound **27a**



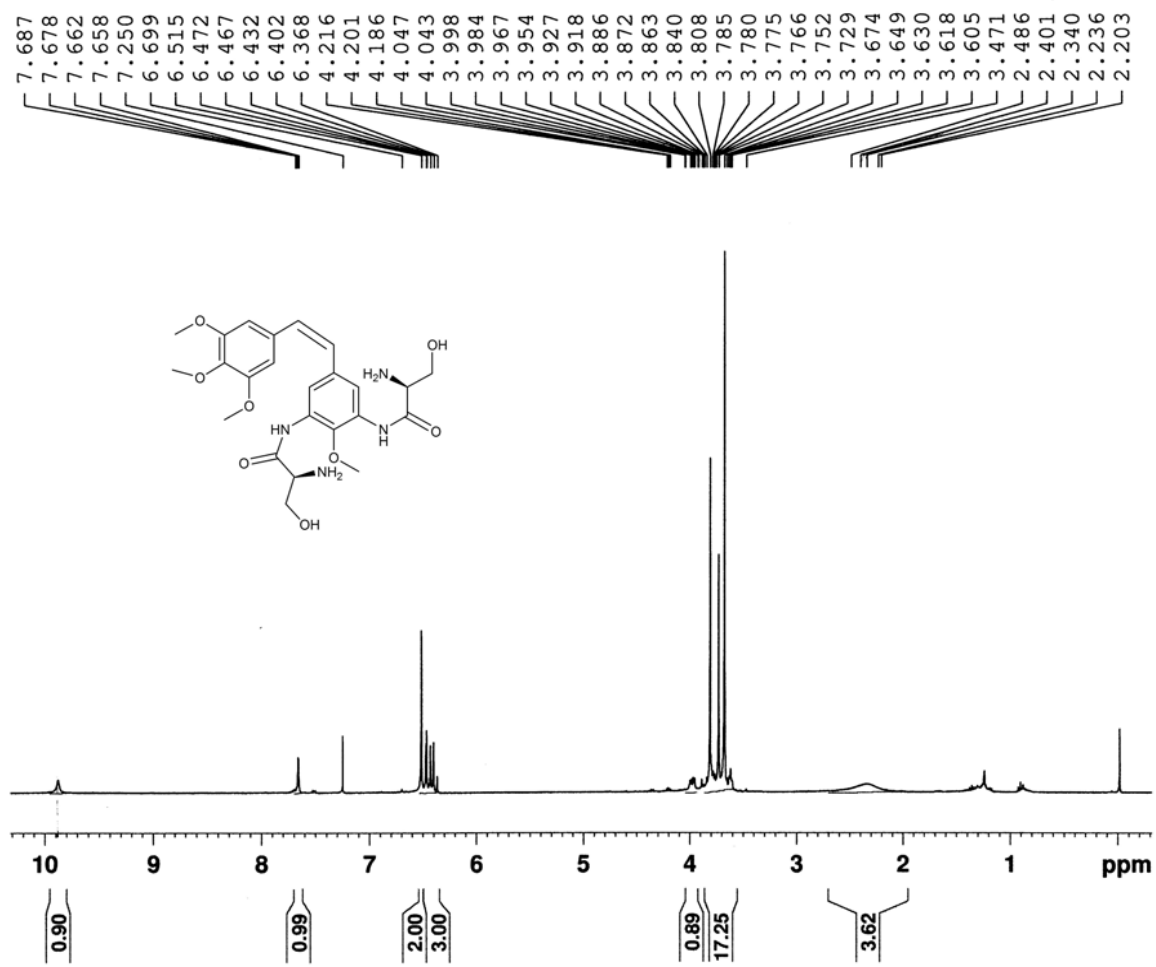
¹H-NMR (300 MHz, MeOH-d₄) of Compound **27b**



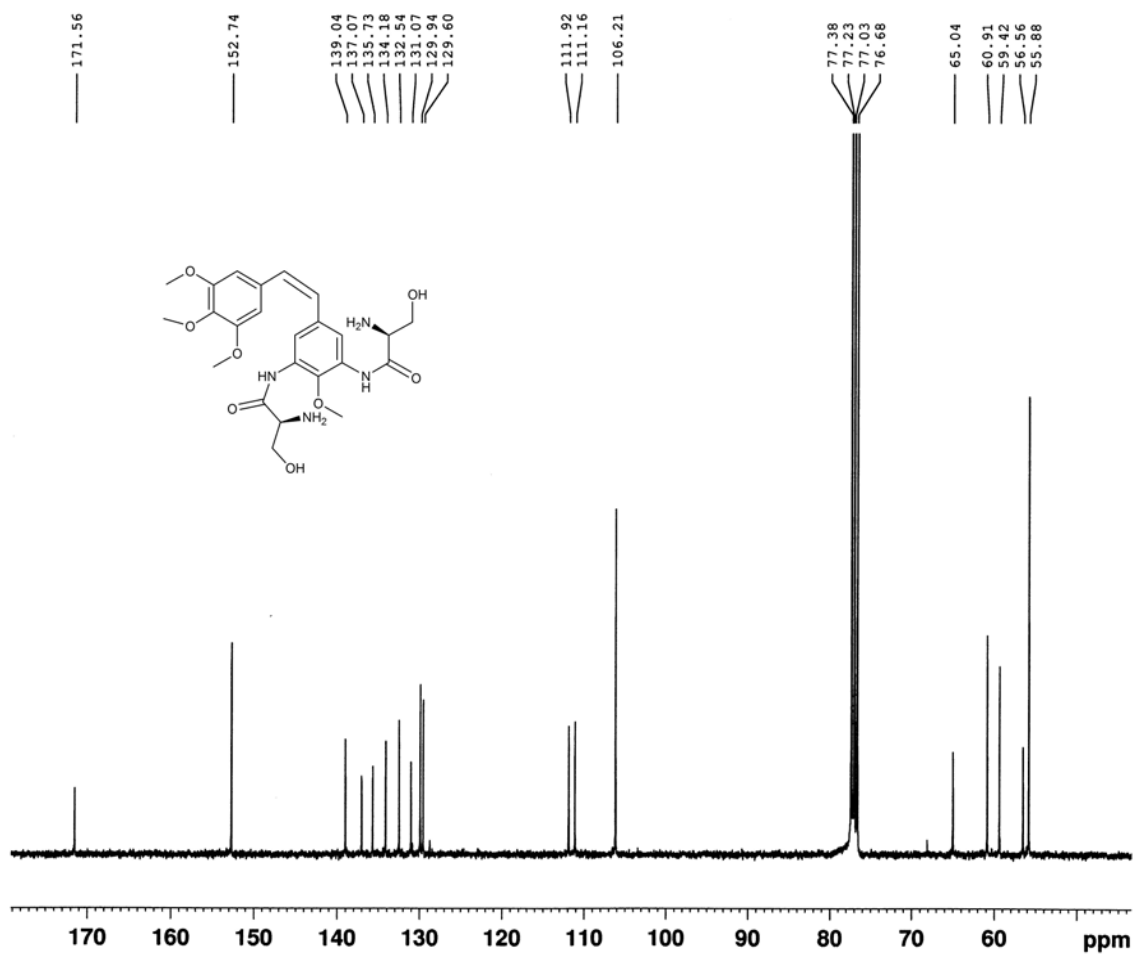
Dept 45-NMR (75 MHz, MeOH-d₄) of Compound **27b**



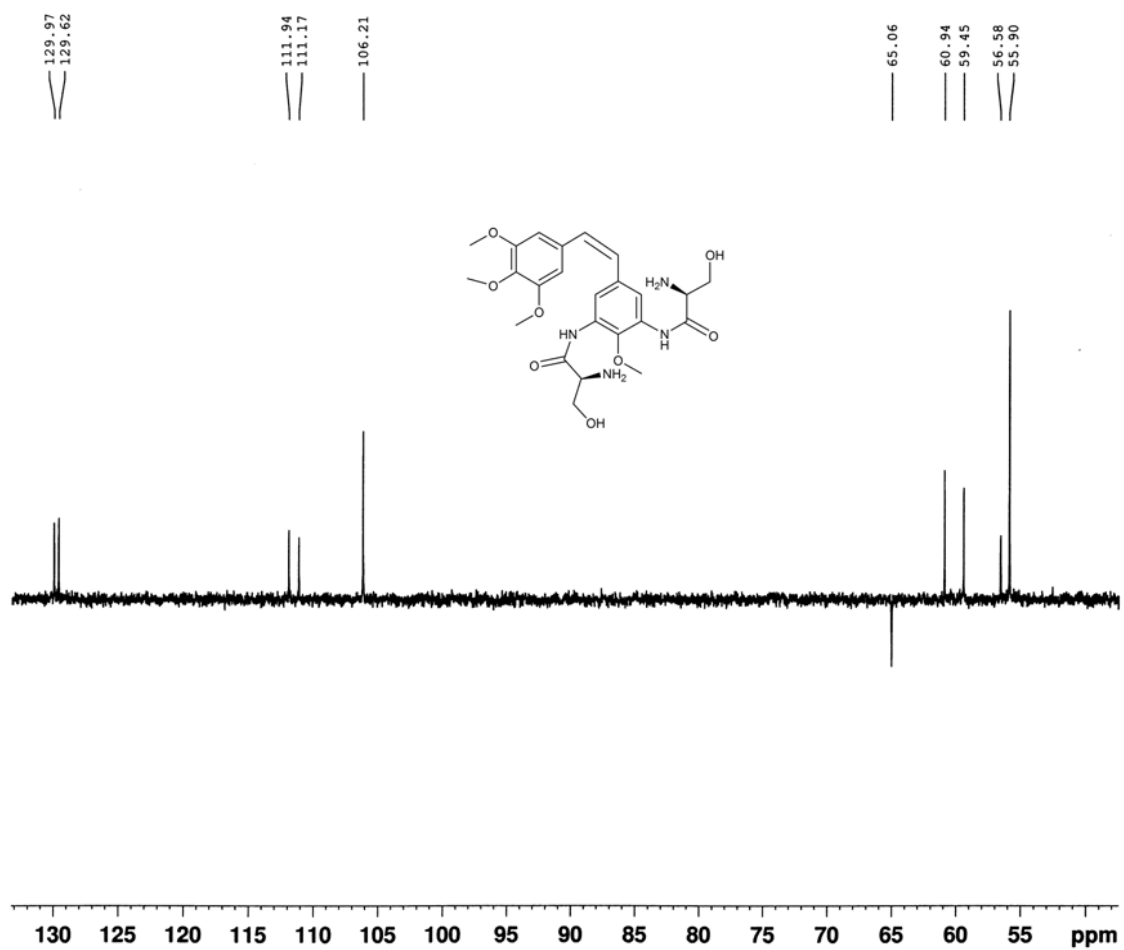
¹H-NMR (360 MHz, CDCl₃) of Compound **29**



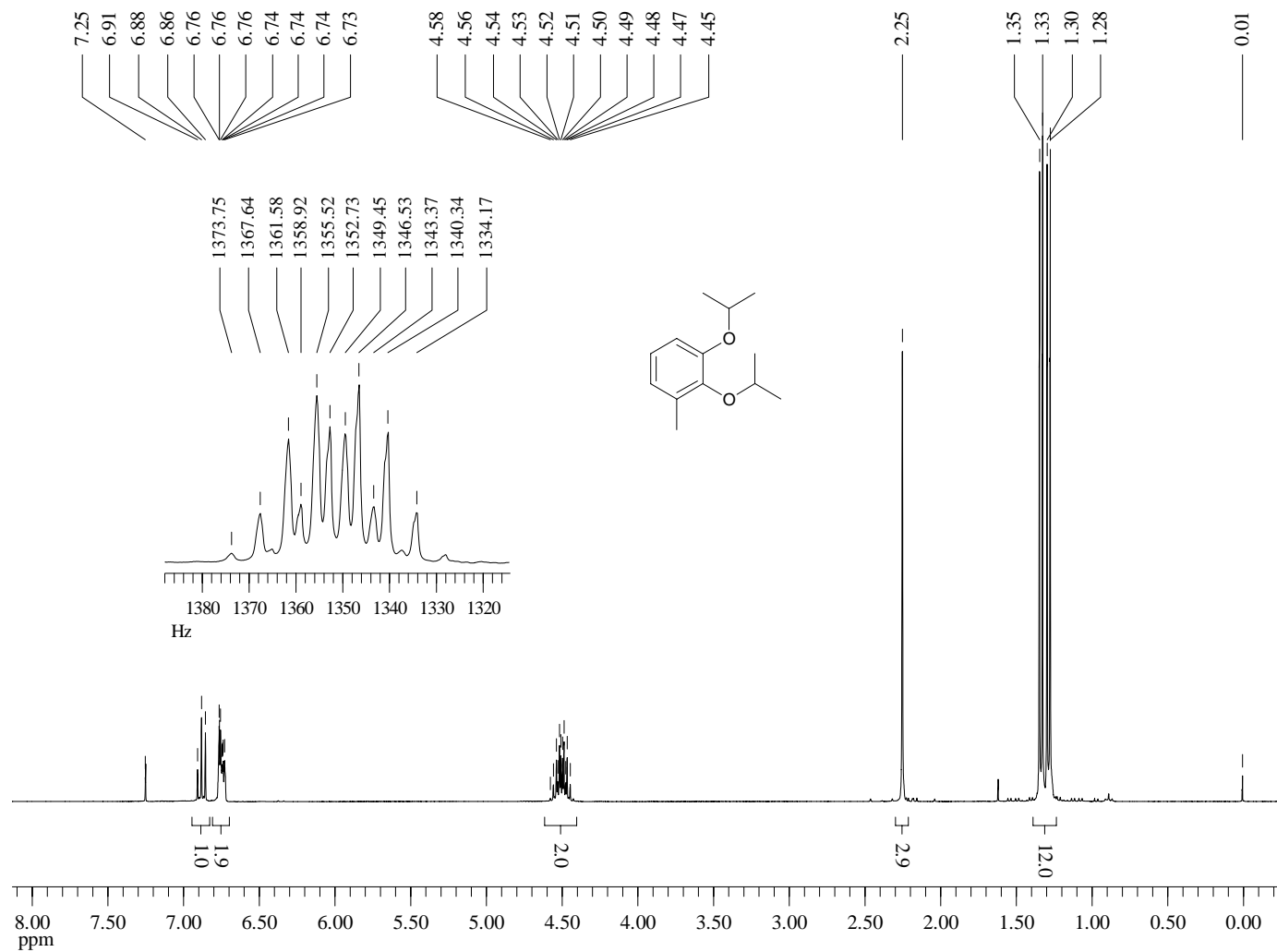
^{13}C -NMR (90 MHz, CDCl_3) of Compound **29**



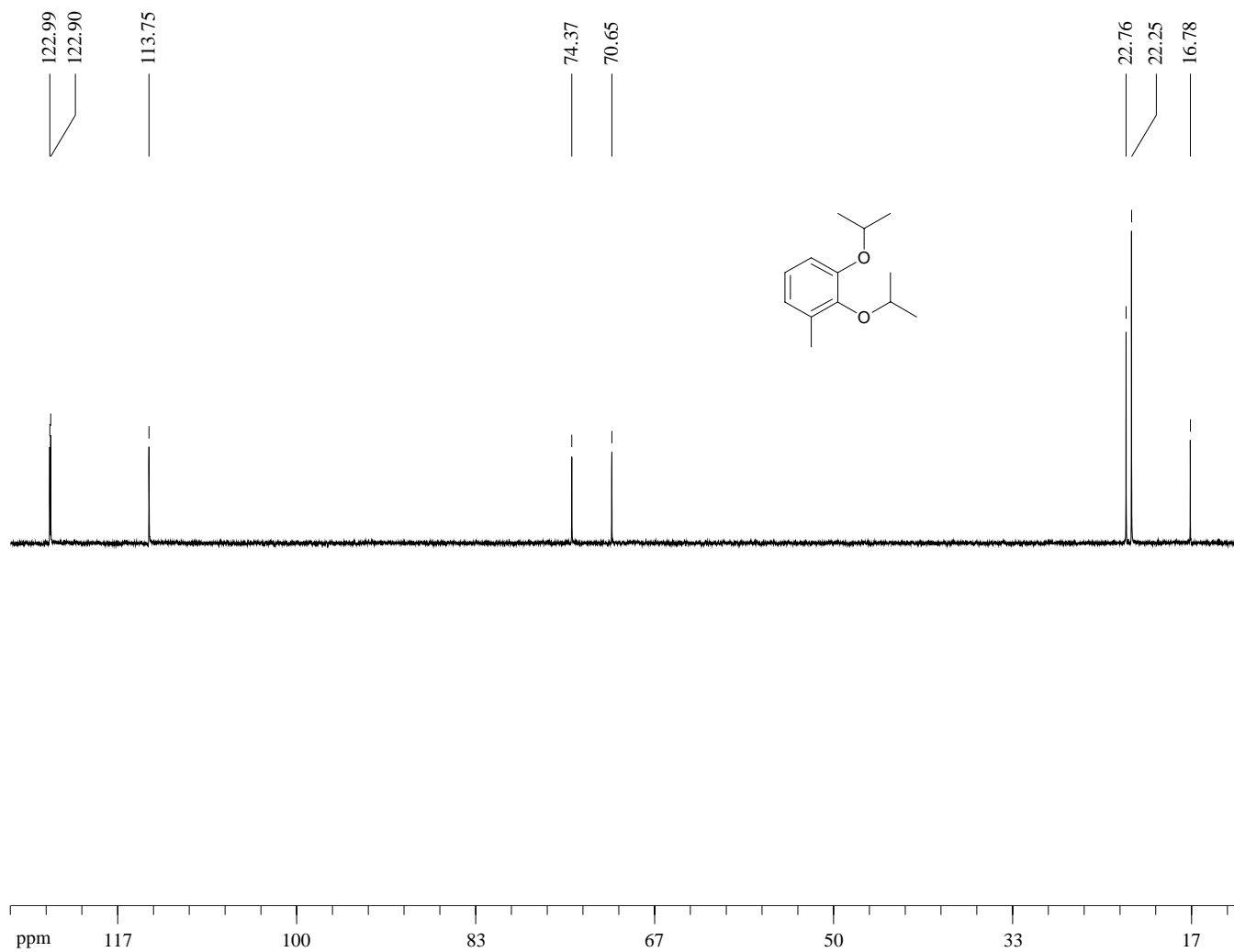
Dept 135-NMR (90 MHz, CDCl₃) of Compound 29



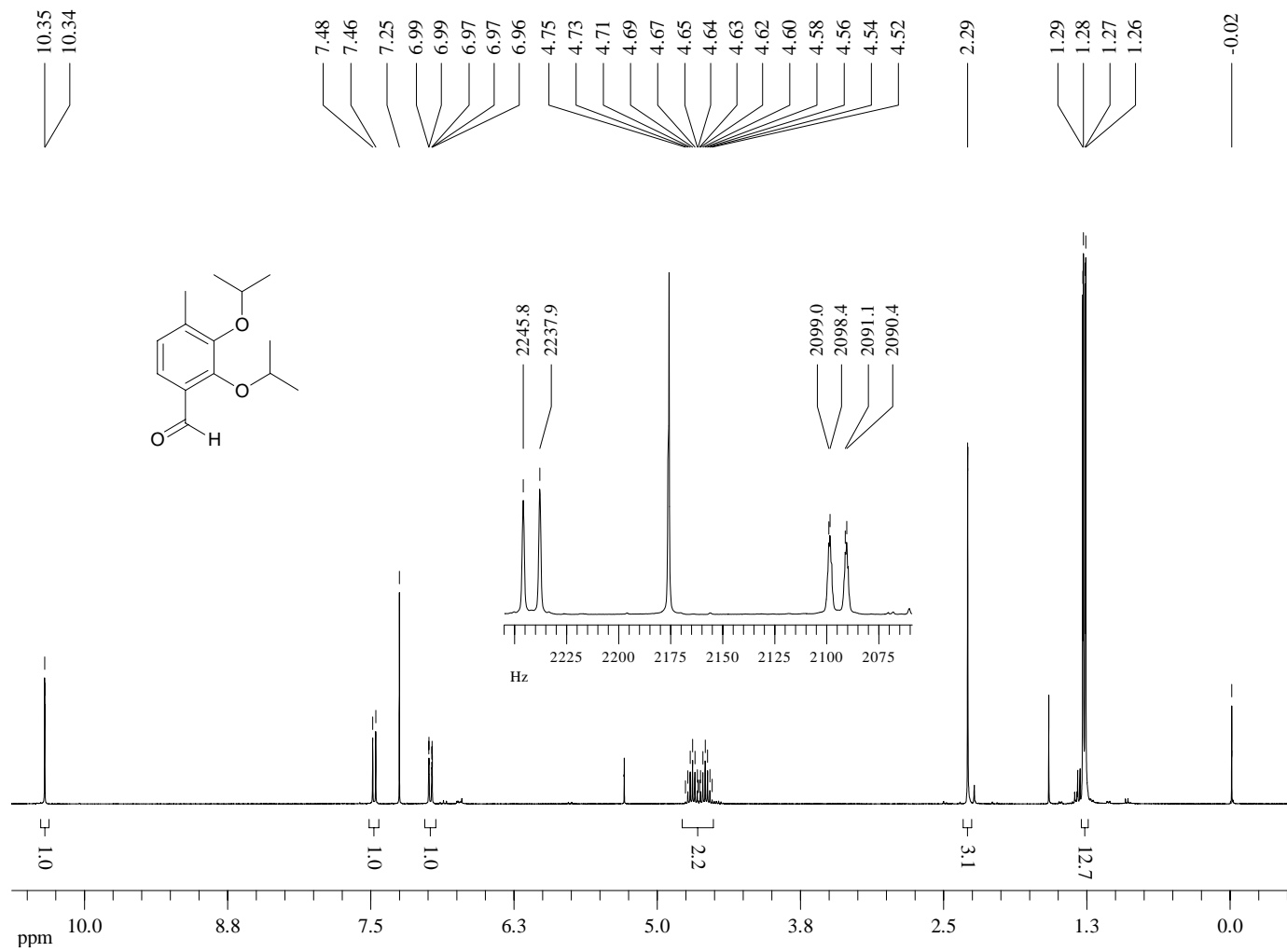
¹H-NMR (300 MHz, CDCl₃) of Compound **30**



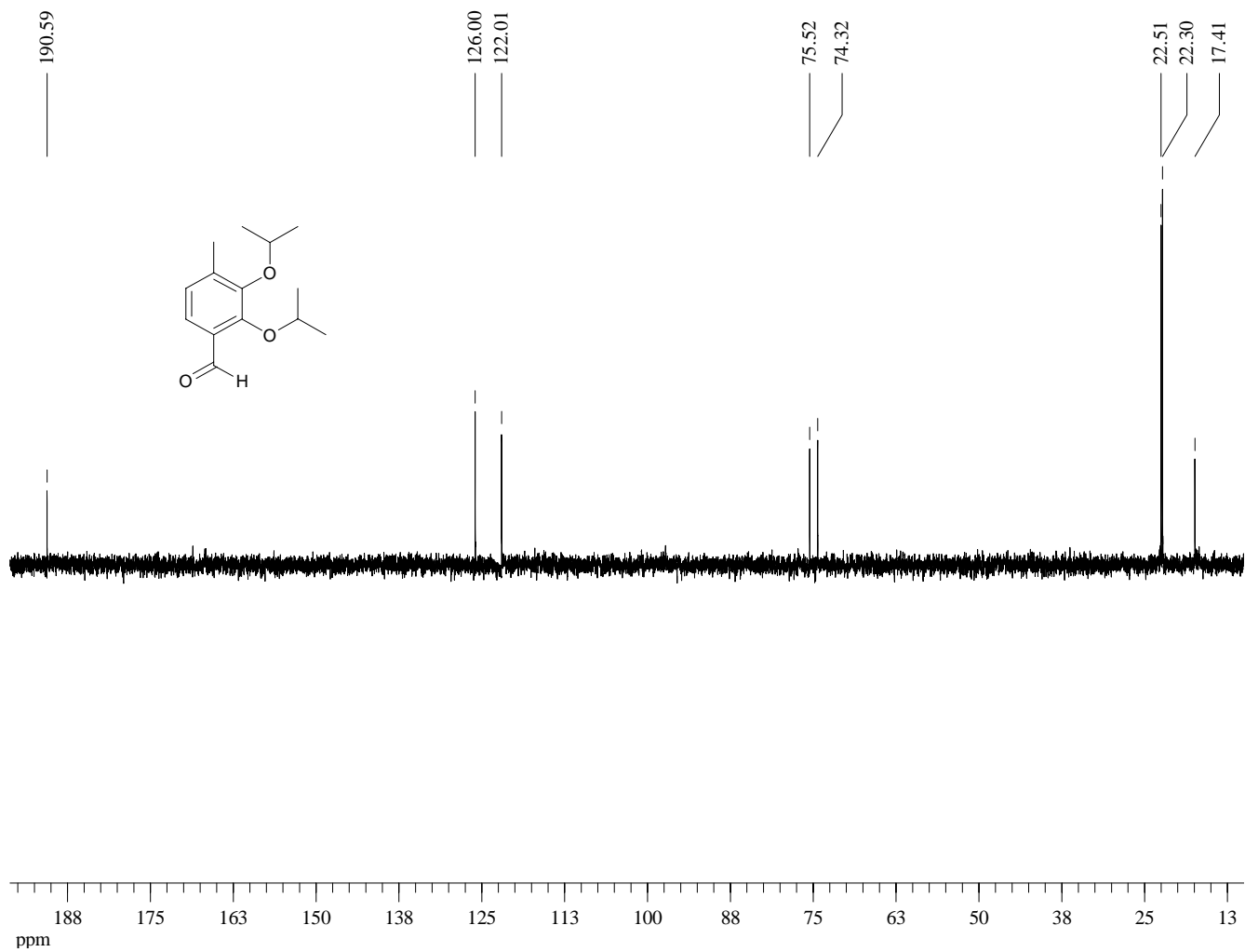
Dept 135-NMR (75 MHz, CDCl₃) of Compound **30**



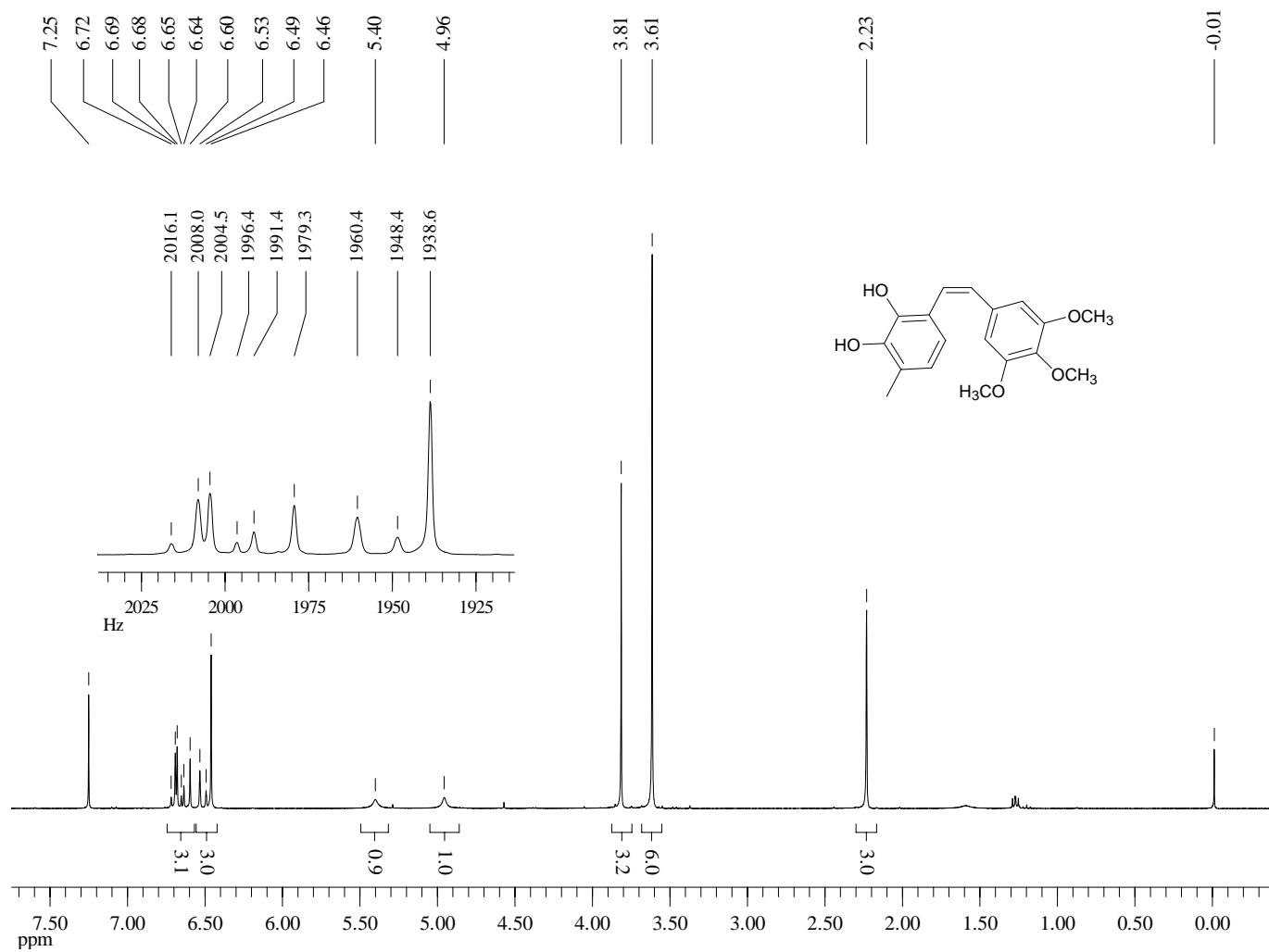
¹H-NMR (300 MHz, CDCl₃) of Compound **31**



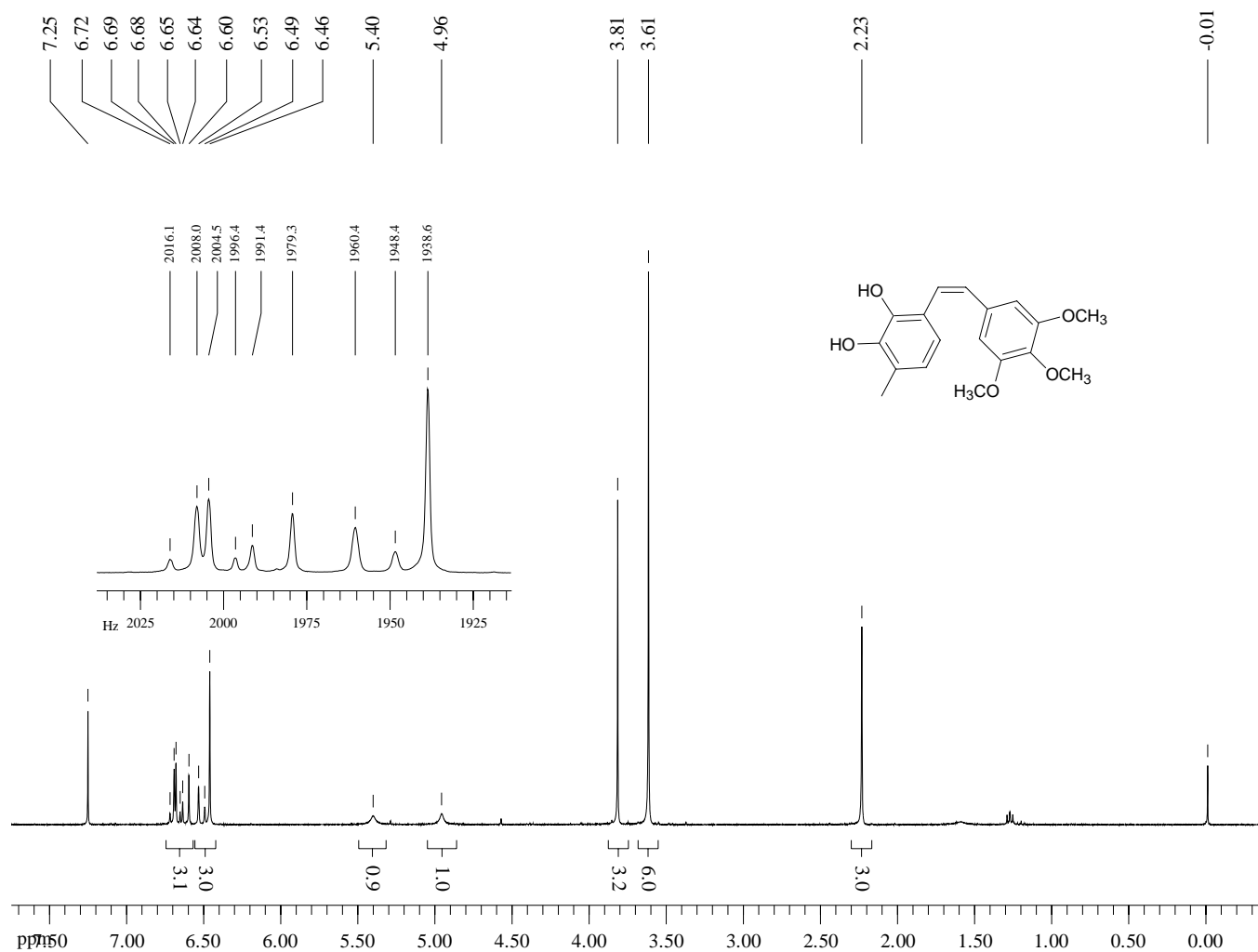
Dept 135-NMR (75 MHz, CDCl₃) of Compound **31**



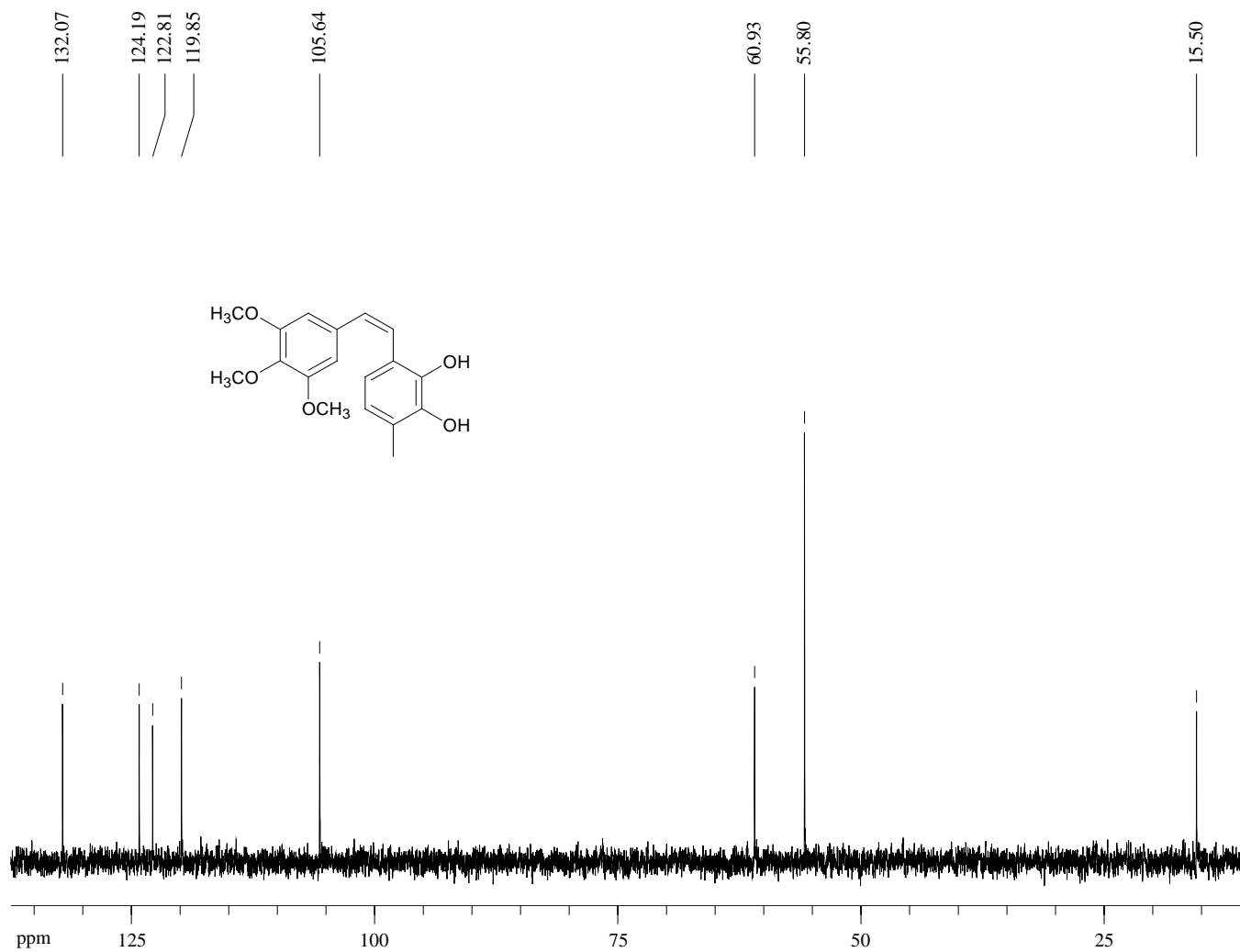
¹H-NMR (300 MHz, CDCl₃) of Compound **32**



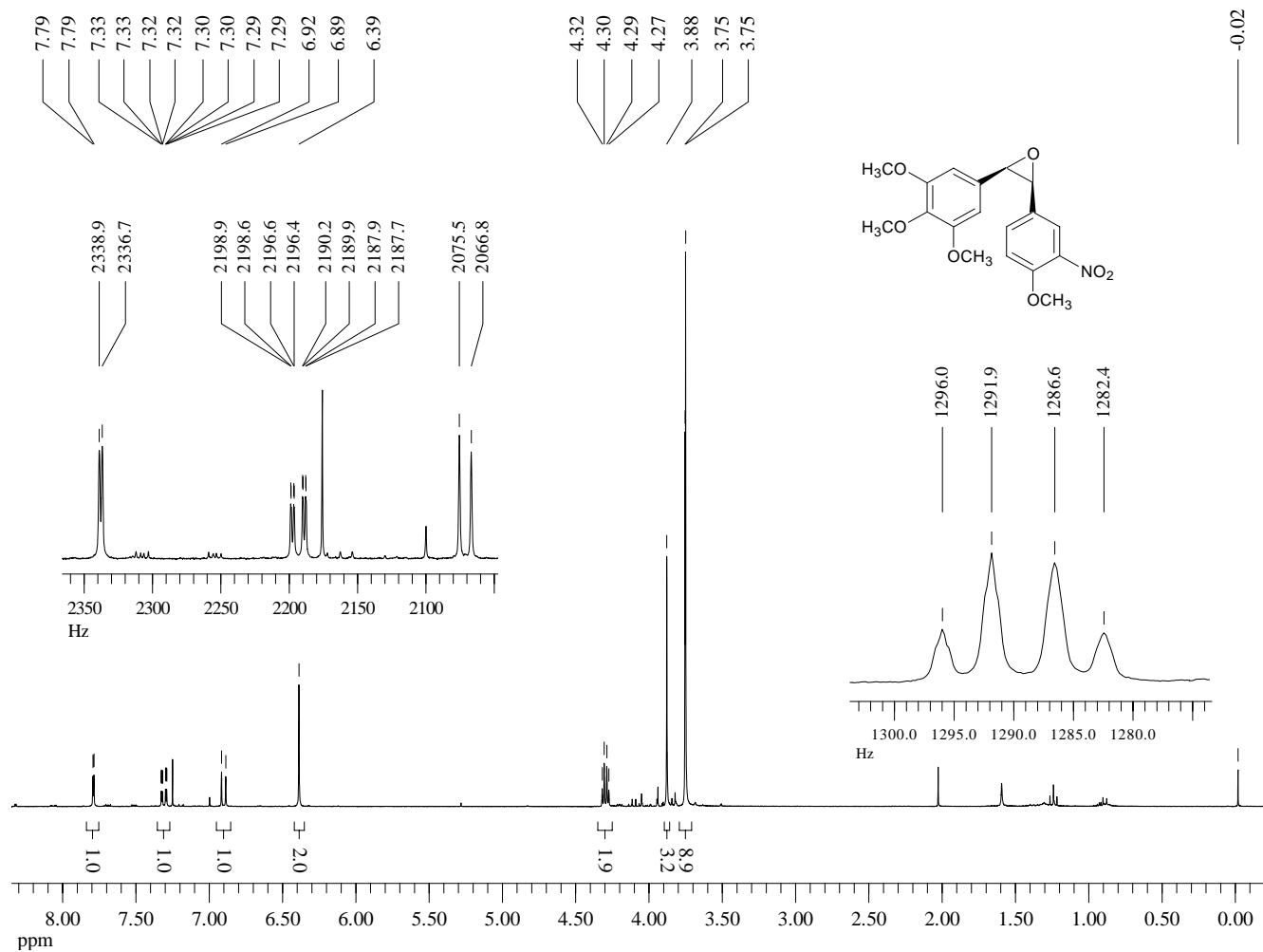
¹H-NMR (300 MHz, CDCl₃) of Compound **33**



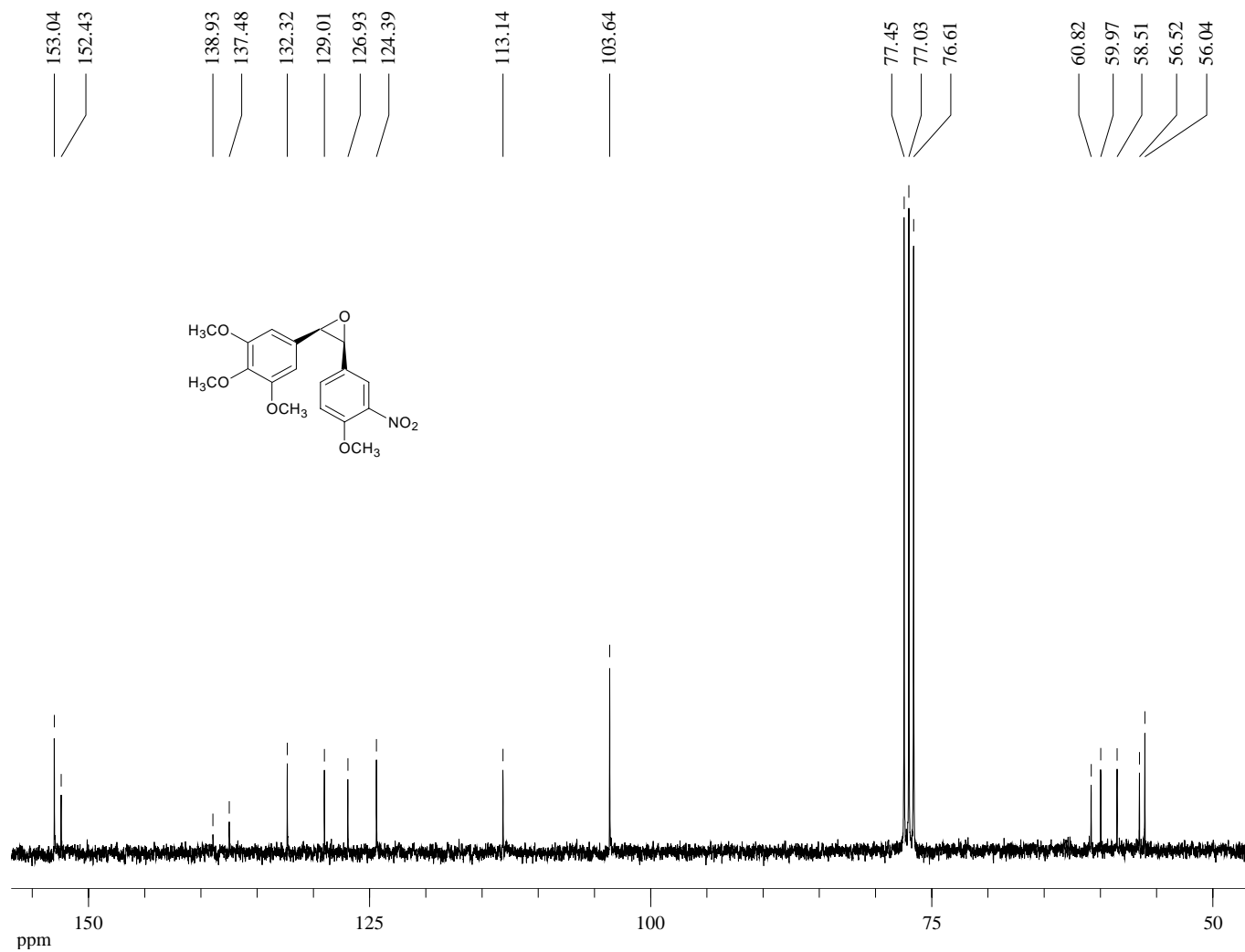
Dept 45-NMR (75 MHz, CDCl₃) of Compound **33**



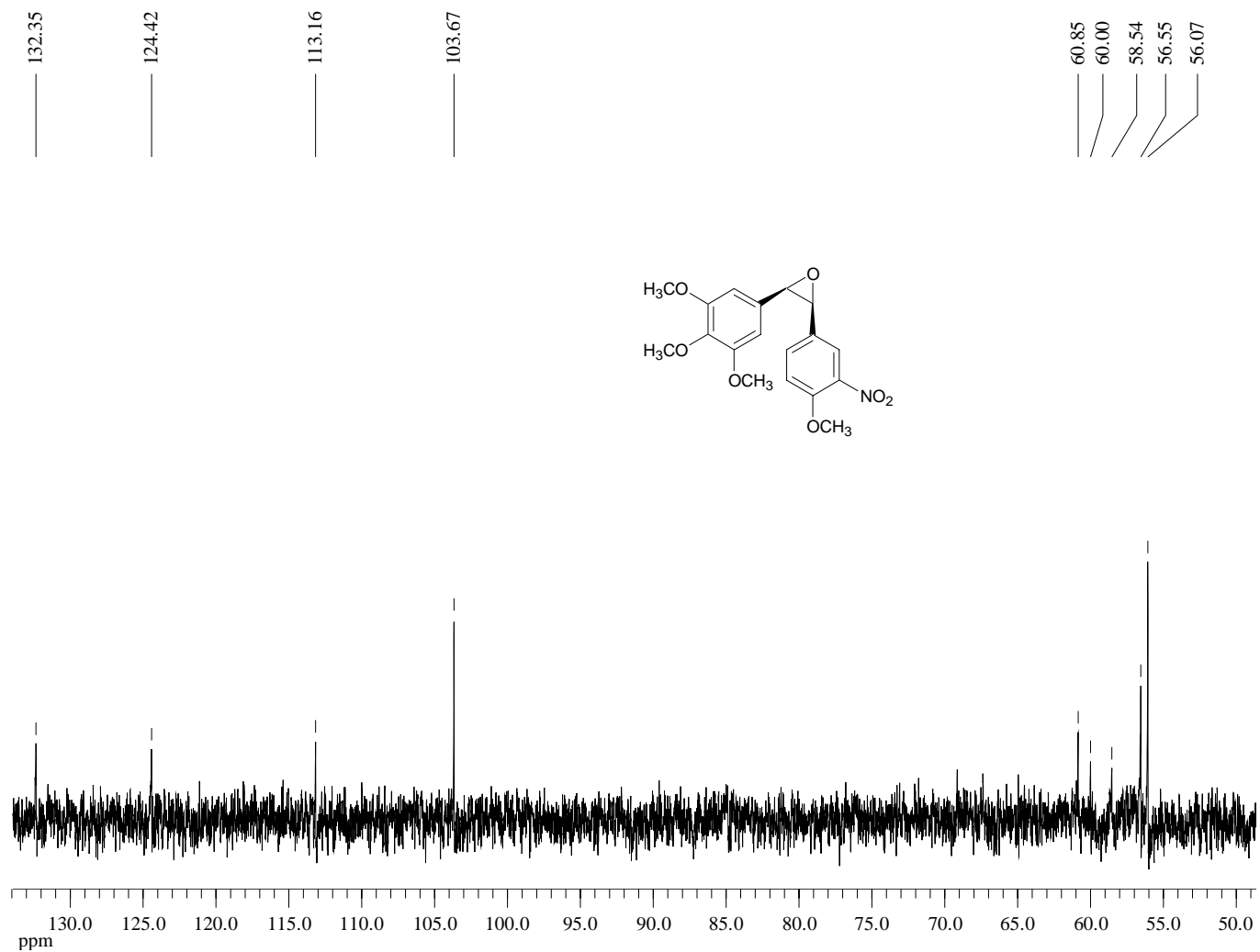
¹H-NMR (300 MHz, CDCl₃) of Compound **34**



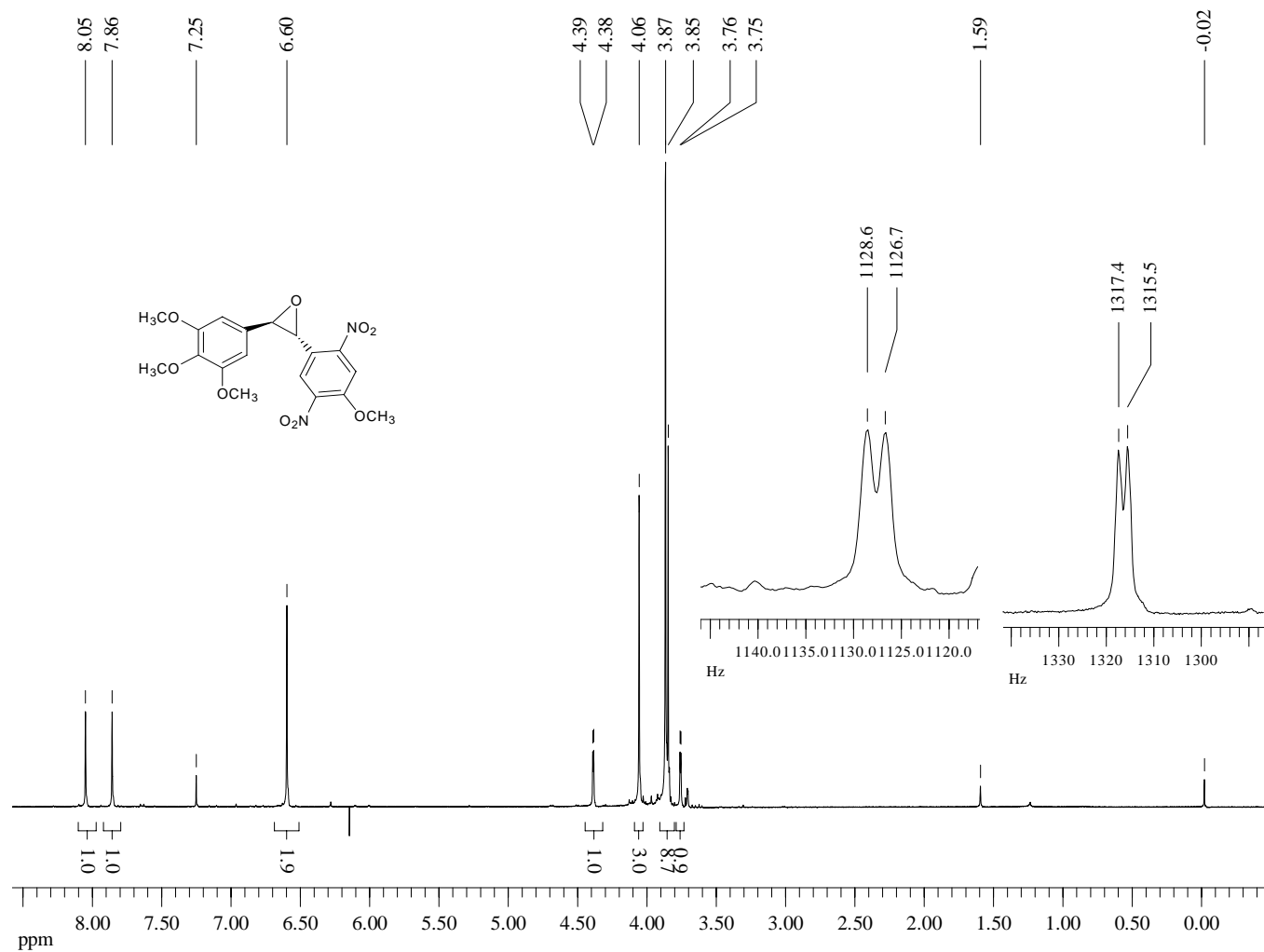
¹³C-NMR (75 MHz, CDCl₃) of Compound **34**



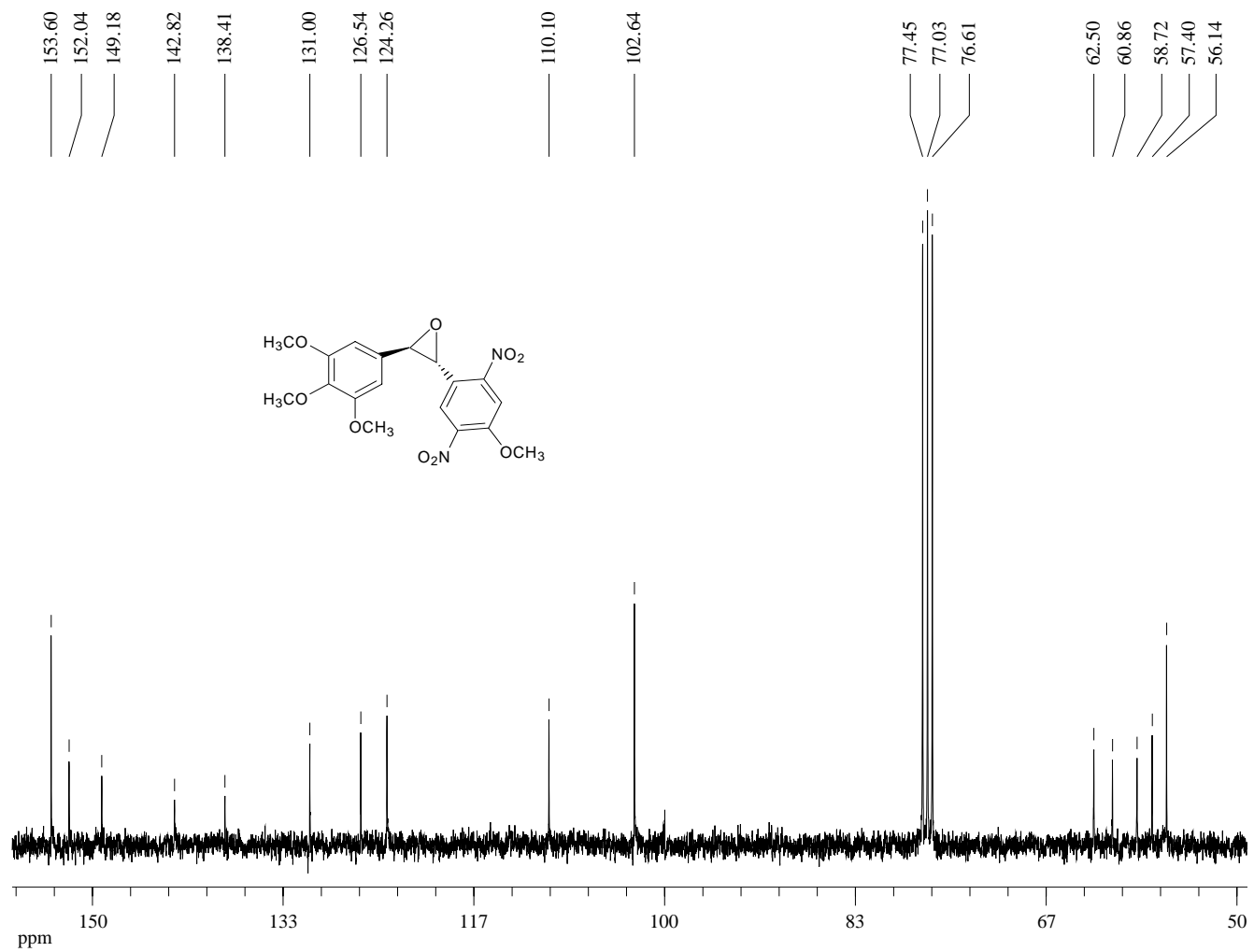
Dept 45-NMR (75 MHz, CDCl₃) of Compound **34**



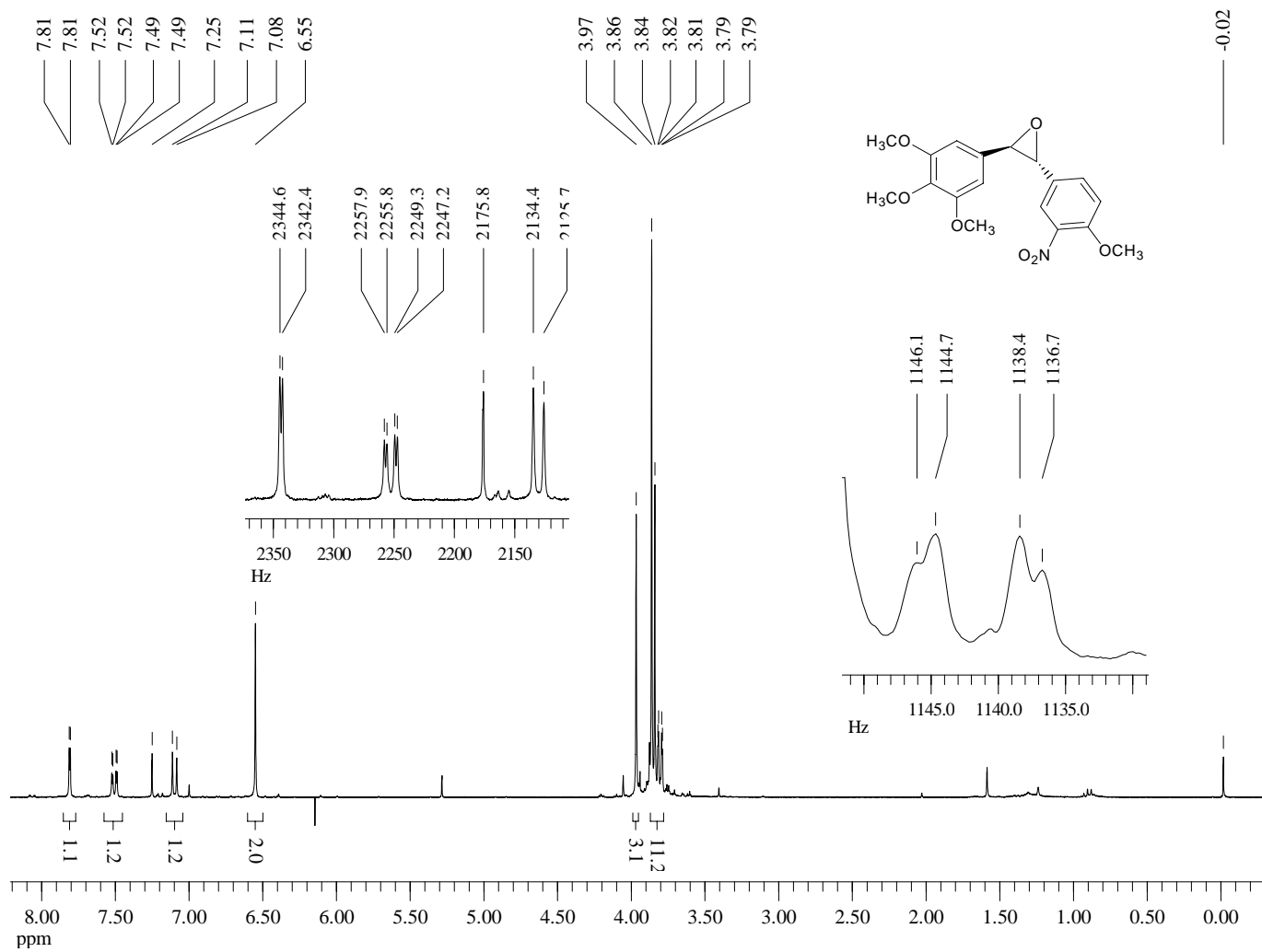
¹H-NMR (300 MHz, CDCl₃) of Compound **35**



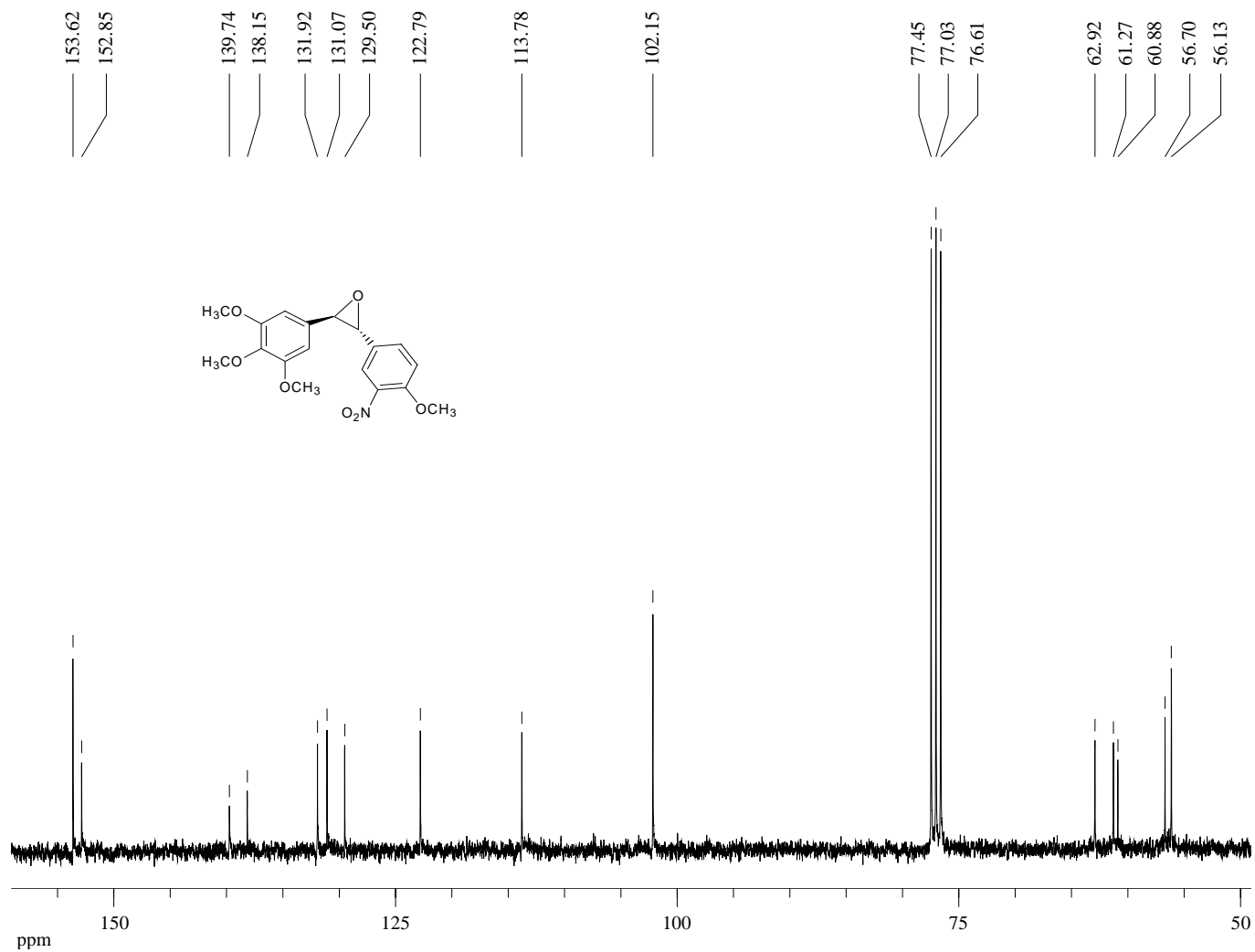
¹³C-NMR (75 MHz, CDCl₃) of Compound **35**



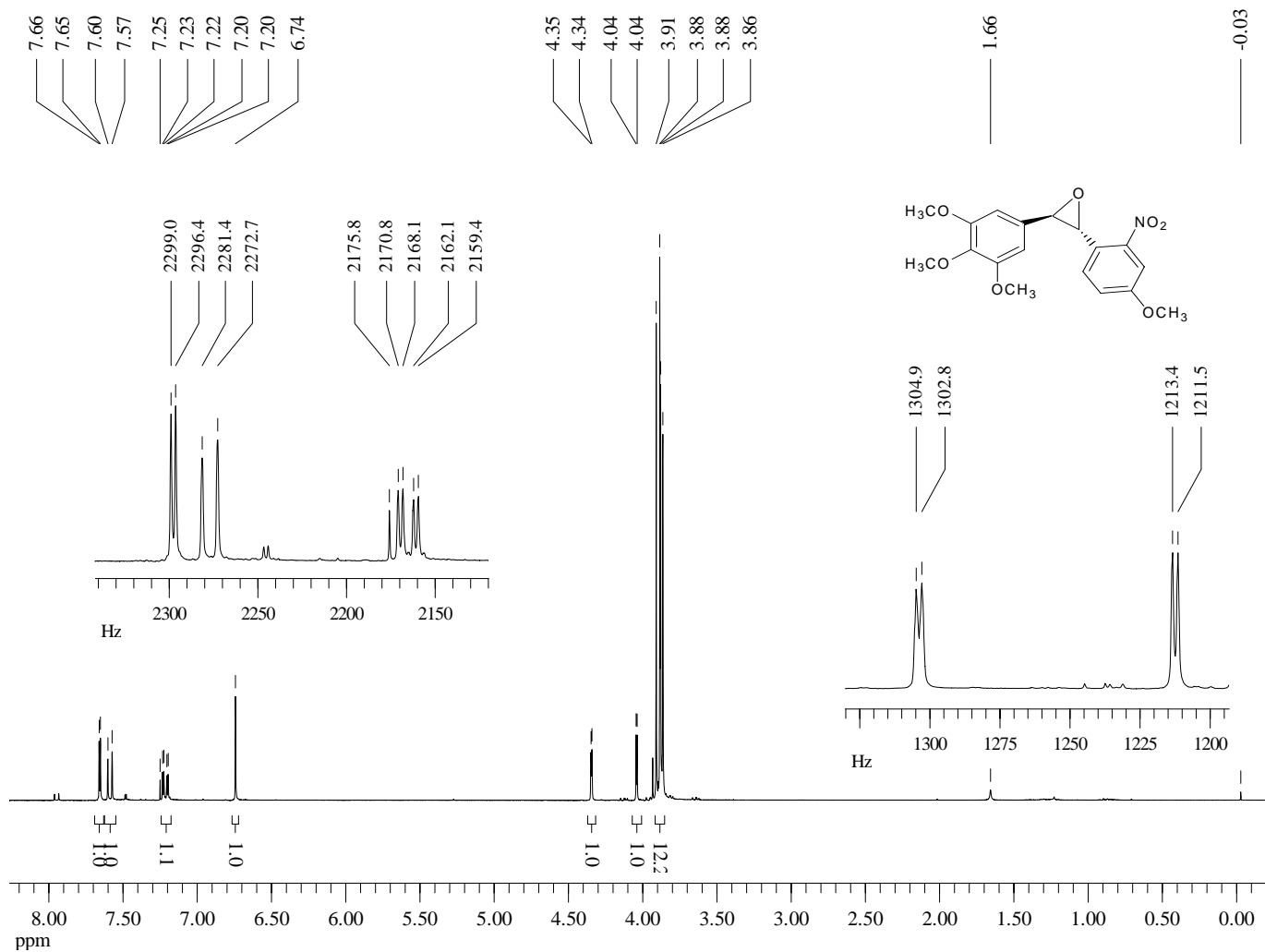
¹H-NMR (300 MHz, CDCl₃) of Compound **36**



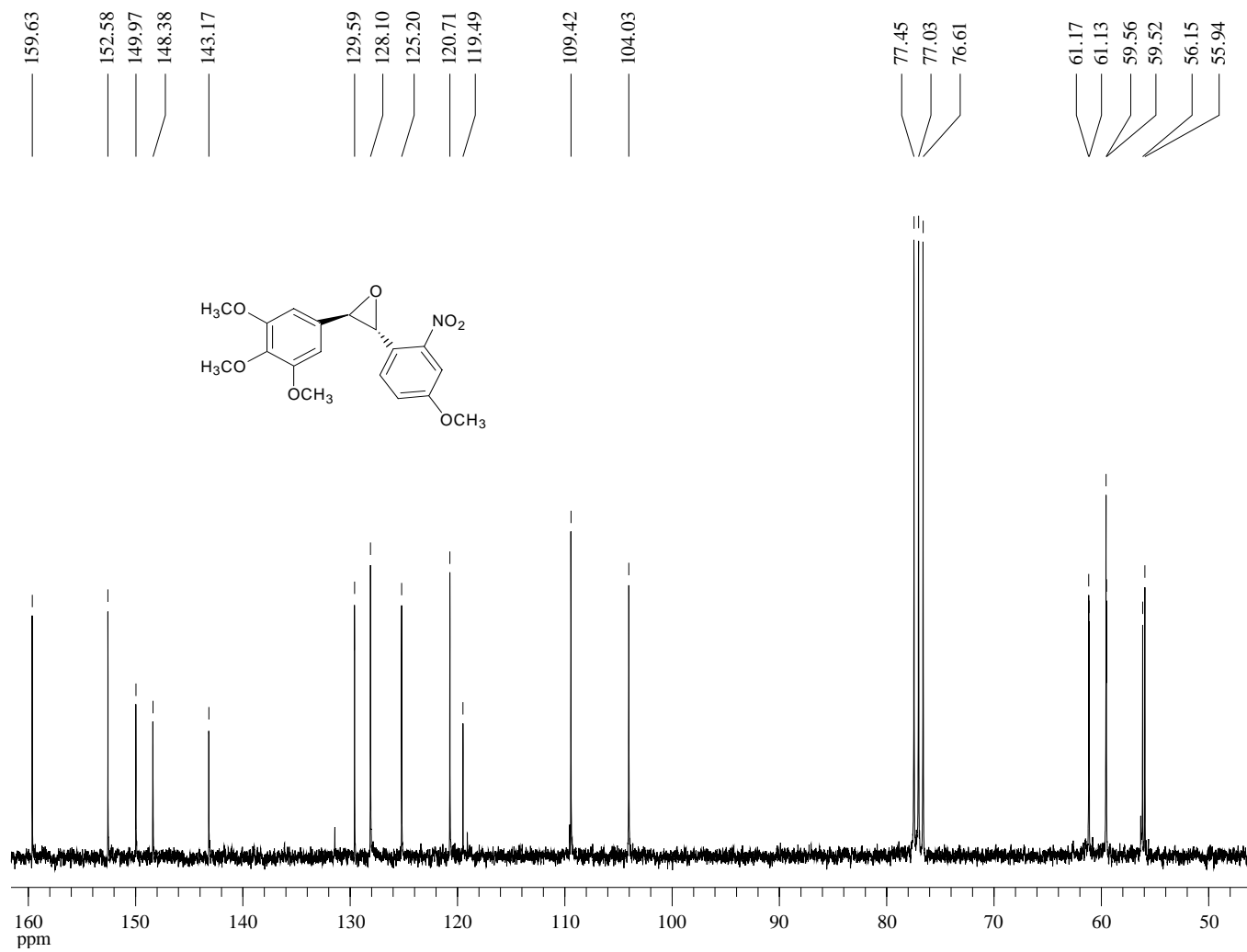
¹³C-NMR (75 MHz, CDCl₃) of Compound **36**



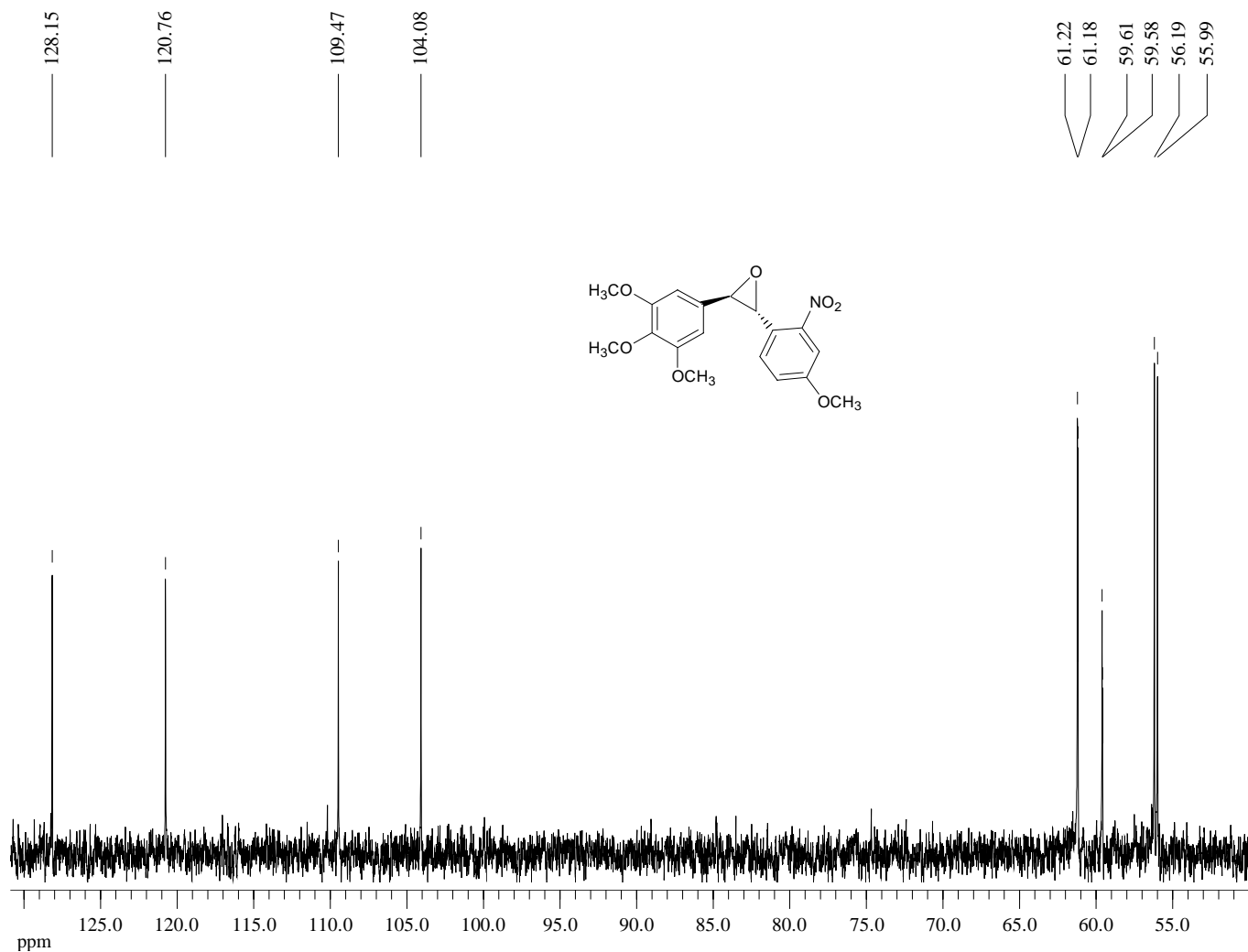
¹H-NMR (300 MHz, CDCl₃) of Compound **37**



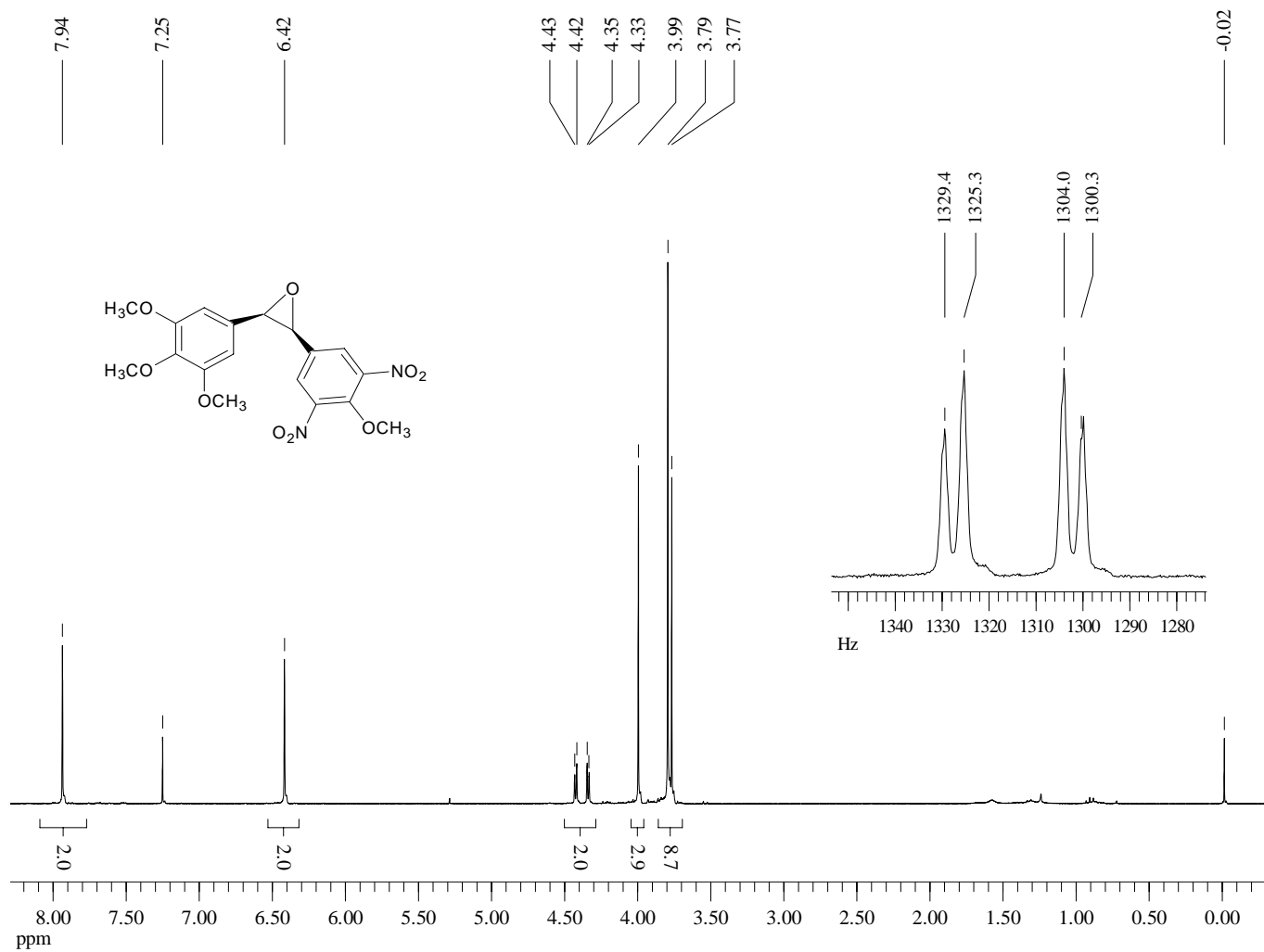
¹³C-NMR (75 MHz, CDCl₃) of Compound **37**



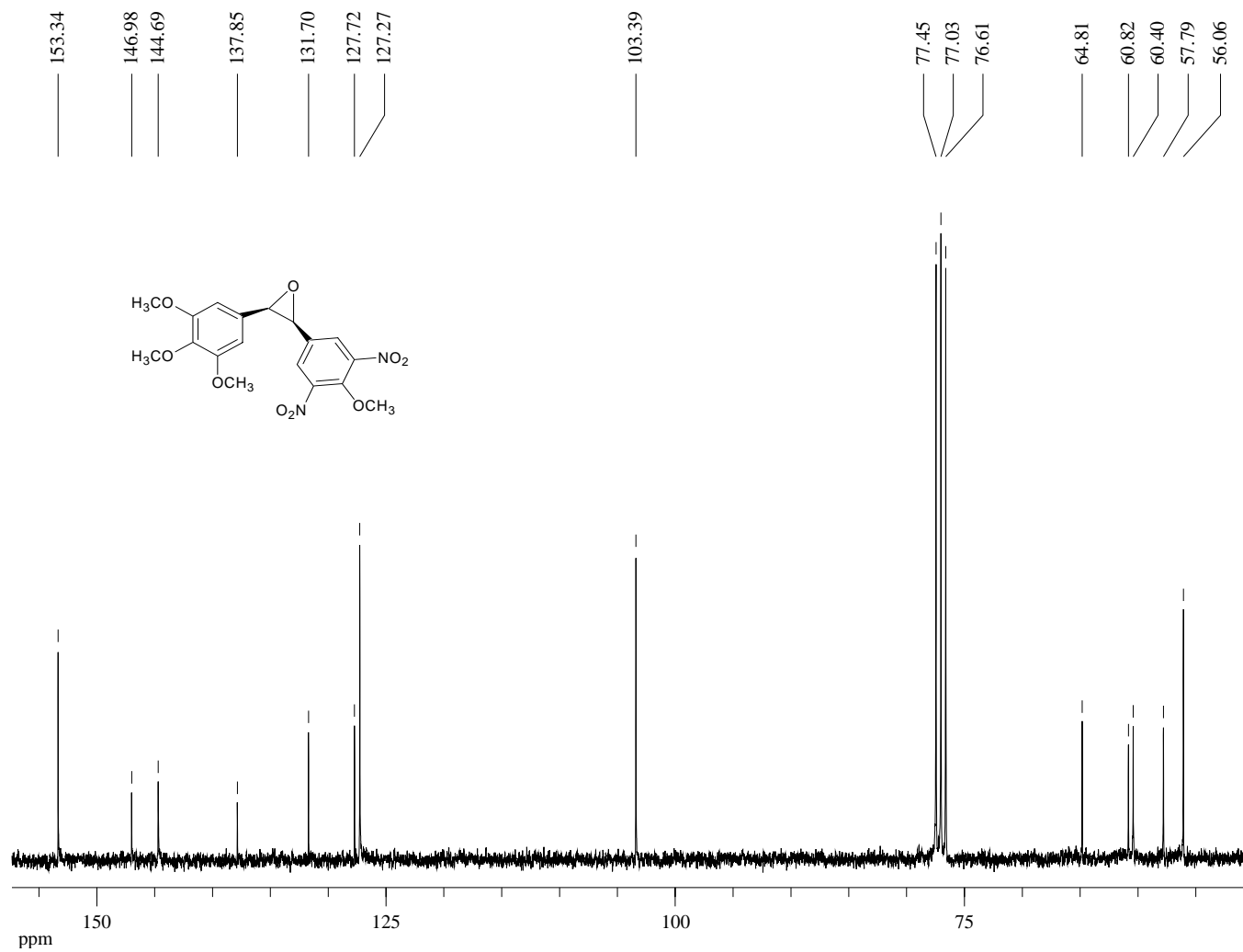
Dept 45-NMR (75 MHz, CDCl₃) of Compound **37**



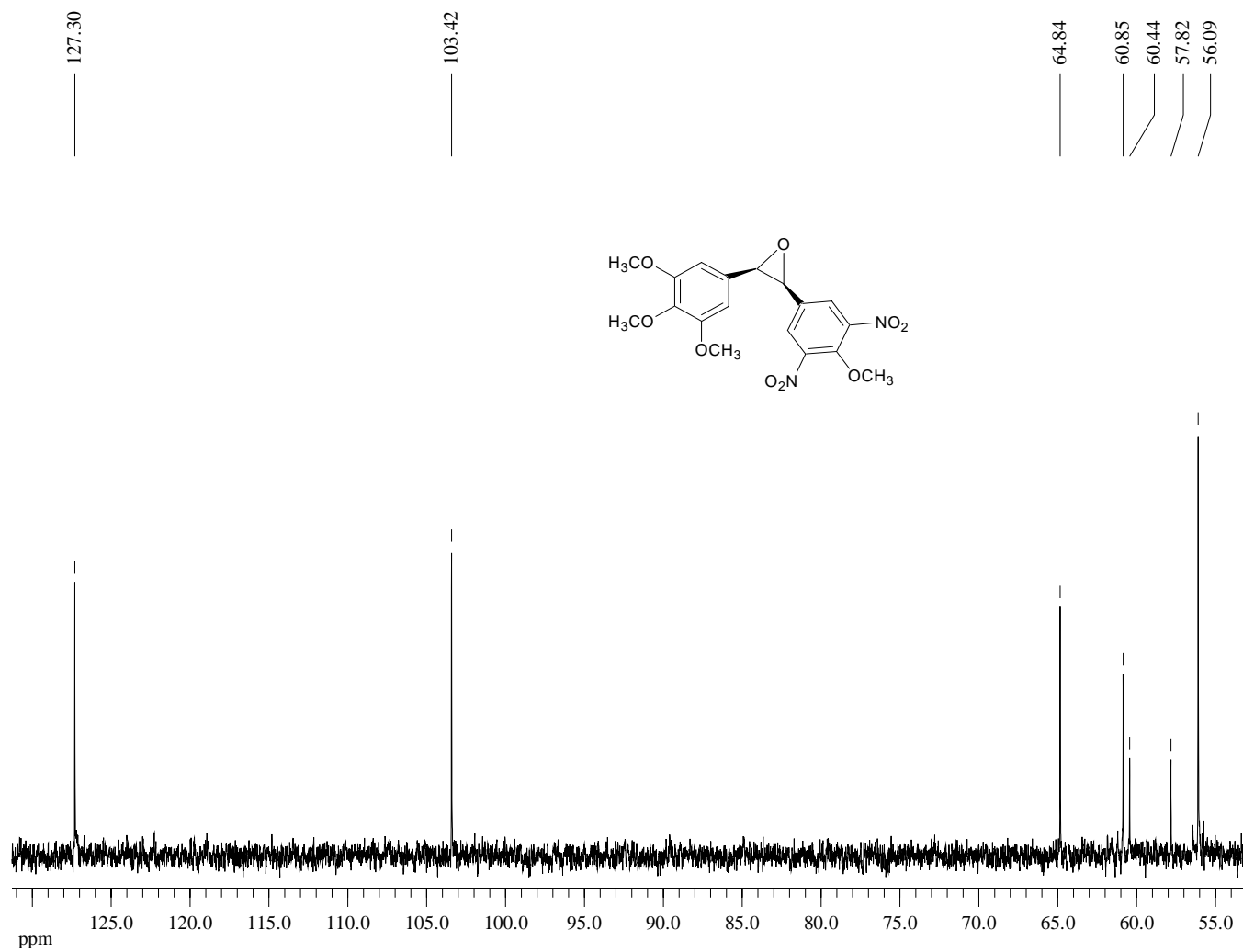
¹H-NMR (300 MHz, CDCl₃) of Compound **38**



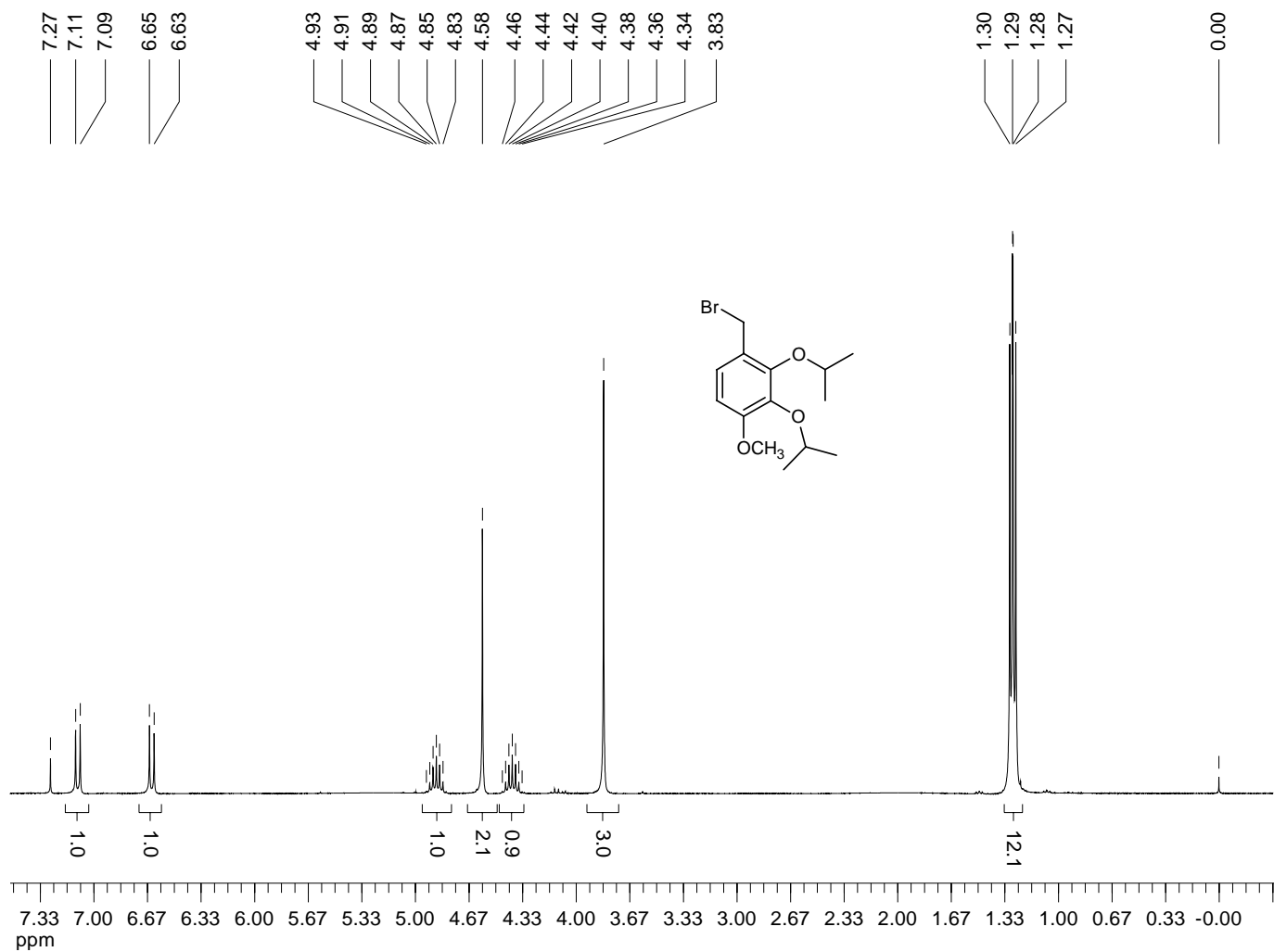
^{13}C -NMR (75 MHz, CDCl_3) of Compound **38**



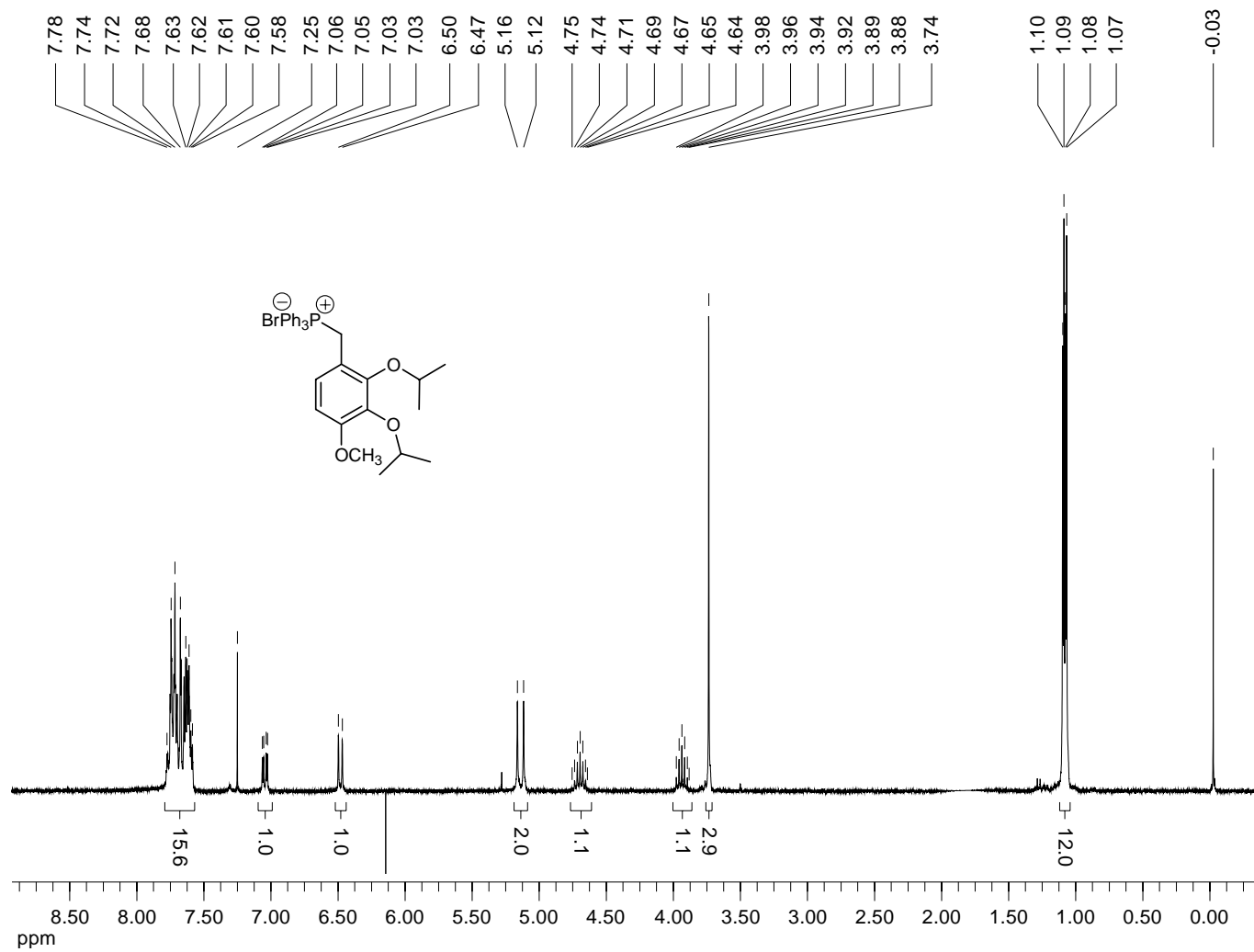
Dept 45-NMR (75 MHz, CDCl₃) of Compound **38**



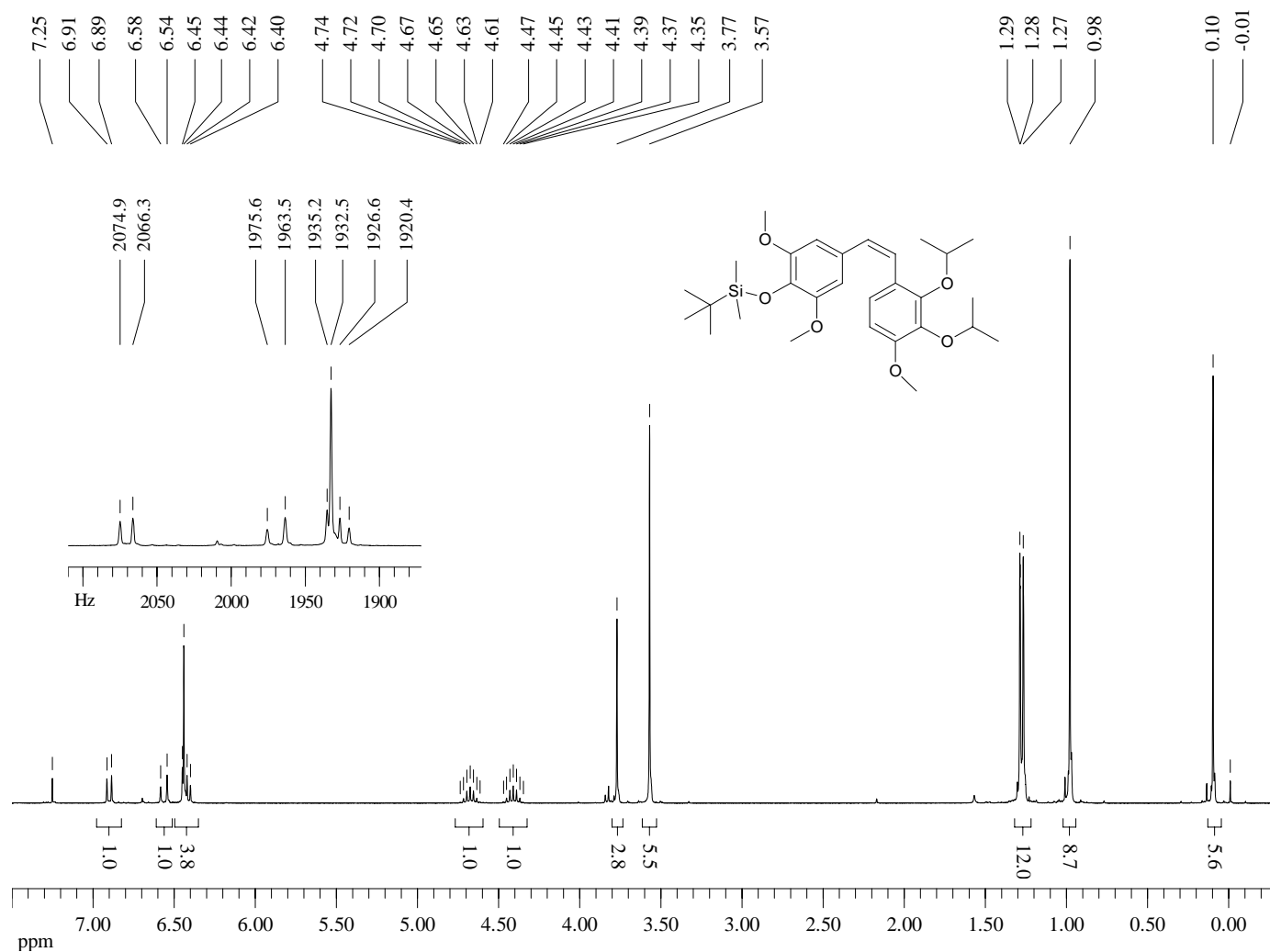
¹H-NMR (300 MHz, CDCl₃) of Compound **39a**



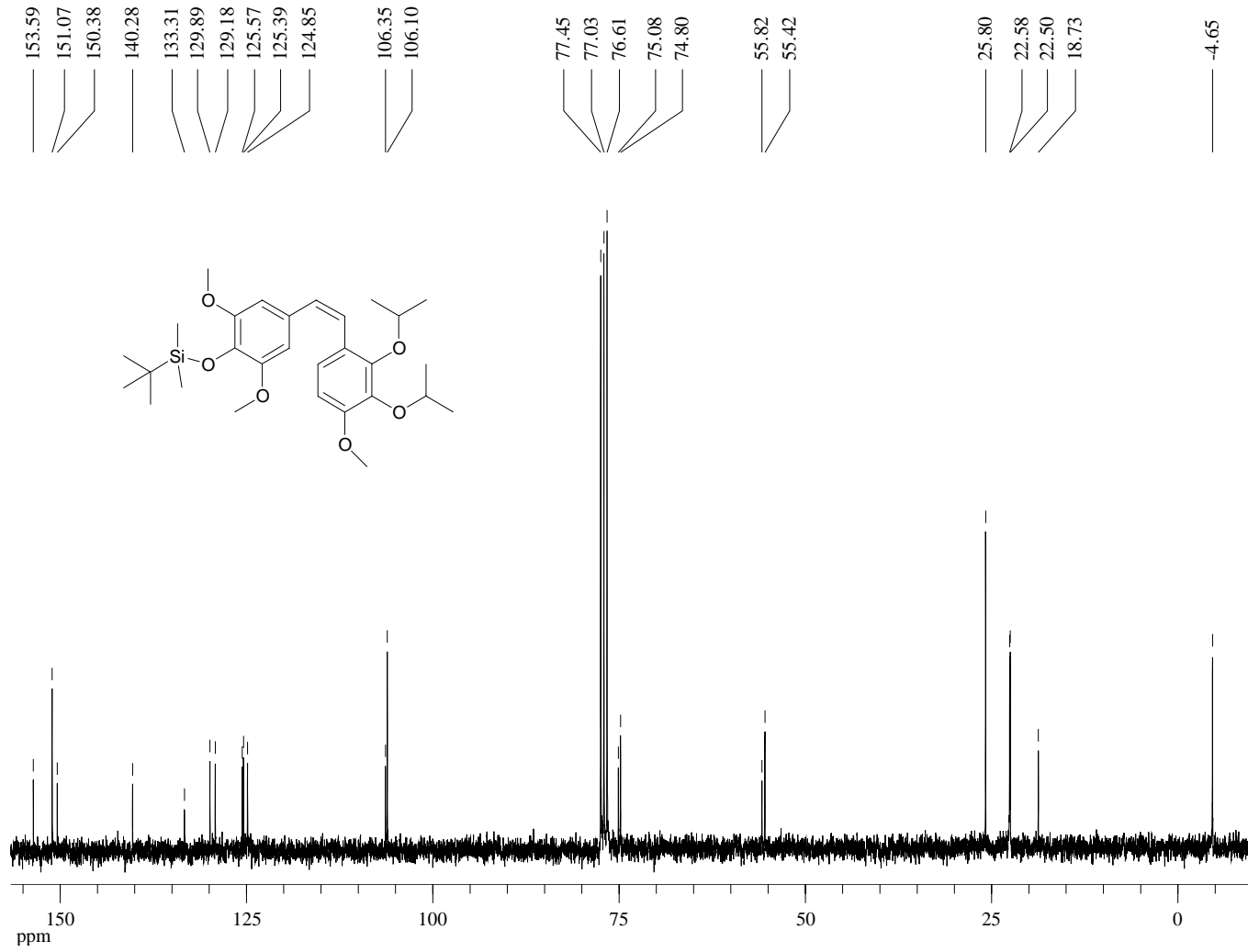
¹H-NMR (300 MHz, CDCl₃) of Compound **39b**



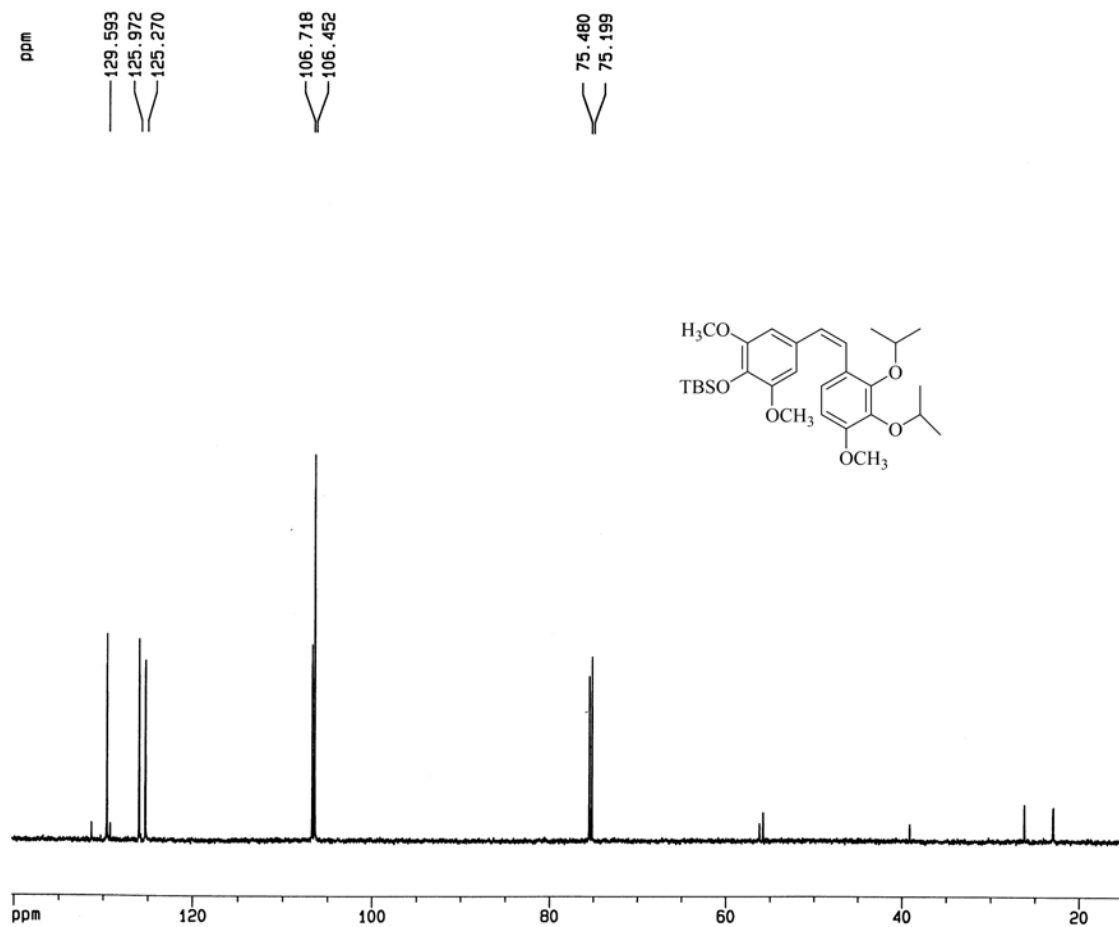
¹H-NMR (300 MHz, CDCl₃) of Compound **40a**



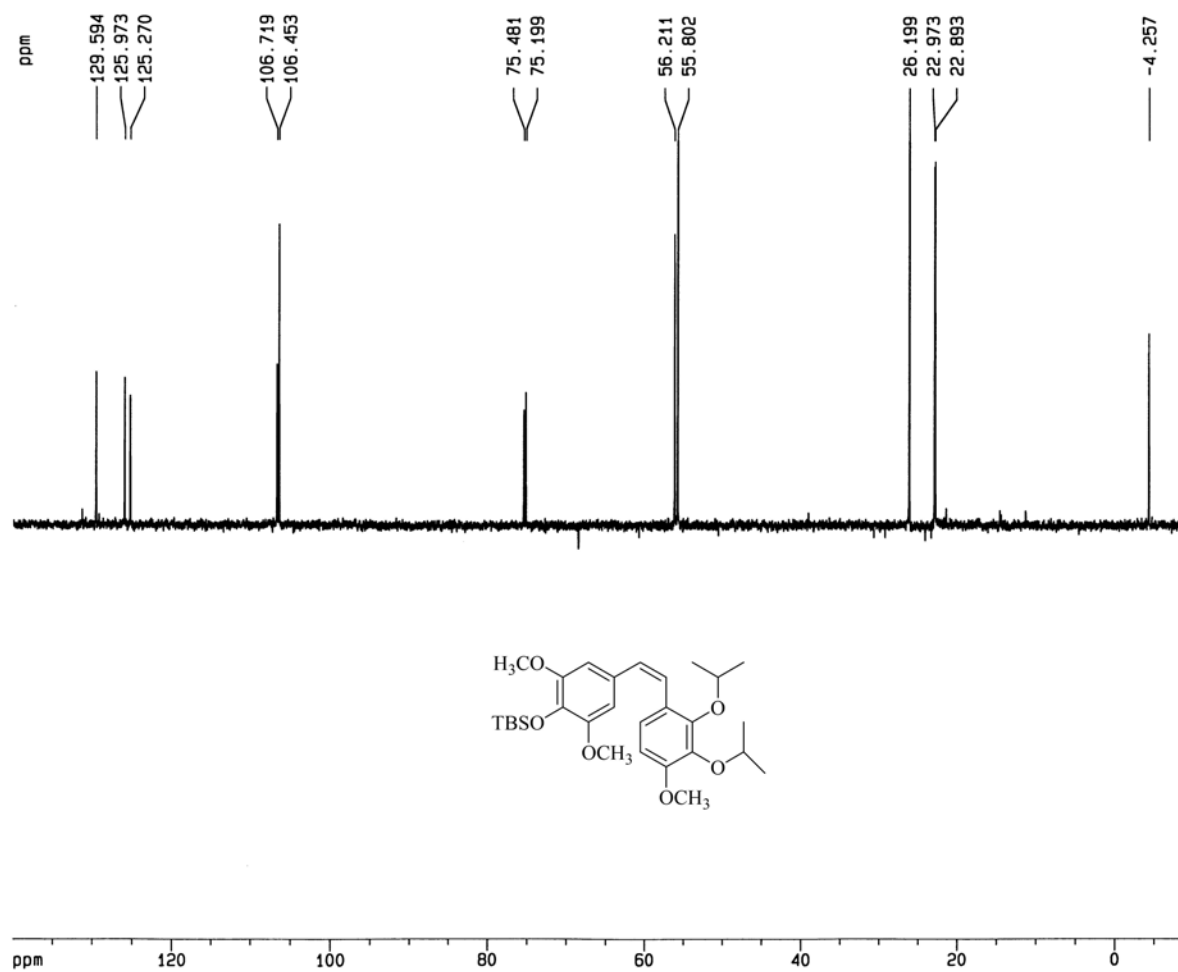
¹³C-NMR (75 MHz, CDCl₃) of Compound **40a**



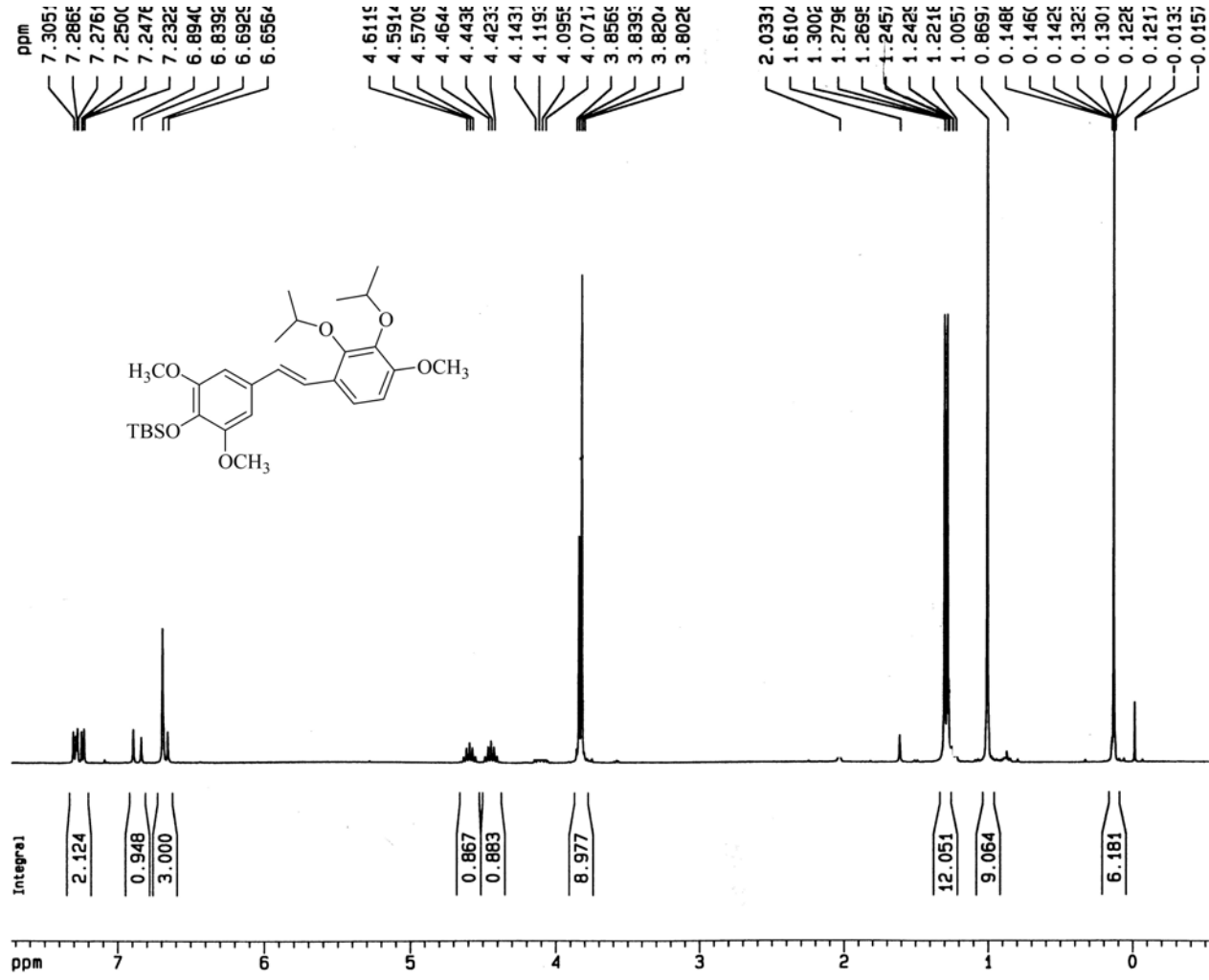
Dept 90-NMR (75 MHz, CDCl₃) of Compound **40a**



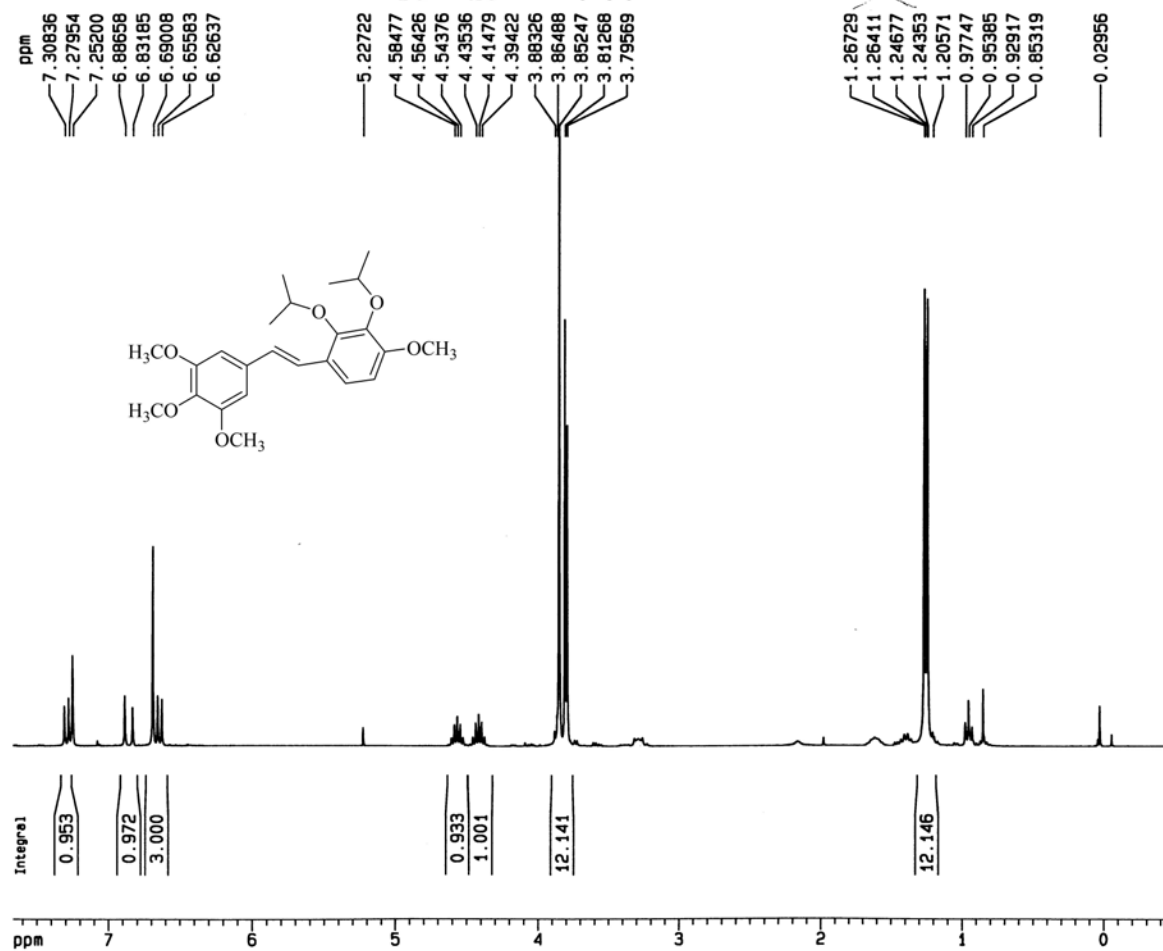
Dept 135-NMR (75 MHz, CDCl₃) of Compound **40a**



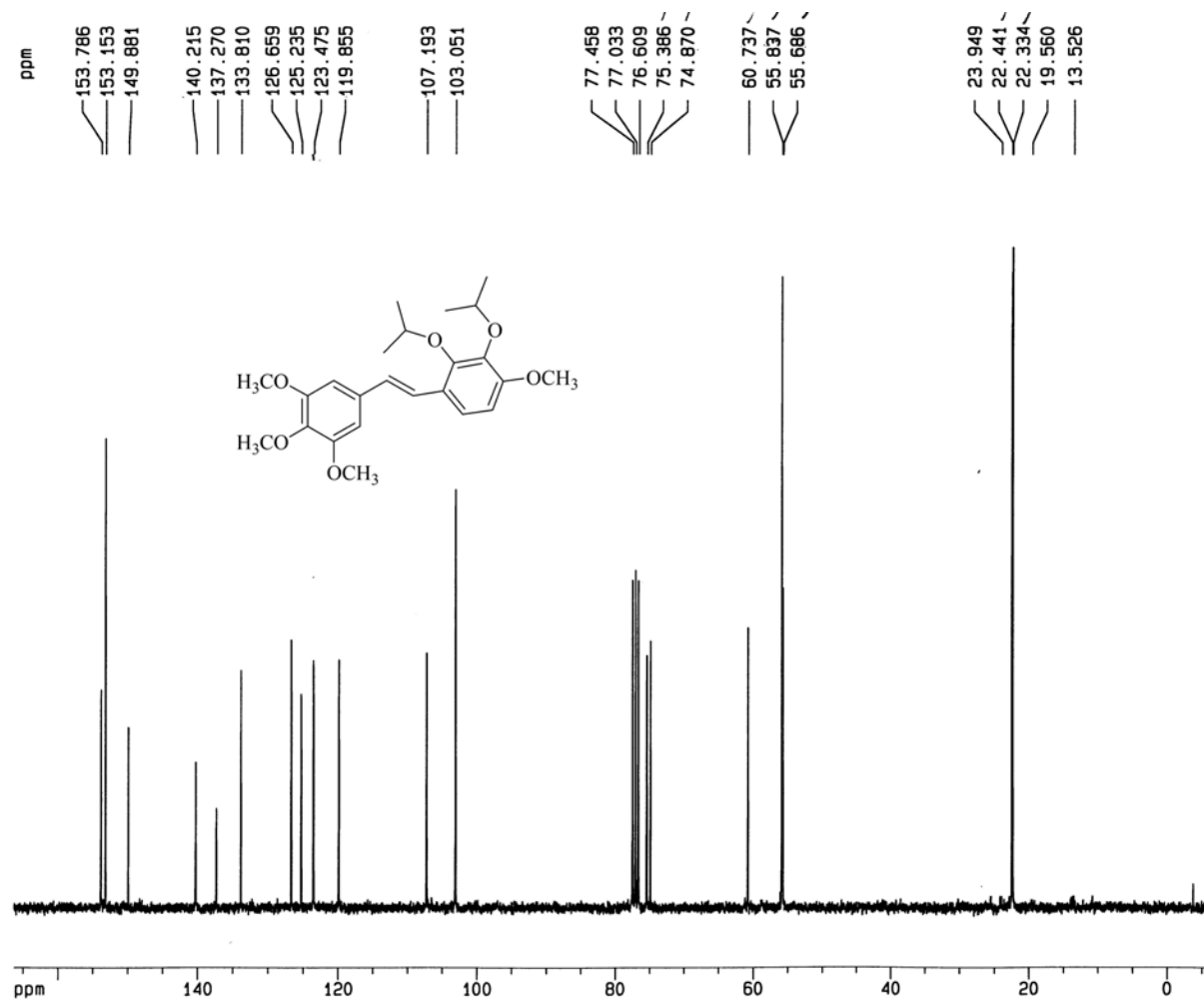
¹H-NMR (300 MHz, CDCl₃) of Compound **40b**



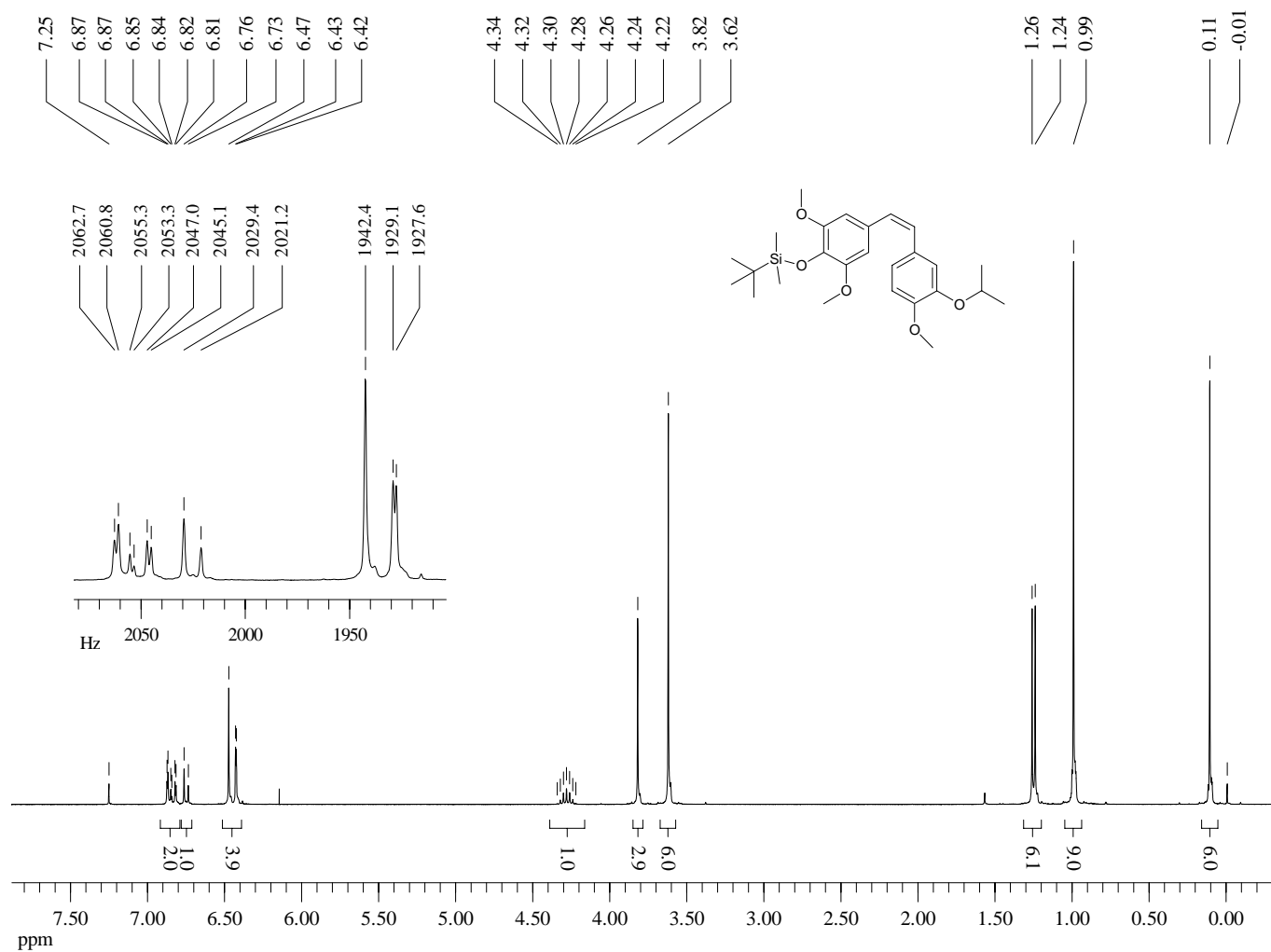
¹H-NMR (300 MHz, CDCl₃) of Compound 40c



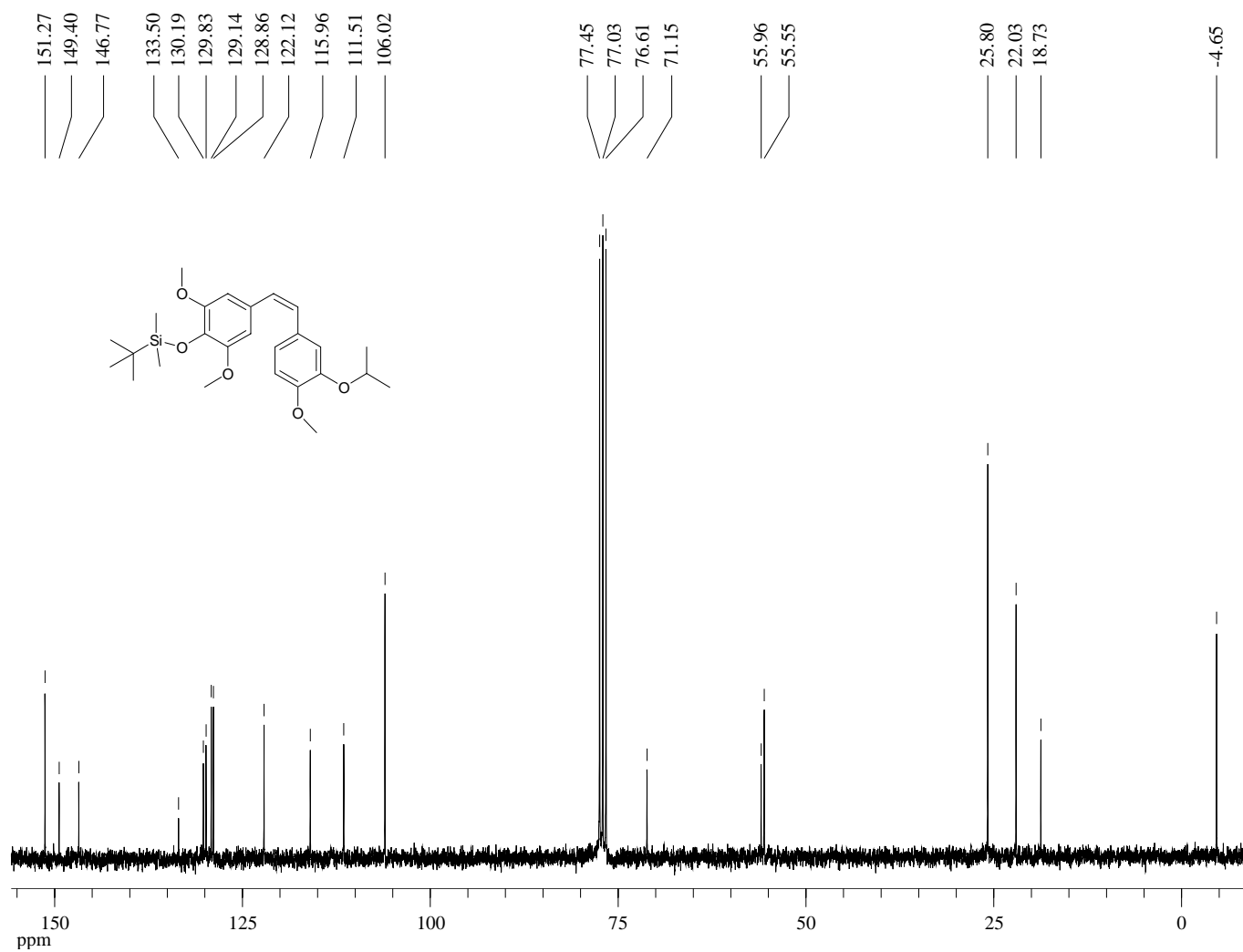
$^{13}\text{C-NMR}$ (75 MHz, CDCl_3) of Compound **40c**



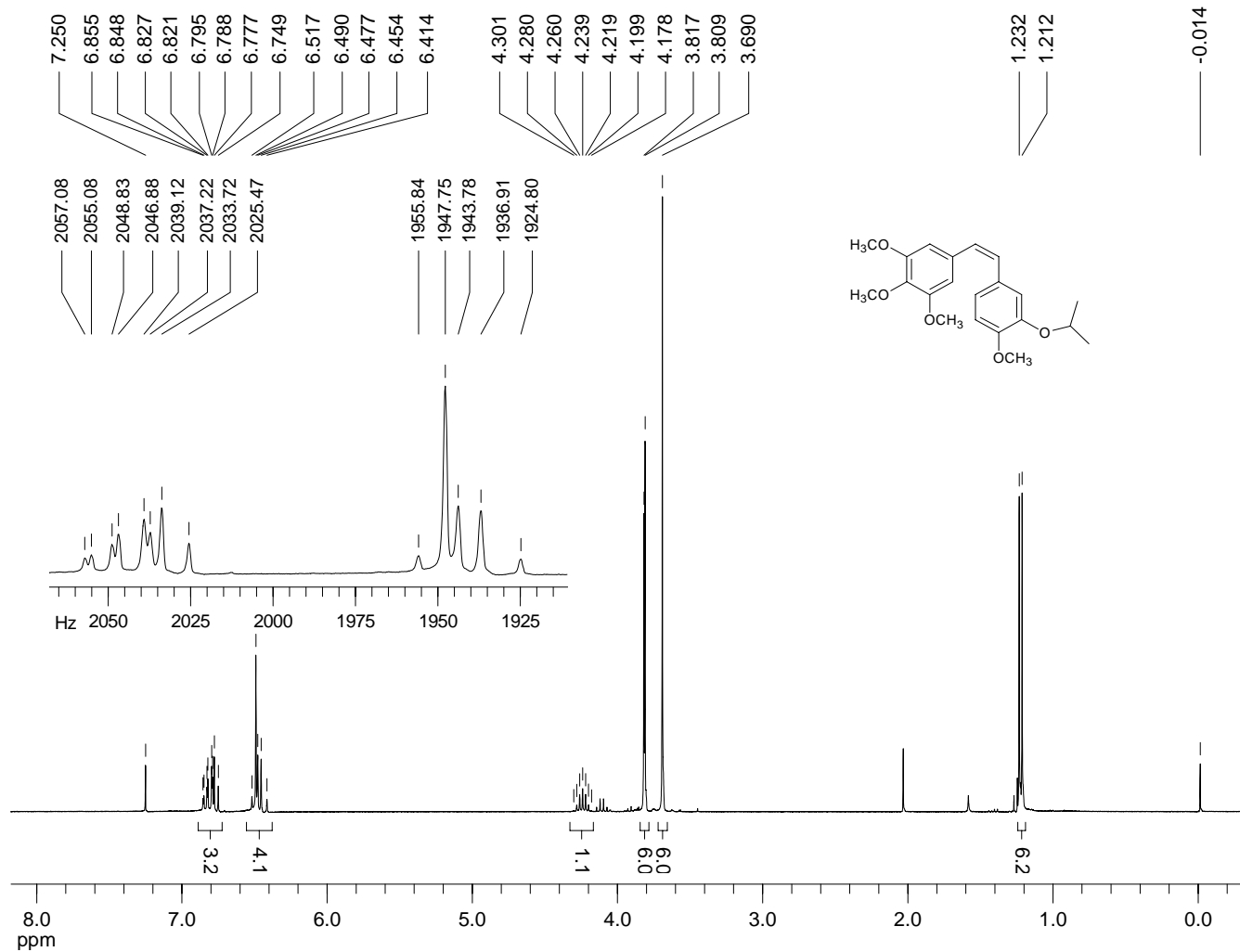
¹H-NMR (300 MHz, CDCl₃) of Compound **40d**



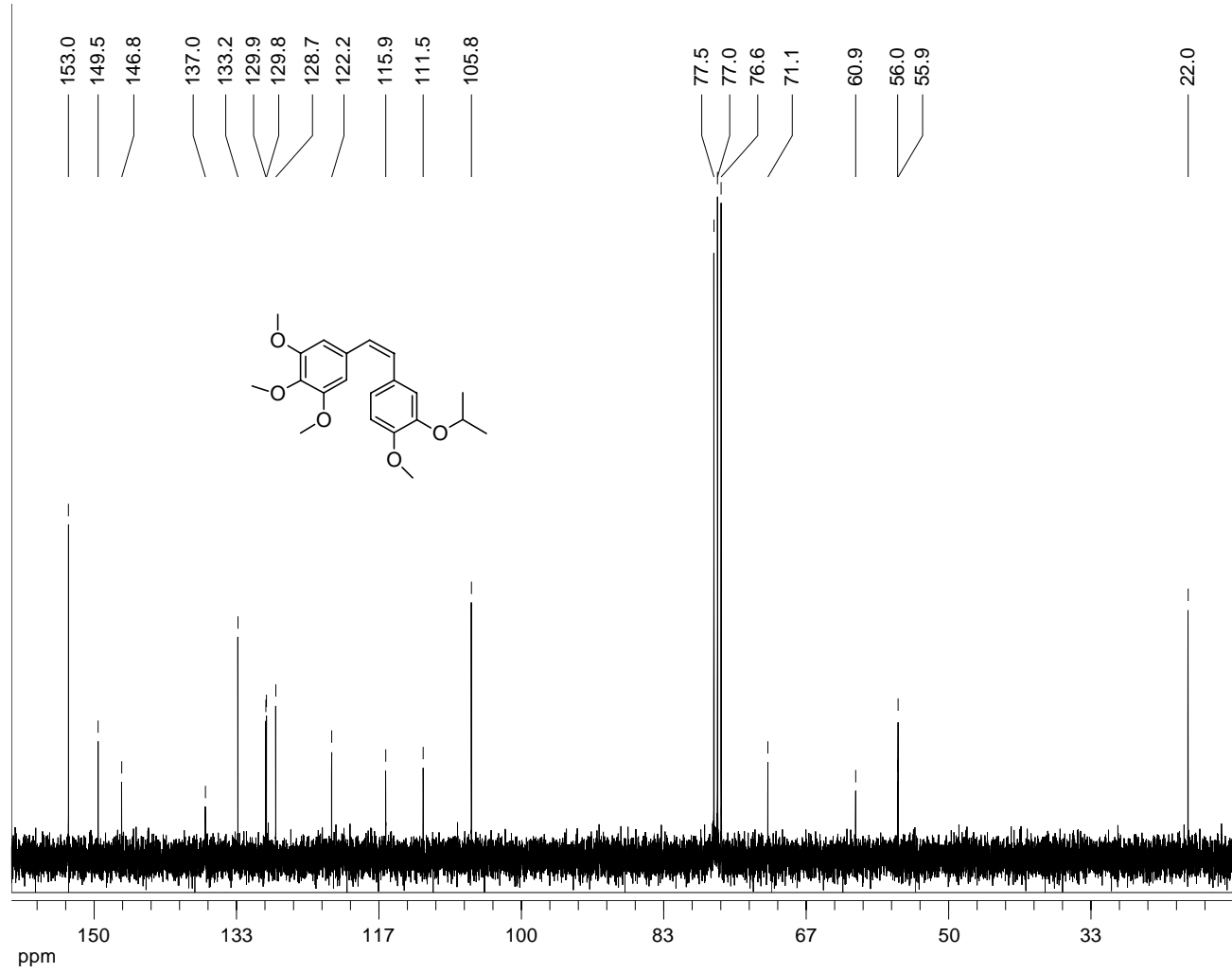
¹³C-NMR (75 MHz, CDCl₃) of Compound **40d**



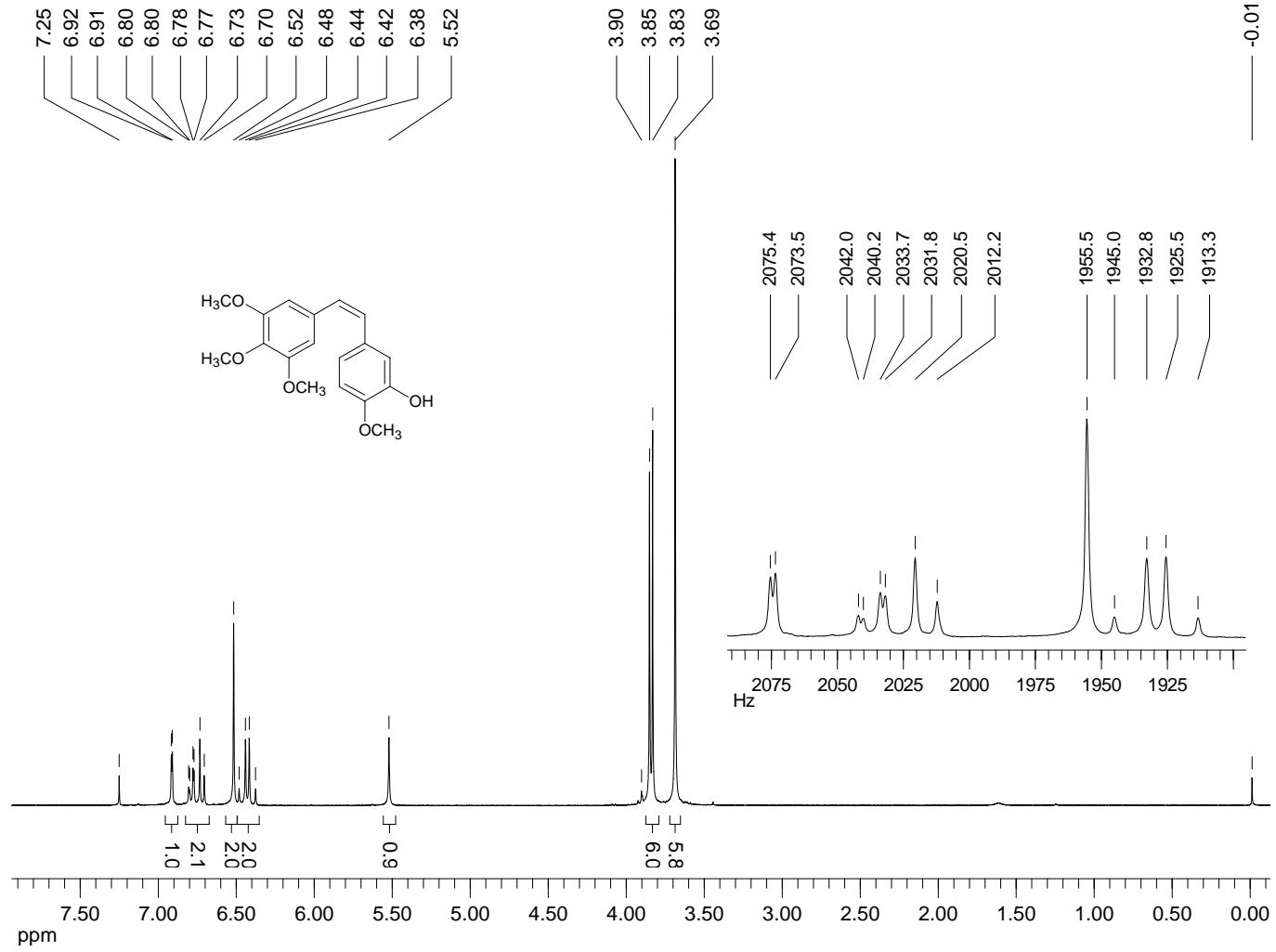
¹H-NMR (300 MHz, CDCl₃) of Compound **40e**



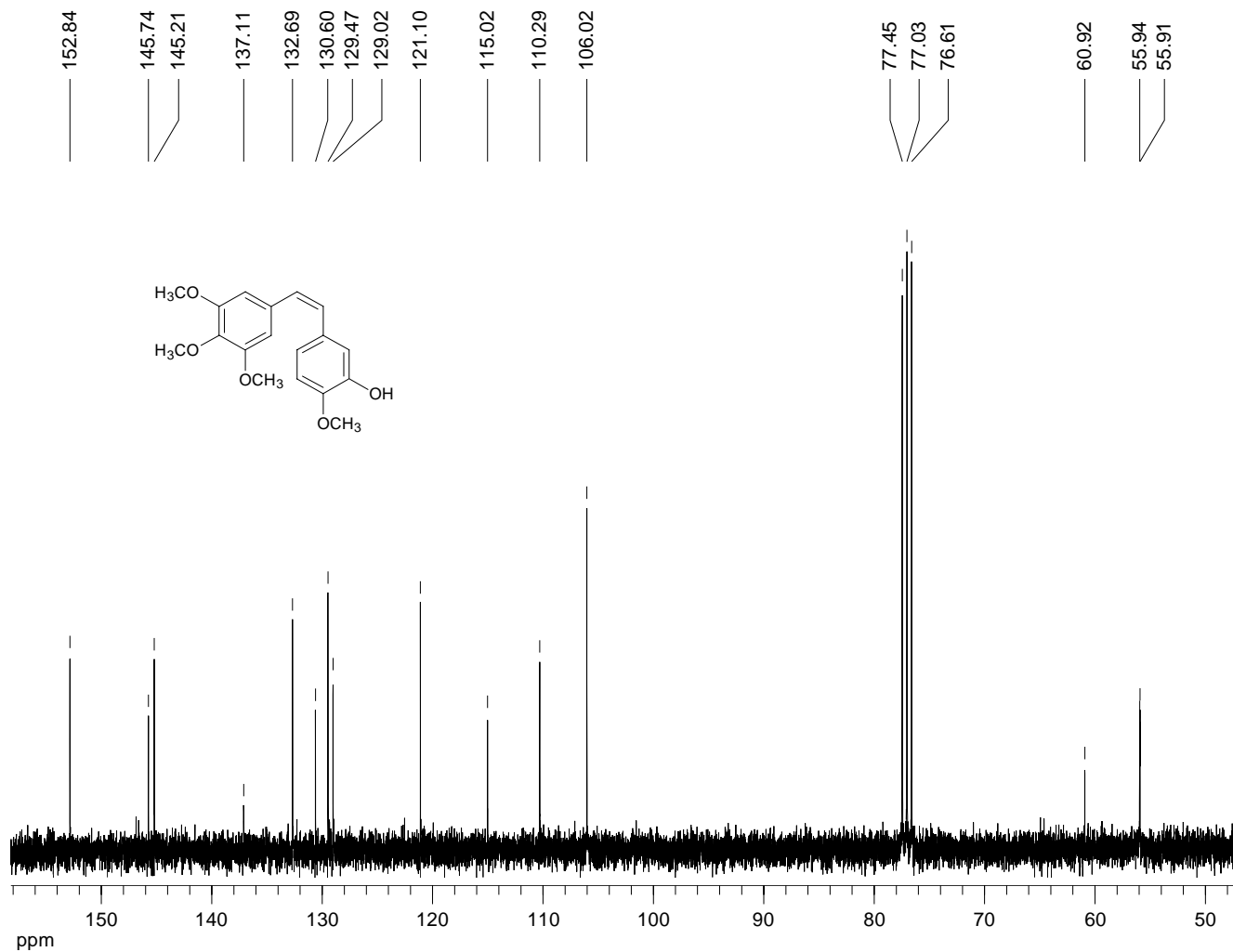
$^{13}\text{C-NMR}$ (75 MHz, CDCl_3) of Compound **40e**



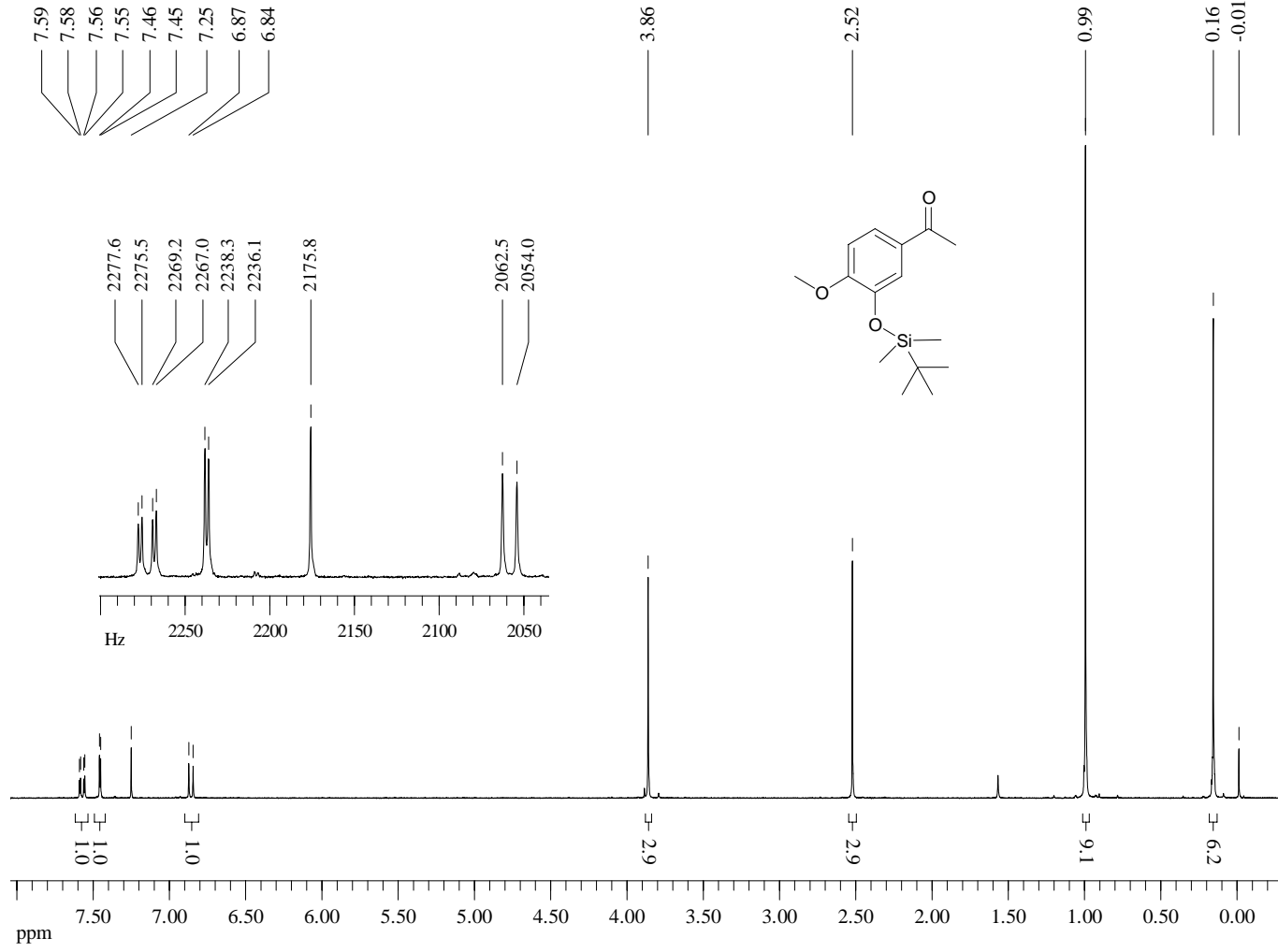
¹H-NMR (300 MHz, CDCl₃) of Compound **40f**



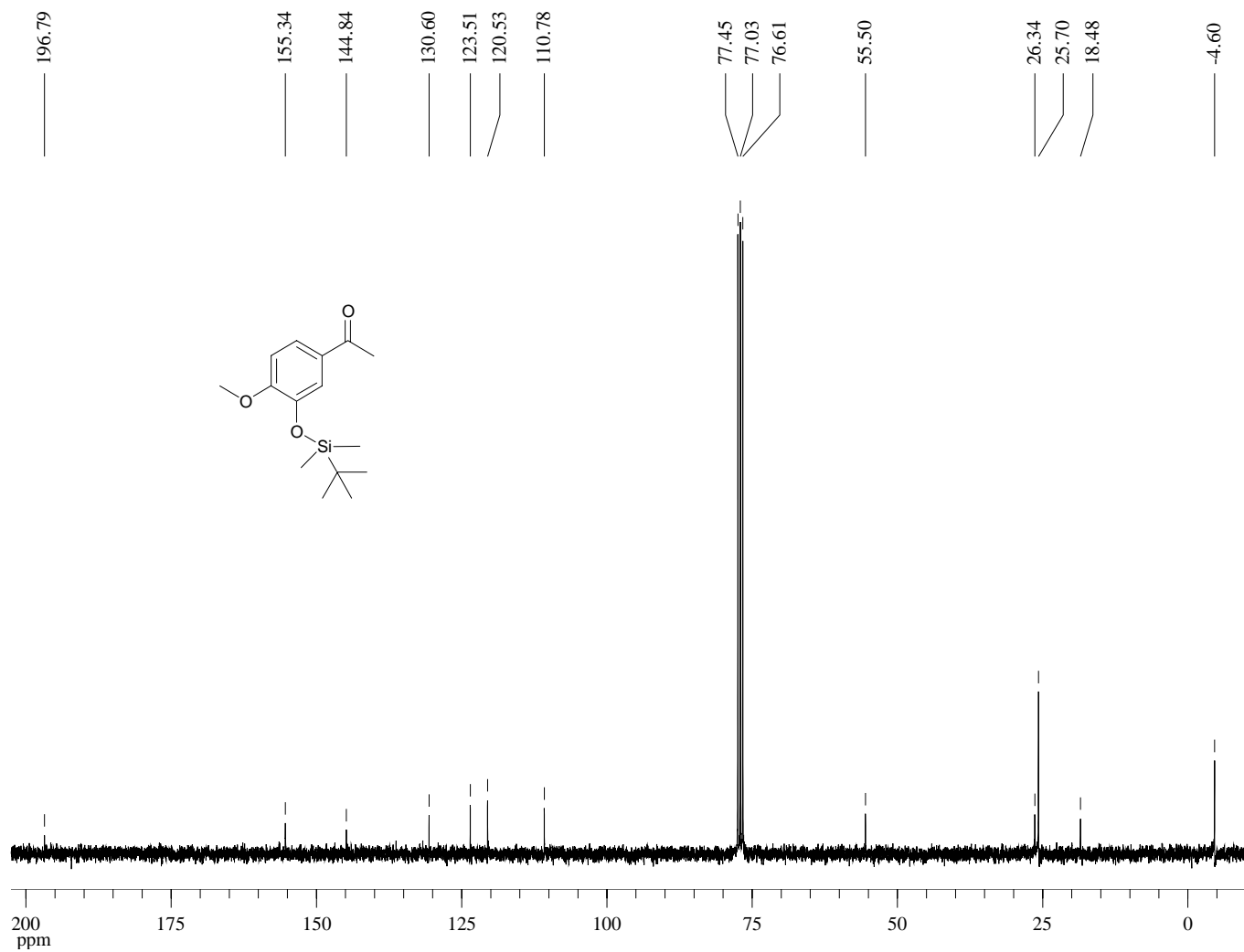
^{13}C -NMR (75 MHz, CDCl_3) of Compound **40f**



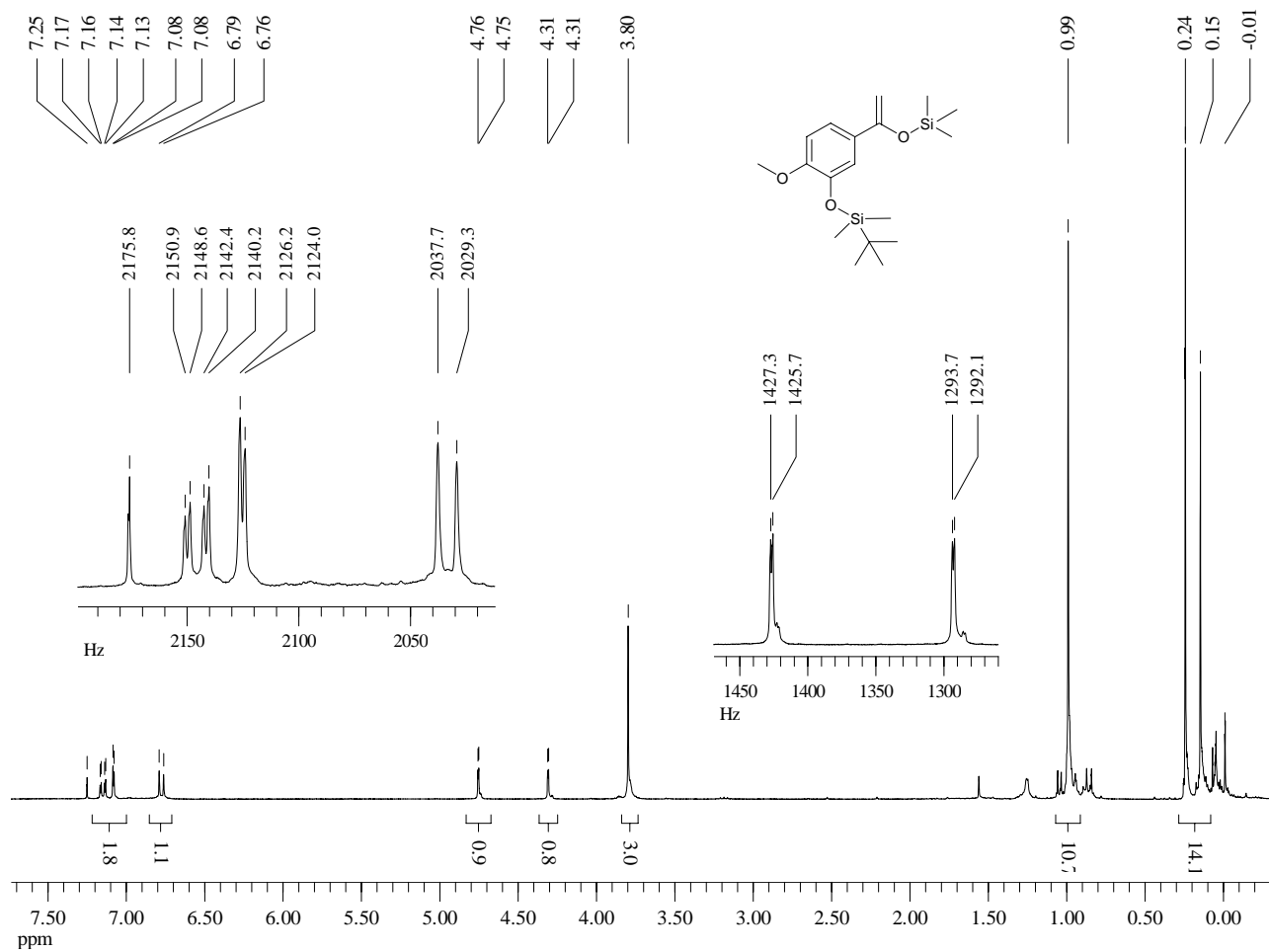
¹H-NMR (300 MHz, CDCl₃) of Compound **41a**



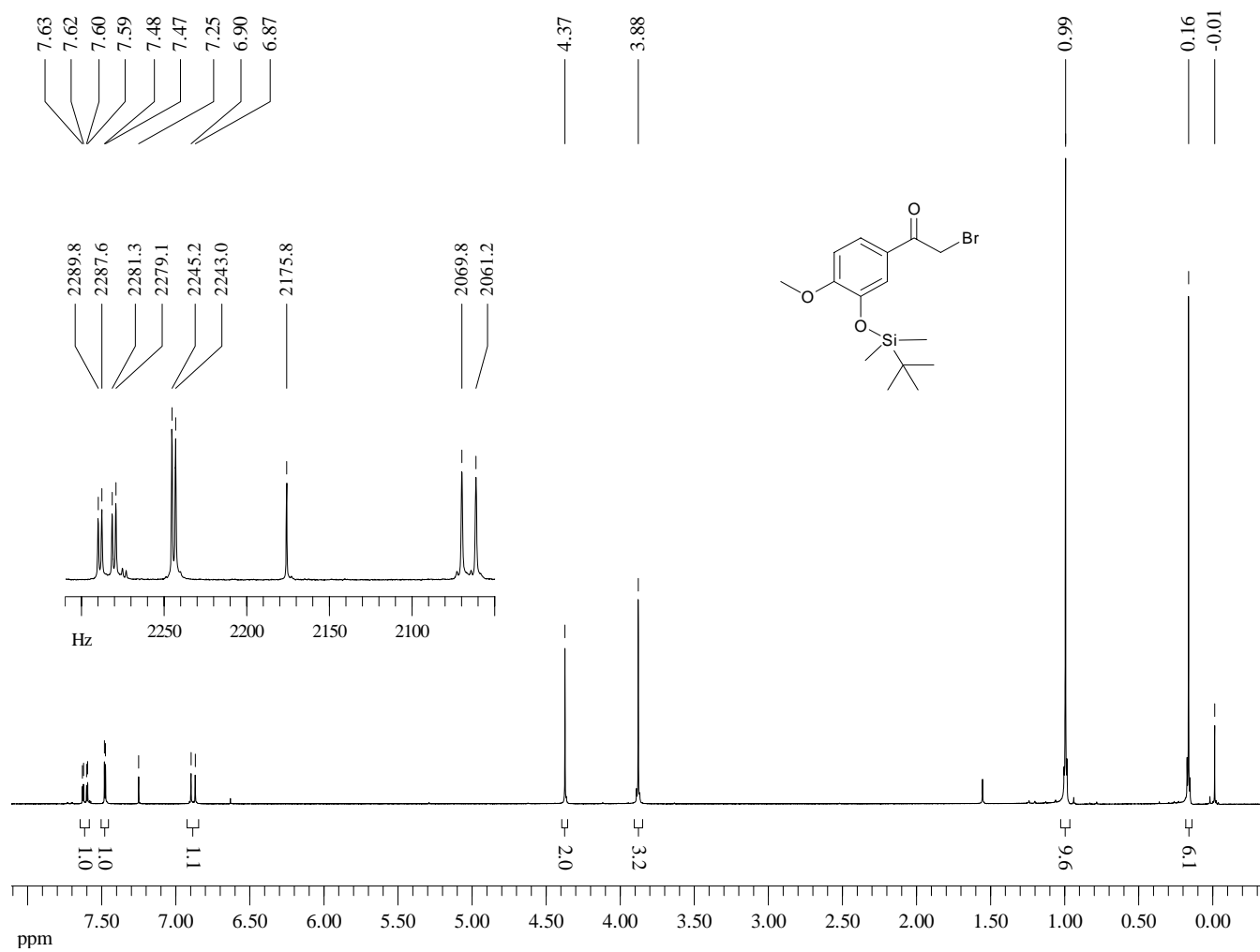
¹³C-NMR (75 MHz, CDCl₃) of Compound **41a**



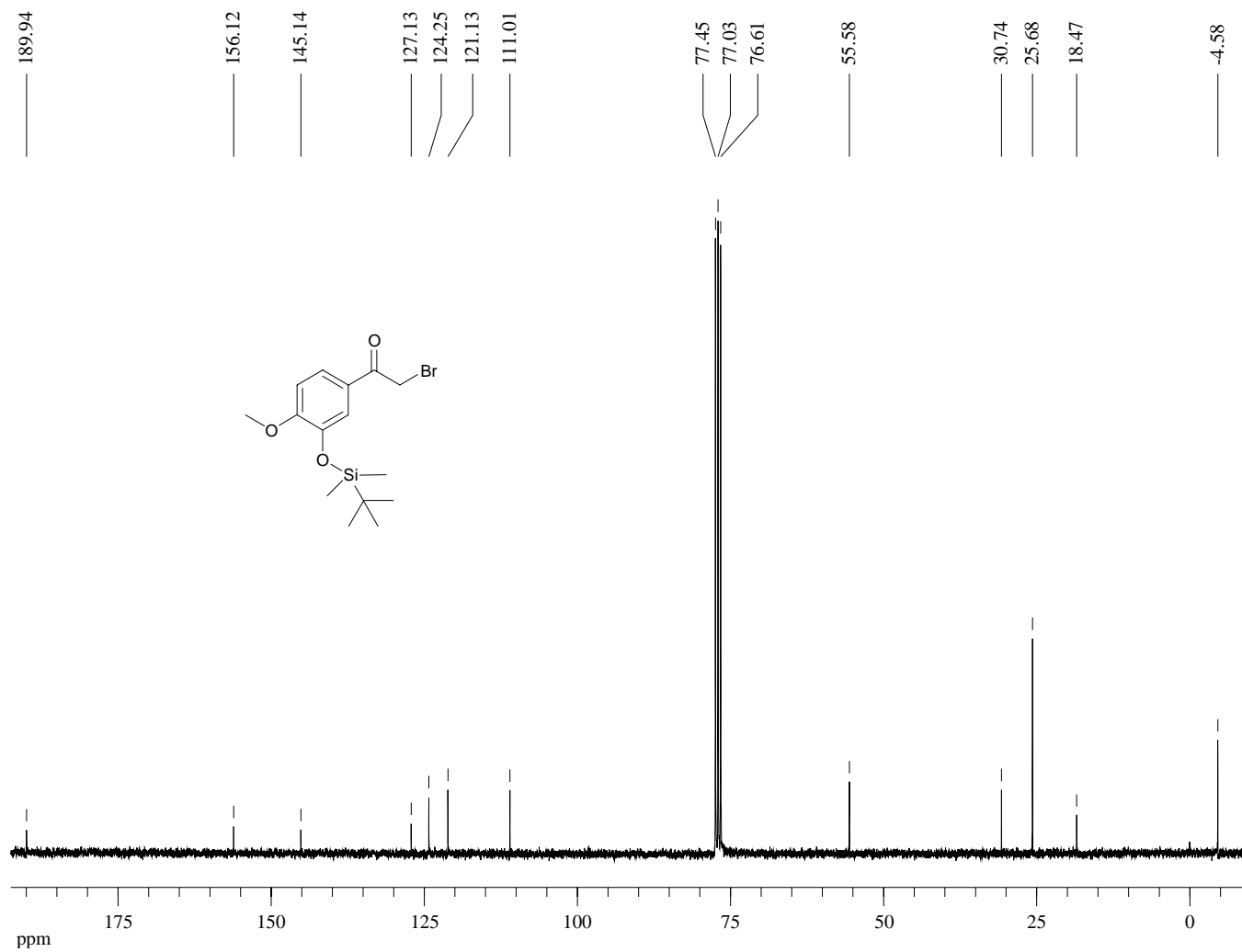
¹H-NMR (300 MHz, CDCl₃) of Compound **41b**



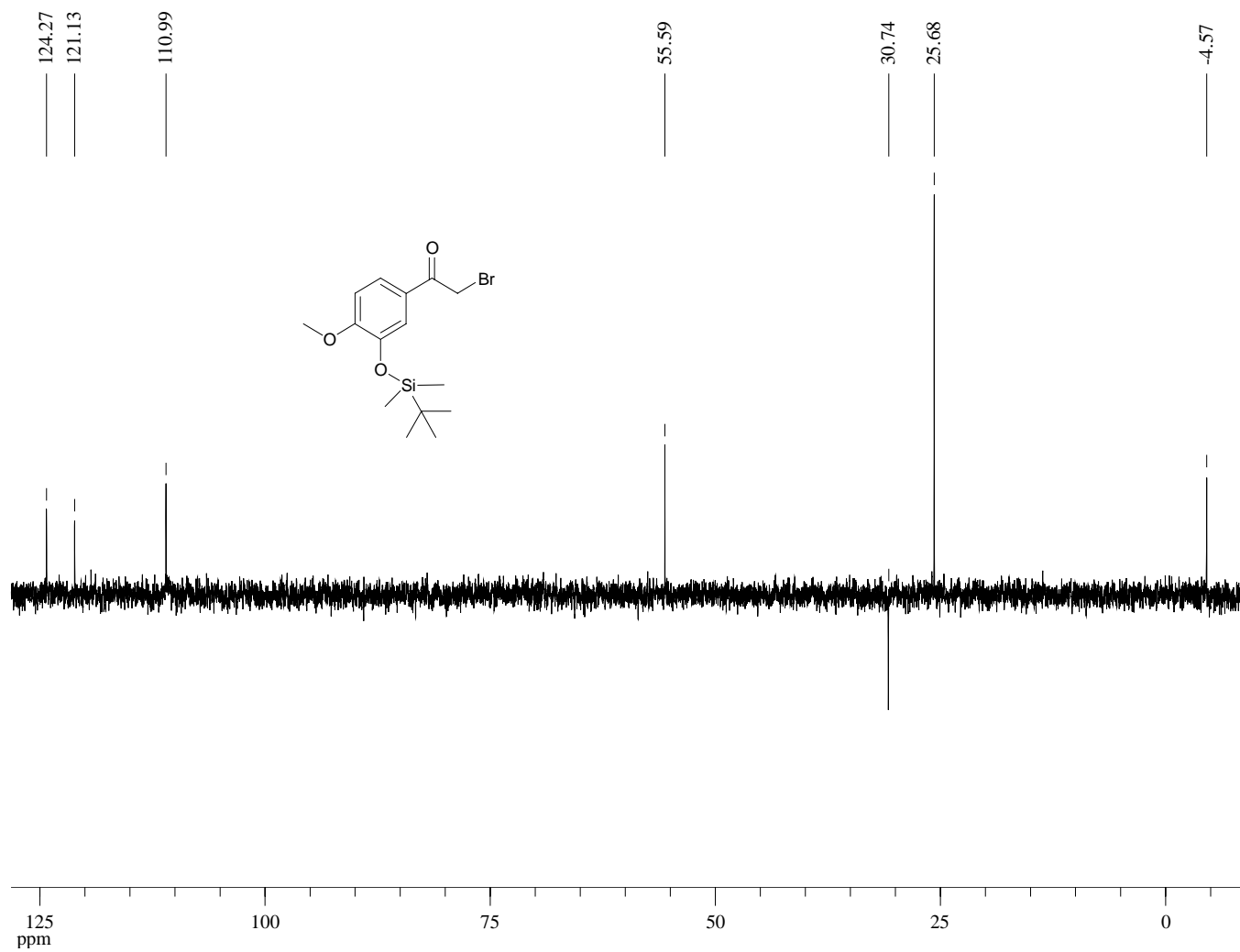
¹H-NMR (300 MHz, CDCl₃) of Compound **41c**



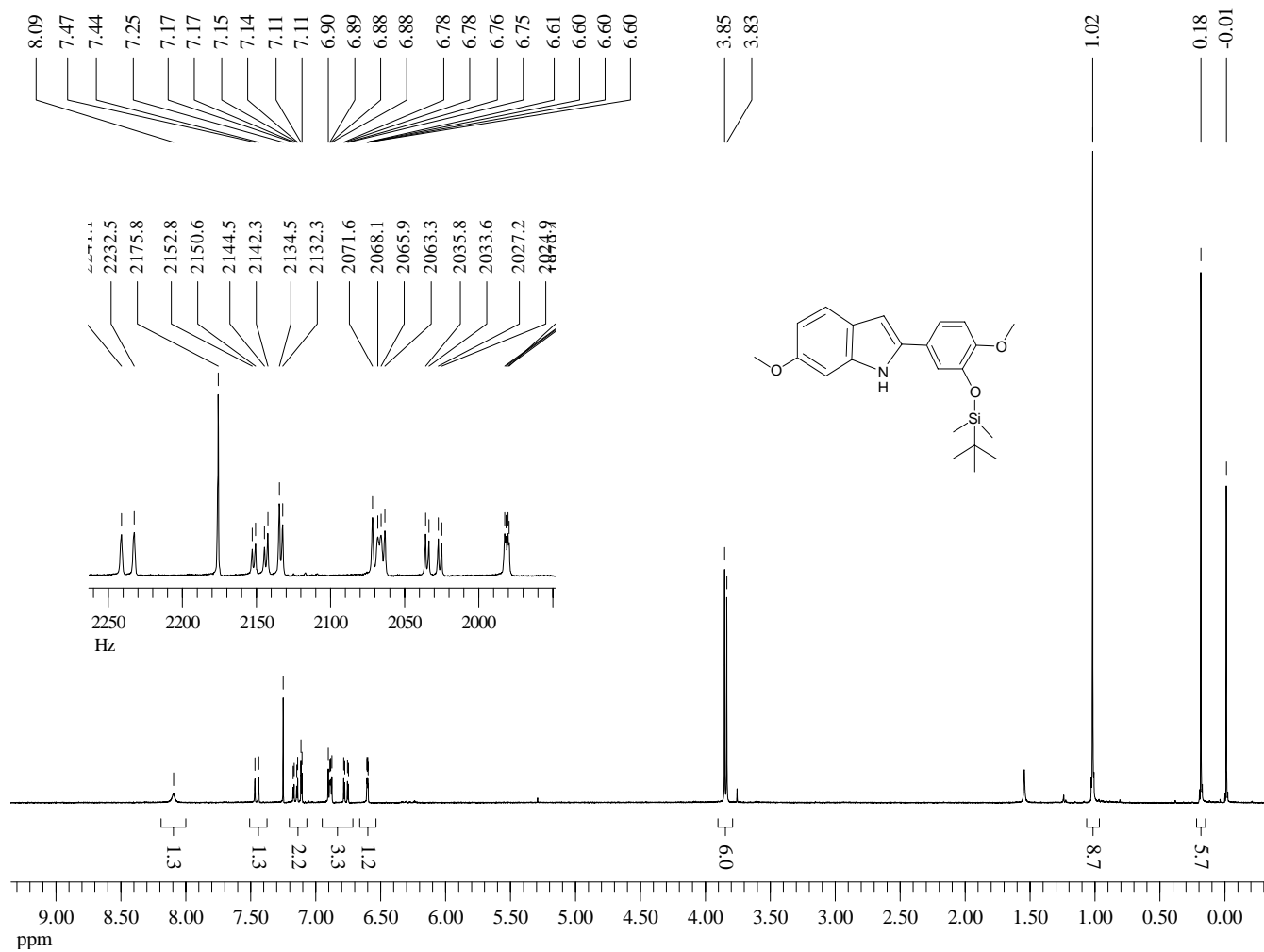
¹³C-NMR (75 MHz, CDCl₃) of Compound **41c**



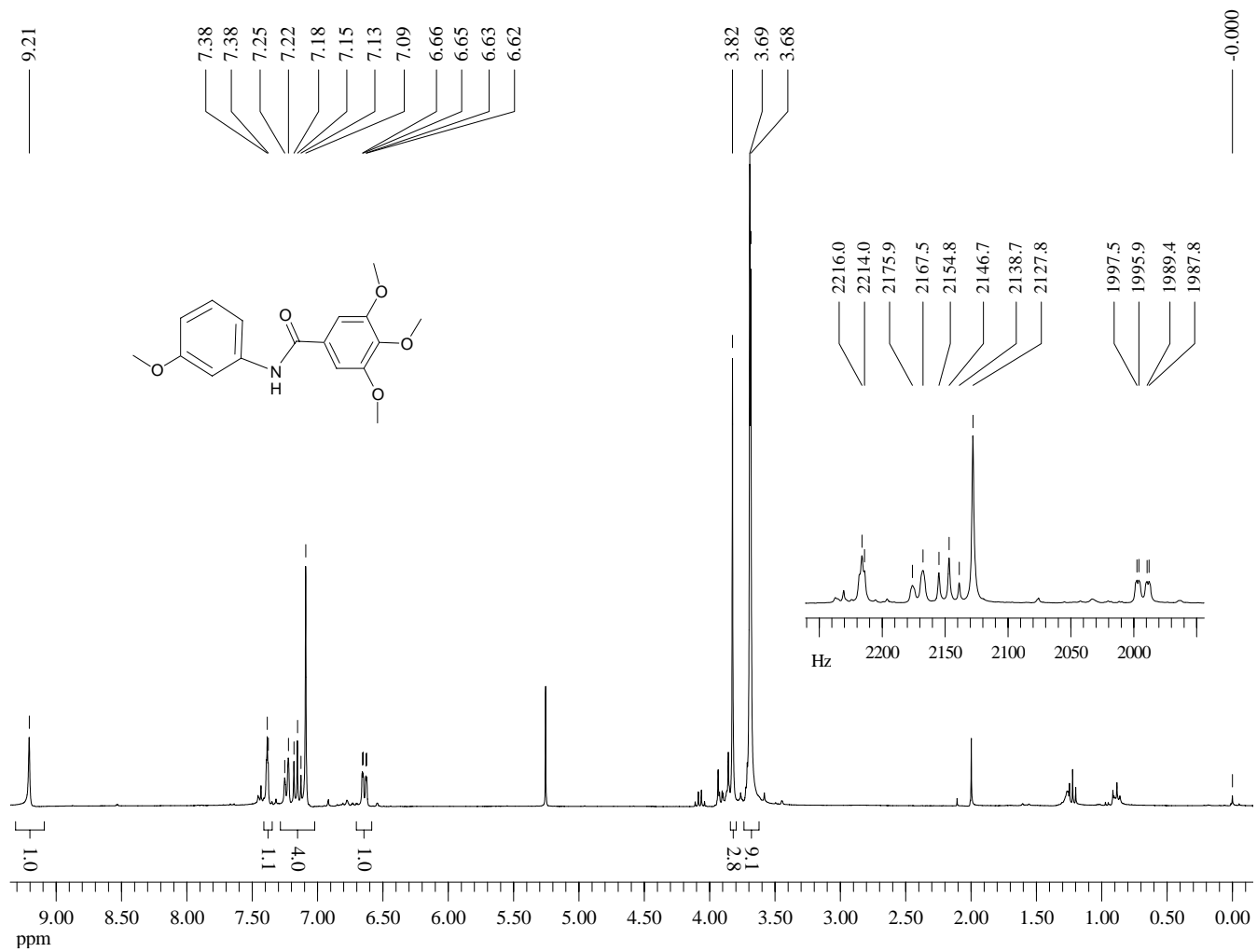
Dept 135-NMR (75 MHz, CDCl₃) of Compound **41c**



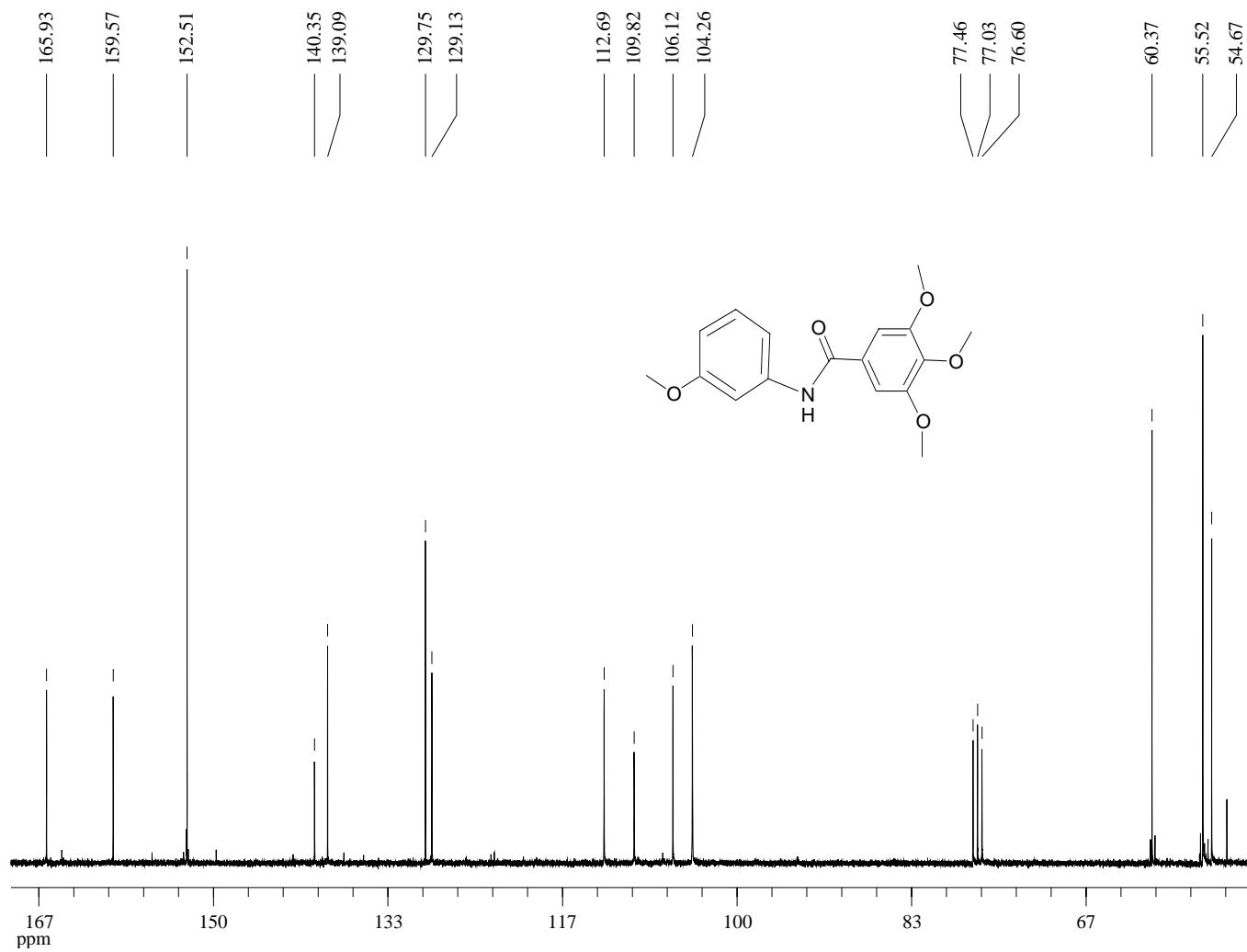
¹H-NMR (300 MHz, CDCl₃) of Compound **41d**



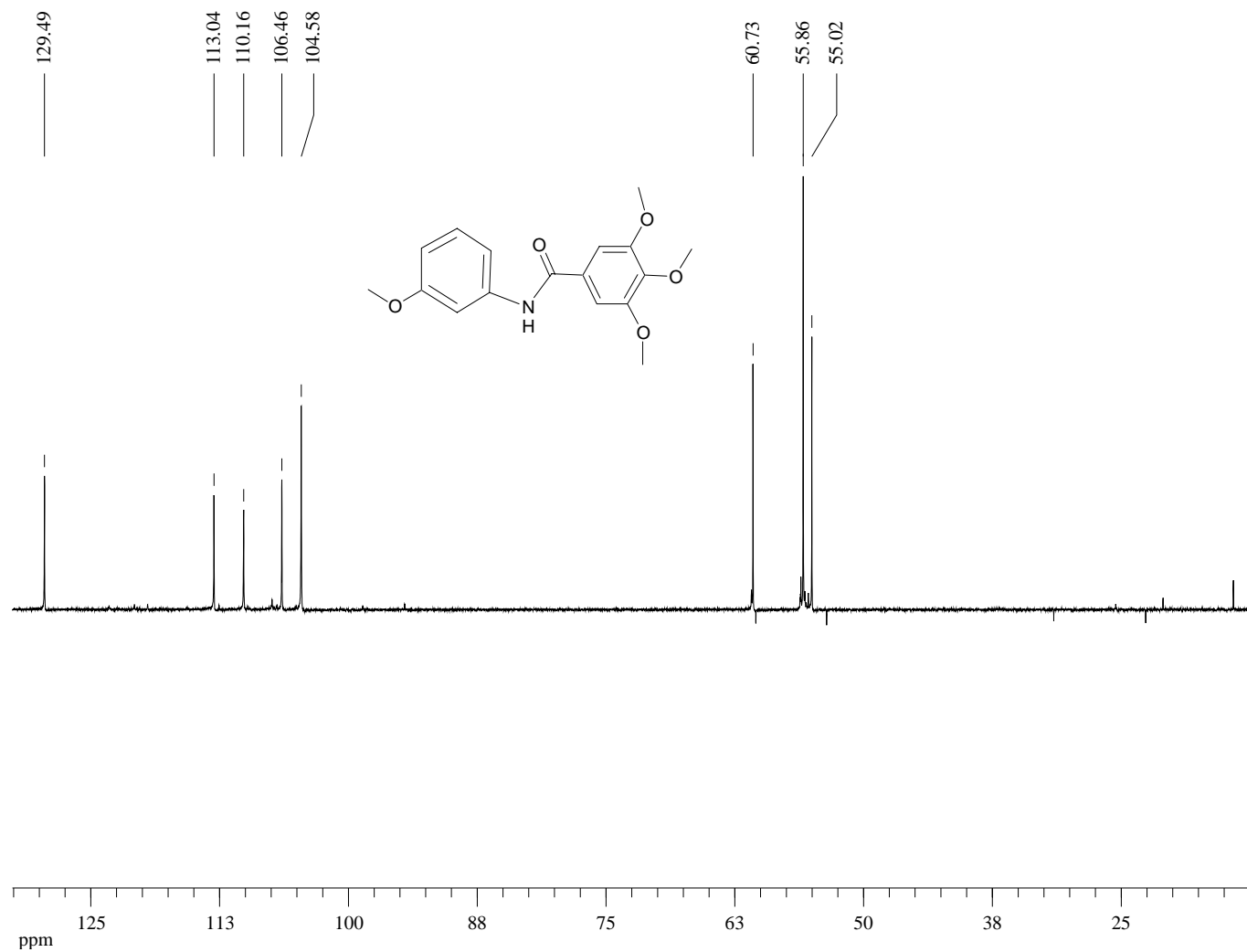
¹H-NMR (300 MHz, CDCl₃) of Compound 42



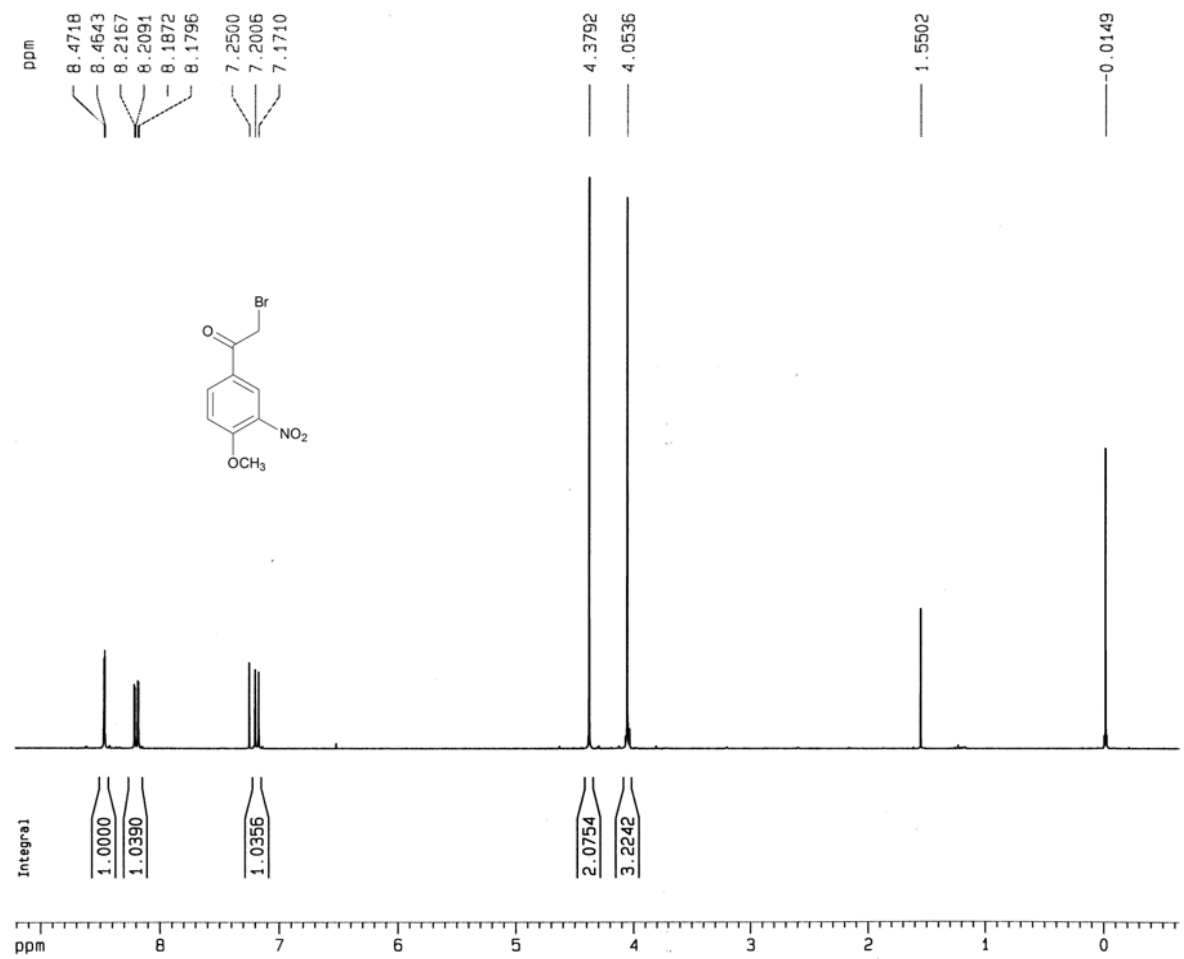
¹³C-NMR (75 MHz, CDCl₃) of Compound **42**



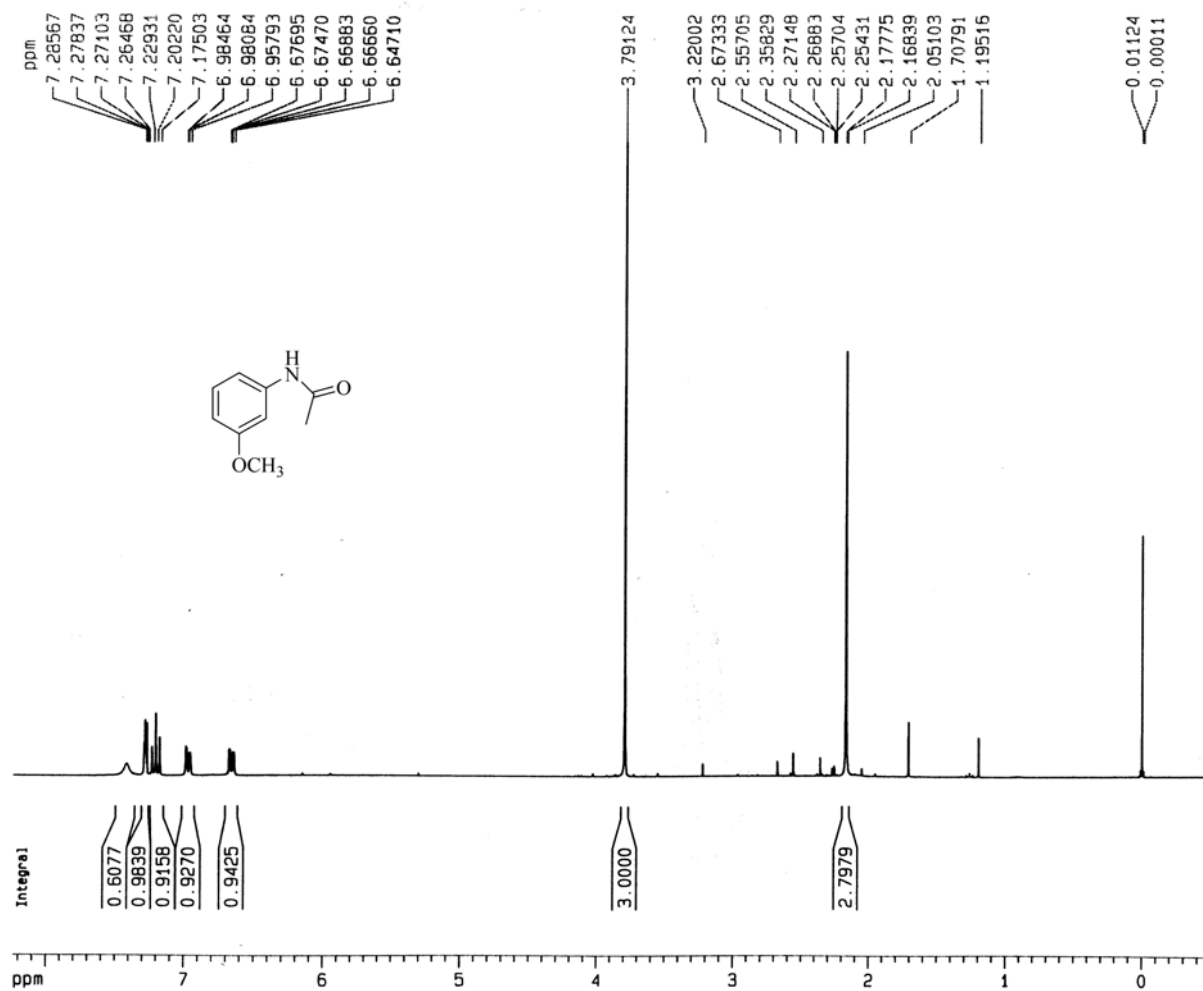
Dept 135-NMR (75 MHz, CDCl₃) of Compound 42



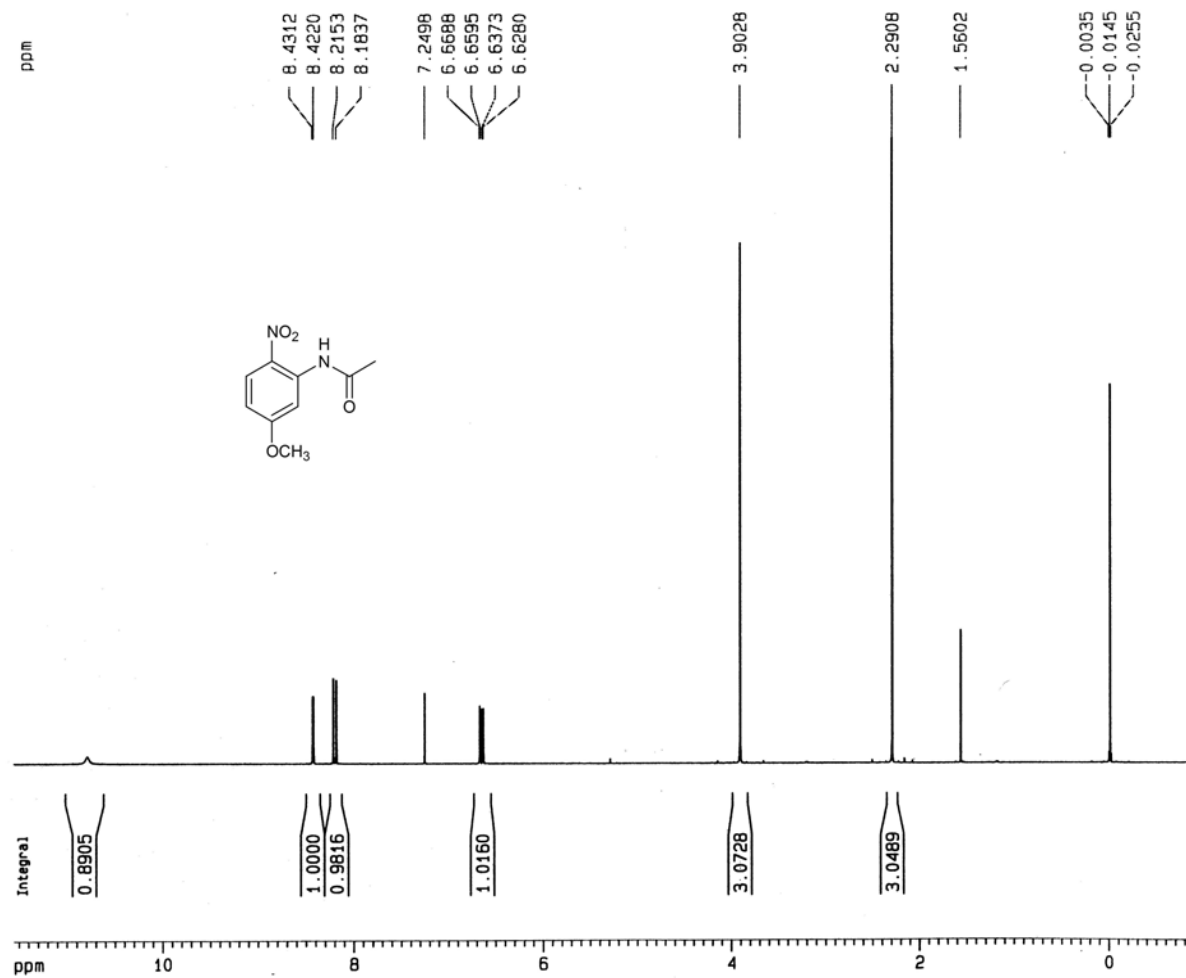
¹H-NMR (300 MHz, CDCl₃) of Compound **43**



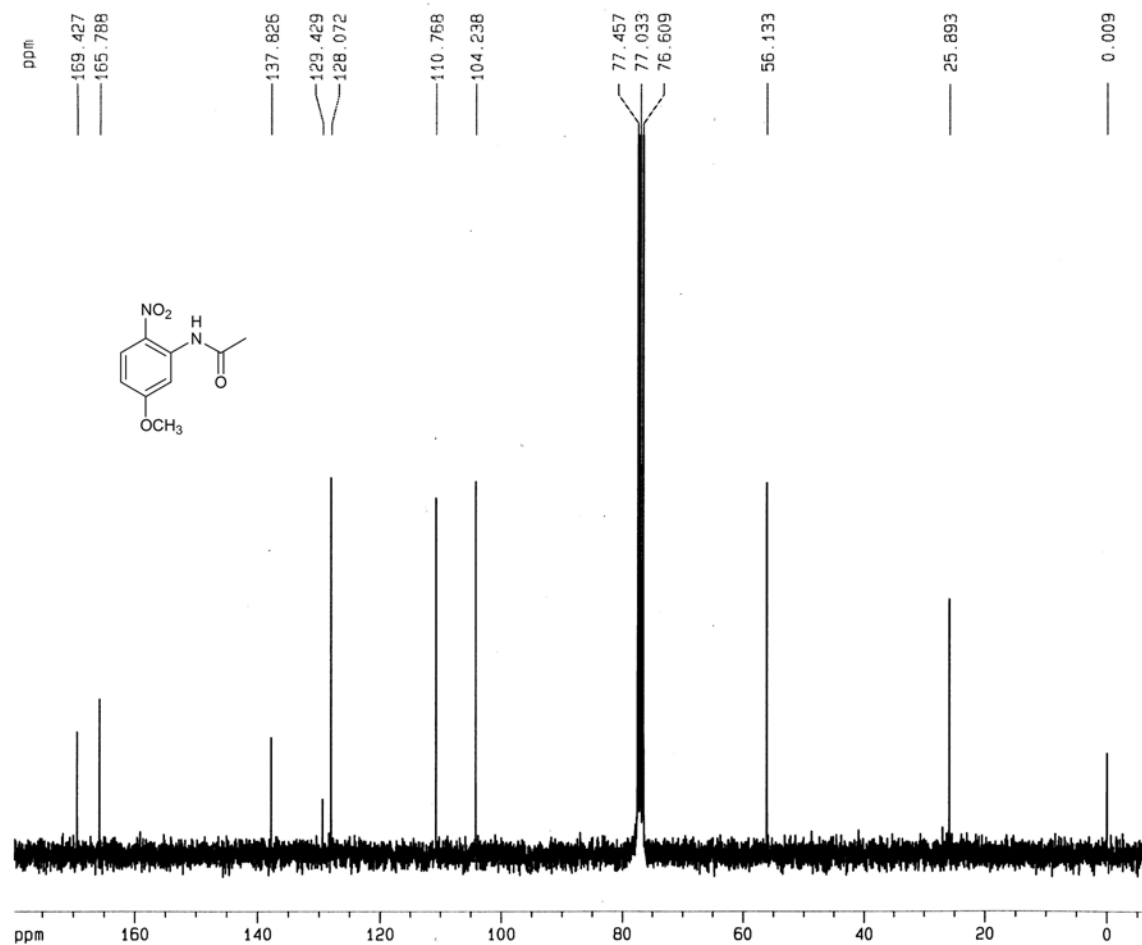
¹H-NMR (360 MHz, CDCl₃) of Compound **44**



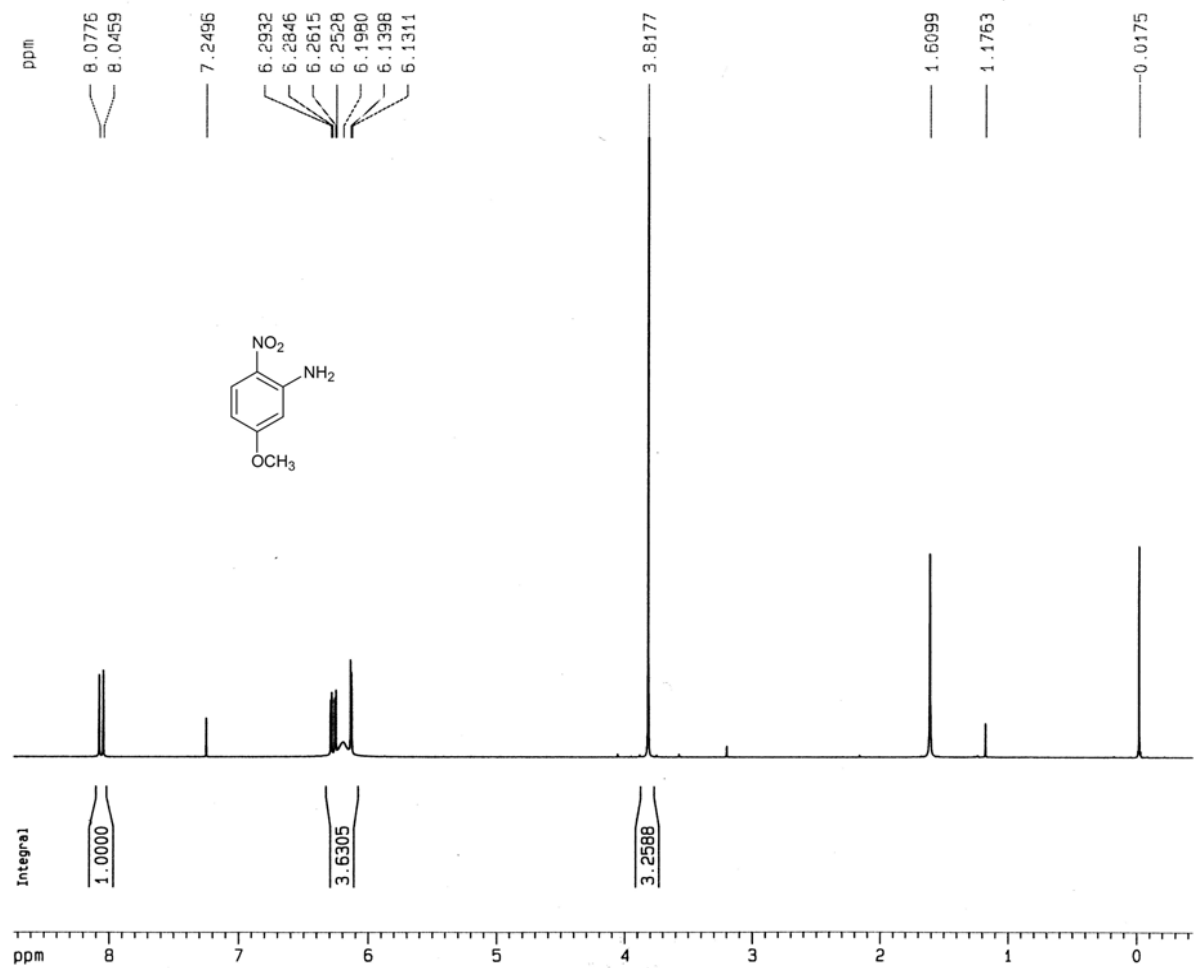
¹H-NMR (300 MHz, CDCl₃) of Compound **45**



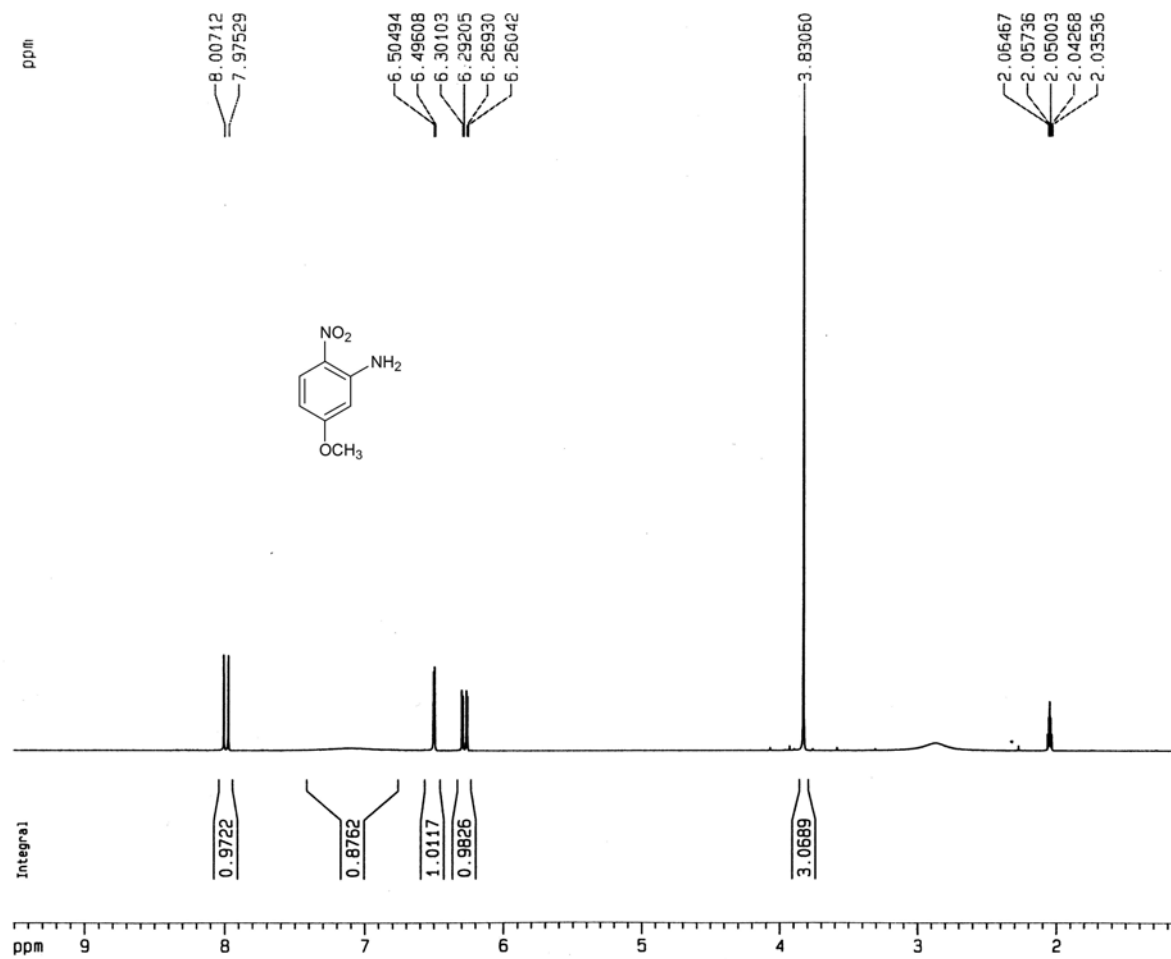
$^{13}\text{C-NMR}$ (75 MHz, CDCl_3) of Compound **45**



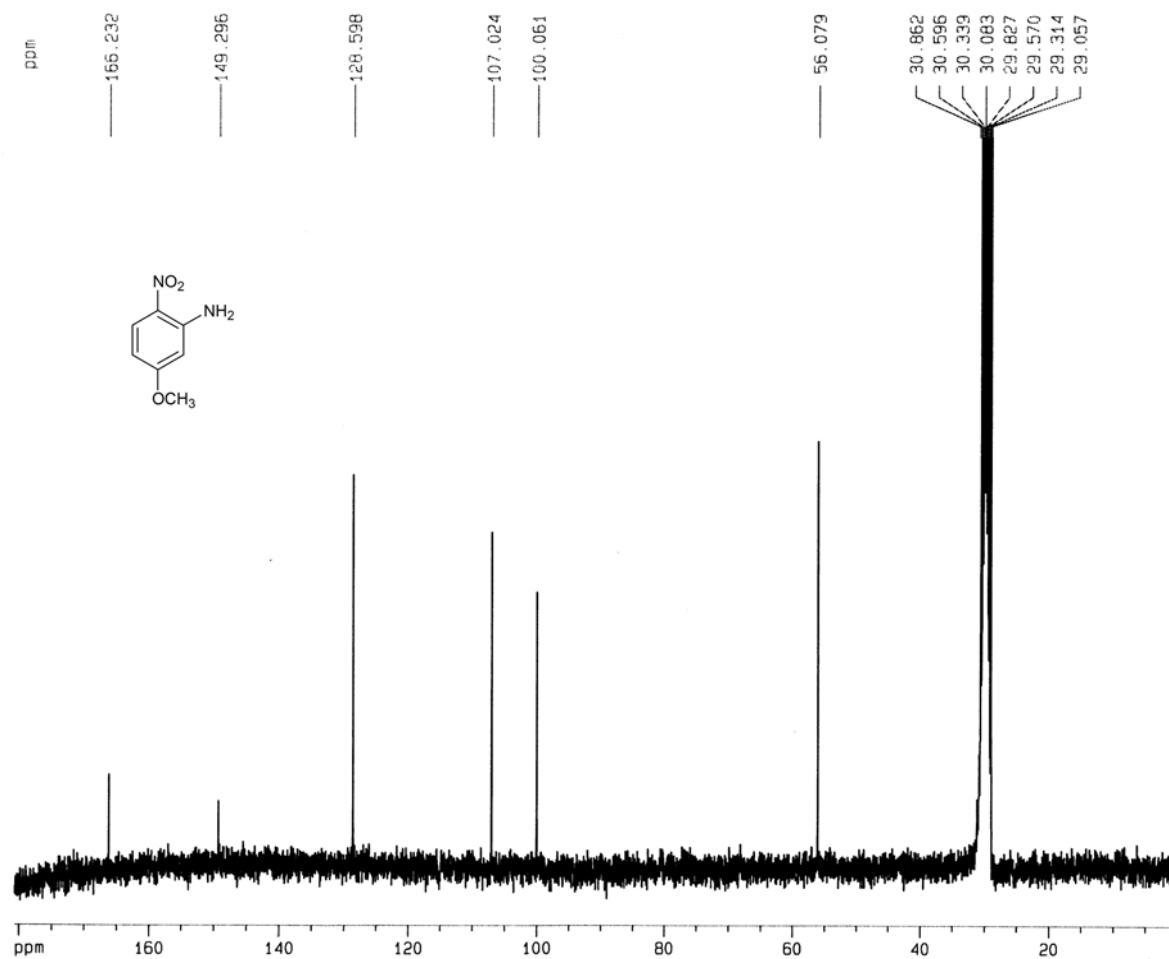
¹H-NMR (300 MHz, CDCl₃) of Compound **46**



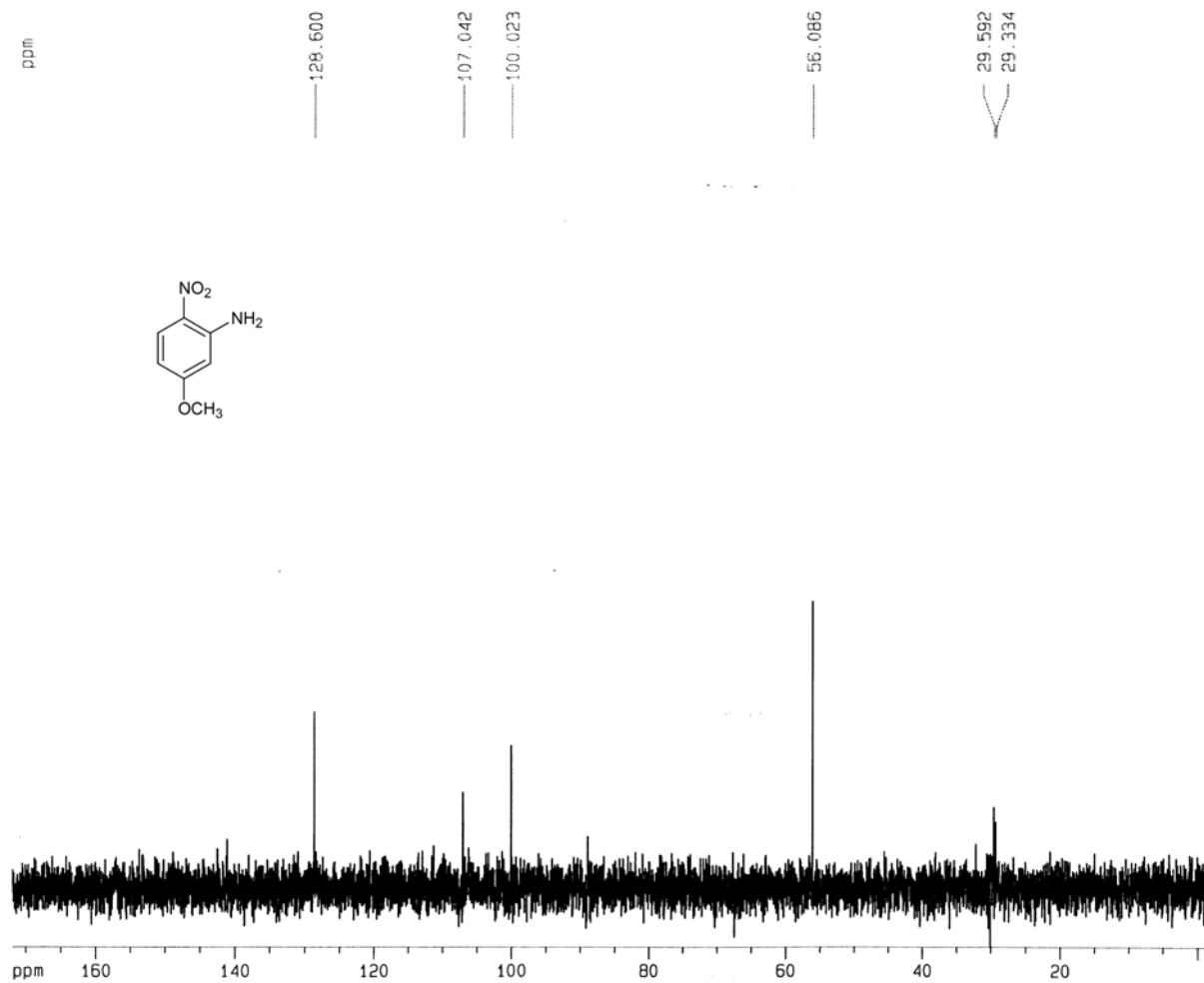
¹H-NMR (300 MHz, Acetone-d₆) of Compound 46



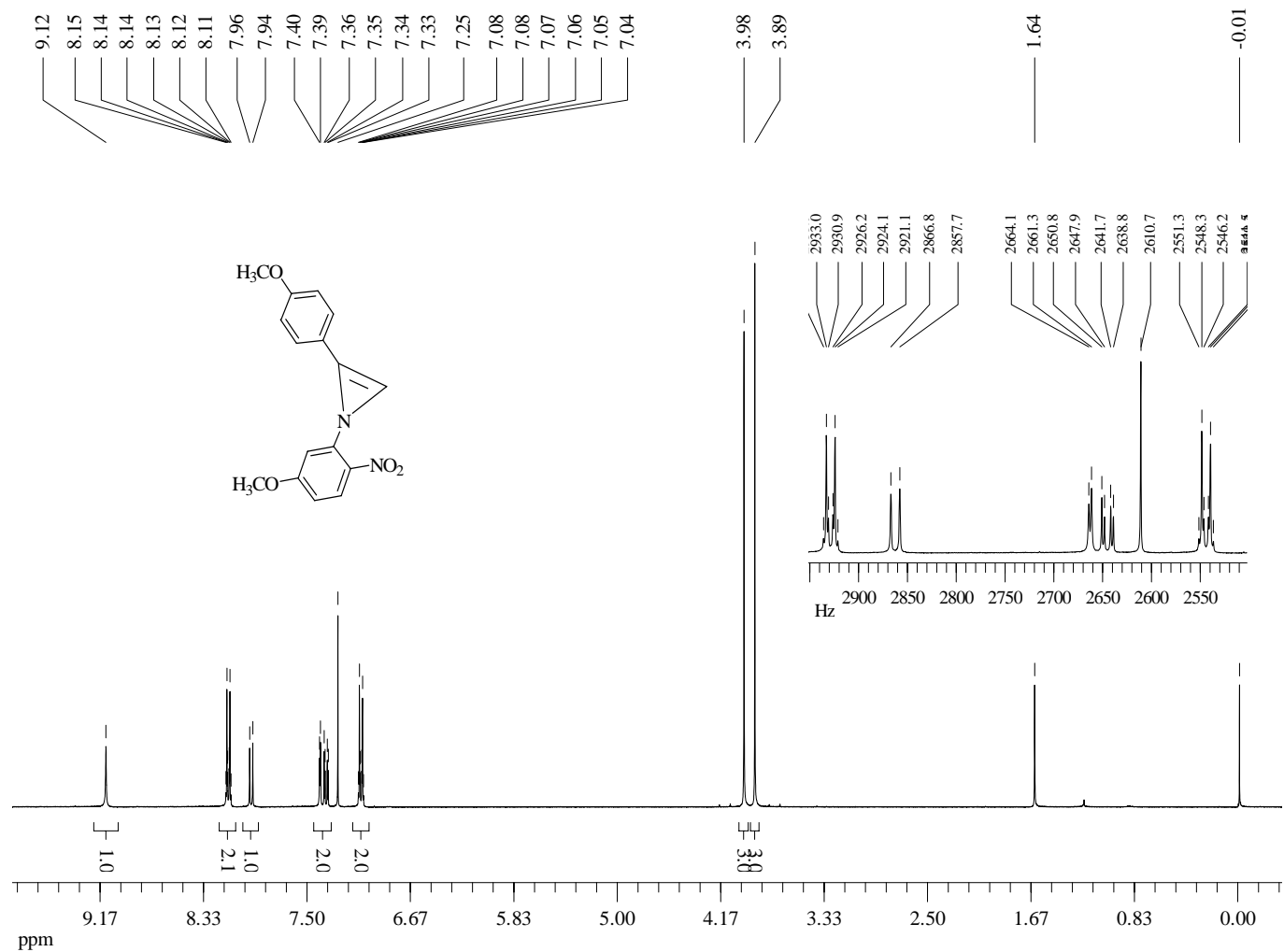
^{13}C -NMR (75 MHz, Acetone- d_6) of Compound **46**



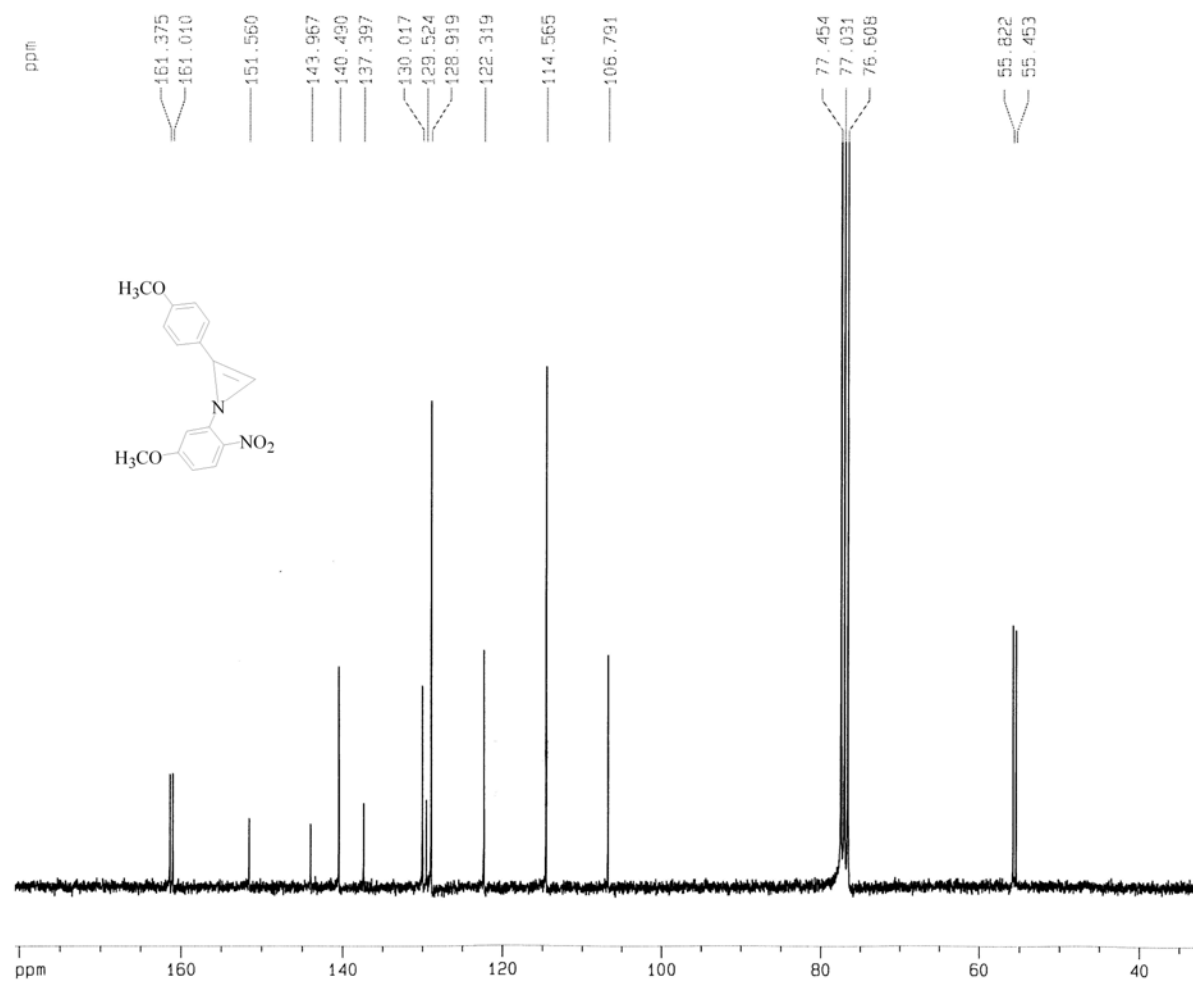
Dept 45-NMR (75 MHz, Acetone-d₆) of Compound **46**



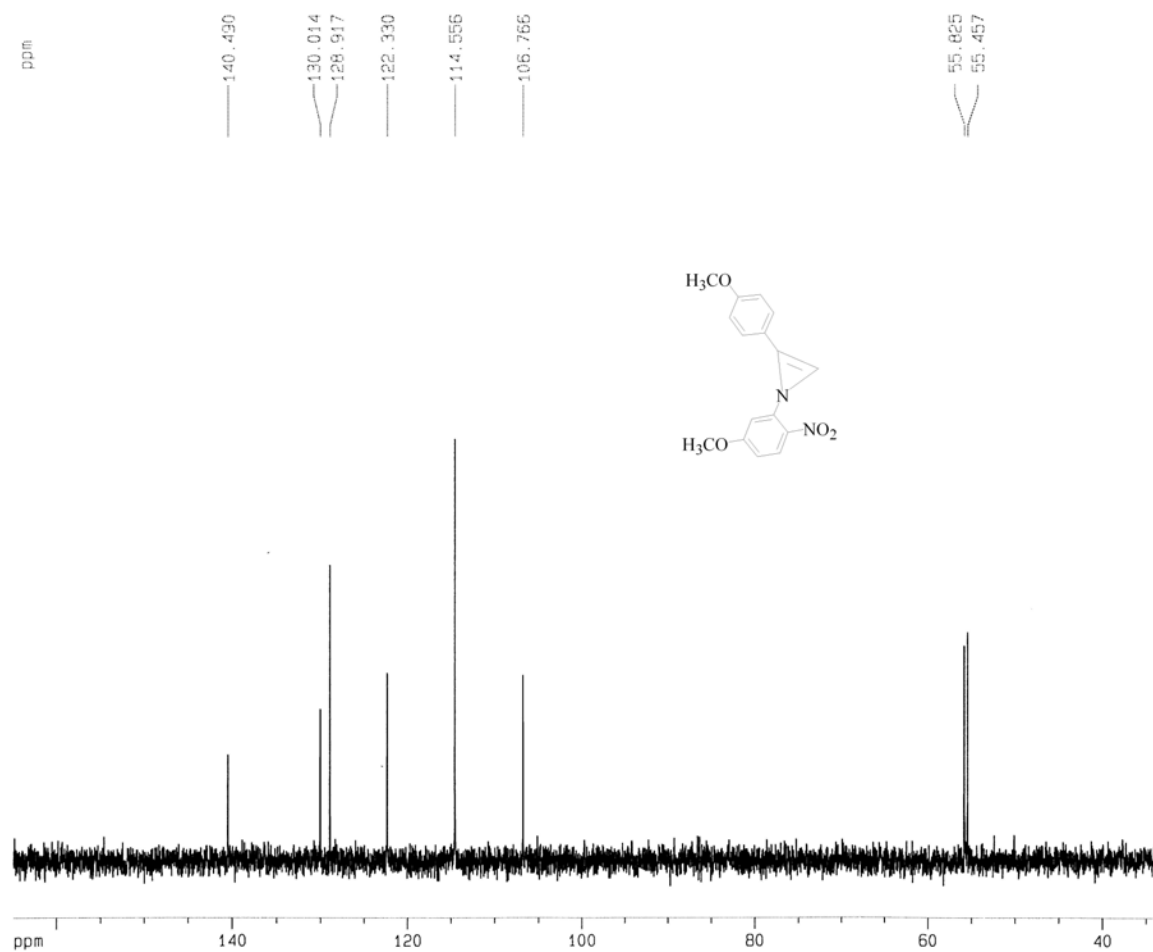
¹H-NMR (360 MHz, CDCl₃) of Compound **47**



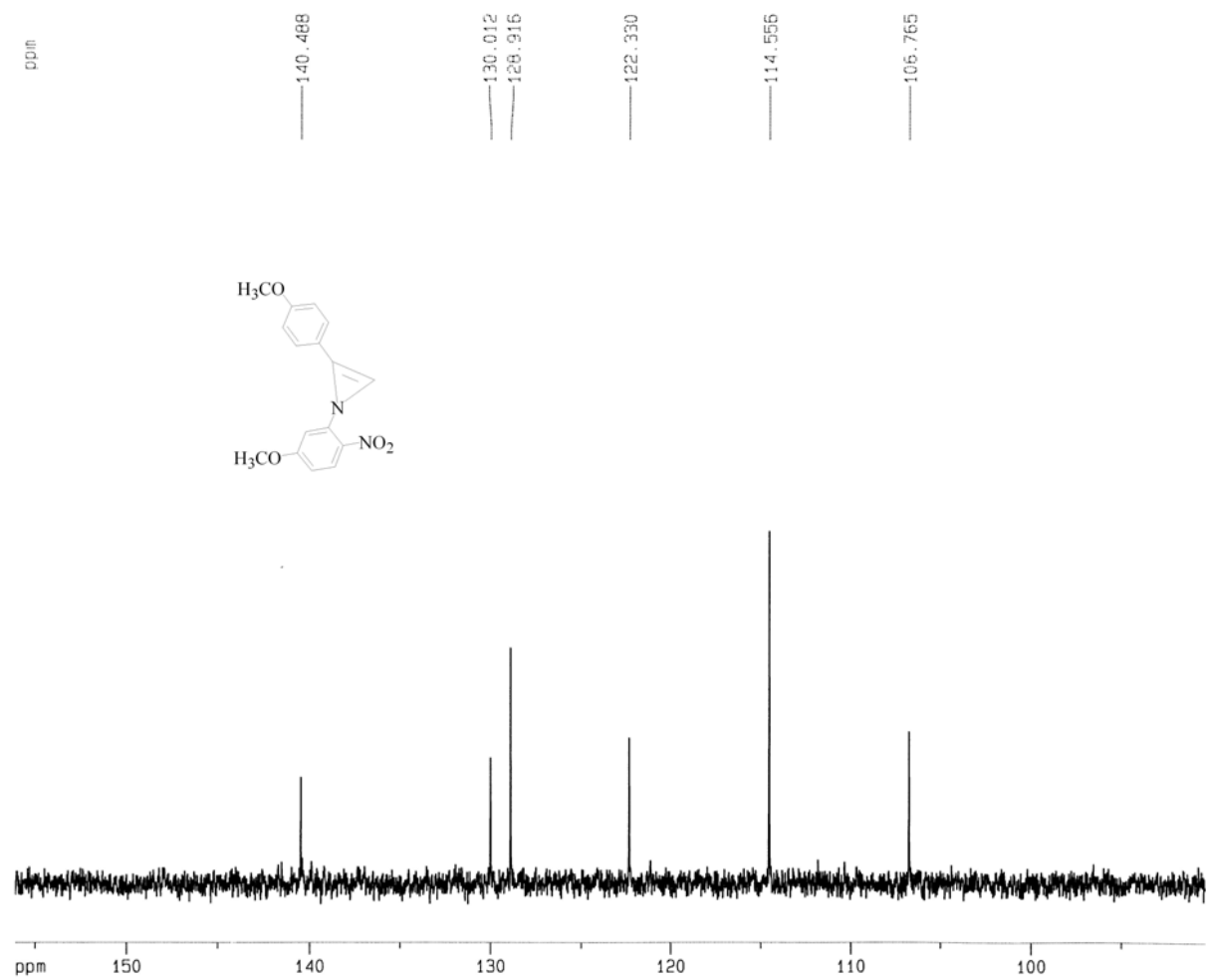
$^{13}\text{C-NMR}$ (75 MHz, CDCl_3) of Compound **47**



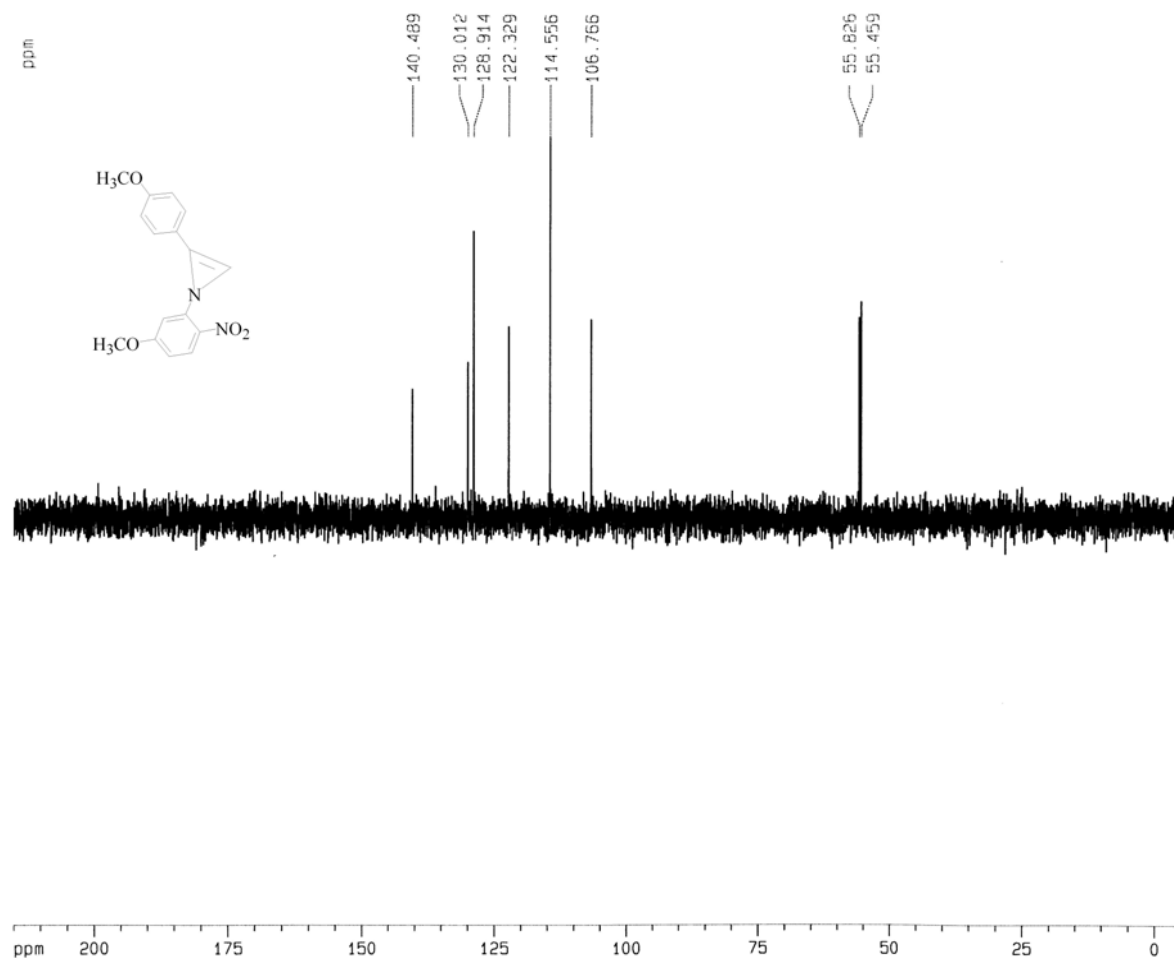
Dept 45 -NMR (75 MHz, CDCl₃) of Compound **47**



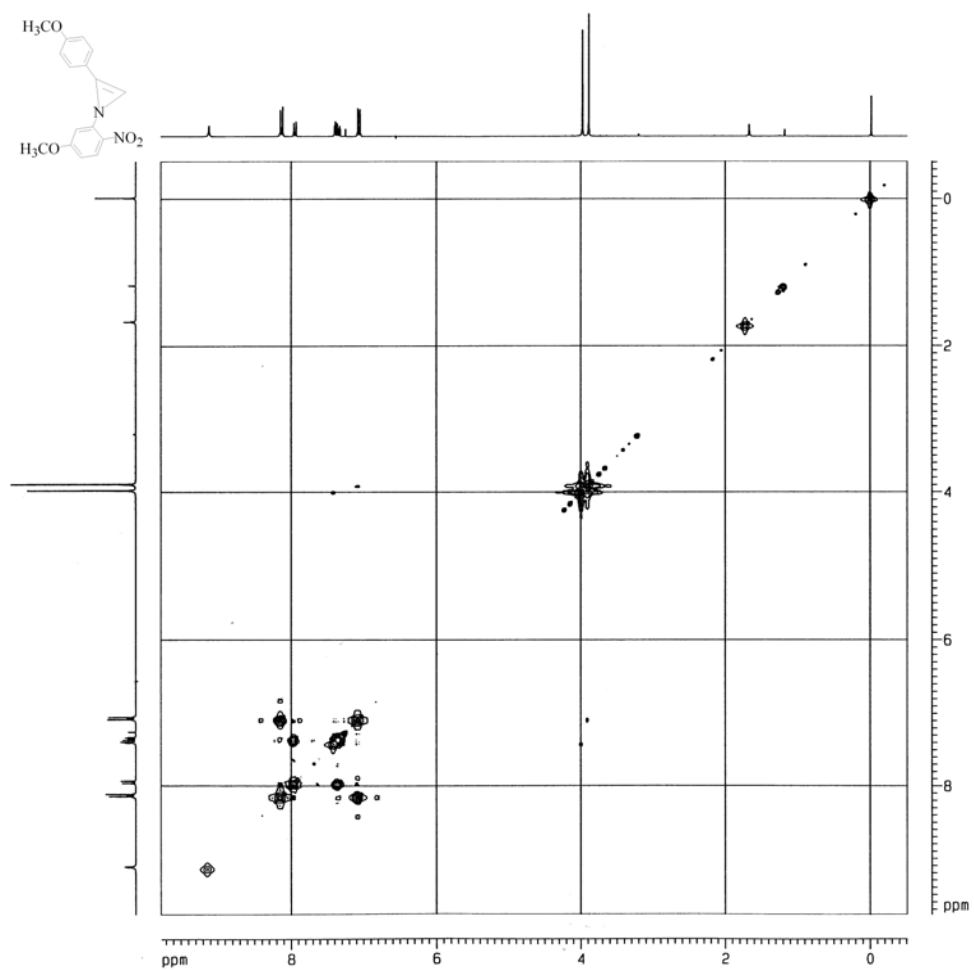
Dept 90 -NMR (75 MHz, CDCl₃) of Compound **47**



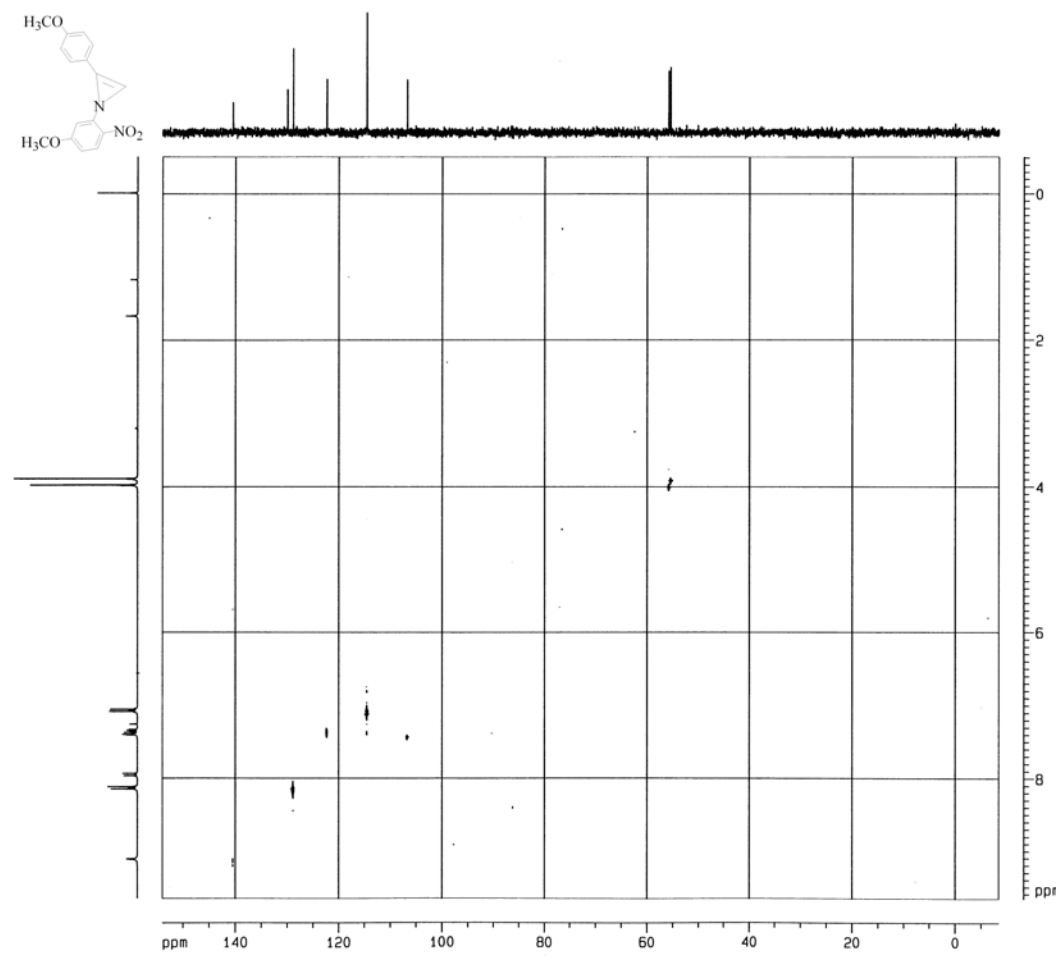
Dept 135 -NMR (75 MHz, CDCl₃) of Compound 47



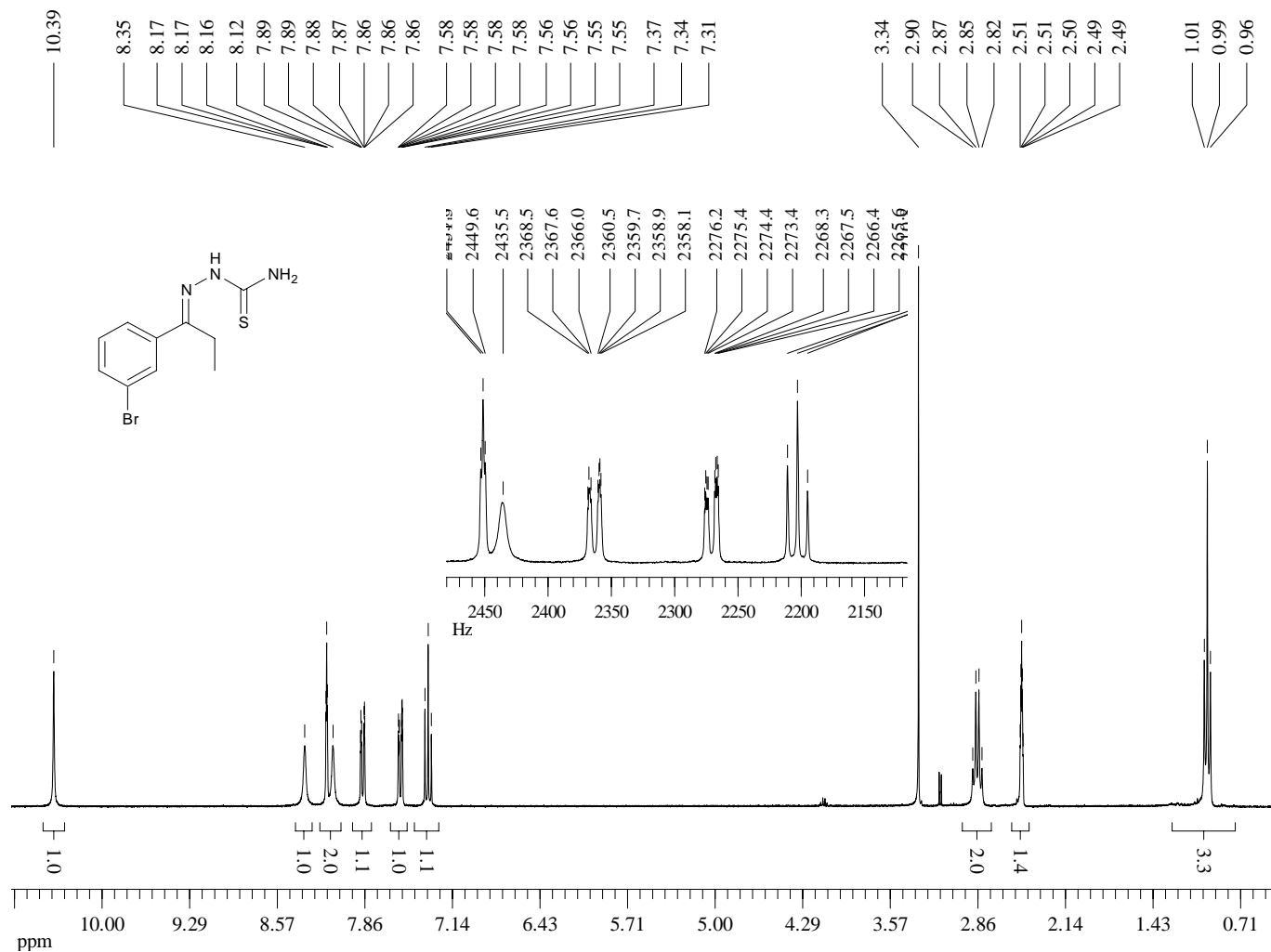
COSY ^1H - ^1H NMR (300 MHz, CDCl_3) of Compound **47**



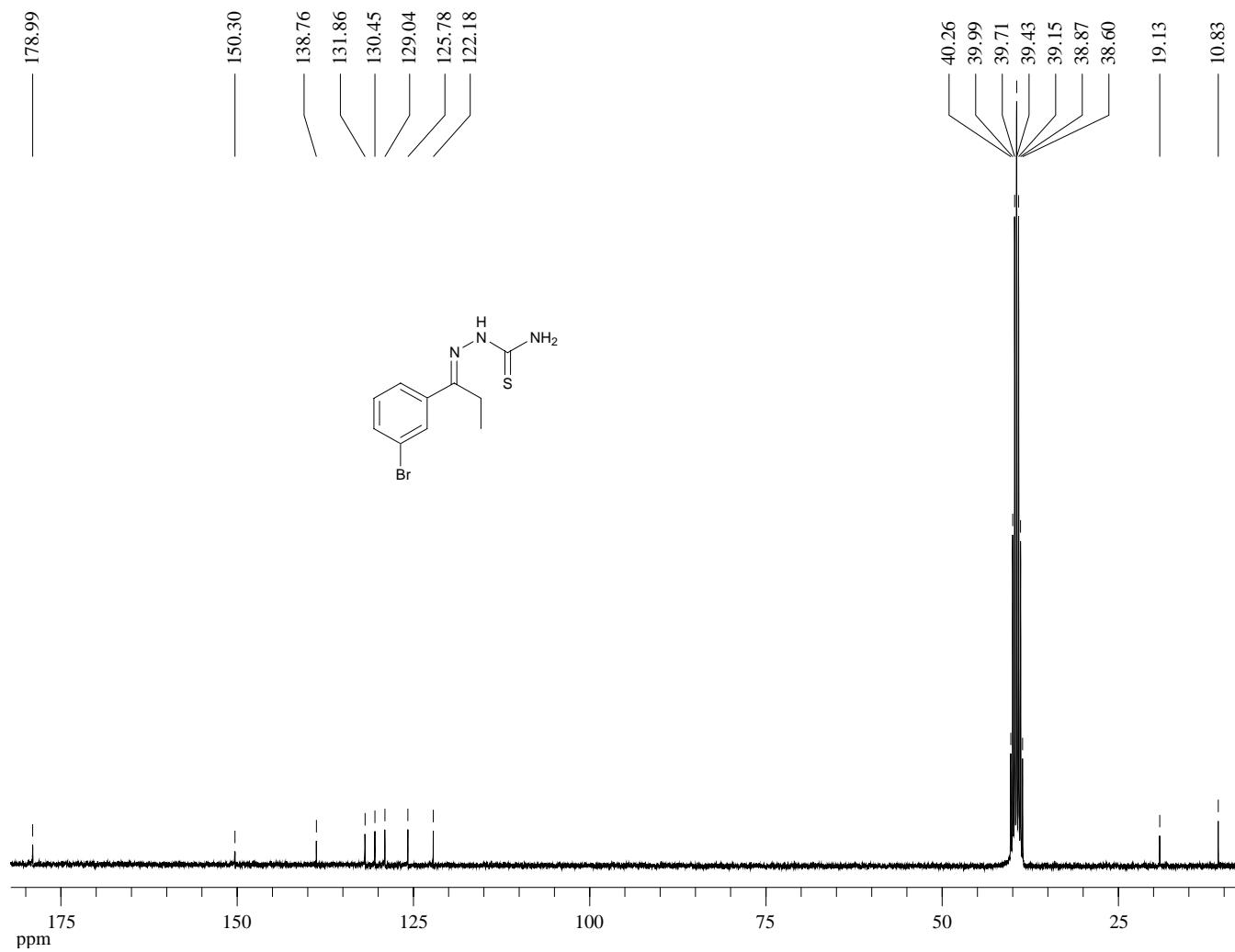
COSY ^1H - ^{13}C NMR (75 MHz, CDCl_3) of Compound **47**



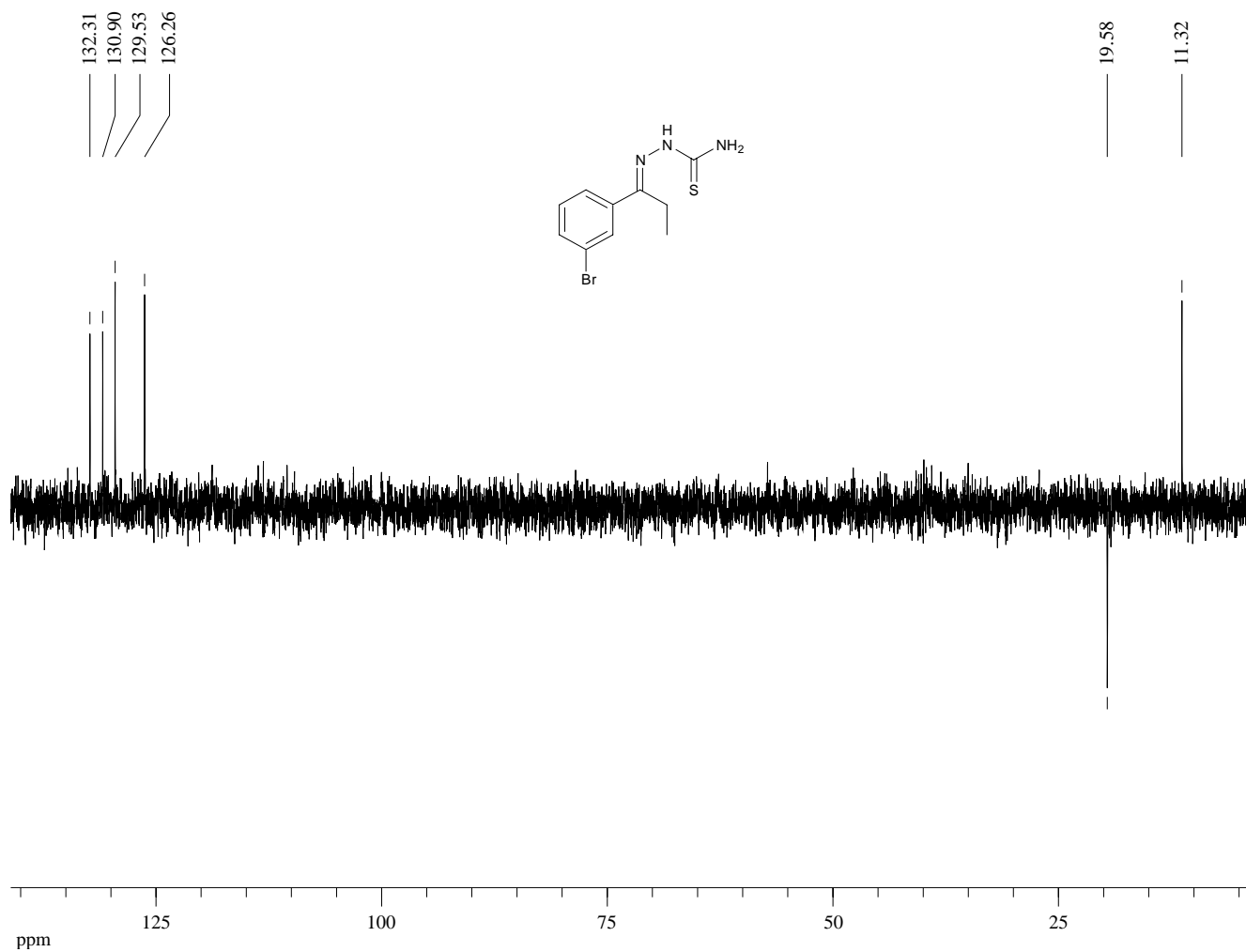
¹H-NMR (300 MHz, Methyl Sulfoxide-d₆) of Compound **49**



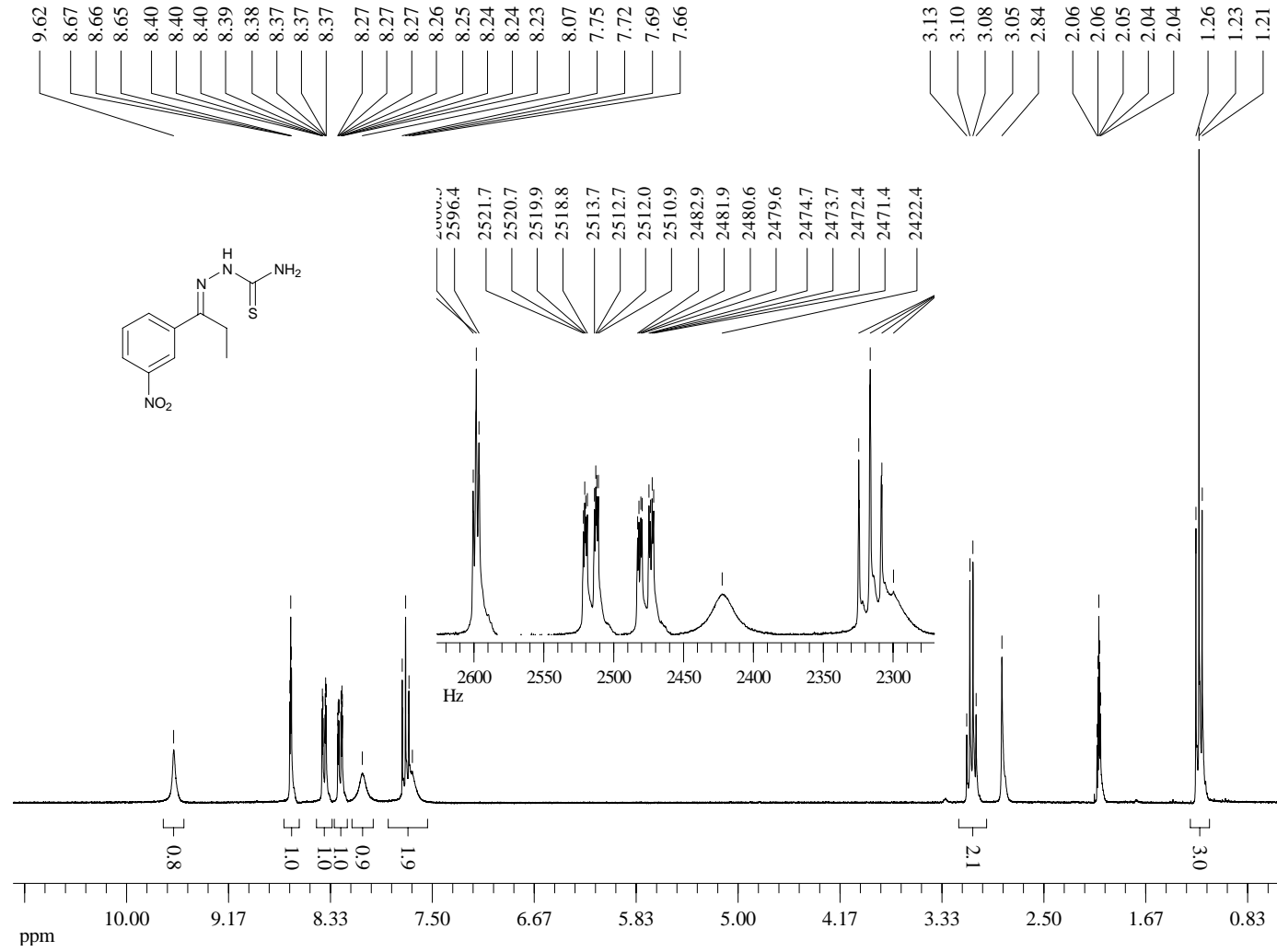
¹³C-NMR (75 MHz, Methyl Sulfoxide-d₆) of Compound **49**



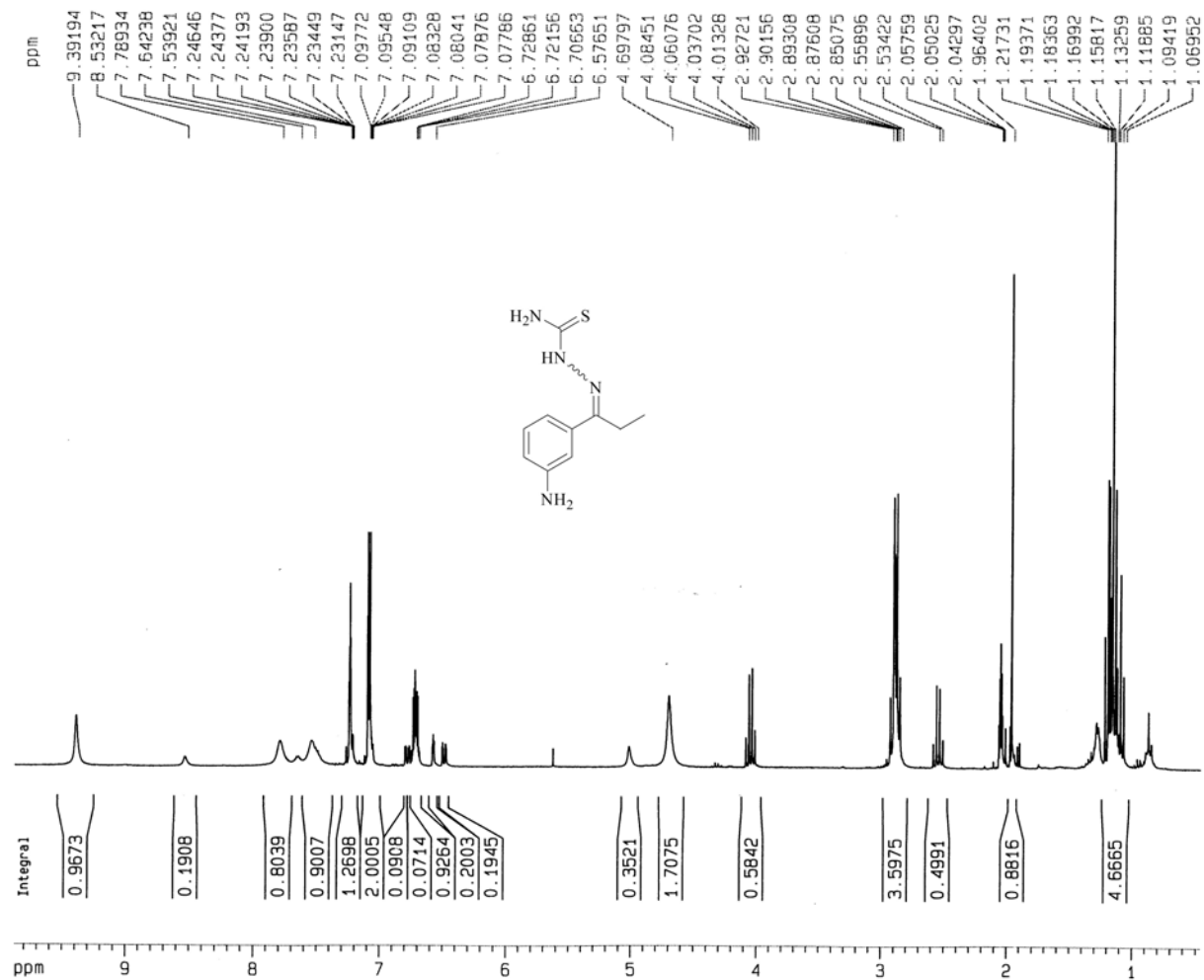
Dept 135-NMR (75 MHz, Methyl Sulfoxide-d₆) of Compound **49**



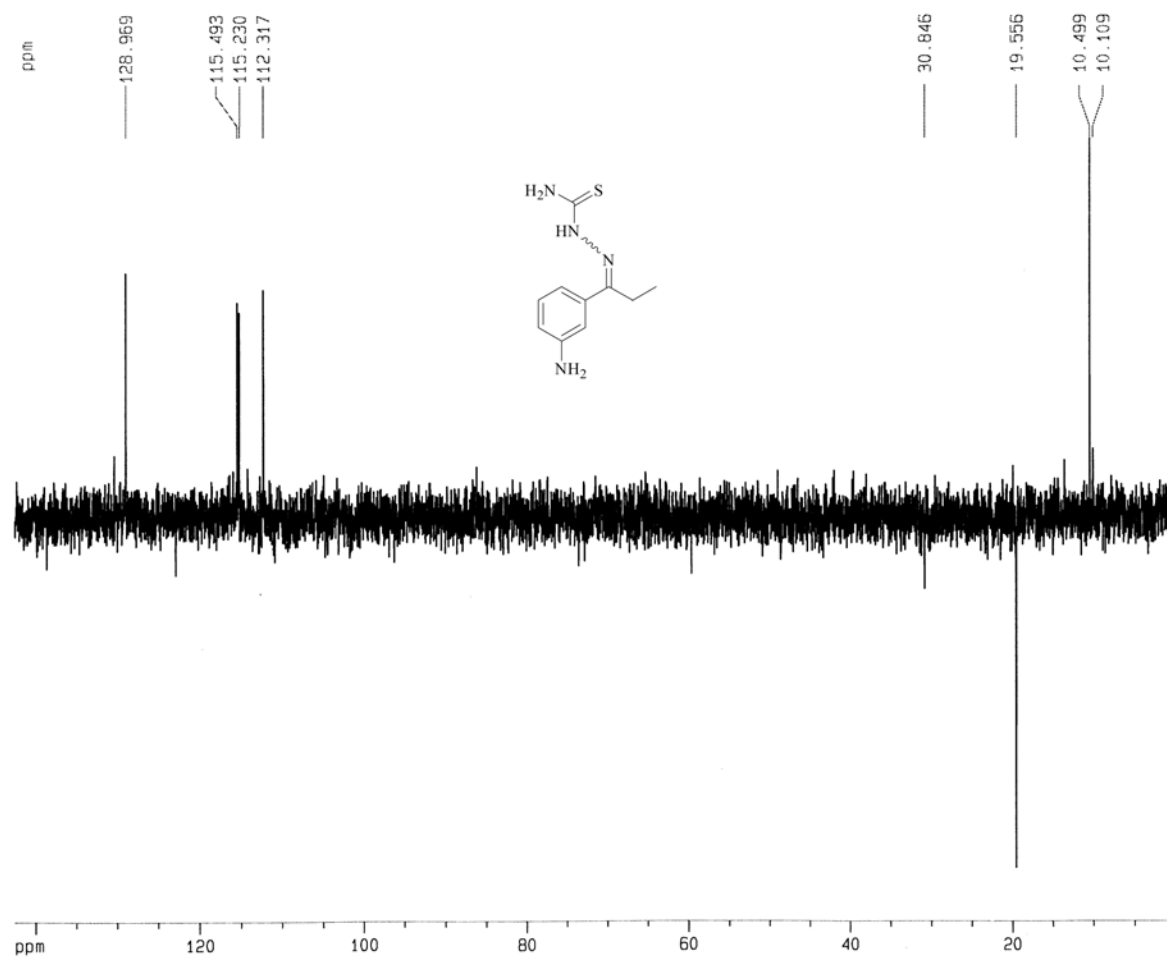
¹H-NMR (300 MHz, Acetone-d₆) of Compound **50**



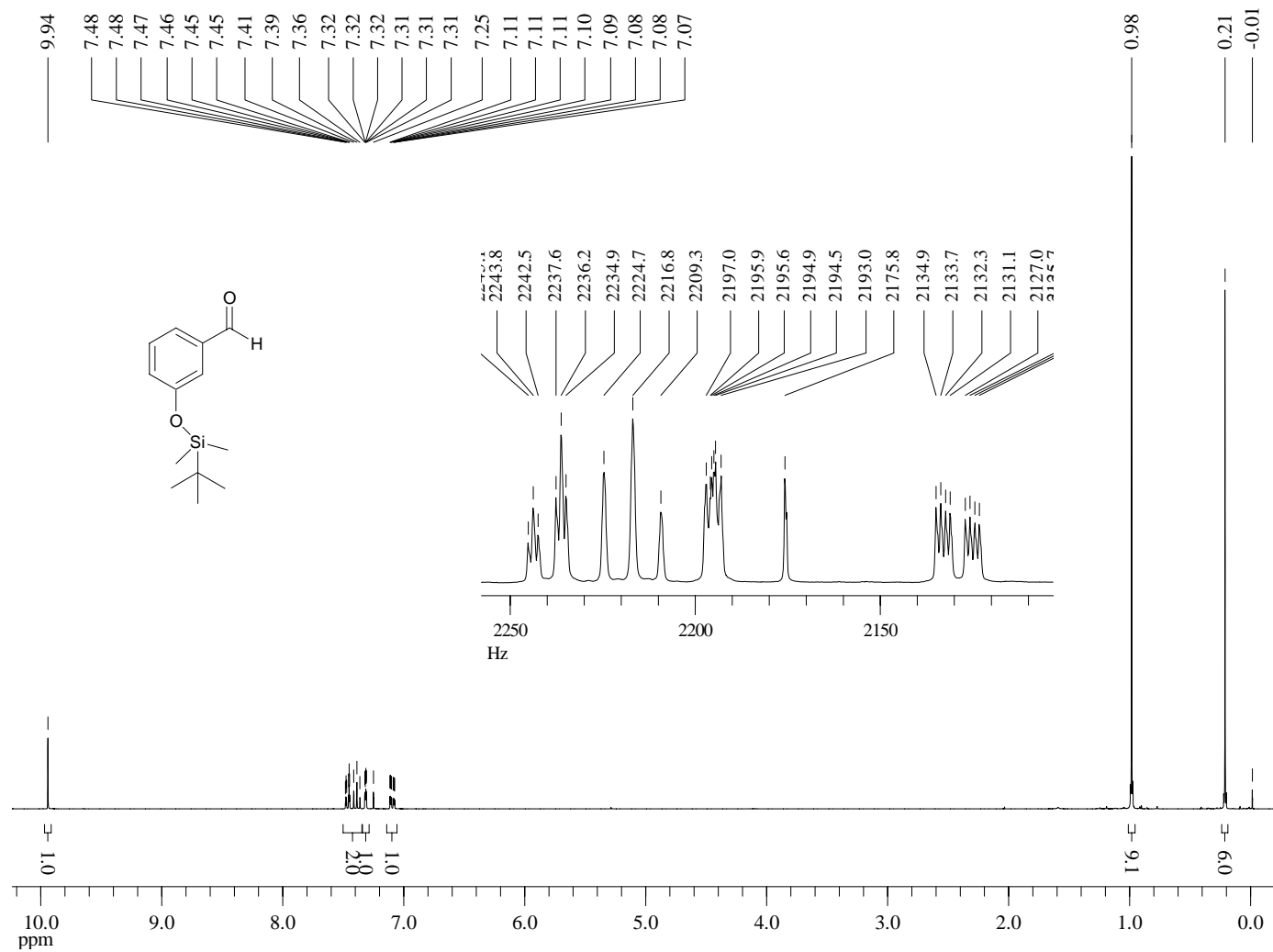
¹H-NMR (300 MHz, Acetone-d₆) of Compound 51



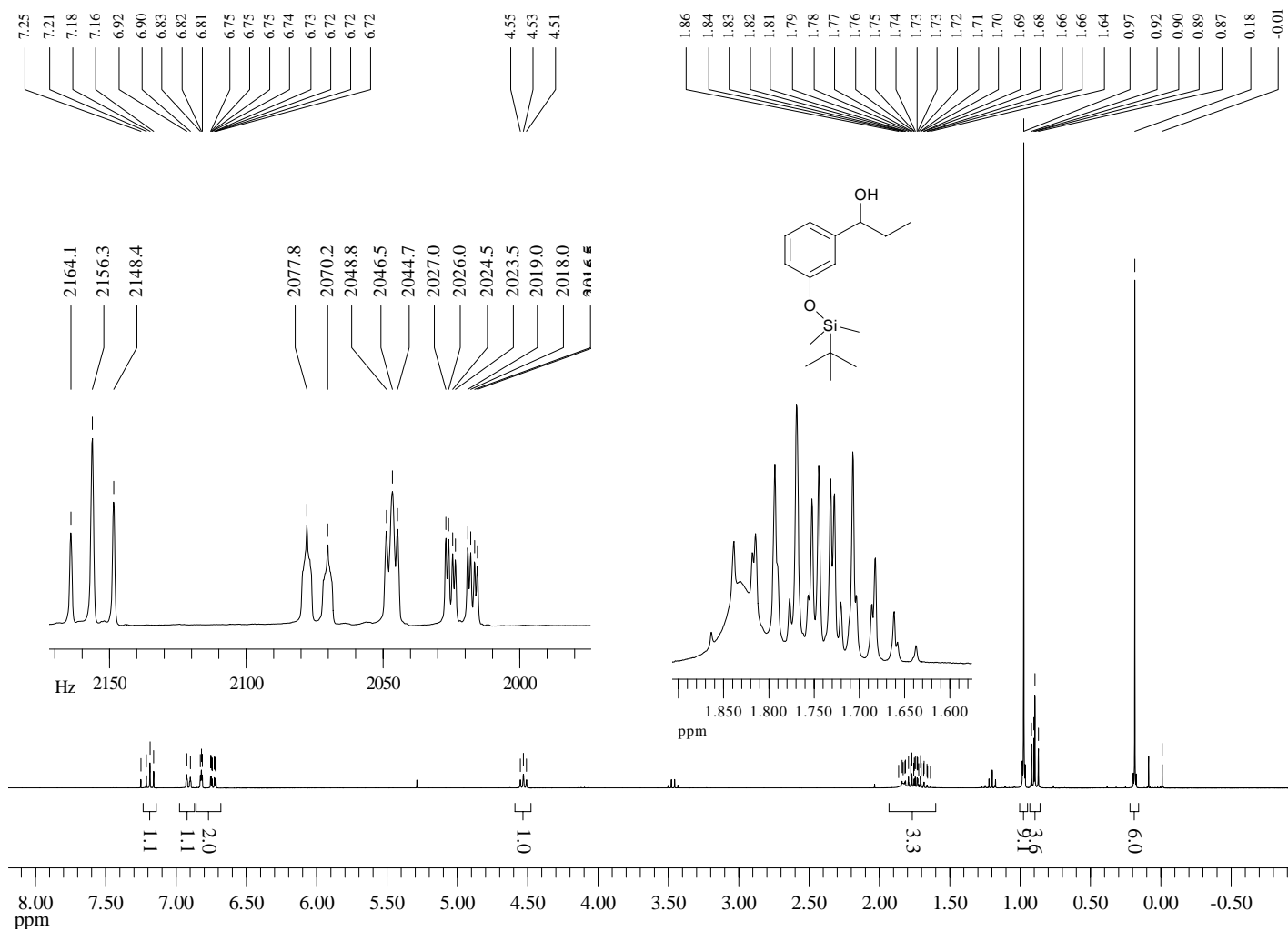
DEPT-135 NMR (75 MHz, Acetone-d₆) of Compound **51**



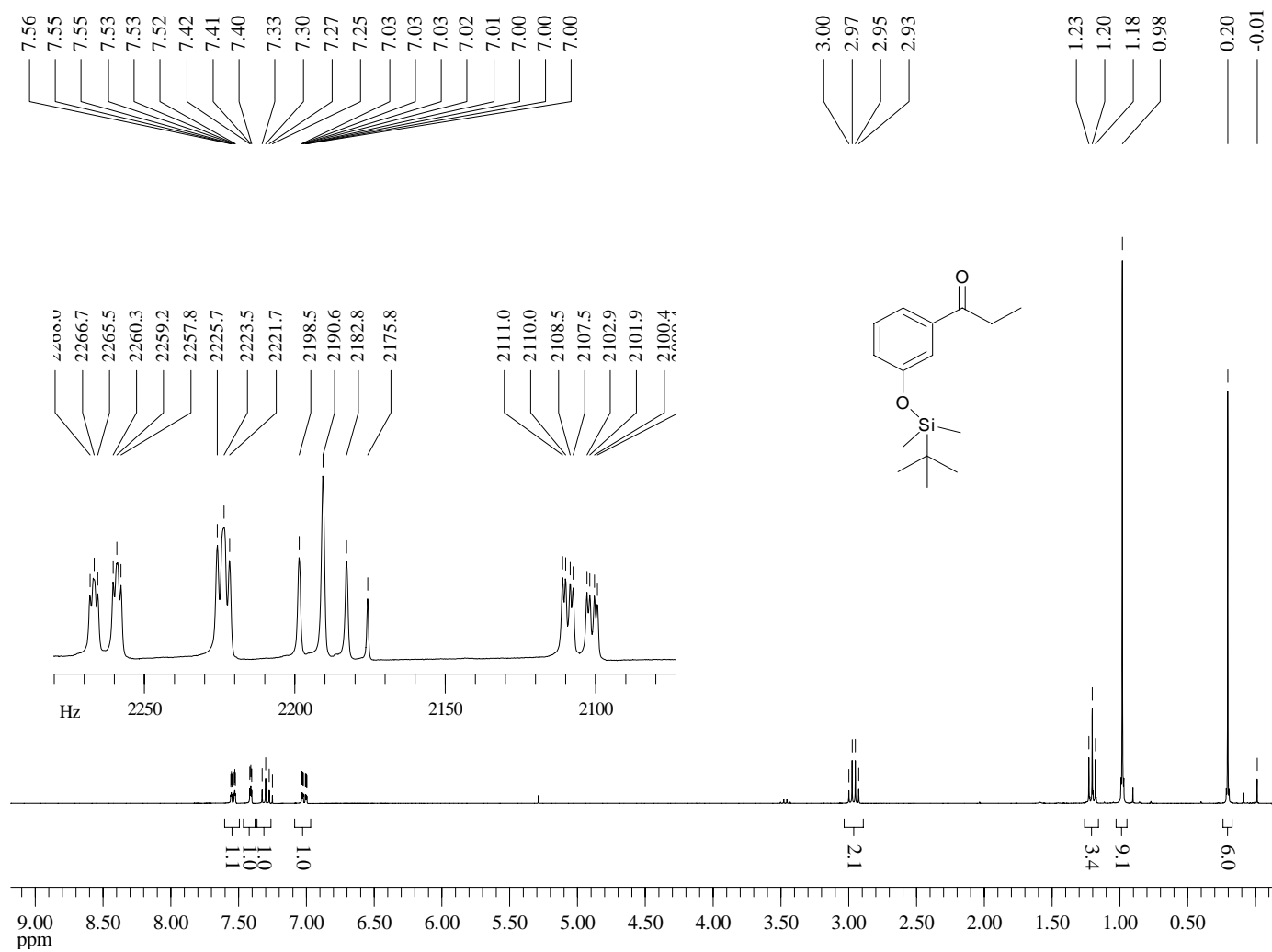
¹H-NMR (300 MHz, CDCl₃) of Compound **52**



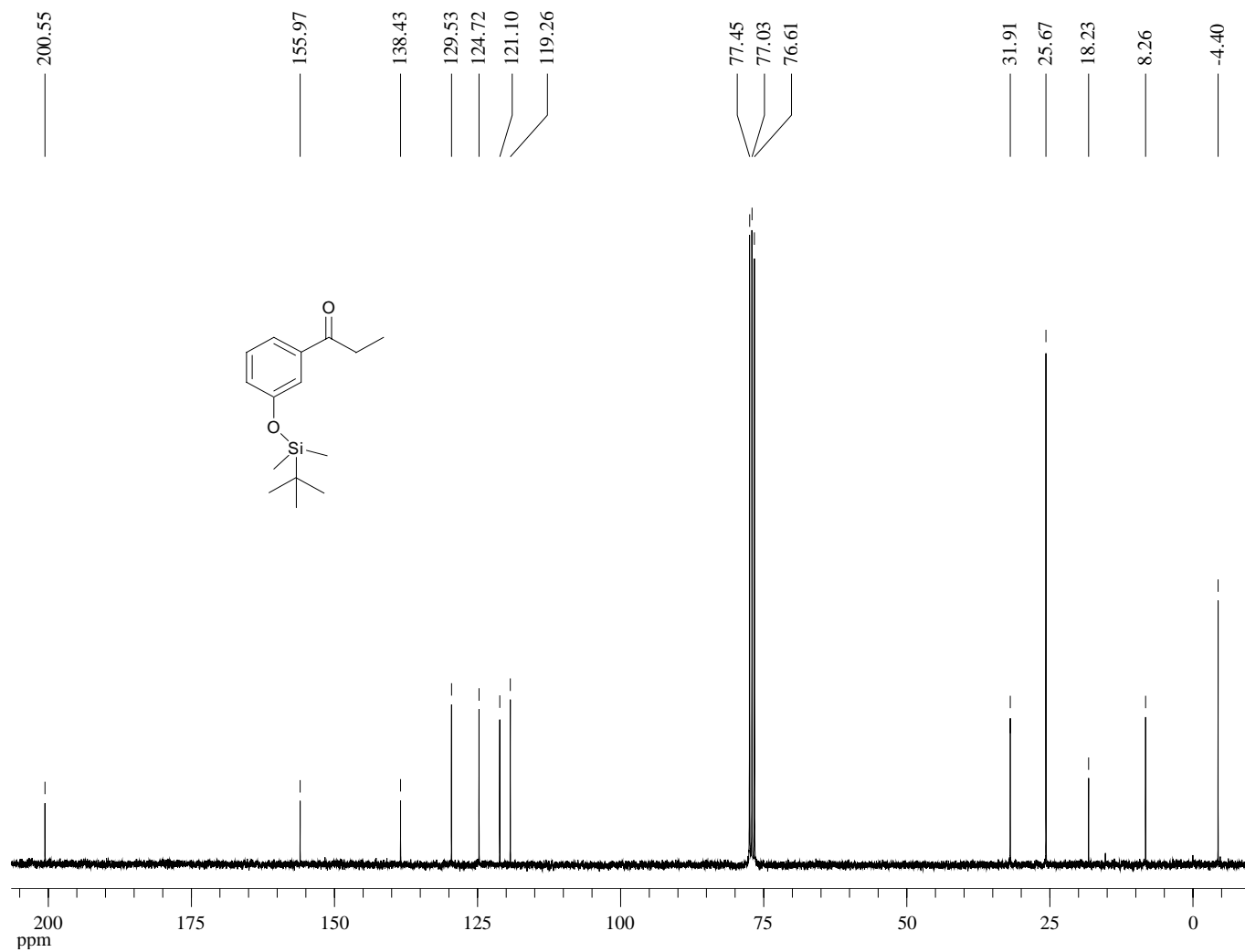
¹H-NMR (300 MHz, CDCl₃) of Compound **53**



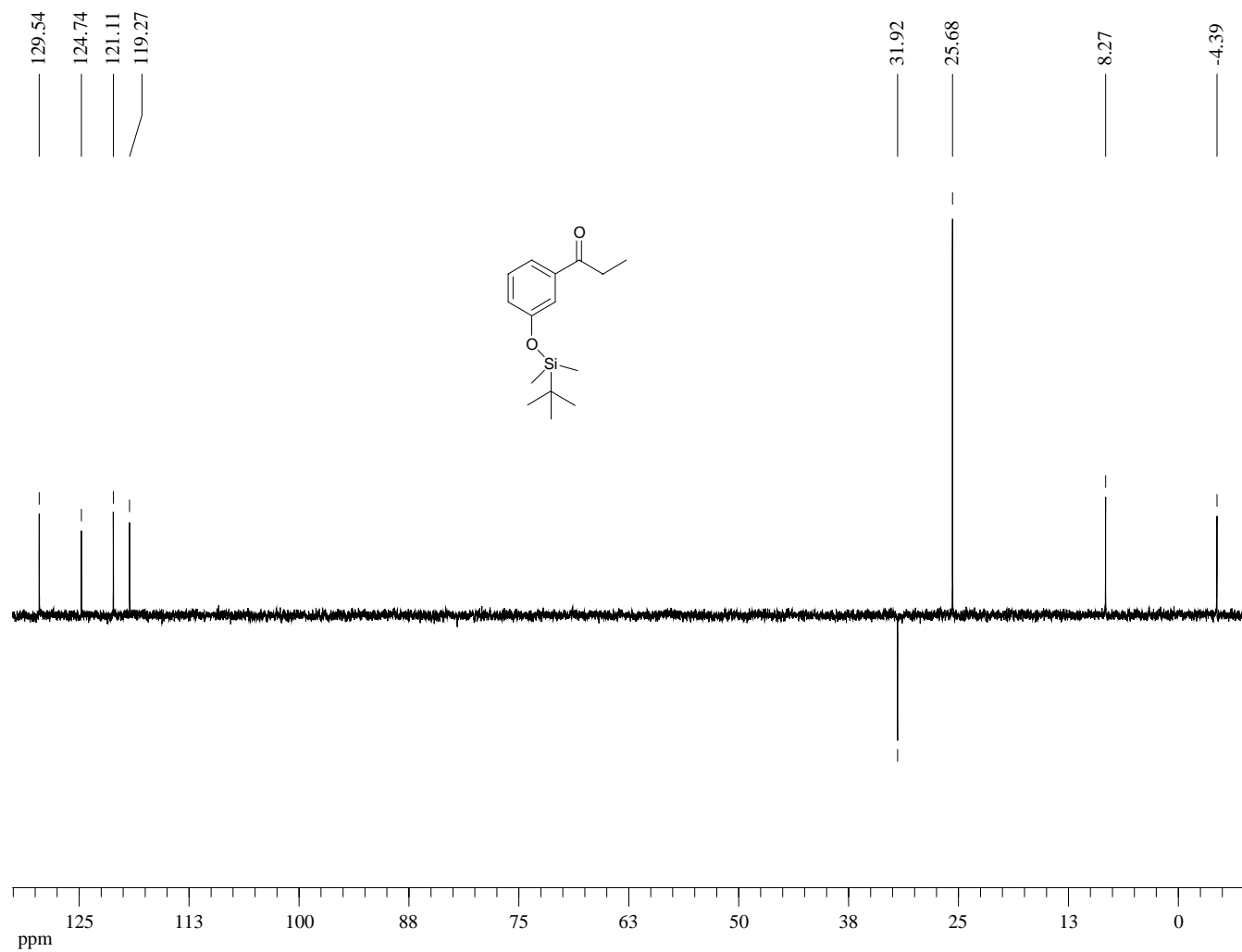
¹H-NMR (300 MHz, CDCl₃) of Compound **54**



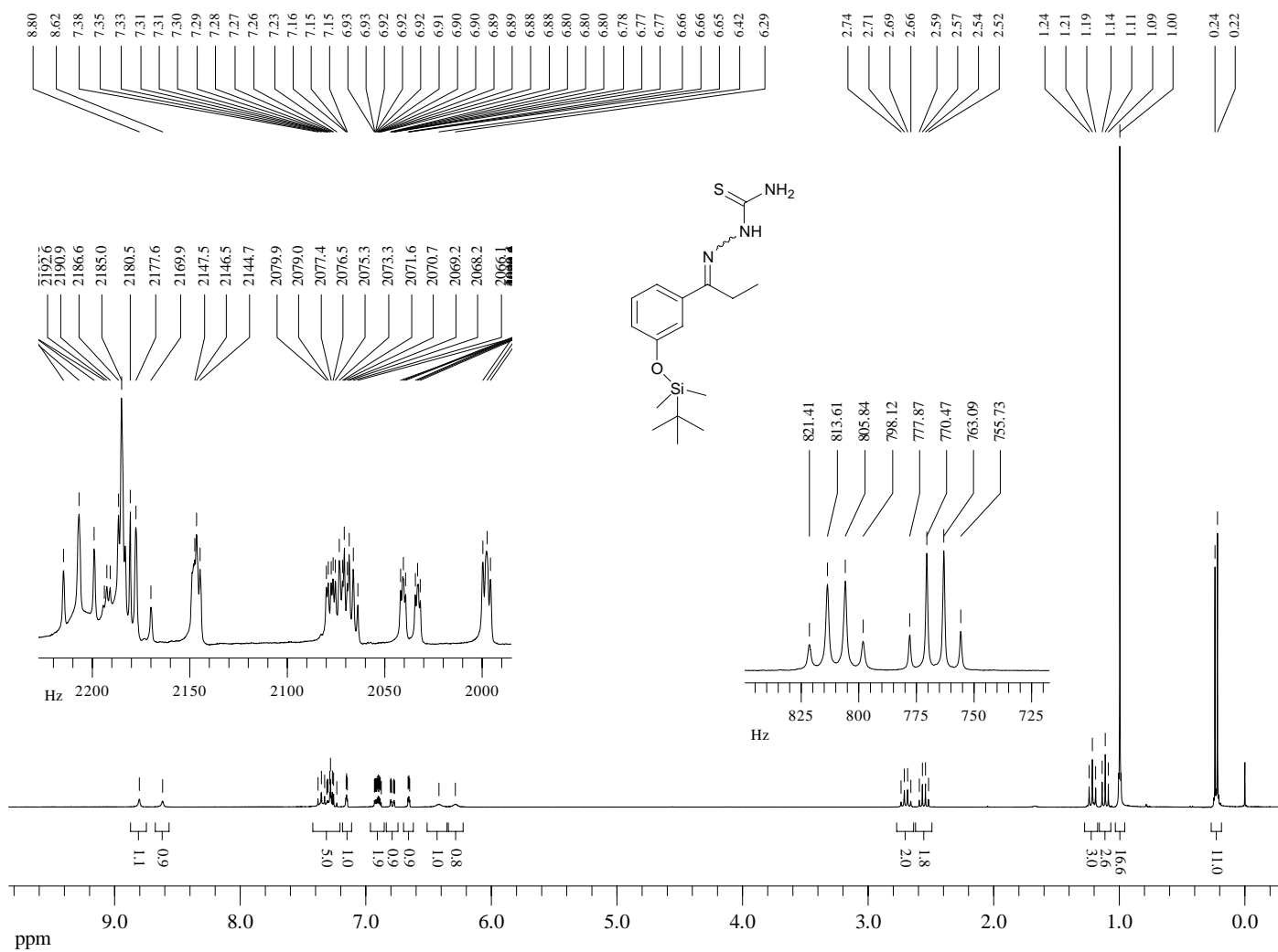
^{13}C -NMR (75 MHz, CDCl_3) of Compound **54**



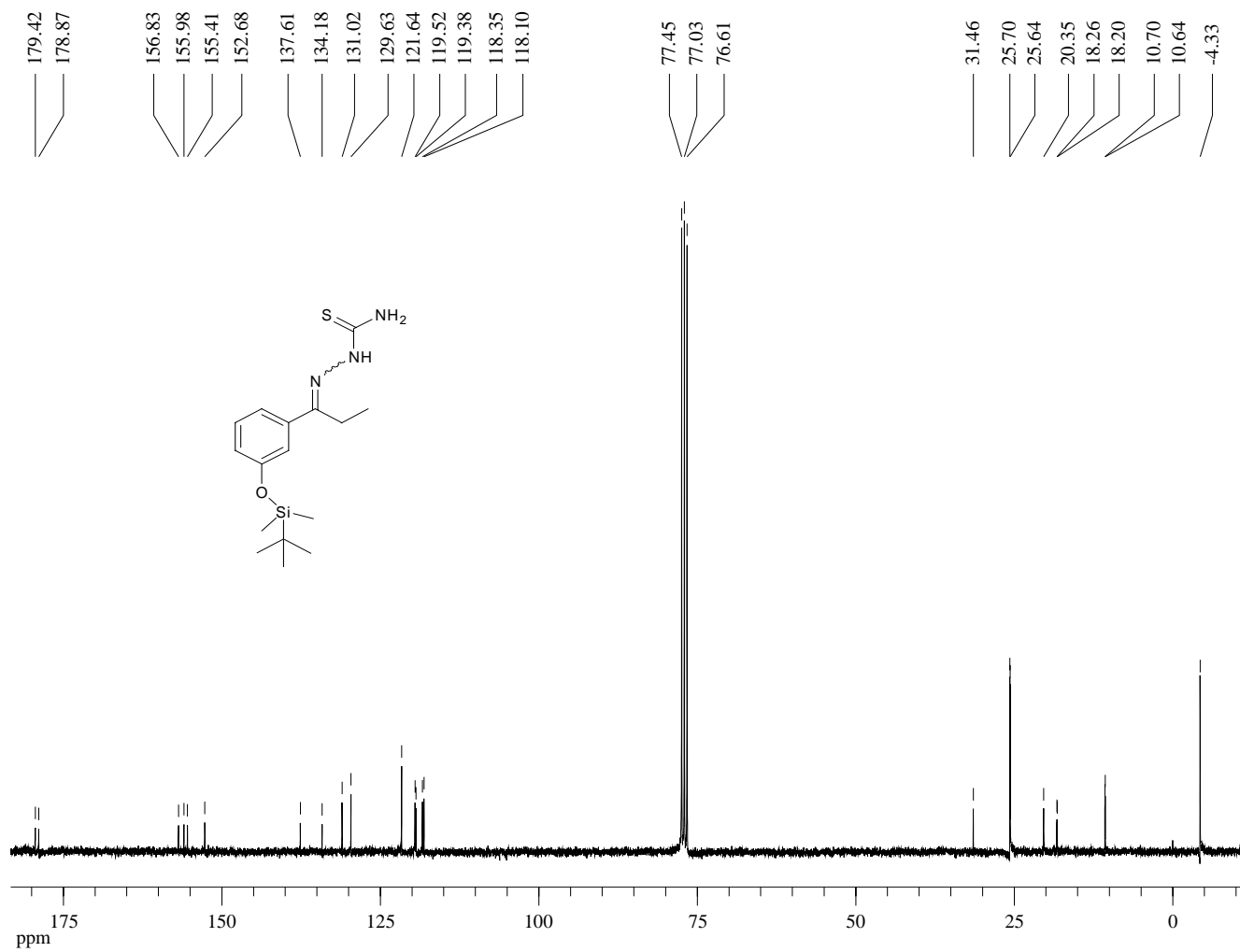
Dept 135-NMR (75 MHz, CDCl₃) of Compound **54**



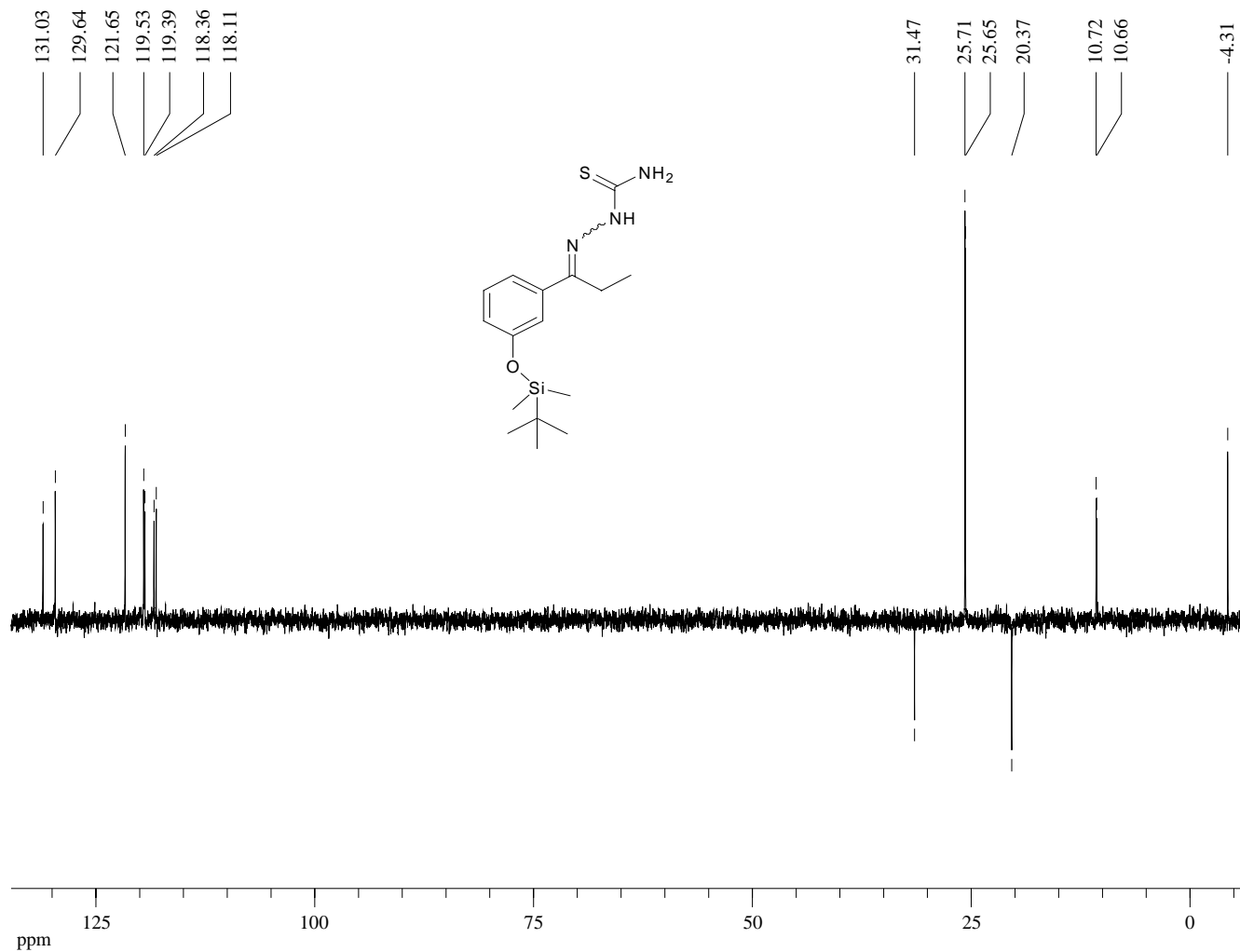
¹H-NMR (300 MHz, CDCl₃) of Compound **55**



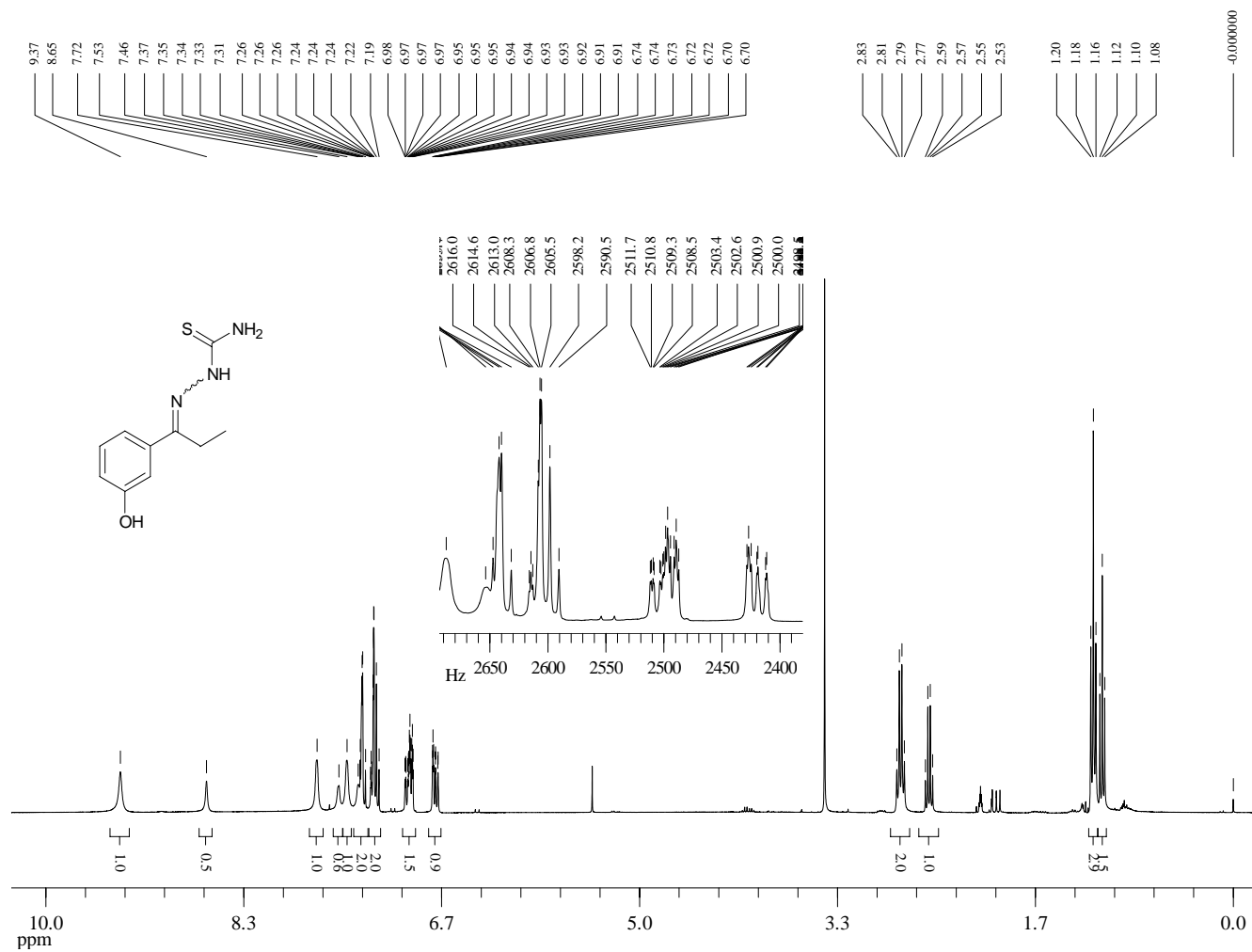
¹³C-NMR (75 MHz, CDCl₃) of Compound **55**



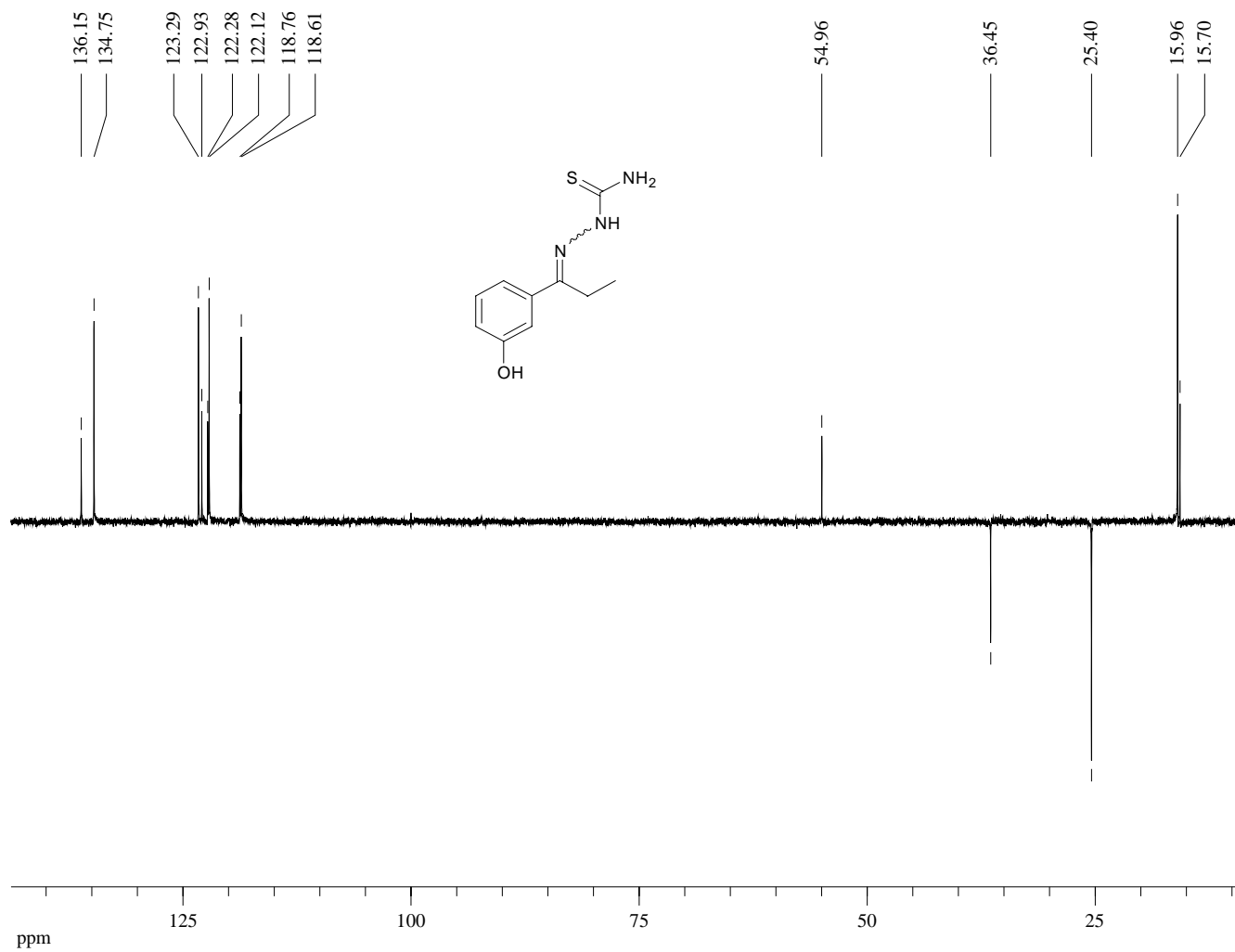
Dept 135-NMR (75 MHz, CDCl₃) of Compound **55**



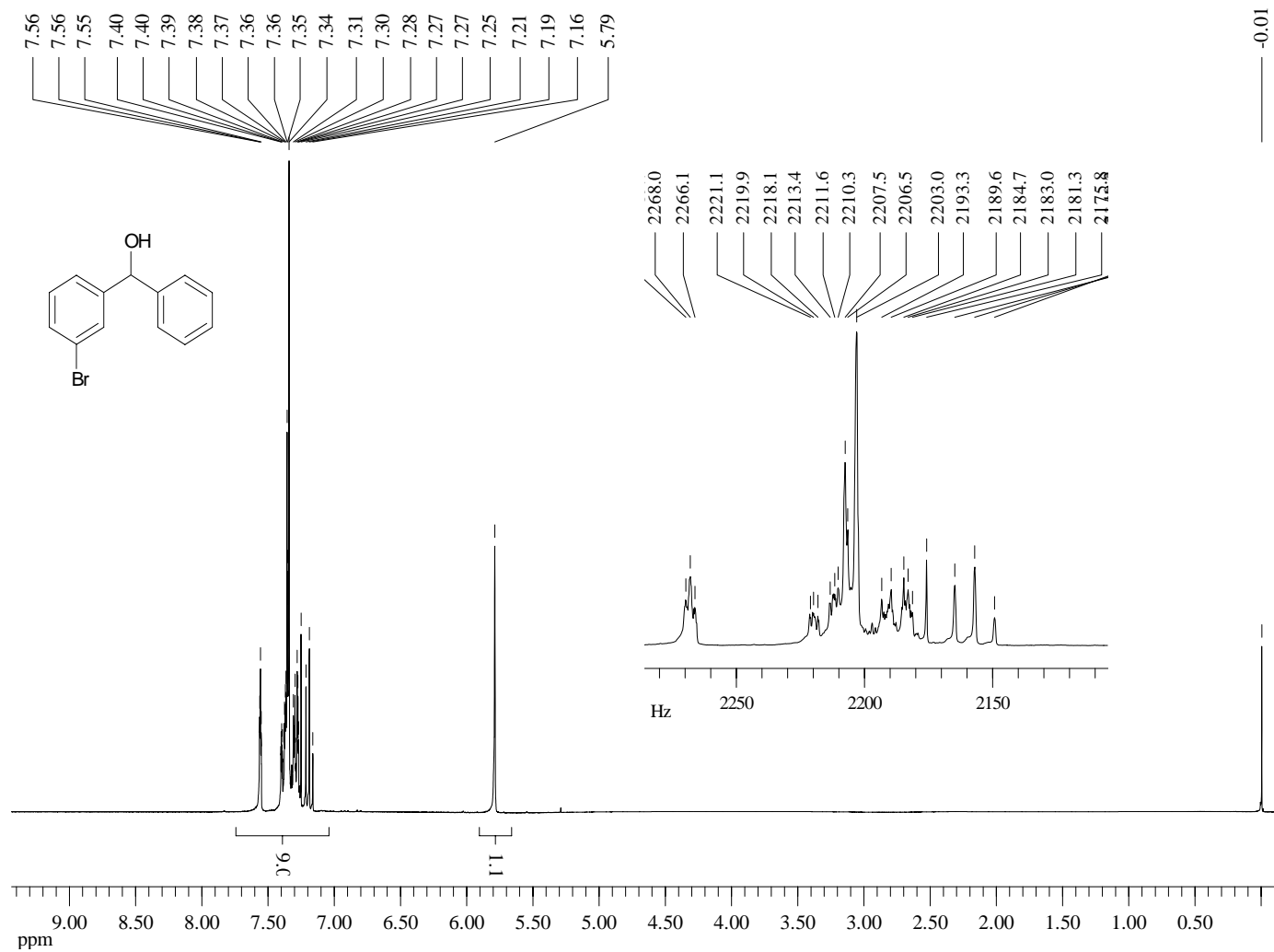
¹H-NMR (360 MHz, CDCl₃) of Compound **56**



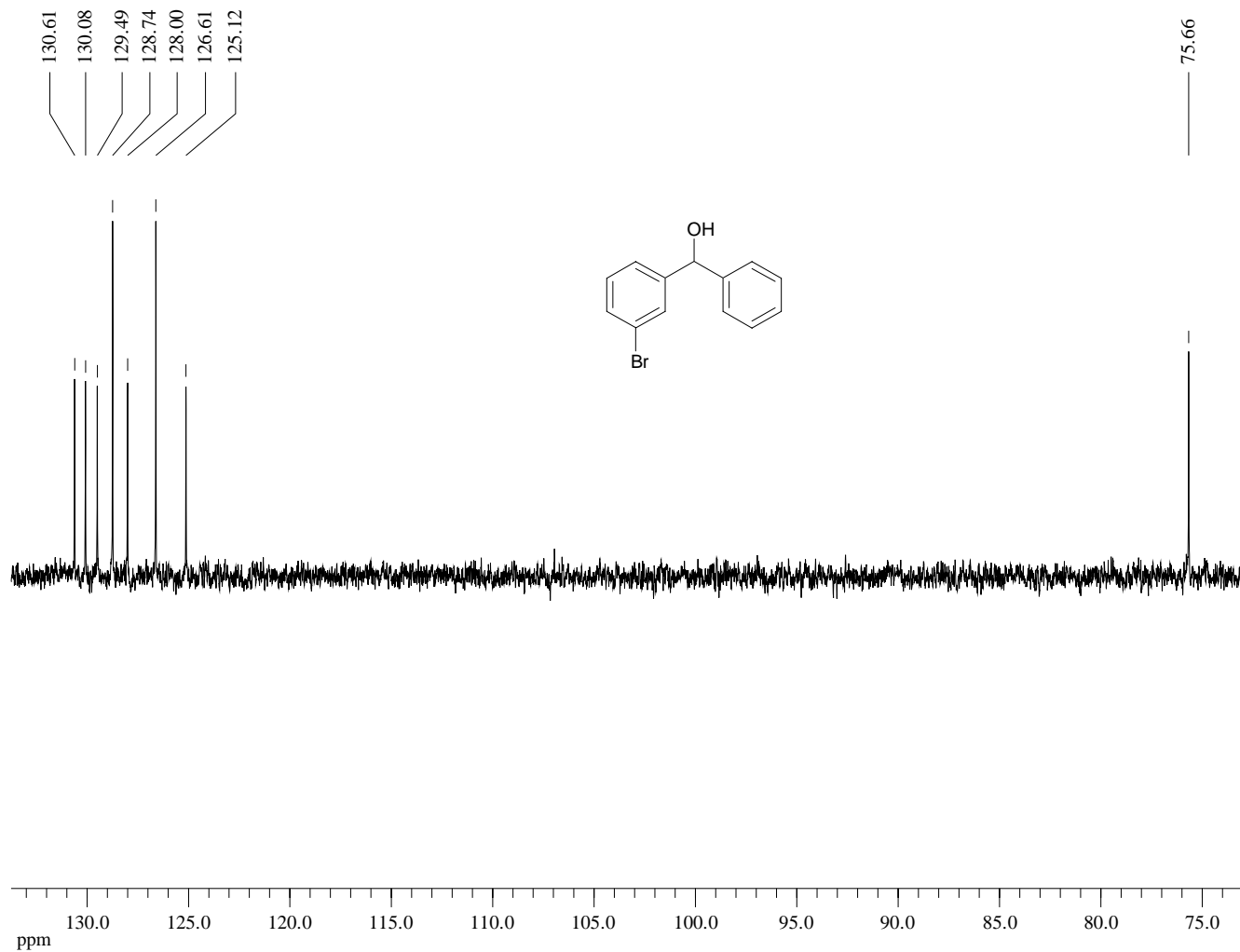
Dept 135-NMR (75 MHz, CDCl₃) of Compound **56**



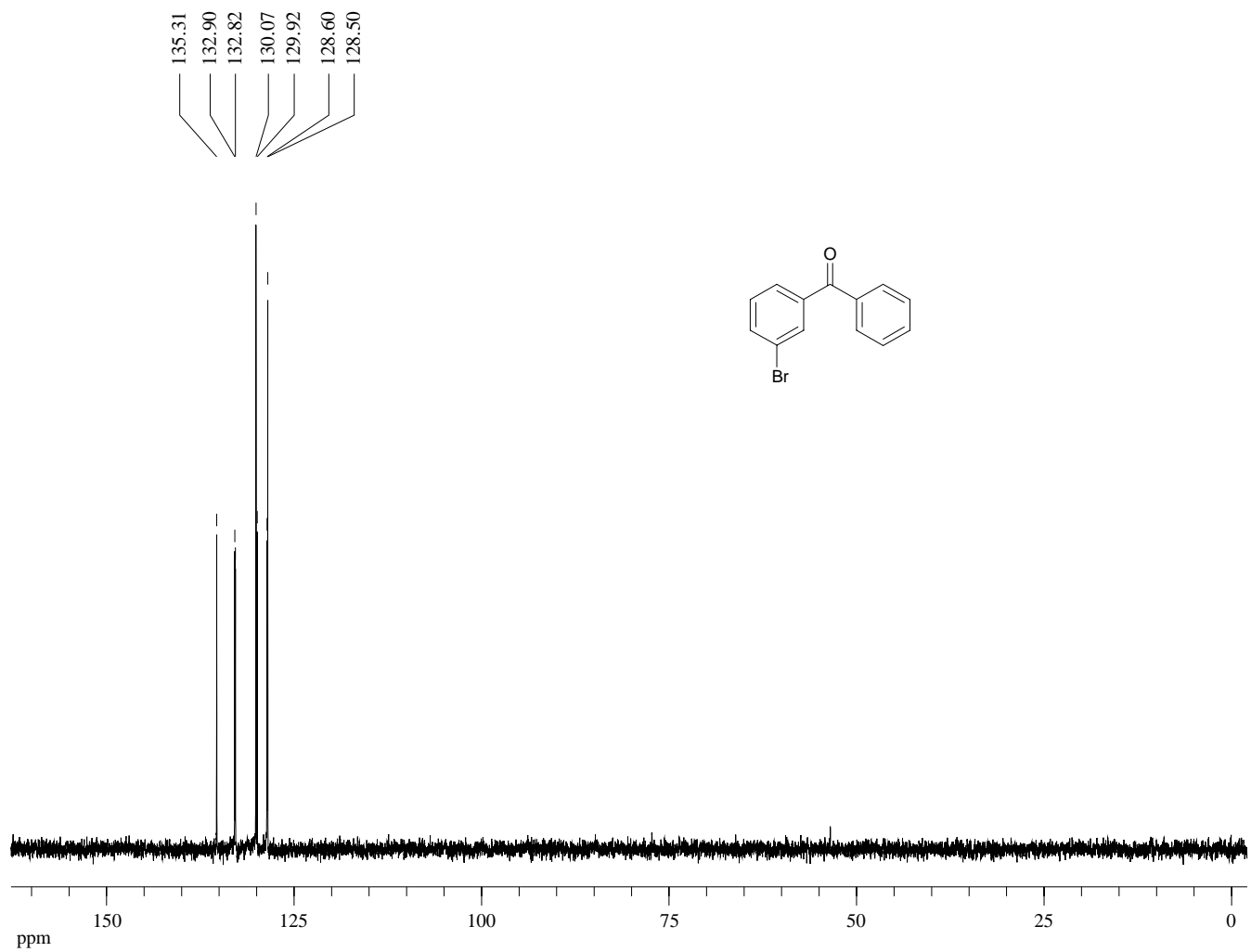
¹H-NMR (300 MHz, CDCl₃) of Compound **57**



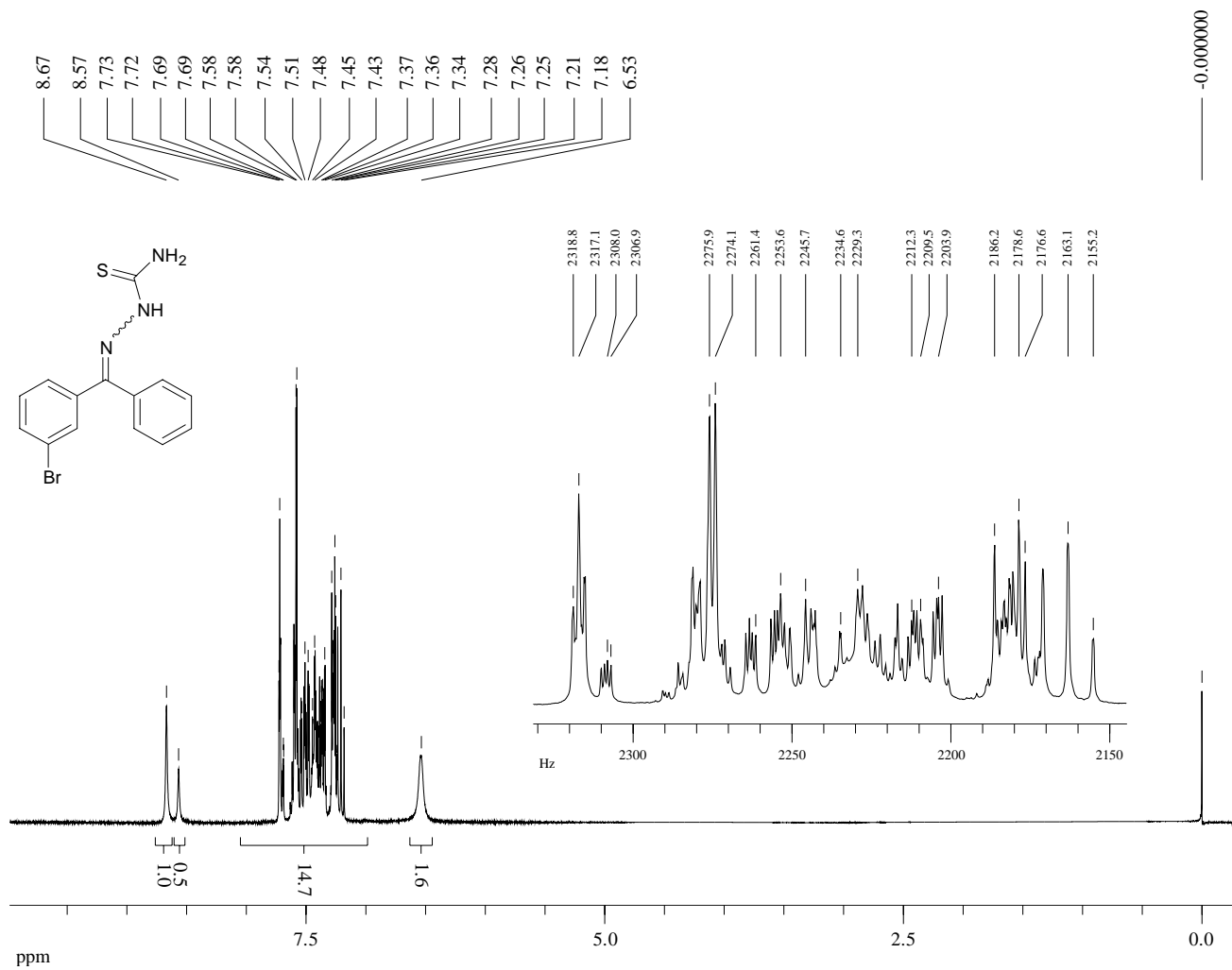
Dept 135-NMR (75 MHz, CDCl₃) of Compound **57**



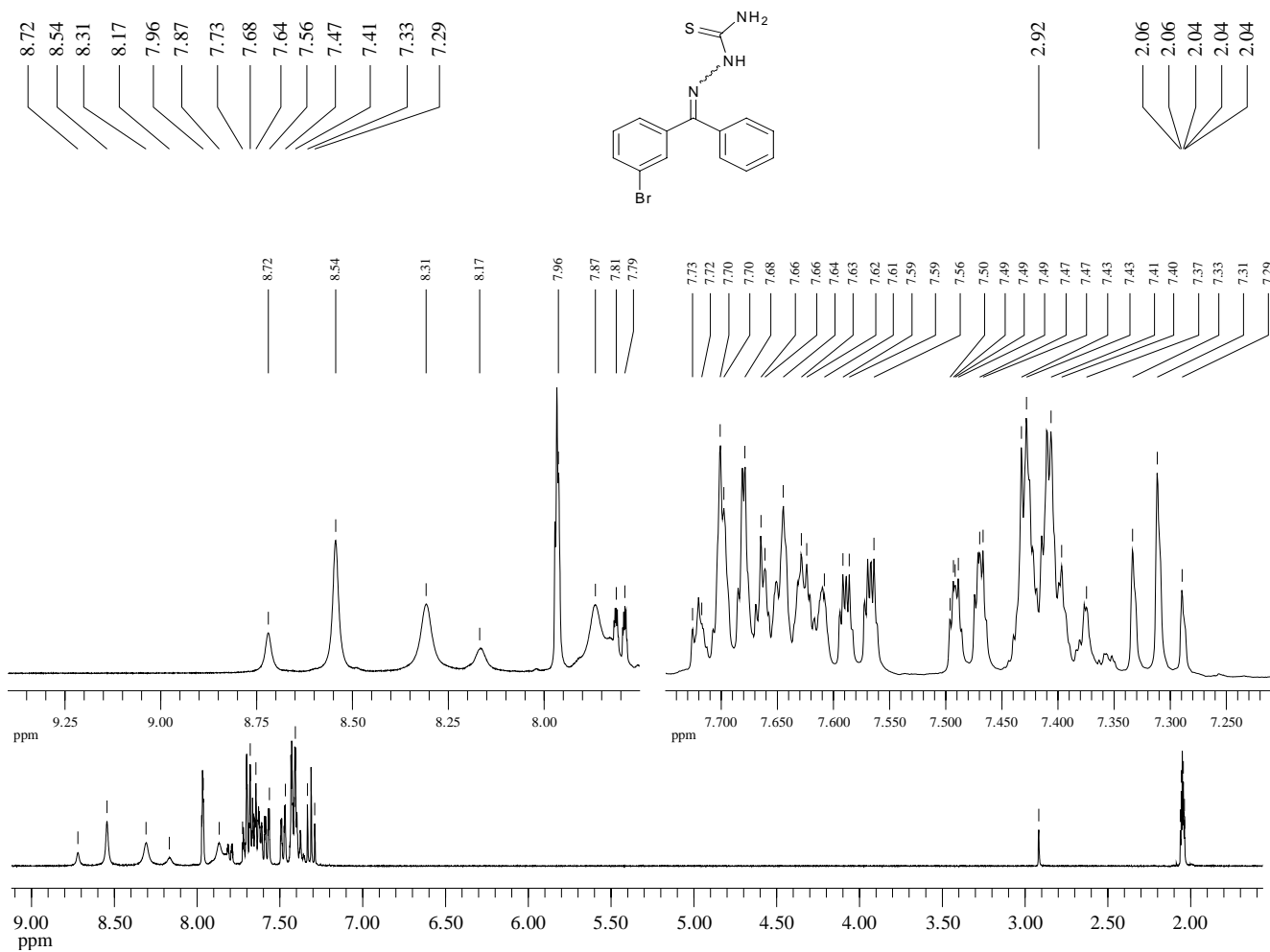
Dept 45-NMR (75 MHz, CDCl₃) of Compound **58**



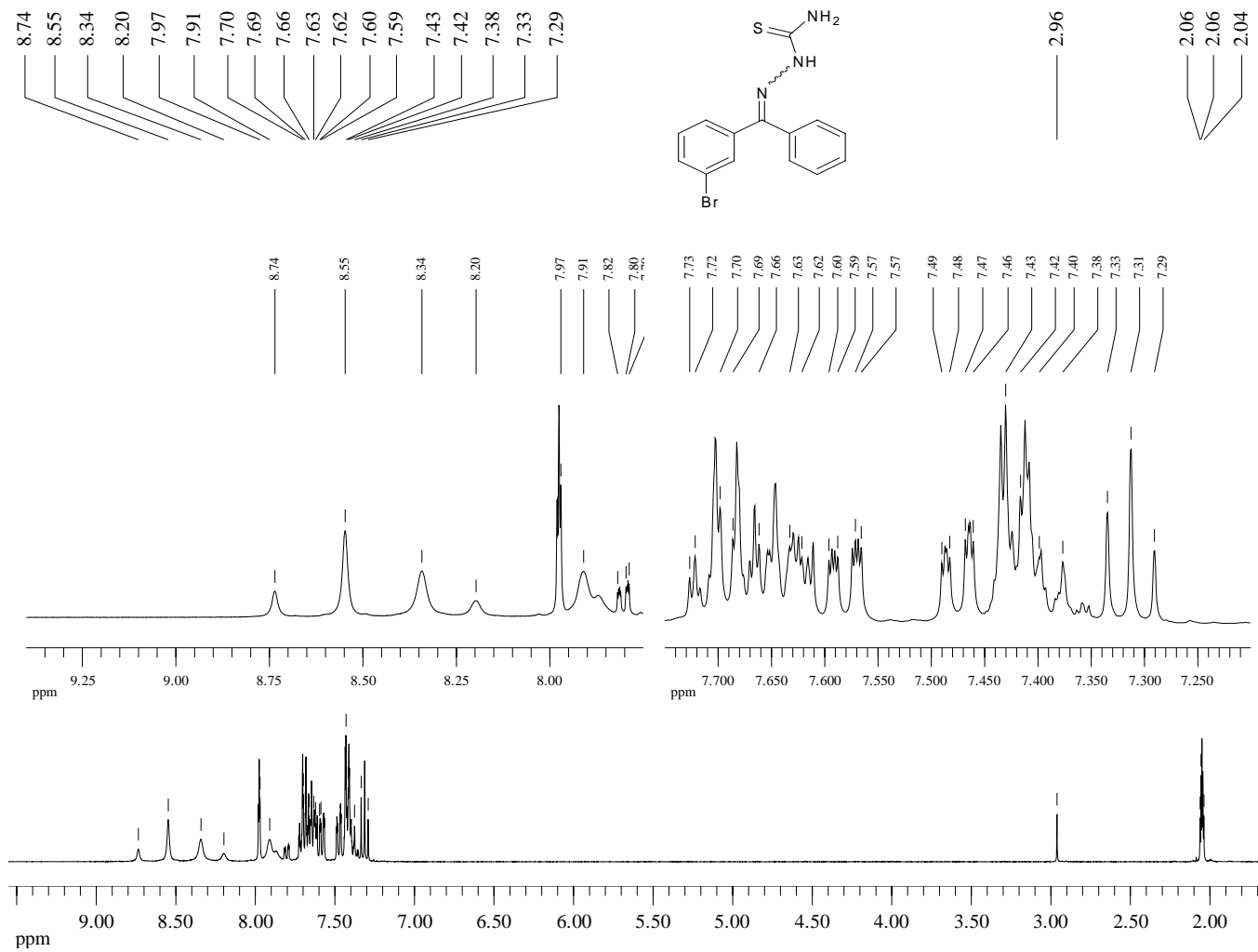
¹H-NMR (300 MHz, CDCl₃) of Compound **59**



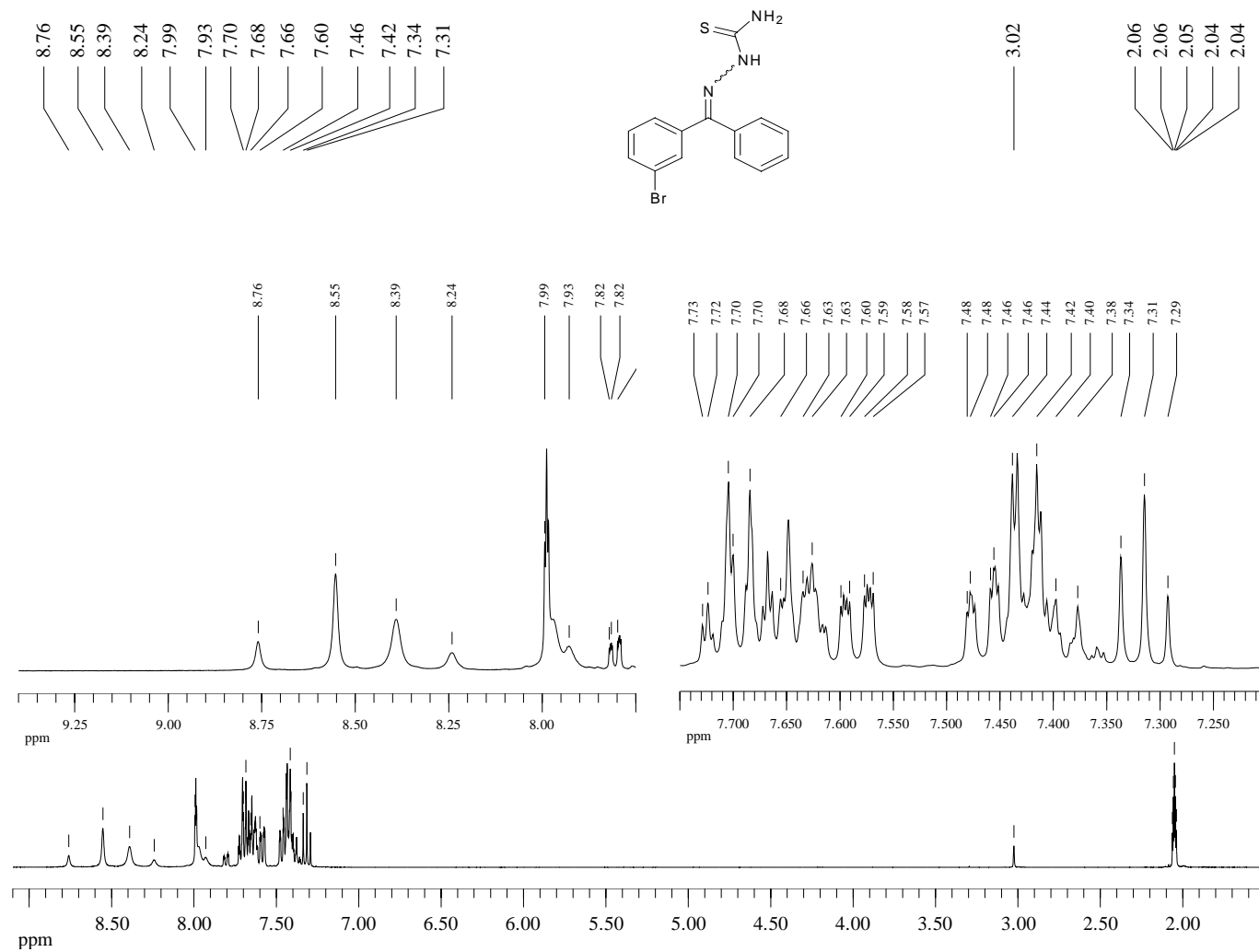
¹H-NMR (360 MHz, Acetone-d₆) at 17°C of Compound **59**



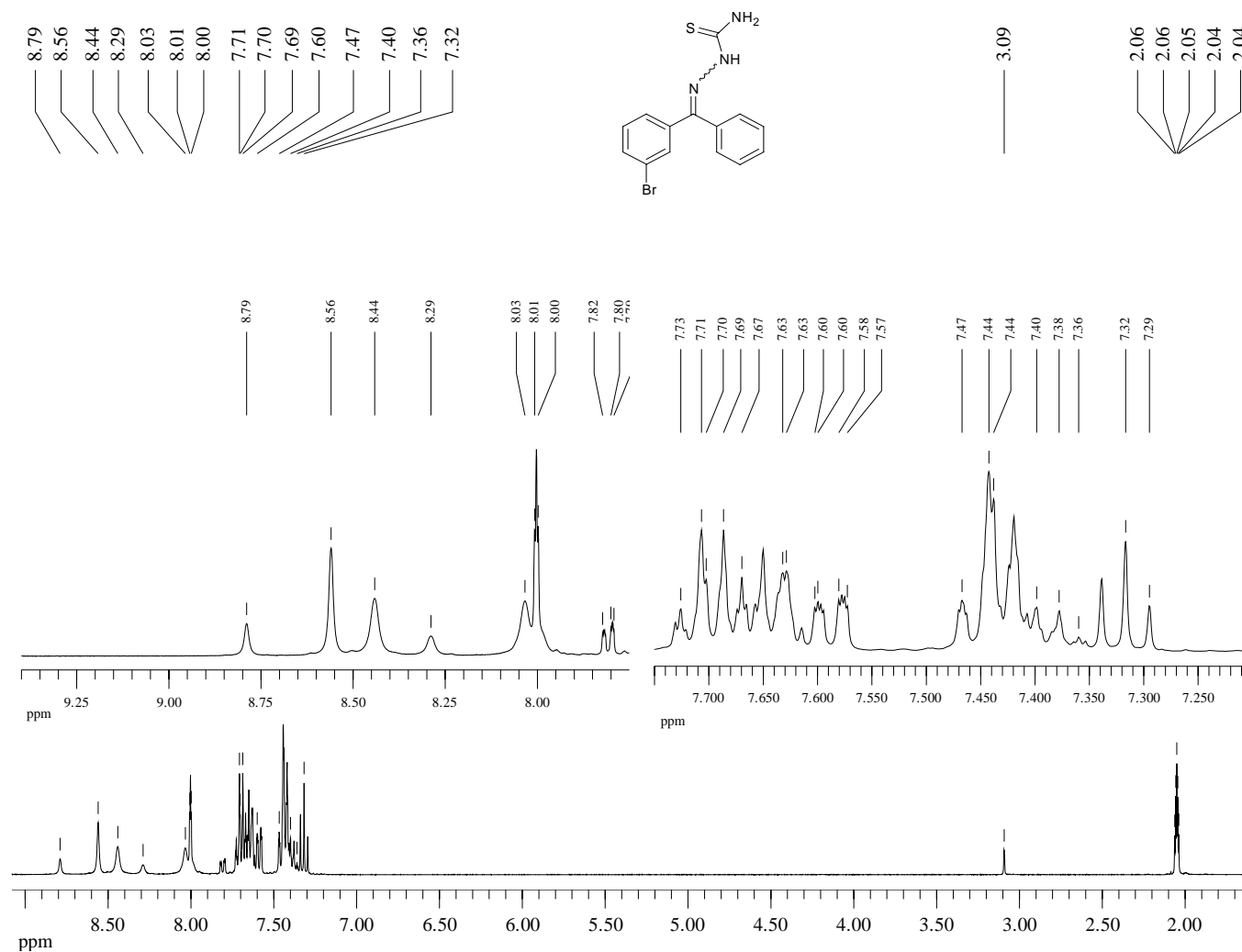
¹H-NMR (360 MHz, Acetone-d₆) at 10°C of Compound **59**



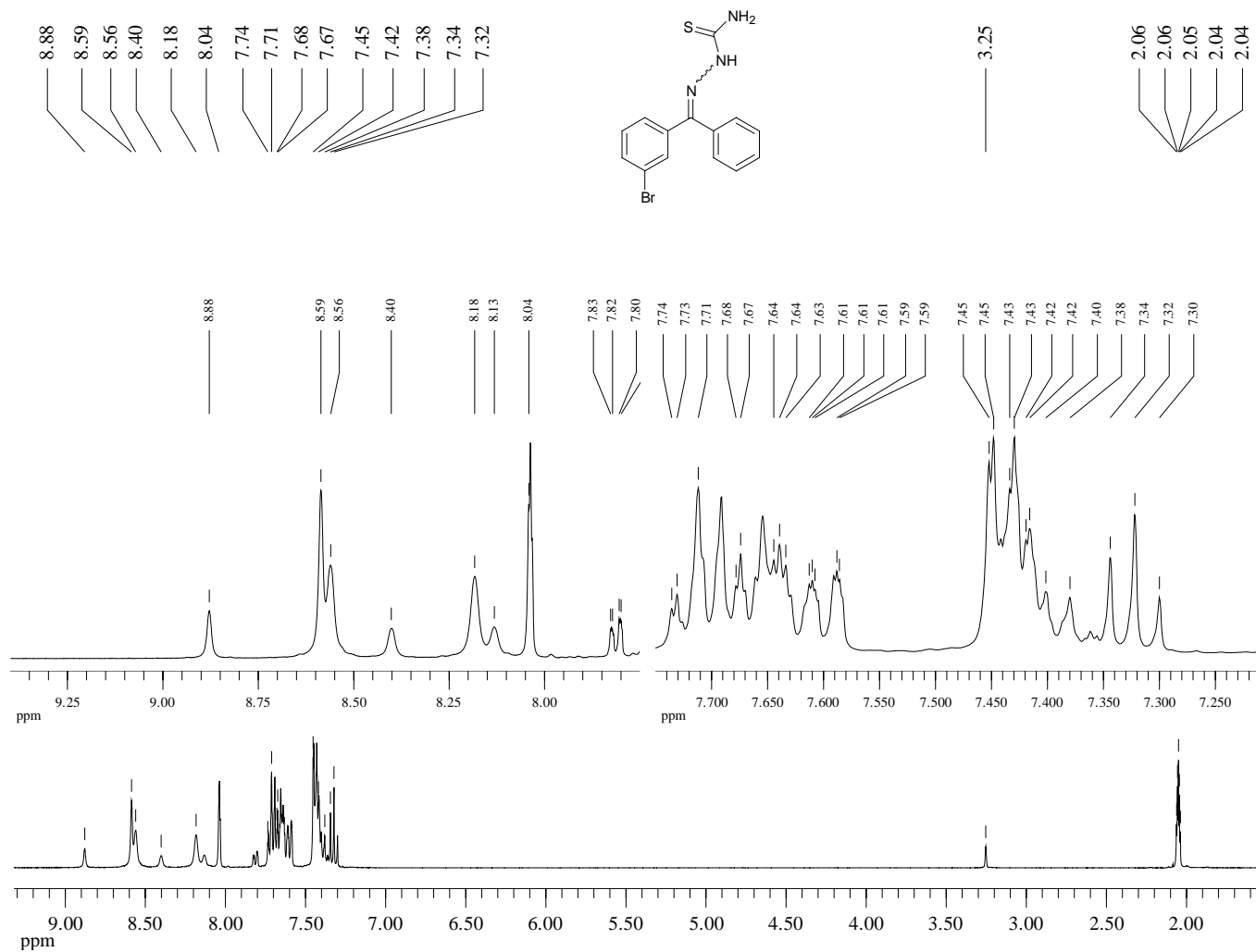
¹H-NMR (360 MHz, Acetone-d₆) at 0°C of Compound **59**



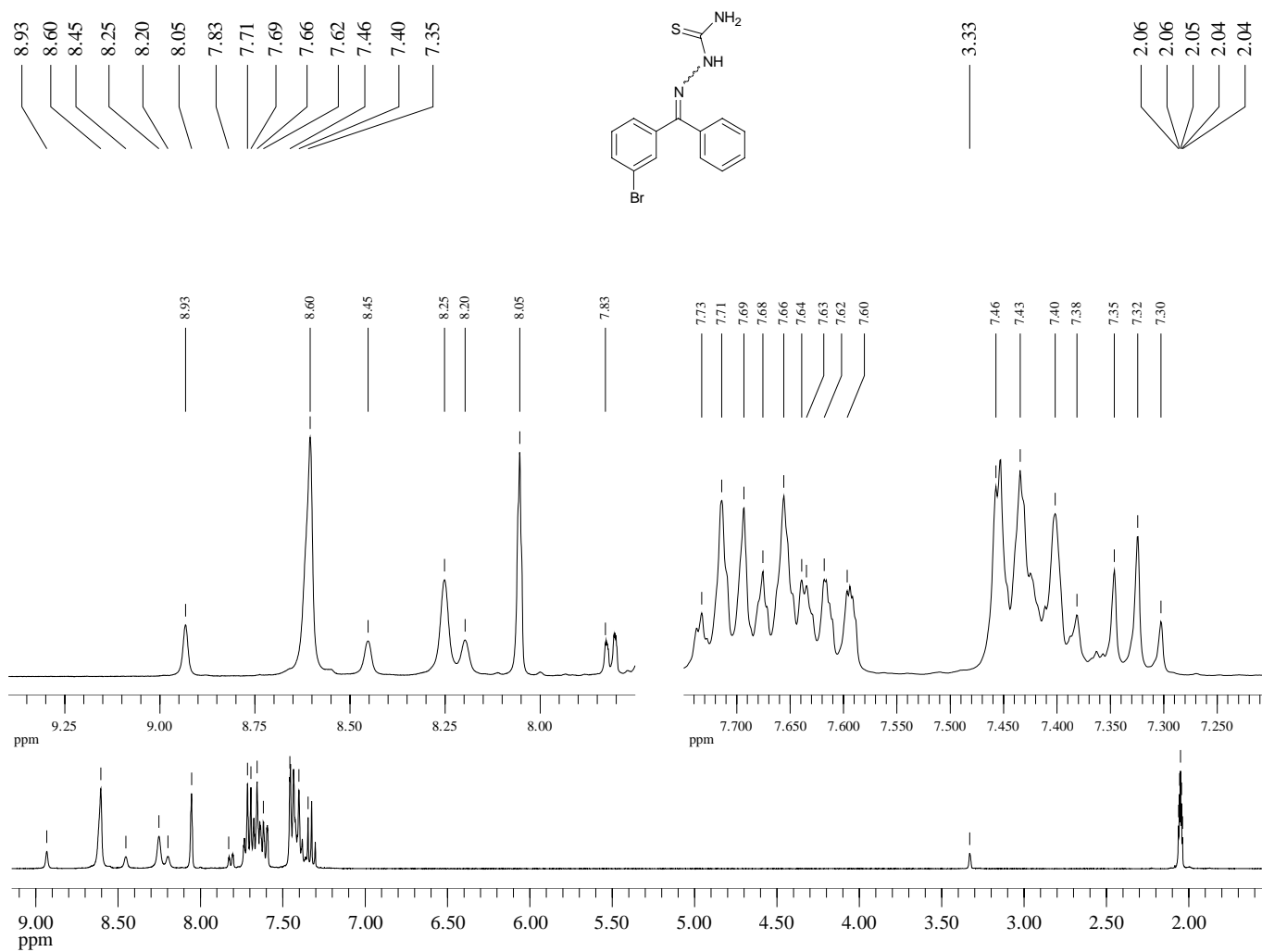
¹H-NMR (360 MHz, Acetone-d₆) at -10°C of Compound **59**



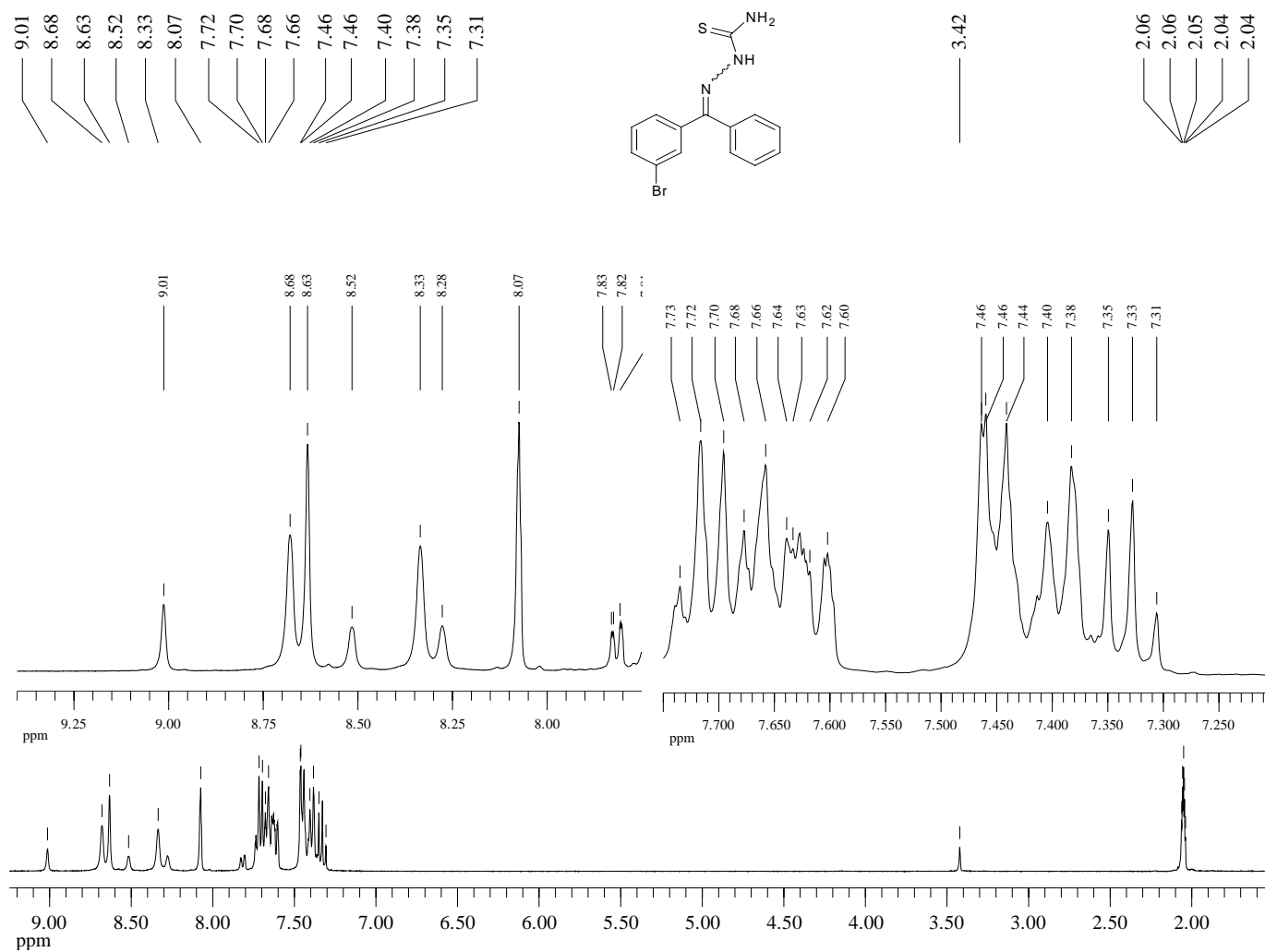
$^1\text{H-NMR}$ (360 MHz, Acetone- d_6) at -30°C of Compound **59**



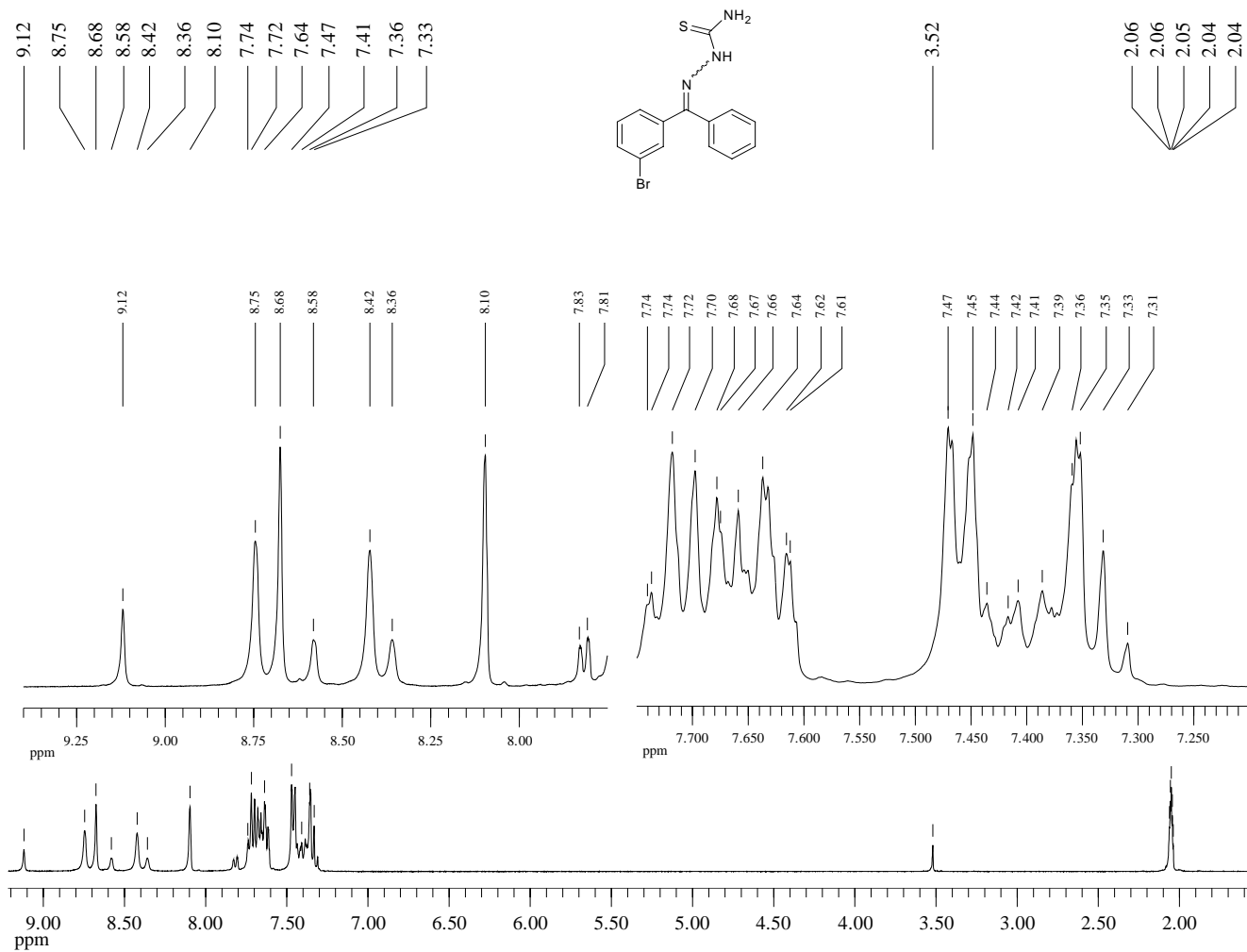
¹H-NMR (360 MHz, Acetone-d₆) at -40°C of Compound **59**



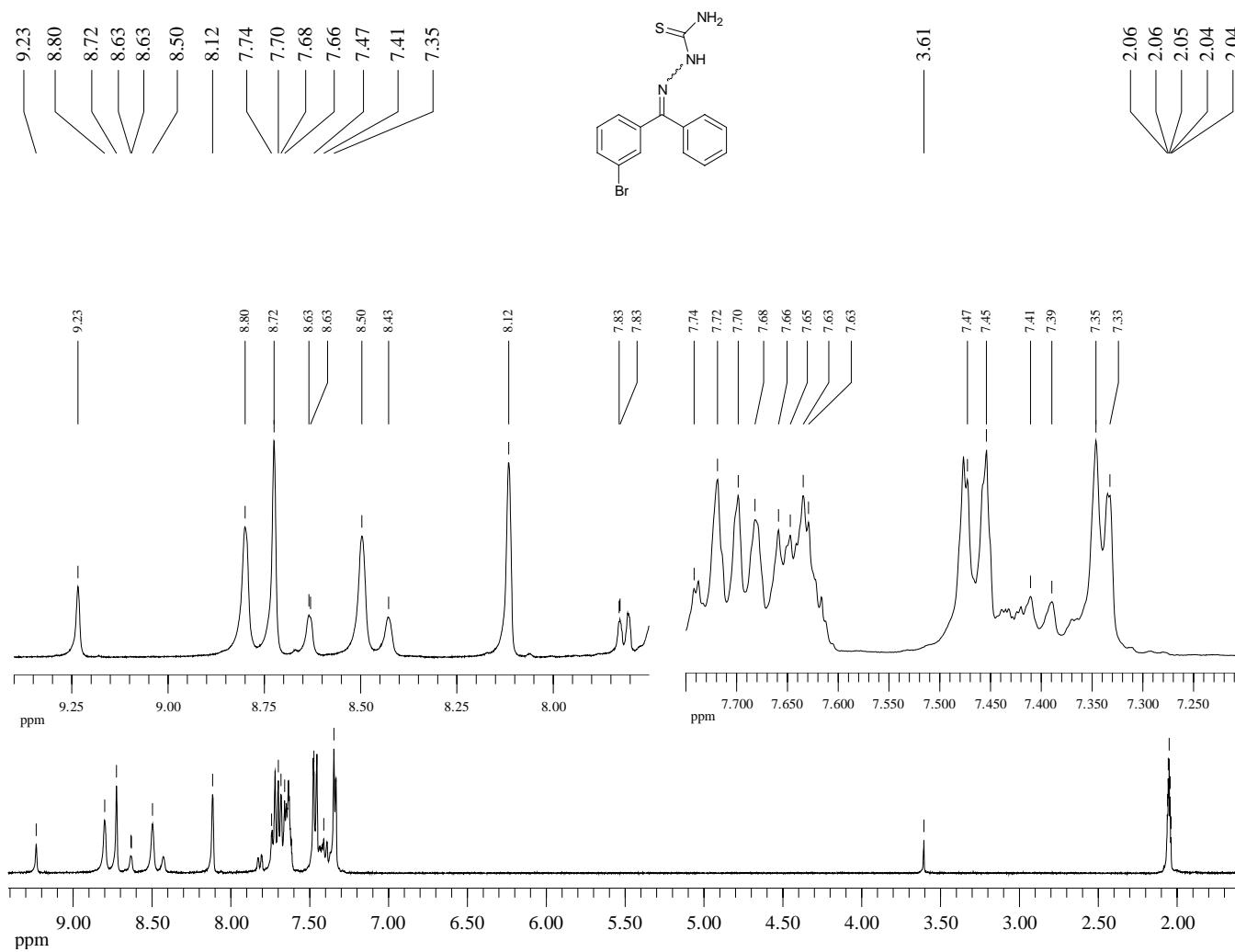
¹H-NMR (360 MHz, Acetone-d₆) at -50°C of Compound **59**



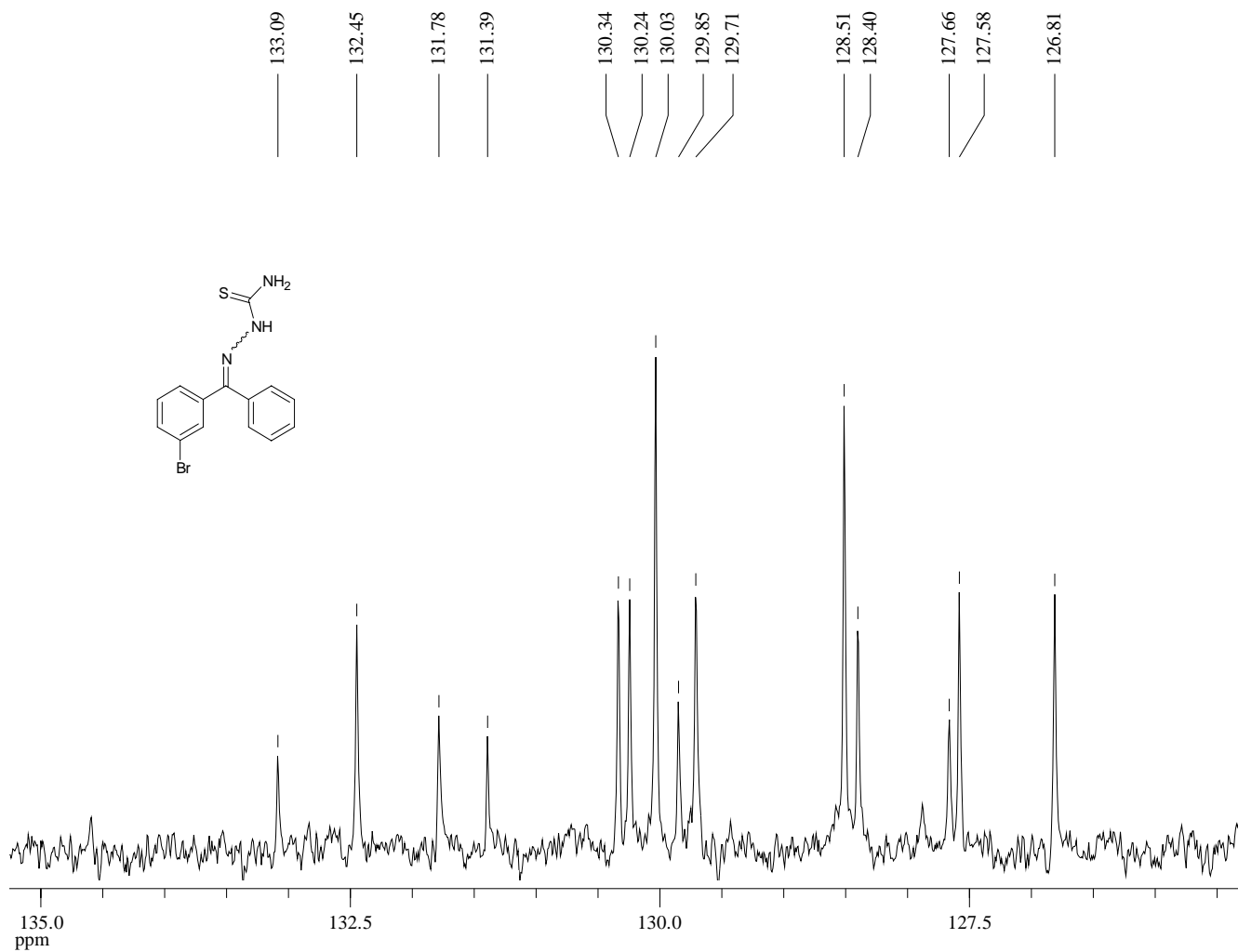
$^1\text{H-NMR}$ (360 MHz, Acetone- d_6) at -60°C of Compound **59**



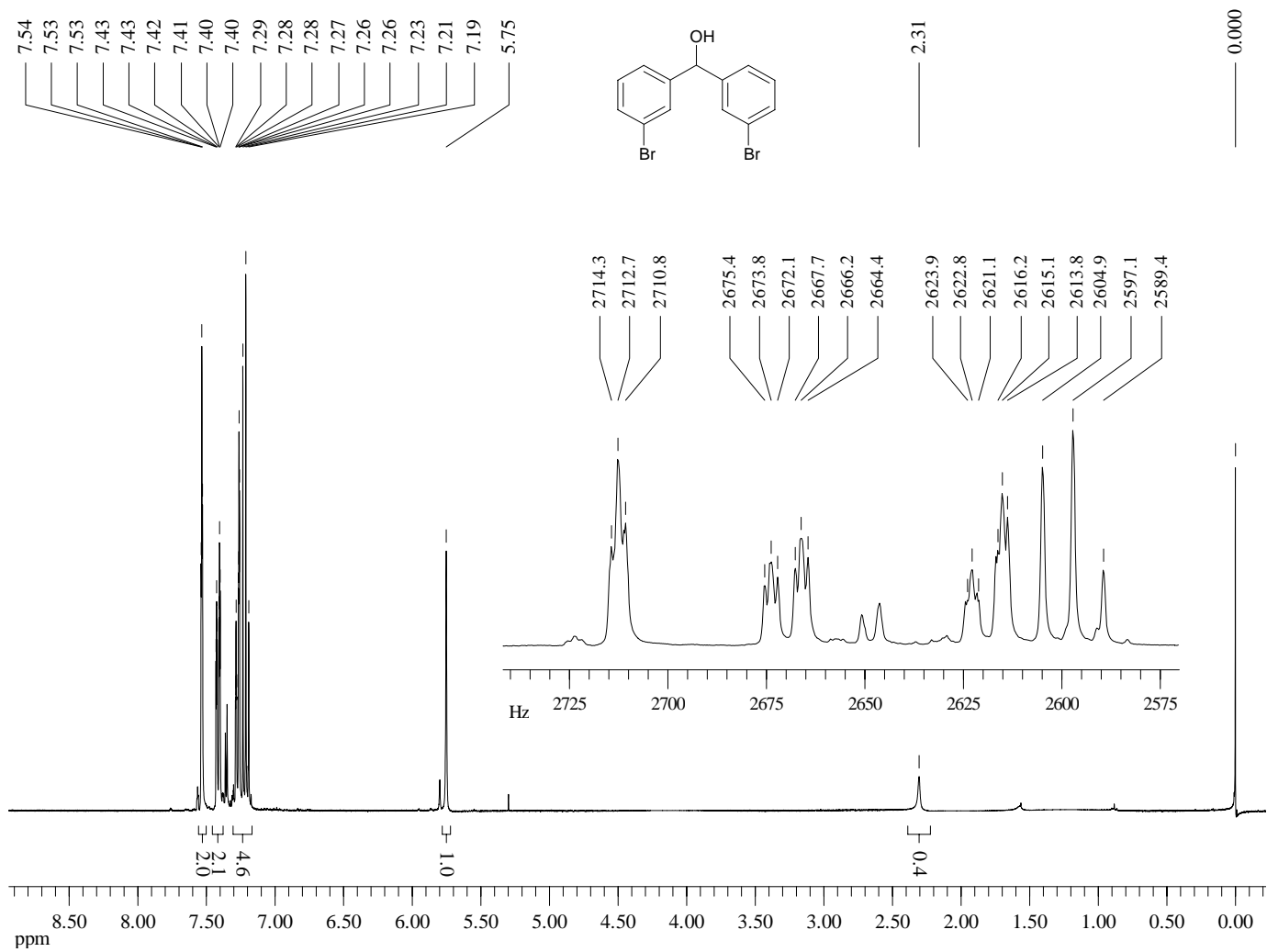
$^1\text{H-NMR}$ (360 MHz, Acetone- d_6) at -70°C of Compound **59**



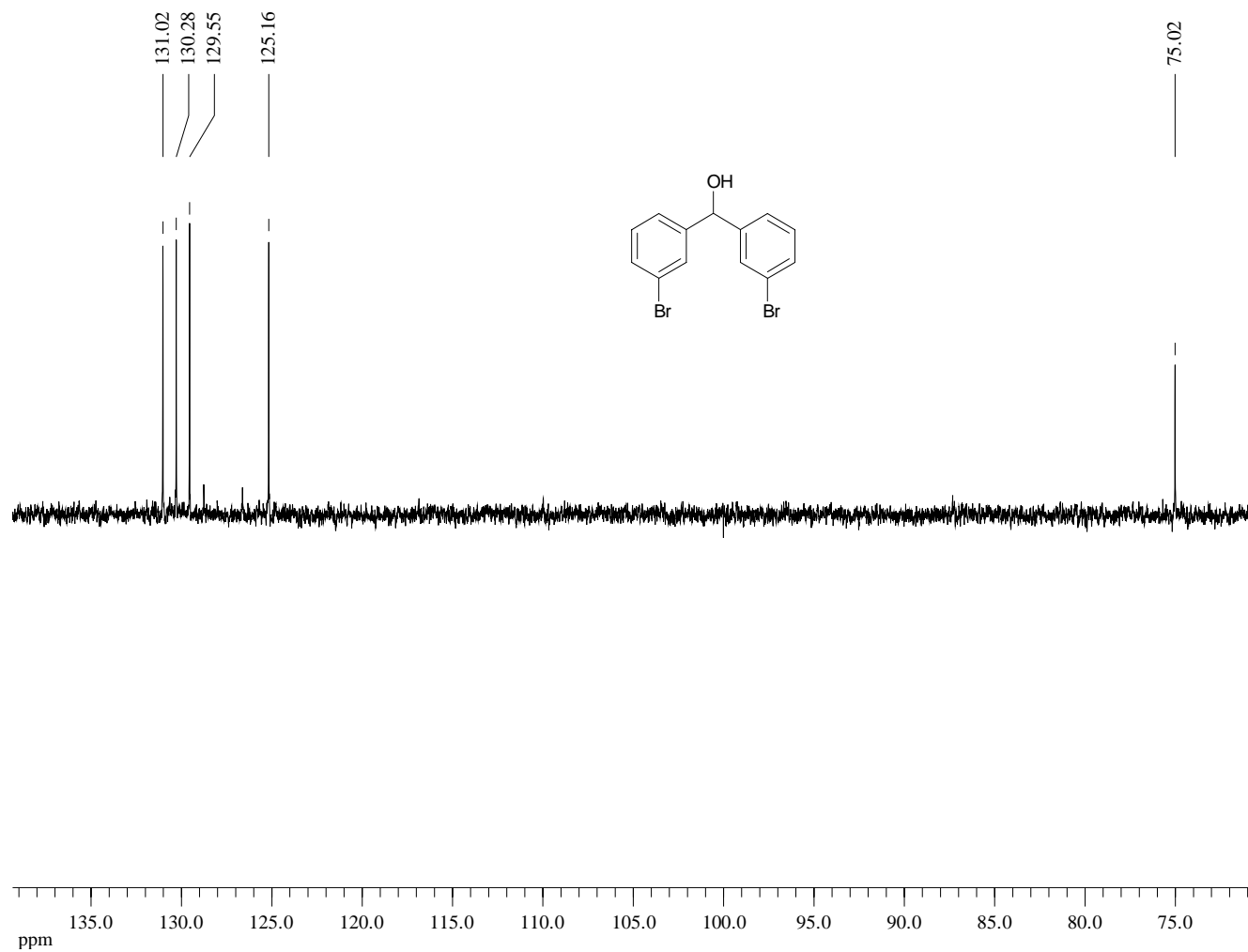
Dept 45-NMR (75 MHz, Acetone-d₆) of Compound **59**



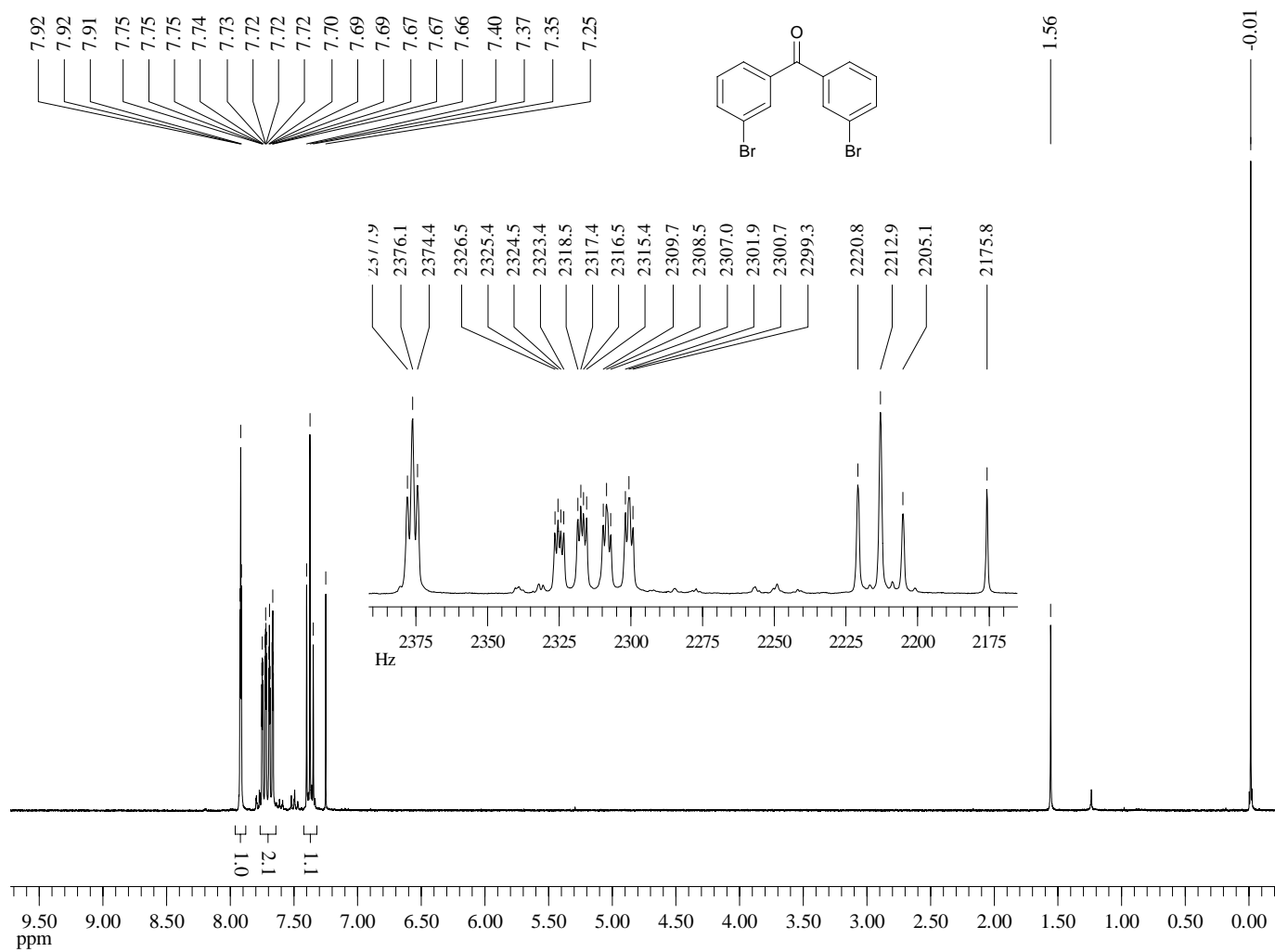
¹H-NMR (360 MHz, CDCl₃) of Compound **60**



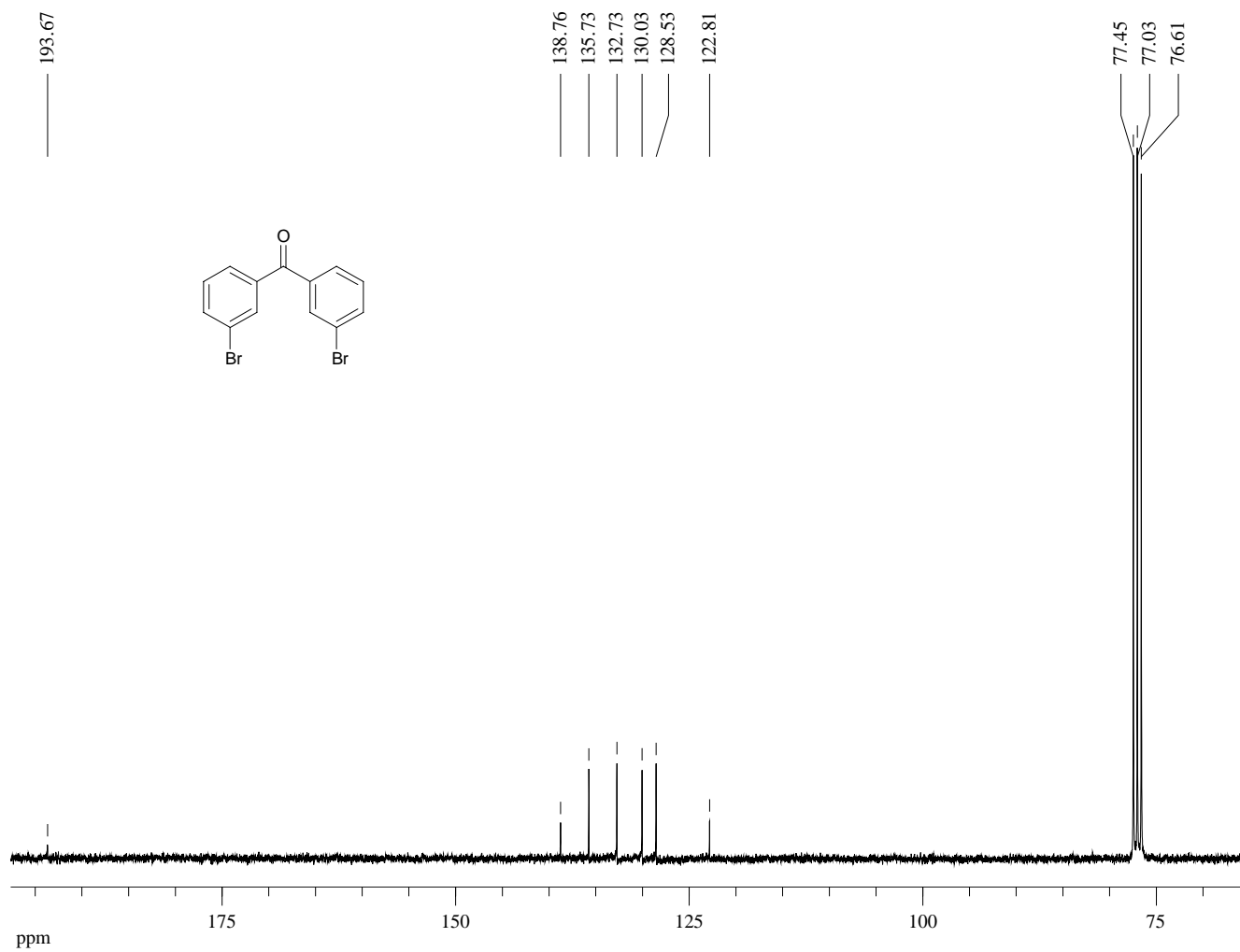
Dept 135-NMR (90 MHz, CDCl₃) of Compound **60**



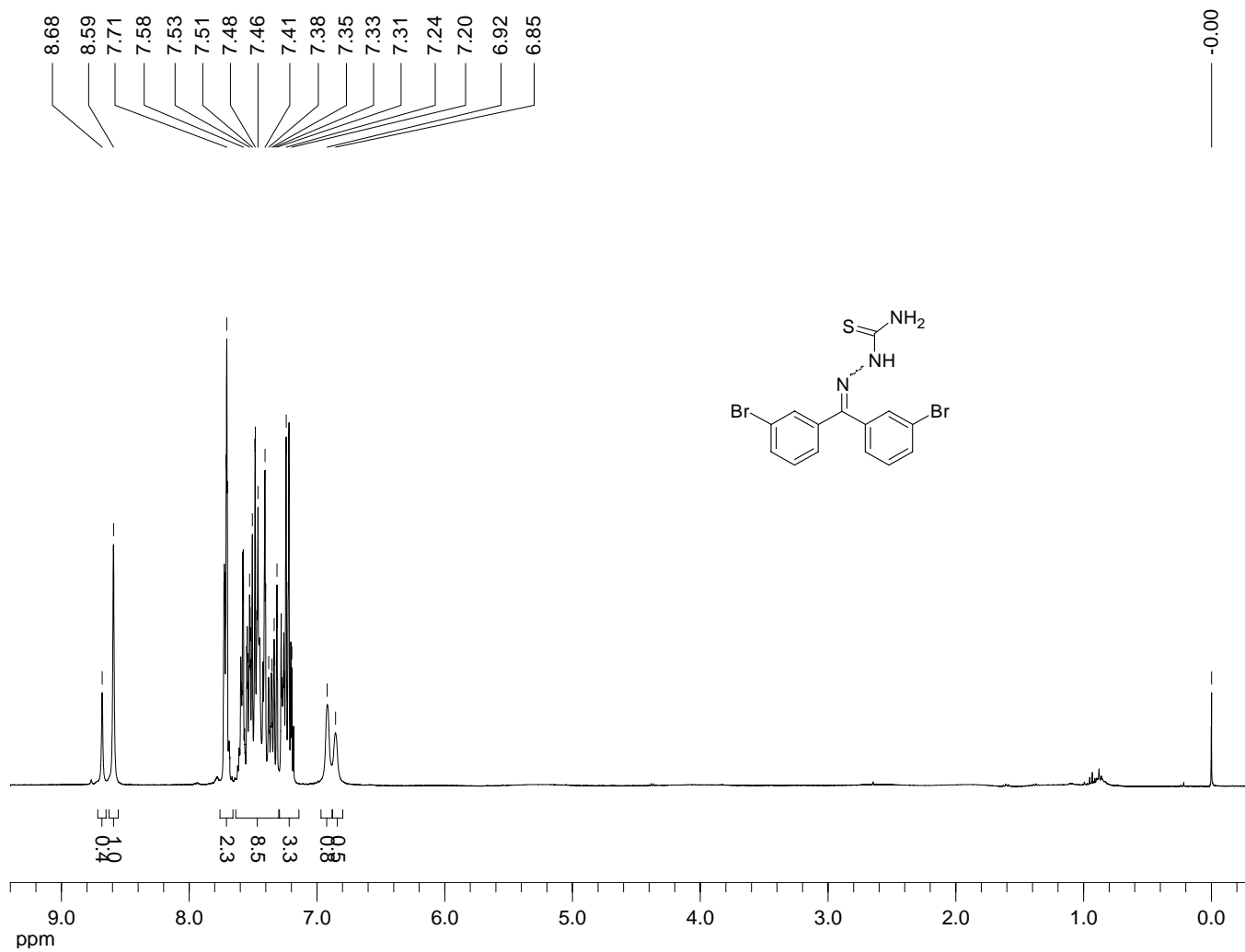
¹H-NMR (300 MHz, CDCl₃) of Compound **61**



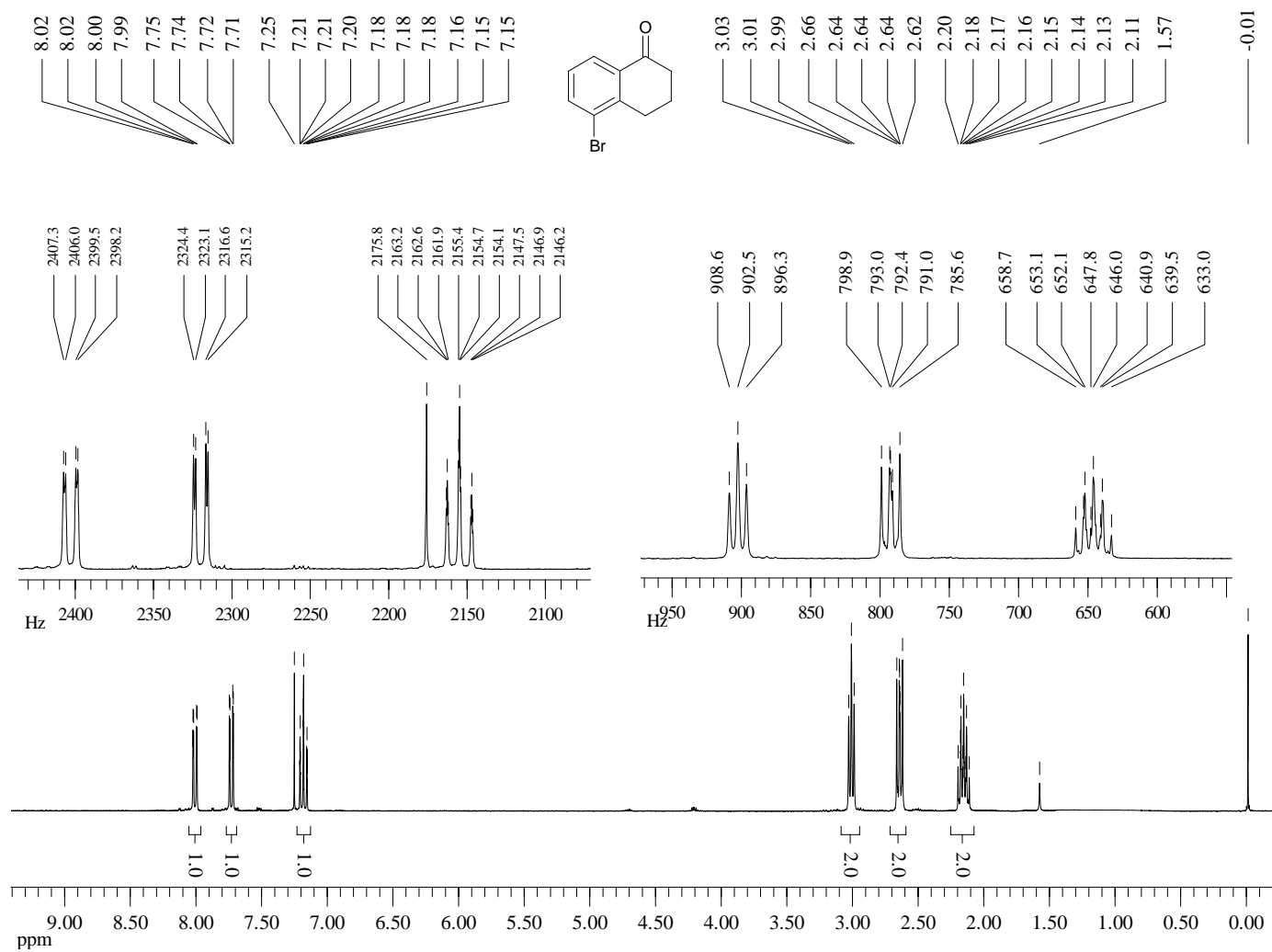
^{13}C -NMR (75 MHz, CDCl_3) of Compound **61**



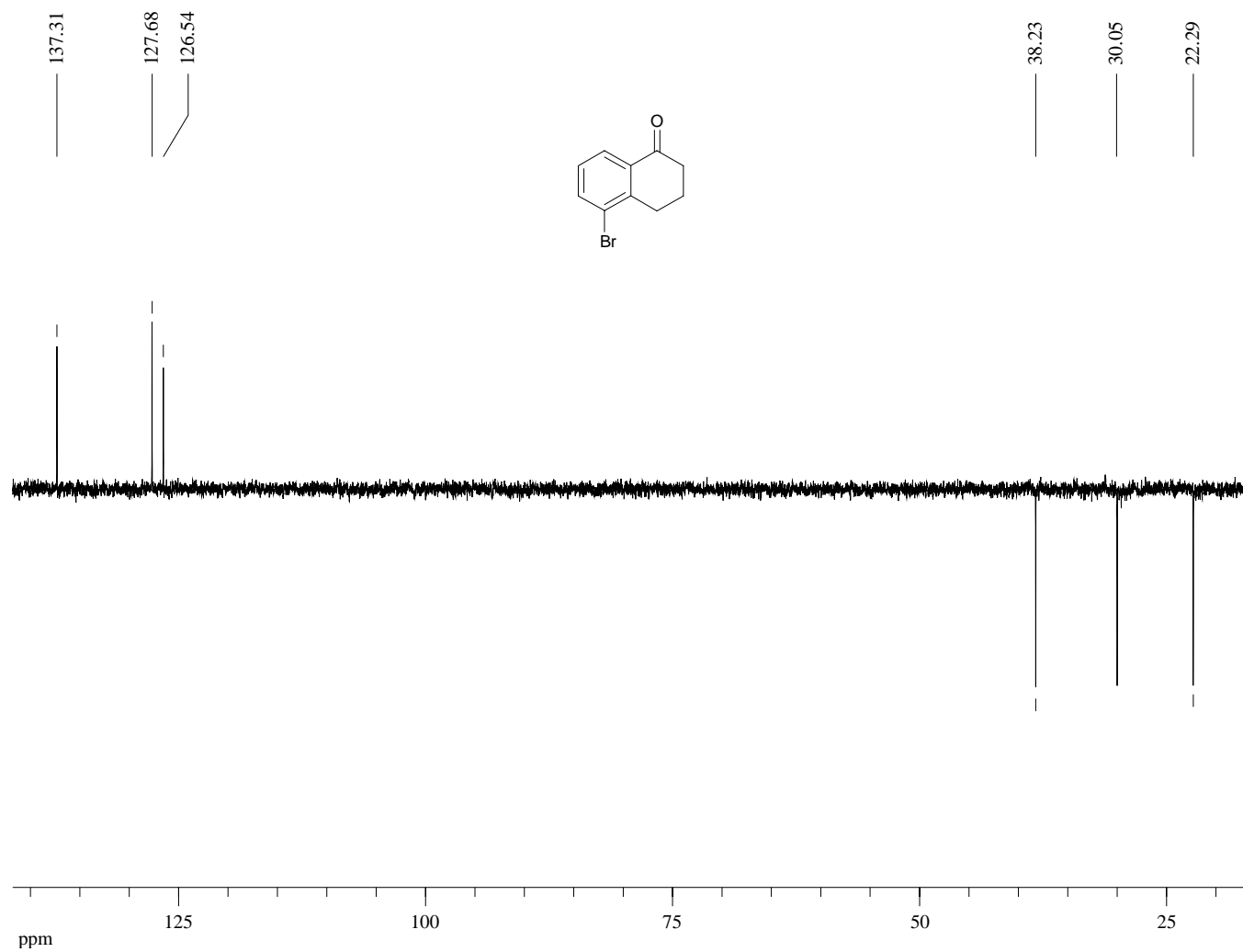
¹H-NMR (360 MHz, CDCl₃) of Compound **62**



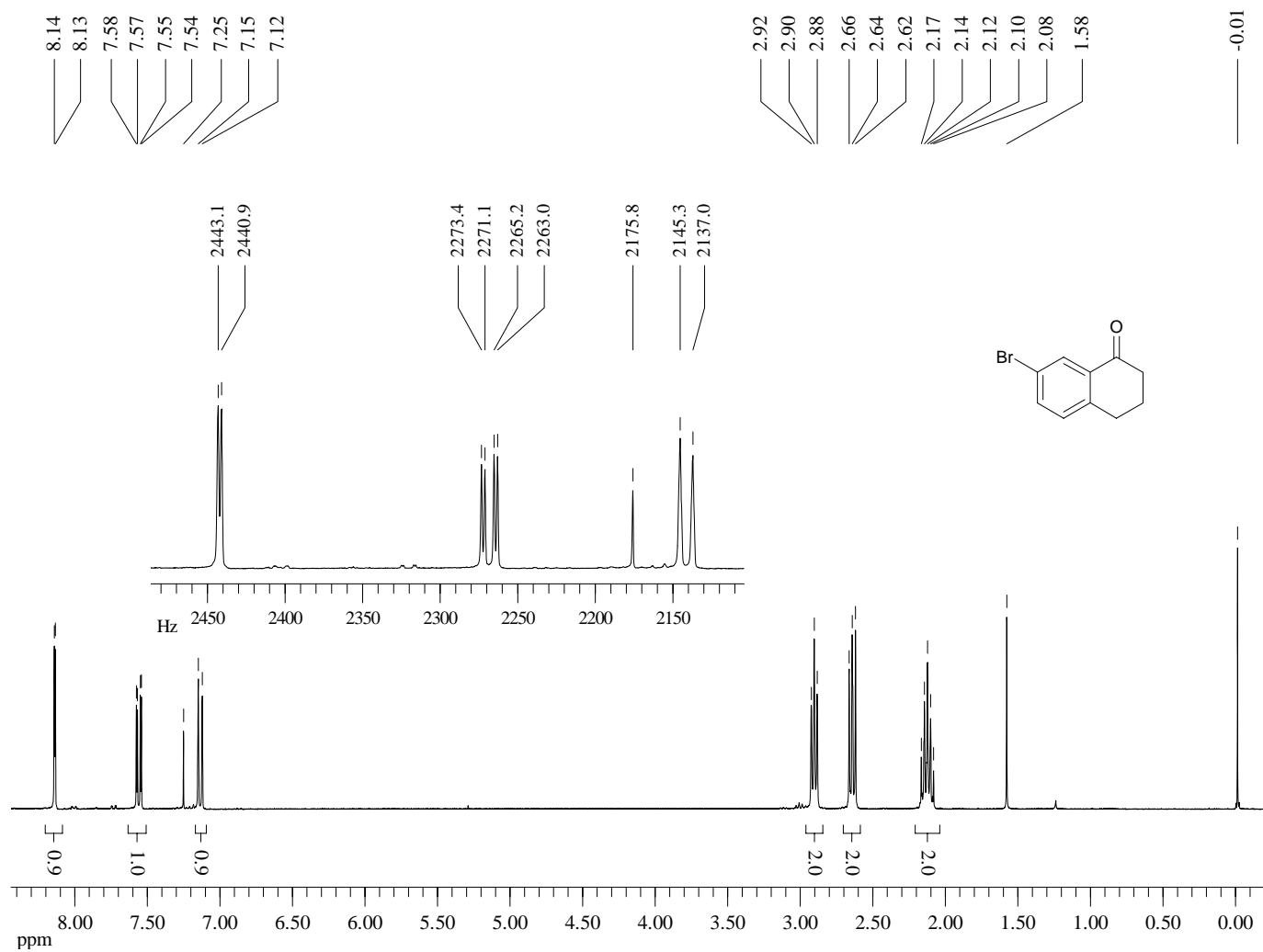
¹H-NMR (300 MHz, CDCl₃) of Compound **63**



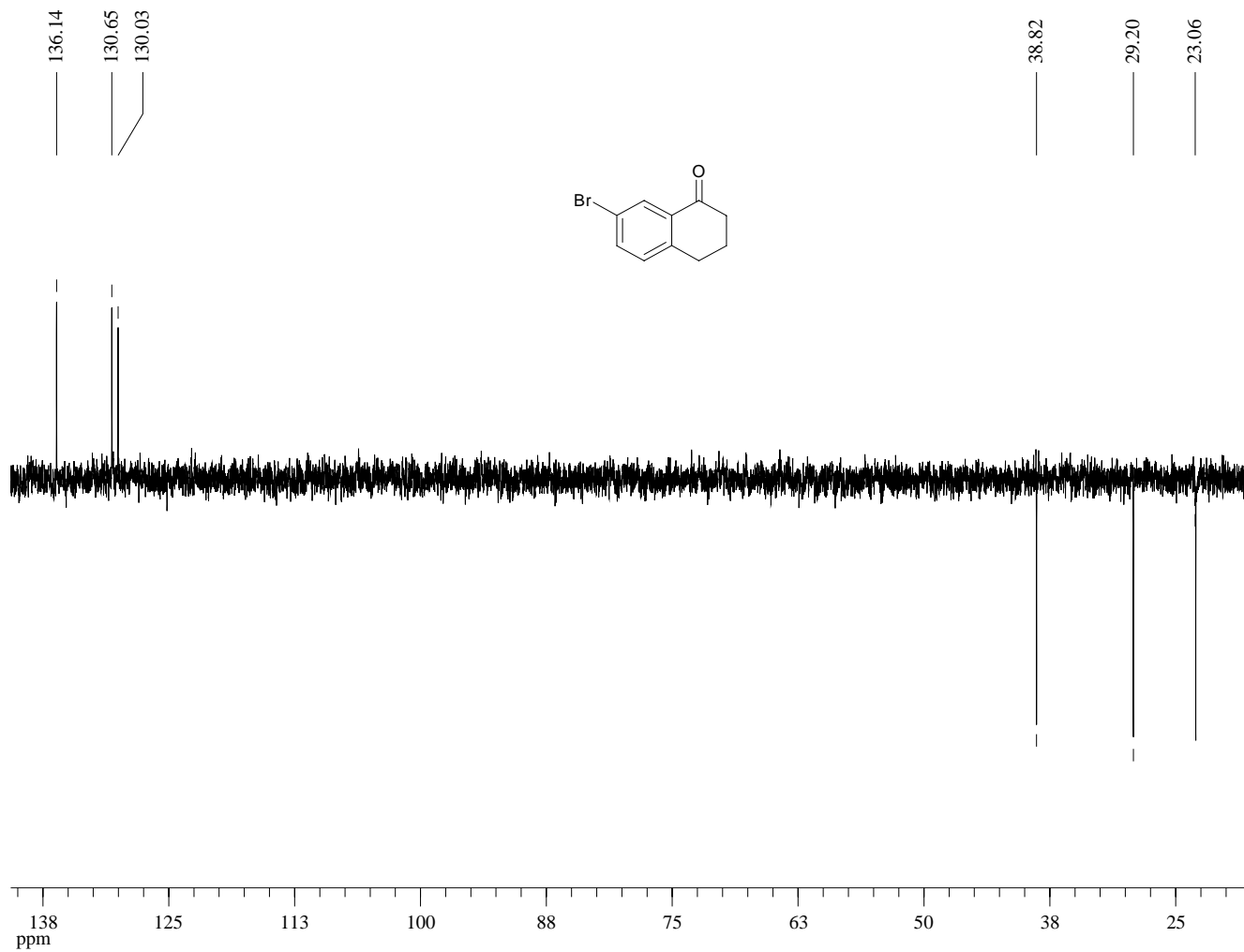
Dept 135-NMR (75 MHz, CDCl₃) of Compound **63**



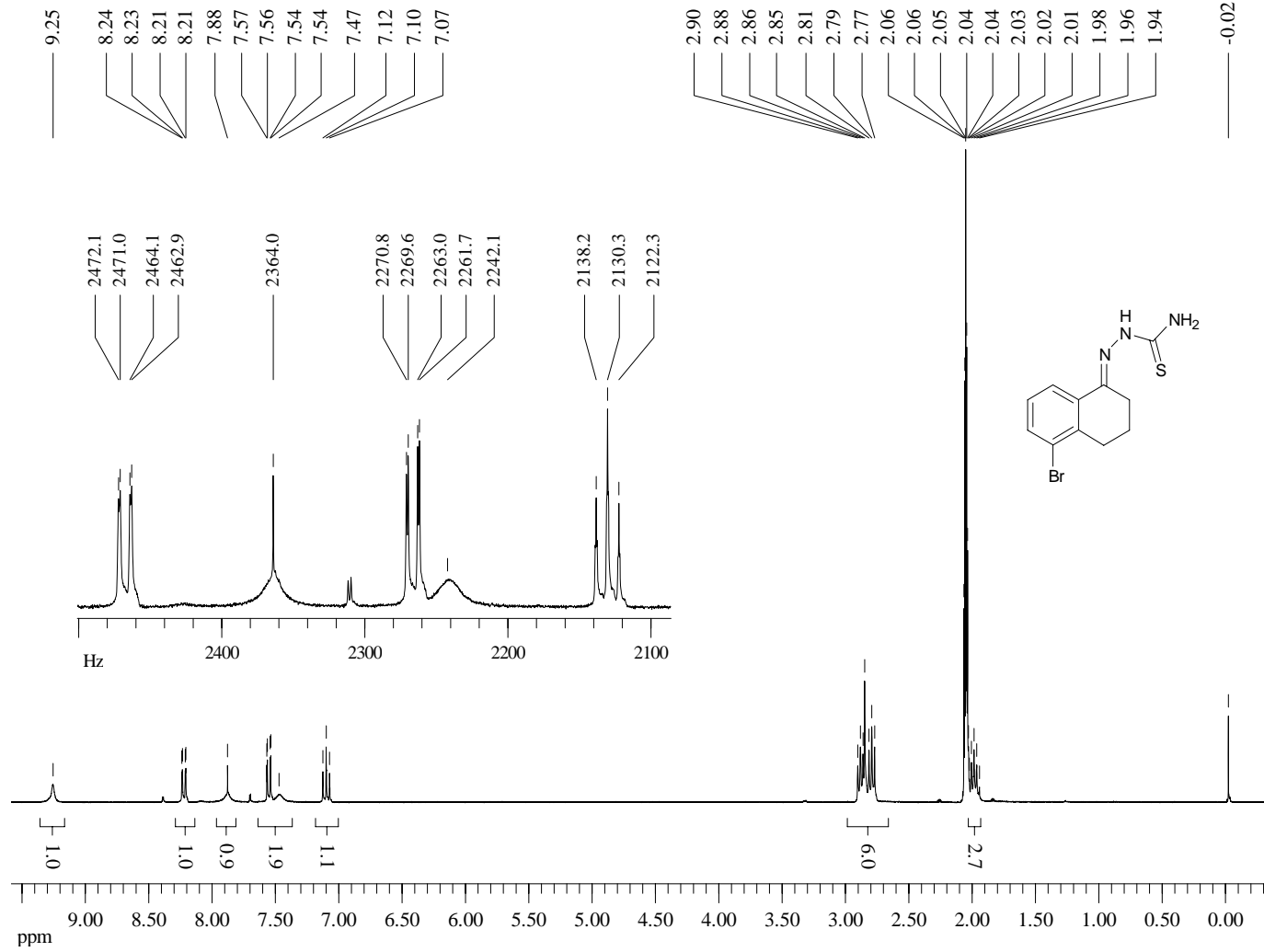
¹H-NMR (300 MHz, CDCl₃) of Compound **64**



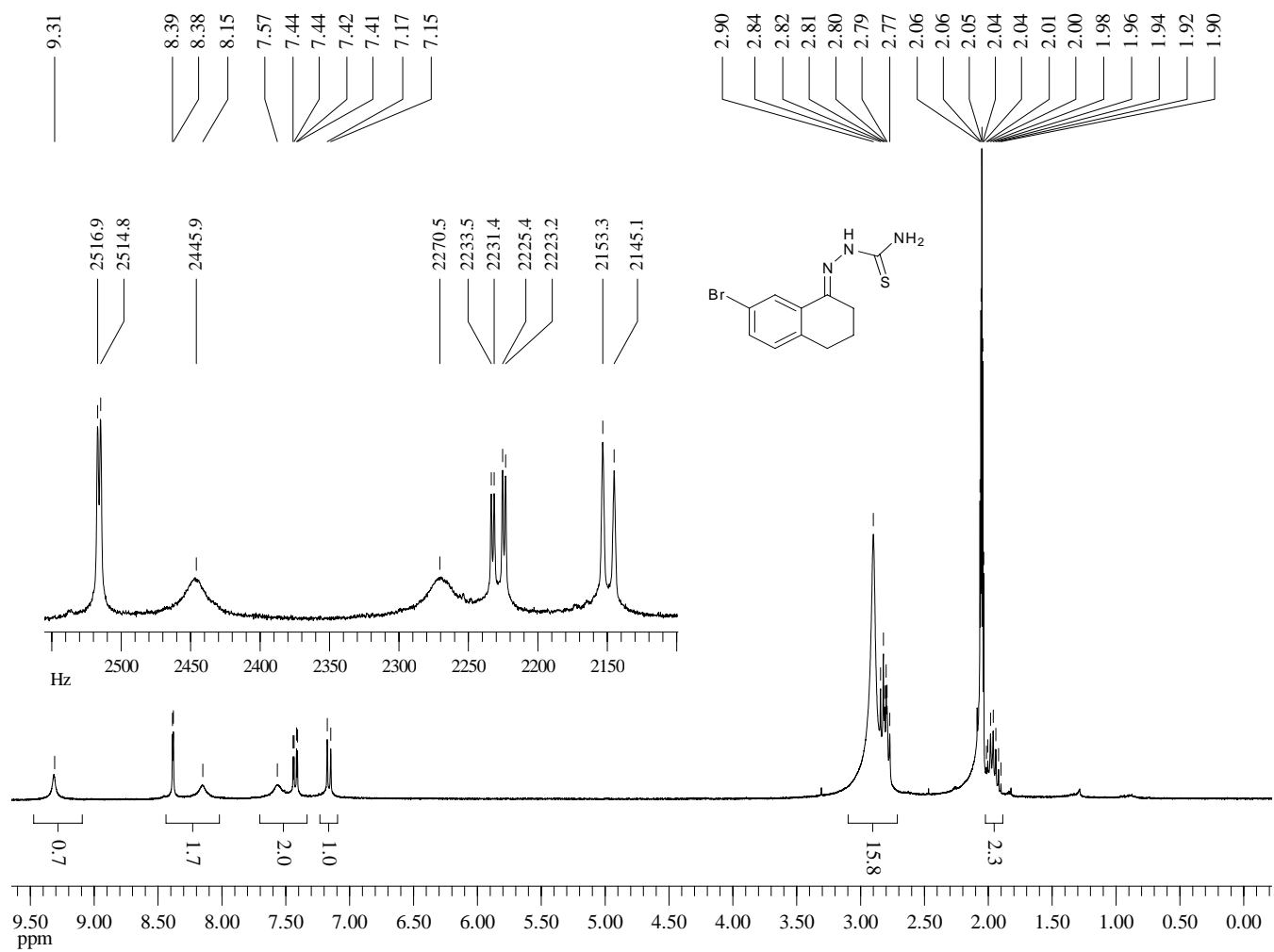
Dept 135-NMR (75 MHz, CDCl₃) of Compound **64**



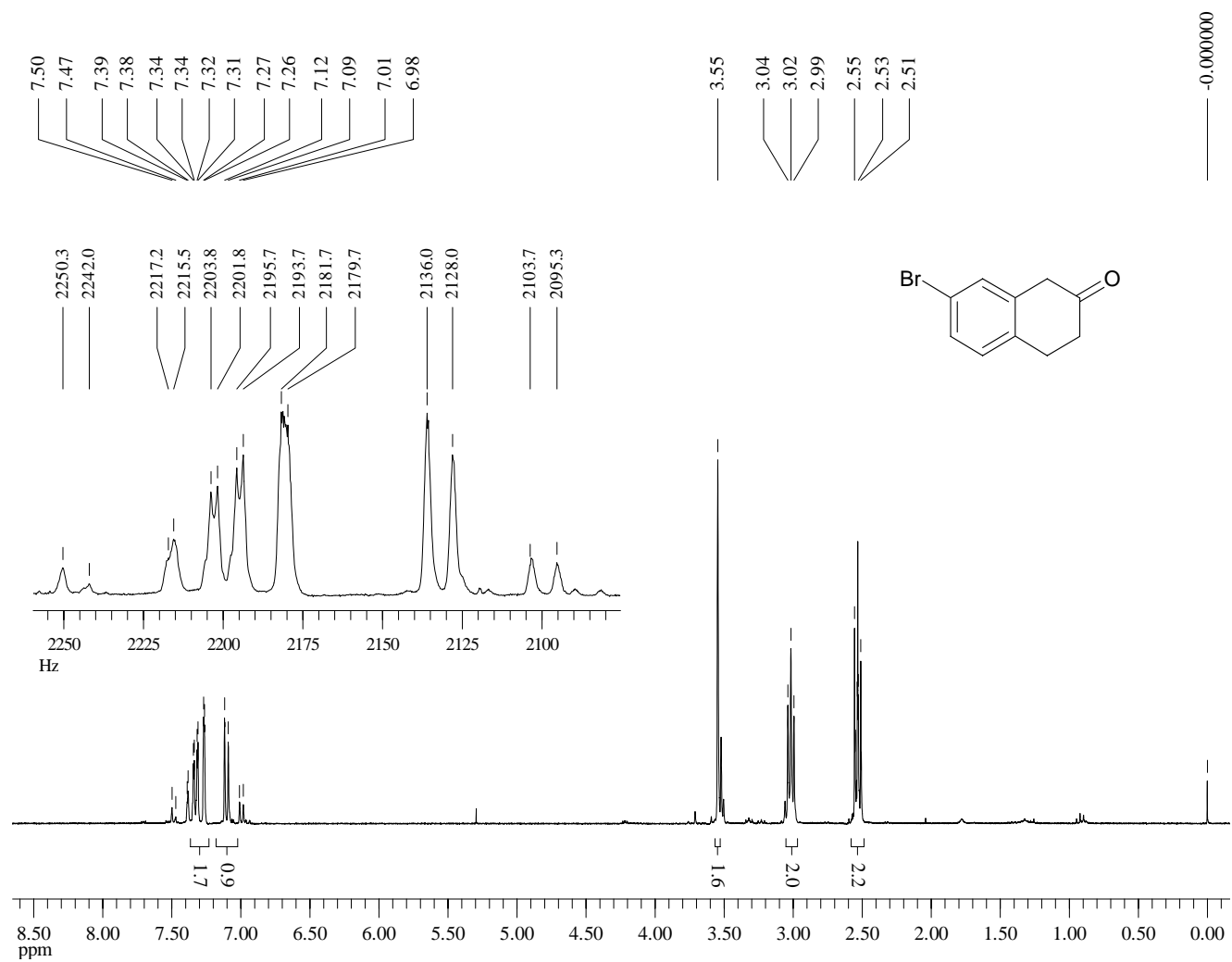
¹H-NMR (300 MHz, Acetone-d₆) of Compound **65**



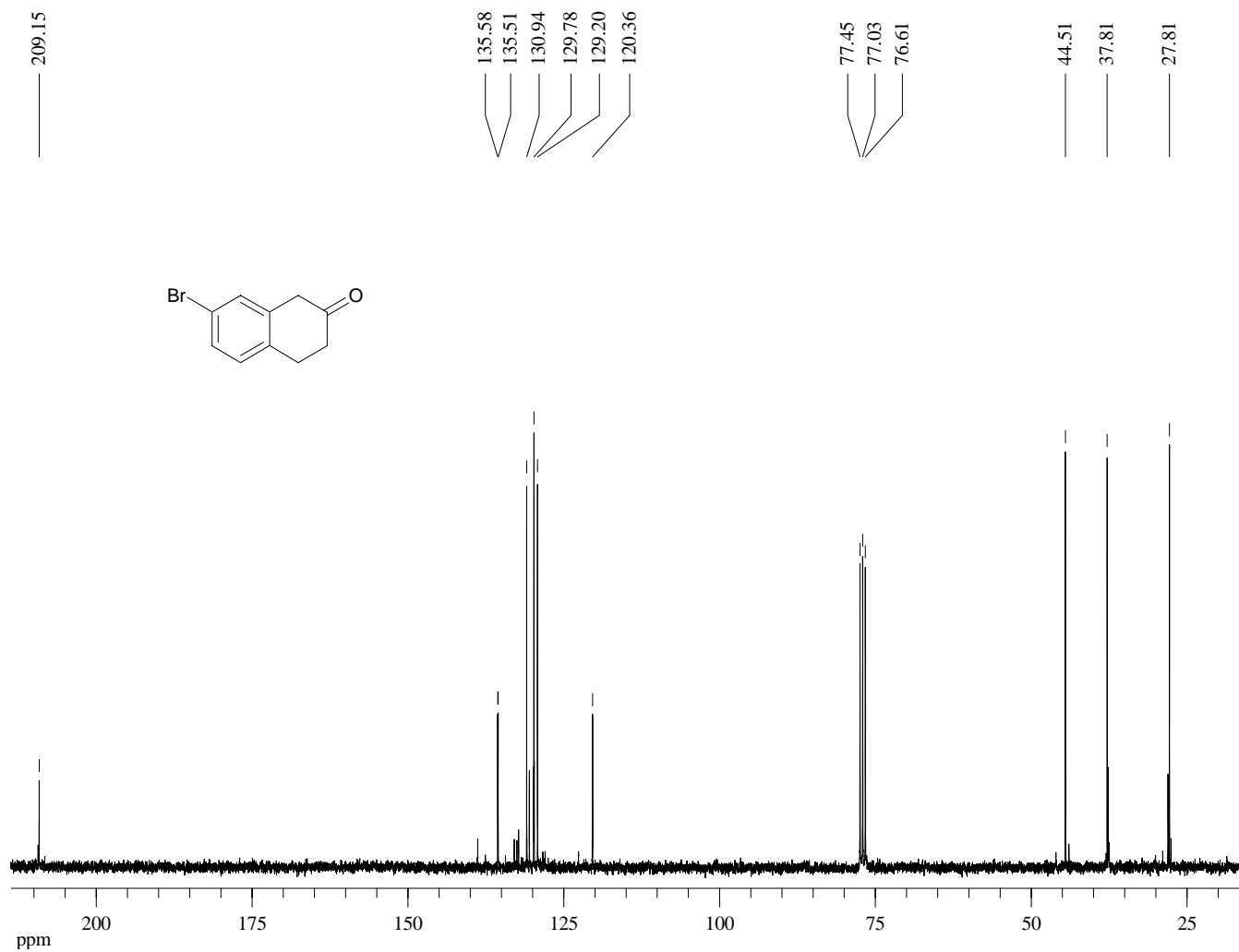
¹H-NMR (300 MHz, Acetone d₆) of Compound **66**



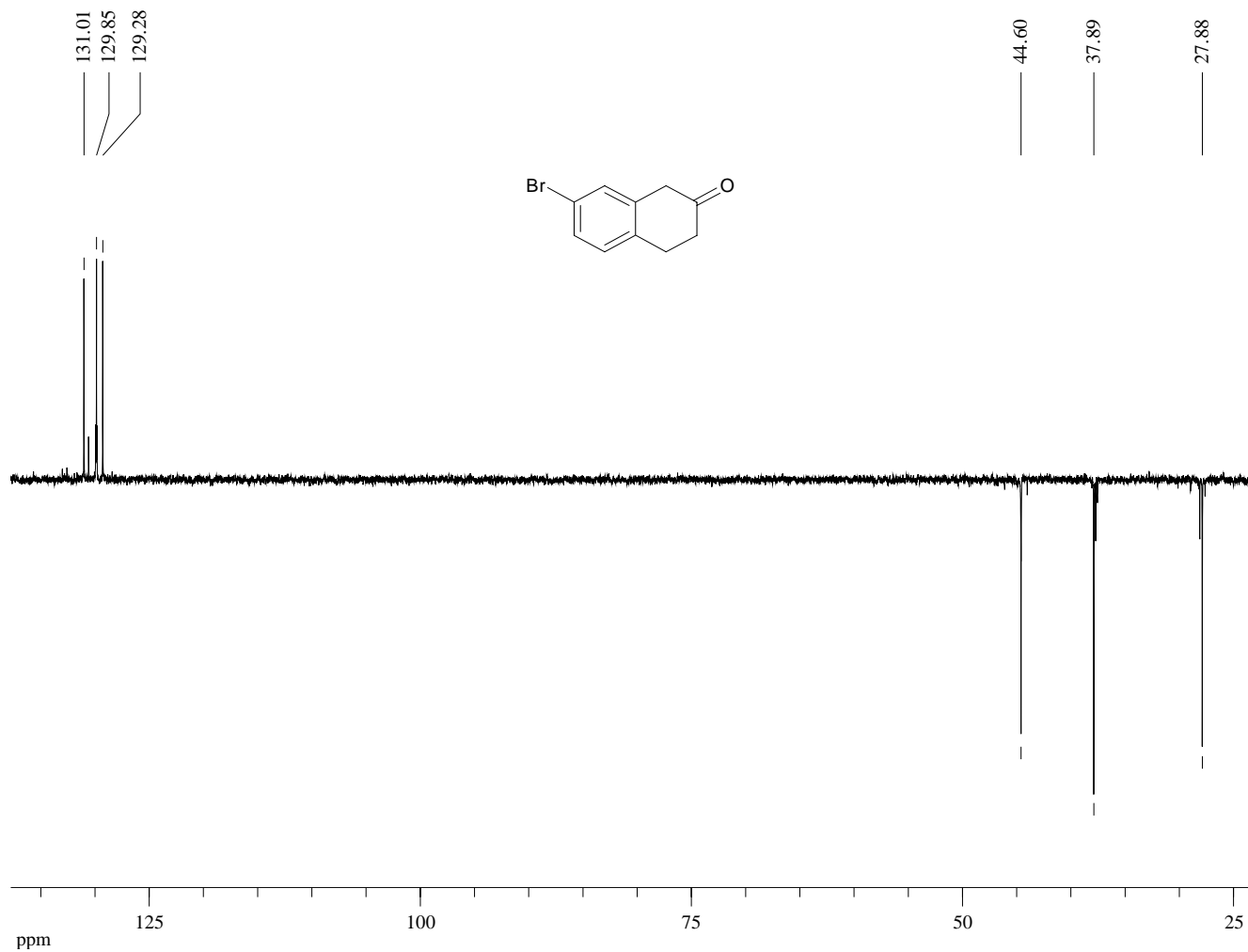
¹H-NMR (300 MHz, CDCl₃) of Compound **67**



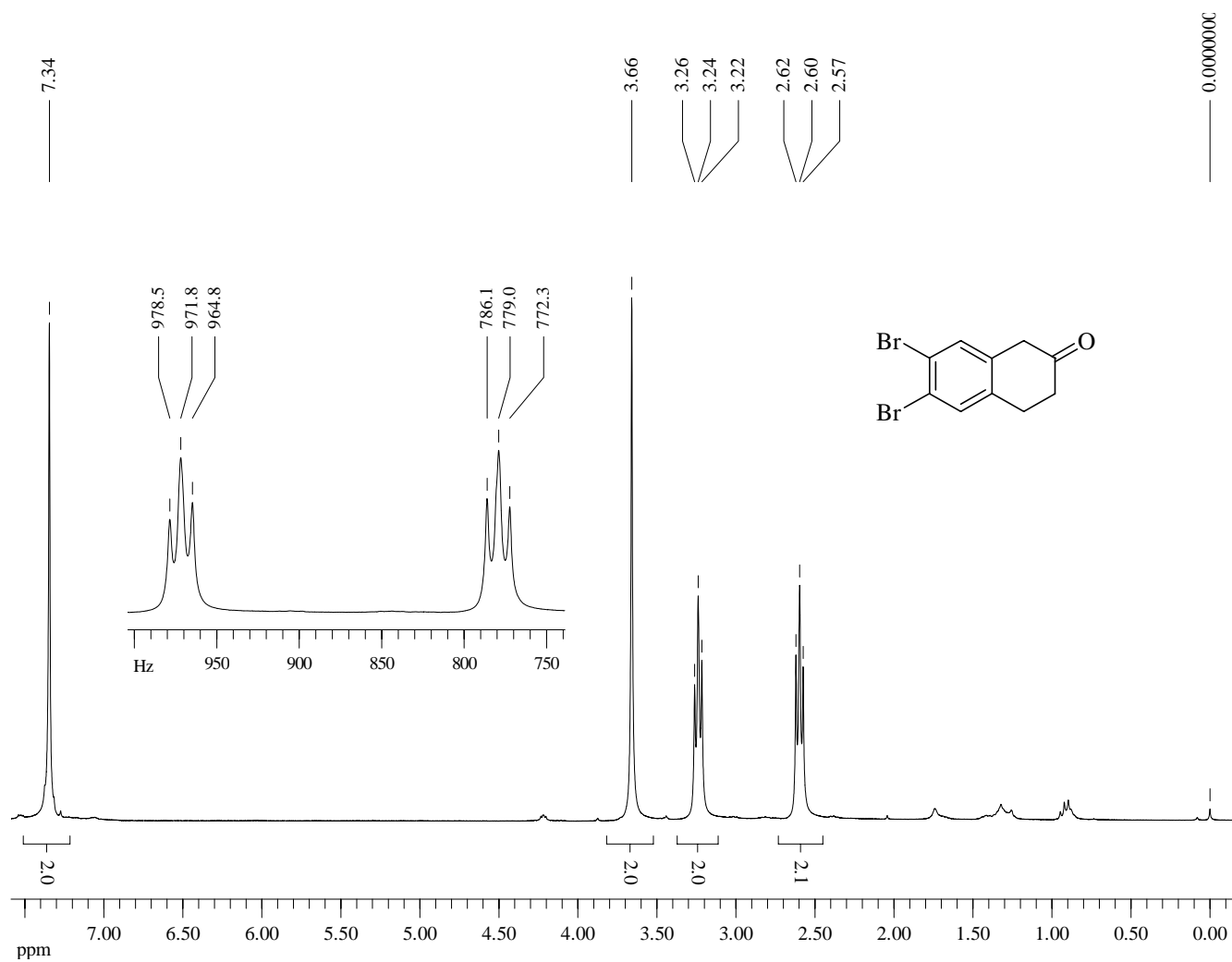
^{13}C -NMR (75 MHz, CDCl_3) of Compound **67**



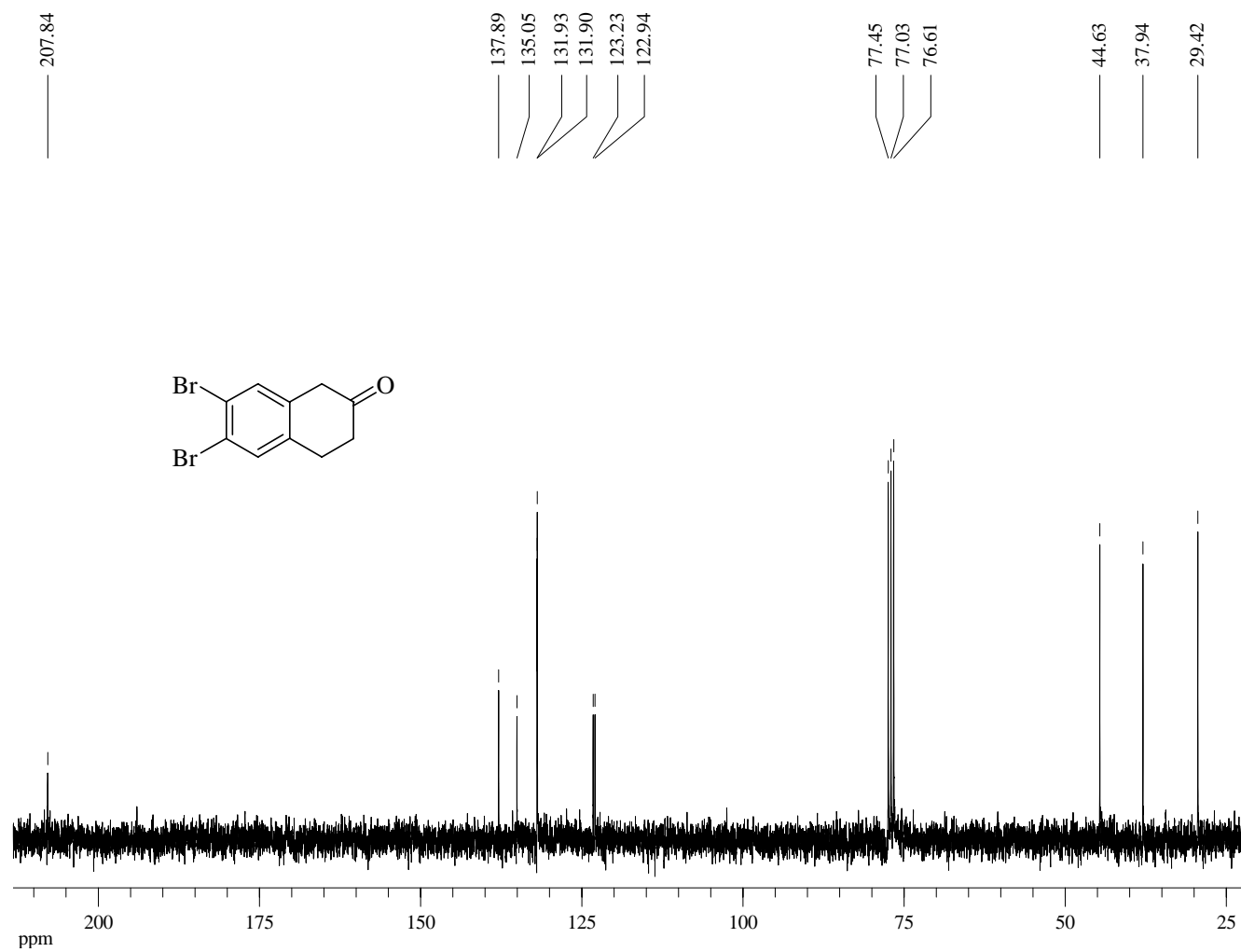
Dept 135-NMR (75 MHz, CDCl₃) of Compound **67**



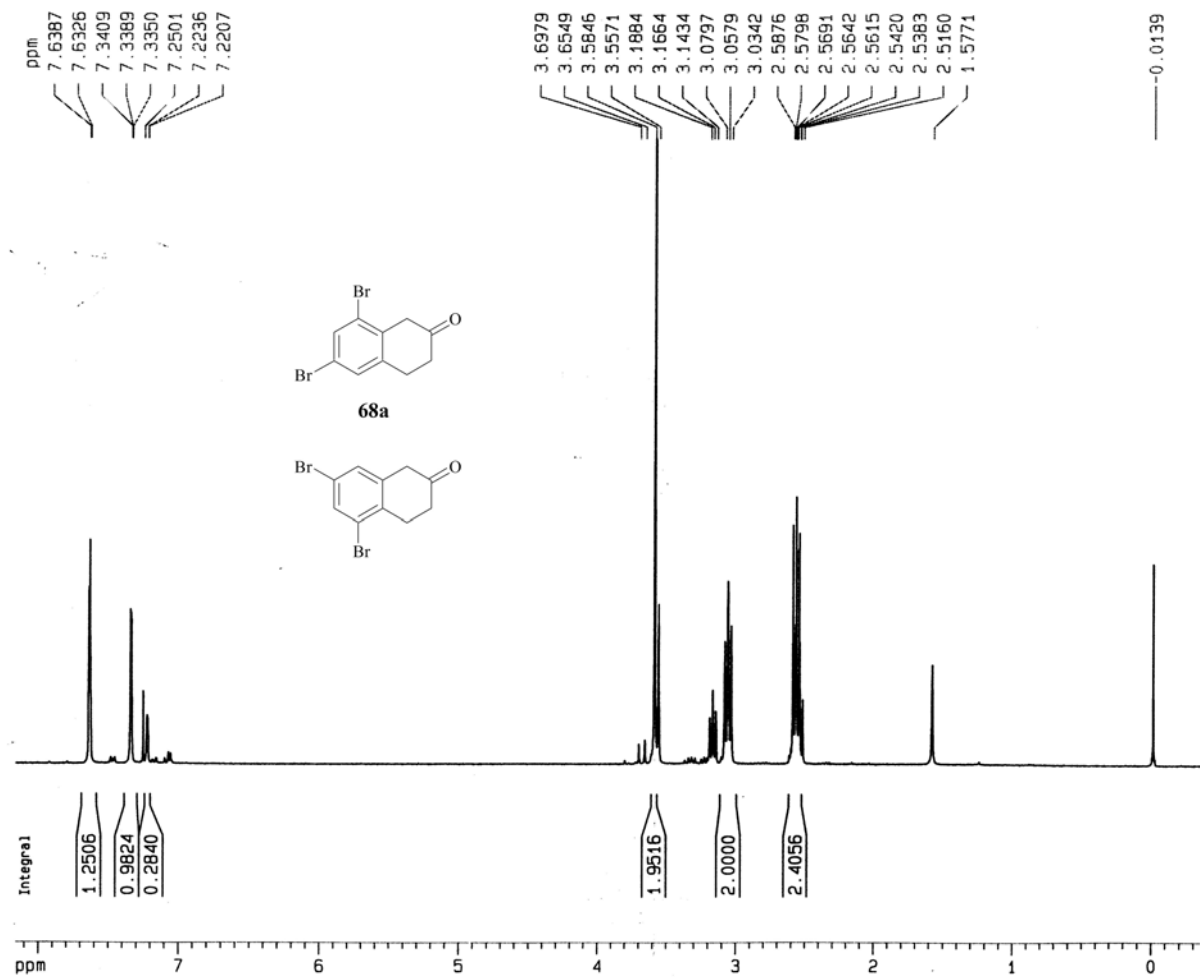
¹H-NMR (300 MHz, CDCl₃) of Compound **68**



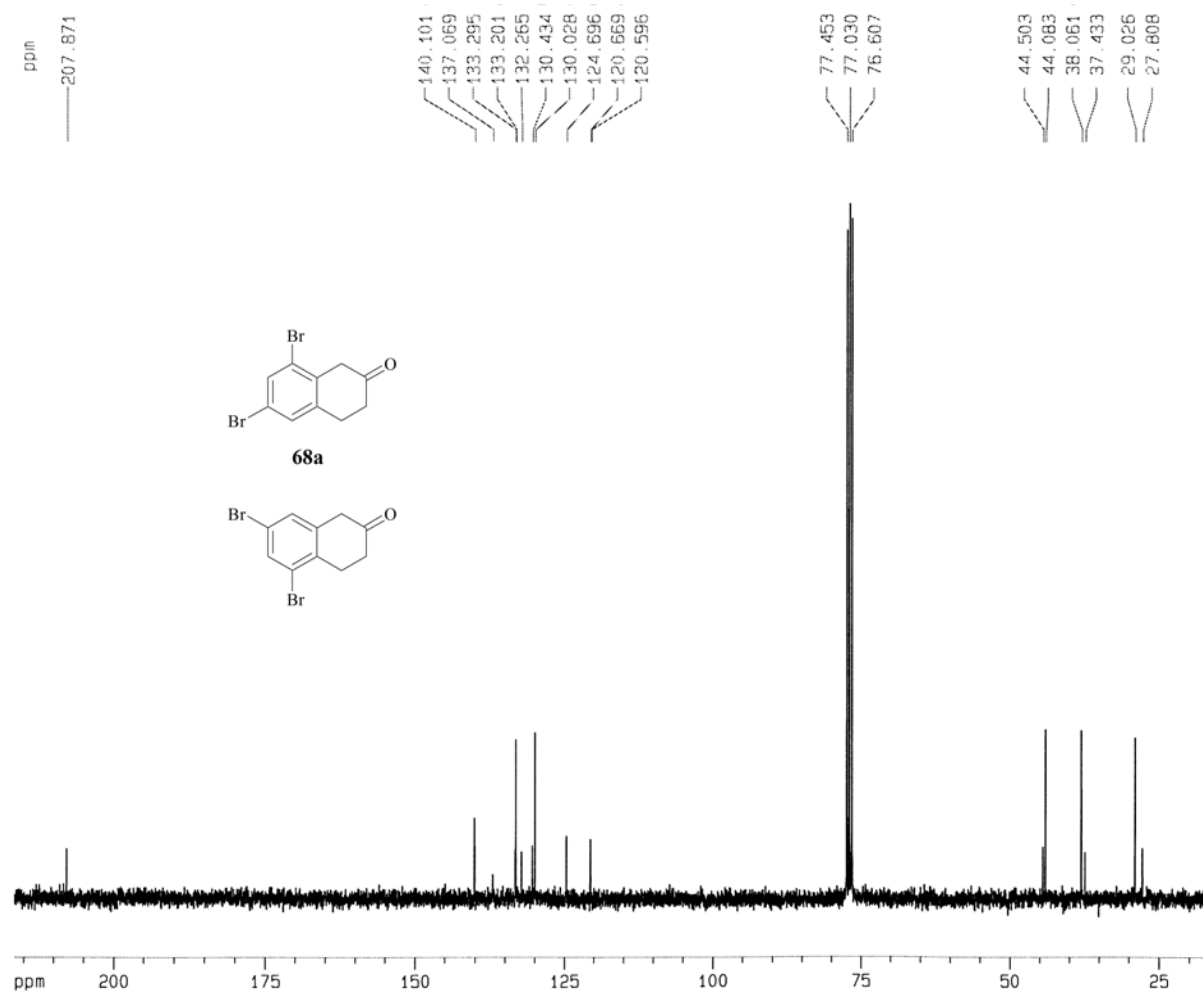
¹³C-NMR (75 MHz, CDCl₃) of Compound **68**



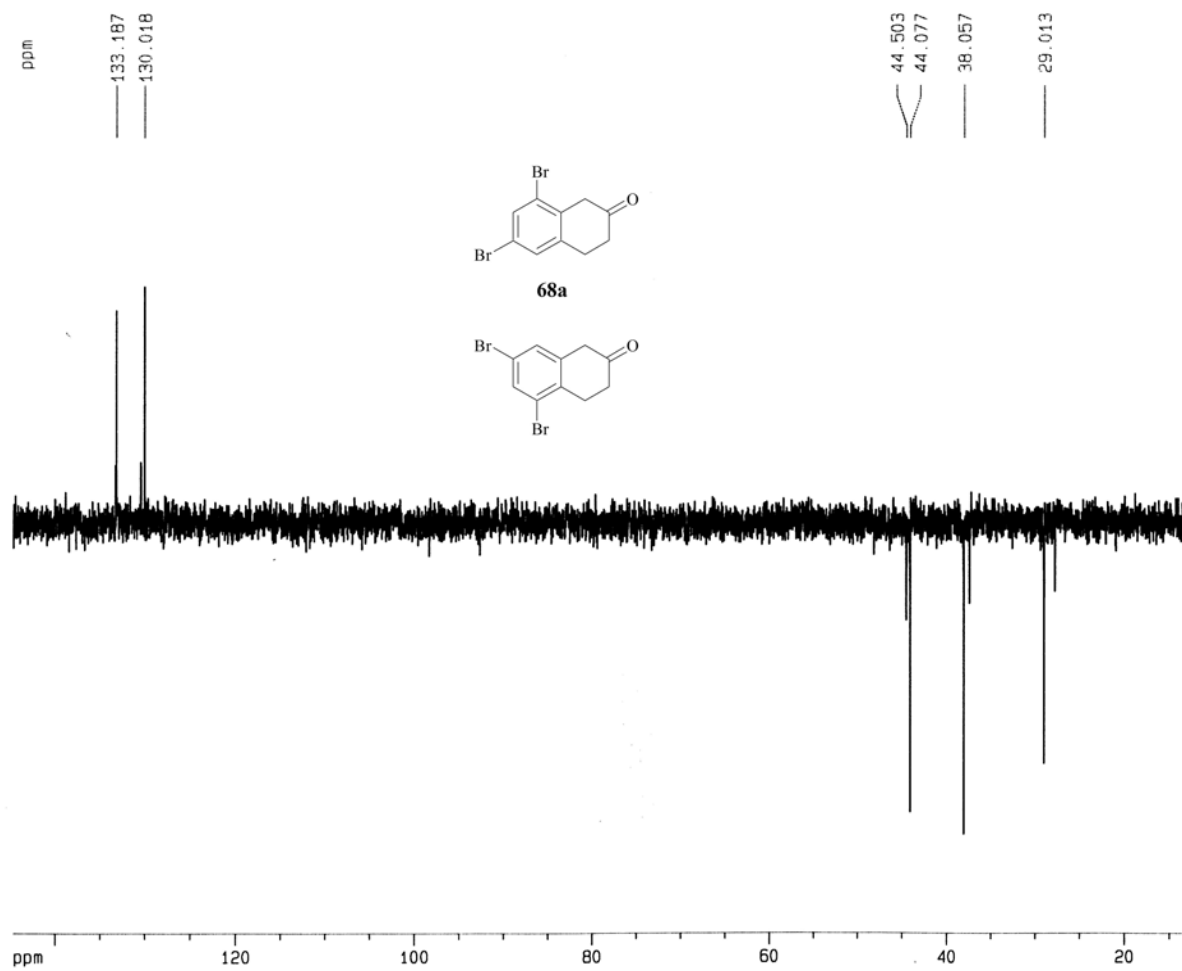
¹H-NMR (300 MHz, CDCl₃) of Compound **68a**



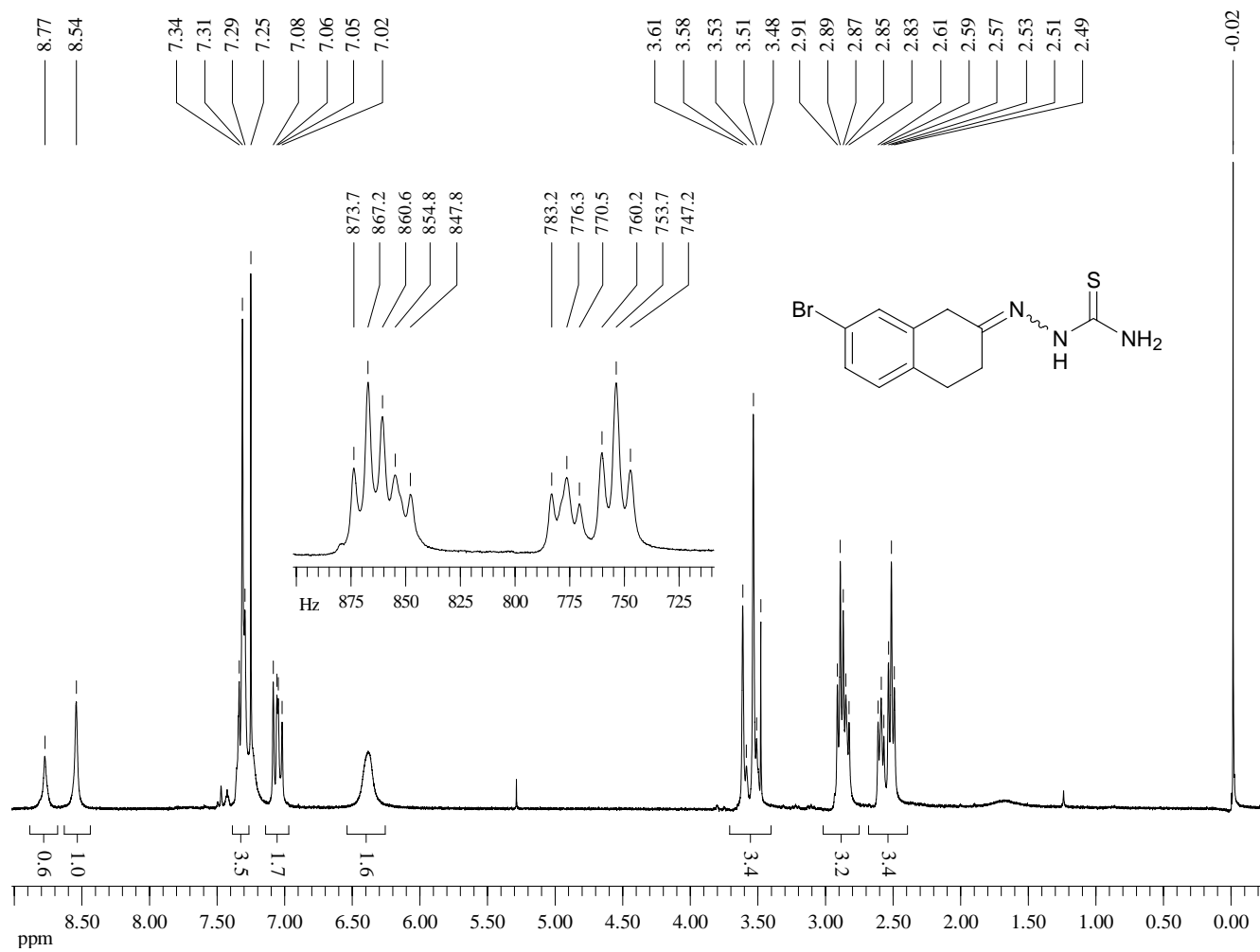
¹³C-NMR (75 MHz, CDCl₃) of Compound **68a**



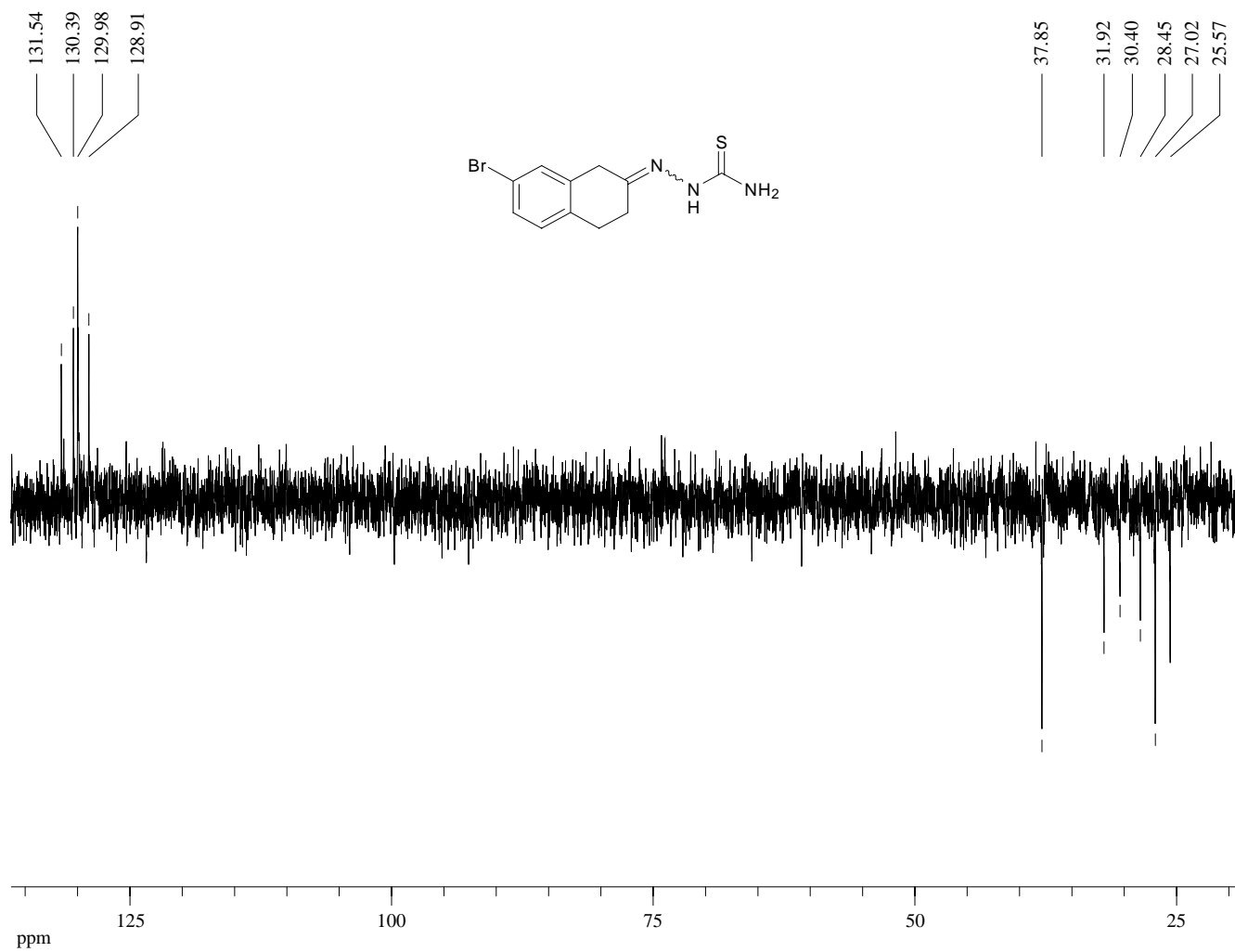
Dept 135-NMR (75 MHz, CDCl₃) of Compound **68a**



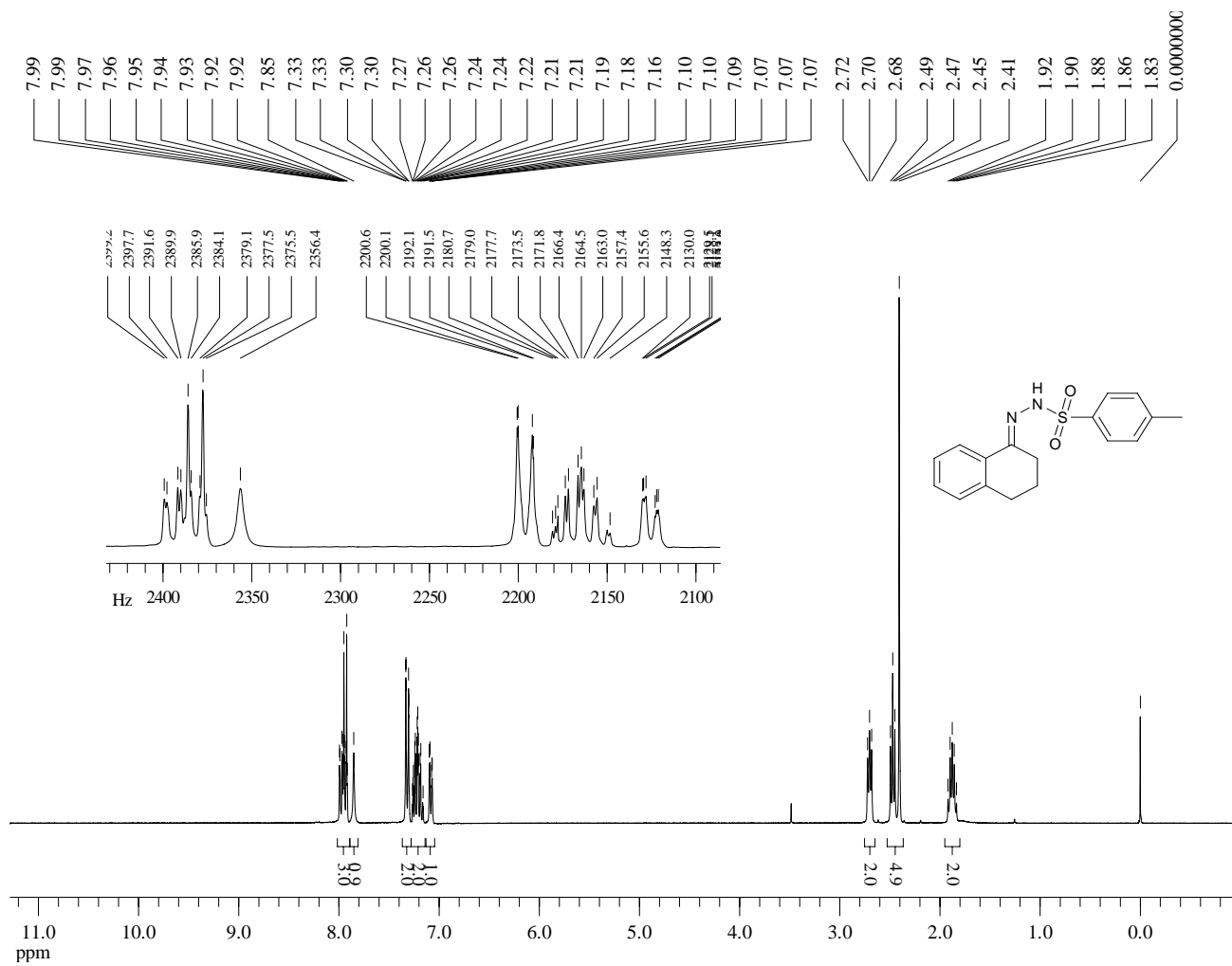
¹H-NMR (300 MHz, CDCl₃) of Compound **69**



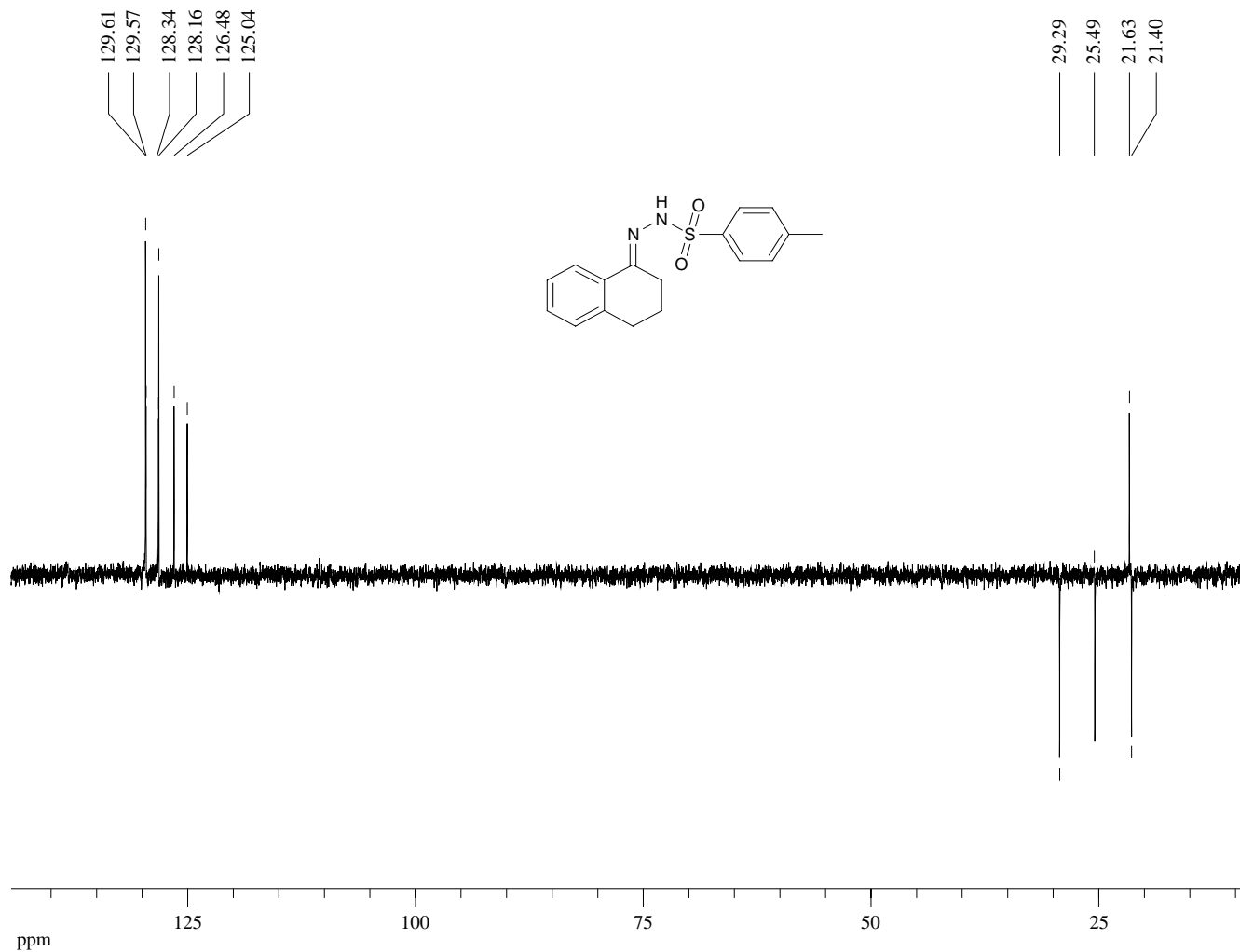
Dept 135-NMR (75 MHz, CDCl₃) of Compound **69**



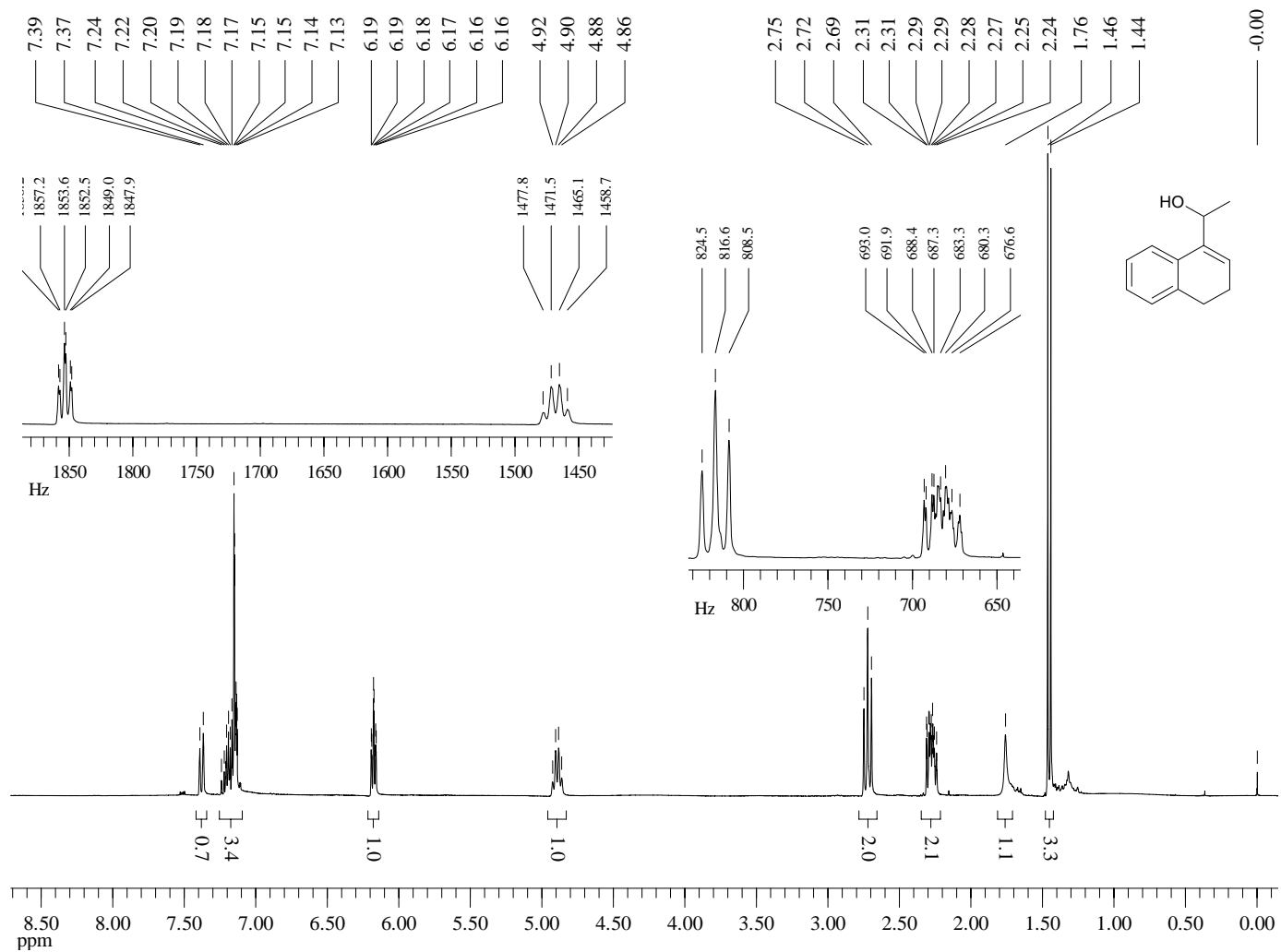
¹H-NMR (300 MHz, CDCl₃) of Compound **71**



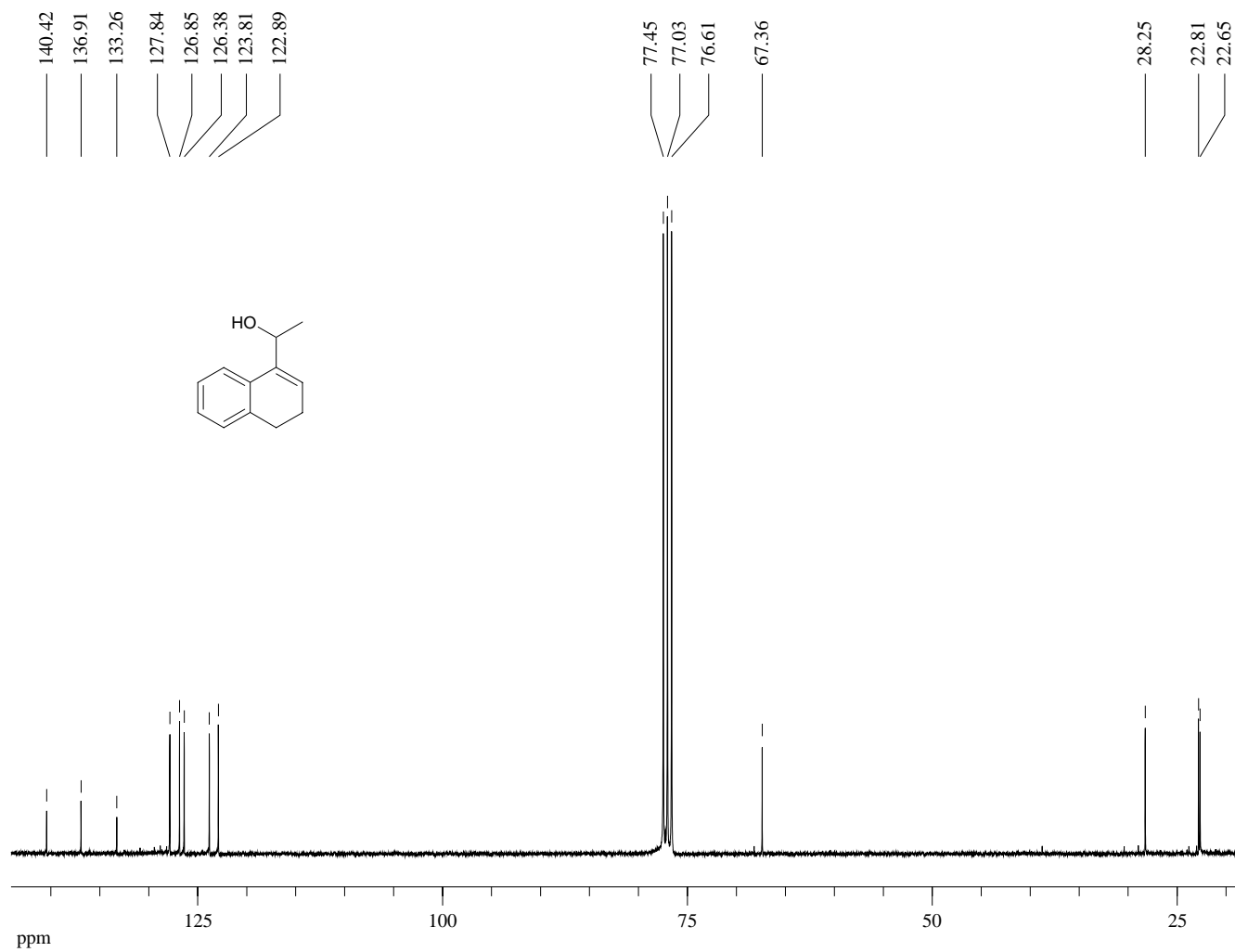
Dept 135-NMR (75 MHz, CDCl₃) of Compound **71**



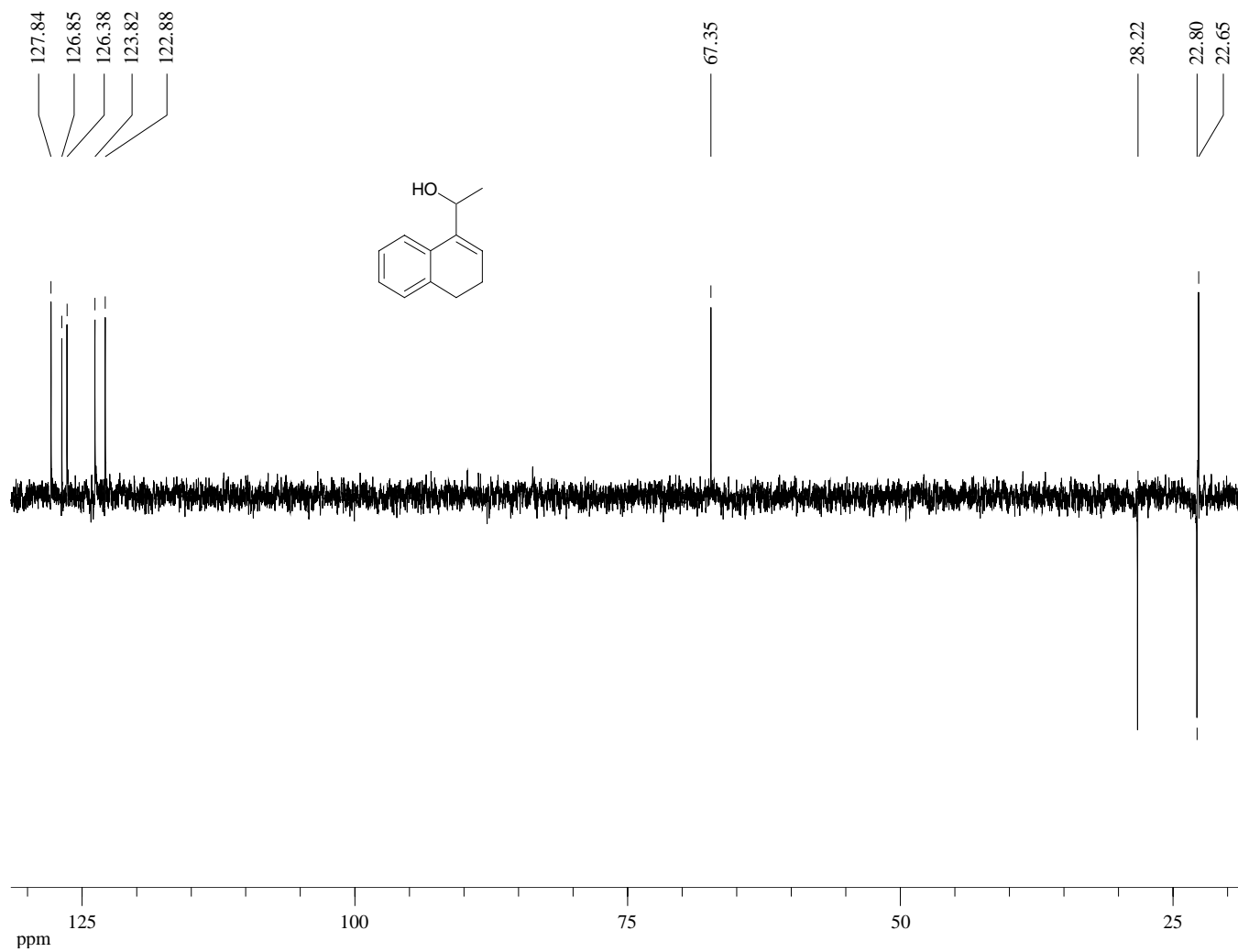
¹H-NMR (300 MHz, CDCl₃) of Compound **72a**



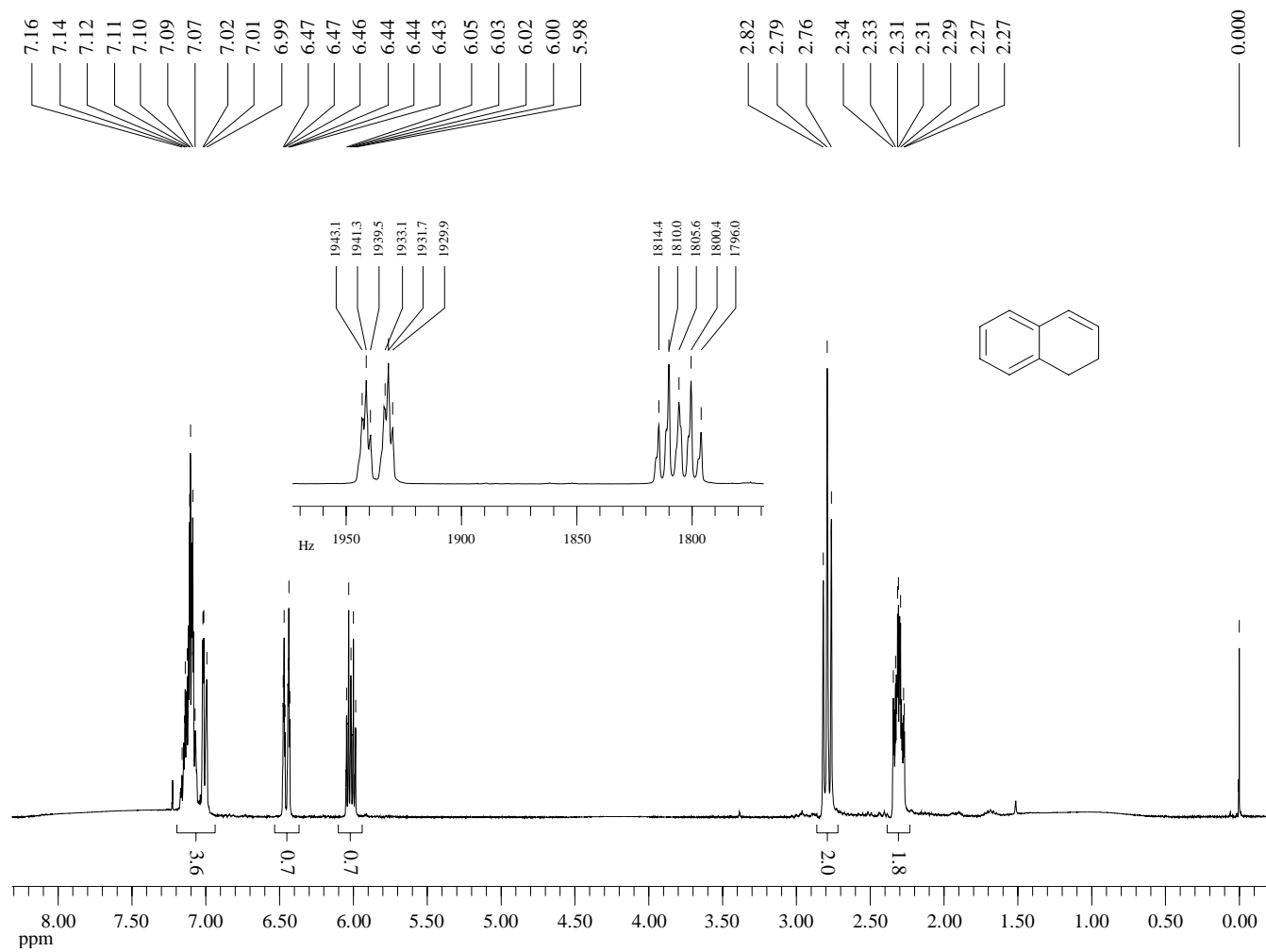
^{13}C -NMR (75 MHz, CDCl_3) of Compound **72a**



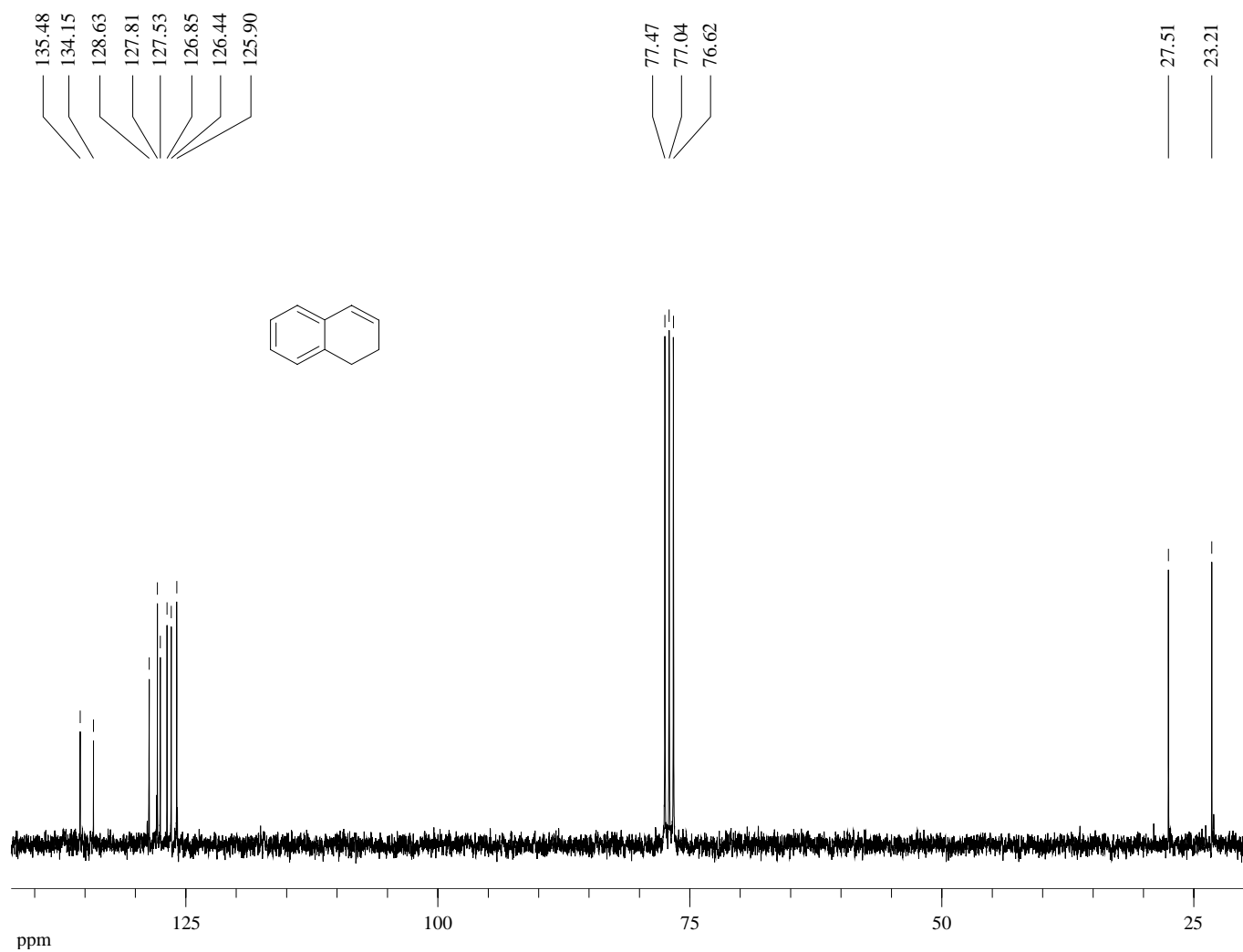
Dept 135-NMR (75 MHz, CDCl₃) of Compound **72a**



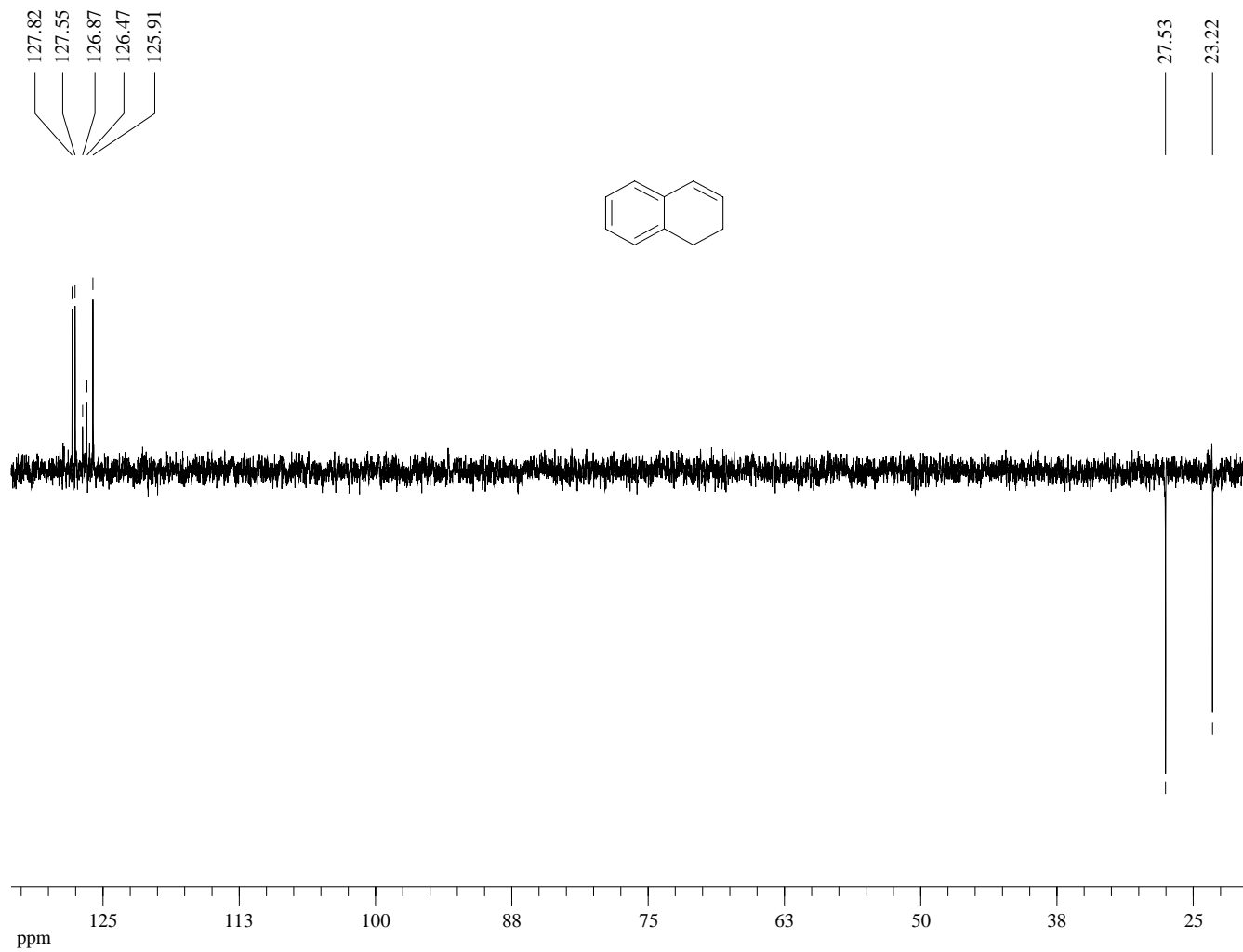
¹H-NMR (300 MHz, CDCl₃) of Compound **72b**



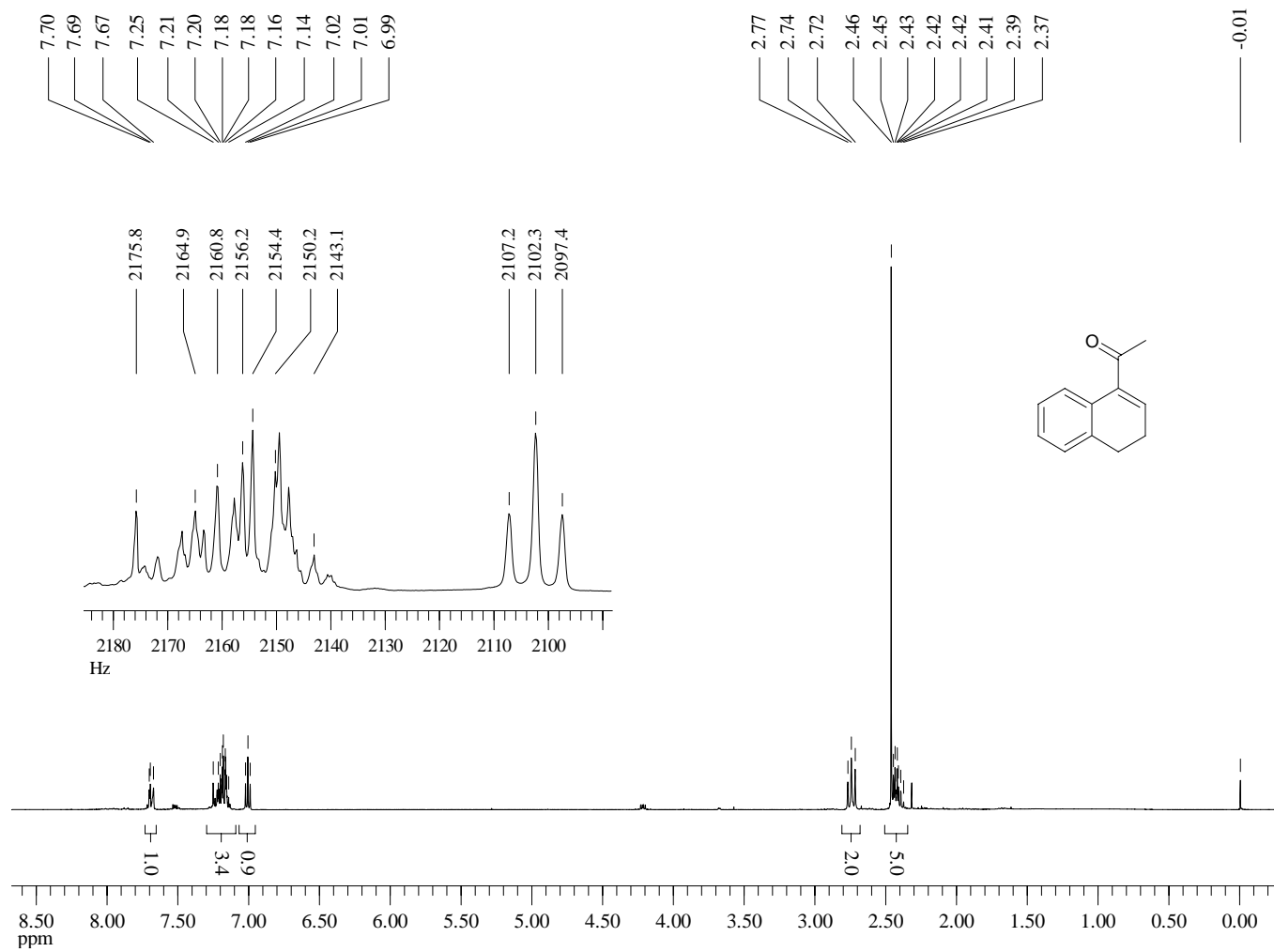
¹³C-NMR (75 MHz, CDCl₃) of Compound **72b**



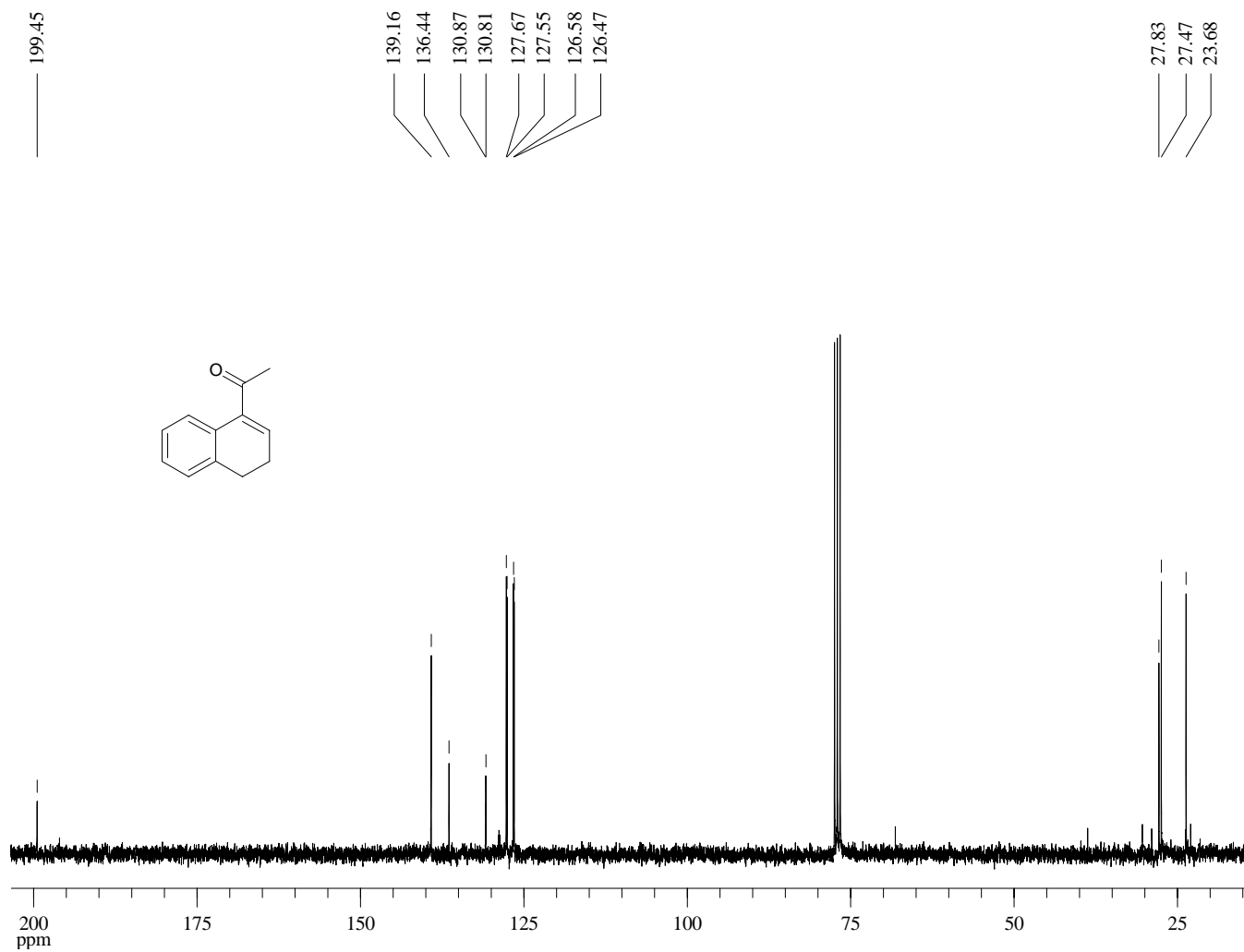
Dept 135-NMR (75 MHz, CDCl₃) of Compound **72b**



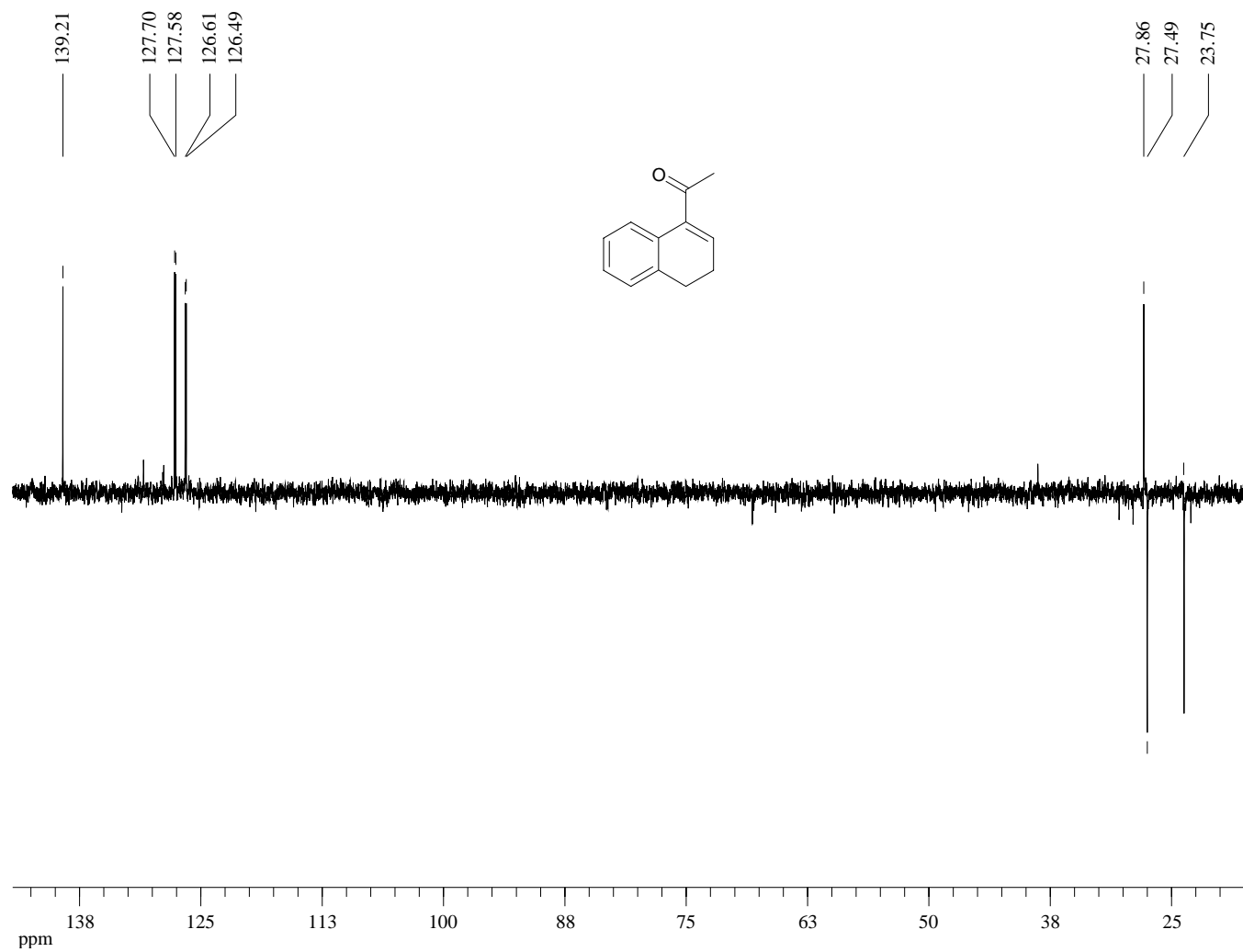
¹H-NMR (300 MHz, CDCl₃) of Compound **73**



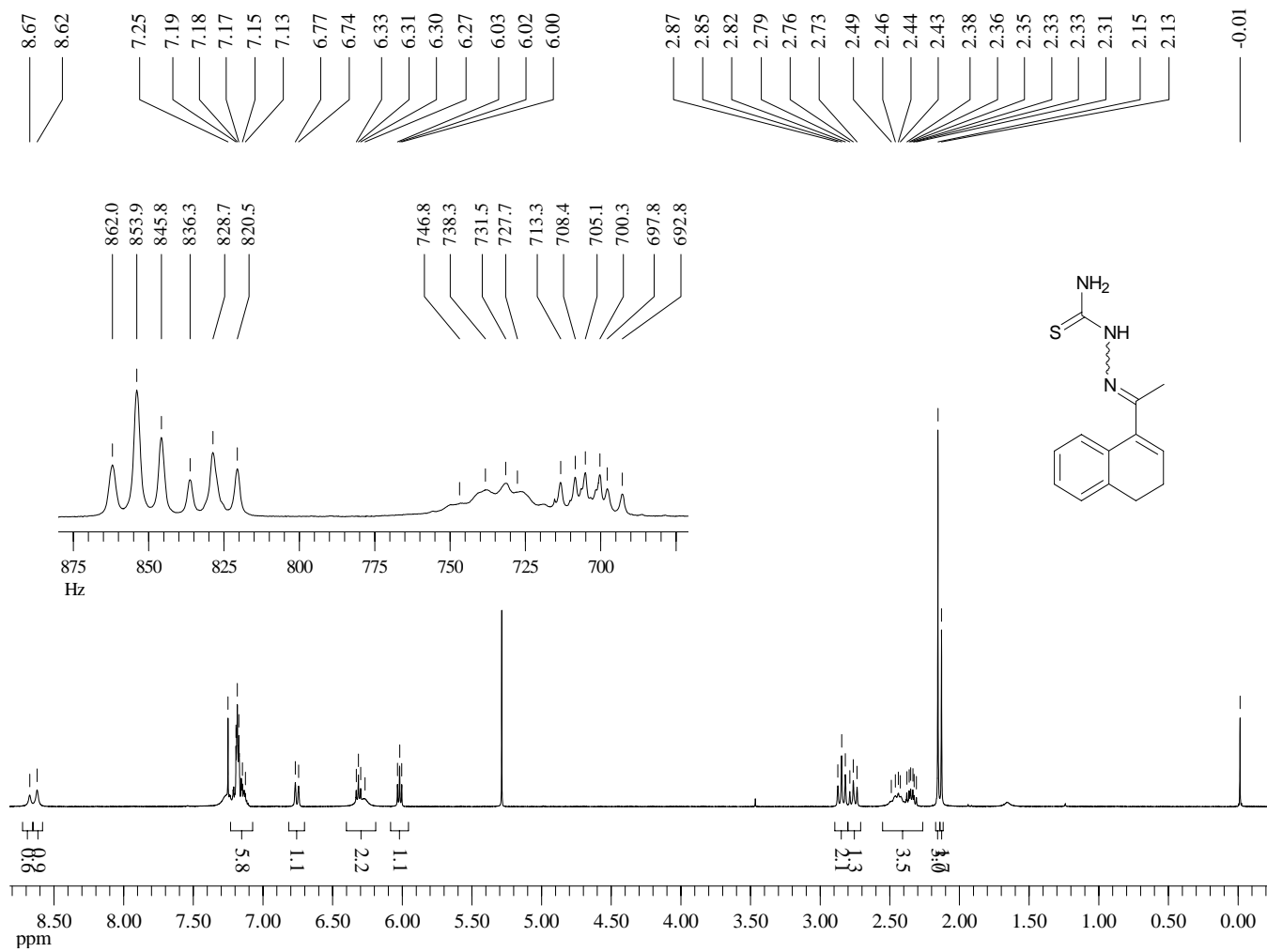
^{13}C -NMR (75 MHz, CDCl_3) of Compound **73**



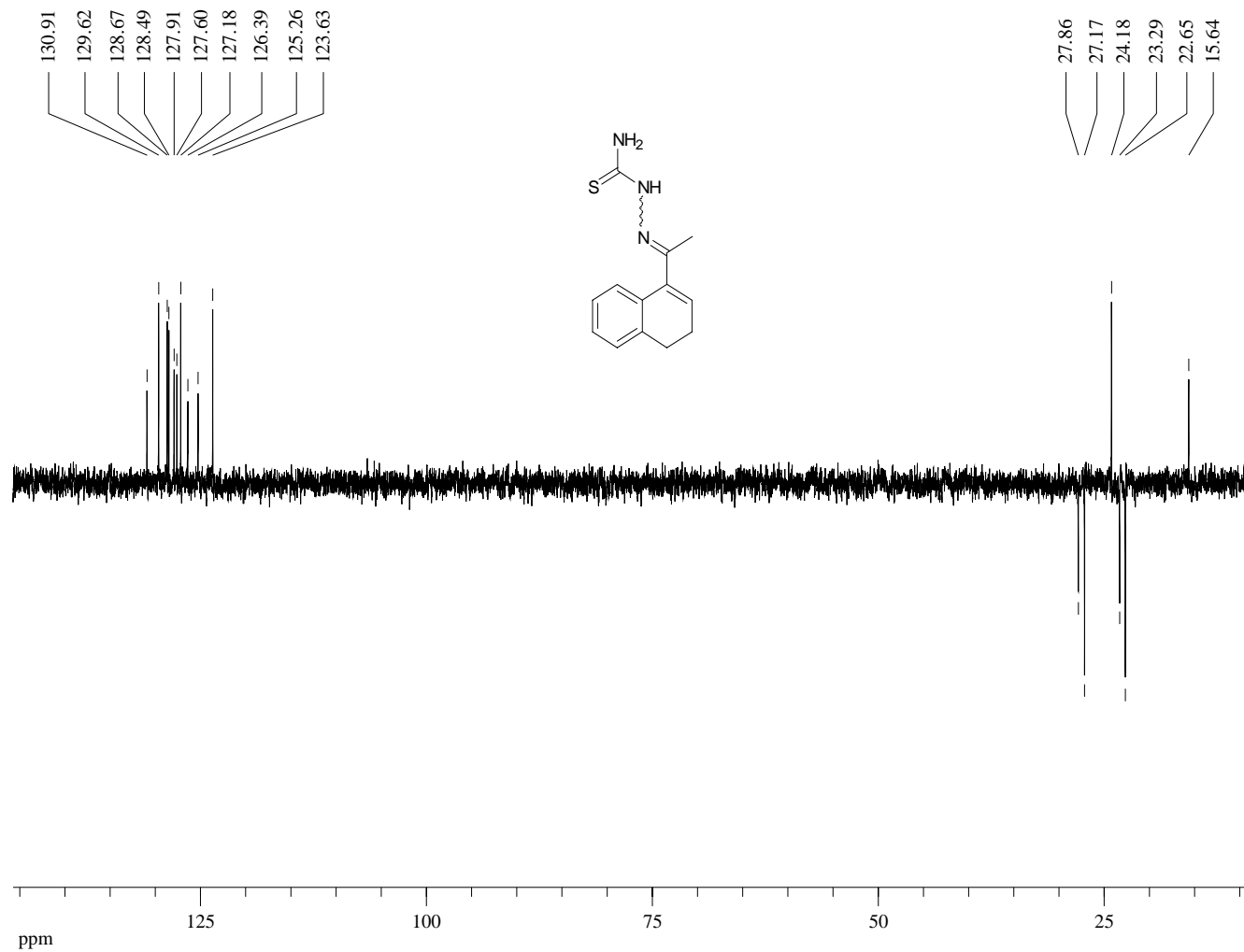
Dept 135-NMR (75 MHz, CDCl₃) of Compound **73**



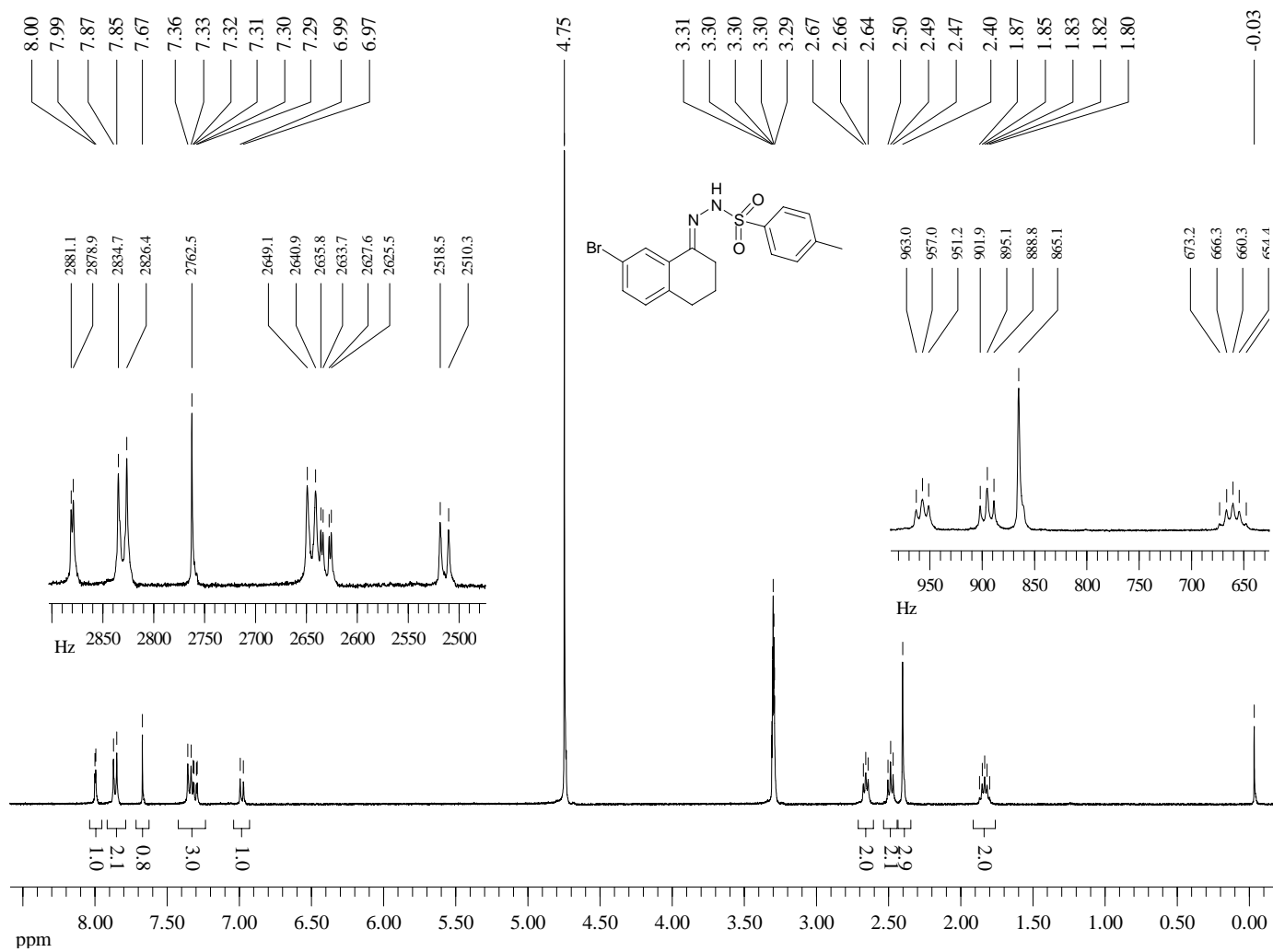
¹H-NMR (300 MHz, CDCl₃) of Compound **74**



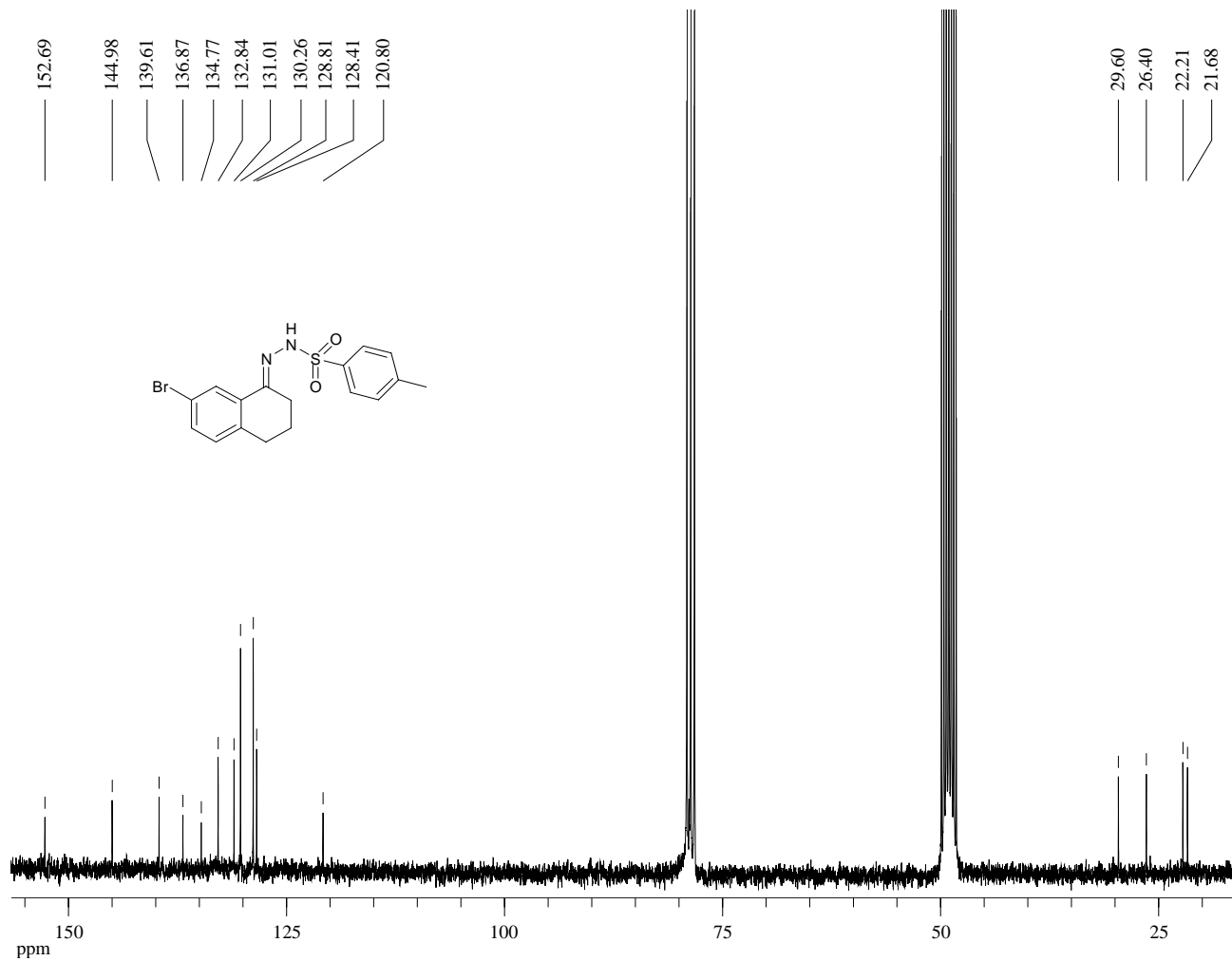
Dept 135-NMR (75 MHz, CDCl₃) of Compound **74**



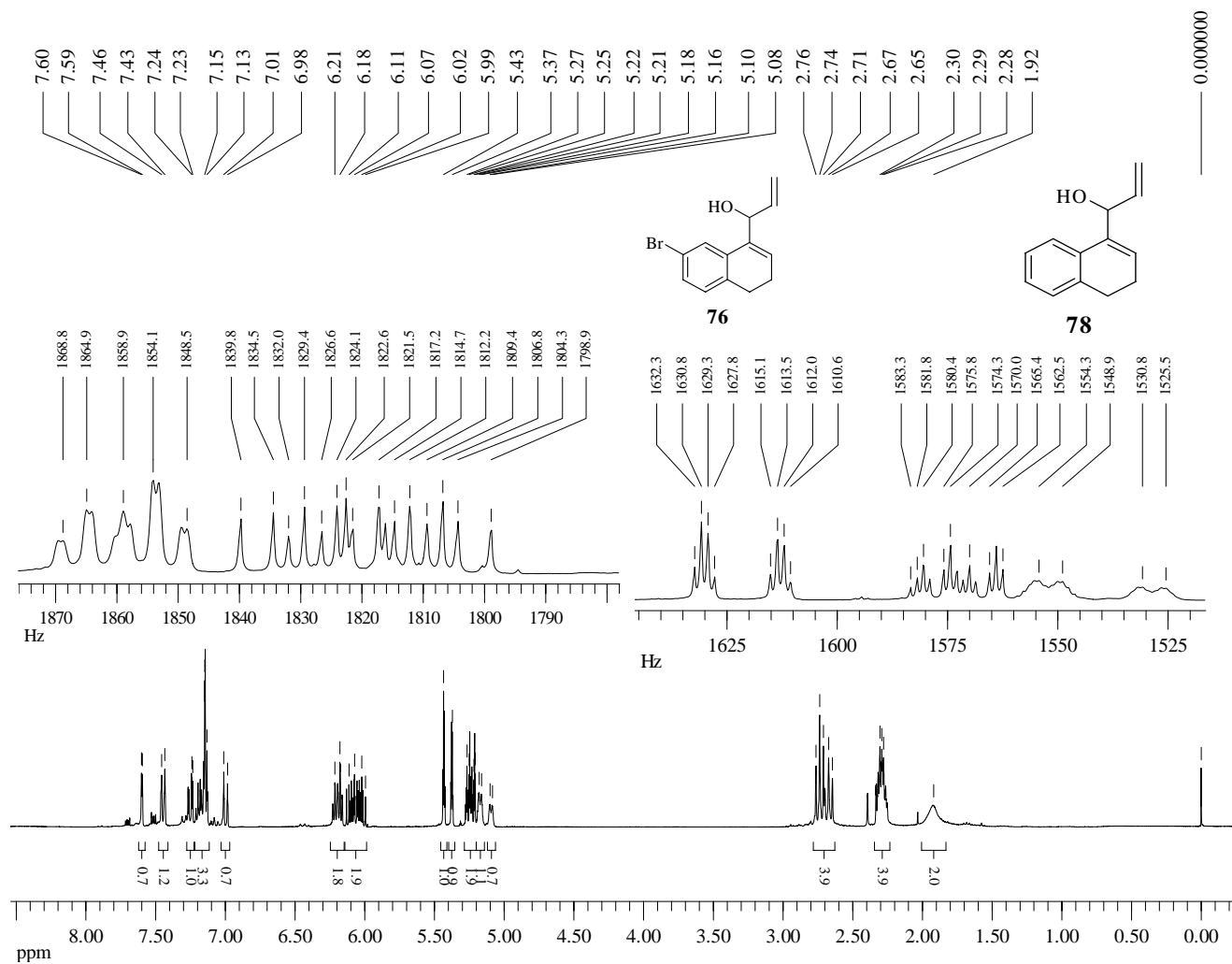
¹H-NMR (360 MHz, Methanol-d₆) of Compound **75**



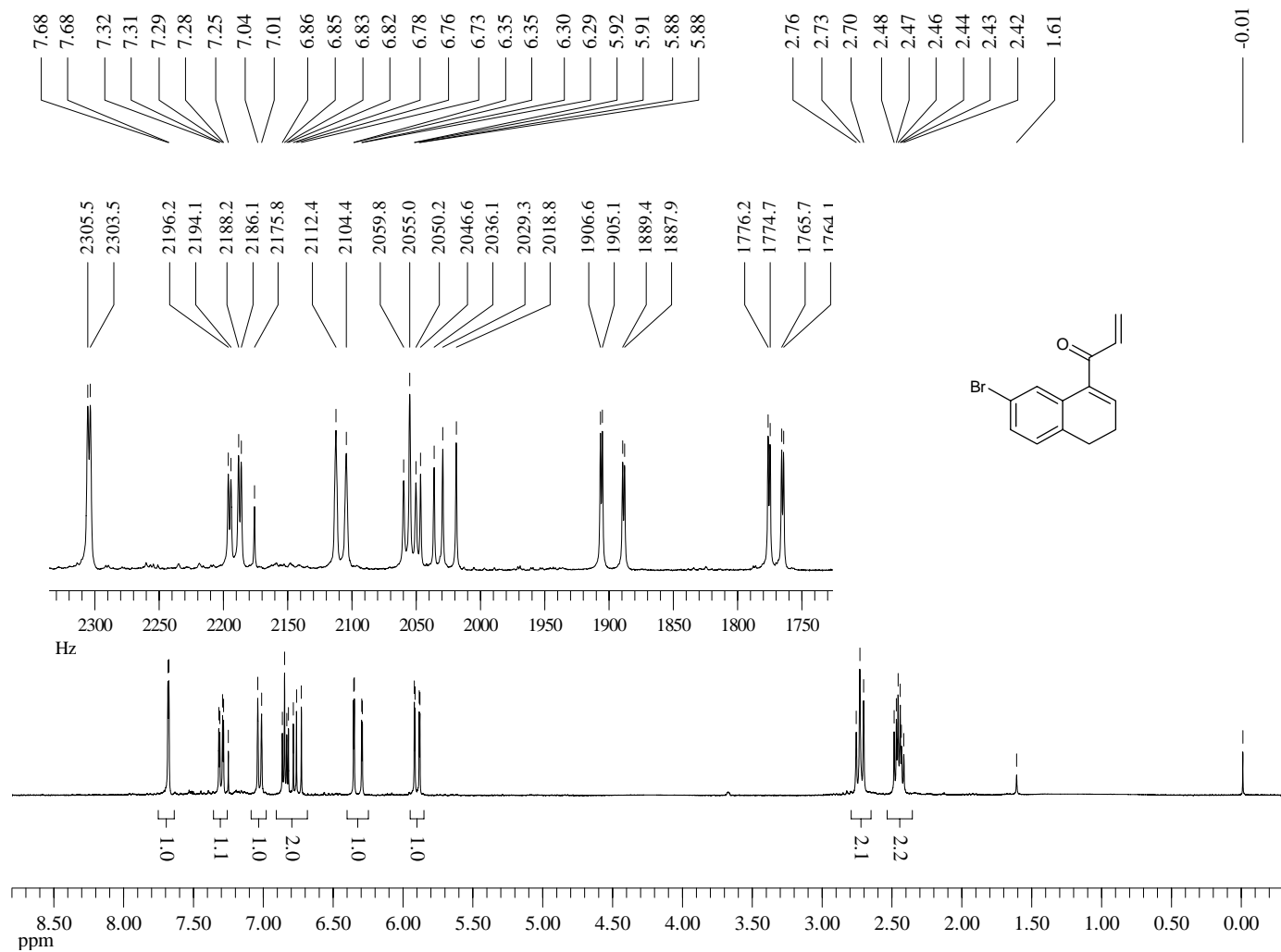
¹³C-NMR (75 MHz, Methanol-d₆) of Compound **75**



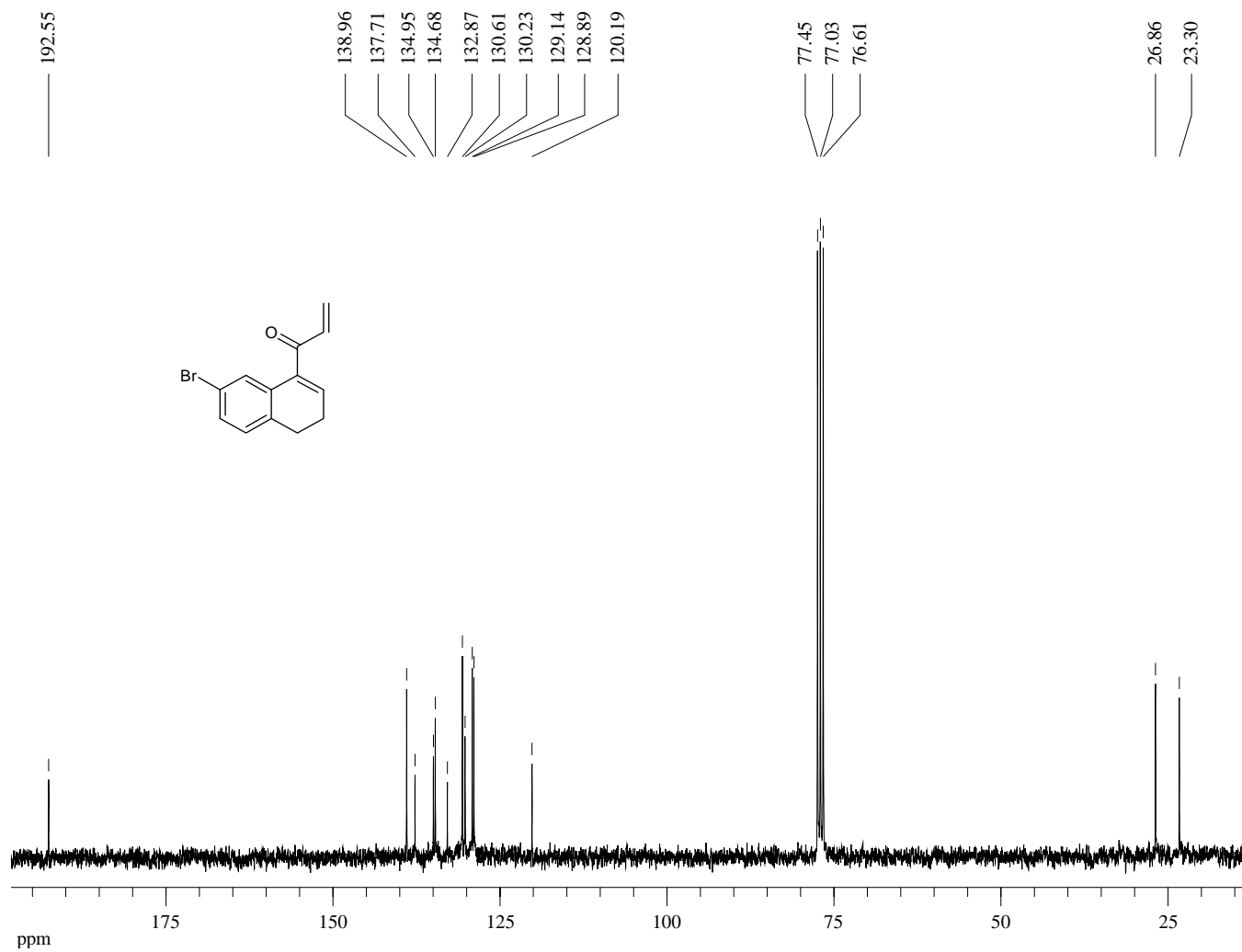
¹H-NMR (300 MHz, CDCl₃) of Compound **76**



¹H-NMR (300 MHz, CDCl₃) of Compound **77**

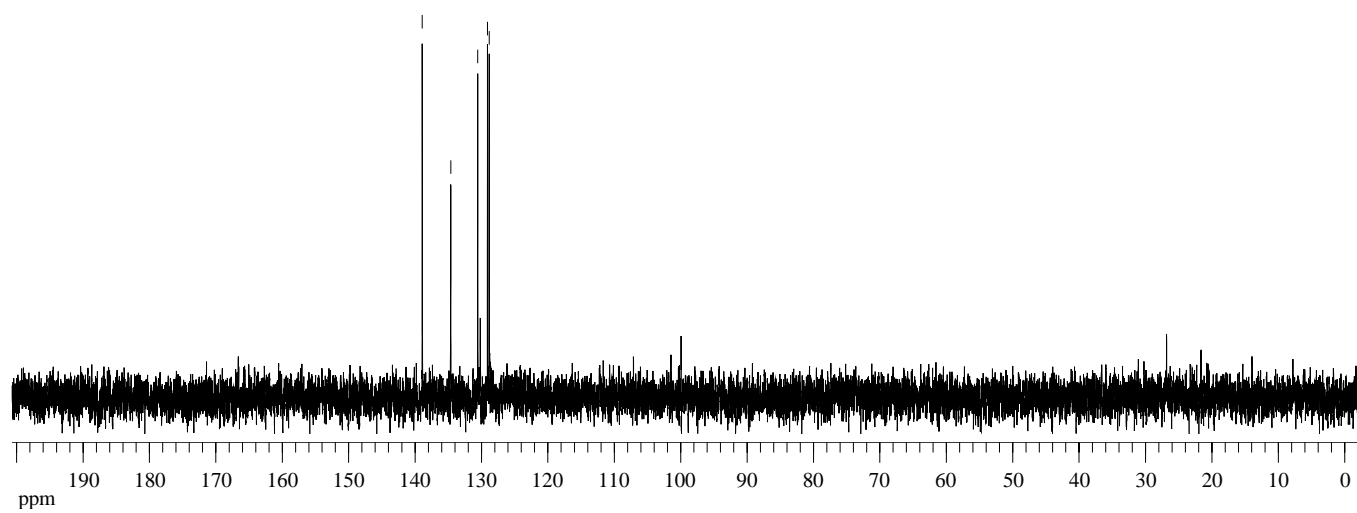
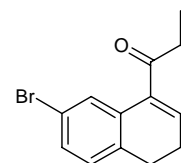


$^{13}\text{C-NMR}$ (75 MHz, CDCl_3) of Compound **77**

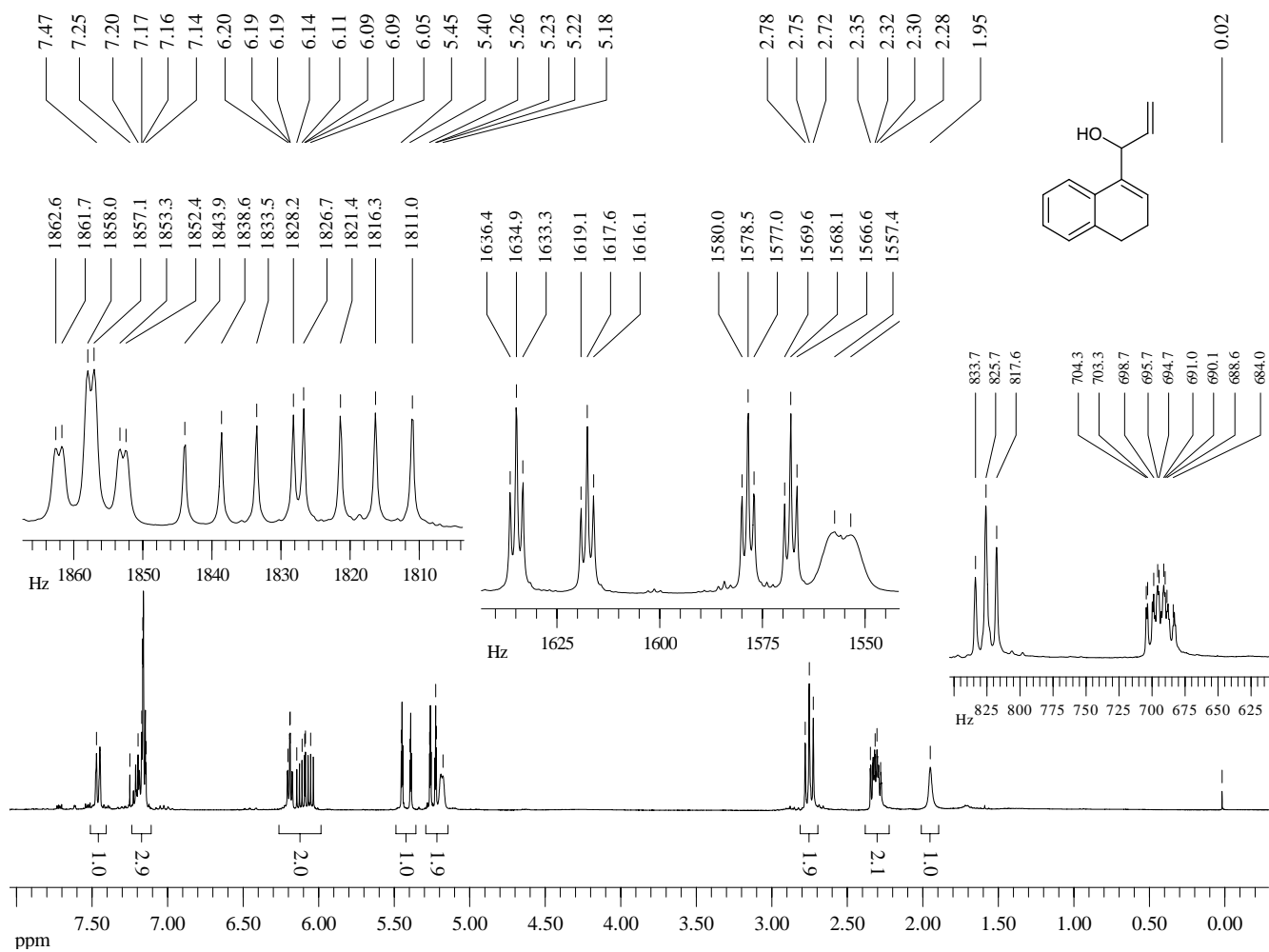


Dept 90-NMR (75 MHz, CDCl₃) of Compound **77**

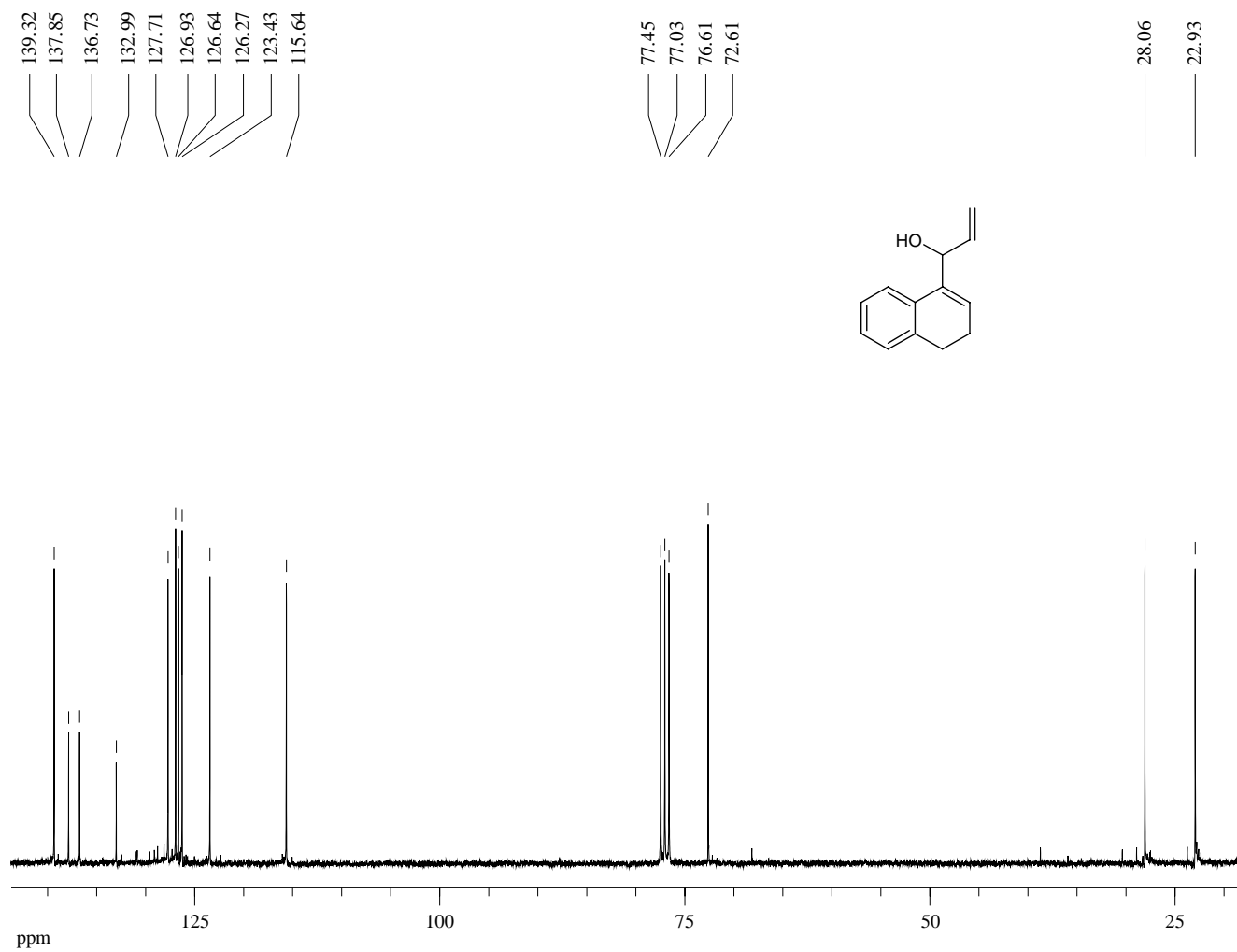
138.91
134.62
130.56
129.09
128.83



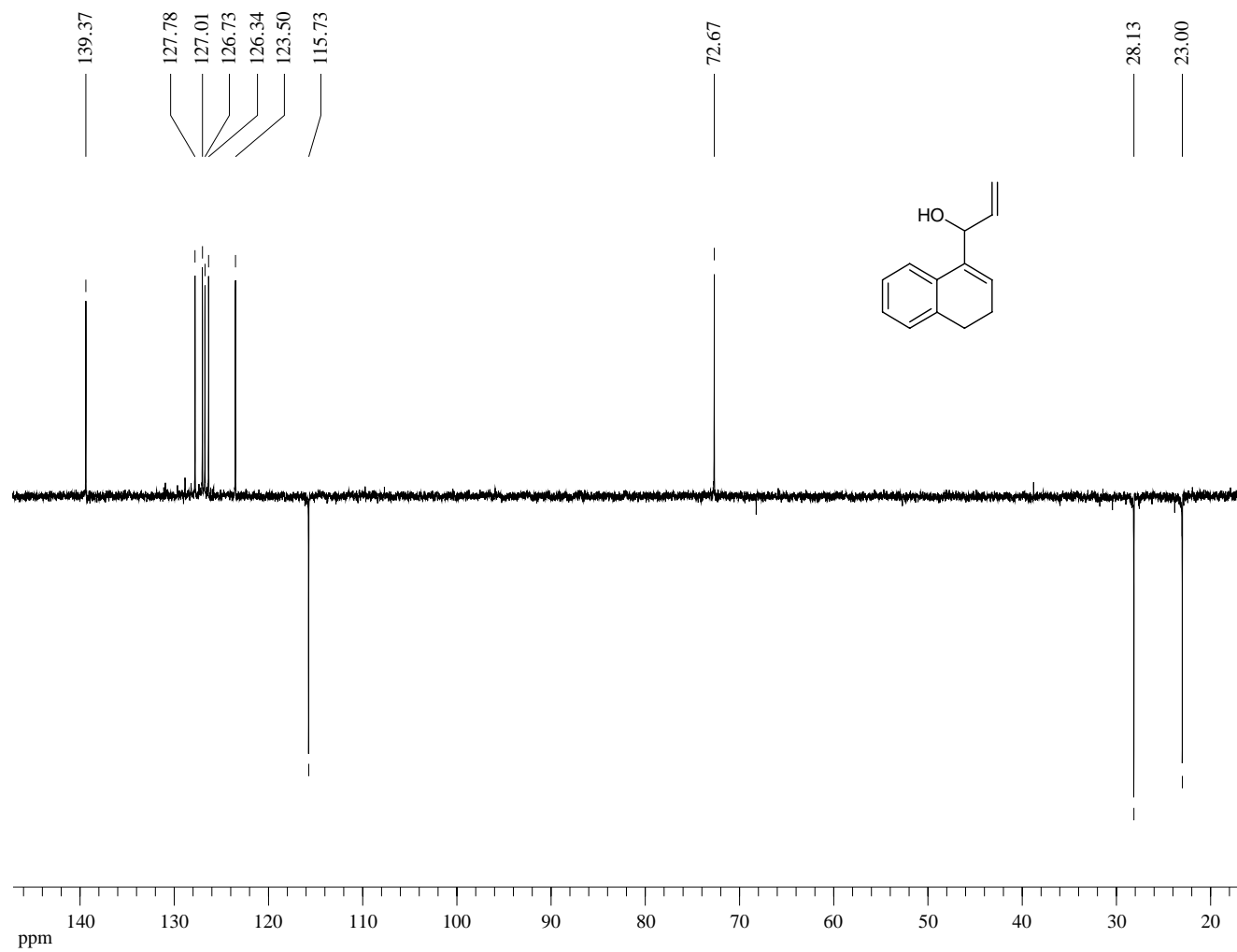
¹H-NMR (300 MHz, CDCl₃) of Compound **78**



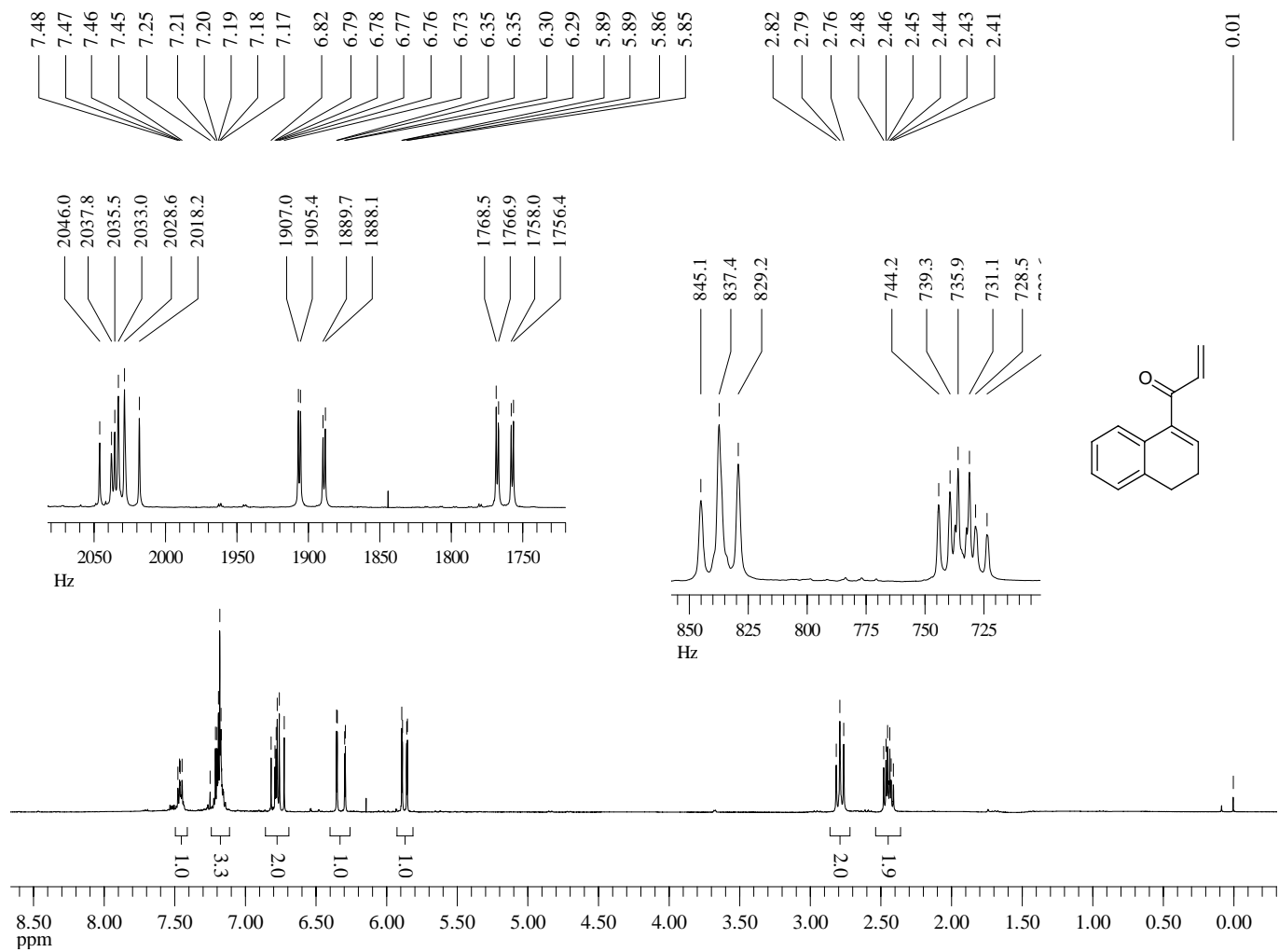
^{13}C -NMR (75 MHz, CDCl_3) of Compound **78**



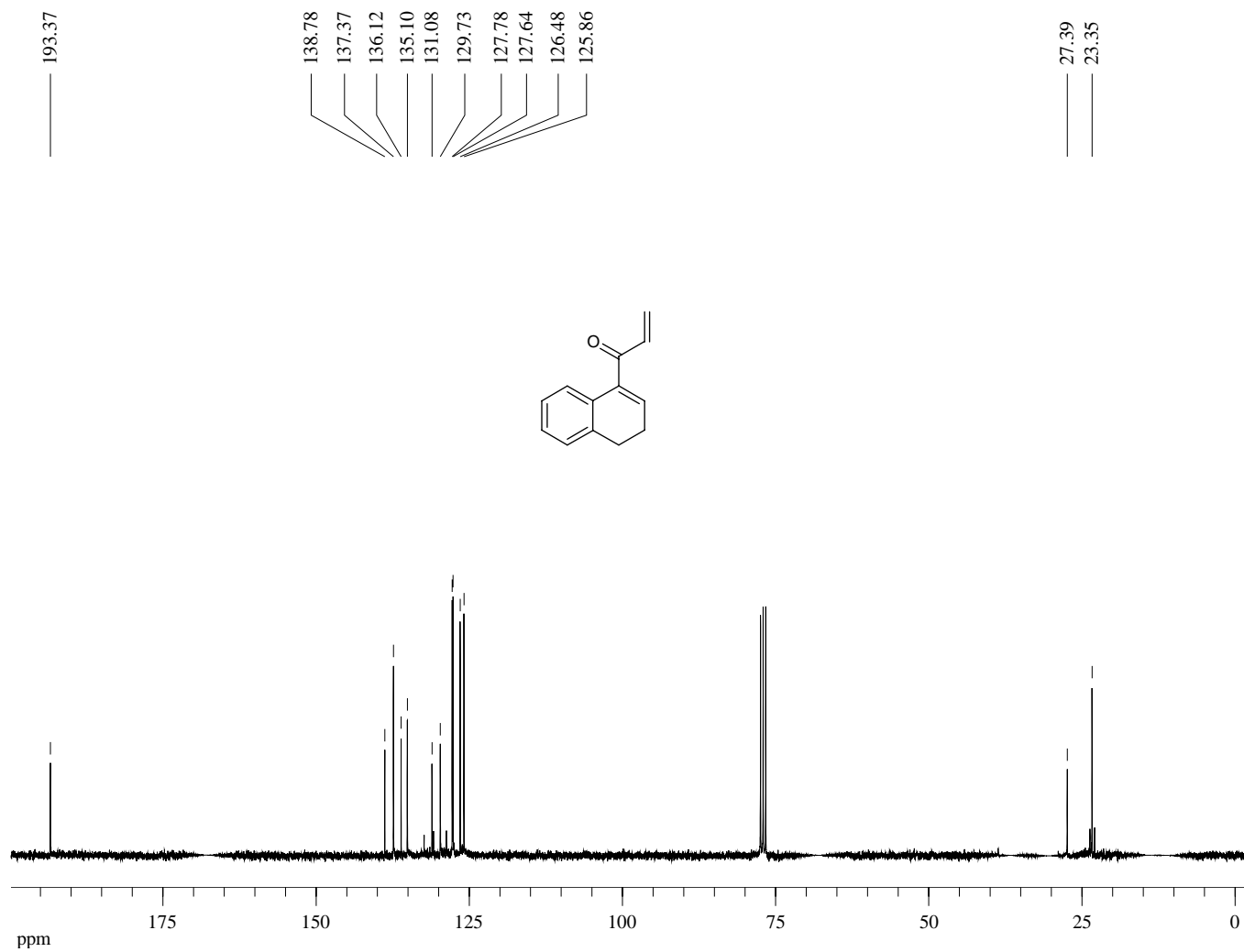
Dept 135-NMR (75 MHz, CDCl₃) of Compound **78**



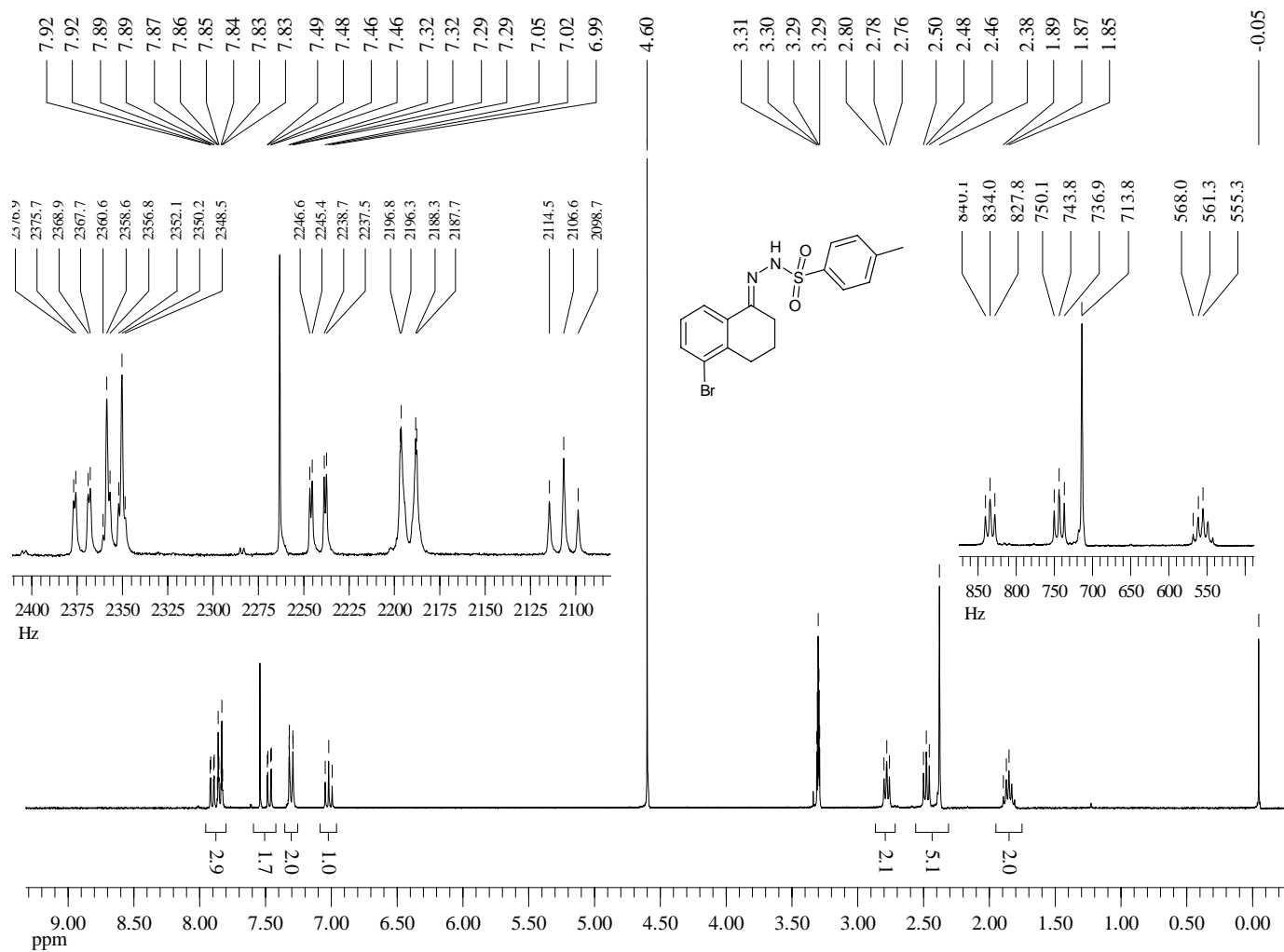
¹H-NMR (300 MHz, CDCl₃) of Compound **79**



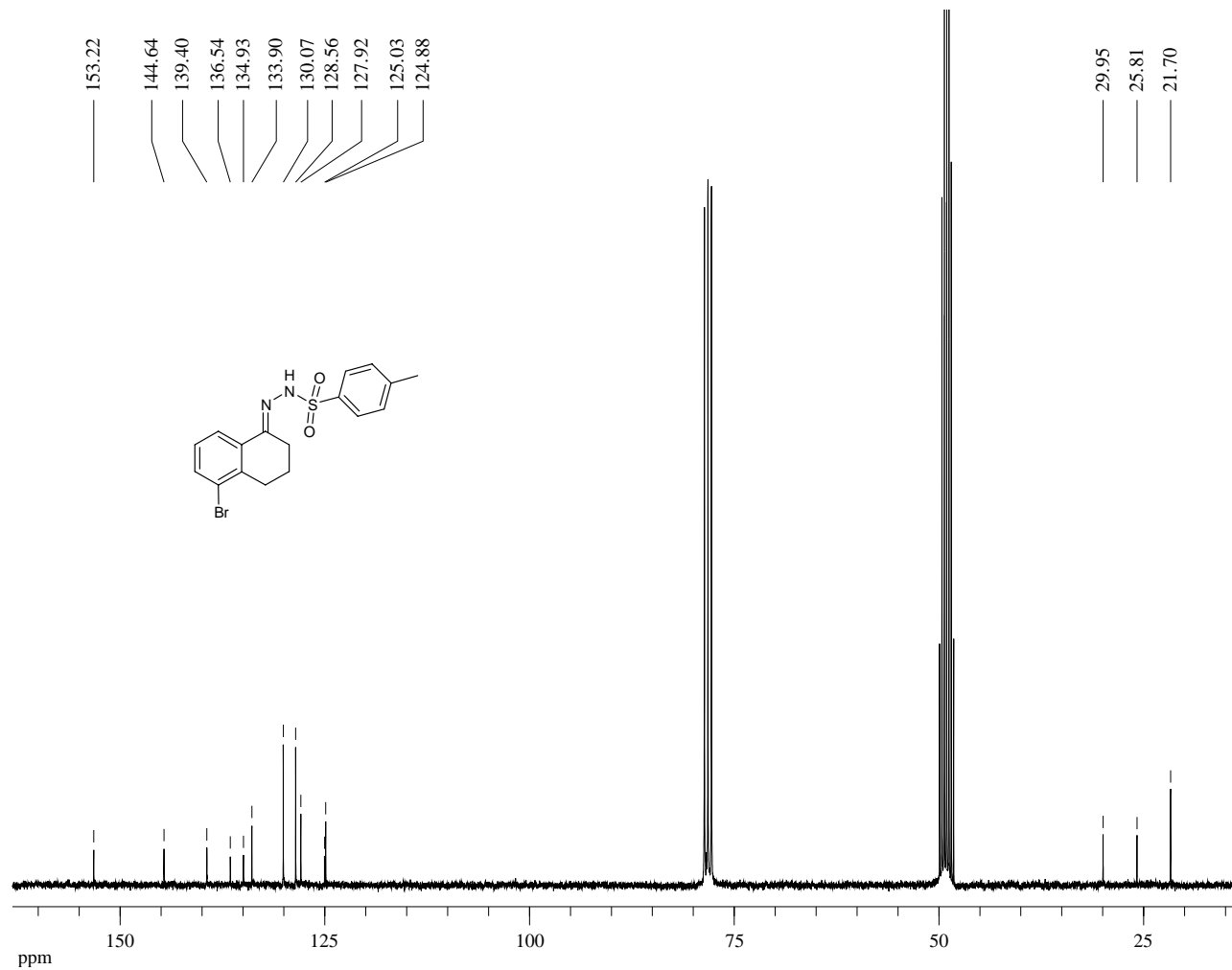
^{13}C -NMR (75 MHz, CDCl_3) of Compound **79**



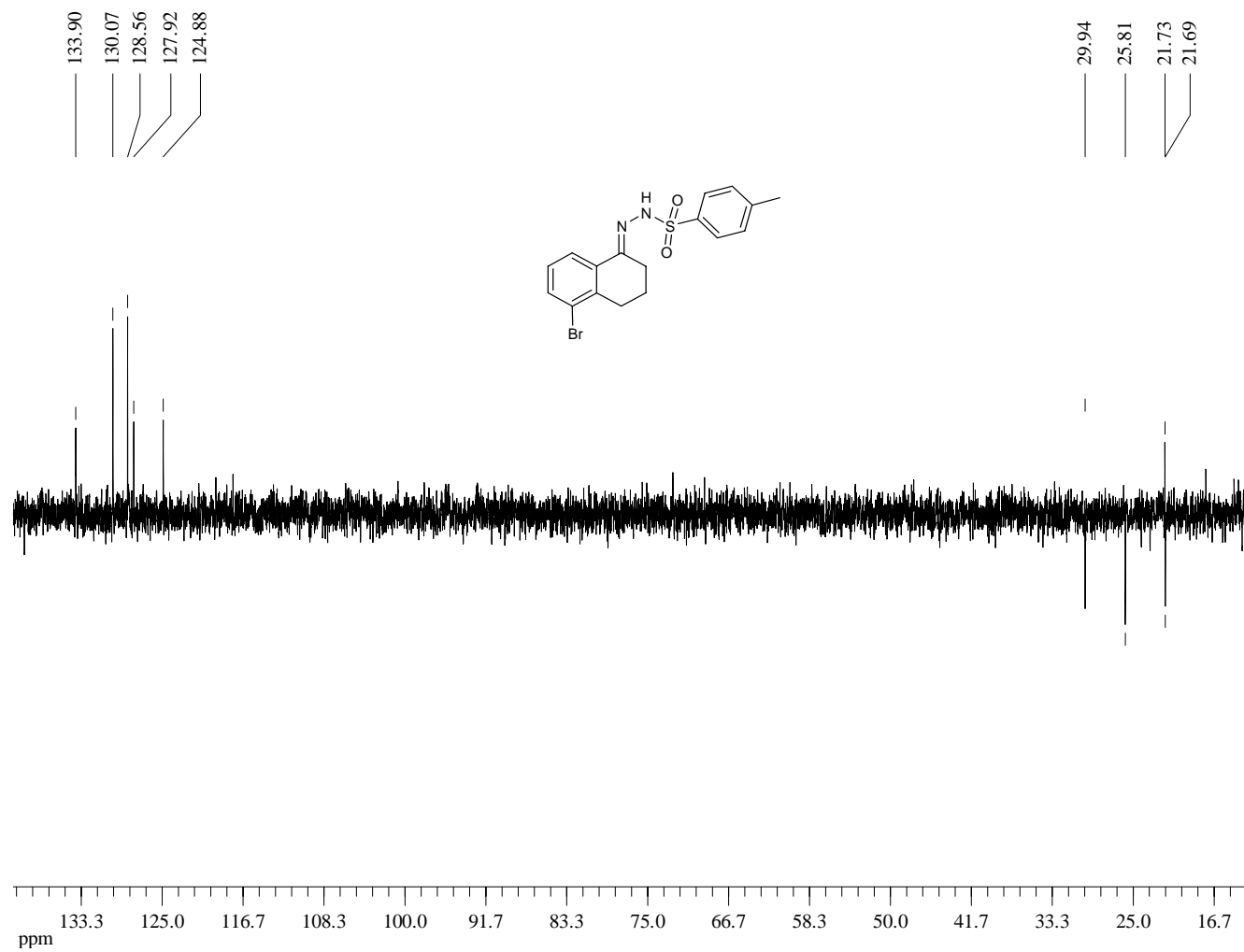
¹H-NMR (300 MHz, Methanol-d₆) of Compound **80**



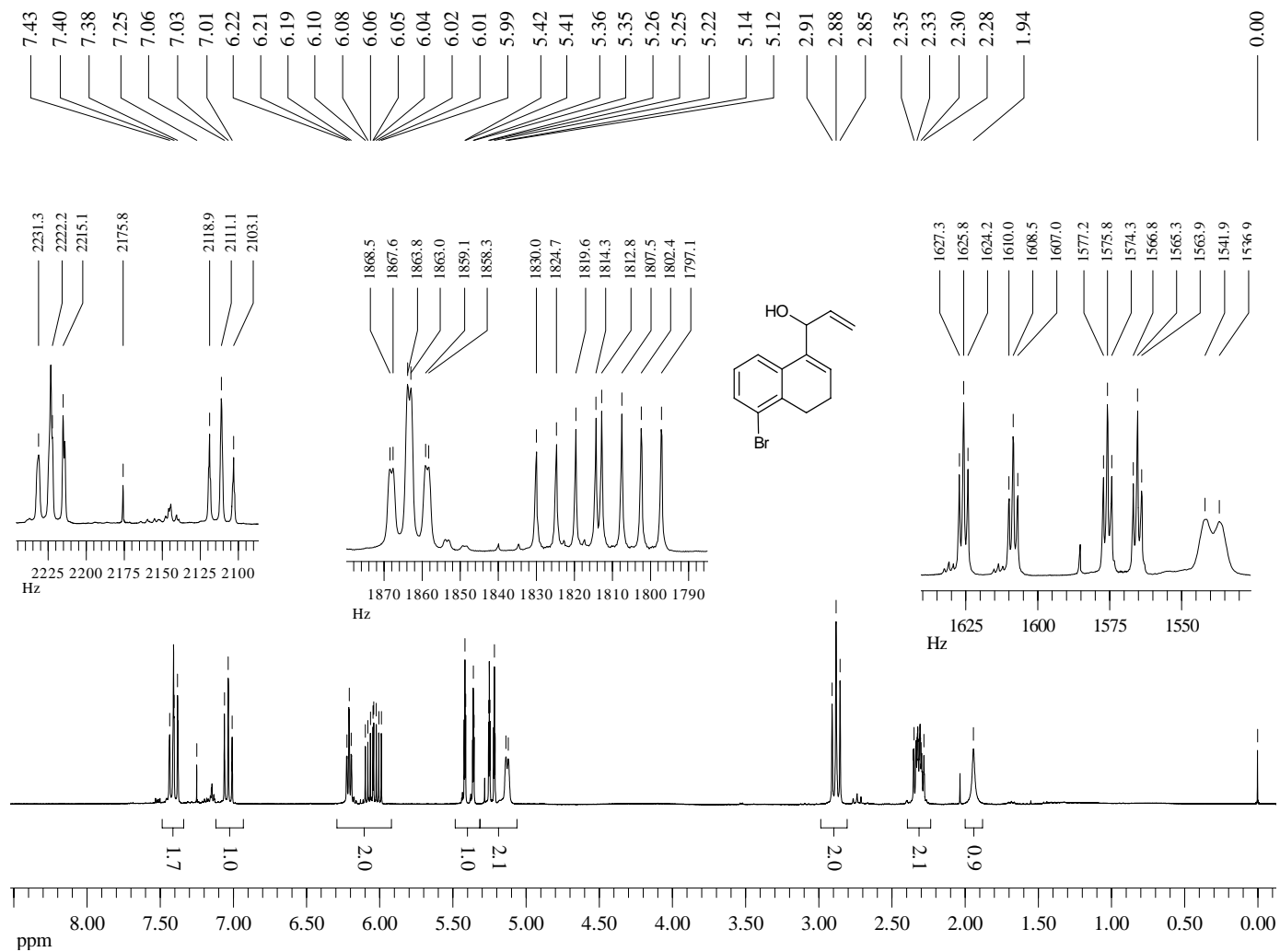
¹³C-NMR (75 MHz, Methanol-d₆) of Compound **80**



Dept 135-NMR (75 MHz, Methanol-d₆) of Compound **80**



¹H-NMR (300 MHz, CDCl₃) of Compound **81**

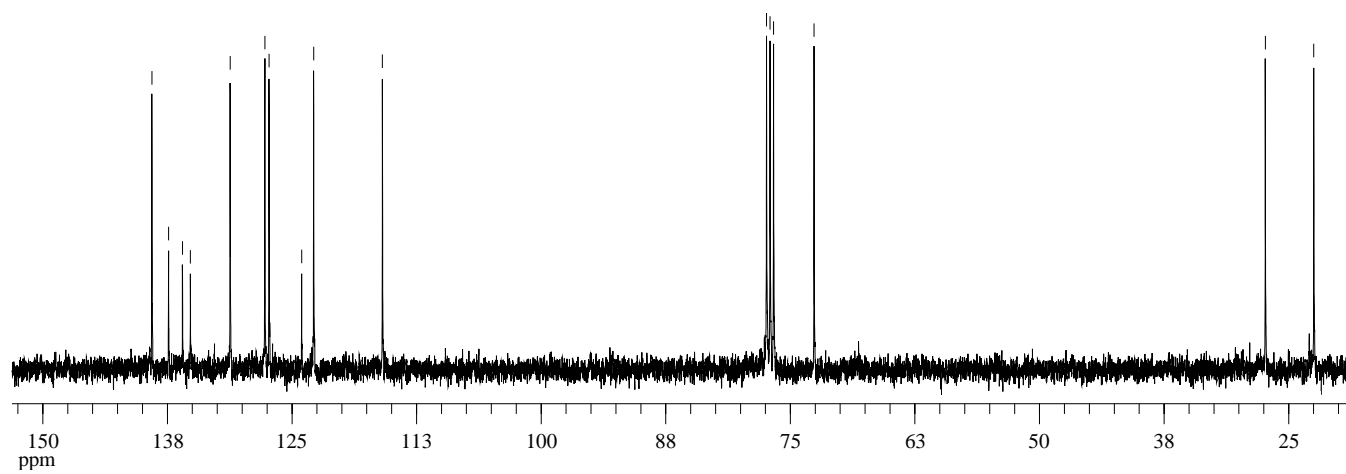
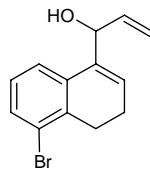


^{13}C -NMR (90 MHz, CDCl_3) of Compound **81**

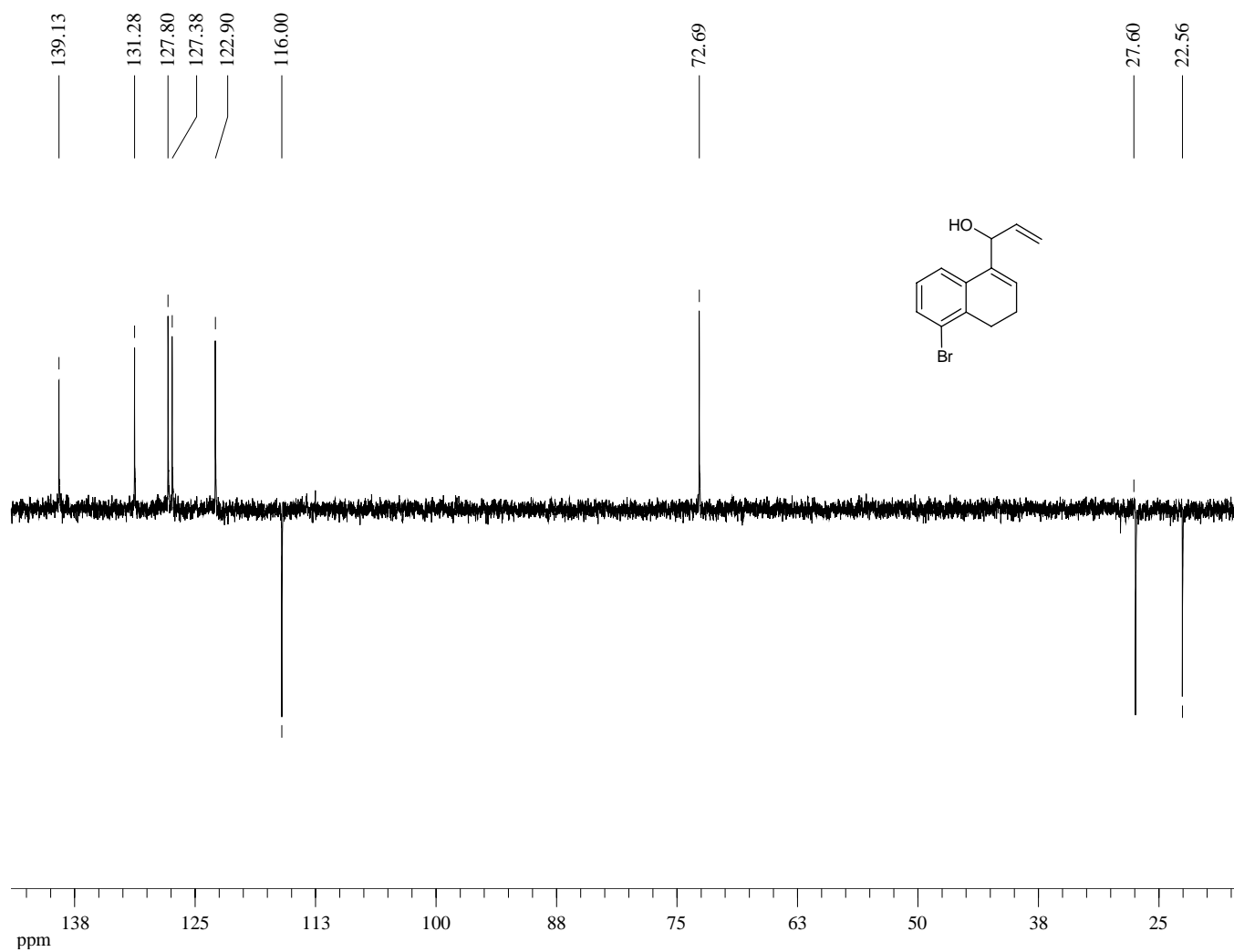
139.05
137.38
135.98
135.19
131.20
127.72
127.30
124.02
122.82
115.92

77.38
77.03
76.68
72.61

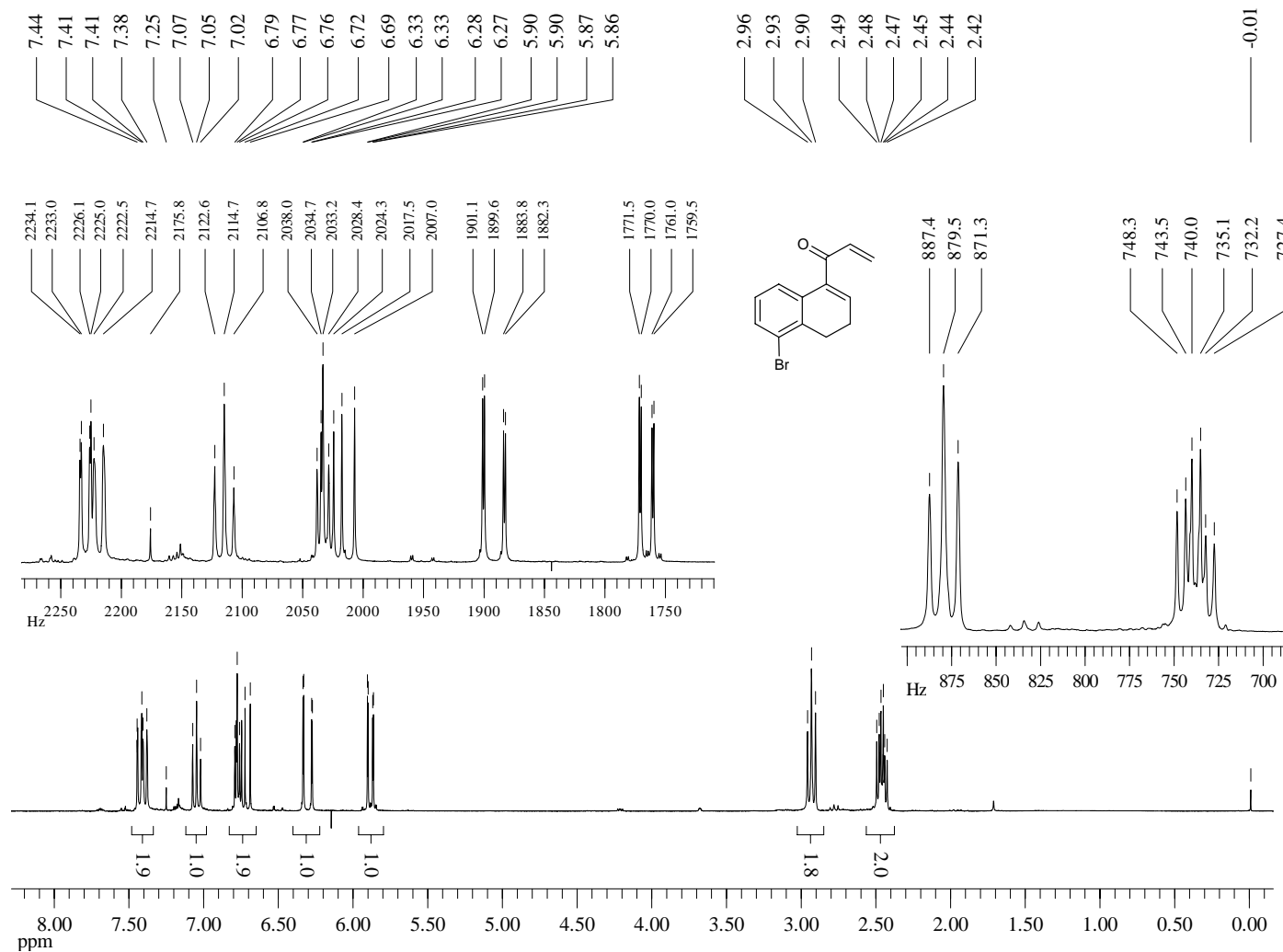
27.34
22.48



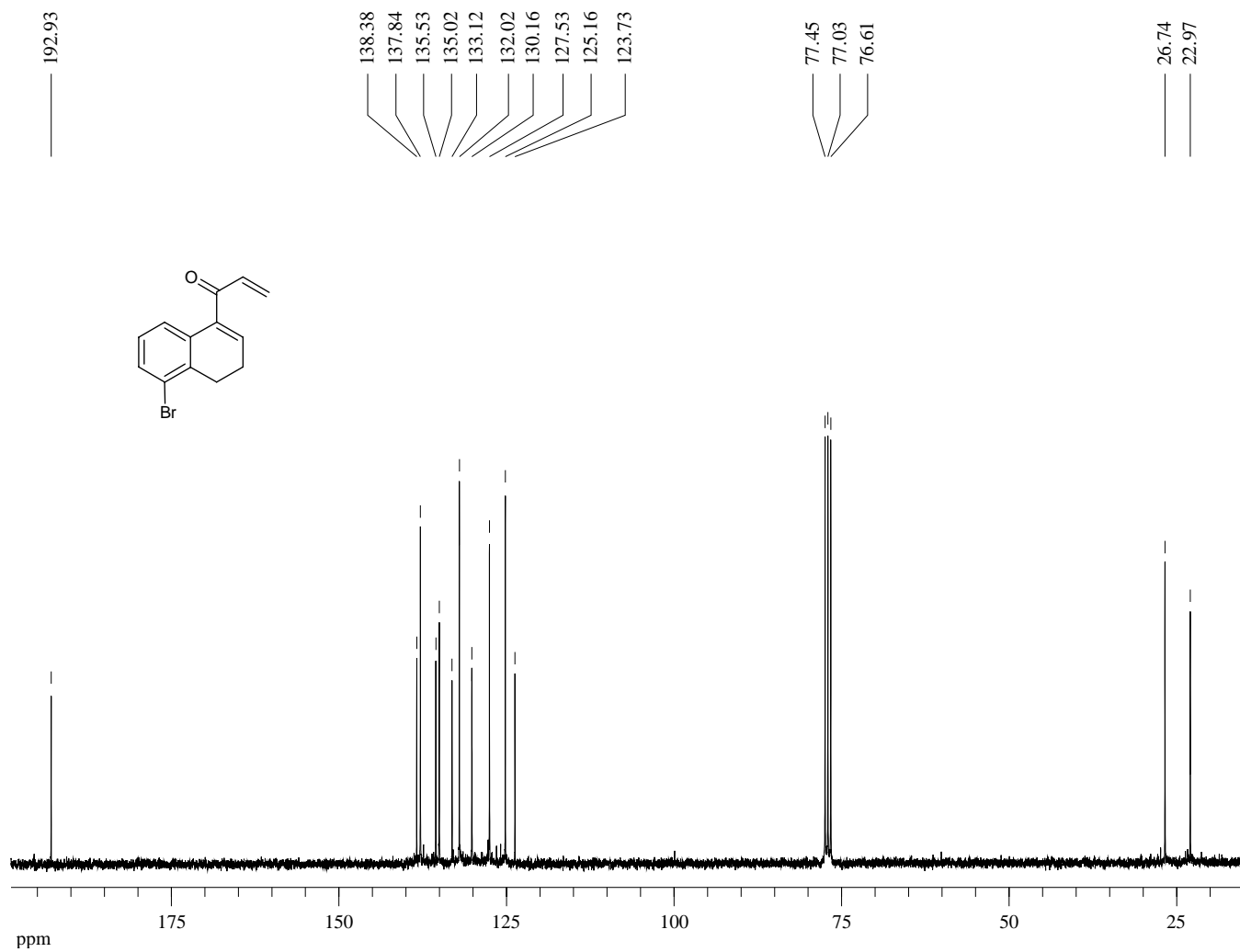
Dept 135-NMR (90 MHz, CDCl₃) of Compound **81**



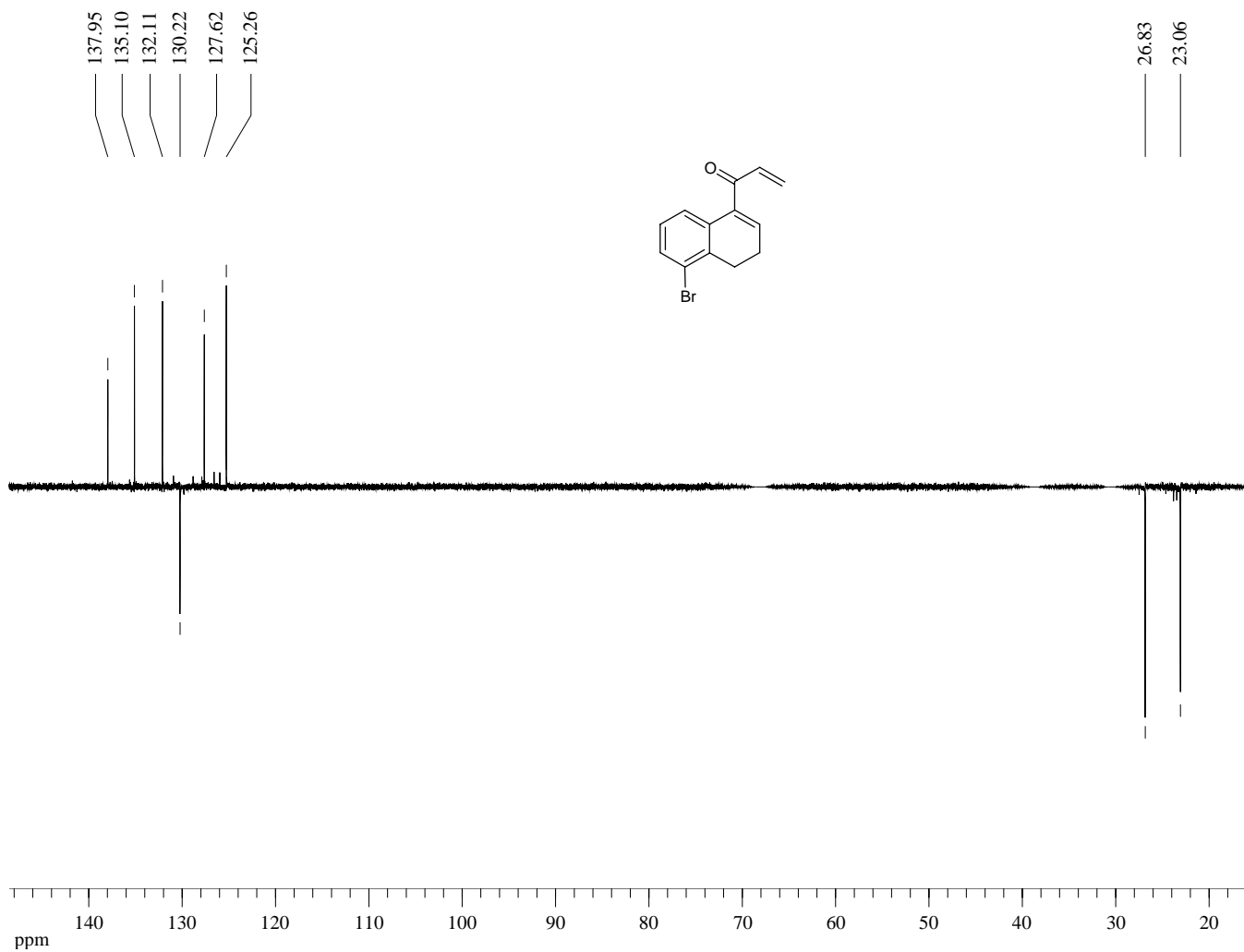
¹H-NMR (300 MHz, CDCl₃) of Compound **82**



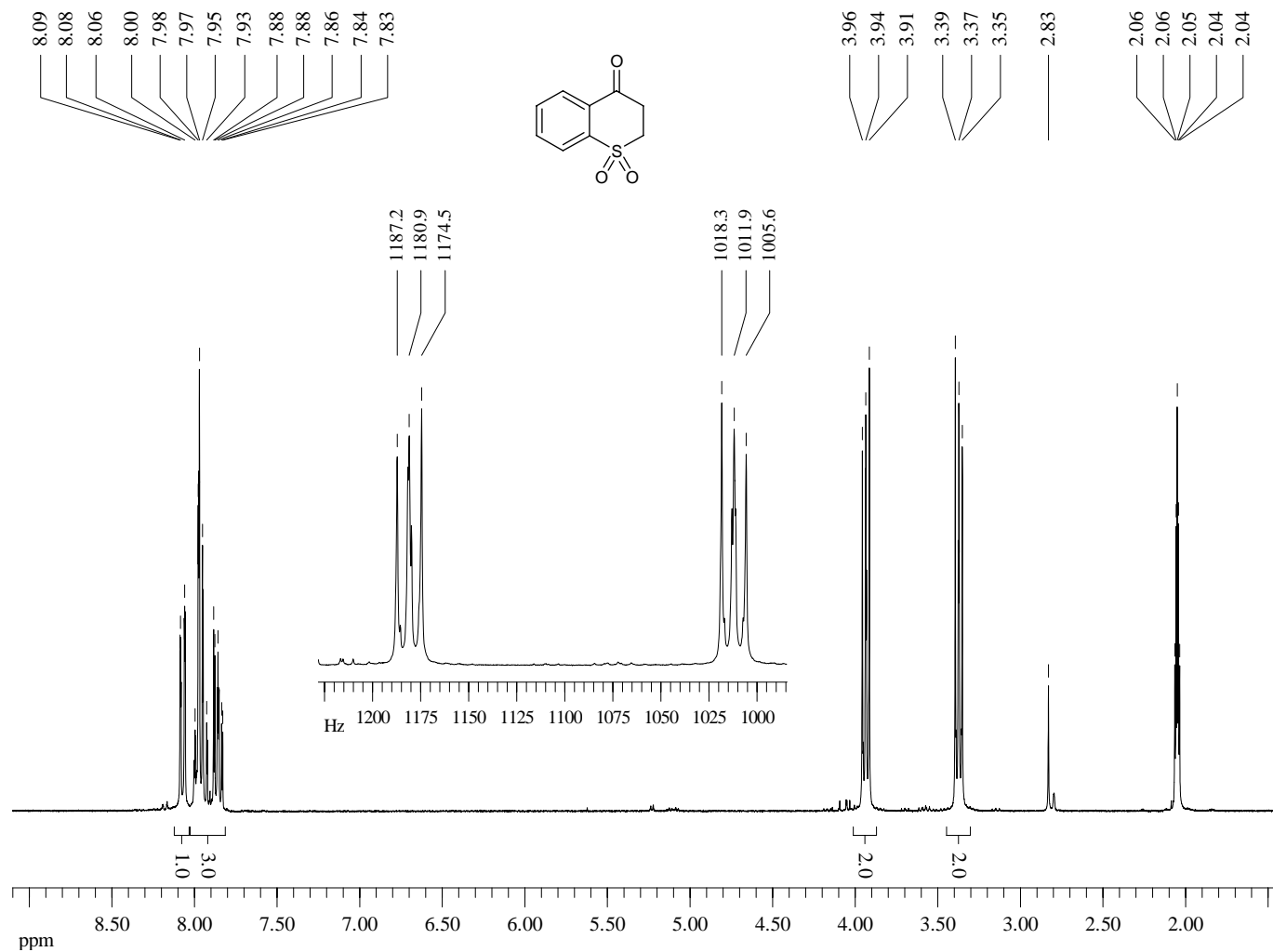
¹³C-NMR (75 MHz, CDCl₃) of Compound **82**



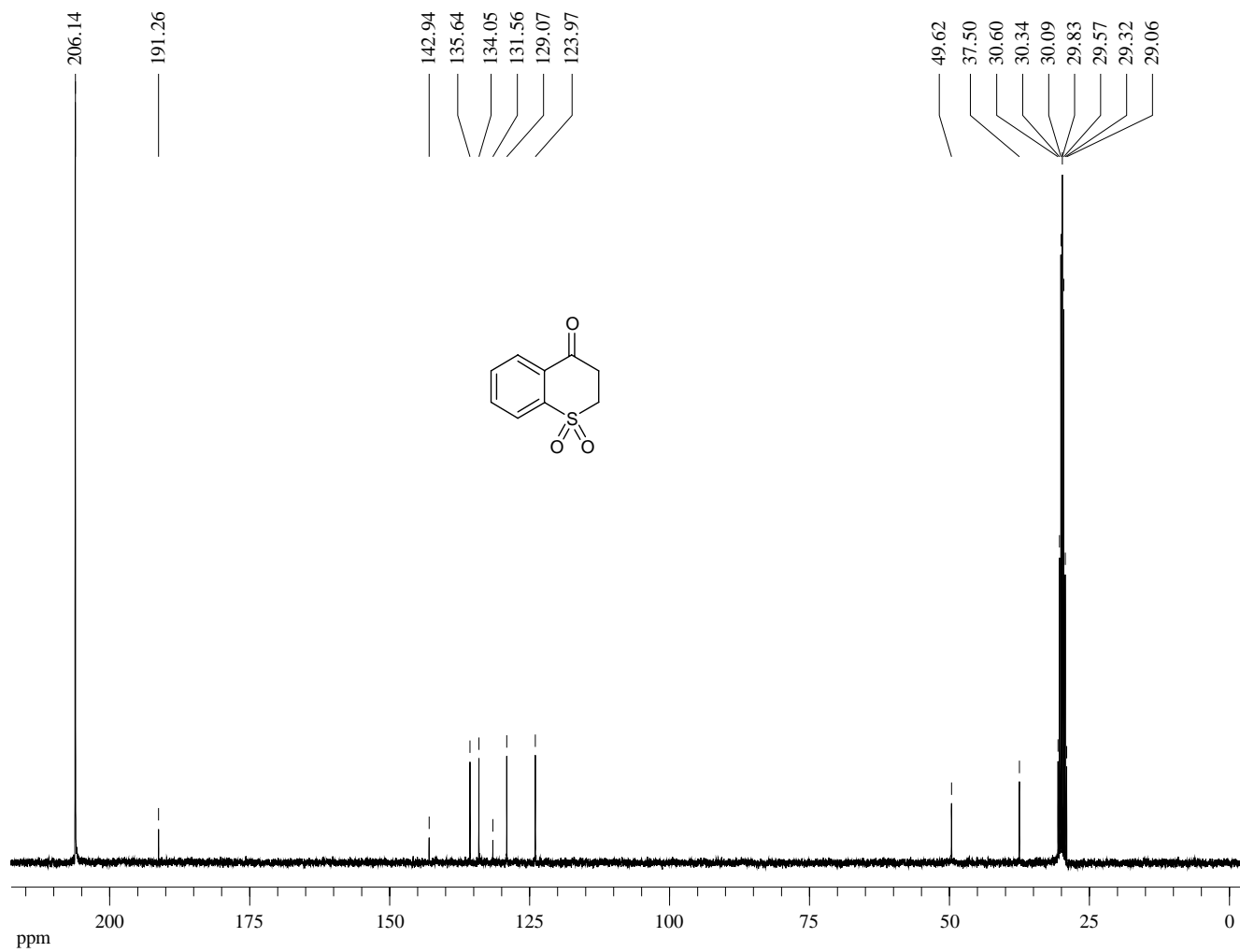
Dept 135-NMR (75 MHz, CDCl₃) of Compound **82**



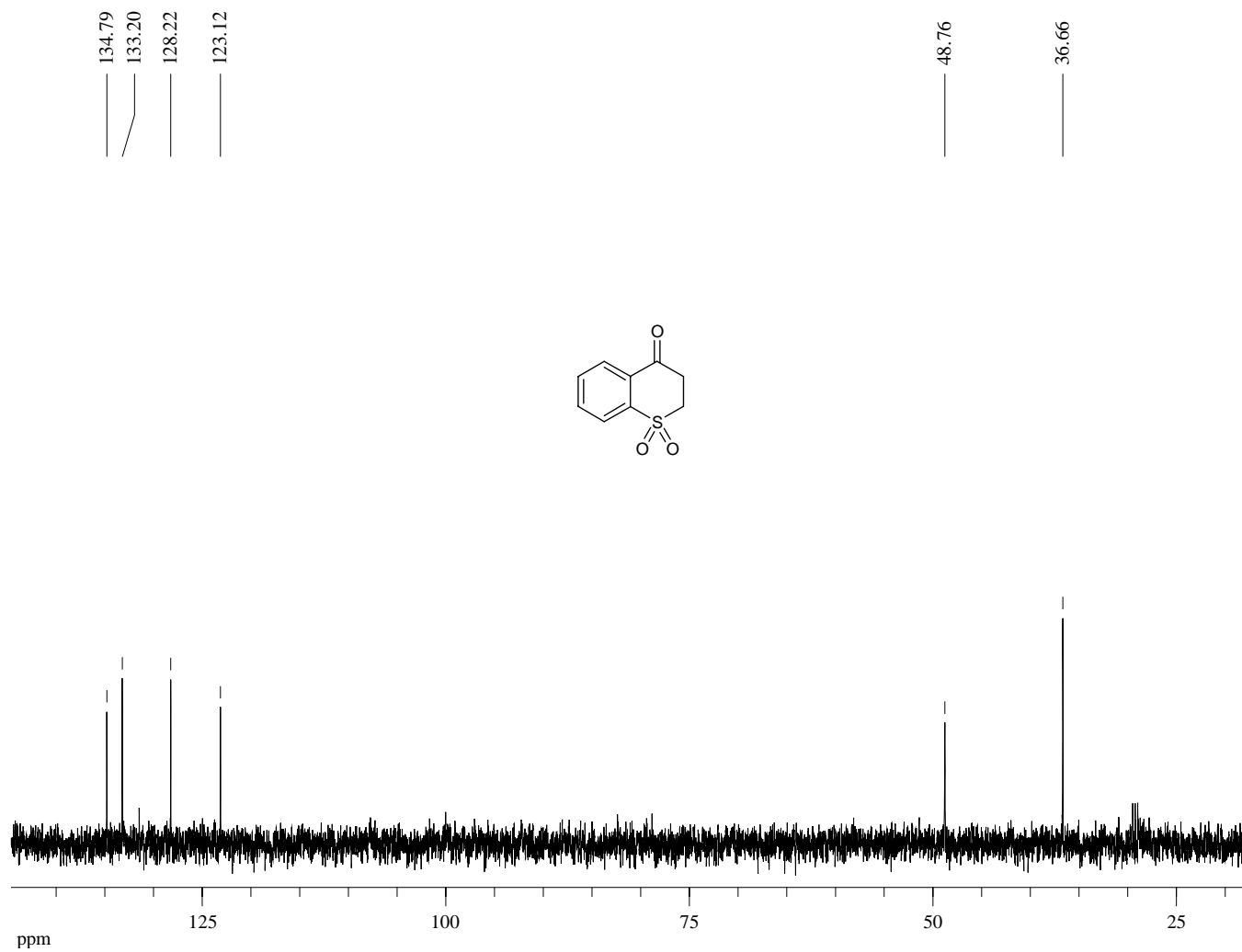
¹H-NMR (300 MHz, Acetone-d₆) of Compound **83**



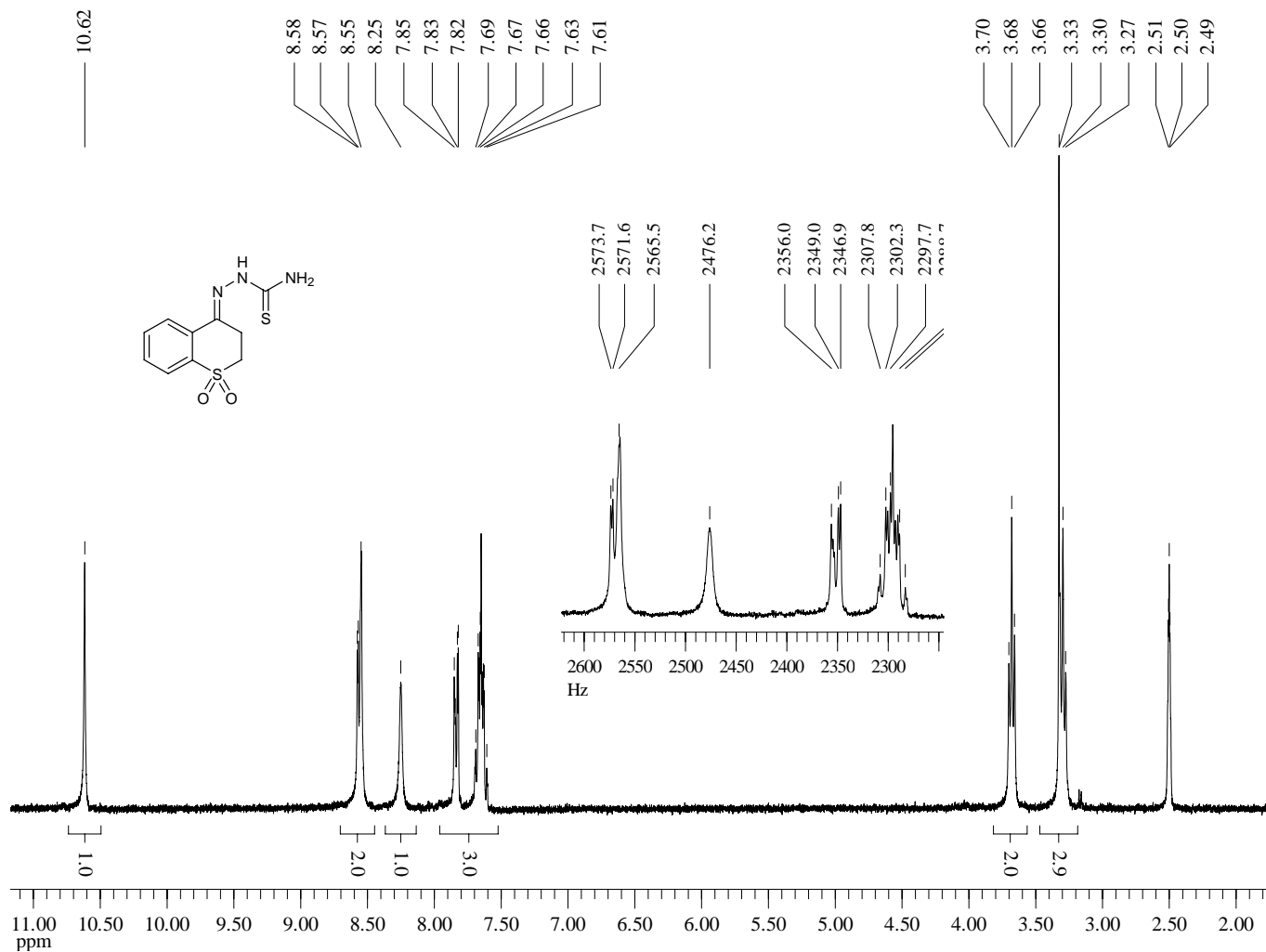
^{13}C -NMR (75 MHz, Acetone- d_6) of Compound **83**



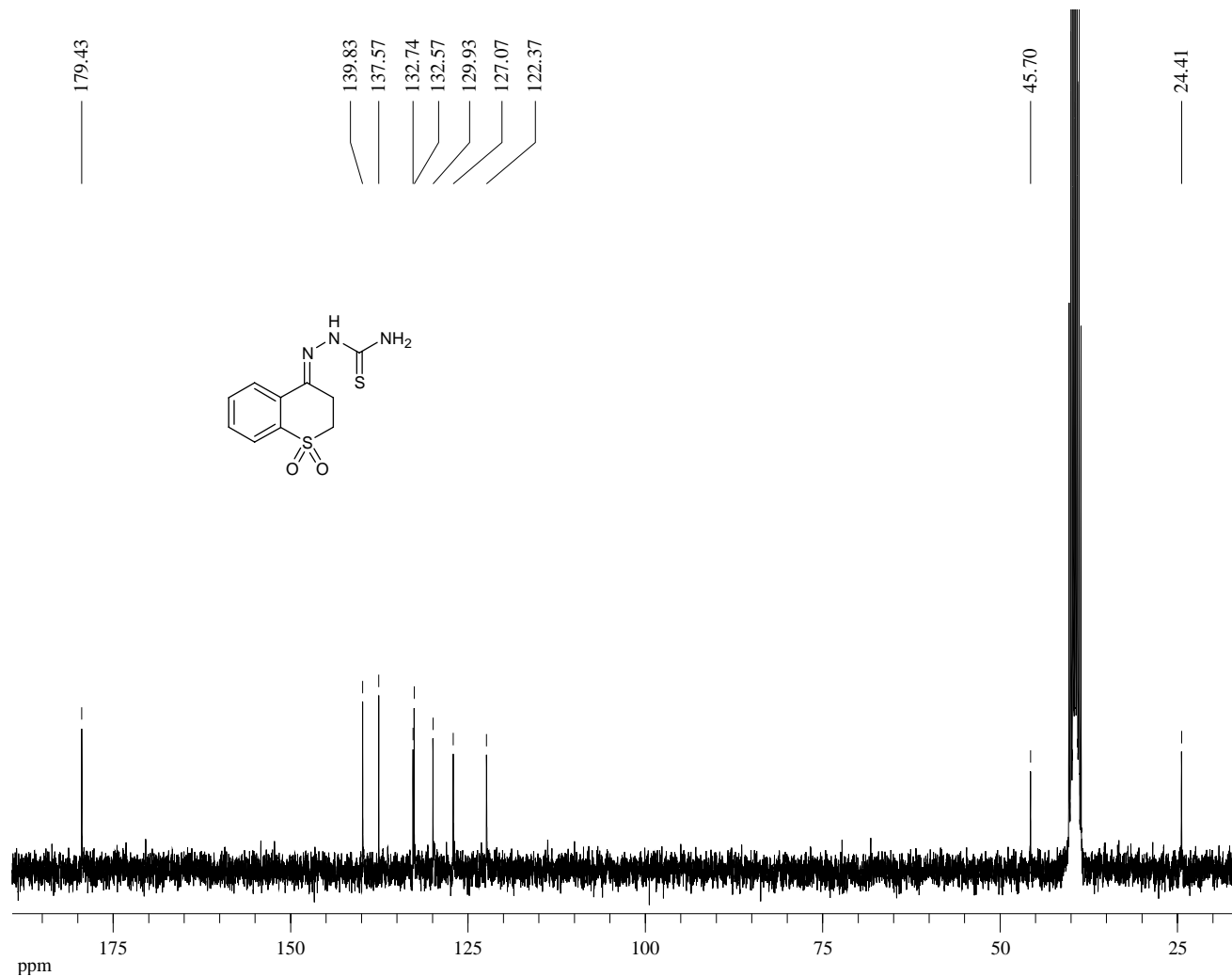
Dept 45-NMR (75 MHz, Acetone-d₆) of Compound **83**



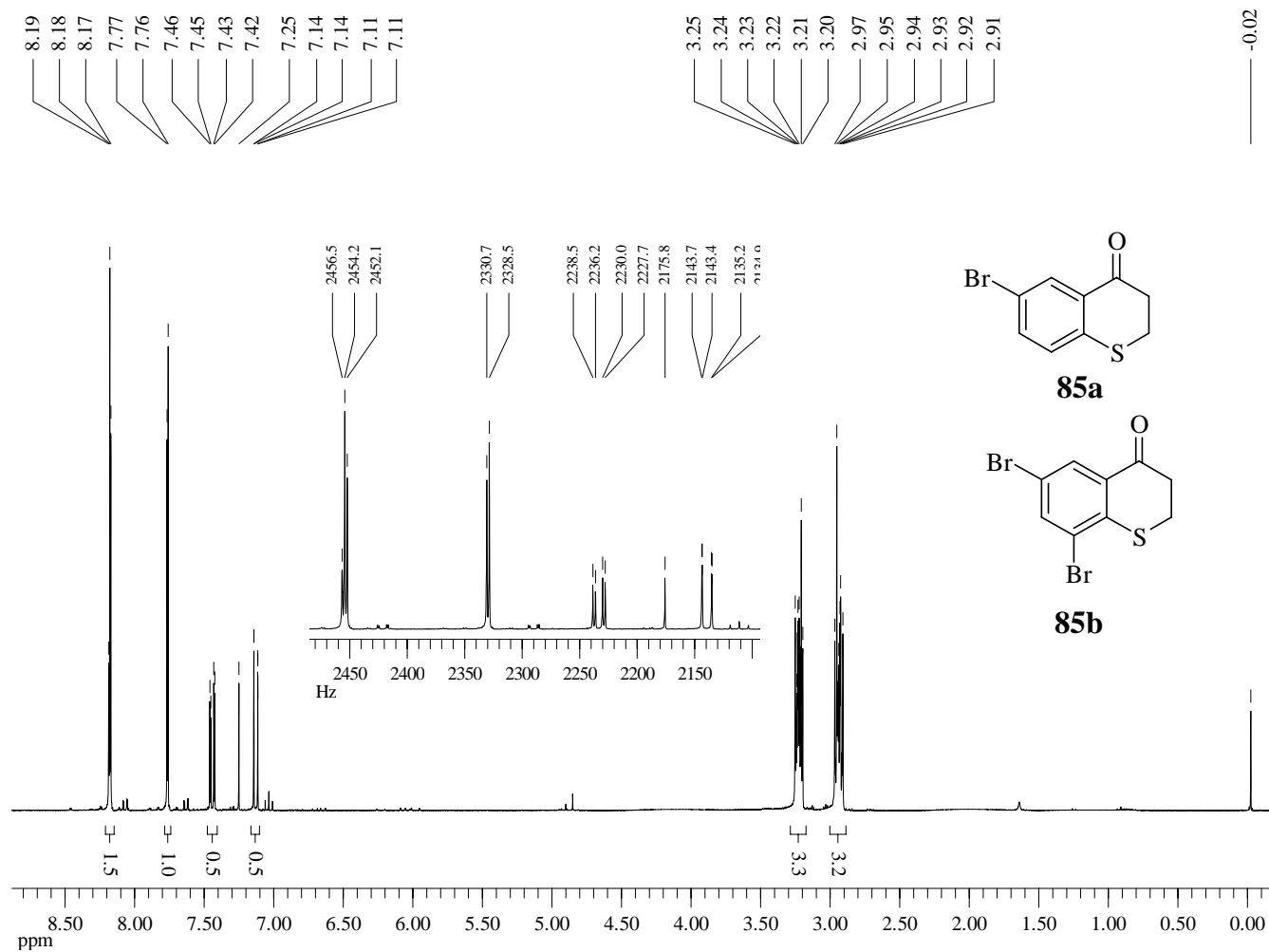
¹H-NMR (300 MHz, Methyl Sulfoxide-d₆) of Compound **84**



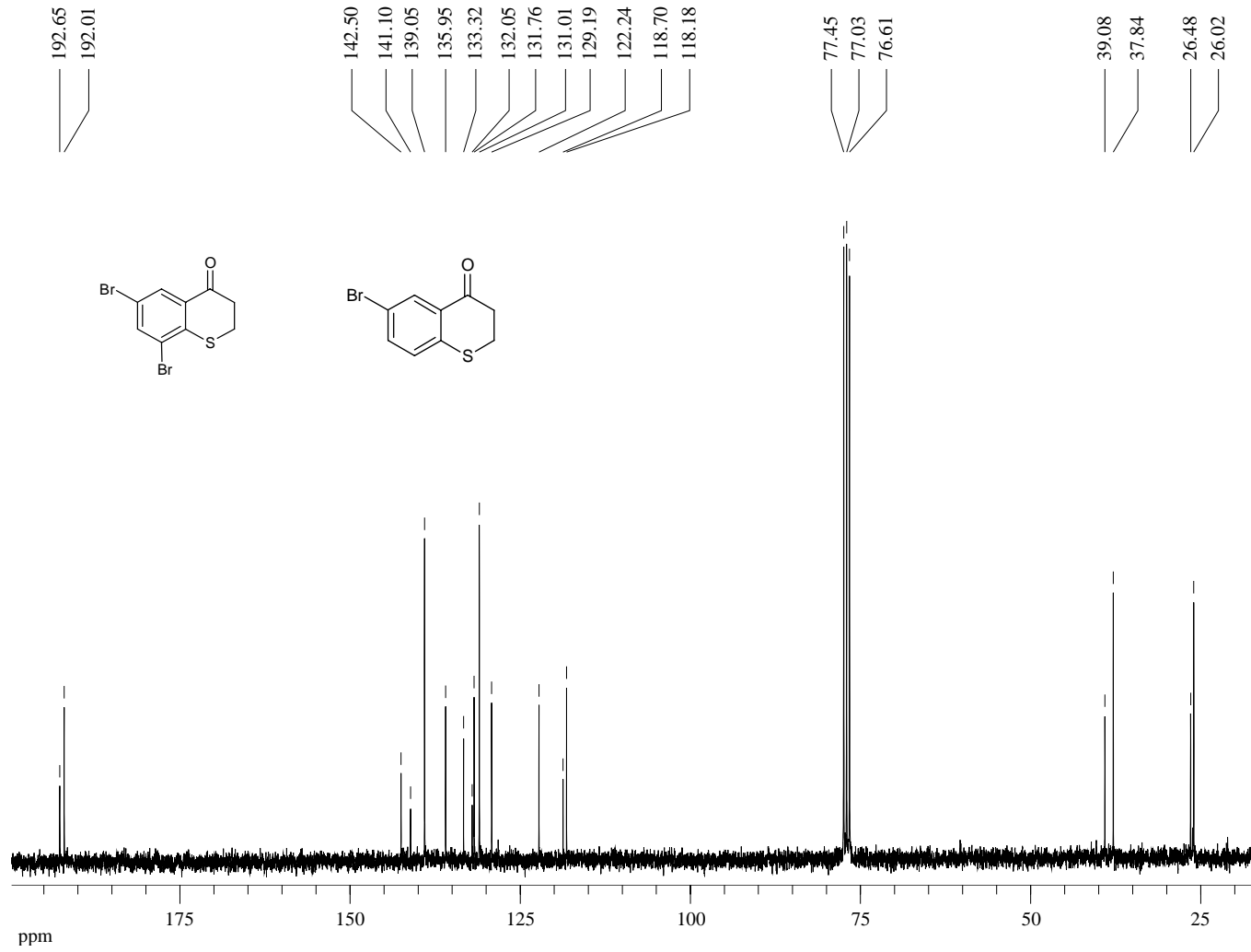
^{13}C -NMR (75 MHz, Methyl Sulfoxide- d_6) of Compound **84**



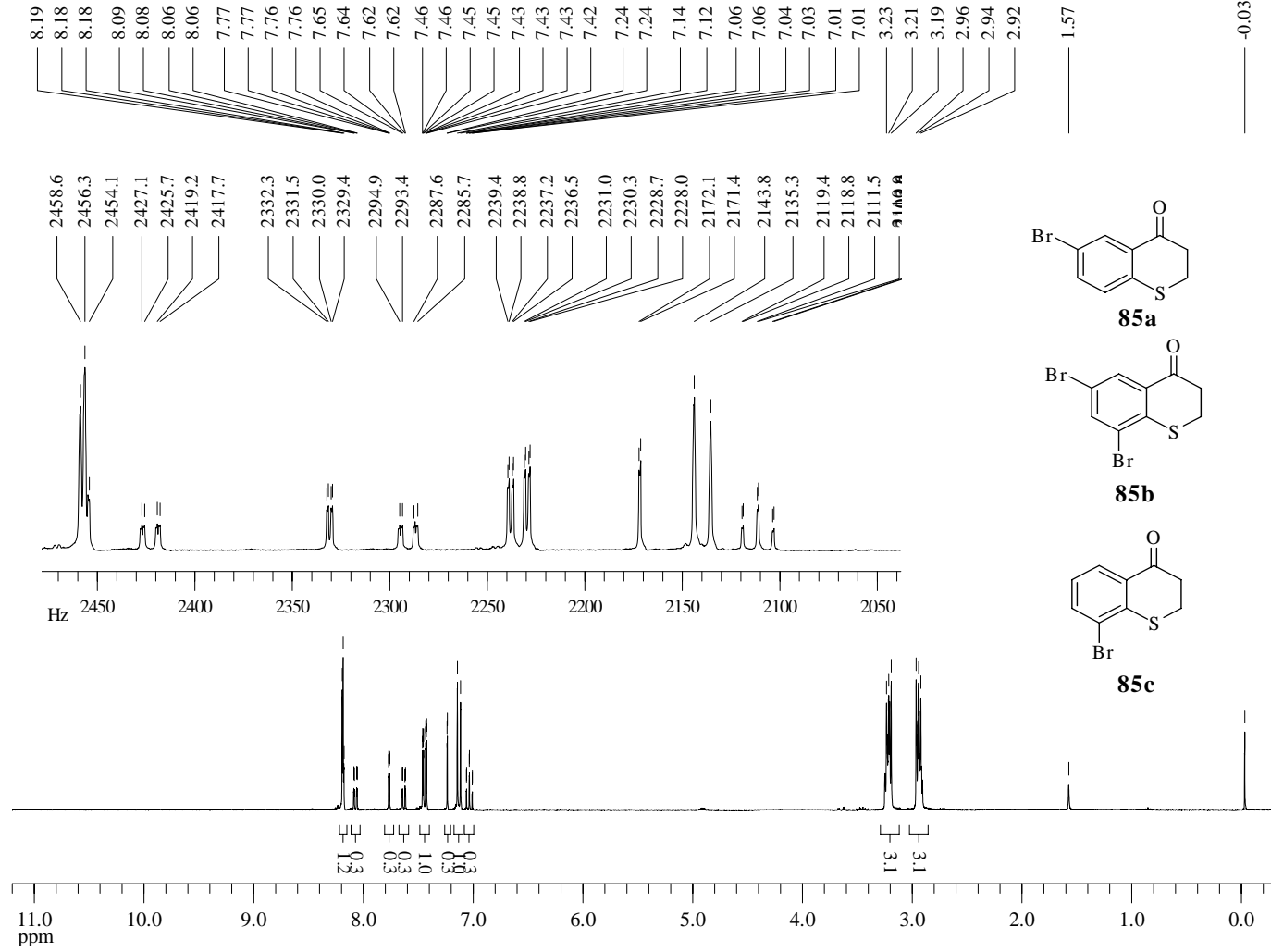
¹H-NMR (300 MHz, CDCl₃) of Compound **85a**



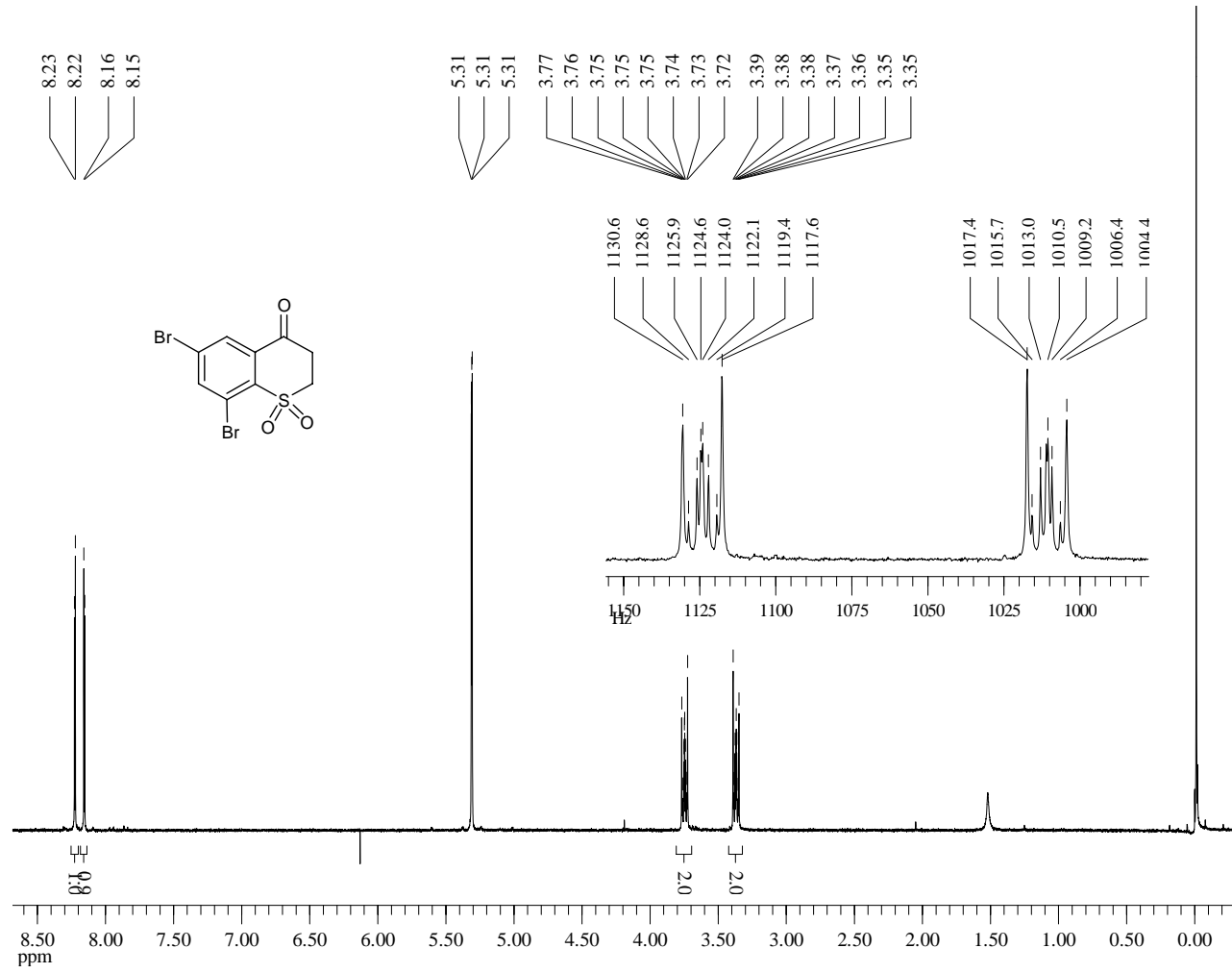
¹³C-NMR (75 MHz, CDCl₃) of Compound **85a**



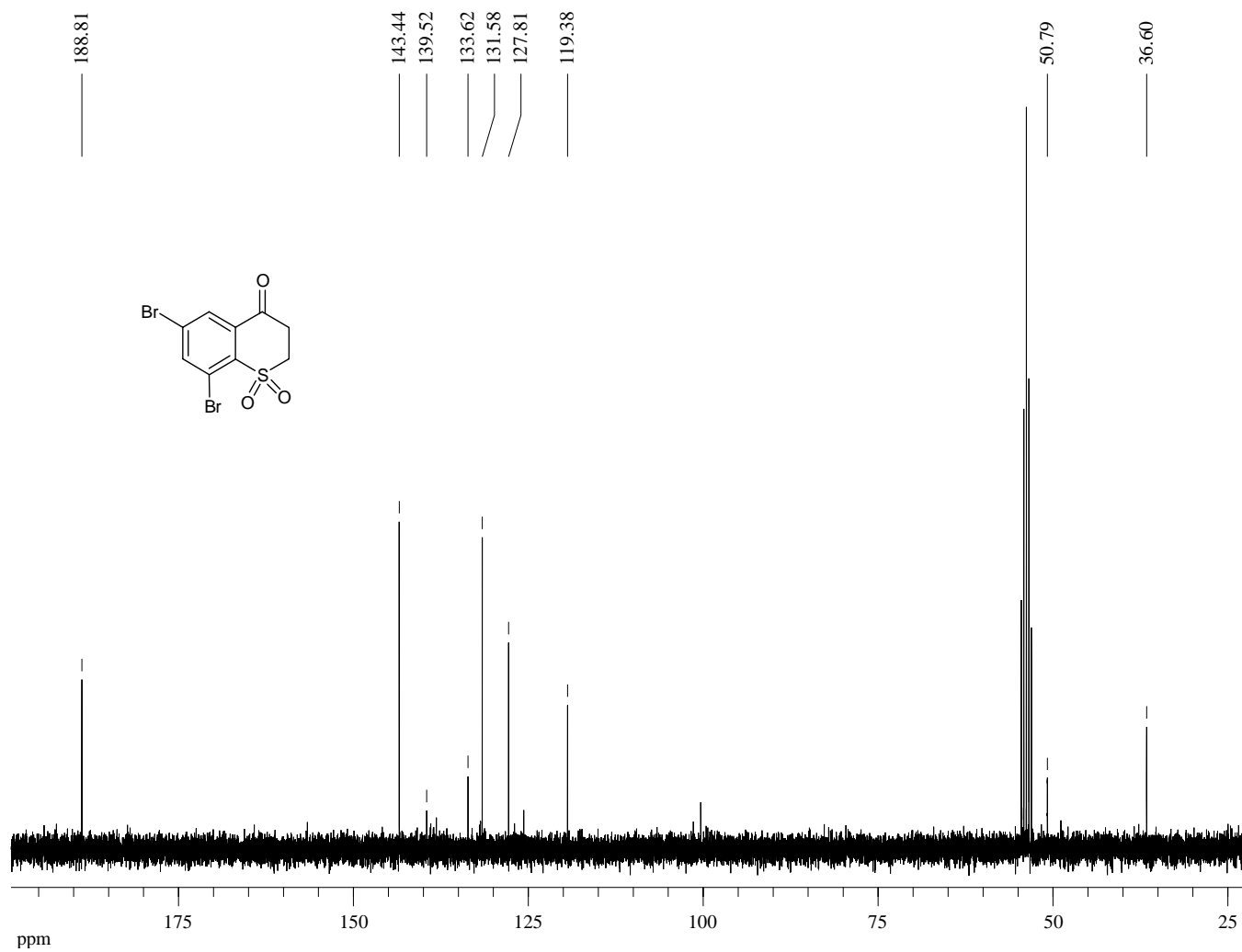
¹H-NMR (300 MHz, CDCl₃) of Compound **85b**



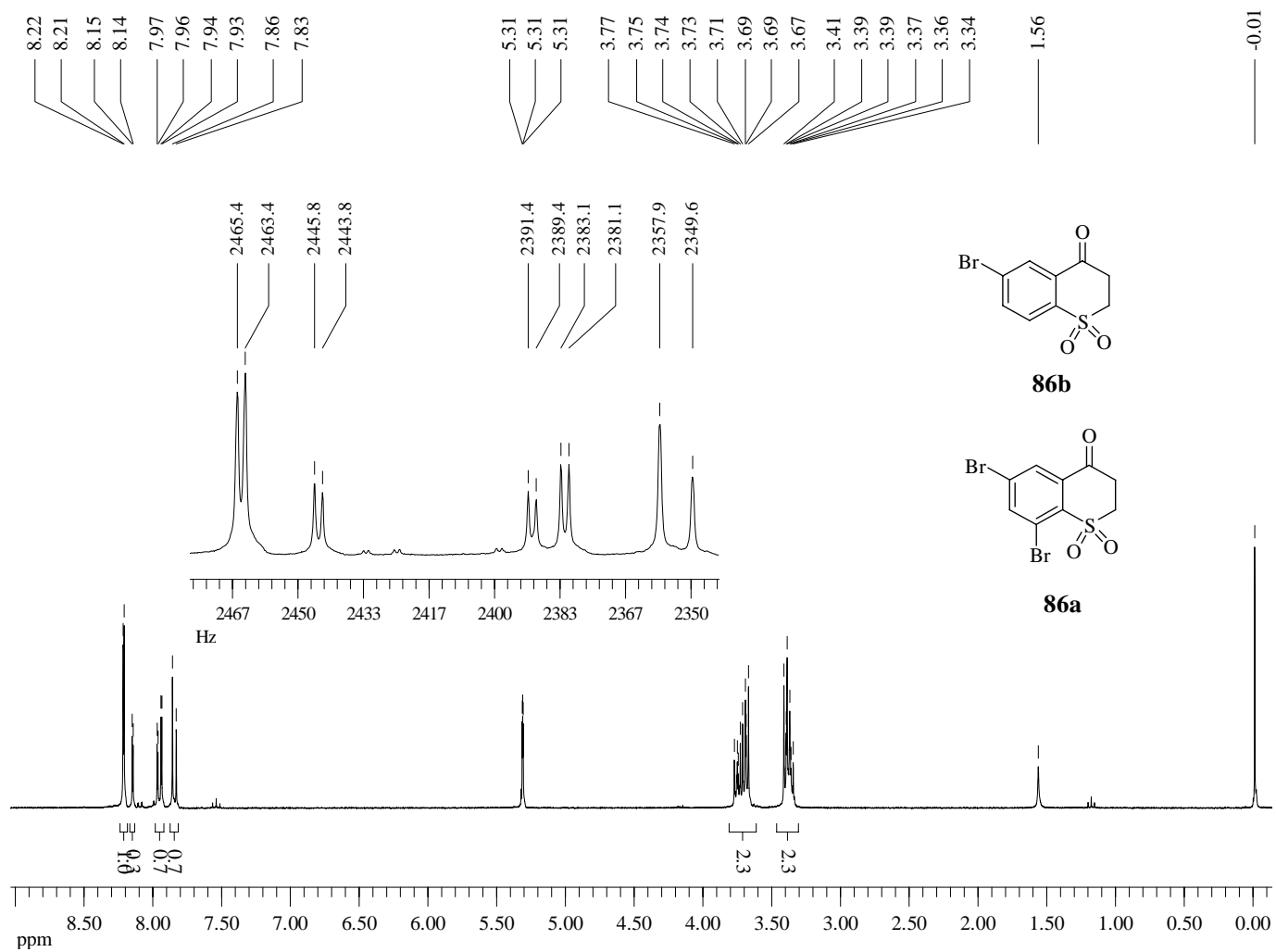
¹H-NMR (300 MHz, CD₂Cl₂) of Compound **86a**



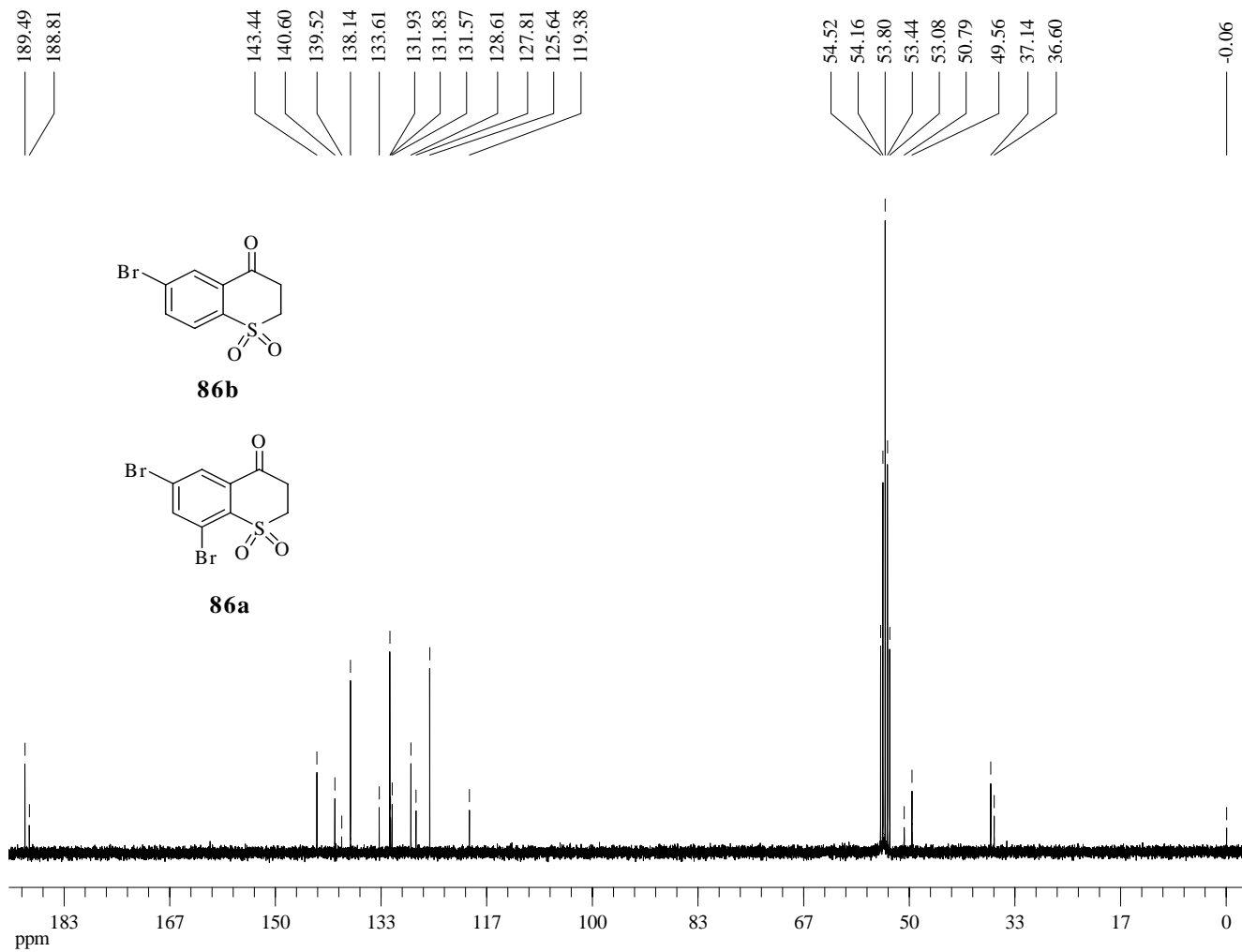
¹³C-NMR (75 MHz, CD₂Cl₂) of Compound **86a**



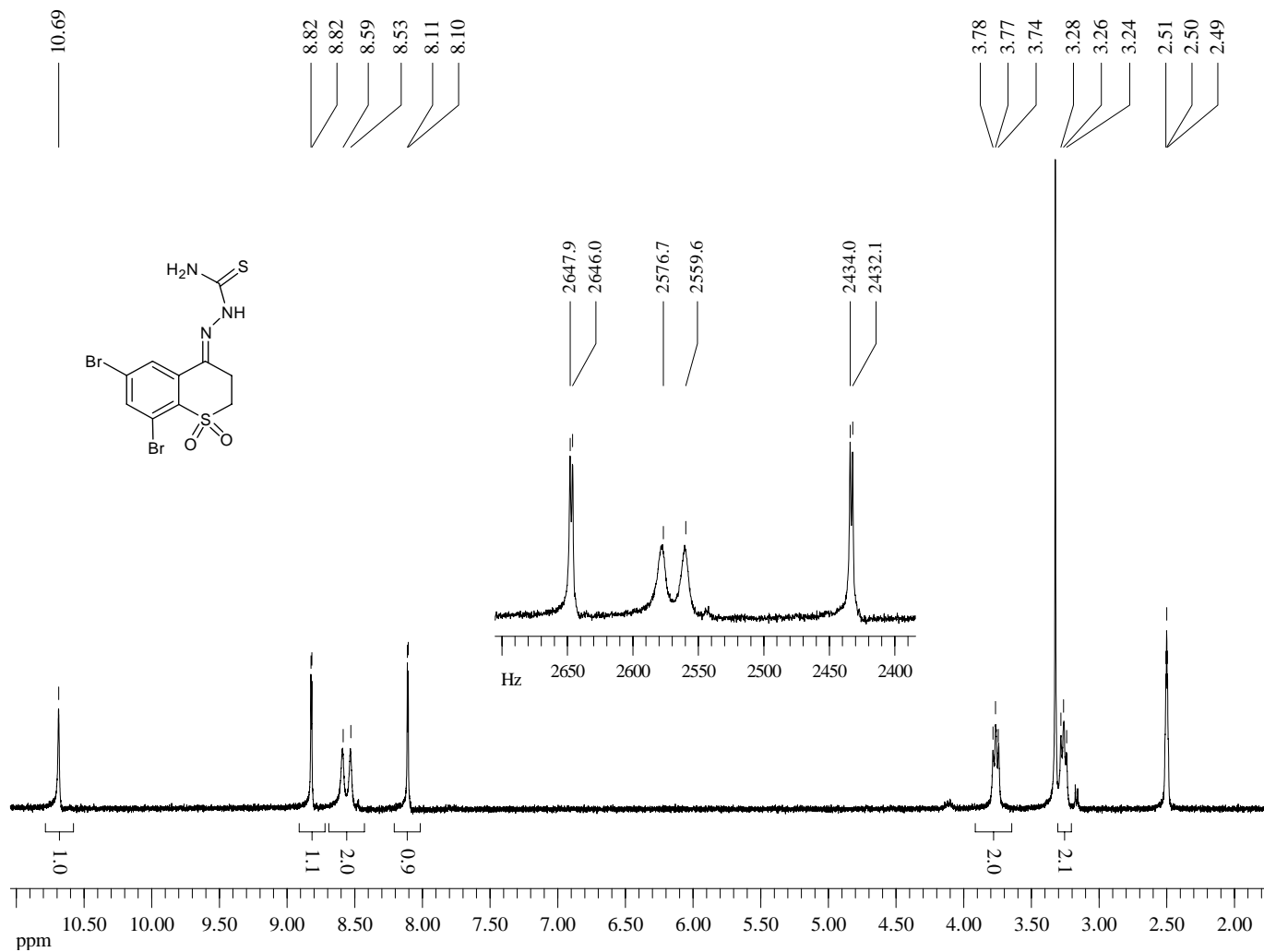
¹H-NMR (300 MHz, CD₂Cl₂) of Compound **86b**



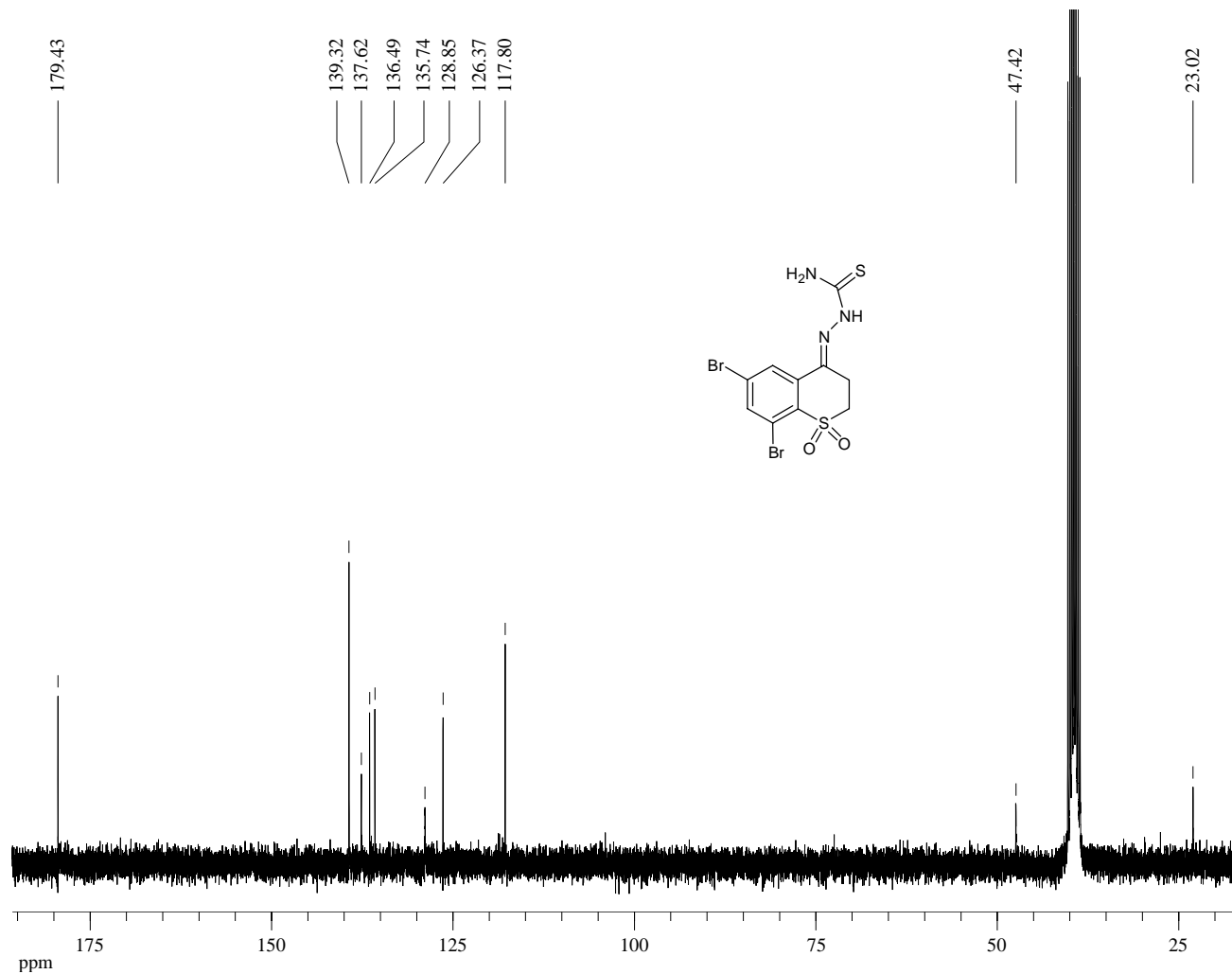
¹³C-NMR (75 MHz, CD₂Cl₂) of Compound **86b**



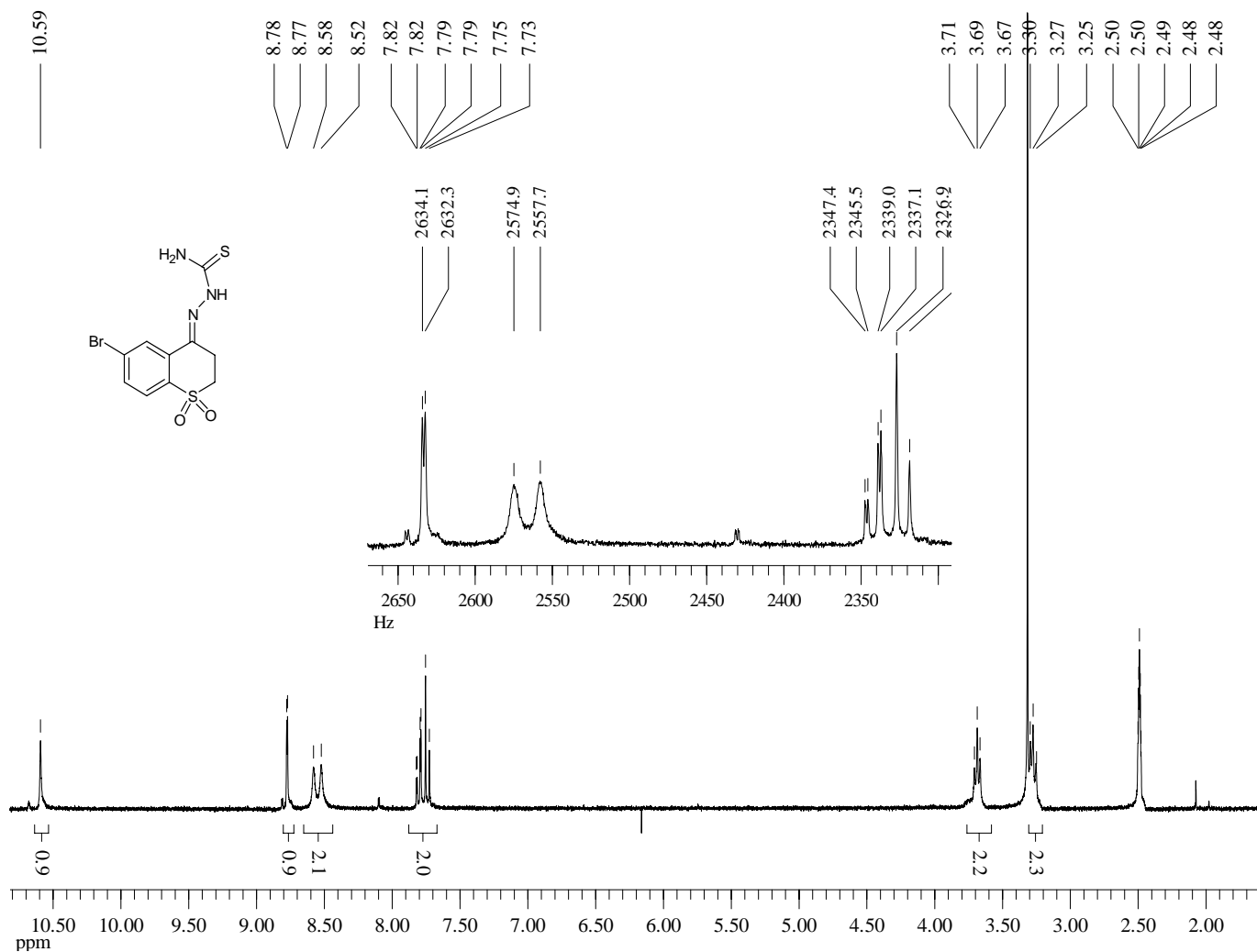
¹H-NMR (300 MHz, Methyl Sulfoxide-d₆) of Compound **87**



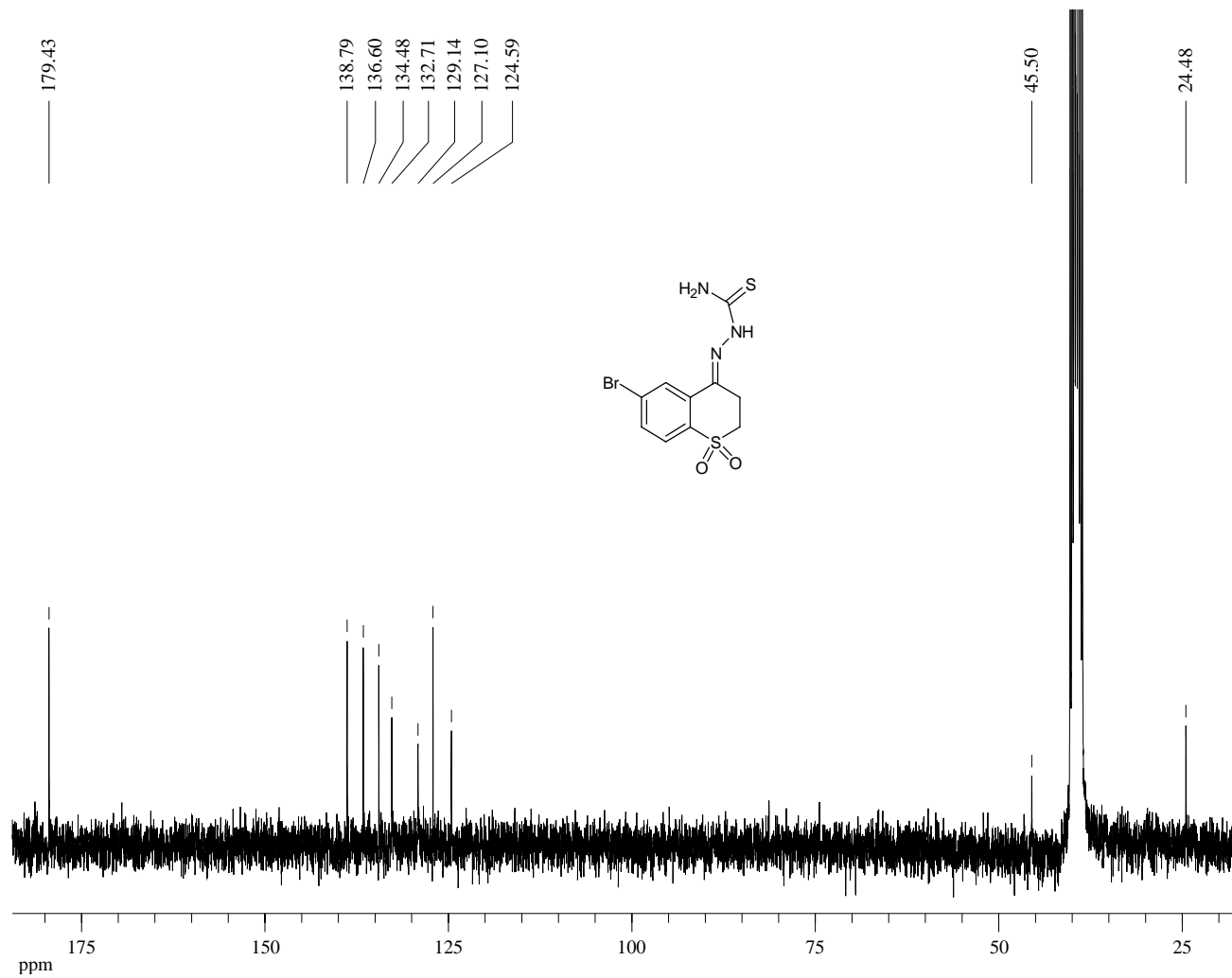
^{13}C -NMR (75 MHz, Methyl Sulfoxide- d_6) of Compound **87**



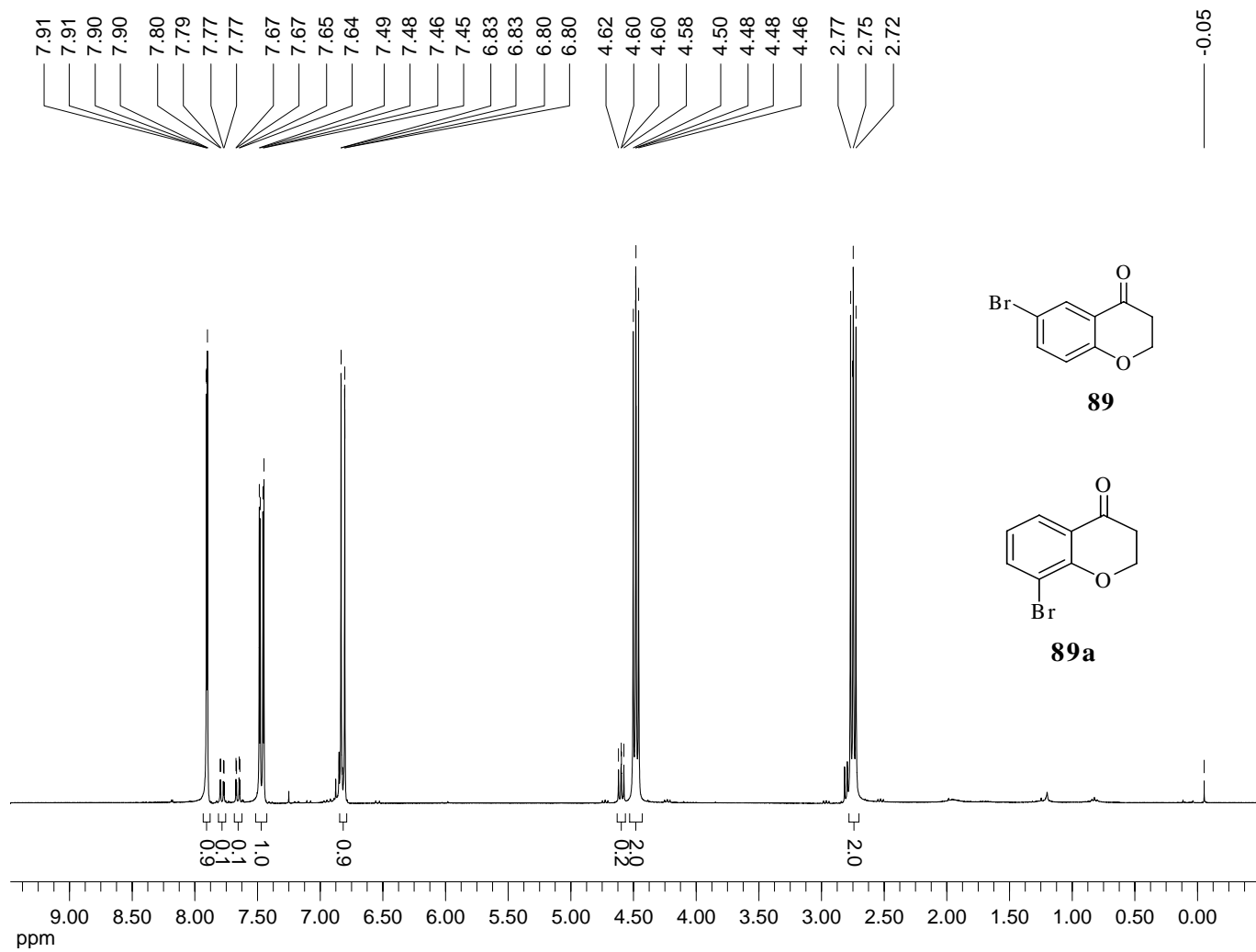
¹H-NMR (300 MHz, Methyl Sulfoxide d₆) of Compound **88**



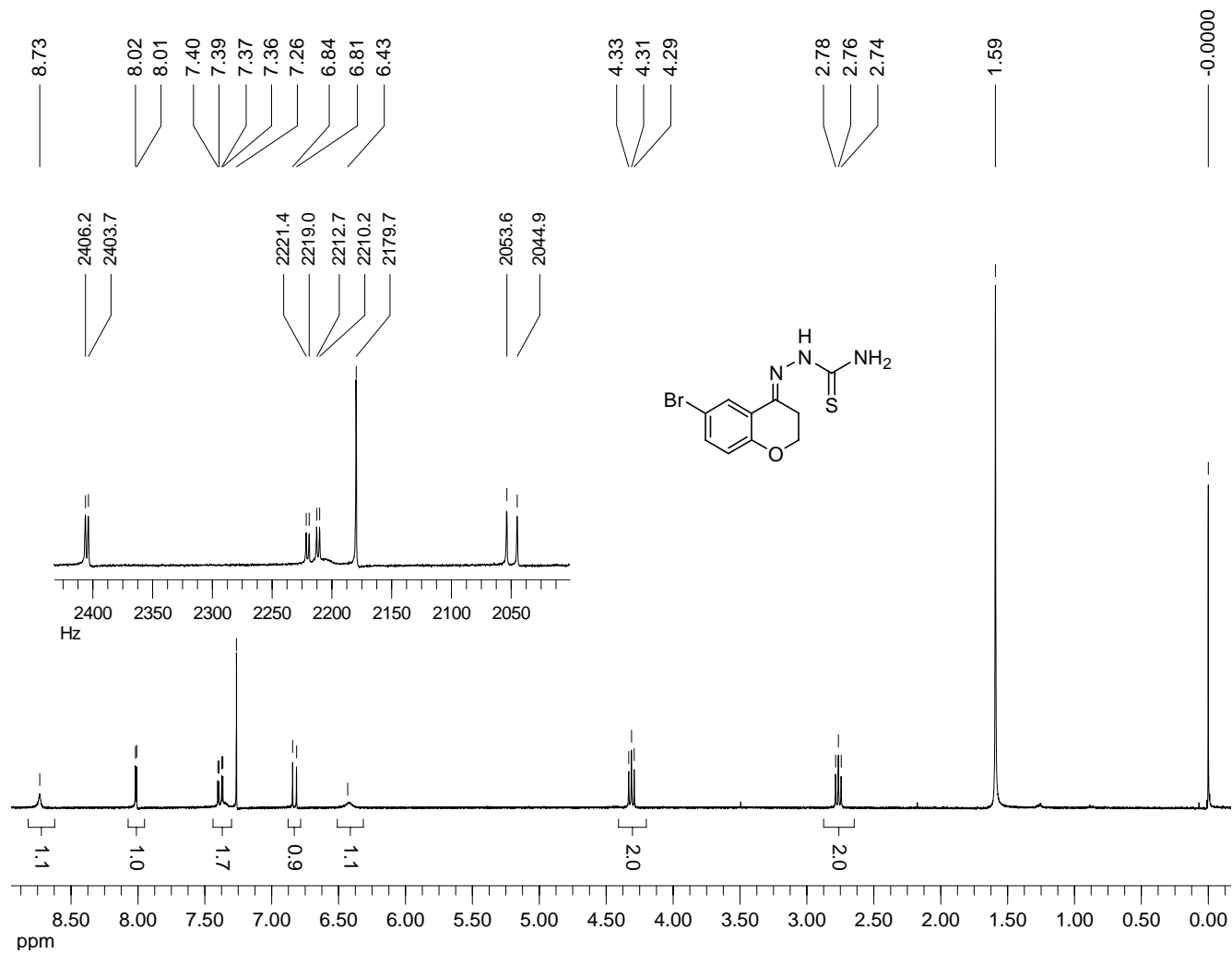
^{13}C -NMR (75 MHz, Methyl Sulfoxide d_6) of Compound **88**



¹H-NMR (300 MHz, CDCl₃) of Compound **89**



¹H-NMR (300 MHz, CDCl₃) of Compound **90**



References

1. Breslow, R. *J. Chem. Ed.* **1998**, 75, 705-718.
2. Roberts, S. M.; Ganellin, C. R. *Medicinal chemistry : the role of organic chemistry in drug research*; Academic Press: London ; San Diego, 1993.
3. King, F. D.; RSC Medicinal Chemistry School (7th : 1993 : University of Kent at Canterbury) In *Medicinal chemistry : principles and practice*; Royal Society of Chemistry: Cambridge, 1994.
4. Werbovetz, K. A. *Curr. Med. Chem.* **2000**, 7, 835-860.
5. Kevin G. Pinney, Christopher Jelinek, Klaus Edvardsen, David J. Chaplin, and George R. Pettit, Chapter 3 entitled: The Discovery and Development of the Combretastatins. pages 23-46, Published in *Antitumor Agents from Natural Products*, **2005**, edited by David Kingston, David Newman, and Gordon Cragg, CRC Press, Taylor and Francis Group, Boca Raton, Florida.
6. Pettit, G.R.; Singh, S.B. *Can. J. Chem.* **1987**, 65, 2390-2396.
7. Singh, S.B.; Pettit, G.R. *J. Org. Chem.* **1989**, 54, 4105-4114.
8. Gaukroger, K.; Hadfield, J.A.; Lawrence, N.J.; Nolan, S.; Mc Gown, A.T. *Org. Biomol. Chem.* **2003**, 1, 3033-3037.
9. Urbina, J. A. *Curr. Pharm. Des.* **2002**, 8, 287-295.
10. Copeland, R. A. *Evaluation of enzyme inhibitors in drug discovery : a guide for medicinal chemists and pharmacologists*; J. Wiley: Hoboken, N.J, 2005.
11. Clayman, C. B., *The American Medical Association Encyclopedia of Medicine*; Random House, Inc: New York, 1989.
12. Postlethwait, J. H.; Hopson, J. L. *Explore Life*; Rose, N., Ed.; Thomson Brooks/Cole: USA, 2003.
13. Weinreb, E. L. *Anatomy and Physiology*; Moore, J. A., Pinette, M., Eds.; Addison-Wesley Publishing Company, Inc: USA, 1984.
14. Encyclopedia Britannica, Encyclopedia Britannica Online. cancer. <<http://search.eb.com/eb/article-9106118>> (accessed 9/16, 2005).

15. Jemal, A.; Murray, T.; Ward, E.; Samuels, A.; Tiwari, R. C.; Ghafoor, A.; Feuer, E. J.; Thun, M. J. *CA Cancer. J. Clin.* **2005**, *55*, 10-30.
16. National Center for Health Statistics, Division of Vital Statistics. Centers for Disease Control and Prevention US Mortality Data in 1950 and 2002. <http://www.cdc.gov/nchs/nvss.htm> (accessed 9/17, 2005).
17. Baquiran, D. C. *Lippincott's cancer chemotherapy handbook*; Lippincott: Philadelphia, 2001.
18. Aggarwal, B. B.; Takada, Y.; Oommen, O. V. *Expert Opin. Investig. Drugs* **2004**, *13*, 1327-1338.
19. Johnson, J. G. The Cell Cycle Model Project <http://www.sirinet.net/~jgjohnso/cellcycleproject.html> (accessed 9/19, 2005).
20. Nygren, P. *Acta Oncol.* **2001**, *40*, 166-174.
21. Eckhardt, S. *Curr. Med. Chem-Anti-Cancer Agents* **2002**, *2*, 419-439.
22. Ross, J.; Schenkein, D.; Pietrusko, R.; Rolfe, M.; Linette, G.; Stec, J.; Stagliano, N. *Am. J. Clin. Pathol.* **2004**, *122*, 598-609.
23. Novotny, L.; Szekeres, T. *Expert opinion on therapeutic targets* **2005**, *9*, 343-357.
24. Arbuck, S. G.; Dancey, J.; Pluda, J. M.; Grochow, L.; Murgo, A. J.; Ivy, P.; Wright, J.; Blaylock, B.; Via, L. E.; Sausville, E. A. *Cancer Chemother. Biol. Response Modif.* **2001**, *19*, 237-288.
25. Liscovitch, M.; Lavie, Y. *IDrugs : investigational drugs journal* **2002**, *5*, 349-355.
26. Mellinghoff, I. K.; Sawyers, C. L. *Pharmacogenomics* **2002**, *3*, 603-623.
27. Siemann, D. W.; Shi, W. *Int. J. Radiat. Oncol. Biol. Phys.* **2004**, *60*, 1233-1240.
28. Siemann, D. W.; Chaplin, D.J. and Horsman, M. R. *Cancer* **2004**, *100*, 2491-2499.
29. Gaya, A. M.; Rustin, G. J. S. *Clin. Oncol.* **2005**, *17*, 277-290.
30. Siemann, D. W.; Horsman, M. R. *Expert review of anticancer therapy* **2004**, *4*, 321-327.
31. Blakey, D. C.; Ashton, S. E.; Westwood, F. R.; Walker, M.; Ryan, A. J. *International Journal of Radiation Oncology, Biology, Physics* **2002**, *54*, 1497-1502.

32. Siemann, D. W.; Bibby, M. C.; Dark, G. G.; Dicker, A. P.; Eskens Ferry, A. L. M.; Horsman, M. R.; Marme, D.; Lorusso, P. M. *Clinical cancer research : an official journal of the American Association for Cancer Research* **2005**, *11*, 416-420.
33. Tozer, G. M.; Kanthou, C.; Baguley, B. C. *Nature Reviews Cancer* **2005**, *5*, 423-435.
34. Ching, L.; Wilson, W. R.; Baguley, B. C. *Methods Mol. Med.* **2000**, *25*, 133-157.
35. Rowinsky, E. K.; Siemann, D. W.; Remick, S. C.; Ziats, N. P. *Horizons in Cancer Therapeutics* **2002**, *3*, 1-27.
36. Zhou, J.; Giannakakou, P. *Current Medicinal Chemistry - Anti-Cancer Agents* **2005**, *5*, 65-71.
37. Allan Jordan, John A. Hadfield, Nicholas J. Lawrence, Alan T. McGown *Med. Res. Rev.* **1998**, 259-296.
38. Anderson, P. J. *J. Biol. Chem.* **1979**, *254*, 2168-2171.
39. Lowe, J.; Li, H.; Downing, K. H.; Nogales, E. *J. Mol. Biol.* **2001**, *313*, 1045-1057.
40. Luduena, R. F.; Banerjee, A.; Khan, I. A. *Curr. Opin. Cell Biol.* **1992**, *4*, 53-57.
41. Li, H.; DeRosier, D. J.; Nicholson, W. V.; Nogales, E.; Downing, K. H. *Structure* **2002**, *10*, 1317-1328.
42. Checchi, P. M.; Nettles, J. H.; Zhou, J.; Snyder, J. P.; Joshi, H. C. *Trends Pharmacol. Sci.* **2003**, *24*, 361-365
43. Downing, K. H.; Nogales, E. *Curr. Opin. Struct. Biol.* **1998**, *8*, 785-791.
44. Desai, A.; Mitchison, T. J. *Annu. Rev. Cell Dev. Biol.* **1997**, *13*, 83-117.
45. Von Angerer, E. *Expert Opinion on Therapeutic Patents* **1999**, *9*, 1069-1081.
46. Giannakakou, P.; Sackett, D.; Fojo, T. *J. Natl. Cancer Inst.* **2000**, *92*, 182-183.
47. Ravelli, R. B. G.; Gigant, B.; Curmi, P. A.; Jourdain, I.; Lachkar, S.; Sobel, A.; Knossow, M. *Nature* **2004**, *428*, 198-202.
48. Shi, Q.; Chen, K.; Morris-Natschke, S. L.; Lee, K. H. *Curr. Pharm. Des.* **1998**, *4*, 219-248.
49. Desbene, S.; Giorgi-Renault, S. *Curr. Med. Chem-Anti-Cancer Agents* **2002**, *2*, 71-9.
50. Hamel, E.; Lin, C.M. *Biochemistry* **1984**, *23*, 4173.

51. Barbier, P.; Peyrot, V.; Dumortier, C.; D'Hoore, A.; Rener, G. A.; Engelborghs, Y. *Biochemistry* **1996**, *35*, 2008.
52. Harrisson, C. M. H.; Page, B. M.; Keir, H. M. *Nature* **1976**, *260*, 470-476.
53. Verdier-Pinard, P.; Lai, J-Y.; Yoo, H-D.; Yu, J.; Marquez, B.; Nagle, D. G.; Nambu, M.; White, J. D.; Falck, J. R.; Gerwick, W. H.; Day, B. W.; Hamel, E. *Molec. Pharmacol.* **1998**, *53*, 62.
54. Hamel, E. *Cell Biochem. Biophys.* **2003**, *38*, 1-21.
55. Mosmann, T. *Journal of Immunological Methods* **1983**, *65*, 55-63.
56. Pinney, K. G.; Mejia, M. P.; Villalobos, V. M.; Rosenquist, B. E.; Pettit, G. R.; Verdier-Pinard, P.; Hamel, E. *Bioorganic Med. Chem.* **2000**, *8*, 2417.
57. Silverstein, R.M.; Webster, F.X. *Spectrometric Identification of Organic Compounds*, 6th Ed., John Wiley & Sons, U.S.A., 1998.
58. Pavia, D.L.; Lampman, G.M.; Kriz, G.S. *Introduction to Spectroscopy: a Guide for Students of Organic Chemistry*, 2nd Ed. Sanders Collegue, U.S.A., 1996.
59. Schewerman, R.A.; Tumelty, D. *Tetrahedron Letters*, **2000**, *41*, 6531-6535.
60. Louis-Andre, O.; Gelbard, G. *Bulletin de la Societe Chimique de France*, **1986**, *4*, 565-577.
61. Whitten, K.W.; Gailey, K.D.; Davis, R.E. *General Chemistry*, Sauders Collegue, 3rd Ed., U.S.A., 1980.
62. Leonard, J.; Lygo, B.; Procter, G. *Advanced Practical Organic Chemistry*, 2nd Ed., Chapman and Hall, Great Britain, 1995.
63. Ohsumi, K.; Nakagawa, R.; Fukuda, Y.; Hatanaka, T.; Morinaga, Y.; Nihei, Y.; Ohishi, K.; Suga, Y.; Akiyama, Y.; Tsuji, T. *J. Med. Chem.* **1998**, *41*, 3022-3032.
64. Hatanaka, T.; Ohsumi, K.; Tsuyi, T.; Nihei, Y.; Nakagawa, R.; Ohishi, K. US Patent 5674906, 1995.
65. Ohsumi, K.; Hatanaka, T.; Fujita, K.; Nakagama, R.; Fukuda, Y.; Nikei, Y.; Suga, Y.; Morinaga, Y.; Akiyama, Y.; Tsuyi, T. *Bioorganic & Medicinal Chemistry Letters*, **1998**, *8*, 3153-3158.
66. Hatanaka, T.; Fujita, K.; Ohsumi, K.; Nakagawa, R.; Fukuda, Y.; Nihei, Y.; Suga, Y.; Akiyama, Y.; Tsuji, T. *Bioorg. Med. Chem. Lett.* **1998**, *8*, 3371-3374.

67. Ohsumi, K.; Hatanaka, T.; Nakagawa, R.; Fukuda, Y.; Morinaga, Y.; Suga, Y.; Nihei, Y.; Ohishi, K.; Akiyama, Y.; Tsuji, T. *Anti-Cancer Drug Design* **1999**, *14*, 539.
68. Hori, K.; Saito, S.; Sato, Y.; Kubota, K. *Med. Sci. Monit.* **2001**, *7*, 26-33.
69. Nihei, Y.; Suga, Y.; Morinaga, Y.; Ohishi, K.; Okamo, A.; Ohsumi, K.; Hatanaka, T.; Sato, Y.; Tsuruou, T. *Jpn. J. Cancer Res.* **1999**, *90*, 1016-1025.
70. Hori, K.; Saito, S.; Nihei, Y.; Suzuki, M.; Sato, Y. *Jpn. J. Cancer Res.* **1999**, *90*, 1026-1038.
71. Hori, K.; Saito, S. *Br. J. Cancer* **2003**, *89*, 1334.
72. Hori, K.; Saito, S. *Br. J. Cancer* **2004**, *90*, 549-553.
73. Hori, K.; Saito, S.; Kubota, K. *Br. J. Cancer* **2002**, *86*, 1604.
74. Nihei, Y.; Suga, Y.; Morinaga, Y.; Ohishi, K.; Suzuki, M.; Okamo, A.; Ohsumi, K.; Hatanaka, T.; Nakagawa, R.; Tsuyi, T.; Akiyama, Y.; Tsuruo, T. *Proceedings of the American Association for Cancer Research* **1998**, *39*, 167.
75. Nihei, Y.; Suzuki, M.; Okamo, A.; Morinaga, Y.; Ohishi, K.; Suzuki, M.; Ohsumi, K.; Hatanaka, T.; Nakagawa, R.; Tsuyi, T.; Akiyama, Y.; Tsuruo, T. *Proceedings of the American Association for Cancer Research* **1998**, *39*, 47.
76. Monk, K.A.; Siles, R.; Hadimani, M.; Mugabe, B.E.; Ackley, F.; Studerus, S.W.; Edvarlsen, K.; Trawick, M.L.; Garner, C.M.; Rhodes, M.R.; Pettit, G.R.; Pinney, K.G. *Bioorganic & Medicinal Chemistry* 2005, in press.
77. Chaplin, D.J.; Garner, C.M.; Kane, R.B.; Pinney, K.G.; Prezioso, J.A.; Edvarlsen, K. US Patent 6919324B2, 2005.
78. Crews, P.; Rodriguez, J.; Jaspars, M. *Organic Structure Analysis*, Oxford University, U.S.A., 1998.
79. *Chem 3D Molecular Modeling and Analysis*, Cambridge Scientific Computing, U.S.A. Copyright 1986-2000.
80. Sakowski, J.; Bohm, M.; Sattler, I.; Dahse, H.; Schlitzer, M. *J. Med. Chem.* **2001**, *44*, 2886-2899.
81. Wiesner, J.; Kettler, K.; Sakowski, J.; Ortmann, R.; Jomaa, H.; Schlitzer, M. *Biorganic & Medicinal Chem. Letters* **2003**, *13*, 361-363.
82. Somei, M.; Yamada, F.; Koneko, C. *Chemistry Letters*, **1979**, 943-944.

83. Meghani, P.; Street, J.D.; Joule, J.A. *J. Chem. Soc. Chem. Commun.*, **1987**, 1406-1407.
84. Somei, M.; Kato, K.; Inoue, S. *Chem. Pharm. Bull.* **1980**, 28, 2515-2518.
85. Yue, E. W.; Higley, C. A.; DiMeo, S. V.; Carini, D. J.; Nugiel, D. A.; Benware, C.; Benfield, P. A.; Burton, C. R.; Cox, S.; Grafstrom, R. H.; Sharp, D. M.; Sisk, L. M.; Boylan, J. F.; Muckelbauer, J. K.; Smallwood, A. M.; Chen, H.; Chang, C. -.; Seitz, S. P.; Trainor, G. L. *J. Med. Chem.* **2002**, 45, 5233-5248.
86. Pettit, G. R.; Anderson, C. R.; Herald, D. L.; Jung, M. K.; Lee, D. J.; Hamel, E.; Pettit, R. K. *J. Med. Chem.* **2003**, 46, 525-531.
87. Pettit, G.R. and Lippert, J.W. *Anti-Cancer Drug Des.* **2000**, 15, 203-216.
88. Monk, K.; Siles, R.; Pinney, K.G.; Garner, C.M. *Tetrahedron Letters* **2003**, 44, 3759-3761.
89. Siles, R.; Hadimani, M.; Pinney, K. G. 58th Southwest Regional Meeting of The American Chemical Society, (Abstract No. 236), Austin, TX, November 4, **2002**.
90. Ohta, A.; Tonomura, Y.; Sawaki, J.; Sato, N.; Akiike, H. *Heterocycles* **1991**, 32(5), 965-973.
91. Singh, S.B.; Pettit, G.R. *Synthetic Communications* **1987**, 17(7), 877-892.
92. Perez-Melero, C.; Maya, B.S.; Del Rey, B.; Pelaez, R.; Caballero, E.; Velarde, M. *Bioorganic & Medicinal Chemistry Letters* **2004**, 14(14), 3771-3774.
93. Toda, N.; Tazo, K.; Maremoto, S.; Takami, K.; Ori, M.; Yamada, N.; Kaneko, T.; Kogen, H. *Bioorganic & Medicinal Chemistry* **2003**, 11, 1935-1955.
94. Grossman, R.B. *The Art of Writing Reasonable Organic Reaction Mechanisms*, Springer-Verlag, New York, U.S.A., 1999.
95. X-ray crystallographic analysis was carried out by Feazell, R. and Klausmeyer, K., Baylor University.
96. Adler, E.; Bjorkqvist, K.J. *Acta Chimica Scandinavica* **1951**, 5, 241-252.
97. Voet, D.; Voet, J. G. *Biochemistry*; John Wiley & Sons, USA, 1995.
98. Little, R.D.; Muller, G.W. *J. Am. Chem. Soc.* **1981**, 103(10), 2748.
99. Corey, E.J.; Suggs, W. *Tetrahedron Letters* **1975**, 31, 2647-2650.

100. Fernandes, R.A.; Kumar, P. *Tetrahedron Letters* **2003**, 44, 1275-1278.
101. Luzzio, F.A.; Fitch, R.W.; Hoore, W. J.; Hudd, K.D. *J. Chem. Ed.* **1999**, 76(7), 974-975.
102. Riesgo, E. C.; Jin, X.; Thummel, R. P. *J. Org. Chem.* **1996**, 61, 3017-3022.
103. ChewDraw Ultra Chemical Structure Drawing Standard, Cambridge software, U.S.A., Copyright,1985-2000.
104. Hadimani, M. B., Ph.D dissertation, Studies toward the discovery of new classes of privileged molecules as colchicine-site binding ligands for tubulin : structure-based design, synthesis and bioactivity of small ligands targeted at tumor vasculature, Baylor University, 2004.
105. Shirali, A. R. Inhibitors of tubulin assembly : designed ligands featuring benzo[b]thiophene, dihydronaphthalene and aroylchromene molecular core structures, Baylor University, 2002.
106. Kaufman, T.S. *J. Chem. Soc. Perkin Trans 1: Organic and Bio-Organic Chemistry* **1996**, 20, 2497-2505.
107. Pettit, G. R.; Toki, B.; Herald, D. L.; Verdier-Pinard, P.; Boyd, M. R.; Hamel, E.; Pettit, R. K. *J. Med. Chem.* **1998**, 41, 1688-1695.
108. Lynch, J.E.; Choi, W.B.; Churchill, H.R.O.; Volante, R.P.; Reamer, R.A.; Ball, R.G. *J. Org. Chem.* **1997**, 62, 9223-9228.
109. Brandes, B.D.; Jacobsen, E.N. *J. Org. Chem.* **1994**, 59, 4378-4380.
110. Corey, E.J.; Venkateswaren, A. *J. Am. Chem. Soc.* **1972**, 94(17), 6190-6191.
111. Pinney, K.G.; Shirali, A.; Sriram, M.; Hadimani, M.; Jelinek, C.; Siles, R.; Arthasery, P. Report submitted to Oxygene Inc., February 9th, 2004.
112. Chen, Z.; Mocharla, V. P.; Farmer, J. M.; Pettit, G. R.; Hamel, E.; Pinney, K. G. *J. Org. Chem.* **2000**, 65, 8811-8815.
113. Pinney, K.G.; Wang, F.; Hadimani, M. (2005b). Indole-containing and combretastatin-related anti-mitotic and anti-tubulin polymerization agents.US Patent 6849656.
114. Pinney, K.G.; Edvardsen, K.; Chaplin, D.J.; Hadimani, M.B.; Kessler, R.J.; Jelinek, C.; Arthesary, P. (2004c). Molecular recognition of the colchicine binding site as a design paradigm for the discovery and development of new vascular targeting

(disrupting) agents. Second International Vascular Targeting Conference, Miami Beach, Florida, May 15-18, 2004.

115. Hadimani, M.; Kessler, R.J.; Kautz, J.A.; Ghatak, A.; Shirali, A.; O'Dell, H.; Garner, C.M.; Pinney, K.G. (2002). 2-(3-tert-Butyldimethylsiloxy-4-methoxyphenyl)-6-methoxy-3-(3,4,5-trimethoxybenzoyl)indole. *Acta Cryst., Sec. C: Crystal Structure Comm.* **C58**, 330-332.
116. Gupta, R.R.; Kumar, M.; Gupta, V. *Heterocyclic Chemistry II*, Springer-Verlag, Germany, 1999
117. Julian, P.L.; Meyer, E.W.; Magnani, A.; Cole, W. *J. Am. Chem. Soc.* **1945**, 67(7), 1203-1211.
118. Bashford, K.E.; Cooper, A.L.; Kane, P.D.; Moody, C.J. *J. Chem. Soc. Perkin Trans. I*, **2002**, 1672-1687.
119. Gribble, G.W. *J. Chem. Soc. Perkin Trans. I*, **2000**, 1045-1075.
120. Olive, D.L.J.; Hisanidee, S.; Coltart, D.M. *J. Org. Chem.* **2003**, 68(24), 9247-9254.
121. Hofle, G.; Steglich, W.; Vorbruggen, M. *Angew. Chem. Int. Ed. Engl.* **1978**, 17, 569-583.
122. Leclerc, G.; Marciniak, G.; Decker, N.; Schwartz, J. *J. Med. Chem.* **1986**, 29, 2433-2438.
123. Leclerc, G.; Marciniak, G.; Decker, N.; Schwartz, J. *J. Med. Chem.* **1986**, 29, 2427-2432.
124. Smith, K.; Musson, A.; DeBoss, G.A. *J. Org. Chem.* **1998**, 63, 8448-8454.
125. Smith, K.; Musson, A.; DeBoss, G.A. *Chem. Commun.* **1996**, 469-470.
126. Perez, R.S.; Fernandez-Alvarez, F.; Nieto, O.; Piedrahita, F.J. *J. Med. Chem.* **1992**, 35, 4584-4588.
127. Gokhale, U.B.; Joshi, A.A. *Indian Journal of Chemistry* **1993**, 32B, 1073.
128. Bartels-Keith, J.; Ciecuch, F.W. *Canadian Journal of Chemistry* **1968**, 46, 2593-2600.
129. Pettit, G.R.; Singh, S.B.; Boyd, M.R.; Hamel, E.; Pettit, R.K.; Schmidt, J.M.; Hogan, F. *J. Med. Chem.* **1995**, 38, 1666.

130. Pettit, G. R.; Singh, S. B.; Niven, M. L.; Hamel, E.; Schmidt, J. M. *J. Nat. Prod.* **1987**, *50*, 119.
131. Pettit, G.R.; Temple, C. Jr.; Narayanan, V.L.; Varma, R.; Simpson, M.J.; Boyd, M.R.; Rener, G.A.; Bansal, N. *Anti-Cancer Drug Des.* **1995**, *10*, 299.
132. Ohsumi, K.; Nakagawa, R.; Fukuda, Y.; Hatanaka, T.; Morinaga, Y.; Nihei, Y.; Ohishi, K.; Suga, Y.; Akiyama, Y.; Tsuji, T. *J. Med. Chem.* **1998**, *41*, 3022.
133. Hatanaka, T.; Fujita, K.; Ohsumi, K.; Nakagawa, R.; Fukuda, Y.; Nihei, Y.; Suga, Y.; Akiyama, Y.; Tsuji, T. *Bioorganic & Medicinal Chemistry Letters* **1998**, 3371-3374.
134. Cushman, M.; Nagarathman, D.; Gopal, D.; Lin, C.M.; Hamel, E. *J. Med. Chem.* **1991**, *34*, 2579-2588.
135. Sheng, Y.; Hua, J.; Pinney, K. G.; Garner, C. M.; Kane, R. R.; Prezioso, J. A.; Chaplin, D. J.; Edvardsen, K. *Int. J. Cancer* **2004**, *111*, 604.
136. Chagas disease. <http://www.pennhealth.com/ency/article/001372.htm> (accessed 10/29, 2005).
137. Mendoza, I.; Moleiro, F.; Marques, J.; Guerrero, J.; Matheus, A.; Rodriguez, F. Implications of Sudden Death in Chagas Disease. <http://www.caibco.ucv.ve/articulo/implicat.htm> (accessed 8/31, 2002).
138. Rodriques, C. J.; de Castro, S. L. *Mem. Inst. Oswaldo Cruz* **2002**, *97*, 3-24.
139. Werbovetz, K. A. *Curr. Med. Chem.* **2000**, *7*, 835-860.
140. Huang, L.; Lee, A.; Ellman, J. A. *J. Med. Chem.* **2002**, *45*, 676-684.
141. Urbina, J. A. *Curr. Pharm. Des.* **2002**, *8*, 287-295.
142. Urbina, J. A. *Expert Opinion on Therapeutic Patents* **2003**, *13*, 661-669.
143. Cazzulo, J. J. *Proteases of Infectious Agents* **1999**, 189-203.
144. Jose, C. J.; Stoka, V.; Turk, V. *Curr. Pharm. Des.* **2001**, *7*, 1143-1156.
145. Cerecetto, H.; Gonzalez, M. *Current topics in medicinal chemistry* **2002**, *2*, 1187-1213.
146. Engel, J. C.; Doyle, P. S.; McKerrow, J. H. *Medicina* **1999**, *59 Suppl 2*, 171-175.

147. The Kiss of death: chagas' disease in the Americas
<http://www.uta.edu/chagas/html/chagDoYa.html> (accessed 10/29, 2005).
148. http://www.dpd.cdc.gov/dpdx/HTML/TrypanosomiasisAmerican.asp?body=Frames/S-/TrypanosomiasisAmerican/body_TrypanosomiasisAmerican_page1.htm
(accessed 10/29, 2005).
149. Historical aspects. <http://www.dbbm.fiocruz.br/tropical/chagas/chapter.html> (accessed 10/29, 2005).
150. WHO Chagas Disease. <http://www.who.int/tdr/diseases/chagas/default.htm> (accessed 10/29, 2005).
151. Urbina, J. A. *Expert Opinion on Therapeutic Patents* **2003**, *13*, 661-669.
152. Urbina, J. A.; Docampo, R. *Trends Parasitol.* **2003**, *19*, 495-501.
153. Urbina, J. A. *Curr. Opin. Infect. Dis.* **2001**, *14*, 733-741.
154. Docampo, R. *Curr. Pharm. Des.* **2001**, *7*, 1157-1164.
155. Cerecetto, H.; Gonzalez, M. *Current topics in medicinal chemistry* **2002**, *2*, 1187-1213.
156. De Castro, S. L. *Acta Trop.* **1993**, *53*, 83-98.
157. Stoppani, A. O. *Medicina* **1999**, *59 Suppl 2*, 147-165.
158. McGrath, M. E.; Eakin, A. E.; Engel, J. C.; McKerrow, J. H.; Craik, C. S.; Fletterick, R. J. *J. Mol. Biol.* **1995**, *247*, 251-259.
159. Gillmor, S. A.; Craik, C. S.; Fletterick, R. J. *Protein science : a publication of the Protein Society* **1997**, *6*, 1603-1611.
160. Brinen, L. S.; Hansell, E.; Cheng, J.; Roush, W. R.; McKerrow, J. H.; Fletterick, R. *J. structure Fold. Des.* **2000**, *8*, 831-840.
161. Sajid, M.; McKerrow, J. H. *Mol. Biochem. Parasitol.* **2002**, *120*, 1-21.
162. Harris, J. L.; Backes, B. J.; Leonetti, F.; Mahrus, S.; Ellman, J. A.; Craik, C. S. *Proc. Natl. Acad. Sci. U. S. A.* **2000**, *97*, 7754-7759.
163. Powers, J. C.; Asgian, J. L.; Ekici, O. D.; James, K. E. *Chem. Rev.* **2002**, *102*, 4639-4750.
164. Leung, D.; Abbenante, G.; Fairlie, D. P. *J. Med. Chem.* **2000**, *43*, 305-341.

165. McKerrow, J. H. *Int. J. Parasitol.* **1999**, *29*, 833-837.
166. Serveau, C.; Lalmanach, G.; Juliano, M. A.; Scharfstein, J.; Juliano, L.; Gauthier, F. *Biochem. J.* **1996**, *313*, 951-956.
167. McKerrow, J. H.; Engel, J. C.; Caffrey, C. R. *Bioorg. Med. Chem.* **1999**, *7*, 639-644.
168. Barr, S.C.; Warner, K.L.; Kornreic, B.G.; Piscitelli, J.; Wolf, A.; Benet, L.; McKerrow, J.H. *Antimicrobial Agents and Chemotherapy* **2005**, *49*(12), 5160-5161.
169. Du, X.; Guo, C.; Hansell, E.; Doyle, P. S.; Caffrey, C. R.; Holler, T. P.; McKerrow, J. H.; Cohen, F. E. *J. Med. Chem.* **2002**, *45*, 2695-2707.
170. Chiyanzu, I.; Hansell, E.; Gut, J.; Rosenthal, P. J.; McKerrow, J. H.; Chibale, K. *Bioorg. Med. Chem. Lett.* **2003**, *13*, 3527-3530.
171. Fujii, N.; Mallari, J. P.; Hansell, E. J.; Mackey, Z.; Doyle, P.; Zhou, Y. M.; Gut, J.; Rosenthal, P. J.; McKerrow, J. H.; Guy, R. K. *Bioorg. Med. Chem. Lett.* **2005**, *15*, 121-123.
172. Palmer, J. T.; Rasnick, D.; Klaus, J. L. PCT, Patent 9523222, 1995.
173. Cornelius, L.A.H.; Combs, D.W. *Synthetic Communications* **1994**, *24*(19), 2777-2788.
174. Pavia, D.L.; Lapman, G.M.; Kriz, G.S. Introduction to Organic laboratory Techniques, 3rd Ed.; Engel, R.G.; Ed., Edmonds Community Collegue, Lynnwood, Washington, 1999.
175. Karabatsos, G.J.; Vane, F.M.; Taller, R.A.; His, N. *J. Am. Chem. Soc.* **1964**, *86*, 3351-3357.
176. Karabatsos, G.J.; Graham, J.D. Vane, F.M. *J. Am. Chem. Soc.* **1962**, *84*, 753-755.
177. Karabatsos, G.J.; Taller, R.A.; Vane, F.M. *J. Am. Chem. Soc.* **1963**, *85*, 2326-2327.
178. Karabatsos, G.J.; Shapiro, B.L.; Vane, F.M.; Fleming, J.S.; Ratka, J.S. *J. Am. Chem. Soc.* **1963**, *85*, 2784-2788.
179. Karabatsos, G.J.; Taller, R.A. *J. Am. Chem. Soc.* **1963**, *85*, 3624-3629.
180. Faul, M.M.; Ratz, A.M.; Sullivan, K.A.; Trankle, W.G.; Winneroski, L.L. *J. Org. Chem.* **2001**, *66*(17), 5572-5782.

181. Mocharla, V.P. Design, Synthesis, and Biological Evaluation of Diverse Small Molecular Frameworks as Tubulin Binding Ligands, Ph.D., Dissertation, Baylor University, 1999.
182. Kolonko, K.J.; Shapiro, R.M. *J. Org. Chem.* **1978**, 43(7), 1404-1408.
183. Siemiling, U.; Newmann, B.; Stammler, H.G. *J. Org. Chem.* **1997**, 62, 3407-3408.
184. Shapiro, R.M.; Heath, M.J. *J. Am. Chem. Soc.* **1967**, 89(22), 5734-5735.
185. Dess, D.B.; Martin, J.C. *J. Org. Chem.* **1983**, 48, 4155-4156.
186. Dess, D.B.; Martin, J.C. *J. Am. Chem. Soc.* **1991**, 113, 7277-7287.
187. Hurd, C.D.; Hayao, S. *J. Am. Chem. Soc.* **1954**, 76, 5065-5069.
188. Greenbaum, D. C.; Mackey, Z.; Hansell, E.; Doyle, P.; Gut, J.; Caffrey, C. R.; Lehrman, J.; Rosenthal, P. J.; McKerrow, J. H.; Chibale, K. *J. Med. Chem.* **2004**, 47, 3212-3219.
189. Siles, R.; Chen, S.E.; Zhou, M.; Trawick, M.L.; Pinney, K.G. 229th National Meeting of the American Chemical Society, San Diego, CA, March 13-17, 2005.
190. Tyndall, J. D. A.; Nall, T.; Fairlie, D. P. *Chem. Rev.* **2005**, 105, 973-1000.
191. King, F. D.; RSC Medicinal Chemistry School (7th : 1993 : University of Kent at Canterbury) *Medicinal chemistry : principles and practice*; Chemistry, Pharmaceutical congresses; Pharmaceutical chemistry; Royal Society of Chemistry: Cambridge, 1994.